

**Identification and functional characterization of novel
ionotropic glutamate receptor subunits at *Drosophila*
neuromuscular synapse**

Dissertation
zur Erlangung des Doktorgrades
der Mathematisch-Naturwissenschaftlichen Fakultäten
der Georg-August-Universität zu Göttingen

Vorgelegt von
Gang Qin
aus Tianjin, V.R. China

Göttingen 2004

D7

Referent: Prof. Dr. F. W. Schürmann

Korreferent: Prof. Dr. H. Jäckle

Tag der mündlichen Prüfung: 26 JAN 2005

Table content	1
Summary	4
List of Figures	5
List of Tables	6
Acknowledgements	7
1 Introduction	8
1.1 Molecular basics of Synaptogenesis	8
1.1.1 The making of a synapse	8
1.1.2 Development of vertebrate NMJ	11
1.1.2.1 Initial AchR clustering	11
1.1.2.2 Agrin-MuSK signalling pathway	13
1.1.2.3 Developmental role of AchR per se	16
1.1.3 Development of mammalian CNS excitatory synapse	16
1.1.3.1 Cell adhesion molecules in the axon-dendrite contact	18
1.1.3.2 Assembly of synapse	21
1.1.3.2.1 Presynaptic assembly	21
1.1.3.2.2 Postsynaptic assembly	23
1.1.3.3 Time sequence of pre- and postsynaptic assembly	25
1.1.4 <i>Drosophila</i> NMJ as one model for synaptogenesis	25
1.1.4.1 Structural properties of <i>Drosophila</i> NMJ	25
1.1.4.2 Initiation and maintenance of neuromuscular connection	28
1.1.4.2.1 Initiation of neuromuscular contact---target recognition (pathfinding)	28
1.1.4.2.2 Stabilization and maintenance of neuromuscular connection by cell adhesion molecules	29
1.1.4.3 Synapse formation	31
1.2 Structure and functional relevance of ionotropic glutamate receptors	33
1.2.1 Modular design of ionotropic glutamate receptors during evolution	33
1.2.2 Molecular mechanisms underlying selective assembly and transport of ionotropic glutamate receptors	34
1.2.3 Properties of ionotropic glutamate receptors expressed at <i>Drosophila</i> neuromuscular synapses	36
1.3 The aim and strategy of this work	37

2	Materials and methods	39
2.1	Materials (Chemicals, enzymes and molecular kits)	39
2.2	Methods	39
2.2.1	Genechip analysis and quantitative real-time RT-PCR	39
2.2.1.1	Genechip analysis	39
2.2.1.2	Real-time RT-PCR	45
2.2.2	Fly stocks and genetics	46
2.2.2.1	Fly stocks, crosses and rearing conditions	46
2.2.2.2	Mutagenesis screening	47
2.2.3	Molecular constructs and transgenes	48
2.2.4	In situ hybridization	50
2.2.5	Biochemistry (collaborated with Tobias Schwarz)	53
2.2.6	Immunohistochemistry	54
2.2.6.1	Embryonic and Larval filet preparation	54
2.2.6.2	Confocal epifluorescent microscopy	56
2.2.7	Ultrastructural analysis (collaborated with Carolin Wichmann)	56
2.2.8	Electrophysiology (collaborated with Robert Kittle)	57
3	Results	58
3.1	Establishing the tissue specific transcriptome of <i>Drosophila</i> larval body wall muscle	58
3.2	Identification of novel ionotropic glutamate receptor subunits expressed at the <i>Drosophila</i> neuromuscular synapse	59
3.2.1	Enrichment of various transcripts encoding novel ionotropic glutamate receptor subunits in larval body wall muscles	60
3.2.2	Expression pattern of new ionotropic glutamate receptor genes	61
3.2.3	The GluR-IIID and GluR-IIIE represent a new type of muscle expressed glutamate receptor subunits	63
3.2.4	GluR-IIC, GluR-IIID and GluR-IIIE are specifically localized at postsynaptic densities of neuromuscular synapses	65
3.3	GluR-IIID and GluR-IIIE are essential for viability	67
3.4	Reciprocal dependence of all essential glutamate receptor subunits for glutamate receptor expression and function at synapse	70
3.4.1	Complete absence of all the other glutamate receptor subunits at synapse in knockout of any essential subunit genes	70
3.4.2	Genetically depriving the expression level of any single essential glutamate receptor subunits results into tight reduction of all of the other subunits at synapse	72
3.4.3	Depriving synaptic glutamate receptor subunits results into dramatic weakness of postsynaptic activity	77

3.5 Structural role of ionotropic glutamate receptor during pre- and postsynaptic differentiation of neuromuscular synapse	77
3.5.1 Normal differentiation of presynaptic transmitter release machinery at glutamate receptor deprived synapse	77
3.5.2 Defective assembly of PSD specialization at glutamate receptor deprived but not presynaptic neurotransmission deprived synapse	79
3.5.3 Ultrastructural evidence of abnormal synaptic differentiation at glutamate receptor deprived synapse	84
3.5.4 Defective compartmentation of the synaptic and perisynaptic area at glutamate receptor deprived but not neurotransmission deprived synapse	87
3.5.5 Similar defects in synaptic differentiation in the complete absence of glutamate receptors	89
4 Discussion	90
4.1 Genomic tools could speed up identifying essential genes involved in synapse formation and modulation	90
4.2 GluR-IID and GluR-IIIE are novel glutamate receptor subunits crucial for glutamate receptor assembly and thus neurotransmission at neuromuscular synapse	91
4.3 Implications in the in vivo stoichiometry of <i>Drosophila</i> glutamate receptor based on genetic analysis	93
4.4 Structural role of ionotropic glutamate receptor per se in organizing synaptic assembly and time sequence of pre- and postsynaptic assembly	95
References	99
Appendix: Genes enriched in larval body wall preparations	107
<i>Lebenslauf</i>	127

Summary

The molecular mechanisms triggering the formation of synapses *in vivo* are crucial for understanding the development as well as the activity dependent remodelling of synaptic circuits. The *Drosophila* neuromuscular junction (NMJ) provides an excellent platform for investigating fundamental aspects of how glutamatergic synapse form *in vivo*. The molecular mechanisms relevant to synaptogenesis and growth control of the *Drosophila* NMJ were addressed by combining genome-wide transcript analysis with functional genetics. This allowed the identification of two novel postsynaptic muscle expressed ionotropic glutamate receptor subunits, GluR-IID and GluR-IIE. Genetic elimination of either of the two novel subunits resulted in paralyzed lethal embryos, indicating that both new subunits are essential for forming the postsynaptic glutamate receptor complex. Further genetic, cell biological and electrophysiological studies then uncovered a tight interdependence of all NMJ glutamate receptor subunits for synaptic localization and function. These results imply that the NMJ glutamate receptor complex has strictly hetero-tetrameric stoichiometry. This so far was not described for mammalian ionotropic glutamate receptors which are usually considered to be dimers of dimers. In the second part of the thesis, glutamate receptor deprived synapses were closer inspected. Surprisingly, depleting glutamate receptors (but not depleting synaptic neurotransmission activity) provoked severe ultrastructural and molecular defects of postsynaptic membrane organization and compartment formation. Thus, the glutamate receptor complex *per se* but not its ligand-gated ion channel activity seemingly plays an instructive role for assembling mature postsynaptic specializations. Such a ‘structural’ role of glutamate receptor complexes in synaptic differentiation is novel. It might be relevant for the role

ionotropic glutamate receptors play during synaptic plasticity of the mammalian brain, which is considered to be a cellular correlate of learning and memory processes.

List of Figures

Fig.1-1 Basic structure of chemical synapse	9
Fig. 1-2 Representative molecular composition of CNS glutamatergic Synapse	10
Fig.1-3 Vertebrate neuromuscular junction	12
Fig. 1-4 Spiny dendrites from hippocampal pyramidal neuron	18
Fig. 1-5 Structure of <i>Drosophila</i> NMJ	27
Fig.1-6 Structure of iGluR subunit and model of iGluR assembly	34
Figure 3-1. <i>GluR-IID</i> and <i>GluR-IIE</i>: novel glutamate receptor subunits with muscle specific expression	62
Figure 3-2 Sequence analysis of <i>GluR-IID</i> and <i>GluR-IIE</i>	64
Fig.3-3 <i>GluR-IID</i> and <i>GluR-IIE</i> are expressed within postsynaptic Densities	66
Figure 3-4 Genetic analysis of <i>GluR-IID</i> and <i>GluR-IIE</i>	68
Figure 3-5 Interdependence between glutamate receptor subunits for NMJ expression	71
Figure 3-6 A partial reduction of either <i>GluR-IIE</i> or <i>GluR-IID</i> provokes a significant reduction of all glutamate receptor subunits at the NMJ	73
Fig.3-7 Minimal mounts of <i>GluR-IIA</i> and no- <i>IIB</i>: expression of all glutamate receptor subunits and postsynaptic sensitivity are strongly reduced	76
Fig. 3-8 Normal organization of presynaptic neurotransmitter release machinery components at glutamate receptor deprived synapses	79
Fig.3-9 Defective PSD assembly at glutamate receptor deprived but not transmission deprived synapses	81
Fig. 3-10 Glutamate receptor <i>per se</i> but not presynaptic vesicle release are important for proper synapse formation at embryo NMJ	84
Fig.3-11 Electron microscopy: defective postsynaptic assembly at glutamate receptor deprived synapses	85
Fig.3-12 Defective synaptic compartments at glutamate receptor deprived but not neurotransmission deprived synapses	88

List of Tables

Table 3-1 Described muscle / cuticle-specific transcripts displaying enrichment in gene chip analysis of body-wall-preparations	59
Table 3-2 GluR-IID and GluR-IIIE are enriched in larval body wall mRNA	61

Acknowledgements

First of all, I would like to express my gratitude to my advisors, Dr. Stephan Sigrist, Prof. Dr. F. W. Schürmann and Prof. Dr. H. Jäckle for their consistent support, helpful tips, kind advices and comments.

My very special thanks are to Dr. Stephan Sigrist, who provides me the opportunity to join his group and do exciting cutting-edge science. As one talented and serious scientist, Stephan taught me not only how to perform successful experiments but also how to ask the right question and address it in a logic way. During my whole thesis period, I was encouraged by our extensive and enthusiastic discussion, from which I really have learned a lot. Also, for me it is really nice to witness the rapid growth of our young group.

I would like to thank several collaborators, Robert Kittel for electrophysiology, Dr. Carolin Wichmann for Electron Microscopy and Tobias Schwarz for biochemistry. Without their excellent contributions, I could hardly reach current stage. The Gene Chip experiments were performed in Max-Planck Institute for Biophysical Chemistry, I am really indebted to Dr. Ronald Kühnlein and Dr. Sebastian Grönke for their warm and patient help.

I am also grateful to my colleagues Carlos Melino, Tobias Rasse, Andreas Schmid, Sara Mertel, Wernher, Laura Swan and Manuela Schmidt, with whom I can freely exchange ideas and reagents, which greatly facilitate my work. I want to express my kindest gratefulness to Christine Quentin, Miriam Richter and Jasmin for their highly professional technical assistance.

Finally, my very special thanks are addressed to my family and my friends.

1 Introduction

1.1 Molecular basics of Synaptogenesis

1.1.1 The making of a synapse

The human brain comprises a huge network of neurons (about 10^{11}) which link with each other structurally and functionally through the special type of cell-cell junctions called synapses. Synapses transmit electrical signals between neurons, mediating neuronal signaling and computation, also they are able to undergo long-term changes (synaptic plasticity) that underlie aspects of learning and memory (Li and Sheng, 2003). Although many of these synaptic contacts are highly specialized, all neurons make use of one of the two basic forms of synaptic transmission: electrical or chemical. Synaptic communication in the brain is mainly dependent on chemical mechanisms, that is, synaptic transmission is mediated via a chemical substance that is released by presynaptic terminal and diffuses through the synaptic cleft to activate relevant receptors on the postsynaptic membrane. Like other cell-cell junctions, synapses contain a wide variety of transmembrane proteins, cytoskeletal units and signaling components. However, they differ from most other junctions in being structurally asymmetric (Fig. 1-1): the presynaptic specialization, usually on the axon, contains a complex apparatus called active zone, which controls the transmitter-filled vesicles docking, fusing and the release of transmitter into the synaptic cleft. In contrast, the postsynaptic reception specialization, just juxtaposed to the active zone and recognized ultrastructurally by the presence of an electron-dense thickening called the postsynaptic density (PSD), is made of receptors, ion channels, signaling components and scaffold proteins clustered all together (Garner et al., 2002; Yamagata et al., 2003).

On average, each neuron forms about 1000 synaptic connections and receives even more, perhaps as many as 10,000 connections (Kandel ER et al. 2001). These synapses include excitatory, inhibitory and modulatory type. Most

of them are excitatory and utilize glutamate as neurotransmitter. The inhibitory neurotransmission is mediated by glycine or GABA, whereas modulatory neurotransmission is mediated by 5-HT, dopamine, acetylcholine (Ach) and neuropeptides etc. Notably, although presynaptic terminals from any given neuron generally release one type of transmitter, neurons usually receive multiple forms of synaptic input, which can be excitatory, inhibitory or modulatory. Moreover, anatomical evidence has shown that the number of cellular contacts often exceeds the number of synaptic connections formed onto a single cell, suggesting that neurons are able to distinguish synaptic contact site and nonsynaptic site (White et al., 1976; Benson et al., 2001). Thus, for efficient and accurate neurotransmission, the site where synaptic contact forms is carefully selected, and, within an individual synapse, appropriate pre- and postsynaptic apparatus is assembled highly coordinately and precisely.

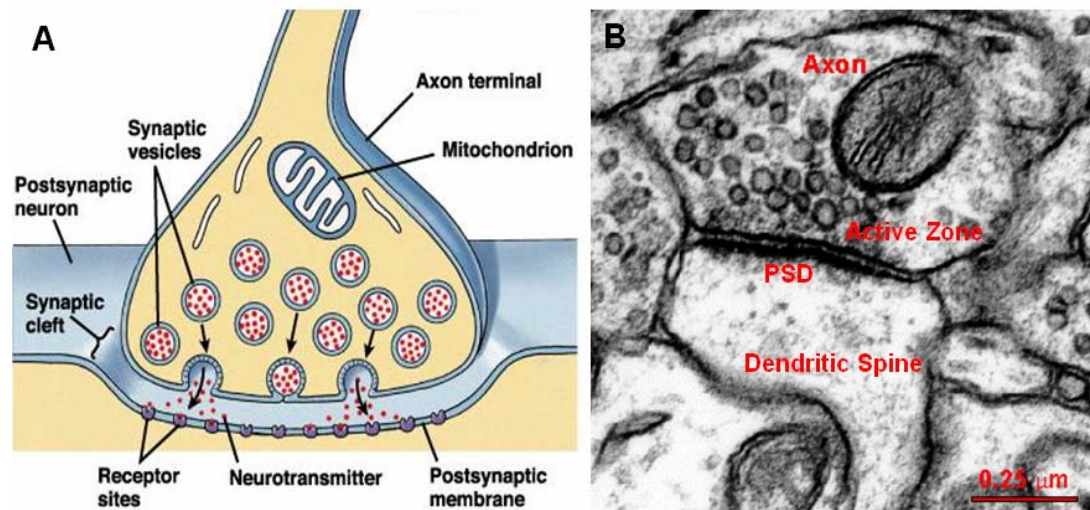


Fig.1-1 Basic structure of chemical synapse. A, diagram of a central nervous system chemical synapse. B, ultrastructure of a central chemical synapse (Adapted from www.synapses.mcg.edu/)

What is the molecular mechanisms controlling the site and type specific assembly of chemical synapses? To answer this fundamental question in neurobiology, extensive efforts have been invested to identify the molecular

constituents of synapses and define their functional significance via the combination of molecular, biochemical and genetic approaches (Fernandez-Chacon and Sudhof, 1999; Scannevin and Huganir, 2000; Phillips et al., 2001; Sheng, 2001; Garner et al., 2002) (Fig. 1-2). Furthermore, recently the adoption of newly developed optical imaging technique has provided a way to track the dynamics of individual synaptic protein trafficking and targeting during synapse formation even in real-time resolution (Ahmari et al., 2000; Okabe et al., 2001; Prange and Murphy, 2001; Rosenberg et al., 2001; Zhai et al., 2001).

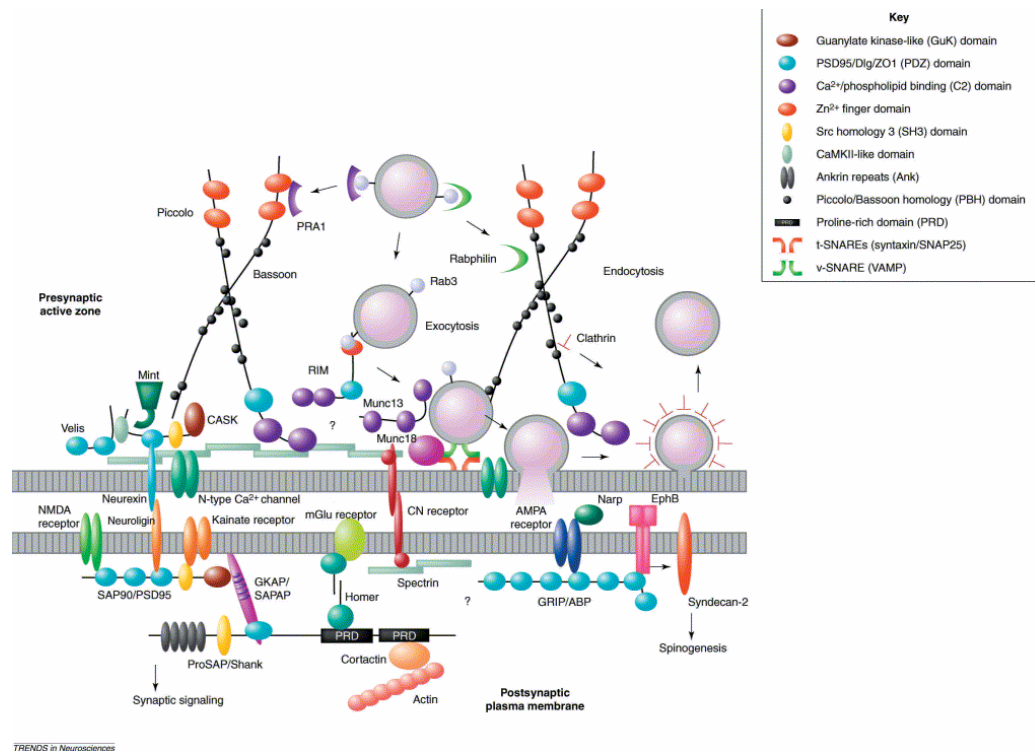


Fig. 1-2 Representative molecular composition of CNS glutamatergic synapse (Adapted from Garner et al., 2002).

Historically, much of what we know about the development of chemical synapses is based on studies of the vertebrate neuromuscular junction (NMJ)—a large peripheral synapse formed between a motor neuron and a skeletal muscle fibre. However, in recent years, with the incremental technical

advances a picture of the synaptogenesis in the mammalian central nervous system has also begun to emerge.

1.1.2 Vertebrate NMJ

The vertebrate NMJ (Fig. 1-3) is ideal for studying chemical synaptogenesis because it is large, relatively simple and unparalleled accessible to experimentation. During development (starting at about E11 in mice) multinucleated skeletal muscle fibres form by fusion of precursor myoblasts, shortly after myotubes begin to form (at E12-13 in mice), motor neurons innervate the muscle at a specialized region of the muscle membrane called the end-plate. At the region where the motor axon approaches the muscle fibre, the axon loses its myelin sheath and splits into several fine branches. The ends of the fine branches form multiple expansions or varicosities, called synaptic boutons, from which the neurotransmitter (here is Ach) is released from the motor neuron. Each bouton is positioned over a postjunctional fold, a deep and narrow depression of muscle cell membrane that contains high densities of transmitter receptors (here is acetylcholine receptors, AchRs), and this precise apposition of postsynaptic specializations to the motor nerve terminal insures that transmitter comes into contact with its receptor within microseconds after release, thereby facilitating efficient synaptic transmission.

1.1.2.1 Initial AchR clustering

Once the myotube forms, the AchR is starting to be expressed and inserted into the muscle surface, but with low density (usually about 1000 per μm^2); after synaptic maturation, by contrast, the AchRs are highly concentrated at the synaptic sites (to a density up to 10,000 per μm^2) and depleted at the extrasynaptic membrane (10 per μm^2 or less). One of the central questions is the contribution of muscle versus motor nerve in initiating

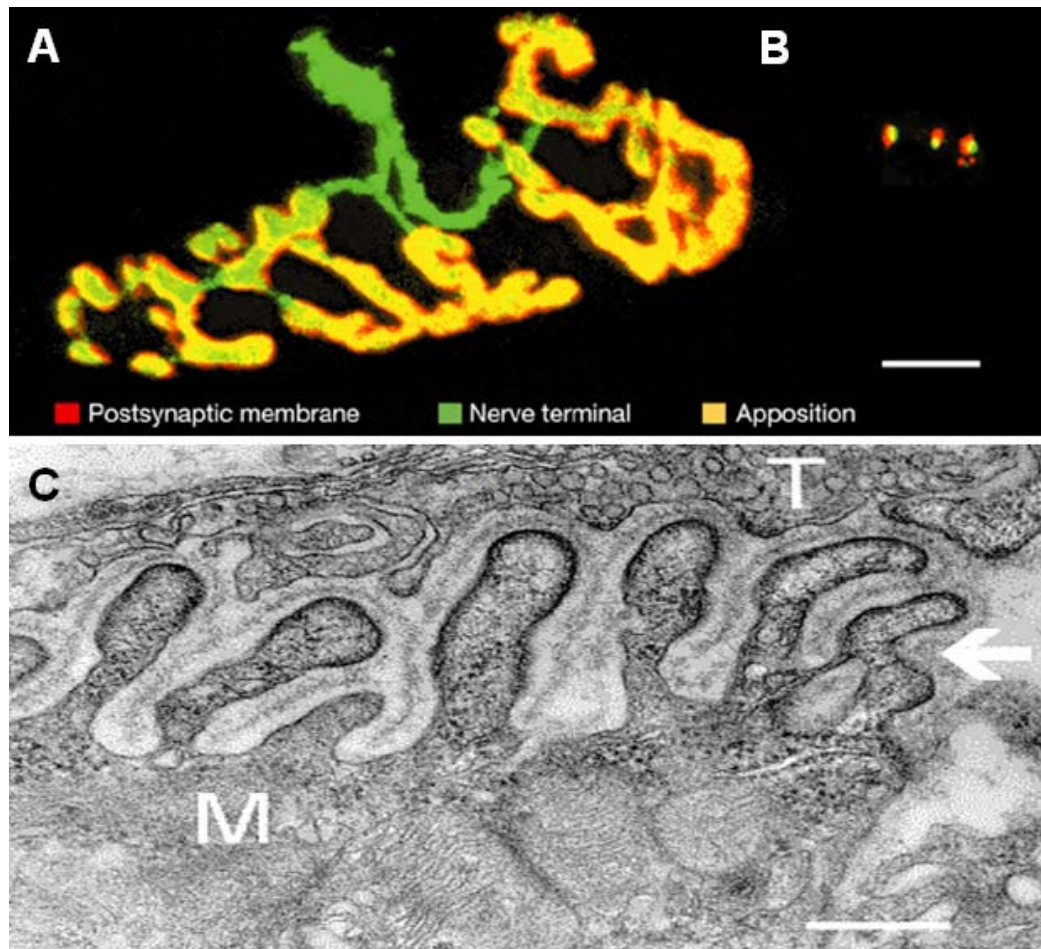


Fig.1-3 Vertebrate neuromuscular junction. A, The neuromuscular junction of an adult mouse. Scale = 5 μm . B, Three synapses on cultured mouse hippocampal neurons shown at the same scale (Adapted from Sanes J et al. 2001). C, Electron micrograph of motor end plate of abdominal muscle of frog. T - axon terminal, M - muscle fiber, arrow - foldings covered with basal lamina. Scale = 0.3 μm (Adapted from www.synapses.mcg.edu/)

and maintaining postsynaptic differentiation. Recently, more and more evidences suggest that the muscle itself has the capacity to be prepatterned. Particularly pertinent observations are, during the brief period when synaptogenesis begins in mouse muscle, some AchR clusters are not apposed by nerves and some nerve endings are not opposed to AchR clusters; moreover, the AchR clusters are present in muscles even without innervation, most of these

small clusters aggregate in the central end-plate band of the muscle, although this central band appears to be wider and more poorly defined than the one in innervated muscle (Lin et al., 2001; Yang et al., 2001).

1.1.2.2 Arin-MuSK Signaling Pathway

Upon innervation, AchR clusters are restricted to the central band of muscle. In the past three decades, numerous studies have established that motor nerve plays a major role in organizing this type of postsynaptic differentiation via two intramuscular mechanisms: clustering of AchRs at the synaptic contact sites; and selective transcription of AchR genes by myonuclei associated with synaptic sites (Burden, 1998; Sanes and Lichtman, 1999; Lin et al., 2001). Several nerve derived molecules have been identified and agrin is proved to be crucial *in vivo*. Agrin, isolated by McMahan and colleagues, is a large heparan sulphate proteoglycan that is synthesized by motor neurons, transported down motor axons, and released from nerve terminals, where it stably associates with the basal lamina of the synaptic cleft (Wallace, 1989; McMahan, 1990; Bowe and Fallon, 1995; Sanes and Lichtman, 2001). Agrin was identified from its ability to induce the aggregation AchRs on cultured myotubes, and was soon found to also aggregate many other components of the postsynaptic apparatus (Wallace, 1989). In Agrin-deficient mice, the number and density of AchR clusters, as well as synapse-specific transcription, are reduced markedly, which convincingly demonstrates that Agrin is crucial for AchR clustering in the muscle membrane opposite the presynaptic terminals (Gautam et al., 1996; Ruegg and Bixby, 1998).

MuSK, a transmembrane receptor tyrosine kinase, was discovered due to its selective abundance in synapse-rich Torpedo electric organ, whose principal cells are modified muscle cells that are innervated by cholinergic synapses (Jennings et al., 1993). Studies in mice reveal that MuSK is specifically expressed in skeletal muscles and is colocalized with AchRs in the postsynaptic membrane at the NMJ (Valenzuela et al., 1995).

Unexpectedly, muscles in MuSK-null mutant mice show totally no detectable signs of postsynaptic differentiation, although the AchR genes are expressed at normal level (DeChiara et al., 1996; Lin et al., 2001; Yang et al., 2001). Several studies have established the linkage between Agrin and Musk signaling: application of Agrin to myotubes leads to rapid activation of MuSK; expression of a dominant negative form of MuSK inhibits Agrin-induced cluster formation in cultured myotubes (Glass et al., 1996); MuSK^{-/-} myotubes are completely unresponsive to agrin, but agrin sensitivity is restored by introducing wild-type MuSK (Zhou et al., 1999). Taken together, these results demonstrate that MuSK is essential for agrin-induced postsynaptic differentiation.

A crucial component downstream of MuSK that affects the postsynaptic differentiation is rapsyn, a 43-kDa membrane associated cytoplasmic protein. Rapsyn is identified from its tight connection with AchR. It appears as soon as AchR starts clustering, perfectly colocalizes with AchR clusters, and in the electric organ it follows 1:1 stoichiometry (LaRochelle and Froehner, 1986; Noakes et al., 1993). Co-expression of AchR and rapsyn in all of the heterologous cells tested so far results into the formation of AchR- Rapsyn co-clusters, whereas AchRs are diffusely distributed when expressed alone (Froehner et al., 1990; Phillips et al., 1991). Consistently, in rapsyn mutant mice, no AchR clusters form on the muscle surface (Gautam et al., 1995). Thus, rapsyn is necessary for all forms of AchR clustering. Intriguingly, rapsyn can cluster AchRs when they are co-expressed in heterologous non-muscle cells that lack agrin and MuSK (Apel et al., 1997). By contrast, not even spontaneous (agrin-independent) AchR clusters form in MuSK deficient myotubes (Zhou et al., 1999), and overexpression of rapsyn in wild-type myotubes induces virtually no further cluster formation (Yoshihara and Hall, 1993; Han et al., 1999). This raises the possibility that muscles contain intrinsic activity to prevent the MuSK signaling independent clustering of rapsyn, which might be an efficient way to avoid the AchR clustering at the

wrong sites.

How does activation of Agrin-MuSK signaling lead to the clustering of AchRs? Previously it has been shown that cytoskeletal components are closely associated with AchR clusters, and disruption of cytoskeleton prevents the AchR cluster formation (Bloch and Pumplin, 1988). Thus, it is plausible that the activation of MuSK signaling upon agrin binding provide intrinsic cytoskeletal regulatory capacity required for remodelling and postsynaptic assembly. Consistent with this view, it has been found that agrin induces the polymerization of actin at the AchR clustering sites (Dai et al., 2000), moreover, it has been demonstrated that agrin-mediated clustering of AchRs depends on activation of Rac/ Cdc42, leading to the formation of AchR microclusters, followed by Rho activation, resulting in the consolidation of these microclusters into larger AchR clusters (Weston et al., 2000; Weston et al., 2003).

Although there is little doubt that Agrin/ MuSK signaling is the major pathway that is crucial for NMJ synaptogenesis, the intracellular signaling mechanisms downstream of MuSK have only begun to be elucidated recently. In response to agrin binding, MuSK undergoes tyrosine phosphorylation, this might create docking sites for signaling molecules or promote proper folding of the kinase. As an example, the juxtamembrane tyrosine (Y553) is required for agrin-induced AchR clustering (Zhou et al., 1999; Herbst and Burden, 2000). Very recently, the Abl kinases were shown to be required for the agrin/ MuSK dependant synaptic assembly, Abl kinases and MuSK can effect reciprocal tyrosine phosphorylation and form a complex after agrin engagement (Finn et al., 2003). Dishevelled (Dvl), a signaling molecule important for planar cell polarity, has also been found to interact directly with MuSK and PAK, forming a signaling scaffold which is important for agrin/ MuSK mediated AchR clustering (Luo et al., 2002). Additionally, evidences have been provided that geranylgeranyltransferase I (GGT), a zinc

metalloenzyme that tethers proteins to plasma membrane by prenylation (Zhang and Casey, 1996), serves as one important component in the agrin/MuSK pathway, which reveals an important role of prenylation in regulating synapse formation and/ or maintenance (Luo et al., 2003).

1.1.2.3 Developmental role of AchR *per se*

During postsynaptic differentiation, do AchRs only occupy the slots within assembled scaffold and contribute nothing for the assembly? In tested non-muscle cells, this seems true, but in muscle cells it is obviously not the case: Rapsyn fails to cluster at synaptic sites in zebrafish mutants deficient in the AchRs, suggesting the requirement of AchRs for proper synaptic localization of postsynaptic components (Ono et al., 2001); consistently, in the variants of C2 myotubes virtually lacking AchRs, agrin also fails to aggregate rapsyn (Marangi et al., 2001); moreover, in mutant mice that lack an adult AchR subunit, the postsynaptic membrane undergoes a profound reorganization in which levels of several membrane and cytoskeletal components decline in parallel with AchR loss, and residual material forms abnormal small islands at the NMJ (Missias et al., 1997). Therefore, the AchR *per se* is not merely a passive ligand, but plays an active role in organizing synaptic assembly. Interestingly, this is reminiscent of the assembly of inhibitory CNS synapses, in which GABA_A receptor subtypes are localized at synapses through their interaction with gephyrin (Kneussel et al., 1999). Gephyrin is not clustered at postsynaptic sites of mice lacking GABA_A receptor γ subunits, suggesting that gephyrin requires the presence of GABA_A receptors to efficiently form synaptic aggregates (Essrich et al., 1998). Thus, neurotransmitter receptors of both vertebrate NMJ and inhibitory CNS synapses are actively involved in postsynaptic assembly during synaptogenesis.

1.1.3 Mammalian CNS excitatory synapses

In the central nervous system, most excitatory synapses utilize glutamate

as the neurotransmitter. Glutamatergic synapses contain excitatory, glutamate responsive ionotropic and metabotropic receptors (Hollmann and Heinemann, 1994; McGee and Brecht, 2003). Ionotropic glutamate receptors are supposed to be tetrameric complexes, and are categorized into three major classes, on the basis of pharmacology, electrophysiology and sequence homology: AMPA (α -amino-3-hydroxy-5-methyl-4-isoxazolepropionic acid) receptors, NMDA (N-methyl-D-aspartic acid) receptors and kainate receptors.

Morphologically, most mature excitatory synapses are constructed on the characteristic tiny actin-rich structures---dendritic spines---the small lateral dendritic protrusions. Spines have variable size (up to a few μm in length and $0.8 \mu\text{m}^3$ in volume) and shape (such as thin, stubby or mushroom-like) (Harris and Kater, 1994; Hering and Sheng, 2001; Li and Sheng, 2003) (Fig. 1-4). During brain development, there is morphological transition in spines. During the first two postnatal weeks, synapses are frequently observed on the dendritic shaft, on stubby spines and on filopodia (Fiala et al., 1998), with maturation of the brain, such synapses are gradually substituted by, or converted to, synapses on mushroom-like spines (Harris and Kater, 1994).

As described before, the pre- and postsynaptic membrane of vertebrate NMJ are separated by an extracellular basal membrane, the extracellular-matrix molecule agrin is secreted from the nerve terminal and induces the postsynaptic differentiation. However, in central synapses, the extracellular matrix is not well characterized and, so far, no secreted molecules has been convincingly shown to be crucial for the development of mammalian central synapses. Narp (neuronal activity-regulated pentraxin), a secreted molecule that accumulates at synaptic sites, can interact with and cluster AMPA receptors (O'Brien et al., 1999; O'Brien et al., 2002). However, just as its name implied, Narp is a neuronal activity-regulated molecule, it recruits AMPA receptors only when a synapse is undergoing activity-dependant changes. Narp is less likely to play a major role during synaptogenesis, since AMPA receptor clustering is not essential for initial

synapse formation (see below for details).

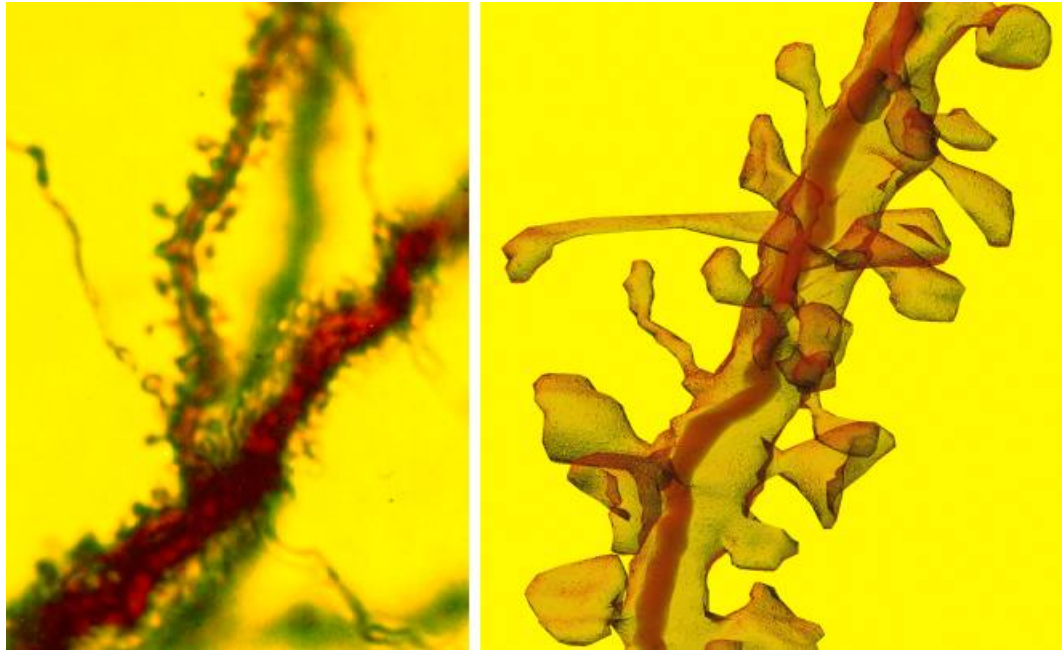


Fig. 1-4 Spiny dendrites from hippocampal pyramidal neuron.

Left: Light microscope image. *Right:* Reconstruction from serial electron microscopy (Adapted from www.synapses.mcg.edu/).

1.1.3.1 Cell adhesion molecules in the axon-dendrite contact

Synaptic assembly appears to be a multi-step process that is initiated from the axon-dendrite contact. Initial contact is followed by a stabilization step at the contact site and, subsequently, by further pre- and postsynaptic differentiation. Each process seems to require the interaction of various classes of cell adhesion molecules (CAMs). The Cadherin family of homophilic cell adhesion molecules is essential for the formation and stability of epithelial cell junctions. Cadherins are found to localize at both pre- and postsynaptic side, dominant-negative studies of the neuronal cadherins indicate that they are important for synapse integrity and morphological maturation of dendritic spines (Togashi et al., 2002). However, due to the large number of various Cadherin and Cadherin-related genes that are expressed in the central nervous system, it is still not possible to conclude

whether cadherin plays an initiating role in synapse formation or a promoting role in subsequent synaptic growth.

Various types of integrins are expressed in the brain with different distribution patterns (Pinkstaff et al., 1999). Integrins function as cell-matrix or cell-cell adhesion molecules by binding, respectively, to extracellular matrix proteins or to immunoglobulin superfamily proteins (Aplin et al., 1998). Based on our current understanding, integrins have diverse functions in early stage of CNS development, including neuronal migration (Milner and Campbell, 2002), axon pathfinding and outgrowth (Hoang and Chiba, 1998; Pasterkamp and Kolodkin, 2003), they also appear to have a role in synapse maturation (Chavis and Westbrook, 2001).

Immunoglobulin superfamily molecules contain certain numbers of extracellular cyctein-looped domains first found in immunoglobulins. Synaptic cell adhesion molecule (SynCAM) belongs to such a superfamily and is found to be localized on the synaptic membranes. Importantly, expression of SynCAM in nonneuronal cells both induces neighboring neurons to form functional presynaptic terminals and, if gluamate receptors are coexpressed, endows the postsynaptic membranes with the capacity of responding to glutamate (Biederer et al., 2002). Thus, SynCAM seems an ideal candidate initiating central synapse formation, although its *in vivo* role has yet to be examined. Very recently, another two immunoglobulin superfamily members, SYG-1 and SYG-2 were isolated in genetic screen for *C. elegans* mutants defective in targeting specificity during synaptogenesis (Shen and Bargmann, 2003; Shen et al., 2004). SYG-1 is present at the presynaptic neuron HSNL and localizes to synaptic sites at the early stages of synaptic formation, while SYG-2 is expressed transiently in the guidepost epithelial cells during synapse formation. SYG-2 can interact with SYG-1 and thus instruct the accumulation of synaptic vesicles and the subsequent synaptic assembly at proper site.

Presynaptic neurexins and postsynaptic neuroligins represent another group of synaptic CAMs proposed to function in synapse differentiation. The extracellular domain of presynaptic beta-neurexin interacts directly with the extracellular AchE-like domain of postsynaptic neuroligin (Nguyen and Sudhof, 1997). In a co-culture system, the overexpression of neuroligin in heterologous cells can induce the structural and functional presynaptic specialization in contacting axons (Scheiffele et al., 2000). More convincingly, in the context of intracellular interactions, the cytoplasmic tail of β -neurexin binds with PDZ protein CASK, a presynaptic scaffold protein; comparably, the intracellular part of neuroligin binds with PSD-95, which is an important PDZ domain scaffold protein of the postsynaptic density. Thus the direct ‘talk’ between β -neurexin and neuroligin across the synaptic cleft might bridge the adhesive and signaling components of both presynaptic transmitter release machinery and postsynaptic reception apparatus, allowing for a stepwise assembly of trans-synaptic complexes (Dean et al., 2003). Recent studies in knock-out mice have revealed that, in the absence of α -neurexins the central synapse morphology is largely normal, but the presynaptic calcium channel activity and neurotransmitter release are severely impaired (Missler et al., 2003). Therefore, α -neurexins probably have a role in organizing the molecular machinery at presynaptic side. Up to now, the in vivo role of β -neurexin in synaptic assembly remains to be answered.

Finally, Ephrin-Bs (EphB) are small transmembrane proteins identified as ligands for the EphB receptor tyrosine kinase. Through binding to EphB receptor, EphB can induce the clustering of NMDA receptors on the surface of fibroblasts and immature cultured hippocampal neurons (Dalva et al., 2000). The NMDA receptor clustering is mediated by a ligand-induced association of the extracellular domain of EphB receptor with the large extracellular domain of NR1 subunit, while the tyrosine kinase activity of EphB receptor are not necessary for this process. EphBs are unlikely to be the general inducers of postsynaptic differentiation, since in immature neurons it can only facilitate the

clustering of NMDA receptors and its partner Ca^{2+} -calmodulin-dependant protein kinase II (CaMKII) but not the other known PSD components (such as SAP90/ PSD95), moreover, although EpgB2 knock-out mice show deficits in activity-dependant synaptic plasticity, they have normal synapse density and structure, as well as largely intact synaptic function (Grunwald et al., 2001; Henderson et al., 2001). Syndecan2, a cell-surface heparan sulfate proteoglycan, is able to enhance the maturation of dendritic spines: when syndecan2 is overexpressed in cultured immature hippocampal neurons, dendritic spines display morphology typical of mature spines (Ethell and Yamaguchi, 1999). Interestingly, EphB receptor is shown to be the upstream activators of syndecan2 (Ethell et al., 2001), thus EphB receptor pathway might not only function during the initial formation of synapses but also participate in their maturation process.

1.1.3.2 Assembly of synapse

The development of the time-lapse imaging techniques has allowed one to obtain information on the dynamic behavior of essential biological processes in living cells. Synaptic transmission can be detected within an hour of initial axon-dendrite contact, so the accumulation of certain pre- and postsynaptic proteins must occur even earlier. The time-lapse studies have shown that many synaptic components are assembled within tens of minutes after the initial contact of axons and dendrites, much faster than previous estimation (Friedman et al., 2000; Okabe et al., 2001; Washbourne et al., 2002).

1.1.3.2.1 Presynaptic assembly

Recently, evidence is growing to support the opinion that the presynaptic specialization is constructed from essentially two types of preassembled ‘packets’ of vesicles and/ or proteins (Hannah et al., 1999; Jahn and Sudhof, 1999; Sudhof, 2000). The biogenesis of these two precursor complexes occurs in the soma, apparently through the Golgi body.

Using time-lapse imaging of green fluorescent protein (GFP) tagged VAMP (vesicle associated membrane protein, a synaptic vesicle protein), it has been found that even before the period of peak synaptogenesis in culture, VAMP-GFP is present in axons as mobile clusters (about 0.5-1.5 μm) larger than single synaptic vesicles. These VAMP labelled puncta have varied vesicular and tubular membrane structures, as shown by EM, and they colocalize with presynaptic membrane proteins (such as the voltage-gated calcium channels) and other synaptic vesicle associated proteins (such as synaptic vesicle protein 2 and synapsin I). It is estimated that the amount of VAMP required in a single presynaptic bouton corresponds to 1-4 such precursor packets (Ahmari et al., 2000).

A second type of precursor packet, which is associated with dense-core vesicles that have a diameter of about 80 nm, has been visualized and purified (Zhai et al., 2001). In contrast to synaptic vesicles, these dense-core vesicles contain many active zone components, including the presynaptic scaffold proteins Piccolo, Bassoon and RIM (Rab3-interacting molecule), the SNARE (soluble N-ethylmaleimide-sensitive-factor attachment protein receptor) proteins syntaxin and SNAP-25 (synaptosomal-associated protein 25), and the CAM N-Cadherin, suggesting that they constitute 'active zone precursor vesicles' that, upon fusing with the presynaptic plasma membrane, lead to rapid formation of active zones (Zhai et al., 2001). It was proposed that incorporation of only 2-3 of these transport vesicles supplies enough material for an active zone of average size (Shapira et al., 2003).

A common feature of these two types of precursor packets is that they are mobile along axons prior to synaptogenesis, but promptly immobilized at nascent synapses. During neuronal development, the Piccolo/ Bassoon dense-core vesicles are present earlier than the VAMP containing synaptic vesicle precursor packet, which might suggest that the formation of new neurotransmitter release sites is preceded by the recruitment and assembly of

active zone components. The molecular mechanisms that target these precursor complexes to the nascent synaptic site still remain elusive, however, studies from immunoglobulin superfamily proteins (SYG-1 and SYG-2, see above) have already provided possible clue.

1.1.3.2.2 Postsynaptic assembly

Compared to the assembly of presynaptic specialization, the process of postsynaptic assembly is not well characterized yet, which is at least partially due to the fact that postsynaptic specialization is more complex and heterogeneous than presynaptic active zone. One of the best-studied complexes is associated with NMDA receptors. This complex comprises molecules such as SAP90/ PSD95, alpha-actinin, and CaMKII, neuroligin, the microtubule-binding protein Cript, the guanylate kinase domain-binding proteins GKAP/ SAPAPs, and other proteins such as ProSAP/ Shank, Homer and cortactin (which provide additional links to the actin cytoskeleton and other glutamate receptor complexes (Garner et al., 2002). The rapid recruitment of PSD-95 and the presence of non-synaptic clusters of PSD-95 (Rao et al., 1998; Marrs et al., 2001) are consistent with the idea that ‘prefabricated’ complexes are used to assemble the PSD---which is analogous to presynaptic differentiation. However, it is not known whether the non-synaptic clusters of PSD-95 represent real packets of PSD proteins in delivery. In sharp contrast to this view, however, independent studies suggest that although some synaptic PSD-95 clusters might be derived from the transport of pre-existing non-synaptic precursor packets, the *de novo* accumulation of PSD-95 clusters at nascent synapses seems to usually occur from diffuse ‘cytoplasmic pools’ (Bresler et al., 2001; Marrs et al., 2001). Notably, this model is supported by an updated report in which more PSD components have been examined, all the tagged PSD components tested are recruited to new synaptic sites gradually, with no discernable discrete transport packets involved (Bresler et al., 2004). Interestingly, in this new study, the non-synaptic PSD clusters are also observed, but they appear no more mobile than synaptic clusters, hence unlikely representing the transport intermediates.

Ionotropic glutamate receptors are essential components of postsynaptic apparatus, in addition to converting the chemical signal released from presynaptic terminal to an electrical response in the postsynaptic neuron, they are critically involved in activity-dependant, long-term changes in synaptic strength, which may represent a central physiological correlate to learning and memory. Time-lapse imaging of GFP-tagged NR1 (one subunit of NMDA receptors) and GluR1 (one subunit of AMPA receptors) indicates that NMDA receptors and AMPA receptors are present in largely non-overlapping mobile clusters before synaptogenesis starts, NMDA receptors are recruited earlier than AMPA receptors to the axon-dendrite contact sites (Washbourne et al., 2002). It is still uncertain whether these glutamate receptor clusters represent prefabricated packets of synaptic components, or just reflect distinct classes of transport vesicles containing certain types of glutamate receptors. The fact that, the NMDA receptor scaffolding protein PSD-95 is transported to synaptic sites largely independently of NMDA receptors (Rao et al., 1998; Friedman et al., 2000; Rao et al., 2000; Washbourne et al., 2002), supports the latter interpretation. The non-overlapping of mobile AMPA and NMDA receptor clusters and the different dynamics of their recruitment to synaptic sites reflect the presence of distinct regulatory mechanisms controlling their synaptic traffic and localization. Consistently, the cytoplasmic parts of AMPA and NMDA receptor subunits bind to very different sets of structural and regulatory proteins (Scannevin and Huganir, 2000; Sheng, 2001; Sheng and Lee, 2001). The AMPA receptor binding protein, Stargazin, is crucial for the synaptic targeting of AMPA receptors, but not for the morphological development of synapses (Chen et al., 2000). Also combining with the discovery of 'silent synapses' present in rat hippocampus and somatosensory cortex, which only contain NMDA receptors but lack AMPA receptors (Liao et al., 1995; Isaac et al., 1997), it is clear that the AMPA receptor incorporation at the synaptic sites is not required for initial synaptic assembly.

1.1.3.3 Time sequence of pre- and postsynaptic assembly

Although more and more pre- and postsynaptic proteins have been tagged with fluorescent probes and recorded in living cells, there is incomplete agreement on the time course of pre- and postsynaptic assembly. For example, DsRed tagged NMDA receptors have been reported to cluster at nascent synapses within a few minutes of axon-dendrite contact in young cortical culture (3-4 days *in vitro*) (Washbourne et al., 2002). However, another study in more mature hippocampal neurons (about 14 days *in vitro*) showed that the accumulation of NMDA receptors at nascent synapses takes 1-2 hours, and therefore lags behind the accumulation of presynaptic markers (Okabe et al., 2001). Thus, it is still not absolutely sure whether one synaptic side differentiates before the other, or whether the synaptic assembly undergoes simultaneously on both sides. Because the discrepancy raised here is at least partially due to the difference of experimental materials, it is also possible that divergent mechanisms for synaptic assembly are used by different neuron types, or even different stages of the same type. Further studies are apparently required to determine this basic issue in synaptogenesis, and it will be much more beneficial to analyze, if possible, this process *in vivo*. Despite the uncertainty of the time course of pre- and postsynaptic assembly, as soon as a synapse is established, presynaptic active zone and PSD are exquisitely overlapped, indicating a close coordination of presynaptic and postsynaptic maintenance.

1.1.4 *Drosophila* NMJ as a model for studying synaptogenesis

1.1.4.1 Structural properties of *Drosophila* NMJ

The *Drosophila* neuromuscular junction (NMJ) is an excellent model system for addressing fundamental mechanisms governing synapse formation and growth. The advantageous features of *Drosophila* NMJ include its structural accessibility and amenability to powerful genetic, electrophysiological and microscopic techniques.

In *Drosophila* late stage embryo and larva, body wall musculature shows a segmentally repeated pattern of 30 muscle cells (in each symmetric hemisegment) innervated by about 45 motor axons. Each of these muscles is easily identified by its distinct position and size, and is innervated by specific motorneurons. The NMJ morphology is highly stereotyped, the axons of motorneurons spread onto the muscle surface, forming a synaptic arbor composed of series of varicosities connected by thin axonal processes (Fig. 1-5 A). These varicosities, or called synaptic boutons, are categorized by three classes (Gramates and Budnik, 1999; Rheuben et al., 1999). The major class of boutons (type I) contain clear vesicles and are glutamatergic, and at larval stage, they are surrounded by the characteristic subsynaptic reticulum (SSR), an elaborately layered structure formed from the muscle membrane at the junctional region (Atwood et al., 1993; Jia et al., 1993)(Fig. 1-5 B). All 30 body wall muscles are innervated by type I glutamatergic boutons, some muscles are also innervated by type II and type III boutons, which contain octopamine or peptide neurotransmitters (Koh et al., 2000). The neuromuscular contact differentiates into distinct boutons containing functional synapses in late stage embryo, and the boutons continuously grow and sprout throughout the whole larval life. Extensive studies have been made on the third instar larval type I glutamatergic synapses, detailed analysis revealed that type I boutons can be further divided into type I small (Is) and type I big (Ib) by size, the extent of the folding of SSR, and electrophysiological properties. Due to the tiny size of embryo, it is not used as frequently as larva, however, it has been proved to be invaluable in understanding molecular events relevant to initial synapse formation. Unlike the vertebrate NMJ, the NMJ of *Drosophila* is not covered by glial cells, leaving 10–20 μm of neuronal surface without insulation from the hemolymph. (Hall and Sanes, 1993; Auld et al., 1995).

Notably, *Drosophila* NMJ shares several important features with the excitatory central synapses in vertebrate brain: it is glutamatergic (unlike the cholinergic NMJ in vertebrate) and contains homologous ionotropic glutamate

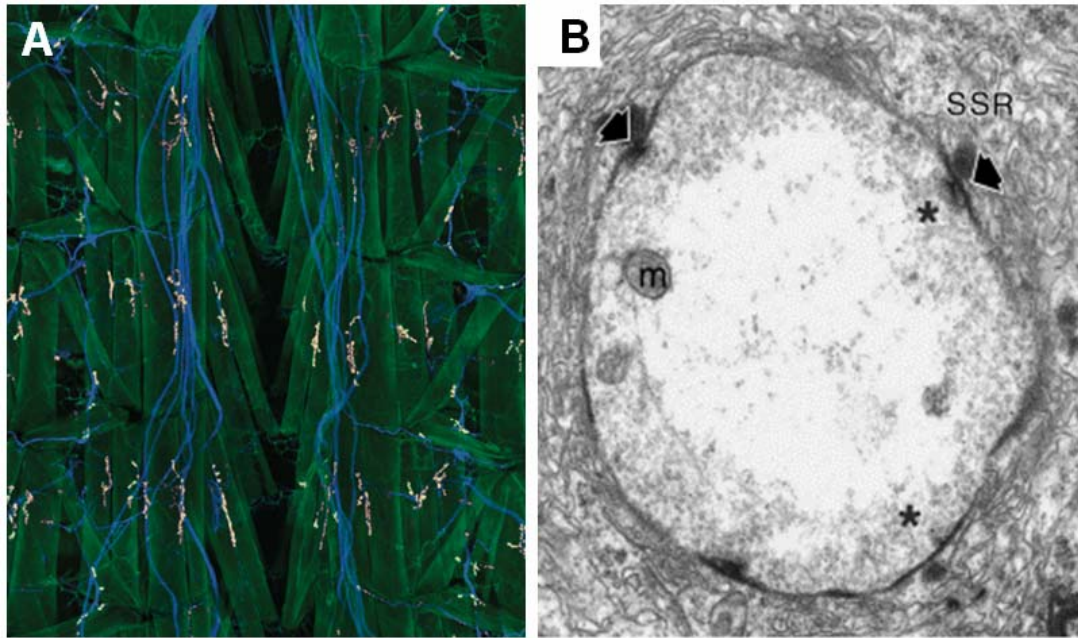


Fig.1-5 Structure of *Drosophila* NMJ.

A, Three segments of a dissected third instar *Drosophila* larva. Muscles are stained as green, neuromuscular junctions stained as red and nerves stained as blue (Adapted from (Daniels et al., 2004)). B, Electron micrographs depicting cross-sections through a type-I bouton on muscle 6 in wild-type larvae. The subsynaptic reticulum (SSR), active zones (asterisks), T-bars (thick arrows), and mitochondria (m) are marked (Adapted from (Aberle et al., 2002)).

receptors; there is no obvious basal lamina layer that separates pre- and postsynaptic membrane, so the synapse appears close membrane-membrane apposition ultrastructurally (Fig. 1-5 B); it is organized into a series of boutons that can be added or eliminated during development and plasticity (Petersen et al., 1997). During the period that larva grows from first instar to third instar, which normally takes several days, the muscles undergo a dramatic increase in size (more than 100 folds), therefore requiring a concomitant addition of more synaptic boutons and further elaboration of NMJ branches to efficiently depolarize the muscles.

Although the NMJ architecture changes dramatically during postembryonic

development, the characteristics of individual neuromuscular synapses are rather similar between embryo and larva at ultrastructural level (Prokop, 1999): the pre- and postsynaptic membranes appear smoother and more electron dense compared to the extrasynaptic areas, indicating that the molecular composition of synaptic fields differs from extrasynaptic membranes. The intracellular face of presynaptic membrane harbors active zones, which contain characteristic T-shaped electron-dense structures (T-bars) surrounded by clusters of synaptic vesicles (Fig. 1-5 B). T-bars can still be seen in neuronal terminals that are depleted of synaptic vesicles and therefore appear to be independent molecular structures (Poodry and Edgar, 1979). The exact molecular composition and function of T-bars still remain unclear.

1.1.4.2 Initiation and maintenance of neuromuscular connection

1.1.4.2.1 Initiation of neuromuscular contact---target recognition (pathfinding)

So far, most studies on NMJ formation have been carried out on the ventral longitudinal muscles 6 and 7, which are innervated exclusively by glutamatergic type I boutons. It is believed that most NMJs, if not all, develop in a similar way and share the common architecture. At embryonic stage 15/ 16, muscles start sending out myopodia preferentially from the future innervation site (Ritzenthaler et al., 2000), and they are contacted by filopodia sent out from the motoneuronal growth cones in a random fashion. Those motoneuronal processes which are in contact with inappropriate muscles are soon withdrawn (Broadie and Bate, 1993; Yoshihara et al., 1997). This specific targeting recognition process is suggested to be mediated by both repulsion from inappropriate target muscle and contact-mediated attraction to the right target muscle (Bate and Broadie, 1995; Keshishian et al., 1996). Example of repellent molecule is the Toll, which is present on the surfaces of certain muscles and can prevent innervating by irrelevant motoneurons, removal of Toll leads to the ectopic

innervation. Fasciclin III (FasIII), one homophilic cell adhesion molecule, appears to be mediate attractive cell-cell recognition, since misexpression of FasIII introduces innervation at the non-target cell. Up to now, many targeting cues have been identified, such as caspricious, semaphorins, connectin, neuromusculin and netrins (Bate and Broadie, 1995; Chiba and Rose, 1998), acting as either repellent or attractive molecules.

1.1.4.2.2 Stabilization and maintenance of neuromuscular connection by cell adhesion molecules

As soon as the initial neuromuscular contact is established, it has to be stabilized for further differentiation. This process, which should be also required for the new bouton growth during postembryonic period, is believed to be largely mediated by multiple cell adhesion molecules. Upon initial neuromuscular contact at embryonic stage 13, usually the junction consists of only short stretches of apposed membranes, often interrupted by stretches of non-connected cell surfaces (Schuster et al., 1996; Yoshihara et al., 1997; Prokop A et al., 1998). While at the mature NMJ of late stage 17 embryo such contact develops into an extended cell-cell junction, indicating that adhesive properties change during NMJ maturation. Consistent with this notion, FasIII, which contributes to target recognition and potentially also early phase of contact stabilization, disappears from NMJs of later stages (Broadie and Bate, 1993). In contrast, FasII, another homophilic CAM belonging to the immunoglobulin superfamily, is initially expressed strongly on the surfaces of all motor axons and at low levels in muscles during NMJ formation (Schuster et al., 1996). As synaptic connections are established, FasII is progressively clustered at pre- and postsynaptic membranes. The late junctional maintenance of FasII is largely, but not all, mediated by the scaffold protein Discs large (Dlg), the *Drosophila* Membrane-Associated Guanylate Kinase (MAGUK) homologous to mammalian PSD-95/ SAP90 family proteins (Budnik et al., 1996; Thomas et al., 1997; Zito et al., 1997), which itself is not detectable at the NMJ until late stage 17 (Guan et al., 1996). Deleting FasII does not interfere with

NMJ formation, but strongly affects postembryonic stabilization and maintenance of NMJs, suggesting its crucial role in controlling synaptic stability and growth (Schuster et al., 1996). Furthermore, it seems to be of developmental importance that FasII function is restricted to the late phase of NMJ differentiation: overexpression of FasII in muscles during initial NMJ formation seems to render muscle surfaces too 'sticky' and interferes with precise neuromuscular target recognition, as a result, ectopic motoneuronal branches (which normally occur only transiently) become trapped and form NMJs on inappropriate muscles (Davis et al., 1997). Apparently, there must exist other yet unidentified adhesion molecule(s) required for initial events of synapse formation.

Another example relevant to switch in adhesive properties at NMJ comes from analysis of *mef2* mutant embryos, where the initial neuromuscular contact can be genetically separated from the late phase of neuromuscular adhesion. In *mef2* mutant embryos, muscle founder cells form, and motoneurons establish initial contact with proper target cells (Prokop et al., 1996). However, the muscle founder cells remain immature and fail to acquire properties of general muscle differentiation. In late-stage 17 *mef2* mutant embryos, proper cell junctions between motoneurons and improperly differentiated muscle fibers are never observed, but instead the abnormal muscle surfaces are covered by basement membrane. This phenotype could be explained by lack of *mef2*-dependent late synaptic CAMs, which directly maintain the established neuromuscular connection. Alternatively, *mef2* might be required to exclude basement membrane receptors from the NMJ, thus preventing dissociation of the pre- and postsynaptic membranes from competitive invasion of basement membrane material. No matter which explanation is true, it is clear that appropriate adhesive strength is the prerequisite for proper NMJ maturation and further maintenance.

1.1.4.3 Synapse formation

Synapse formation involves the coordinated assembly of pre- and postsynaptic apparatus. Positioning cues are required to direct the juxtaposition of synaptic components at the pre- and postsynaptic membranes. In *Drosophila* NMJ, candidate that might serve as positioning cue is the special type of cleft-spanning adhesion molecules, as supposed by the function of Neuroligin/ Neuexin at vertebrate central synapses and immunoglobulin superfamily members SYG-1/ SYG-2 in *C. elegans* (see above), but this still remains to be proved.

In contrast to the essential role that nerve-secreted factor agrin plays in vertebrate NMJ differentiation, no agrin orthologue seems to be present in the *Drosophila* genome. However, recent evidence indicates that other sets of secreted molecules, Wnts and members of the TGF-beta family might take similar responsibility in the development of glutamatergic synapses at *Drosophila* NMJ. Wingless (Wg), a member of the Wnt family of ligands, is secreted from motorneuron, loss of Wg leads to dramatic impairment of synapse formation, with boutons lacking active zones and postsynaptic structures (Packard et al., 2002). In consistence with this, a mammalian Wg homologue Wnt7a has been implicated in presynaptic differentiation in the cerebellum (Hall et al., 2000). Wishful thinking (wit) encodes a BMP (bone-morphogenetic-protein) type II receptor, which is present in a subsets of neurons, including motorneurons; its ligand, the BMP ortholog Glass Bottom Boat (Gbb), mainly fuctions in muscles. Mutations in both wit and Gbb result in much smaller NMJs, defective synaptic transmission and presynaptic abnormalities (such as synaptic membrane detachment at active zone region, presence of floating T-bodies) (Aberle et al., 2002; McCabe et al., 2003). Taken together, these studies indicate that Wg and Gbb function in opposite directions at *Drosophila* NMJ to assure proper differentiation of pre- and postsynaptic structures.

Before motorneuron innervation, low amounts of glutamate receptors are already expressed in muscles and diffusely distributed over the muscle surfaces (Broadie and Bate, 1993; Currie et al., 1995; Saitoe et al., 1997). Upon the initial neuromuscular contact, glutamate receptors begin clustering rapidly at the innervation sites, and within a few hours, new glutamate receptors are synthesized and inserted into newly formed synapses. Compared to the innervation-independent spontaneous AchR clustering at vertebrate NMJ, the clustering of glutamate receptors is innervation-dependent, the aneural muscles neither cluster existing receptors nor synthesize additional receptors. Intriguingly, disruption or complete elimination of neurotransmission does not seem to inhibit glutamate receptor field formation (Broadie et al., 1995; Featherstone and Broadie, 2000), however, the glutamate receptors will not cluster if the action potential of the neuron is blocked genetically or with tetrodotoxin (Broadie and Bate, 1993). Thus, glutamate receptor clustering appears to require an electrical activity dependant signal derived from motorneuron, and this signal is not related to neurotransmission. The latter notion is completely consistent with findings in mammalian central synapses: in Munc-13 or Munc-18 null mutant mice, in which neurotransmitter release is completely absent, both brain anatomy and synapses appear normal (Verhage et al., 2000; Varoqueaux et al., 2002). Thus, evidences from both *Drosophila* and vertebrates highly suggest that, at least in glutamatergic synapses, synaptic activity is not necessary for initiating synaptogenesis.

Analysis on mutants deficient in muscle development indicates that the presynaptic apparatus can be assembled independently of the postsynaptic cell (Prokop et al., 1996), which again contrasts with vertebrate NMJ differentiation. In the latter case, muscular secretion of α -laminin into synaptic basement membrane is essential for the assembly of morphologically normal active zones (Noakes et al., 1995). Anyhow, although the assembly of active zones at *Drosophila* NMJ can be independent of muscle cells, the precise apposition of

pre- and postsynaptic apparatus must rely on the close communication between motorneuron and target muscle.

1.2 Structure and functional relevance of ionotropic glutamate receptors

The ionotropic glutamate receptors (iGluRs), including AMPA, NMDA and Kainate types, mediate excitatory synaptic transmission at most mammalian central synapses. In addition to converting transmitter released from presynaptic terminal to electrical response in the postsynaptic neuron, these receptors are thought to contribute to the activity-dependant, long-term changes in synaptic strength which is proposed to underlie learning and memory (Contractor and Heinemann, 2002). Besides the physiological importance of iGluRs, their dysfunction is implicated in various neuropathologies, including epilepsy, stroke damage and the perception of pain (Dingledine et al., 1999).

1.2.1 Modular design of ionotropic glutamate receptors during evolution

Ligand-gated ion channels are generally formed as homo- or hetero-oligomeric assemblies of integral membrane protein subunits. One important feature of iGluR structure is its modular construction. As illustrated in Fig.1-6 A, one typical iGluR subunit consists of an amino-terminal domain (NTD), a ligand-binding domain (S1S2), three transmembrane domains, a re-entrant pore loop, and a carboxy-terminal domain (Hollmann and Heinemann, 1994; Madden, 2002). The NTD shows homology to the leucine/ isoleucine/ valine-binding protein LIVBP, one of the bacterial periplasmic binding proteins (PBPs). In NR2 subunits, it forms or contributes to the binding site of many NMDA receptor modulators and affects receptor desensitization. For the non-NMDA receptors, it is supposed to be involved in receptor assembly. The S1S2 ligand-binding domain is formed by two sequences (the S1 region which is the N-terminal of transmembrane domain 1, and the S2 region which is C-terminal of transmembrane domain 2) sharing sequence and structural

homology with the glutamine-binding protein QBP. The re-entrant pore loop is homologous to the P-loop sequences of other channels, the P-loop sequence lines the channel and determines many of its electrophysiological properties. In addition, the cytoplasmic carboxy-terminal contains various interaction domains and phosphorylation sites, which likely controls the transport and localization of these receptors. The modular feature of iGluR indicates that it might have been assembled from discrete components during evolution, consistent with the ‘genes-in-pieces’ hypothesis (Gilbert, 1978). Supporting this notion, a prokaryotic glutamate receptor ion channel (GluR0) was found, which lacks NTD and has only two transmembrane domains but is indeed glutamate-gated and selective for potassium ions (Chen et al., 1999).

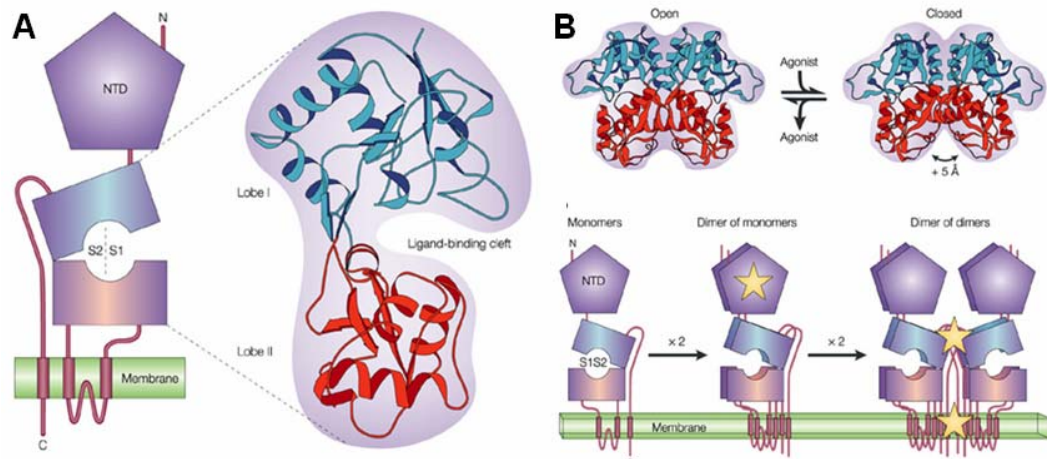


Fig.1-6 Structure of iGluR subunit and model of iGluR assembly. A, The modular structure of iGluR subunit. B, ‘Dimer of dimers’ model of iGluR assembly (Adapted from Madden, 2002).

1.2.2 Molecular mechanisms underlying selective assembly and transport of ionotropic glutamate receptors

Despite the schematic understanding of the sequence of building blocks that constitutes glutamate receptor subunits, still little is known about the spatial disposition of these domains within individual subunit and assembled functional

ion channel. Recently, dissecting the molecular details underlying the functional assembly and cell surface trafficking of various types of iGluRs has become one of the central focuses in molecular neuroscience.

On the basis of electrophysiological, biochemical and hydrodynamic analysis, iGluRs are proposed to be tetramers (Laube et al., 1998; Mano and Teichberg, 1998; Rosenmund et al., 1998; Kuusinen et al., 1999; Safferling et al., 2001). AMPA receptors are homo- or hetero-tetramers composed of GluR1-4 (Hollmann and Heinemann, 1994; Dingledine et al., 1999). Kainate receptors are homo- or hetero-tetramers of the subunits GluR5-7, KA1 and KA2. NMDA receptors require both NR1 and at least one type of the four NR2 subunits (A-D) to form functional channels, in some cases NR3 subunits are also included (Meguro et al., 1992; Monyer et al., 1992; Perez-Otano et al., 2001; Matsuda et al., 2003). Recently, using a series of epitope-tagged receptor chimeras (Ayalon and Stern-Bach, 2001), Ayalon and Stern-Bach provided evidence of sequential assembly of tetrameric iGluRs as dimmer of dimmers (Fig.1-7 B). In this model, initial subunit dimerization is mediated primarily by interactions between compatible NTDs. Then, assembly of functional receptors requires that these dimmers undergo a second dimerization, this time requiring compatibility between the S2 and transmembrane domains of the subunits. This secondary dimerization is not observed in the absence of NTD compatibility, indicating that it might be weaker than the primary dimerization. This dimmer-of-dimmers model of iGluR assembly is consistent with images of GluR2 homomers determined by electron microscopy (Safferling et al., 2001).

In non-neuronal cells, the step of exit from the endoplasmic reticulum (ER) is often under the most stringent control during transport of membrane proteins to the cell surface (Ellgaard and Helenius, 2003). Like other multimeric cell membrane proteins, glutamate receptors are synthesized, folded, assembled in the ER; similarly, traffic of glutamate receptors through ER is also tightly regulated, which decides the type and number of glutamate receptor at synapse

(Vandenberghe and Bredt, 2004). ER contains rigorous quality control system to ensure that only correctly folded and assembled proteins exit to the Golgi body, which in the case of glutamate receptors is evidenced by the presence of various ER retention and export signals in NMDA, AMPA and Kainate receptor subunits. For NMDA and Kainate receptors, both ER retention and export signals localize within the intracellular tails (Standley and Baudry, 2000; Scott et al., 2001; Xia et al., 2001; Ren et al., 2003; Hawkins et al., 2004; Jaskolski et al., 2004). Intriguingly, AMPA receptor subunit GluR2 contains a unique ER retention motif which just localizes in the re-entrant membrane loop (Greger et al., 2002), this single arginine (R607) is generated by mRNA editing and critically controls the ion permeability (Burnashev et al., 1992). Unlike other known ER export signal, the ER export signal of AMPA receptor subunit Glu1 appears within the extra-cellular NTD (Xia et al., 2002).

1.2.3 Properties of ionotropic glutamate receptors expressed at *Drosophila* neuromuscular synapses

In contrast to mammalian acetylcholinergic NMJ, the *Drosophila* type I junctional bouton is glutamatergic. So far, three ionotropic glutamate receptor subunits have been identified to be specifically expressed at the postsynaptic muscle cell (Schuster et al., 1991; Marrus et al., 2004). These glutamate receptor subunits are structurally and functionally similar to mammalian AMPA-/ Kainate-type receptors. *GluR-IIA* and *GluR-IIB* are genomic neighbors and their encoding proteins share 44% amino acid identity, animals with double knock-out of both genes die at late embryonic stage, while the lethality can be fully rescued by transgenic expression of either gene; moreover, modulation of subunit composition via genetically changing the copy number of *GluR-IIA* and *GluR-IIB* gene results into distinct single channel kinetic properties and is able to trigger long term changes of synaptic strength (Petersen et al., 1997; DiAntonio et al., 1999; Sigrist et al., 2002). GluRIII (also called GluR-IIC) is crucial for animal vitality and required for synaptic localization of GluR-IIA and GluR-IIB; while GluR-IIA and GluR-IIB do not precisely colocalize at

many synapses, they both perfectly colocalize with GluR-III, implicating that GluR-III acts as a obligate subunit for functional receptor assembly (Marrus et al., 2004).

1.3 The aim and strategy of this work

The purpose of this study is to improve our understanding of the molecular mechanisms relevant to the synaptogenesis and growth control/ regulation of *Drosophila* NMJ. To this end, newly developed DNA microarray technique was applied to sort potential genes relevant to the NMJ formation and functioning through the whole genome. Via RNA profiling of postsynaptic cell (here is the somatic body wall muscle), a pool of genes with specific or enriched expression pattern were obtained, which would greatly facilitate systematic characterization of certain interesting functional groups. Data mining from these obtained RNA profiles and online genomic resources resulted into the identification of several muscle expressed but uncharacterized ionotropic glutamate receptor subunit genes. The expression pattern of these subunits were further verified at both RNA and protein level, via quantitative RT-PCR, in situ hybridization and immunohistochemistry. Ionotropic glutamate receptors play the major roles in mediating the signal transmission at excitatory glutamatergic synapses in the central nervous system, moreover, these receptors are also thought to contribute to the activity-dependant, long-term plasticity of neuronal circuits which is proposed to underlie learning and memory (Contractor A et al., 2002). The *Drosophila* neuromuscular synapse provides an excellent platform for investigating the behavior of glutamate receptors, due to its structural and functional similarity to excitatory central synapse and its rather simple organization. Reasonably, characterizing the functional significance of these newly identified glutamate receptor subunits at *Drosophila* NMJ in principle would help better understand their orthologs in the central synapses and thus became the main body of this thesis work.

To study the *in vivo* roles of these novel glutamate receptor subunits, knock-out animals were generated via standard transposon-based mutagenesis screening. The null mutant animals of either subunit die at late embryonic stage, indicating that they are all essential genes. Further genetic, cell biological and electrophysiological studies were performed and uncovered a tight interdependence of all essential glutamate receptor subunits for synaptic localization and functioning, implying a novel “strictly hetero-tetrameric stoichiometry” model which is so far not reported in mammalian ionotropic glutamate receptors.

Closer inspection on glutamate receptor deprived synapses was also performed, with the combination of immunohistochemistry and electron microscopy based ultrastructural analysis. Surprisingly, it was found that with deprivation of glutamate receptors, the typical postsynaptic differentiation and synaptic compartmentation displayed severe defects, further analysis of a series of neurotransmission deficient mutant backgrounds excluded the involvement of neurotransmission activity in instructing differentiation of synaptic specializations. Thus, the glutamate receptor *per se*, but not its ligand-gated ion channel activity, is essential for normal synaptic construction. This important ‘structural’ role of glutamate receptor in organizing synaptic differentiation is firstly reported, raising highly interesting questions such as, which part of glutamate receptor is responsible for facilitating synaptic assembly? Do the ionotropic glutamate receptors in mammalian central synapses play similar roles during synaptogenesis?

1 Materials and methods

2.1 Materials (Chemicals, enzymes and molecular biology kits)

All of the chemicals were purchased from Roth and Sigma unless stated elsewhere. For molecular cloning, all of the enzymes, including various restriction endonuclease enzymes, T4 DNA ligases, Alkaline Phosphatase were purchased from Roche (Mannheim, Germany). The Vent polymerase used for PCR cloning was from NEB (USA). All of the oligonucleotides were synthesized from MWG (Germany). The E. Coli strains used for transformation were either self-made DH5 α chemical competent cell or SURE electroporation competent cell from Stratagene (USA). Unless described elsewhere all of the molecular biology kits were from Qiagen (Germany).

2.2 Methods

2.2.1 Genechip analysis and real-time RT-PCR

2.2.1.1 Genechip analysis

Part I Protocol for the Affymatrix GeneChip Target Preparation

Material and Reagents:

Qiagen RNeasy RNA purification kit

3M Sodium Acetate, pH 5.2 Sigma

80% ethanol kept cold

Absolute ethanol kept cold

Glycogen 5mg/ml, Roche

Ethidium bromide

7.5M Ammonium Acetate, Sigma

1). Synthesis of Double-Stranded cDNA from Total RNA

Materials and Reagents:

T7- (dT)₂₄ Primer, (MWG Corp) HPLC purified DNA

Phase lock Gel, Eppendorf

Phenol/ Chloroform/isoamyl alcohol, Roth
Superscript Choice System, Invitrogen
Ice bath
Heat/cool block for 70°C, 42°C, 16°C
PE 9700 PCR machine

1.1. First strand cDNA synthesis

Prepare an Rnase- free 0.5 ml reaction tube containing the following reagents. They are to be added in the order listed. The total reaction volume is 20µl.

1. In a 0.5ml Rnase-free tube add total volume of 10µl of total RNA sample (2.5µg).
2. Add 1µl of T7- (dT) 24 primer (100 pmol/µl).
3. Incubate at 70°C for 10 Min, quick spin and place on ice.
4. Add 4µl of 5X First strand cDNA buffer.
5. Add 2µl of 0.1 M DTT.
6. Then add 1µl of 10mM dNTP mix.
7. Add this mixture to the RNA sample then Incubate at 42°C for 2 min.
8. While in the bath Add 2µl SSII
9. Incubate for 1 hour at 42°C.
10. Place reaction on ice and proceed onto second strand synthesis.
11. Equilibrate a 16°C bath.

1.2. Second Strand Synthesis

12. Briefly centrifuge first strand reaction and return to ice.
13. Add the following reagents in the order listed to the first strand reaction.
14. Make sure to add the reagents while the reaction is on ice.

91µl of DEPC-treated dH₂O

30µl of 5X Second Strand Reaction Buffer

3µl of 10mM dATP, dCTP, dGTP, DTTP

1µl of DNA ligase (10U/µl)

4µl of DNA polymerase I (10U/µl)

1µl of Rnase H (2U/µl)

To yield a final reaction volume of 150µl.

15. Gently tap tube to mix. Briefly spin to remove condensation.
16. Incubate the reaction at 16°C for 2 hours in a cooling water bath
17. While in the bath add 2µl of T4 DNA Polymerase.
18. Incubate for an additional 5 minutes at 16°C.
19. Add 10µl of 0.5M Na₂EDTA

The reaction product can be stored at -20°C for later use.

1.3 Clean Up of Double-Stranded cDNA

STEP 1-Phase Lock Gels Phenol/Chloroform Extraction

1. Pellet the Phase lock gel in a micro-centrifuge tube by spinning it at full speed (1,3200rpm) for 20 to 30 seconds.
2. Add 162µl of Phenol: Chloroform: isoamyl alcohol (saturated with 10mM Tris-HCl pH 8.0/ 1mM EDTA) to the cDNA reaction sample, mix by vortexing for one minute.
3. Transfer the entire cDNA Phenol Chloroform mixture into the PLG tube. Spin the PLG tube at full speed for 2minutes
4. Avoiding contact with the gel transfer the aqueous upper phase to a fresh 1.5 ml tube (Tilt the tube for better recovery).

Proceed to step 2.

STEP 2 - Ethanol precipitation

1. Add 1µl of glycogen to the sample.
2. Add 0.5 volumes of 7.5M NH₄Ac plus 2.5 volumes of absolute ethanol (stored at -20°C) to the sample and vortex.
3. Immediately spin at full speed in a micro-centrifuge at room temp for 20 min, discard supernatant.
4. Wash pellet with 500µl of 80% ethanol (stored at -20°C)
5. Spin at full speed for 5minutes at room temp.
6. Remove the ethanol very carefully so as not to disturb the pellet and repeat the wash. (This is an optional stopping point. The pellet may be left in the wash

at -20°C overnight.)

7. Air dry the pellet at room temp completely (this may require over an hour).

8. Resuspend the pellet in 12µl of Rnase-free water.

9. Proceed onto Synthesis of biotin-labeled cRNA.

To reduce overdrying leave the pellet in a very small volume of the last wash.

2). Synthesis of biotin-labeled cRNA

Materials and Reagents:

Enzo RNA transcript labeling Kit 9 (BioArray High Yield RNA Transcript Labeling Kit)

Rneasy Mini Kit, Qiagen

DEPC-treated water

10X TBE, BioWhittaker

Reagent preparation

5X Fragmentation Buffer:

In an Rnase-free vessel combine

4.0 ml of 1M Tris-acetate pH 8.1 (adjusted with glacial acetic acid).

0.64 g MgOAc.

0.98 g KOAc.

DEPC-treated water to make a final volume of 20mL.

Mix thoroughly then filter through a 0.2µm vacuum filter unit. This reagent should be aliquoted and stored.

2.1 protocol for the IVT reaction

1. Equilibrate a 37°C bath / block

2. Thaw the Enzo reagents on ice.

3. When thawed check for precipitate, vortex if necessary.

4. The volume of cDNA to be used in the IVT reaction should corresponding to the total RNA range of 8.0 and 16.0 µg.

5. From the Enzo BioArray RNA labeling kit add the following reagents in the

order listed.

Reagent Volume

Template DNA Variable to give 1 μg of cDNA (10 μl)

Deionized water To make final volume equal to 40 μl (~12 μl)

10X HY Buffer 4 μl

10X Biotin-labeled nucleotides 4 μl

10X DTT 4 μl

10X RNase inhibitor 4 μl

20X T7 RNA polymerase 2 μl

Total volume 40 μl

6. Carefully mix the reagents in the tube then spin the sample briefly
7. Immediately place the tube in a water bath at 37°C incubate for 5.5 hours gently mixing every 30 to 45 minutes
8. Remove 1 μl aliquot for gel analysis
9. At the end of the incubation the reaction may be stored at -20.0°C for later use.

2.2 Purification and Quantification of in vitro Transcription

STEP 1 - Column purification of RNA

1. Pre-heat a small working stock of RNase-free water at 60-65°C.
2. Pre-heat elution buffer at 60-65°C.
3. Aliquot one half (~20 μl) of the cRNA reaction into a 1.5 ml tube.
4. Adjust volume to 100 μl with RNase-free water.
5. Add 350 μl of buffer RLT (lysis buffer) to the sample. Mix thoroughly.
6. Add 250 μl of ethanol (96-100%) to the lysate and mix well by pipetting up and down.
7. Apply sample (700 μl) to Rneasy mini-spin column sitting in a 2ml-collection tube.
8. Centrifuge for 30 sec at 10,000 rpm.
9. Reapply the flow-through onto the column and spin again.
10. Transfer the column into a new 2ml-collection tube.
11. Add 500 μl of buffer RPE (ensure ethanol has been added to the buffer) and

let stand for 1 min.

12. Spin at max for 30s and discard flow-through.

13. Add another 500µl of buffer RPE onto the column and let it stand for 1 min.

14. Centrifuge and discard flow-through.

15. Spin at full speed for an additional 3min.

16. Transfer the column to a new 1.5 ml tube and pipet 33 µl of the pre-heated Rnase free water directly onto the membrane. Let stand for 1 min.

17. Spin at full speed for 1 min.

18. Repeat elution using the flow-through from the first elution.

STEP 2 - Ethanol precipitation: if the cRNA yield is poor

19. Add 0.5 volume of 7.5M Ammonium Acetate and 2.5 times volume of absolute ethanol

20. Incubate at -20°C for 60 min then spin at full speed for 30 minutes.

21. Decant the supernatant then wash the pellet by adding 500µl of 80% Ethanol and spin at full speed for 5 minutes.

22. Decant the supernatant and repeat the wash step

23. Decant the final wash and dry the pellet at room temperature.

STEP 3 – Electrophoresis

24. Prepare sample in a RNA gel-loading buffer.

25. Heat sample 65°C , 5 min.

26. Run one lane of unpurified labeled cRNA (0.5 µl) along side a lane of the purified labeled probe (1.5 µl) on standard 1% agarose gel.

Fragmentation of cRNA for target preparation

27. Add 2µl of 5X Fragmentation buffer to every 8µl of RNA plus water. The final RNA concentration in the reaction can range between 0.8 µg/µl and 2 µg/µl.

28. The following are guidelines that should be followed:

20µg cRNA 1 to 16µl

5X Fragmentation buffer 4µl

Rnase-free water to 20µL

Component Volume

15 µg cRNA (extreme case) 1 to 12 µl

5X Fragmentation buffer 3 µl

Rnase-free water 15 µl

29. Incubate the reaction at 94°C for 35min, quick spin and place on ice immediately following the incubation.

30. Run 1 µg of the fragmented RNA on a 1% agarose gel to check the completion of fragmentation.

31. The fragmented RNA is ready for hybridization.

Hybridization was performed in Affymetrix hybridization oven at 50°C for 16 hours. The hybridized Gene chips were then stained and washed in Affymetrix fluidics station following the standard program. Data analysis was performed via Microarray Suite 4.0 and exported via Excel.

2.2.1.2 Real-time RT-PCR

1. Extract total RNAs using QIAGEN's RNeasy kit (as described in 2.2.1.1), check the concentration of each sample.

2. Perform reverse transcription using QIAGEN's Omniscript Reverse Transcriptase:

Master mix:

10X Buffer RT	2.0µl
dNTP Mix (5mM each dNTP)	2.0µl
Random hexamer	2.0µl
Rnase inhibitor (40 units /µl)	0.25µl
Ominiscript Reverse Transcriptase	1.0µl
Rnase-free H ₂ O	Xµl

Template RNA 2μg

Incubate the mixture for 1 hour at 37°C, then inactivate the Reverse Transcriptase by heating the reaction mixture to 93°C for 5 min followed by rapid cooling on ice.

3. Perform the real-time PCR in 96 well plate :

Master mix (50μl):

2X PCR mixture 25μl

H₂O 22μl

Primer (forward) 1.0μl

Primer (reverse) 1.0μl

cDNA template 1.0μl

4. Quantitate the relative transcript level by analyzing Ct value of each sample.

5. Check the amplified products by agrose gel electrophoresis.

2.2.2 Fly stocks and genetics

2.2.2.1 Fly stocks, crosses and rearing conditions

Fly stocks used are: All of the wild type control strain used is w¹ (B) except stated elsewhere. w⁻;Df(2L)^{SP22} (*Gglur-IIA*^{-/-}, *Gglur-IIB*^{-/-})/ Cyo, Kr::GFP (Petersen et al., 1997). w⁻;Df(2L)c1^{h4}/ Cyo, Kr::GFP. w⁻;OK319-Gal4. w⁻;UAS-TNTE (Sweeney et al., 1995). *Syx*²²⁹ is a null mutation allele of *syx-IA* that completely eliminates mRNA and protein expression (Schulze et al., 1995). *Shi*^{ts1} mutants were shifted from a permissive (25°C) to a non-permissive temperature (32°C) after 13 h of embryogenesis (Featherstone D et al., 2002). III¹/ Gla Bc (Marrus et al., 2004).

Double mutants in *GluR-IIA* and *GluR-IIB* were described previously (Petersen et al., 1997; DiAntonio et al., 1999). In short, *GluR-IIA* and *GluR-IIB*

double mutant embryos were recovered by crossing *Df(2L)GluR-IIA&B^{SP22}* to *Df(2L)cl^{h4}*, mutant embryos were selected using GFP marked balancer chromosomes.

To generate *GluRIIA^{hypo}*, *GluR-IIB^{null}* condition having an extremely reduced amount of GluR-IIA and no GluR-IIB expression, genomic fragment of GluR-IIA encompassing promoter region and the whole open reading frame while missing most part of the 3'-UTR was used. This transgene still produces full length GluR-IIA while in dramatically reduced amount due a loss of message stability (see 3.4.2 for details). This construct was expressed from *pUAST* vector (using the *GluR-IIA* endogenous promoter). A single transgene copy rescues embryos null for both *GluR-IIA* and *GluR-IIB* (*Df(2L)GluRIIA&B^{SP22}/Df(2L)cl^{h4}*) giving *GluRIIA^{hypo}*, *GluR-IIB^{null}* larvae (see results).

Unless stated elsewhere, all of the crosses were established at 25 °C with 60% humidity.

2.2.2.2 Mutagenesis screening

The *GluR-IIID* and *GluR-IIIE* loci are situated at 92F4. In a recently released pBac transposon insertion collection (Thibault et al., 2004), a *piggyBac* transposon (pBac{RB}e01443, #17952,) was found to be inserted into intron 6 at amino acid position 427 of the *GluR-IIID* open reading frame. This allele *GluR-IIIDe⁰¹⁴⁴³* is embryonic lethal both homozygous or over *Df(3R)H-B79* (Bloomington *Drosophila* stock center) which deletes a large genomic region including the *GluR-IIID* and *GluR-IIIE* locus, and over deficiency *GluRIID&-IIIE^{E3}* (see below). For *GluR-IIIE*, imprecise excision screening was performed using the P element line GE28753 (commercially available with Genexcel), which is inserted ~150bp downstream of the end of the *GluR-IIIE* transcript. In brief, P-element GE28753 was remobilized by crossing to the Δ 2-3 transposase source, white eye progenies were selected and mated individually,

then single fly genomic PCR reactions were performed to map deletions flanking the P-element insertion site. Nearly 1,000 eye color revertants were checked, one line (*GluR-IIE^{E1}*) was found to delete 1.2 kb flanking region in direction of the *GluR-IIE* gene, removing the C-term and transmembrane domain 4 of GluR-IIE. *GluR-IIE^{E1}* is embryonic lethal homozygously, over *df(3R)H-B79* and over *GluR-IID&-IIE^{E3}*. *GluR-IID&-IIE^{E3}* is a larger deletion also recovered from excision mutagenesis of GE28753, which removes both *GluR-IIE* and *GluRIID* and thus was used in combination with either *GluR-IID^{e01443}* or *GluR-IIE^{E1}* as deficiency.

2.2.3 Molecular Constructs and Transgenes

A genomic fragment covering the DGluR-IIA gene (containing 1.3 kb sequence 5' of the ATG) was firstly subcloned into pSL1180 as EcoRI/ XhoI fragment (5.6 Kb) from a BAC clone RPCI-98-35L07. The wild type rescue construct was made by directly inserting the EcoRI/ XhoI fragment into pUAST (Brand and Perrimon, 1993). For the 3' UTR deleted version, the subclone was cut with NcoI and XhoI, end-blunted and religated, then the EcoRI/ Asp718 fragment (4.7 Kb) was inserted into pUAST. All constructs were confirmed by double-strand sequencing, transgenic flies were produced in w1 background via standard procedures and crossed into the Df(2L)c1^{h4}/ Gla, Bc background.

Genomic fragments covering the *GluR-IID* gene and *GluR-IIE* gene were generated by PCR using for IID

5'GGTCTAGAGCGGCCGCGGCCACGAAGTACCCACGGTTTC3' and

5'GCGGCCCTCGAGCGACGTCAAGGATGTGCCAC3'

and for IIE

5'GGTCTAGAGCGGCCGACCTCCCCAAGCTGTCAACTTC3' and

5'GCGGCCCTCGAGACTGCTCAAAGCTGCTGCCCTG3'. The products

were double strand sequenced and cloned into *pUAST*. Several independent lines of transgenic animals were generated. For overexpression studies,

UAS-GluRIID and *UAS-GluRIIE* were generated by introducing the full length cDNA into the transformation vector *pUAST*. Full-length cDNAs of *GluR-IID* (RE24732) and *GluR-IIE* (RE07945) were obtained from Berkeley *Drosophila* Genome Project cDNA libraries.

The construct for inducible RNA interference (*RNAi-GluR-IIE*) was made based on the *pUASTi* plasmid (contains an intron between insertion sites for sense and antisense fragments; generous gift by Amin Ghabria, Krasnow lab). Selected cDNA fragments covering part of 5'-UTR and coding region were PCR-amplified by using the following primer pairs:

5'GCGCGCCTCGAGCTGTTCGGGAAACTCAAGAAT3' and
5'GGTCTAGAGCGGCCCGCCGTGGTTAGCTCGTTCAAATG3'
and

5'GCTGGTACCTGTTCGGGAAACTCAAGAAT3' and
5'GCGTCTAGATCGTGGTTAGCTCGTTCAAATG3'

The two fragments were inserted into *pUASTi* plasmid sequentially and verified by sequencing. Several independent lines of transgenic animals carrying *UAS-GluR-IIE* were generated.

To generate *GluR-IIE::EGFP* fusion. The EGFP ORF was inserted into the C-terminal of *GluR-IIE* coding sequence (the insertion site and the linker sequences are as described in (Sheridan et al., 2002) via 'blunt-end ligation' strategy. Briefly, a *HindIII* fragment covering the C-terminal region of *GluRIIE* was cut from full-length cDNA (RE07945) and subcloned into *pSL1180*; PCR reaction was performed to generate the whole length linear fragment using the following primers which are standing at the EGFP insertion site but opposite in direction:

GGCAGATGTGTATAAGAGACAGTCGCCAGTCCTCGATGTCAGTAGCTT
and

AGATGTGTATAAGAGACAGGACTGGCGACTGCGCGAGTAGATGG,

at the same time EGFP coding sequence was amplified from EGFP vector (Clontech) using the following primers with 5' phosphate modification:

pGGCGCGCCGAGCAAGGGCGAGGAGCTGTTACCCGG

and

pCGGGCGCGCCGCCCTTGTACAGCTCGTCCATGCCGAGA,

the two PCR products were put together for blunt-end ligation and the positive clones with right orientation of EGFP were verified by PCR and sequencing; then the HindIII fragment (now containing EGFP insert) was put back into the full-length cDNA backbone and the reading frame was verified by PCR and sequencing; finally the full-length DGluRIIE cDNA tagged with EGFP was PCR cloned into the NotI/ XbaI site of pUAST and pFasBac vector and verified by sequencing. Several independent lines of transgenic animals were generated from injecting the pUAST construct. The pFastBac construct was used for driving expression in Sf9 cells (for details see 2.2.5)

2.2.4 In Situ Hybridization

I. Preparation of embryos

1. Collect embryos every 3 hours for 24 hours and wash 3X with 0.02% Triton X (Tx)
(15ml for up to 2ml embryos in a 50ml falcon tube).
2. Dechorionate 3 min. in 50% bleach.
3. Wash 3X with 0.02% Tx.
4. Fill tube with equal parts heptane and 4% formaldehyde/PBS (filtered).
5. Incubate 25 min. with frequent shaking.
6. Remove LOWER aqueous phase and replace with equal volume methanol.
7. Shake for 1 min. allowing embryos to settle. Do not vortex.
8. Remove UPPER phase along with embryos and vitelline membranes and remaining at the interphase.
9. Rinse settled embryos 3X with methanol (Embryos can be stored at -20 degrees C at this point).
10. Rehydrate in 3:1 (MeOH: 4% formaldehyde/PBS) for 2 min., then 1:3 (MeOH: 4% formaldehyde/PBS) for 5 min.

11. Fix 10 min. in 4% formaldehyde/PBS.
12. Rinse 6X with PBS + 0.1% Tween 20 (PBT).

II. Preparation of Probe

1. Perform restriction digestion of the vectors containing the sequences of interest. For preparing antisense RNA probes of, *GluR-IIID* and *GluR-IIIE*, RE24732 (*GluR-IIID*) and RE07945 (*GluR-IIIE*) plasmids were cut with *NotI*, respectively.
2. Run the digest on agarose gel and extract the DNA (elute the DNA in 10 μ l of H₂O)
3. Run 1 μ l of DNA on a test gel.
4. In-vitro transcription:

Set the following reaction mixture:

DNA	9 μ l
RNase free water	3 μ l
10xTranscription Buffer	2 μ l
RNase inhibitor	2 μ l
DIG-labelling mix	2 μ l
T3 RNA polymerase	2 μ l

Incubate at 37°C for 2 hours.

5. Then add 2 μ l RNase free DNase and incubate at 37°C for 15 minutes.
6. Extract the RNAs by using RNeasy Kit.
7. Fragmentation of RNA

RNA sample in Rnase free water	25 μ l
2xcarbonate buffer	25 μ l
8. Divide the above mixture into two parts. Incubate 25 μ l at 60°C for 5 min and incubate other 25 μ l at 60°C for 15 min.
9. Add Rnase free water to the fragmented RNA sample to get a final volume of 100 μ l, add 10 μ l of NaAc buffer (PH 5.2) and 1 μ l of LPA, and 250 μ l of

absolute ethanol. Mix and centrifuge for 5 min at full speed, remove supernatant and wash the pellet with 75% ethanol.

10. Dissolve the RNAs sample with 25 μ l of probe resuspension buffer.

III. Hybridisation of embryos (fillets)

1. Wash the prepared embryos (fillets) in 1ml Pre-hybridisation Buffer(-DS)

Formamide	25 ml
20x SSC	10ml
50x Denhardtts	1 ml
tRNA 10 mg/ml	1.25 ml
ssDNA 10 mg/ml	1.25 ml
(preheated for 10 min at 100°C, followed by chilling in icewater)	
Heparin 50 mg/ml	0.05 ml
20% Tween	0.25 ml
Water	6.20 ml

Combine 9 ml with 1 ml water to get the Pre-hybridisation Buffer (-DS)

2. Incubate the samples in 1 ml of Pre-hybridisation Buffer(-DS) for 1 hr at room temperature.

3. Add 1 μ l of probe to 0.5 ml hybridisation Buffer (+DS) (9:1). Incubate overnight at 55°C.

4. 2x wash with 0.5 ml Washbuffer prewarmed at 55°C.

Wash buffer:

Formamide	250 ml
20x SSC	50 ml
Water	200 ml
20% Tween 20	2.5 ml

5. 7x 0.5 ml warmed wash buffer 1hr at 55°C.

6. Incubate in 0.5 ml warmed wash buffer overnight at 55°C.

7. 2x wash with PBTw.

8. Incubate for 30 min in PBTw at RT.
9. Incubate in 0.5 ml PBTw + 5% NGS + Antikörper (1:2000) (anti-DIG-AP FAB-Frag.) for 2 hrs. at RT.
10. 2x wash with PBTw.
11. 9x 10 min. PBTw at RT.
12. 2x wash with Alkaline Phosphatase Buffer + 0.1% Tween-20
 - 100 mM NaCl (= 20 ml 5M NaCl)
 - 5 mM MgCl₂ (=5 ml MgCl₂)
 - 100 mM Tris/HCl pH 9.5 (= 100 ml 1M Tris + 875 ml water)
 - 1/100 V 10% Tween-20
13. 5 min of incubation in AP buffer at RT.
14. Transfer the samples into 24 well plates, wash one time with 0.2 ml of BM Purple AP substrate, then add 0.2 ml of BM Purple AP substrate.
15. At proper stages, stop staining by 3 times of wash with PBTw and add 80% Glycerin/ H₂O. Store the plate at 4 degrees.

III. Mounting and light microscopy

2.2.5 Biochemistry (collaborated with Tobias Schwarz)

GluR-IIID and GluR-IIIE-EGFP were inserted into pFastbac1 vector (Invitrogen) and transformed into DH10Bac cells. Then the recombinant bacmid DNA was used for transfecting Sf9 cells with the aid of the Bac-to-Bac Baculovirus expression system (Invitrogen). For immunoblot experiments Sf9 cells were infected with the recombinant GluR-IIID and GluR-IIIE-EGFP baculovirus at a MOI (multiplicity of infection) of 1. Sf9 cells were harvested 40 hours post-infection washed twice with PBS, denatured in Laemmli buffer and heated at 100°C for 10 minutes.

Drosophila wild-type embryos were collected and dechorionated 18h AEL, froze in liquid nitrogen and stored at -80°C. Embryo lysates were prepared as described (Gillespie and Wasserman, 1994). The embryonic debris was removed

by centrifugation at 13000rpm for 15minutes and the supernatant was transferred to a new tube and centrifuged again for further purification. A portion of both pellet and supernatant fraction were mixed with an equal volume of 2x Laemmli buffer and heated at 100°C for 10 minutes.

Standard western blot was performed as described before. Anti-IID (1:1000), anti-IIC (1:1000) and rabbit anti-GFP antibodies (1:2000, Abcam) were incubated for 2 hours with the blot membranes at 4°C. For the visualization of the bands horseradish peroxidase conjugated secondary antibodies were used with the ECL Western blot system (Amersham).

2.2.6 Immunohistochemistry

2.2.6.1 Embryonic and Larval preparation

Solutions used for dissection:

Haemolymph-like (HL-3) saline without Ca

14ml 5M NaCl

5ml 1M KCl

20ml 1M MgCl₂

5ml Trehalose

115ml 1M Sucrose

Add distilled and deionized water to 1000ml, adjust PH to 7.2

10X PBS (Phosphate-buffered saline)

80g NaCl

2g KCl

2g KH₂PO₄

11.5g Na₂HPO₄.2H₂O

Add distilled and deionized water to 1000ml, adjust PH to 7.4

PBT

1X PBS

0.05% Tween-20

4% PFA (Fixation solution)

4% paraformaldehyde

1X PBS

Bouwin Fixation solution

Antibodies

Rabbit anti-GluR-IIC/III antibodies were generated against a c-terminal peptide (PRRSLDKSLDRTPKS). Rabbit anti-GluR-IID antibodies were generated against a c-terminal peptide of GluR-IID (ESLKTDSEENMPVED). Both sera were affinity purified and used at 1:500 dilution. Other primary antibodies were used at the following concentrations: mouse monoclonal anti-GluR-IIA antibody (8B4D2, DSHB), 1:100; Goat anti-HRP-Cy5, 1:250; mouse anti-FasII (1D4, DSHB), 1:40; mouse anti-Dlg (DSHB), 1:500; Nc82 (generous gift of Erich Buchner, Würzburg), 1:100. Except for samples stained with 8B4D2, which were fixed for 5 min with cold methanol, all of the other stainings were fixed for 10 min with 4% paraformaldehyd.

Dissection and staining

Mid stage 3rd instar larvae were put on a dissection plate, both ends were fixed by fine pins and the specimen was covered by a drop of ice cold HL-3 solution (see below). Dissection scissors were used to make a small hole at the dorsal midline of the larva (near to the posterior end) which was then completely opened along the dorsal midline from the hole to the anterior end. The epidermis was stretched flat and pinned down, then the internal organs and central nervous system were removed carefully with forceps. Late stage embryos (20- 22hrs after egg laying) were dissected on sylgard plates, fixed

with fine clips and opened using a pair of sharp tungsten needles. The dissected samples were fixed and then incubated with primary antibodies overnight, followed by fluorescence-labelled secondary antibodies (Dianova) and mounted in VectaShield mounting media (Vector Laboratories).

2.2.6.2 Confocal and epifluorescent microscopy

Imaging of embryonic and larval body wall preparations was performed on a Leica DM IRE2 microscope equipped with a Leica TCS SP2 AOBS scan head, using a Leica HCX PL Apo CS 63x 1.32 NA OIL UV objective. Epifluorescence images were taken on a Zeiss Axioscope with AxioCam camera, using a 100x oil objective of NA 1.4. Image processing was performed using ImageJ and Photoshop software.

2.2.7 Ultrastructural analysis (collaborated with Carolin Wichmann)

Dissected preparations were primary fixed in a mixture of 4% paraformaldehyde and 0.5% glutaraldehyde in 0.1M PBS (pH7.2) for 10 min and fixed additionally 60 min with secondary fixative comprising of 2% glutaraldehyde in 0.1 M sodium cacodylate buffer (pH7.2), washed three times for 5min in sodium cacodylate buffer, and postfixed on ice for 1hr with 1% osmium tetroxide, followed by an 1hr washing step in sodium cacodylate buffer and three brief washing steps in distilled water. The samples were stained en bloc with 1% uranyl acetate in distilled water for 1hr on ice. After a brief wash with distilled water, the samples were dehydrated in increasing ethanol concentrations (30%, 50%, 70%, 95%, 100%), infiltrated in Epon resin (100% EtOH/Epon 1:1, 30 min and 90 min; 100% Epon, over night) and embedded for 24hr at 85°C.

The samples were trimmed, and series of 80nm ultrathin sections were cut from muscle 6/7, abdominal segment 2 and 3 with a diamond knife on a Reichert Ultracut Ultramicrotome and mounted on Formvar-coated grids.

The sections were stained in uranyl acetate (4%) and photographed with a Philips (EM 301) transmission electron microscope.

2.2.8 Electrophysiology (collaborated with Robert Kittel)

Intracellular recordings were made at 22°C from muscle fiber 6 of abdominal segments 2 and 3, of late third instar larvae. The larvae were dissected in ice-cold, calcium-free haemolymph-like saline (HL-3) according to Stewart et al. (1994). Larval filets were rinsed with 2ml of HL-3 saline containing 1 mM Ca^{2+} , before being transferred to the recording chamber where two-electrode voltage clamp (TEVC) recordings were performed in 1mM extra cellular Ca^{2+} . The larval NMJ was visualized with a fixed-stage upright microscope (Olympus, 40x water immersion lens). Whole muscle recordings of both miniature and evoked postsynaptic currents were recorded in TEVC mode (AxoClamp 2B, Axon Instruments) using sharp microelectrodes (borosilicate glass with filament, 1,5mm outer diameter) with resistances of 15-35 M Ω and filled with 3M KCL. All cells selected for analysis had resting potentials between -55 and -70 mV. For stimulation, the cut end of the segmental nerve was pulled into a fire-polished suction electrode and brief (300 μs) depolarizing pulses were passed at 0.2 Hz (npi stimulus generator and isolation unit). To ensure the stable recruitment of both innervating motoneurons, the amplitude of the pulse was determined by increasing the stimulation strength to 1.5 times the amplitude needed to reach the threshold of double motoneuron recruitment. The clamp was tuned such that it responded to a voltage step from -60 to -70 mV with settling times of 1ms for mEJCs and 500-750 μs for eEJCs, this gave voltage errors of maximally 4 mV for eEJCs of approx. 100nA. Both eEJCs (voltage clamp at -60mV) and mEJCs (voltage clamp at -80mV) were low-pass filtered at 1 kHz. For each cell, 20 eEJCs and 90s of mEJCs recordings were used for subsequent analysis (pClamp9, Axon Instruments). For the paired-pulse stimulation, responses to 20 consecutive paired stimuli (separated by 4s rest) with 20ms interpulse interval were averaged.

3 Results

3.1 Establishing the tissue specific transcriptome of *Drosophila* larval body wall muscles

The total number of genes in *Drosophila* genome is predicted to be approximately 14,000. The high-density DNA microarray technique provides a fast and high throughput way to identify genes expressed at specific tissues or involved in certain processes (Stathopoulos and Levine, 2002; Butler et al., 2003; Li and White, 2003). Here, initial goal was to obtain a whole genome scaled map of molecular components involved in the construction and regulation of the postsynaptic muscle cells. Thus, using a *Drosophila* wild type strain (CS10), the transcripts of 3rd instar larval epidermis preparations, mainly consisting of body wall somatic muscles (with cuticles) but not central nervous systems, were prepared, amplified, labeled and hybridized to the Affymetrix *Drosophila* Genome arrays, generating the RNA expression profiles. RNA expression profiles of total larvae of *Drosophila* CS10 strain were also produced and set as baseline to compare with those from epidermis samples. Since equal amount of RNAs were utilized for different samples, transcripts displaying higher expression level in epidermis samples might represent the muscle specific or enriched genes and were selected.

The transcripts were ranked by average fold increase. Transcripts showing 2 fold or greater enrichment in epidermis samples were collected and shown in the appendix. One direct way to check the specificity of the data obtained is to check those transcripts with known tissue distribution pattern. As expected, among the pool of nearly 700 transcripts showing increasing abundance in epidermis samples, about one tenth are already known to be specifically (or abundantly) present in muscles or cuticles, thus directly proving the reliability of the data. These genes are categorized into various groups, including RNA-binding proteins, transcription factors, cell adhesion molecules, enzymes,

motor proteins, receptors and ion channels, and structural proteins, etc.(representatively shown in Table 3-1).

Table 3-1 Described muscle / cuticle-specific transcripts displaying enrichment in gene chip analysis of body-wall-preparations

Gene	Fold change	Proposed Function
RNA binding proteins		
How (held out wings)	4.5	RNA binding
Transcription factors		
Mef2	4.4	RNA polymerase II transcription factor
Muscle LIM protein at 84B	4.4	transcription factor
Cell adhesion molecules		
neuromusculin	7.3	cell adhesion
Enzymes		
Mlc-k	12.2	myosin light chain kinse
myosin light chain Kinase	5	myosin light chain kinase
CamKII	3.8	Calcium/ Calmodulin-dependent protein kinase II
dlg1 (discs large 1)	2.9	Synaptic and muscular scaffolding
Motor proteins		
Tropomyosin 1	2.6	Molecular motor
Tropomyosin 2	3.6	Molecular motor
upheld (troponin T)	3.6	tropomyosin binding
sanpodo (tropomodulin)	5.8	tropomyosin binding
Mhc (myosin II heavy chain)	2.5	muscle motor protein
Mlc2 (myosin light chain 2)	2.1	muscle motor protein
Receptors and ion channels		
GluR-IIA	4.3	glutamate receptor
GluR-IIB	2.6	glutamate receptor
GluR-III/ IIC	3.5	glutamate receptor
Structural proteins		
Lcp65Ag1	3.3	structural constituent of larval cuticle
Lcp1	2.9	structural constituent of larval cuticle
Lcp2	2.8	structural constituent of larval cuticle
Lcp65Ag2	2.1	structural constituent of larval cuticle
Lcp4	2.1	structural constituent of larval cuticle
Lcp3	2	structural constituent of larval cuticle
Others		
Mp20 (muscle protein 20)	2.9	calcium-binding
TpnC73F (Troponin C)	4.3	calcium-binding
TpnC47D	2.7	calcium-binding

3.2 Identification of novel ionotropic glutamate receptor subunits expressed at the *Drosophila* neuromuscular synapse

3.2.1 Enrichment of various transcripts encoding novel ionotropic glutamate receptor subunits in larval body wall muscles

The *Drosophila* genome encodes about 30 potential ionotropic glutamate receptor subunits (Littleton, 2000; Littleton and Ganetzky, 2000; Sprengel et al., 2001). Using the Affymetrix *Drosophila* gene chip result, the expression level of each subunit gene was compared between larval body wall and whole larvae RNA pools. As expected, GluR-IIA and GluR-IIB mRNA (Schuster et al., 1991; Petersen et al., 1997) were found to be enriched in body wall preparations. Another subunit annotated as CG4226, first referred to as GluR-IIC (Saitoe et al., 2001) and later as GluR-III (Marrus et al., 2004) was found to be enriched in body walls as well. A recent publication has shown that GluR-III null mutants die at late embryonic stages most likely due to a defect of glutamatergic transmission. In addition to these already described subunits with muscle expression, another glutamate receptor (annotated as CG18039) was found to be also enriched in body wall preparations.

Since the probe design of the *Drosophila* gene chip used here is based on an earlier version of the *Drosophila* genome annotation database, some genes might be omitted. To check if there are any newly annotated glutamate receptor genes which were not represented by the chip used, each of these selected glutamate receptor genes was blasted against the updated *Drosophila* genome annotation database (www.Flybase.com). Indeed, when blasting CG18039 coding sequence one gene annotated as CG31201 was found, which is strikingly similar to CG18039 (see below, Fig3-2). Interestingly, these two genes are located as direct neighbors within the genome, which is reminiscent of the organization of *GluR-IIA* and *GluR-IIB* (Petersen et al., 1997). Recently, it has been found that genes with similar expression pattern often cluster at certain regions of genome (Boutanaev et al., 2002; Roy et al., 2002), likely facilitating

transcriptional control of to be co-expressed genes. Intuitively, CG31201 might thus be expressed in a similar pattern with its neighbor CG18039.

Next, real time quantitative RT-PCR was applied to independently quantify the expression level of these candidate glutamate receptor genes. As shown in table3-2, real time quantitative PCR data were consistent with the observation from gene chip analysis. Moreover, CG31201 was shown to be enriched within body wall mRNA pool as well. From now on we will refer to the locus encoding subunit CG18039 as GluR-IIID and the locus encoding CG31201 as GluR-IIIE. These names are meant to reflect their muscle expression (see below) along with GluR-IIA, -IIB and -IIC/III.

	C _t (body wall)	% control	C _t (total larva)	% control	Body wall /total larva
<i>GluR-IIA</i> (CG6992)	26,7	15,4	28,3	4,4	3,5
<i>GluR-IIB</i> (CG7234)	28,2	5,6	29,5	1,9	3,0
<i>GluR-IIC/III</i> (CG4226)	26,4	18,7	28,9	3,1	6,3
<i>GluR-IIID</i> (CG18039)	25,5	35,5	27,0	10,5	3,4
<i>GluR-IIIE</i> (CG31201)	24,5	73,7	26,3	17,5	4,2
<i>tbp-1</i> (internal control)	23,8	100,0	23,8	100,0	1,0

Table 3-2 GluR-IIID and GluR-IIIE are enriched in larval body wall mRNA.

Abundances of glutamate receptor subunit transcripts estimated using real time PCR. The control transcript (proteasome subunit *tbp-1*) had the same abundance in body wall preps and whole larvae. The glutamate receptor subunits shown were enriched in body wall RNA when compared to whole larva RNA. The abundances of mRNAs are expressed as C_t values indicating the cycle number with which amplification exceeds detection threshold (C_t difference of one indicates a two-fold difference in abundance). All data are averages of three independent experiments where each sample was run two times in parallel.

3.2.2 Expression pattern of new ionotropic glutamate receptor genes

To further confirm the muscle expression of these new subunit genes, *in situ* hybridization on *Drosophila* embryos and larvae was performed. In fact, the mRNAs of GluR-IIID (Fig.3-1A-D) and GluR-IIIE (Fig.3-1E, F) are specifically expressed in somatic muscles of both *Drosophila* embryo (Fig.3-1A-C, E, F) and larva (Fig.3-1D). Expression of GluR-IIID (Fig.3-1C-D) and GluR-IIIE (Fig.3-1E) starts in somatic muscles of late stage 12 embryos (Fig.3-1A, E) and extends throughout embryonic and larval development (Fig.3-1D, F), a pattern very similar to that of GluR-IIA, -IIB and -IIC/III (data not shown; Petersen et al., 1997; Marrus et al., 2004). Intriguingly, in addition to the somatic muscle expression GluR-IIID is also abundantly present in cardiac precursor cells (Fig.3-1A, C), which was not found for the other muscle subunit genes.

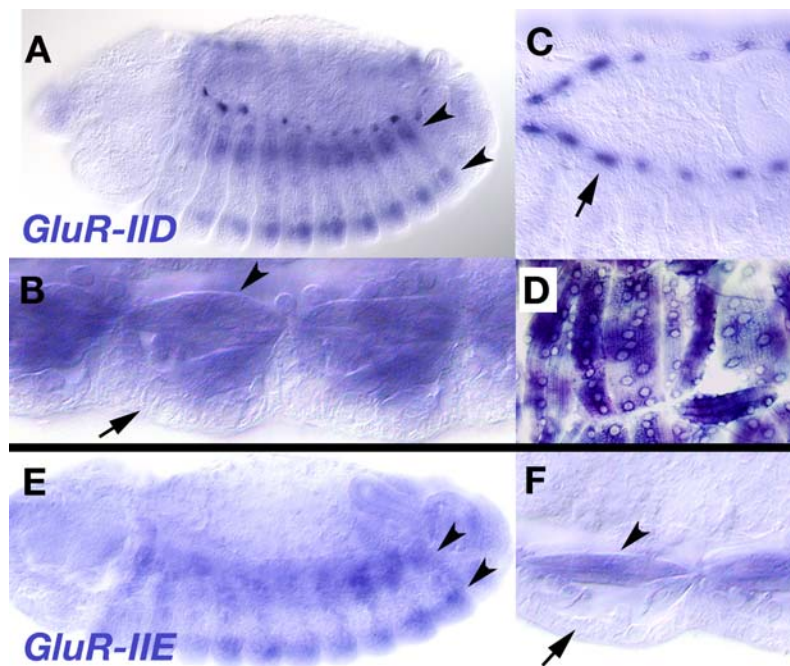


Figure 3-1. *GluR-IIID* and *GluR-IIIE*: novel glutamate receptor subunits with muscle specific expression

In situ hybridizations on *Drosophila* embryos (A-C, E,F) and larvae (D) for *GluRIID* (A-D) and *GluRIIE* mRNA (E,F). Both subunits are expressed specifically in presumptive somatic muscle cells (A, B, E, F, arrowheads) but are for example not found in the adjacent epidermis (A, B, F, arrows). Expression of *GluR-IIID* and *GluR-IIIE* transcript in the presumptive somatic muscles starts in late stage 12 and peaks at around stage 14 (A, E), to then persist during later embryogenesis (B: stage 16; E: stage 17) and larval development (D). *GluR-IIID* is also expressed within heart precursor cells (A and B, arrows).

3.2.3 GluR-IID and GluR-IIE represent a new type of muscle-expressed glutamate receptor subunit

In a 'simple' synaptic model system like the *Drosophila* NMJ the coexistence of so many distinct glutamate receptor subunits is somewhat unexpected. To get a closer view of the relationship among them, full-length cDNA clones of GluR-IIC, GluR-IID and GluR-IIE were obtained, the reading frames were verified by double strand sequencing and the deduced amino acid sequences compared. Clearly, these proteins encode all structural features typical in glutamate receptor subunits. Importantly, all putative transmembrane domains were found at similar positions (see Figure 3-2A). As previously noted (Marrus et al., 2004), the GluR-IIC/III sequence is closely related to GluR-IIA and IIB. GluR-IID and GluR-IIE are also highly related with each other (Fig. 3-2A, B). However, GluR-IID and GluR-IIE are distant from GluR-IIA, IIB and IIC/III group (Fig.3-2B). The fact is, GluR-IID and GluR-IIE are even slightly closer to human kainate receptor GluR6 than they are to the GluR-IIA, -IIB and -IIC/III group (see dendrogram in Fig.3-2B). Thus, in contrast to the GluR-IIA, -IIB, -IIC/III type, GluR-IID and GluR-IIE represent a new type of glutamate receptor subunits which is expressed in somatic *Drosophila* muscle. In a previous alignment entailing all identified ionotropic glutamate receptor subunits of the *Drosophila* genome, several other non-NMDA type subunits group in between GluR-IID, -IIE and GluR-IIA, -IIB, -IIC/III groups (Littleton and Ganetzky, 2000). Notably, all of the muscle glutamate receptor subunits (from GluR-IIA to -IIE) have direct orthologs in *Drosophila Pseudoobscura* (data not shown), suggesting that the differentiation of the insect muscle-expressed glutamate receptor subunits into two structurally different groups might be conserved.

A

**GluR-IIC
GluR-IID
GluR-IIE
GluR-6**

```

MRLCFV--VIVAFIIGFLGILALGGD-DENEIVGATFYENEKE...IEISFDQAFREVNH--MKFSELEFVTIKRYMPTND
MRFVCI--SLILLSLSEVQAQFYGGNAVEAS-QQSRLGLLIDDAATR...IROTFEHAIVVNH...ELGVFVGTETQVAYGN
MFFNHFVILVSLFSHISVVAQYENFGGYDNYQSLSPFLGLLTDQNTQ...MNIIVFDHAIIDVAHQ...EVGSLISLSKEEIVYGD
MKTISFV--SNLVFSSRSLKVLCLLVLGYSQG-NITHVRFGGIFEVYESGFMGAELAEFAVHTIMRNMLTLPFNTITTYDTQKINLYD

RFLIQQITICLLEISNGVAAIFGFSKAAASDVAQIAHATCIPHEIYDLKLEATRQQLNHQMSINVAFRSLVLSLSEALYFEIKKSNVWRITFT
RIVQAFACLCELMQSGVAVFGFAARHTASHLLNACDSKDIPIFIVPHLSV--G...SNPDGPNLHPSP--EDIAIALYLDIVN-QFEVSRFEI
AVIQZYGKLCRMEITGIGAVVFGFSRHTAVHLMISICAMDIPIHEIYZYMS--...-SNAGSGLNHPSP--ADLAALYLSLIT-QFNWTFEII
RFLKXKACQQLLGVAAIFGFSRSEANAVQICNALCQVHEIQTEVWKQVSE--DNRISFVSLYDPSFSLSEALIDLVQ-FEIVKTYT

LIYETPREGARLQDLMNIOALNSDYVXLRNLADYAD-DYRIIVLVEITDITPHEQRIILDCCEFKTLKELKLVSDIFKIQGFENWVPIHLDIT
PCYEAIVKILHLMITRYGLKGFVLEKMRDYDLNHLGNHVESVLRERKESL-DNRKRVVVGRTGMALLERKQAGVGMNNDITTYTIGGNTIN
FYESAIVNINLWETITMLGSSGVITLWLYDMQHLGNKQVLRVRESV-DNRKRVVVGRTGMALLERKQAGVGMNNDITTYTIGGNTIN
VYVDPSGLIRLQELIKAFSSRYNLRKXIRQLPADTK-DAPKLLKEMKRGK-EFHVIFDCRHEMAGILKQALAMGMITVYHYIFTTLDL

MNSGRLIYEDFKANITVRELVVDANPFE-RKTRLRKVDQILG--...-NQTMFLIIFDADVIVASRARNVIAAMQFFPFPNR
HFDLEEK--YSEANITGIRCFSPDQEEVDMEELHQELGERSF-VNRG--SFTITMFMALTYDAVEVIAEITKILFVQFQMLNCSQR
HSFDLEEK--YSEANITGLRLFSPEKMAVKKELMLKLYPTDQDE--FRNG--SCFITVEMALTYDAVQLAQFLKHLFPKFPQNCQR
FALDVEFYR--YSGVNMIGFRLINTENTQSSIEIEMVSMERLQAFPFDRGLDGFMTDAALMADADVHVSVAVQFQOMTVSSLQCNR

HCGSSSEVWMLGAFIVCEMKTISEDDVPEPHFTEENMKLDEYGORHFNHEIYKPTVNEFMVMVTPFNGIKKELNLELESAGTQDFEQR
HNDVQF--DGRFRNMYMRSLEIEKTIYGRVYFEGN--VRKGRTFDVIILQISGLVYKGVVEGKDFEFOR-PPQAVNFNDDGSGSVN
TESVED--DGRFRNMYMRELRLLTDLRLTIGFIYFEGN--VRKGRHLDVIELQFSGIVYKGVVDEDRQYRFPAPPTAQFDRVDR-SLAM
KFWR--FGRFRMRLTKFAHVEG--LIGELTFNKTHGLRDLVIRKKEGELKIGYVDPASGYNMTE--S8QKGRFANI--SLSM

KVVIVV--HYEESYFMMKIDHENFRGEEKYEGYAVDLISKLSRLMEFDVEMIVNG--HNGKYNPITKQVDDIIRKLIIDHRAQIGVCDLTI
KTFIVLISVATKPYASLVESIDTLIGNNQFQGYGVDLIKELADKLGNNFTFRDGSN-DYGSFNKTTNSTRSOMLKEIEISKADLAITDITI
KTFIILSVFKPYAQLVETKQLSWSQYEGYVDLIKELADKLGNNFTFRDGSN-DYGSFNKTTNSTRSOMLKEIEISKADLAITDITI
RSLIVT--IEEYVFKTKDKPILVSGDRFEGCIDLLEELTILGEMFTRVFDGIVGADVDVHGVQVNGMVEELIDKADLAITDITI

TM1
YQMRSEVYDFVFMQLGSLIHVYKSPFPKNOFAFLLEFFAVVWVIMTFAQLTMTLAFVVFARISYSREWLPNFAIQDFDELENIVHVN
TSEELHSAQSTSRERSRSLITVTEKATPFLMDFPSEVWVFLGFLSFLGYSLEFIFLGRSSEVWVFCIFPELEENQFTLG
TSEELHSAQSTSRERSRSLITVTEKATPFLMDFPSEVWVFLGFLSFLGYSLEFIFLGRSSEVWVFCIFPELEENQFTLG
YVREKVIDFSKPFMTLGLSILYRKPNGTNPFGFSLNILSDIWMYLLAYLGVSCVLEVIARFSEVWVYVFPFCIFDQVVENNFLL

TM2
HSLVLMVGSIMQGCIDILFRGPHMRLITGMVVFVIAEMLSYTAHLAAFLYSNHWQSEKRLQDIEIQDKVHGMHGGSEFIFFSSEIN
HSLVFTTGALLQGSSEIAPKALSTRISAVVVFVFLIVSSYTAHLAAFLTIEFPSPINSEVXDLADKDDVQVYGAIKTGFNFFMFTA
HSLVFTTGALLQGSSEIAPKALSTRISAVVVFVFLIVSSYTAHLAAFLTIEFPSPINSEVXDLADKDDVQVYGAIKTGFNFFMFTA
HSLVFGVGAIMQGSSELNKKALSTRISGGIVVVFVFLIVSSYTAHLAAFLTIEFPSPINSEVXDLADKDDVQVYGAIKTGFNFFMFTA

pore
RITDQRLAVNQMKDFNPAFTSTNKEGVAVRKEIKGCVAFLEMTTSLIVNIEENQDLYQIGQIIGEKHYGLAVPLGSDYRINLSVSLFLQIS
RPIYIKMNIYLNAPF-MEMENHQGVQKVKSG-TKYAFLEMTSIEFNYRRCNLTQVGDPLDEKGYGIAMVKNVYFVDRKFNKALLLQ
RERKMKNFMSNFPQ-YITEDNMEGVNEVXTH-THYAFLEMTSIEYNYRRCNLTQIGDALDEKGYGIAMVKNVYFVDRKFNKALLLQ
ISTDQKMAVAFMSRRQGVIVKSNKEGQVRLY--S-YAFLEMTSIEFVYRRCNLTQIGSLIDQKGGYVTFMGSYDRKFITIALLQ

TM4
RRLGLLQKMKKVVKNHN-VTCDSYHVEDGD-EISLIIIGVFLVLAGQVLTIGVILGTFIFLWVQVAVELKVPVQAFKARLIFALKV
RQGVLAELKMKVNEVGAQVCSAESDDDGFSRGGVDEHLSGIYVVLVIGSIIISIIISILCWCVYKAKNHYVPCDALAEERFRIYRFS
RQGVLEKMKVNEVGAQVCIATLSDAPDAPDDNHLISGVFVLLVGSCCALLISILCWCVYKAKNHYVPCDALAEERFRIYRFDH
RSGILHNMKVVRRGSH--EPE-ESEKASAEQVQHLICGIFVLAAGVLSMVFVAVGSEFLKPKKNAQLERKRFCSAMVRELRNRLKQ

VEKFMISSEDSKSSRESE--GRRLKRLKRLKRVSS
EEREELHSAQSTSRERSRSLITVTEKATPFLMDFPSEVWVFLGFLSFLGYSLEFIFLGRSSEVWVFCIFPELEENQFTLG
HYVRLNLSASITSRERSRSL--MVAIVAVQESQ
RRLK-HLFPQAFVIVKTEEVINMHEFNDRRLPGKEMEA

```

B

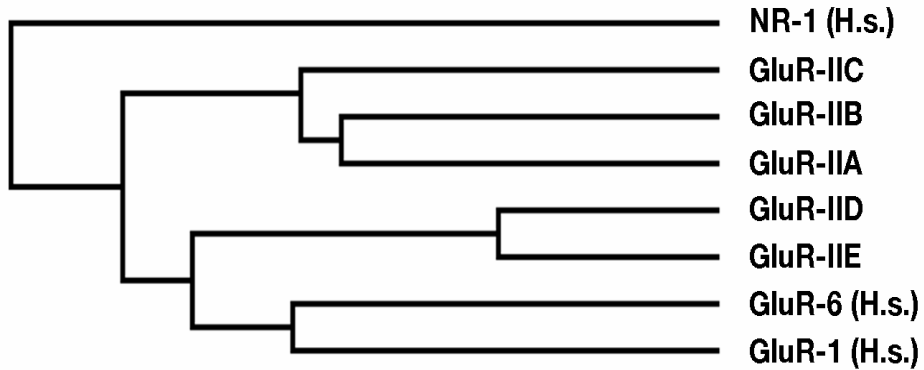


Figure 3-2 Sequence analysis of GluR-IID and GluR-IIE

A, sequence alignment of predicted amino acid sequences of (from top to bottom) GluRIIC/III, GluR-IID, GluR-IIE and human kainate receptor subunit GluR-6, similar amino acids are indicated by shaded boxes. Putative trans-membrane domains (TM1-4), the channel pore region and the c-terminal peptide of GluR-IID which was used for immunization are indicated as well.

B, dendrogram analysis comparing muscle expressed glutamate receptor subunits of *Drosophila*, together with AMPA receptor subunit GluR1, kainate receptor subunit GluR-6 and NMDA receptor subunit NR-1 (all Homo sapiens). Dendrogram was generated using MacVector software.

3.2.4 GluR-IIC, GluR-IID and GluR-IIIE are specifically localized at postsynaptic densities of neuromuscular synapses

To directly test the subcellular distribution of these novel glutamate receptor subunits, polyclonal antibodies were produced. In brief, rabbits were immunized with GluR-IIC/III C-terminus peptide (PRRSLDKSLDRTPKS) and GluR-IID C-terminus peptide (ESLKTDSEENMPVED) respectively. Collected sera were affinity-purified via their corresponding peptides. In western blotting assay, the antibodies against GluR-IIC/III and GluR-IID recognize a single band of about predicted 109 kD and 102 kD in wild type *Drosophila* embryo extracts respectively (Fig.3-3A, right lane). Cross reactivity of our sera between receptor subunits is not observed, since the antiserum against DGluR-IID can specifically recognize SF9-cells infected with recombinant virus containing GluR-IID cDNA but not the SF9-cells with expressing GluR-IIIE (Fig.3-3A, left lanes).

For immuno-fluorescence microscopy studies, previously a monoclonal antibody (8B4D2) against GluR-IIA has been characterized. In both late stage embryos and larvae 8B4D2 stains the postsynaptic membrane along the NMJ with a discrete dotted manner (Fethetherston et al., 2001; Packard et al., 2002). This antibody thus allows direct visualization of PSDs opposite the corresponding active zones. In the wild type larvae and embryos stained with our antibodies against GluR-IIC and GluR-IID, similar findings were obtained: localization of both GluR-IIC and GluR-IID is confined to typical punctae (Fig.3-3B, C, arrow heads) corresponding to individual postsynaptic densities (PSDs), which are surrounded by the HRP labels known to have perisynaptic expression (Sone et al., 2000). Moreover, these punctae are found directly opposite to the presynaptic Nc82 label. The Nc82 monoclonal antibody specifically recognizes the presynaptic active zone (Heimbeck et al., 1999; Wucherpfennig et al., 2003). Thus, it can be concluded that both GluR-IIC and GluR-IID are expressed within the PSD region of individual neuromuscular

synapses.

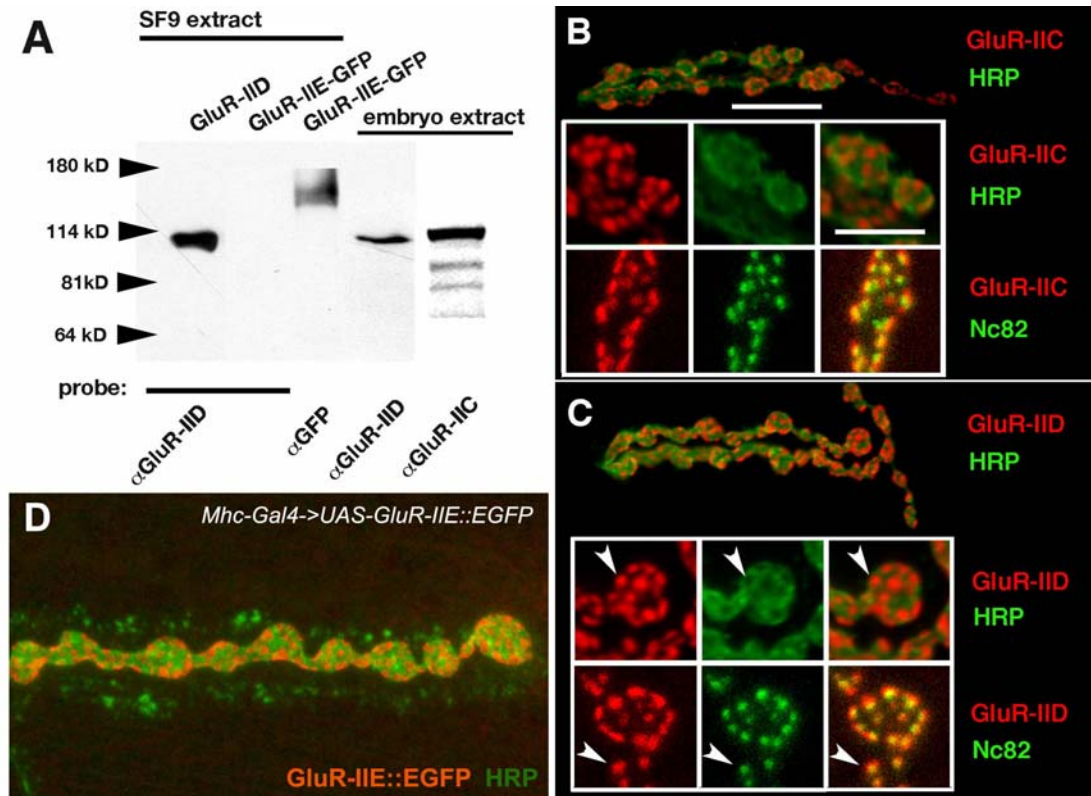


Fig.3-3 GluR-IIID and GluR-IIIE are expressed within postsynaptic densities

A: western blot analysis: the anti-IIID peptide antibody recognizes SF9-cell expressed GluR-IIID and endogenous GluR-IIID from *Drosophila* embryo extract. It does not cross react with the related GluR-IIIE protein, which is SF9-cell expressed as a GFP fusion and is recognized using anti-GFP antibody with the predicted size of about 145 kD. GluR-IIIC/III is recognized with our peptide antibody in *Drosophila* embryo extract with predicted size as well.

B-C, shown are epifluorescence pictures (upper two panels in B and C) and confocal pictures (lower panels in B and C) of receptor subunits GluR-IIIC/III (B, red) and GluR-IIID (C, red) together with the perisynaptic marker HRP (upper panels in B and C, green) or active zone marker Nc82 (lower panels in B and C, green), scale bars: 8 and 4 μ m.

D, confocal picture of GluR-IIIE::EGFP (red) together with perisynaptic marker HRP (green).

Several GluR-IIIE-specific peptides were used to immunize rabbits as well. Unfortunately, specific antibodies could not be obtained, mainly due to the fact that the GluR-IIIE amino acid sequence is closely related to GluR-IIID. In fact, it is hard to find a GluR-IIIE specific peptide sequence which would be proper for

immunization. To overcome this difficulty, the enhanced green fluorescent protein (EGFP) reading frame was inserted into the near C-terminus GluR-IIIE to generate an autofluorescent fusion protein. Fusion of EGFP into the same position of mammalian GluR2 has been previously shown not to interfere with glutamate receptor assembly and function (Sheridan et al., 2002). Indeed, upon overexpressing this GluR-IIIE::EGFP in larval muscle (driven by *MHC-Gal4*), an antibody directed against EGFP strongly labeled the postsynaptic density region (Fig3-3D). This result makes it very likely that the endogenous GluR-IIIE protein localizes to the PSD region as well.

3.3 GluR-IIID and GluR-IIIE are essential for viability

To genetically investigate what roles GluR-IIID and GluR-IIIE play in NMJ glutamatergic transmission, null mutants for each of the two genes were required. For *Drosophila* molecular genetics, transposon mediated mutagenesis often is an efficient way of knocking out a candidate gene function. In the presence of transposase activity, integrated transposons can be remobilized and randomly jump into other chromosomal locations. Upon remobilization, apart from the transposon sequence as well often genomic sequences flanking the insertion site of the mobilized transposon will be eliminated as well. Thus, transposon mapping in the near of candidate loci can be used to produce gene-specific deletions. Here, this strategy was used to obtain mutants of *GluR-IIID* and *GluR-IIIE*.

From a collection of *piggyBac* transposon lines which covers 53% of all loci annotated for *Drosophila* (Thibault et al., 2004), one line (pBac{RB}e01443) was described to have an insertion in the *GluR-IIID* locus. This line was obtained and genomic PCR was performed using one primer corresponding to the flanking region the proposed insertion site and another primer corresponding to the end of the *piggyBac* transposon. The resulting PCR

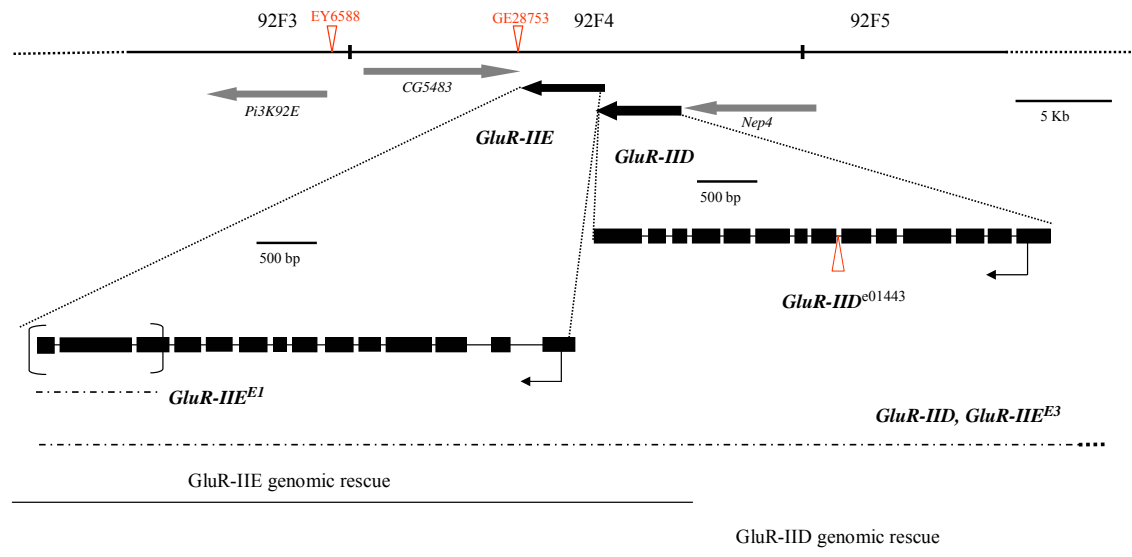


Figure 3-4 Genetic analysis of GluR-IID and GluR-IIIE

GluR-IID and GluR-IIIE map to position 92F on chromosome III. Exon-intron structure of both loci is shown, exons are boxed. The null allele GluR-IIDe01443 is based on a piggyBac transposon insertion within the open reading frame of the GluR-IID locus. Null allele GluR-IIIEE1 lacks c-terminal sequence of the protein including the last transmembrane domain of the receptor subunit. GluR-IIIEE3 deletes at least GluR-IIIE and GluR-IID alleles and thus is used as deficiency allele. The genomic stretches used for genomic rescue constructs are shown below.

product was purified and subjected to sequencing. It was found that in fact in this line the transposon has integrated directly into intron 6 of *DGluR-IID* (Fig.3-4). This could well interfere with normal transcript splicing and hence the generation of GluRIID protein. Interestingly, this line is embryonic lethal in homozygous condition. We from now on refer to this allele as *GluR-IID*^{e01443}.

For *GluR-IIE*, imprecise excision mutagenesis screening was performed using transposon line EY6588 (<http://flypush.imgen.bcm.tmc.edu/pscreen/>) and later GE28753 (<http://www.genexel.com>) whose insertion sites are located 14Kb and 150 bp downstream of the 3' end of *GluR-IIE* transcript, respectively (Fig.3-4). From the screening, about 30 imprecise excision events (Fig.3-4) were recovered, genomic PCR with a series of primer pairs corresponding to the flanking region of GE28753 insertion position were utilized to recover the deleted region in each line. Among them, a line called *GluR-IIE*^{E1} was found to have the genomic sequence encoding the C-terminal part of GluR-IIE including the last transmembrane domain deleted. Importantly however, the *GluR-IIE*^{E1} deletion does not extend into neighboring loci. Similar to *GluR-IID*^{e01443}, *GluR-IIE*^{E1} is also embryonic lethal in homozygous condition. In addition, no GluR-IID protein could be observed at the neuromuscular synapses of either *GluR-IID*^{e01443} or *GluR-IIE*^{E1} homozygous embryos (see 3.4.1 for details). *GluR-IID*^{e01443} and *GluR-IIE*^{E1} are also embryonic lethal over another independent excision allele *GluR-IID&IIE*^{E3} (Fig.3-4), a larger deficiency which deletes both *GluR-IID* and *GluR-IIE* genomic sequences. However, *GluR-IID*^{e01443} is fully viable when crossed over *GluR-IIE*^{E1}. Both *GluR-IID*^{e01443} and *GluR-IIE*^{E1} are fully rescued by transgenic addition of one copy of genomic *GluR-IID* or *GluR-IIE*, respectively; however, neither the *GluR-IID* mutant nor the *GluR-IIE* mutant can be rescued by the respective other transgene. Thus, several lines of evidence (here and 3.4.1) suggest that *GluR-IID*^{e01443} and *GluR-IIE*^{E1} represent specific null mutant alleles for *GluR-IID* and *GluR-IIE*, respectively. While the neighboring loci *GluR-IID* and *GluR-IIE* encode very similar proteins with largely overlapping expression pattern, both of them are essential for embryonic viability.

3.4 Reciprocal dependence of all essential glutamate receptor subunits for synaptic expression and function

3.4.1 Complete synaptic absence of all other glutamate receptor subunits after knockout of any essential subunit genes

Homozygous *GluR-IID*^{e01443} and *GluR-IIE*^{E1} embryos were subjected to further inspection. These embryos, while apparently developing normally, show no coordinated movements and do not hatch. The same phenotype is also observed previously within *GluR-IIC/III* single or *GluR-IIA&IIB* double null mutant embryos. This phenotype was interpreted as failure of neuromuscular neurotransmission due to the absence of functional postsynaptic glutamate receptors (Petersen et al., 1997; Marrus et al., 2004). Consistent with a role in synaptic transmission, *GluR-IID* and *GluR-IIE* mRNA expression starts within embryonic muscles well before the onset of neurotransmission (Fig.3-1), just like the cases of *GluR-IIA*, *-IIB* and *-IIC* (Petersen et al., 1997; Marrus et al., 2004).

In mammals, ionotropic glutamate receptors appear to be composed of rather closely related subunits (Wenthold et al., 1996; Mulle et al., 2000). Hence, whether the rather similar GluR-IID and GluR-IIE subunits directly form glutamate receptors was investigated via immuno-fluorescence microscopy. In principle, if the formation of a certain type of glutamate receptor fails, the synaptic localization of its constituent receptor subunits must be affected. In wild type late stage embryos, GluR-IID proteins stably localize at the PSD region of all NMJ synapses (Fig.3-5B, wild type). In *GluR-IIE*^{E1} embryos, neuromuscular contacts still form, as shown by staining against anti-HRP and Nc82 antibodies (Fig.3-5A, blue and green channel). However, GluR-IID is completely absent from *GluR-IIE*^{E1} embryonic NMJs (Fig.3-5B). This finding suggests that GluR-IIE and GluR-IID might join into a common glutamate receptor which in turn is essential for synaptic neurotransmission at the embryonic NMJ.

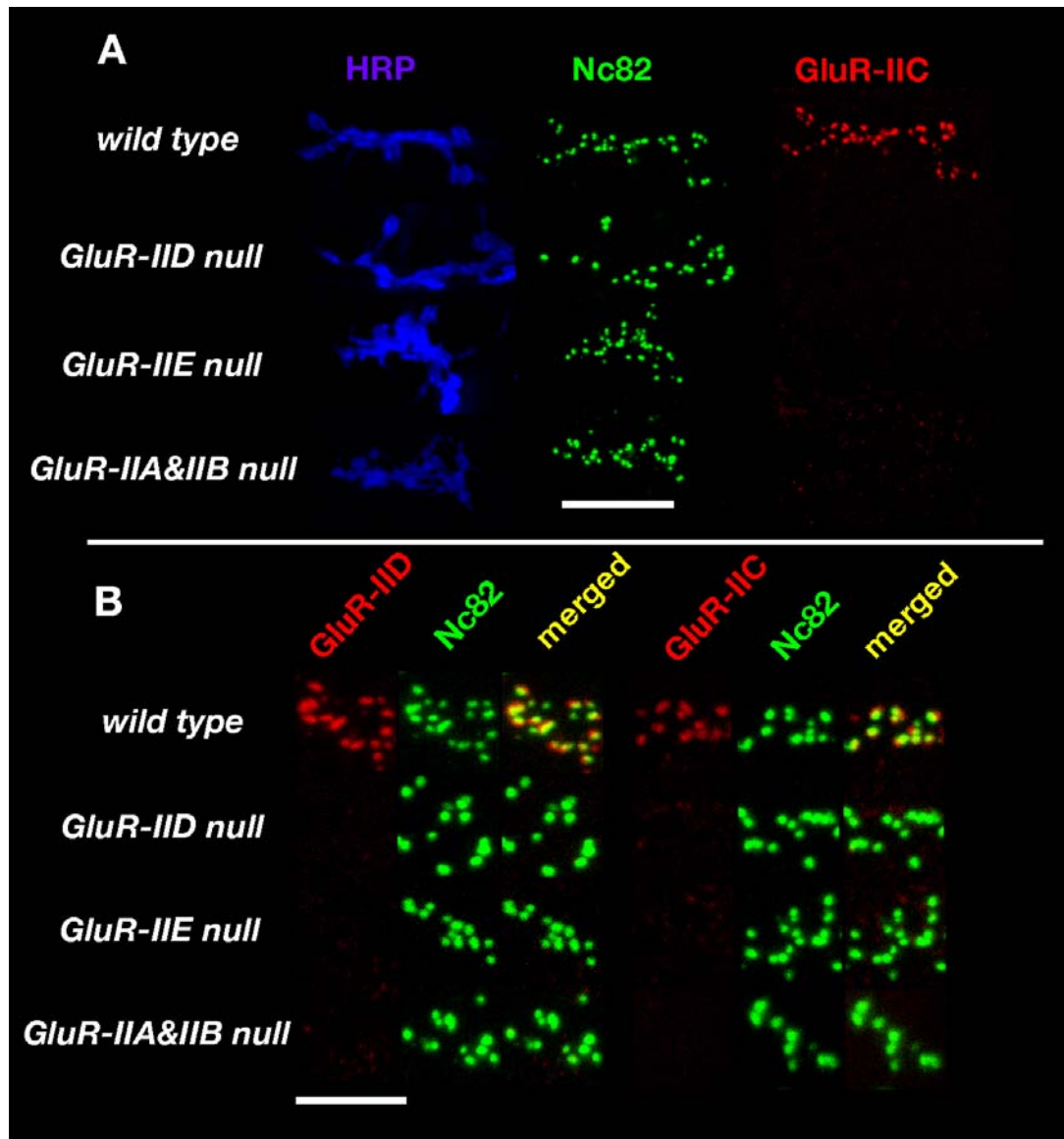


Figure 3-5 Interdependence between glutamate receptor subunits for NMJ expression

A, Confocal images of NMJs in wild-type, *GluR-IID* null, *GluR-IIE* null or *GluR-IIA&IIB* double null mutant embryos (20-22 hrs old) stained with antibodies against *GluR-IIC/III* (red), Nc82 (green) and HRP (blue). Nc82 staining indicates differentiation of presynaptic release sites at the mutant NMJs. Synaptic expression of all glutamate receptor subunits fails at the mutant NMJs. Scale bar: 10 μ m

B, Higher magnifications of confocal stainings similar as in A. Stainings of either *GluR-IID* (left panels) or *GluR-IIC/III* (right panels) are shown together with Nc82. Scale bar: 5 μ m.

Based on the analysis of *GluR-IIC/III* and *GluRII-A* hypomorphic larvae, it

has been suggested that GluR-IIC/III is an obligatory subunit, which associates with either GluR-IIA or GluR-IIB to form functionally distinct glutamate receptors (Marrus et al., 2004). This idea was tested again but **directly** by immunostaining *GluRII-A&IIB* double mutant embryos. Consistent with Marrus et al., GluR-IIC/III label is completely absent from NMJs of *GluRII-A&IIB* null mutant embryos (Fig.3-5A and B). Thus GluR-IIA together with GluR-IIB can be considered a “synthetic essential subunit”. In principle, the two “groups” of subunits (GluR-IID, -IIE versus -IIA, -IIB, -IIC/III) could be independently essential for embryonic neurotransmission. Alternatively, synaptic localization and thus receptor function could be interdependent between both groups. To distinguish these two possibilities, it was first checked whether the synaptic localization of the GluRIIC/III glutamate receptor subunit is dependent on the presence of GluR-IID and GluR-IIE. Clearly, no synaptic localization of GluR-IIC/III can be found in either *GluR-IID* or *GluR-IIE* null mutant embryos (Fig.3-5A and B). *Vice versa*, the synaptic expression of GluR-IID was absent from *GluR-IIA&IIB* double null mutant embryos (Fig. 5B). Thus, at the embryonic NMJ, the synaptic expression of all essential glutamate receptor subunits is absolutely interdependent. The easiest explanation for these data is that at the *Drosophila* NMJ the glutamate receptor is formed by four different essential glutamate receptor subunits: GluR-IIC, GluR-IID, and GluR-IIE together with either GluR-IIA or GluR-IIB.

3.4.2 Genetically depriving the expression level of any single essential glutamate receptor subunit results into corresponding reduction of all other subunits

If the glutamate receptor is indeed assembled from four different subunits, partially suppressing the level of any single such subunit should interfere with the synaptic expression of the other essential subunits and the overall glutamate receptor formation. To test this, several independent experiments have been performed.

First, the expression of GluR-IIIE was knocked down in vivo via transgenic RNA interference technique (Kennerdell and Carthew, 2000). When RNA interference against *GluR-IIIE* was conducted in a muscle-specific manner, the *GluR-IIIE* transcript level was knocked down to about 20% of wild type level while the transcription level of all other muscle subunit genes remained unchanged (not shown), indicating the highly selective RNA degradation mediated by RNA interference. In contrast to the *GluR-IIIE* null mutants, these animals do not die at embryonic stage but instead develop into mature larvae and adult flies. So the effects on the distribution of other subunits in 3rd larvae were examined. Significantly, all of the other known subunits (GluR-IIA, GluR-IIB, GluR-IIC/III and GluR-IID) were greatly reduced at NMJ when the RNA interference was driven in muscles (using *G14-Gal4* or *MHC-Gal4*), while

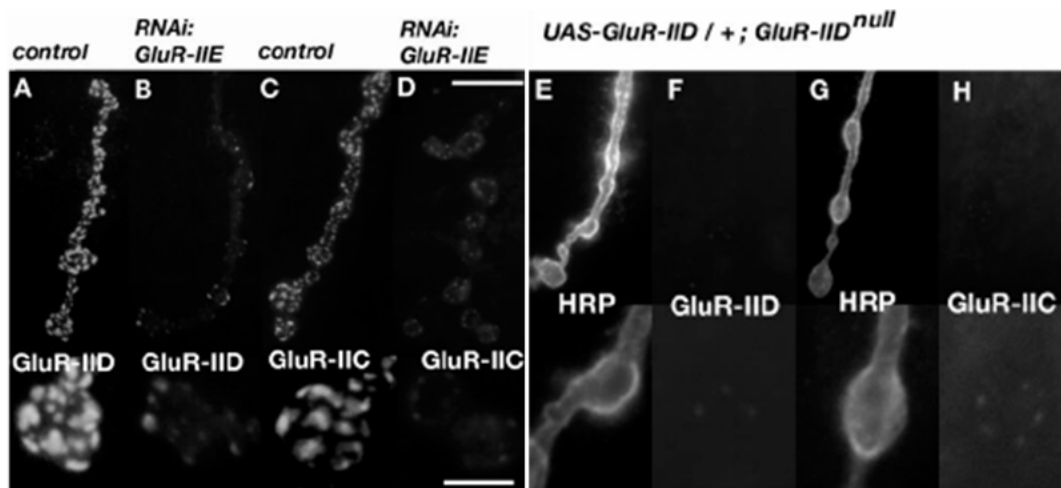


Figure 3-6 A partial reduction of either GluR-IIIE or GluR-IID provokes a significant reduction of all glutamate receptor subunits at the NMJ

(A-D) Larval NMJs (muscle 4, abdominal segment 2) stained for GluR-IID (A, B) or GluR-IIC/III (C, D) in control larvae (*G14-gal4/+*, A and C) or larvae experiencing muscle specific RNA interference against GluR-IIIE (*G14-gal4/+; UAS-GluR-IIIE-RNAi*, B and D). Suppression of *GluR-IIIE* leads also to a reduction in the NMJ expression of GluR-IIC/III and GluR-IID. Lower pictures represent higher magnifications.

(E-H) Shown are NMJs (muscle 4, abdominal segment 2) of *GluR-IID* null mutant larvae rescued with a single copy of *UAS-GluR-IID* (*UAS-GluR-IID/+; GluR-IID^{e01443}/GluR-IID&IIE^{E3}*). Only trace amounts of GluR-IID (F) and GluR-IIC (H) are expressed at the NMJ, HRP stainings (E, G) are added to visualize the NMJ. Non-linear contrasting had to be used to make the trace amounts of GluR-IID (F) and GluR-IIC (H) visible. Scale bar in upper panel 7,5 μm , in lower panel showing higher magnification 2,5 μm .

there is no obvious effects when driving the expression of RNA interference construct in the central nervous system (using *ELAV-Gal4*) (Fig.3-6B, D; data not shown)., which further verify that GluR-IIE functions specifically in somatic muscles and intrinsically associates with other subunits.

For a second experiment, it was found that minimal amounts of GluR-IID (produced by the “leaky” expression from pure *UAS-cDNA* transgenes) can already rescue *GluR-IID* null mutant embryos into mature larvae (Fig.3-6E-H). In these rescued larvae, both GluR-IID and all other glutamate receptor subunits were strongly reduced at the NMJs (Fig.3-6H). Re-expressing GluR-IID to **normal** level by using the muscle specific *Gal4*-driver line *Mhc-Gal4* at 18°C restored the synaptic localization of GluR-IID and all other glutamate receptor subunits (not shown; overexpression of GluR-IID cDNA in both wild type and *GluR-IID* null background at 25°C resulted into significant reduction of synaptic glutamate receptor level with abnormal accumulation of GluR-IID proteins within the ER). Thus, the levels of GluR-IID and GluR-IIE within the muscles directly control the overall amount of glutamate receptors that localize at the NMJ.

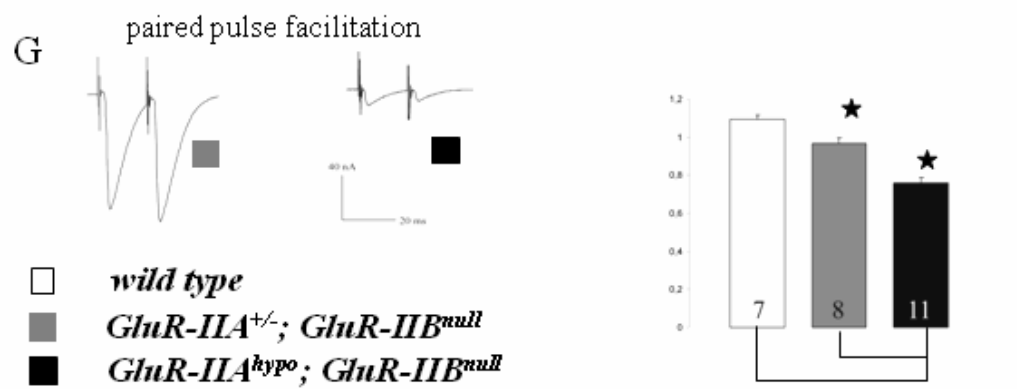
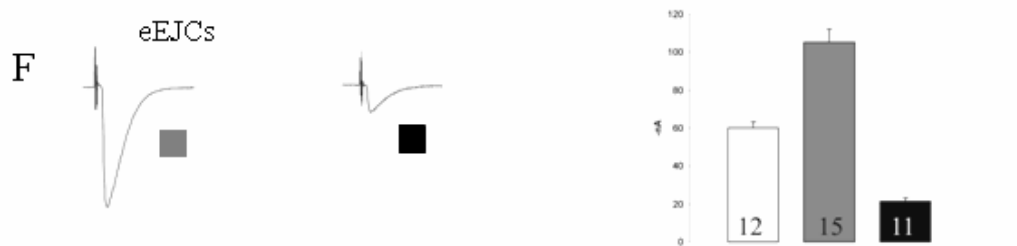
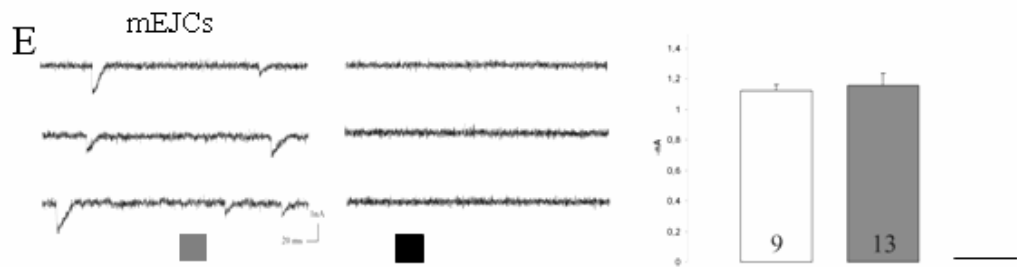
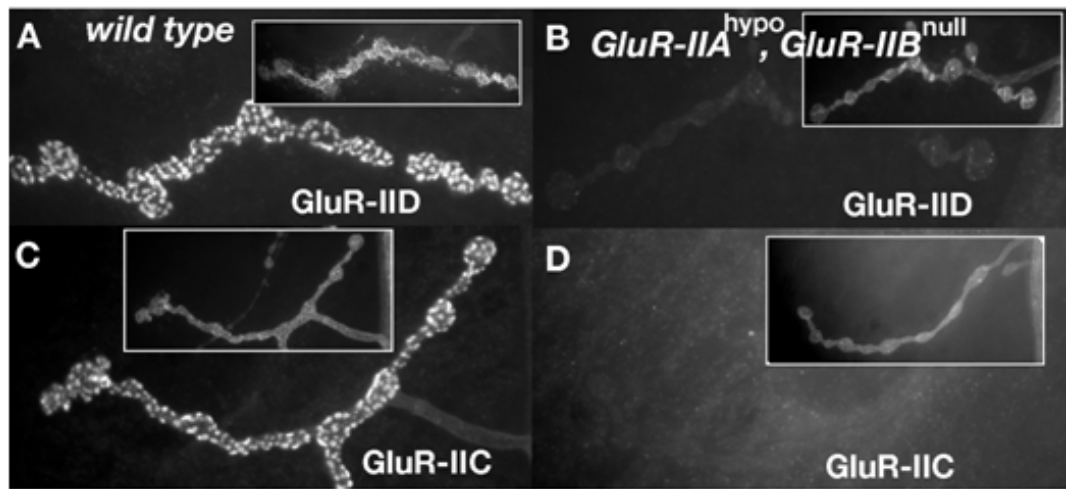
The next question addressed is, whether *vice versa* the amounts of muscle GluR-IIA, -IIB and -IIC/III can control synaptic level of GluR-IID and -IIE. To this end, a genetic situation in which *GluR-IIB* was fully absent and simultaneously *GluR-IIA* was suppressed to dramatically low level (*GluR-IIA^{hypo}*, *GluR-IIB^{null}*, see 2.2.2.1) was used. Previously it has been proposed that local postsynaptic translation plays important roles in controlling the growth and transmission efficacy of synapses at *Drosophila* NMJ. *GluR-IIA* appears might be a substrate under subsynaptic translational control (Sigrist et al., 2000). Since translational control elements often localize within the 3'UTR region of a gene, transgenic flies expressing *GluR-IIA* lacking most 3'UTR were produced and tested for their ability to rescue the *GluR-IIA&IIB* double null mutants, which is

embryonic lethal (Diantonio et al., 1999). Among several independent transgenic lines tested, only one of them could rescue the embryonic lethality with low rate and the rescued larvae were clearly paralyzed. Real-time quantitative PCR assay showed that the *GluR-IIA* message level was below 5% of endogenous level. In accordance with the low message level, the GluR-IIA protein was hardly detectable at the larval NMJ (not shown). Notably, the level of both GluR-IIC/III and GluR-IID were drastically low (Fig.3-7B, D). Collectively, all the above data suggest all essential glutamate receptor subunits together controls receptor formation and proper synaptic localization. Furthermore, this rule seems true for both initial formation and further development of NMJs, where many new synapses get added continuously (Schuster et al., 1996; Gramates and Budnik, 1999).

Fig.3-7 Minimal mounts of GluR-IIA and no- IIB: expression of all glutamate receptor subunits and postsynaptic sensitivity are strongly reduced

(A-D) Shown are 3rd instar larval NMJs (muscle 4, abdominal segment 2) stained for GluR-IID (A, B) or GluR-IIC/III (C, D) in wild type controls (A, C) or in animals having only about 5% GluR-IIA and no GluR-IIB (GluR-IIA_{hypo}, GluR-IIB_{null}, see Material and Methods). NMJ morphology in HRP labeling is shown in insets to allow NMJ visualization independent of receptor label. In GluR-IIA_{hypo}, GluR-IIB_{null} larvae, the synaptic localization of both GluR-IID and GluR-IIC/III is strongly reduced. Apparent differences in between residual GluR-IID and GluR-IIC/III are likely due to slightly different sensitivity of our antibodies.

E-G, Postsynaptic sensitivity is dramatically reduced at larval NMJs of GluR-IIA_{hypo},GluR-IIB_{null} larvae. E, F, Two-electrode voltage-clamp recordings of eEJCs and mEJCs from muscle 6 of abdominal segment A2 and A3. Representative traces of mEJC recordings (E) and average traces of 10 consecutively recorded eEJCs (F) of the indicated genotypes are shown. The mean amplitudes of mEJCs (white bars) are indistinguishable between wild type and GluR-IIA&IIB double mutant larvae rescued with a complete genomic GluR-IIA transgene (exact genotype: *df(2L)clh4, P[GluR-IIAΔ3'UTR] / GluR-IIA&BSP22*). In all muscle cells of GluR-IIA_{hypo},GluR-IIB_{null} larvae, no signs of mEJCs could be recorded despite extensive and sensitive recording. Evoked responses (F) are also dramatically reduced in GluR-IIA_{hypo},GluR-IIB_{null} larvae compared to both control groups. The increase in evoked response in animals rescued with wild type GluR-IIA (and thus without expressing of GluR-IIB) when compared to wild type has been described before (Petersen et al., 1997; DiAntonio et al., 1999). G, Paired pulses (stimulation interval ms) provoke slight facilitation in the controls but depression in GluR-IIA_{hypo},GluR-IIB_{-/-} larvae. Data are derived from the indicated number of cells (number in the column) and represent means ±SEM.



3.4.3 Depriving synaptic glutamate receptor subunits results into dramatic weakness of postsynaptic activity

To test whether the physiological function of glutamate receptor correlates well with its presence at synapse reflected from the above morphological data, electrophysiological analysis is highly necessary. Among the different genetic situations which partially deprive certain glutamate receptor subunits in embryos and larvae, the *GluRIIA^{hypo}*, *GluR-IIB^{null}* larvae maintain the lowest overall level of glutamate receptors (Fig.3-7 B, D) and display clear signs of paralysis. Thus *GluRIIA^{hypo}*, *GluR-IIB^{null}* larvae were subjected to two-electrode-voltage-clamp recordings in collaboration with Robert Kittle (Fig.3-7 E, F). As expected, compared to wild type conditions, spontaneous miniature junctional currents (mEJCs) in these animals were below the detection limit indicating an extreme drop of postsynaptic glutamate receptor function. Accordingly, evoked currents (eEJCs) were also significantly low (*wild type*: 61 nA, n=12, *GluRIIA^{hypo}*, *GluR-IIB^{null}*: 21 nA, n=11; $p < 0.00005$, Mann-Whitney, two-sided non-parametric test).

In conclusion, strongly reducing the expression of a single ‘essential’ glutamate receptor subunit is sufficient in severely downregulating the overall level of functional glutamate receptors at the NMJ, which in turn results into weakening of postsynaptic activity in response to neurotransmitter release.

3.5 Structural role of ionotropic glutamate receptor during pre- and postsynaptic differentiation of neuromuscular synapse

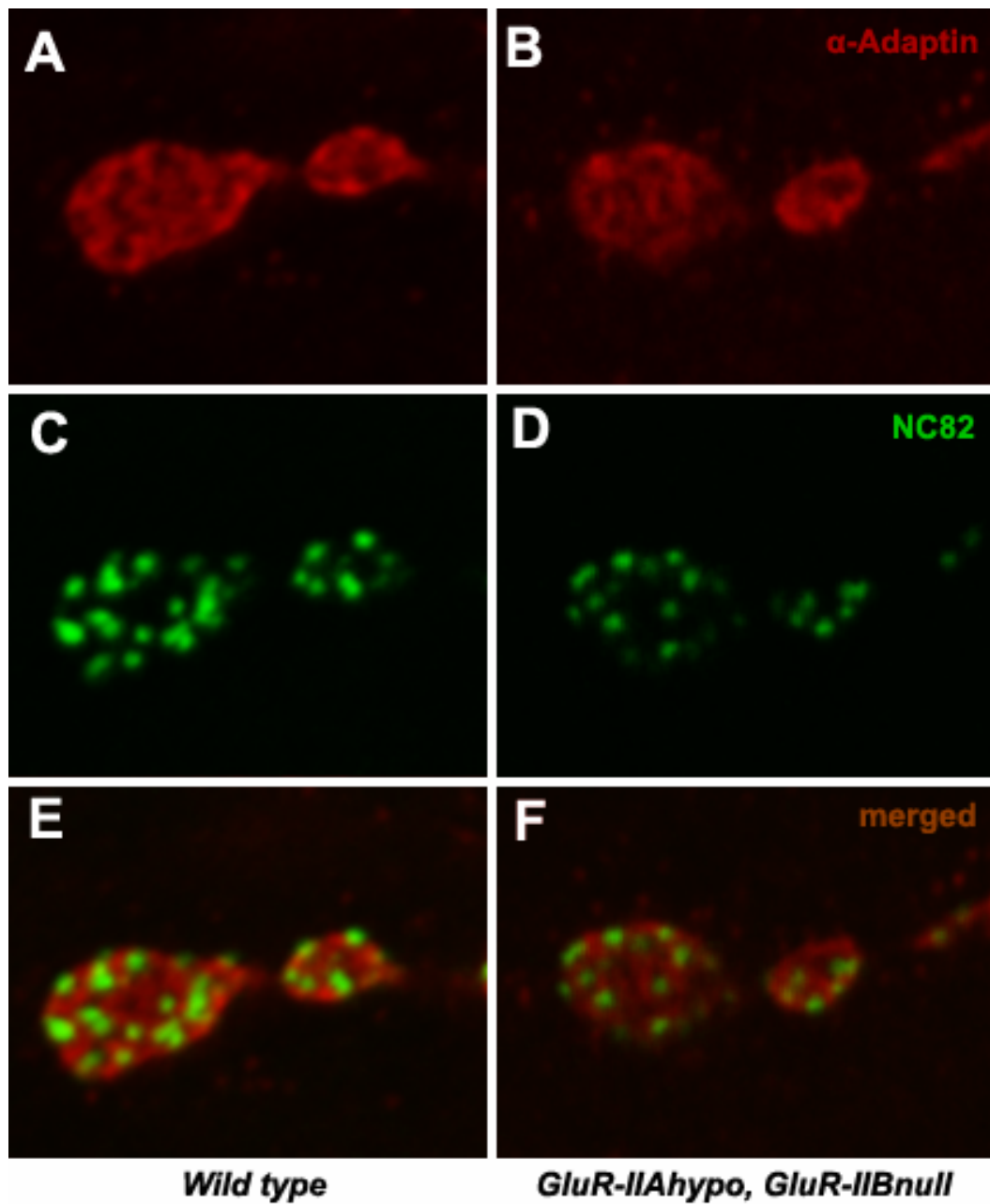
3.5.1 Normal differentiation of presynaptic transmitter release machinery at glutamate receptor deprived synapse

As shown in chapter 3.4, *GluRIIA^{hypo}*, *GluR-IIB^{null}* larval junctions produce evoked currents of about one third of that of wild type junctions. Even more drastically, the spontaneous currents are hardly detectable. We considered the fact that evoked responses appeared less affected than spontaneous responses in

GluRIIA^{hypo}, *GluR-IIB*^{null} larvae as indication of normal or even increased presynaptic transmitter vesicle release as compensation of severe postsynaptic defects. Consistent with the concomitant increase in presynaptic vesicle release, paired pulse stimulation of *GluRIIA*^{hypo}, *GluR-IIB*^{null} NMJ leads to depression of evoked currents while as for wild type controls the currents remain slightly increased in the same condition. The organization of presynaptic release machinery was further characterized morphologically. The active zone is the region of the presynaptic plasma membrane where synaptic vesicles dock, fuse, and release the neurotransmitters (Shapira et al., 2003). Monoclonal antibody NC82 was shown to specifically label the Active zones of synapses of *Drosophila* NMJ (Wucherpfennig et al., 2003) and central synapses (Heimbeck et al., 1999). In *GluRIIA*^{hypo}, *GluR-IIB*^{null} larvae, nc82 labels are clearly present at NMJ with both density and individual size comparable to wild type controls (Fig.3-8 C, D; Fig.3-9 D-E). α -Adaptin is essential for presynaptic endocytosis/vesicle retrieval (Gonzalez-Gaitan and Jackle, 1997) and is restricted to the presynaptic membrane, forming a network-like structure that surrounds the active zones (Gonzalez-Gaitan and Jackle, 1997) (Fig. 3-8 A-C). In *GluRIIA*^{hypo}, *GluR-IIB*^{null} larvae, subcellular distribution of α -Adaptin is not apparently distinct with that of wild type controls (Fig.3-8 A, B), suggesting that the differentiation of presynaptic release apparatus is not affected by depriving postsynaptic glutamate receptor.

Fig. 3-8 Normal organization of presynaptic neurotransmitter release machinery components at glutamate receptor deprived synapses

NMJs double-labeled with the antibodies against presynaptic component α -Adaptin (Gonzalez-Gaintan M et al., 1997; A-B) and Nc82 antibody recognizing an active zone epitope (Wucherpfennig et al., 2003, Heimbeck et al., 1999; C-D). In wild type animals, α -Adaptin is restricted to the presynaptic membrane, forming a network-like structure that surrounds the active zones represented by Nc82 spots (A, C, E). In *GluRIIA*^{hypo}, *GluRIIB*^{-/-} larvae, both Nc82 and α -Adaptin spots appear no different from wild type control (B, D, F).



3.5.2 Defective assembly of PSD specialization at glutamate receptor deprived but not presynaptic neurotransmission activity deprived synapse

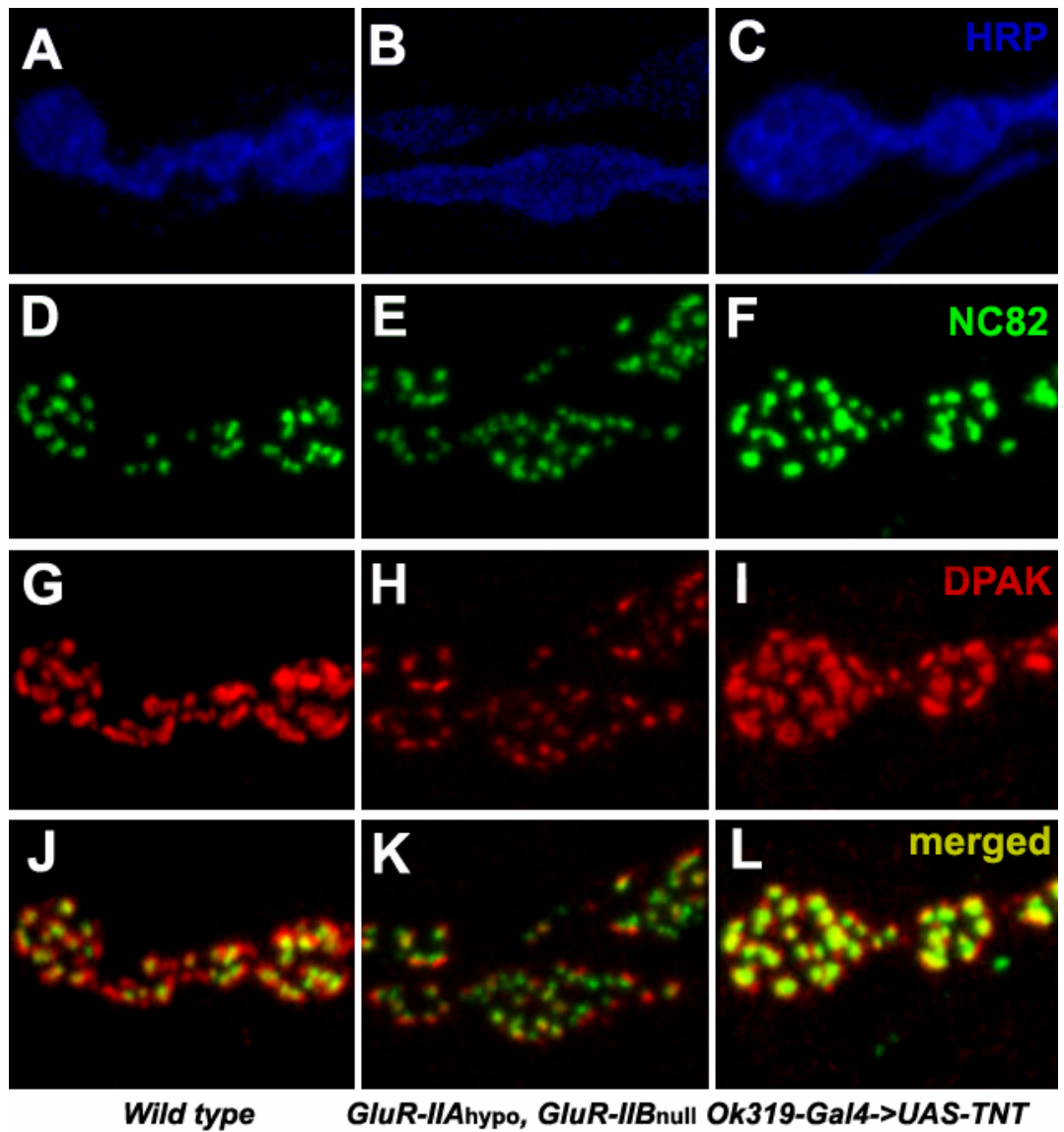
The differentiation of postsynaptic apparatus was also analyzed in *GluRIIA^{hypo}*, *GluR-IIB^{null}* larvae. So far, only a few PSD components have been identified and characterized at *Drosophila* NMJ (Sone et al., 2000; Wan et al.,

2000; Parnas et al., 2001). PAKs are a family of serine/threonine kinases that serve as targets for the small GTP-binding proteins Cdc42 and Rac, they are implicated in modulating the cytoskeleton organization (Bagrodia and Cerione, 1999). In *Drosophila*, dPak has been shown to specifically localize at the PSD of neuromuscular synapse at both immunofluorescence microscopic and immuno-EM level (Sone et al., 2000; Wan et al., 2000). In *dpak* mutants, the levels of DLG and GluRIIA at the synapse are reduced and the SSR folding is also disrupted (Parnas et al., 2001; Albin and Davis, 2004) In wild type larvae, dPAK antibodies labeled the well defined patches with approximately even distribution over the surface of bouton, (Fig. 3-9), and as expected NC82 perfectly colocalized with dPAK staining (Fig.3-9). In *GluRIIA^{hypo}*, *GluRIIB^{null}* bouton, however, the dPAK staining displayed apparently lower density, with the size of individual spots much more diverse---from huge irregular aggregates to tiny dots, and often, at some bouton areas the dPAK even did not aggregate at all but just ‘wrap’ the bouton like cloud, (Fig.3-9 , arrow).

The above data suggest that, when glutamate receptors are deprived from synapse other constitutive components of postsynaptic specialization can not be assembled efficiently. In principle, these defects could be either due to the absence of glutamate receptor *per se* or lack of glutamate mediated transmission activity. To distinguish these possibilities, several genetic situations in which the NMJ transmission was either strongly reduced (survival to larval stage) or

Fig.3-9 Defective PSD assembly at glutamate receptor deprived but not transmission deprived synapses

NMJs triple-labeled with the Nc82 antibody recognizing an active zone epitope (Wucherpfennig et al., 2003, Heimbeck et al., 1999; D-F), antibodies against PSD marker DPAK (Sone et al., 2000; G-I) and HRP (A-C). In wild type animals, Nc82 spots localize at presynaptically juxtaposed to postsynaptic DPAK spots (J). In *GluRIIA^{hypo}*, *GluRIIB^{-/-}* larvae, Nc82 spots localize normally (E), however, DPAK spots display significantly lower density and more variable individual size (H). In *OK319-Gal4->UAS-TNT* larvae, both Nc82 and DPAK spots appear no different from wild type control (F, I, L).



completely suppressed (lethal at late embryonic stage) were analyzed for postsynaptic assembly. Targeted expression of tetanus toxin light chain (TNT) in *Drosophila* neurons completely eliminates evoked, but not spontaneous synaptic vesicle release (Sweeney et al., 1995). When using the motor neuron driver *ok319-Gal4* to drive TNT expression, low number of animals can survive to 3rd instar larval stage (this survival is likely due to the mosaic property of the driver, Cahir O’Kane, personal communication). Surviving larvae were very strongly paralyzed, much stronger than *GluRIIA^{hypo}*, *GluR-IIB^{null}* larvae. However, the distribution of neither postsynaptic components dPAK nor glutamate receptor

show any discernible defects in all the NMJs checked, in contrast they both colocalize well with active zone shown by NC82 staining (Fig.3-9 F, I).

Since the expression of tetanus toxin does not fully eliminate spontaneous synaptic vesicle release (Sweeney et al., 1995), it might be argued that in the above *ok319-Gal4* driven situation remaining activity (especially spontaneous activity) could sufficiently induce the assembly of postsynaptic specializations at normal level. Indeed, recently a tight link between spontaneous vesicle exocytosis and glutamate receptor clustering during *Drosophila* embryonic development has been reported (Saitoe et al., 2001). It should be noted, however, that this report is clearly controversial to some other reports (Broadie et al., 1995; Featherstone et al., 2001). It has been proved previously that, in either null mutants of syntaxin or temperature sensitive allele of dynamin (*shi^{ts1}*) reared at nonpermissive temperature, both spontaneous and evoked vesicle exocytosis and hence synaptic transmission are completely eliminated (Broadie et al., 1995). Using these ‘cleaner’ conditions, the immuno-fluorescence microscopic analysis was performed with our antibodies against GluR-IIC and GluR-IID. In contrast to the findings of Saitoe M et al but consistent with those of Featherstone et al, the glutamate receptor localization within individual PSDs is essentially unaffected as seen in GluR-IIC and GluR-IID staining (Fig.3-10). Moreover, in these animals DPAK proteins also cluster at normal size at the PSD region as evidenced by colocalization with NC82 labels (Fig3-10). Therefore, it is the glutamate receptor per se but not synaptic transmission activity essential for the postsynaptic specialization (including glutamate receptor field) assembly.

Besides the main finding described above, another interesting phenomena found is found. At the NMJs of glutamate receptor deprived larvae (*GluRIIA^{hypo}*, *GluR-IIB^{null}*), often postsynaptic dPAK label was not opposed by presynaptic active zone marker (identified via NC82 staining) (Fig.3-9). One explanation is that these free NC82 labels might represent new synapse growth sites. However,

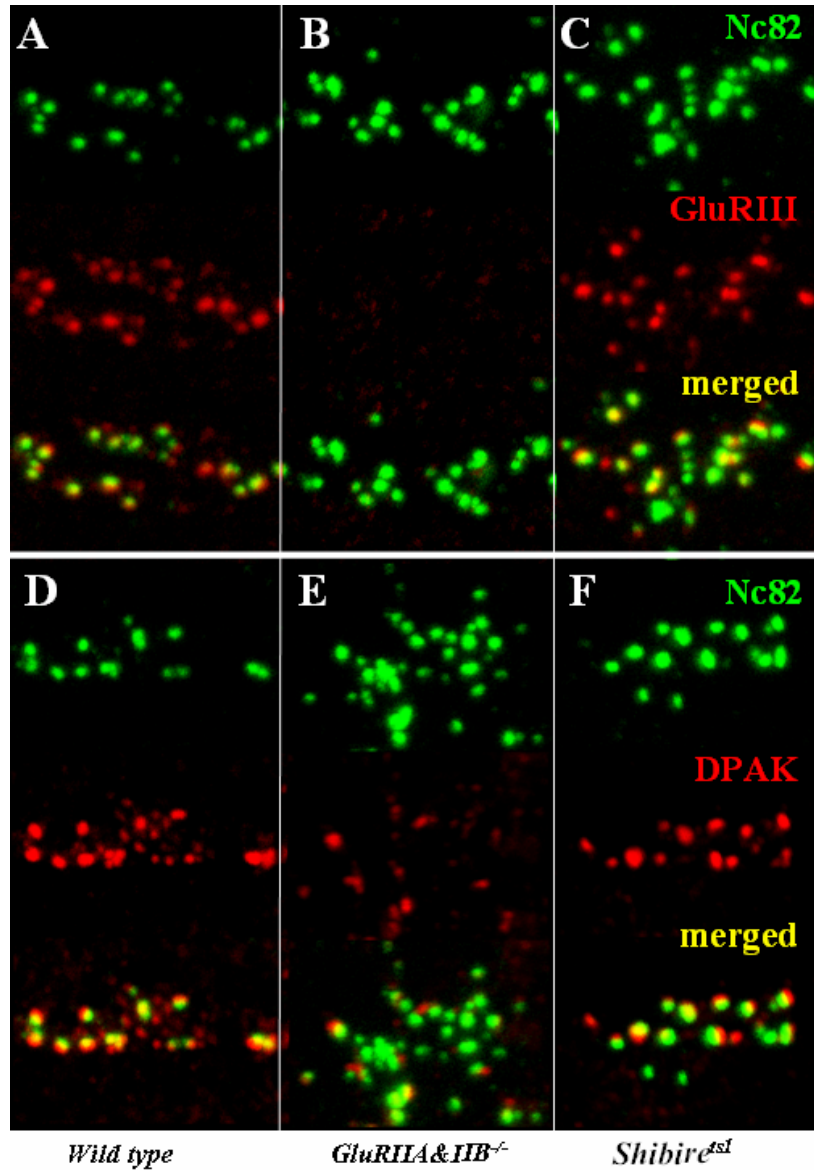
this is quite unlikely since in wild type NMJs stained with same antibodies, the free NC82 labels without aligned dPAK patches were very rarely found (Fig.3-9). Intriguingly, free dPAK labels could be stably detected in wide type NMJs, and in most cases such free dPAK patches are small and localize at the tips of junctions or the linkage regions between boutons, which likely represent the potential growth sites of new synapses. Thus, these free dPAK labels might reflect the precursors of new synapses, which implicates that, in contrast to the finding in synapses of cultured hippocampal neurons, at *Drosophila* NMJ the postsynaptic assembly might precede presynaptic assembly. In *GluRIIA^{hypo}*, *GluR-IIB^{null}* NMJs, the precise coordination of pre- and postsynaptic differentiation is strongly affected. However, it is unlikely that this coordination defect is merely due to absence of glutamate receptor per se, since in embryos with complete loss of presynaptic transmitter release, although individual PSDs are assembled rather normally, there also exist free active zones (Fig.3-10 F). Because the glutamate receptor null mutants lack both glutamate receptor and the concomitant transmission activity, it remains to be further addressed whether the precise coordination of pre- and postsynaptic differentiation is activity-dependant.

Fig. 3-10 Glutamate receptor *per se* but not presynaptic vesicle release are important for proper synapse formation at embryo NMJ

Confocal microscopy on embryonic NMJs (muscle 6 and 7), stained with the synaptic markers in wild type (A-D), in *GluR-IIA&IIB^{-/-}* double mutant embryos (B, E) and in *shibire* temperature sensitive mutant (*shi^{ts1}*) embryos reared at nonpermissive temperature (C, F).

A-C, Embryonic NMJs double labeled with active zone recognizing antibody Nc82, glutamate receptor subunits GluR-IIC/ III. In situation with defective presynaptic release (C), postsynaptic glutamate receptor fields appear identical as in wild type control. As expected, staining for GluR-IIC, which depends on the presence of either GluR-IIA or GluR-IIB expression, is absent from synapses of *dglurIIA&IIB^{-/-}*(B).

D-F, Embryonic NMJs double labeled with the active zone recognizing antibody Nc82 and antibodies against PSD marker DPAK. Wild type embryos show typical DPAK patches juxtaposed to presynaptic Nc82 labels (D). In *GluR-IIA&IIB^{-/-}* and *shibire shi^{ts1}* embryos reared at nonpermissive temperature, Nc82 often is not associated with postsynaptic DPAK spots (E, F), DPAK spots are irregular in size and shape and show lower density in *GluR-IIA&IIB^{-/-}* embryos (E).



3.5.3 Ultrastructural evidence of abnormal synaptic differentiation at glutamate receptor deprived synapse

Next, to check whether such assembly defects of postsynaptic components at glutamate receptor deprived synapse could be directly visualized at the ultrastructural level, neuromuscular junctions 6 and 7 of 3rd instar *GluR-IIA^{hypo}, GluR-IIB^{null}* larvae were subjected to transmission electron microscopy (collaborated with Carolin Wichman). At normal *Drosophila* neuromuscular synapses, active zones are characterized by the presence of

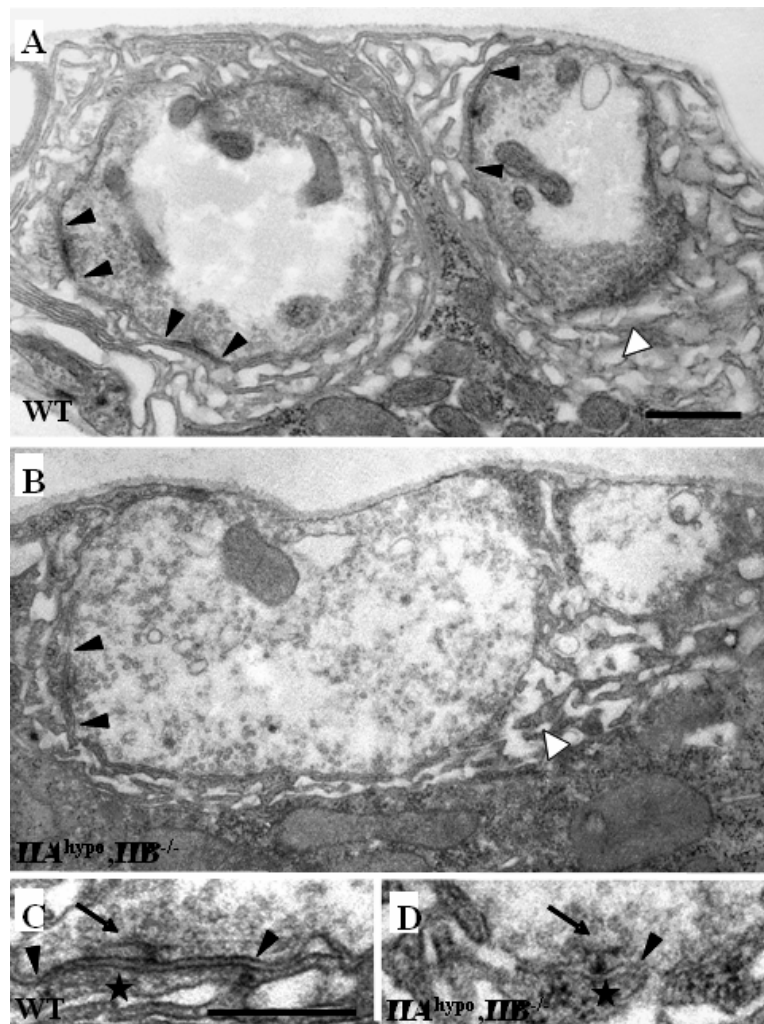


Fig.3-11 Electron microscopy: defective postsynaptic assembly at glutamate receptor deprived synapses

(A) Electron micrograph of type I nerve terminals of NMJ 6/7 in a wild type situation showing several clearly visible electron dense synapses (black arrowheads) and the SSR (white arrowhead). The synaptic vesicles are arranged along the presynaptic membrane. (B) *GluRIIA^{hypo},GluRIIB^{-/-}* type 1b bouton of NMJ 6/7, respectively. The black arrowheads indicate a mutant, clearly electron translucent synapses decorated with a T-bar. The SSR (white arrowhead) is significantly reduced. (C, D) Synaptic sites in wild type (C) and *GluRIIA^{hypo},GluRIIB^{-/-}* (D) larvae. The electron dense T-bars are indicated by arrows. The PSD, in wild type detectable as electron dense material (C, asterisk) is in *GluRIIA^{hypo},GluRIIB^{-/-}* synapses absent (D, asterisk) or in less frequent weaker cases dramatically reduced (not shown). In *GluRIIA^{hypo},GluRIIB^{-/-}* synapses the lack of PSD organization also affects the close alignment of the pre- and postsynaptic membranes, which usually extends over several 100 nm (C, arrowheads). In *GluRIIA^{hypo},GluRIIB^{-/-}* larvae this alignment is severely defective and the SSR formation already begins in direct vicinity to the T-bar (D, arrowhead) or extends asymmetrically.

electron-dense T-shaped structures called ‘T-bars’ at the presynaptic side (Wojtowicz et al., 1994; Cooper et al., 1995; Cooper et al., 1996). PSDs are opposite to the T-bars and easily recognized by electron dense linear membrane-membrane appositions (Fig.3-11), a characteristic structure also found in mammalian CNS glutamatergic synapses. Within the PSD region, pre- and postsynaptic membrane associate closely with each other and are visualized as linear apposition in cross section (Fig.3-11). At most synaptic sites, the PSD diameter clearly exceeds the diameter of the presynaptic T-bar. In region between individual PSDs (so called “perisynaptic region”), pre- and postsynaptic membrane (motorneuron and muscle membrane) are organized into various in-foldings and associate only at restricted contact points. This structure is continuous with the subsynaptic reticulum (SSR).

In *GluR-IIA^{hypo},GluR-IIB^{null}* larvae, apparently normal presynaptic T-bars were observed in boutons. However, PSD organization is severely defective (Fig.3-11) in these animals: the muscle membrane domains juxtaposed to the presynaptic T-bars, where typically PSDs should be formed, show very low amount or even complete absence of electron dense material (Fig. 3-11 D). Moreover, the typical extended and close alignment between pre- and postsynaptic membranes could not be found from *GluRIIA^{hypo},GluRIIB^{null}* larvae, in which with only significantly narrower and “wrinkled” apposition of membranes observed (Fig3-11 D). Thus, the ultrastructural analysis directly shows that in the absence of glutamate receptors, the PSD can not be efficiently assembled. In contrast, in the *dpak* mutants, despite the dramatic reduction of SSR foldings, the ultrastructure of individual synapse appeared rather normal, with smooth electron dense thickening at PSD region (Parnas et al., 2001). Rather normal ultrastructural active zone and PSD assembly was also found in embryos with neuronal TNT expression or lack of Syntaxin (Broadie et al., 1995). In combination of all these data, it is the glutamate receptor per se, obviously independent of transmission activity, controls the normal PSD assembly.

3.5.4 Defective compartmentation of the synaptic and perisynaptic zones at glutamate receptor deprived but not neurotransmission deprived synapse

The ultrastructural analysis showed that the close apposition in between pre- and postsynaptic membrane is largely abolished after reducing glutamate receptor level. It is thus interesting to know, whether the strong defects in ultrastructural PSD organization at glutamate receptor deprived synapses might also reflect defects in the molecular organization of synaptic compartments. Therefore, to address this issue, the *GluRIIA^{hypo},GluRIIB^{null}* larval NMJs were further investigated by antibody staining against compartment specific marker molecules. At normal *Drosophila* NMJ boutons, individual synapses are separated and surrounded by so called “perisynaptic” or “periaxial zone” compartment (Sone et al., 2000; Sigrist et al., 2002), characterized by the presence of various molecular markers such as Fasciclin II (FasII) and Disc Large (Dlg). FasII is one NCAM-related cell adhesion molecule involved in synaptic growth, stabilization and structural plasticity (Shuster et al., 1996). DLG is the *Drosophila* PSD95 homologue, it belongs to the membrane-associated guanylate kinase homologs (MAGUKs) family and is generally involved in synaptic clustering of various molecules such as potassium channel Shaker and FasII through the PDZ domains mediated interactions (Tejedor et al., 1997; Thomas et al., 1997; Zito et al., 1997). As reported previously, in wild type controls both FasII and DLG label the boutons in a characterized network pattern, which is clearly complementary with dPAK staining (Fig.3-12 A, D). Since normally presynaptic active zone is always precisely aligned with DPAK as evidenced by NC82 and DPAK double staining (see Fig.3-9), the perisynaptic components such as FasII and DLG clearly decorate the synaptic region.

At *GluRIIA^{hypo},GluRIIB^{null}* boutons, both FasII and DLG staining appear reduced and lose the typical network pattern, in contrast, they are distributed almost evenly throughout boutons (Fig.3-12 B, E). Notably, this homogeneous distribution pattern of Fas II and DLG indicates the intrusion of perisynaptic

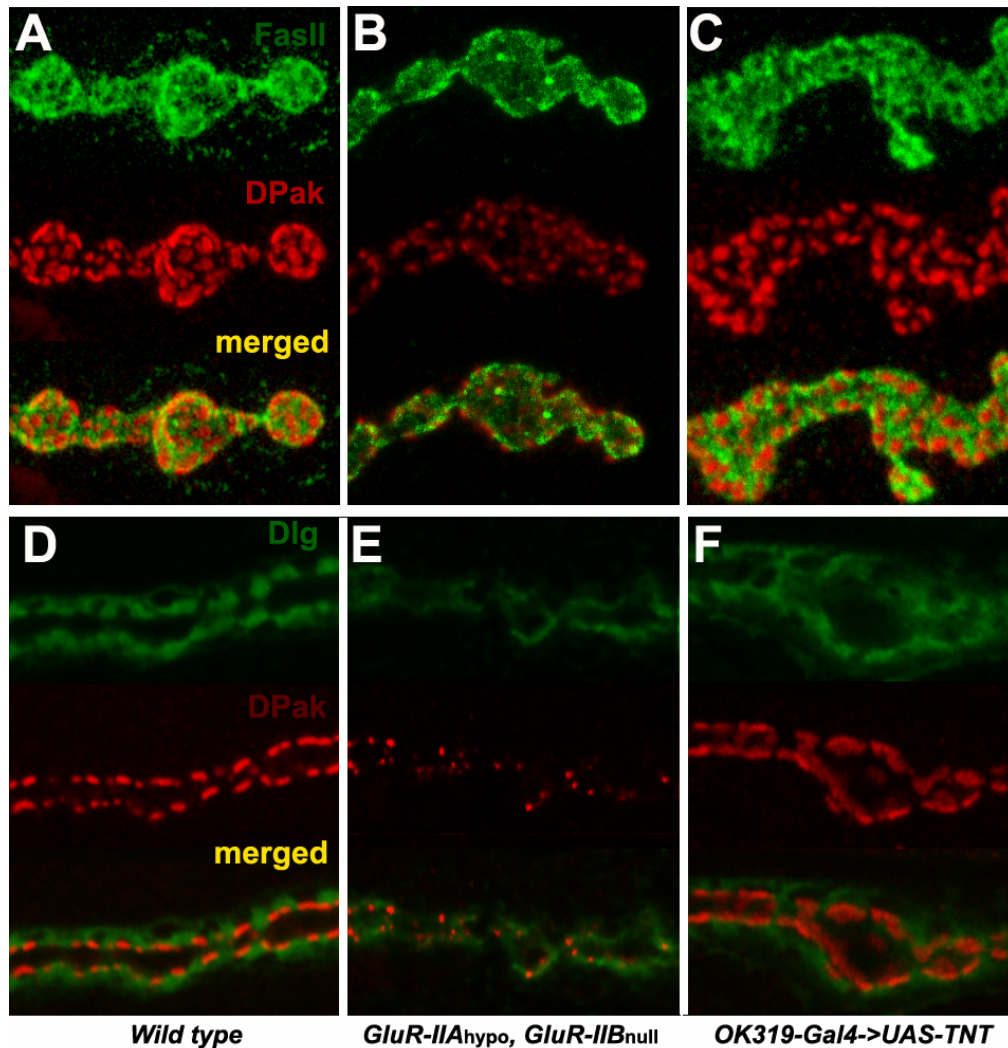


Fig.3-12 Defective synaptic compartments at glutamate receptor deprived but not neurotransmission deprived synapses

Confocal microscopy on NMJs of mid 3rd instar larvae at muscle 4, stained with compartment specific antibodies in wild type (A, D), *GluRIIA^{hypo}, GluRIIB^{-/-}* larvae (B, E) and animals with presynaptic expression of Tetanus-toxin light chain (*OK319-Gal4->UAS-TNT*, Sweeney, et al., 1995) (C, F).

A-C, NMJs double labeled with FASII together with DPAK. In wild type animals, FasII shows typical perisynaptic distribution surrounding individual PSDs which are marked by DPAK expression (A). In *GluRIIA^{hypo}, GluRIIB^{-/-}* larvae, FasII show rather even distribution over the whole bouton (B), DPAK spots display significantly lower density and more variable individual size (B). In *OK319-Gal4->UAS-TNT* larvae, both FasII and DPAK show normal distribution (C).

D-F, single cross section image of larval NMJs double labeled with DLG and DPAK. In wild type animals, DLG shows typical perisynaptic distribution surrounding individual PSDs which are marked by DPAK expression (D). In *GluRIIA^{hypo}, GluRIIB^{-/-}* larvae, DLG show rather even distribution over the whole bouton surface thus invade the synaptic area (E), DPAK spots display significantly lower density and more variable individual size and overlay with DLG labels (E). In *OK319-Gal4->UAS-TNT* larvae, both DLG and DPAK show normal distribution (F).

components into the synaptic/ active zone region, thus destroying the compartmentation of synaptic and perisynaptic area in boutons. Concerning the still rather normal localization of active zones within these boutons, clearly the major driving force to prevent perisynaptic components entering synaptic area comes from the efficiently assembled PSDs, glutamate receptors play either direct or indirect roles in this process.

3.5.5 Similar defects in synaptic differentiation in the complete absence of glutamate receptors

The above studies using glutamate receptor largely deprived larvae strongly support the structural role of glutamate receptor in organizing synaptic differentiation. To further confirm this finding, analysis on synapses with complete loss of all glutamate receptors is needed. To this end, the *GluR-IIA&IIB* double null mutant background was used. At late stage embryos of this mutant, none of any known muscle glutamate receptor subunits can be detected at NMJs (Fig.3-5 B; Fig.3-10). In consistent with the result obtained from *GluRIIA^{hypo},GluRIIB^{null}* larvae, although the active zone localize normally at the presynaptic terminal, much fewer amount of assemble dPAK aggregates are present at junctions compared to control conditions (Fig.3-10 E).

4 Discussion

4.1 Genomic tools could speed up identifying essential genes involved in synapse formation and modulation

Drosophila has long been an excellent model organism due to the availability of well established, classical genetic tools. With the recent release of the whole *Drosophila* genome sequence information and development of systematic functional genomic research tools, reverse genetics has further strengthened the power of this model organism. Recently genomic scale microarray screening has been stably applied to a wide range of studies to obtain molecular insights or identify novel relevant components of complicated regulatory processes (Furlong et al., 2001; Stathopoulos and Levine, 2002; Butler et al., 2003; Li and White, 2003).

Here, to screen genes relevant to synapse formation and growth control at whole genome scale, the microarray technique was applied to the *Drosophila* model synapse system, the NMJ. Thus, the *Drosophila* body wall filets which mainly consist of somatic muscles were sampled and the RNAs were extracted. Tissue specific RNA profiling was performed and pools of genes (about 700) with specific or enriched expression in postsynaptic muscles were obtained. These genes represent wide variety of functional groups, including enzymes, signal transduction components, receptors and ion channels, cell adhesion molecules, transcriptional factors, RNA-binding proteins, structural proteins and so on. Among them, some are previously already shown to be specifically or abundantly expressed within muscle cells, indicating that our strategy is absolutely feasible and the gene chip methodology is highly reliable. Notably, a large body of genes within the pools are not characterized yet, thus the challenge will be to study their functional significance in high-throughput way. To this end, the application of RNA interference (RNAi) will be the best choice since recently *Drosophila* whole genomic RNAi has been set up by various labs and proved to be very efficient assay (Kiger et al., 2003; Kim et al., 2004).

Undoubtedly, the microarray oriented reverse genetics platform can well complement the classical genetic screening based strategy and their application into neuronal system will greatly enhance our precise understanding of molecular details related to synapse construction and modulation. The main part of this thesis work is studying the molecular behaviors of glutamate receptor subunits, which is originated from the microarray screening and thus provide direct proof of its value.

4.2 GluR-IID and GluR-IIE are novel glutamate receptor subunits crucial for glutamate receptor assembly and thus neurotransmission at neuromuscular synapse

The glutamatergic neuromuscular synapses of *Drosophila*, rather similar to the excitatory CNS synapses of vertebrate brain in terms of ultrastructure and molecular composition, have been intensely utilized to investigate synaptic function *in vivo* capitalizing on the efficient genetics and superb experimental accessibility of this model system. At neuromuscular synapses three non-NMDA type glutamate receptor subunits (GluR-IIA, -IIB, -IIC/III) have been described previously. While only *GluR-IIA&IIB* double null mutants but not either single null mutants completely lack neurotransmission (Petersen et al., 1997; DiAntonio et al., 1999), lack of GluRIIC/ III alone is fatal with a phenotype consistent with the absence of neurotransmission at neuromuscular synapses (Marrus et al., 2004). The full picture of subunit composition of synaptic glutamate receptors at the NMJ still remains elusive.

Here via the genomic scale microarray screening, I report the identification of two additional non-NMDA glutamate receptor subunits, GluR-IID and GluR-IIE, which are proved to be specifically localized at the postsynaptic site of all neuromuscular synapses. Interestingly, while GluR-IID and GluR-IIE are genomic neighbors and very similar to each other, they are not particularly close to GluR-IIA, -IIB and -IIC/III. Specific null mutants for both *GluR-IID* and *GluR-IIE* have been obtained to further functional characterization. While both

GluR-IID and *GluR-IIE* null embryos still fully develop, they do not hatch and are incapable of performing any coordinated movement. Consistent with my finding, via embryonic electrophysiological recording, Featherstone et al. have recently demonstrated that no postsynaptic sensitivity to glutamate was detected at the embryonic muscles of one independent *GluR-IID* null mutant allele (personal communication). Thus, *GluR-IID* and *GluR-IIE* appear critically important for mediating glutamate-gated ionic currents at the postsynaptic site of neuromuscular synapses. Since in the case of *GluR-IIA&IIB* double as well as the *GluR-IIC/III* single mutant background the same paralysis phenotype was found, it is therefore most likely, that they also lack any glutamate gated ionic current.

Taken together, lack of either *GluR-IIC/III*, *-IID*, *-IIE* or both *-IIA* and *-IIB* leads to total loss of glutamate receptor function at the embryonic NMJ. The following evidences support that this is directly due to the loss of the respective glutamate receptor subunits hence all the functional glutamate receptors *within* the embryonic muscles. Firstly, despite the fact that *GluR-IID* is also present in cardio-precursor cells, the expression of *GluR-IIA*, *-IIB*, *-IIC/III* and *-IIE* is most likely restricted to the somatic muscles (Petersen et al., 1997; DiAntonio et al., 1999; Fig.3-1). Secondly, the paralysis phenotype of all these null mutants could always be fully rescued by a muscle-specific re-expression of the corresponding cDNAs (DiAntonio et al., 1999; Marrus et al., 2004; 3.4). Thirdly, muscle-specific down-regulation of *GluR-IIE* via RNA interference could effectively down-regulate synaptic expression of *GluR-IID*, *-IIA*, *-IIB* and *-IIC/III* as well. Last, in each of these null mutants, all of the other subunits are also completely absent at NMJ. Thus clearly, lack of any essential glutamate receptor subunits within the postsynaptic muscle cells will result into a complete loss of all glutamate receptors, which is the direct cause of embryonic paralysis.

4.3 Implications in the in vivo stoichiometry of *Drosophila* glutamate receptor based on genetic analysis

Several recent studies have suggested that the mammalian ionotropic glutamate receptors form as a tetramer of subunits (Kuusinen A et al., 1999; Rosenmund C et al., 1998; Laube B et al., 1998; Mano I et al., 1998; Safferling M et al., 2001). At the *Drosophila* Neuromuscular synapses, the synaptic expression of all glutamate receptor subunits is completely abolished after eliminating either *GluR-IID* or *IIE* alone or *GluR-IIA* and *IIB* together (Fig. 3-5), clearly indicating that essential glutamate receptor subunits (GluR-IIC/III, -IID and -IIE) are obligatory part of all postsynaptic glutamate receptors. In addition, the presence of either GluRIIA or GluR-IIB seems obligate for receptor formation as well. One likely scenario therefore is that the glutamate receptor population at the *Drosophila* NMJ is a mix of (IIA)(IIC/III)(IID)(IIE) receptors with (IIB)(IIC/III)(IID)(IIE) receptors. However, since the current tetrameric structure model of ionotropic glutamate receptors was suggested solely on the basis of either electrophysiological and biochemical studies in heterologous system or crystal structure analysis of ligand-binding domains, an unequivocal determination of the stoichiometry of functional glutamate receptor thus still awaits efficient method that reliably resolve the structure of the endogenous receptor itself. In theory, as was proposed in the past (Premkumar et al., 1997), pentameric (or higher) stoichiometry still cannot be totally excluded in the moment. Therefore, stoichiometry as (A)₂(C)(D)(E), (B)₂(C)(D)(E) or (A)(B)(C)(D)(E) still need to be considered.

Previous studies have established that GluR-IIA- and GluR-IIB-containing receptors differ strongly in their biophysical properties, with GluR-IIA-containing receptors showing slow desensitization kinetics and GluR-IIB-containing receptors showing fast desensitization kinetics (DiAntonio et al., 1999). Thus, GluR-IIA and GluR-IIB containing complexes are likely to play different roles in synaptic function and development. Accordingly, it has

been recently found that, increased postsynaptic GluR-IIA level or reduced GluR-IIB gene dosage results into an increased strength of NMJ transmission and an addition of boutons harboring increased numbers of synapses; this phenotypes were suppressed by overexpression of GluR-IIB (Sigrist et al., 2002). Thus, GluR-IIC/III, IID and IIE might establish a “receptor assembly platform” where the incorporation of either the GluR-IIA or the GluR-IIB subunit could determine the specific functions of the respective glutamate receptor.

As discussed above, the interdependency between all essential subunits observed for synaptic localization is easiest explained by assuming the existence of common glutamate receptor. Another possibility might be that eliminating a certain glutamate receptor subunit could provoke an early defect during the developmental set up of neuromuscular synapses, which in turn might interfere with the localization of other glutamate receptor complexes. This way, the genetic elimination of a certain subunit could also cause the loss of synaptic expression (and thus also synaptic function) of another subunit even if these two subunits would not be coassembled in the same glutamate receptor complex. At this juncture, such a scenario appears unlikely because of the following reasons. First, partial suppression of any essential glutamate receptor subunit always provokes a corresponding down-regulation of other essential glutamate receptor subunits at larval neuromuscular synapses (Fig.3-6 and 3-7; Marrus et al., 2004). This suggests that all essential subunits obey a tight stoichiometric relationship, where the availability of the least abundant subunit defines the overall amount of glutamate receptors, and that this relation exists throughout development. Secondly, Featherstone et al. have convincingly demonstrated a *complete* loss of glutamate mediated currents on embryonic muscle surfaces of one independent *GluR-IID* null mutant allele (Featherstone D et al., personal communication). In contrast, extrasynaptic glutamate receptor mediated currents have been stably detected on wild type embryonic muscle membranes using the same experimental settings (Broadie and Bate, 1993; Featherstone et al., personal

communication). Thus, elimination of GluR-IIID abolishes not only synaptic but also extrasynaptic populations of glutamate receptors on embryonic muscles. Therefore, if interaction between independently forming glutamate receptors is involved in their proper targeting, it would have to be absolutely essential already during the intracellular transport and insertion of glutamate receptors. Since all known muscle receptor subunits from GluR-IIA to GluR-IIID (GluR-IIIE also quite likely the case as evidenced by EGFP fusion protein distribution) are clearly expressed in substantial amounts within postsynaptic densities, the existence of subunits evolved only to mediate the intracellular transport or assembly of glutamate receptor complexes appears rather unlikely unless it was omitted from the Gene chip analysis.

Collectively, the *in vivo* data presented here clearly favor the notion that, at *Drosophila* neuromuscular synapses the functional glutamate receptors can be composed of four different subunits. To our knowledge, a “strictly hetero-tetrameric stoichiometry” has so far not been described for other types of ionotropic glutamate receptors in all model synapses. This finding thus potentially reveal that, apart from our current understanding on glutamate receptor behavior mainly based on heterologous studies, the *in vivo* glutamate receptors might have a rather fixed stoichiometry, which is reminiscent of that of other types of ligand-gated ion channels such as the nicotinic acetylcholine receptor (Colquhoun and Sivilotti, 2004).

4.4 Structural role of ionotropic glutamate receptor per se in organizing synaptic assembly

In the brain, huge amount of neurons are precisely connected via synapses, which display respectively characteristic structural properties at both pre and postsynaptic sides. Most excitatory synapses are glutamatergic, and their initial formation, stabilization, and elimination are under strict control all the time. Moreover, the local changes in synapse strength are proposed to be relevant to

the process of learning and memory. Apparently, it is of great importance to understand how the original synaptic contact is initiated at the proper site and how exquisite coordination of presynaptic and postsynaptic development is accomplished. Although up to now great efforts have been devoted in these directions with more and more synaptic components identified and characterized, still the molecular details driving synaptic assembly remain elusive.

At central excitatory synapses, synaptic transmission is mediated by various ionotropic glutamate receptors including AMPA, kainite and NMDA subfamilies. Recent work has revealed that certain classes of AMPA receptors recycle rapidly at the synaptic sites, suggesting that placeholders or 'slots' might be brought to, or assembled at the postsynaptic membrane with *de novo* insertion of AMPA receptors. The molecular identity of the slots is unknown, but is likely to involve one or more receptor-binding or scaffolding proteins (Barry and Ziff, 2002).

Taking the advantages of the powerful *Drosophila* genetic tools and the rather simpler architecture of NMJ, the consequences of losing synaptic glutamate receptor partially or completely *in vivo* were investigated. Despite the rather normal differentiation of transmitter release machinery at the presynaptic membrane, which is consistent with previous findings that the presynaptic differentiation can undergo at the nerve terminal even without contact with the postsynaptic cell (Prokop et al., 1996), the postsynaptic assembly is apparently deficient, as evidenced by not only inefficient clustering of other PSD component (dPAK) but also the intrusion of perisynaptic components (FASII and DLG) into synaptic (active zone) territory. PAK is known to regulate cytoskeleton dynamics, the cytoskeleton organization is crucial for the clustering of synaptic components and /or maintaining the synaptic structure at diverse types of synapses (Kirsch and Betz, 1995; Allison et al., 1998; Dai et al., 2000; Hirai, 2000). Recently it has been proposed that dPAK is important in

clustering glutamate receptors at *Drosophila* NMJ since in *dpak* hypomorphic mutant animals, glutamate receptor subunit GluR-IIA is significantly reduced but still localize normally at synapses (Parnas et al., 2001). Interestingly, the data presented here indicate that proper aggregation and synaptic distribution of dPAK is definitely dependant on the availability of glutamate receptors; with glutamate receptors depleted the dPAK is no longer able to cluster and localize properly. At mammalian neuromuscular synapse it has been shown that agrin-mediated clustering of AchR is mediated by the corporation of various signaling pathways: first the activation of Rac/ Cdc42, leading to formation of AchR microclusters, followed by Rho activation, resulting into combining these microclusters into larger clusters (Weston C et al., 2003). DPAK does not necessarily need to interact directly with glutamate receptors, but via various direct and indirect interactions glutamate receptors might be able to recruit various PSD components (including dPAK, other signaling molecules and scaffold proteins) during synaptogenesis, as soon as these components are recruited together, the relevant signaling cascades are efficiently activated and thus trigger the membrane and cytoskeleton remodeling which finally results into the stable development of mature synaptic structure; in depletion of glutamate receptors, either the dPAK signaling cascade is not efficiently activated to reorganize actin cytoskeleton essential for proper clustering, or activating dPAK cascade along is not sufficient for effective PSD components clustering and maintaining. Currently, it remains elusive whether other signaling pathways are involved in PSD formation, but based on the clear defects in synaptic compartmentation that perisynaptic components intrude into synaptic region, the cytoskeleton organization must have been improperly regulated. This notion is also supported from ultrastructural analysis, the electron dense material typical present at the PSD region is essentially absent from glutamate receptor deprived synapses, implicating that the components of postsynaptic scaffold are either not recruited together at all or no longer stable without the integration of glutamate receptors. Interestingly, at the neuromuscular synapses of *dpak* hypomorphic mutant, despite much fewer SSR, the ultrastructure of

both PSD and active zone appears quite normal, further supporting the relatively minor role of dPAK in postsynaptic differentiation. Notably, the role of glutamate receptor in synaptic development was shown not to be relevant to its ion channel activity, since in all the backgrounds tested which deprive presynaptic neurotransmitter release (partially or completely), the glutamate receptor can be clustered as effectively as wild type control. Correspondingly, the postsynaptic reception apparatus in these transmission depleted conditions appear functional since responses can be stably detected when applying glutamate at junctions (Broadie, 1996).

Another interesting phenomena at glutamate receptor deprived synapse is that the number of presynaptic specializations exceeds postsynaptic ones, thus resulting into free active zones without postsynaptic partners, which is hardly found in normal conditions. In principle, this can be due to either lack of glutamate receptor per se, or that of the transmission activity. The latter idea appears more likely since in complete transmitter release deficient situations, free active zones were also observed although certain levels of PSDs (glutamate receptor fields) were assembled normally.

In conclusion, apart from functioning as ligand-gated ion channel, the glutamate receptor at *Drosophila* NMJ also plays crucial role in organizing and /or maintaining the synaptic architecture, which is reminiscent of AchR at vertebrate NMJ (Ono F et al., 2001; Marangi PA et al., 2001; Missias AC et al., 1997) and glycin and GABA receptor at mammalian central synapses (Essrich et al., 1998). In mammalian CNS synapses similar roles of ionotropic glutamate receptors have not been reported, mainly due to the fact that there exist highly divergent classes of glutamate receptors at central synapses and each type of receptors play distinct roles, therefore it is not easy to obtain a condition with all types of glutamate receptors removed together.

Reference

- Aberle H, Haghighi AP, Fetter RD, McCabe BD, Magalhaes TR, Goodman CS (2002) wishful thinking encodes a BMP type II receptor that regulates synaptic growth in *Drosophila*. *Neuron* 33:545-558.
- Ahmari SE, Buchanan J, Smith SJ (2000) Assembly of presynaptic active zones from cytoplasmic transport packets. *Nat Neurosci* 3:445-451.
- Albin SD, Davis GW (2004) Coordinating structural and functional synapse development: postsynaptic p21-activated kinase independently specifies glutamate receptor abundance and postsynaptic morphology. *J Neurosci* 24:6871-6879.
- Allison DW, Gelfand VI, Spector I, Craig AM (1998) Role of actin in anchoring postsynaptic receptors in cultured hippocampal neurons: differential attachment of NMDA versus AMPA receptors. *J Neurosci* 18:2423-2436.
- Apel ED, Glass DJ, Moscoso LM, Yancopoulos GD, Sanes JR (1997) Rapsyn is required for MuSK signaling and recruits synaptic components to a MuSK-containing scaffold. *Neuron* 18:623-635.
- Aplin AE, Howe A, Alahari SK, Juliano RL (1998) Signal transduction and signal modulation by cell adhesion receptors: the role of integrins, cadherins, immunoglobulin-cell adhesion molecules, and selectins. *Pharmacol Rev* 50:197-263.
- Atwood HL, Govind CK, Wu CF (1993) Differential ultrastructure of synaptic terminals on ventral longitudinal abdominal muscles in *Drosophila* larvae. *J Neurobiol* 24:1008-1024.
- Auld VJ, Fetter RD, Broadie K, Goodman CS (1995) Gliotactin, a novel transmembrane protein on peripheral glia, is required to form the blood-nerve barrier in *Drosophila*. *Cell* 81:757-767.
- Ayalon G, Stern-Bach Y (2001) Functional assembly of AMPA and kainate receptors is mediated by several discrete protein-protein interactions. *Neuron* 31:103-113.
- Bagrodia S, Cerione RA (1999) Pak to the future. *Trends Cell Biol* 9:350-355.
- Barry MF, Ziff EB (2002) Receptor trafficking and the plasticity of excitatory synapses. *Curr Opin Neurobiol* 12:279-286.
- Bate M, Broadie K (1995) Wiring by fly: the neuromuscular system of the *Drosophila* embryo. *Neuron* 15:513-525.
- Benson DL, Colman DR, Huntley GW (2001) Molecules, maps and synapse specificity. *Nat Rev Neurosci* 2:899-909.
- Biederer T, Sara Y, Mozhayeva M, Atasoy D, Liu X, Kavalali ET, Sudhof TC (2002) SynCAM, a synaptic adhesion molecule that drives synapse assembly. *Science* 297:1525-1531.
- Bloch RJ, Pumplin DW (1988) Molecular events in synaptogenesis: nerve-muscle adhesion and postsynaptic differentiation. *Am J Physiol* 254:C345-364.
- Boutanaev AM, Kalmykova AI, Shevelyov YY, Nurminsky DI (2002) Large clusters of co-expressed genes in the *Drosophila* genome. *Nature* 420:666-669.
- Bowe MA, Fallon JR (1995) The role of agrin in synapse formation. *Annu Rev Neurosci* 18:443-462.
- Brand AH, Perrimon N (1993) Targeted gene expression as a means of altering cell fates and generating dominant phenotypes. *Development* 118:401-415.
- Bresler T, Ramati Y, Zamorano PL, Zhai R, Garner CC, Ziv NE (2001) The dynamics of SAP90/PSD-95 recruitment to new synaptic junctions. *Mol Cell Neurosci* 18:149-167.
- Bresler T, Shapira M, Boeckers T, Dresbach T, Futter M, Garner CC, Rosenblum K, Gundelfinger ED, Ziv NE (2004) Postsynaptic density assembly is fundamentally different from presynaptic active zone assembly. *J Neurosci* 24:1507-1520.
- Broadie K, Bate M (1993) Activity-dependent development of the neuromuscular synapse during *Drosophila* embryogenesis. *Neuron* 11:607-619.
- Broadie K, Bate M (1993) Innervation directs receptor synthesis and localization in *Drosophila* embryo synaptogenesis. *Nature* 361:350-353.
- Broadie K, Prokop A, Bellen HJ, O'Kane CJ, Schulze KL, Sweeney ST (1995) Syntaxin and synaptobrevin function downstream of vesicle docking in *Drosophila*. *Neuron* 15:663-673.
- Broadie KS (1996) Regulation of the synaptic vesicle cycle in *Drosophila*. *Biochem Soc Trans* 24:639-645.
- Budnik V, Koh YH, Guan B, Hartmann B, Hough C, Woods D, Gorczyca M (1996) Regulation of

- synapse structure and function by the *Drosophila* tumor suppressor gene dlg. *Neuron* 17:627-640.
- Burden SJ (1998) The formation of neuromuscular synapses. *Genes Dev* 12:133-148.
- Burnashev N, Khodorova A, Jonas P, Helm PJ, Wisden W, Monyer H, Seeburg PH, Sakmann B (1992) Calcium-permeable AMPA-kainate receptors in fusiform cerebellar glial cells. *Science* 256:1566-1570.
- Butler MJ, Jacobsen TL, Cain DM, Jarman MG, Hubank M, Whittle JR, Phillips R, Simcox A (2003) Discovery of genes with highly restricted expression patterns in the *Drosophila* wing disc using DNA oligonucleotide microarrays. *Development* 130:659-670.
- Chavis P, Westbrook G (2001) Integrins mediate functional pre- and postsynaptic maturation at a hippocampal synapse. *Nature* 411:317-321.
- Chen GQ, Cui C, Mayer ML, Gouaux E (1999) Functional characterization of a potassium-selective prokaryotic glutamate receptor. *Nature* 402:817-821.
- Chen L, Chetkovich DM, Petralia RS, Sweeney NT, Kawasaki Y, Wenthold RJ, Brecht DS, Nicoll RA (2000) Stargazin regulates synaptic targeting of AMPA receptors by two distinct mechanisms. *Nature* 408:936-943.
- Chiba A, Rose D (1998) "Painting" the target: how local molecular cues define synaptic relationships. *Bioessays* 20:941-948.
- Colquhoun D, Sivilotti LG (2004) Function and structure in glycine receptors and some of their relatives. *Trends Neurosci* 27:337-344.
- Contractor A, Heinemann SF (2002) Glutamate receptor trafficking in synaptic plasticity. *Sci STKE* 2002:RE14.
- Cooper RL, Marin L, Atwood HL (1995) Synaptic differentiation of a single motor neuron: conjoint definition of transmitter release, presynaptic calcium signals, and ultrastructure. *J Neurosci* 15:4209-4222.
- Cooper RL, Harrington CC, Marin L, Atwood HL (1996) Quantal release at visualized terminals of a crayfish motor axon: intraterminal and regional differences. *J Comp Neurol* 375:583-600.
- Currie DA, Truman JW, Burden SJ (1995) *Drosophila* glutamate receptor RNA expression in embryonic and larval muscle fibers. *Dev Dyn* 203:311-316.
- Dai Z, Luo X, Xie H, Peng HB (2000) The actin-driven movement and formation of acetylcholine receptor clusters. *J Cell Biol* 150:1321-1334.
- Dalva MB, Takasu MA, Lin MZ, Shamah SM, Hu L, Gale NW, Greenberg ME (2000) EphB receptors interact with NMDA receptors and regulate excitatory synapse formation. *Cell* 103:945-956.
- Daniels RW, Collins CA, Gelfand MV, Dant J, Brooks ES, Krantz DE, Diantonio A (2004) Increased Expression of the *Drosophila* Vesicular Glutamate Transporter Leads to Excess Glutamate Release and a Compensatory Decrease in Quantal Content. *J Neurosci* 24:10466-10474.
- Davis GW, Schuster CM, Goodman CS (1997) Genetic analysis of the mechanisms controlling target selection: target-derived Fasciclin II regulates the pattern of synapse formation. *Neuron* 19:561-573.
- Dean C, Scholl FG, Choih J, DeMaria S, Berger J, Isacoff E, Scheiffele P (2003) Neurexin mediates the assembly of presynaptic terminals. *Nat Neurosci* 6:708-716.
- DeChiara TM, Bowen DC, Valenzuela DM, Simmons MV, Poueymirou WT, Thomas S, Kinetz E, Compton DL, Rojas E, Park JS, Smith C, DiStefano PS, Glass DJ, Burden SJ, Yancopoulos GD (1996) The receptor tyrosine kinase MuSK is required for neuromuscular junction formation in vivo. *Cell* 85:501-512.
- DiAntonio A, Petersen SA, Heckmann M, Goodman CS (1999) Glutamate receptor expression regulates quantal size and quantal content at the *Drosophila* neuromuscular junction. *J Neurosci* 19:3023-3032.
- Dingledine R, Borges K, Bowie D, Traynelis SF (1999) The glutamate receptor ion channels. *Pharmacol Rev* 51:7-61.
- Dingledine R, Borges K, Bowie D, Traynelis SF (1999) The glutamate receptor ion channels. *Pharmacol Rev* 51:7-61.
- Ellgaard L, Helenius A (2003) Quality control in the endoplasmic reticulum. *Nat Rev Mol Cell Biol* 4:181-191.
- Essrich C, Lorez M, Benson JA, Fritschy JM, Luscher B (1998) Postsynaptic clustering of major GABAA receptor subtypes requires the gamma 2 subunit and gephyrin. *Nat Neurosci* 1:563-571.
- Ethell IM, Yamaguchi Y (1999) Cell surface heparan sulfate proteoglycan syndecan-2 induces the maturation of dendritic spines in rat hippocampal neurons. *J Cell Biol* 144:575-586.
- Ethell IM, Irie F, Kalo MS, Couchman JR, Pasquale EB, Yamaguchi Y (2001) EphB/syndecan-2

- signaling in dendritic spine morphogenesis. *Neuron* 31:1001-1013.
- Featherstone DE, Broadie K (2000) Surprises from *Drosophila*: genetic mechanisms of synaptic development and plasticity. *Brain Res Bull* 53:501-511.
- Fernandez-Chacon R, Sudhof TC (1999) Genetics of synaptic vesicle function: toward the complete functional anatomy of an organelle. *Annu Rev Physiol* 61:753-776.
- Fiala JC, Feinberg M, Popov V, Harris KM (1998) Synaptogenesis via dendritic filopodia in developing hippocampal area CA1. *J Neurosci* 18:8900-8911.
- Finn AJ, Feng G, Pendergast AM (2003) Postsynaptic requirement for Abl kinases in assembly of the neuromuscular junction. *Nat Neurosci* 6:717-723.
- Friedman HV, Bresler T, Garner CC, Ziv NE (2000) Assembly of new individual excitatory synapses: time course and temporal order of synaptic molecule recruitment. *Neuron* 27:57-69.
- Froehner SC, Luetje CW, Scotland PB, Patrick J (1990) The postsynaptic 43K protein clusters muscle nicotinic acetylcholine receptors in *Xenopus* oocytes. *Neuron* 5:403-410.
- Furlong EE, Andersen EC, Null B, White KP, Scott MP (2001) Patterns of gene expression during *Drosophila* mesoderm development. *Science* 293:1629-1633.
- Garner CC, Zhai RG, Gundelfinger ED, Ziv NE (2002) Molecular mechanisms of CNS synaptogenesis. *Trends Neurosci* 25:243-251.
- Gautam M, Noakes PG, Mudd J, Nichol M, Chu GC, Sanes JR, Merlie JP (1995) Failure of postsynaptic specialization to develop at neuromuscular junctions of rapsyn-deficient mice. *Nature* 377:232-236.
- Gautam M, Noakes PG, Moscoso L, Rupp F, Scheller RH, Merlie JP, Sanes JR (1996) Defective neuromuscular synaptogenesis in agrin-deficient mutant mice. *Cell* 85:525-535.
- Gilbert W (1978) Why genes in pieces? *Nature* 271:501.
- Gillespie SK, Wasserman SA (1994) Dorsal, a *Drosophila* Rel-like protein, is phosphorylated upon activation of the transmembrane protein Toll. *Mol Cell Biol* 14:3559-3568.
- Glass DJ, Bowen DC, Stitt TN, Radziejewski C, Bruno J, Ryan TE, Gies DR, Shah S, Mattsson K, Burden SJ, DiStefano PS, Valenzuela DM, DeChiara TM, Yancopoulos GD (1996) Agrin acts via a MuSK receptor complex. *Cell* 85:513-523.
- Gonzalez-Gaitan M, Jackle H (1997) Role of *Drosophila* alpha-adaptin in presynaptic vesicle recycling. *Cell* 88:767-776.
- Gramates LS, Budnik V (1999) Assembly and maturation of the *Drosophila* larval neuromuscular junction. *Int Rev Neurobiol* 43:93-117.
- Greger IH, Khatri L, Ziff EB (2002) RNA editing at arg607 controls AMPA receptor exit from the endoplasmic reticulum. *Neuron* 34:759-772.
- Grunwald IC, Korte M, Wolfer D, Wilkinson GA, Unsicker K, Lipp HP, Bonhoeffer T, Klein R (2001) Kinase-independent requirement of EphB2 receptors in hippocampal synaptic plasticity. *Neuron* 32:1027-1040.
- Guan B, Hartmann B, Kho YH, Gorczyca M, Budnik V (1996) The *Drosophila* tumor suppressor gene, *dlg*, is involved in structural plasticity at a glutamatergic synapse. *Curr Biol* 6:695-706.
- Hall AC, Lucas FR, Salinas PC (2000) Axonal remodeling and synaptic differentiation in the cerebellum is regulated by WNT-7a signaling. *Cell* 100:525-535.
- Hall ZW, Sanes JR (1993) Synaptic structure and development: the neuromuscular junction. *Cell* 72 Suppl:99-121.
- Han H, Noakes PG, Phillips WD (1999) Overexpression of rapsyn inhibits agrin-induced acetylcholine receptor clustering in muscle cells. *J Neurocytol* 28:763-775.
- Hannah MJ, Schmidt AA, Huttner WB (1999) Synaptic vesicle biogenesis. *Annu Rev Cell Dev Biol* 15:733-798.
- Harris KM, Kater SB (1994) Dendritic spines: cellular specializations imparting both stability and flexibility to synaptic function. *Annu Rev Neurosci* 17:341-371.
- Hawkins LM, Prybylowski K, Chang K, Moussan C, Stephenson FA, Wenthold RJ (2004) Export from the endoplasmic reticulum of assembled N-methyl-D-aspartic acid receptors is controlled by a motif in the c terminus of the NR2 subunit. *J Biol Chem* 279:28903-28910.
- Heimbeck G, Bugnon V, Gendre N, Haberlin C, Stocker RF (1999) Smell and taste perception in *Drosophila melanogaster* larva: toxin expression studies in chemosensory neurons. *J Neurosci* 19:6599-6609.
- Henderson JT, Georgiou J, Jia Z, Robertson J, Elowe S, Roder JC, Pawson T (2001) The receptor tyrosine kinase EphB2 regulates NMDA-dependent synaptic function. *Neuron* 32:1041-1056.
- Herbst R, Burden SJ (2000) The juxtamembrane region of MuSK has a critical role in agrin-mediated signaling. *Embo J* 19:67-77.
- Hering H, Sheng M (2001) Dendritic spines: structure, dynamics and regulation. *Nat Rev Neurosci*

- 2:880-888.
- Hirai H (2000) Clustering of delta glutamate receptors is regulated by the actin cytoskeleton in the dendritic spines of cultured rat Purkinje cells. *Eur J Neurosci* 12:563-570.
- Hoang B, Chiba A (1998) Genetic analysis on the role of integrin during axon guidance in *Drosophila*. *J Neurosci* 18:7847-7855.
- Hollmann M, Heinemann S (1994) Cloned glutamate receptors. *Annu Rev Neurosci* 17:31-108.
- Isaac JT, Crair MC, Nicoll RA, Malenka RC (1997) Silent synapses during development of thalamocortical inputs. *Neuron* 18:269-280.
- Jahn R, Sudhof TC (1999) Membrane fusion and exocytosis. *Annu Rev Biochem* 68:863-911.
- Jaskolski F, Coussen F, Nagarajan N, Normand E, Rosenmund C, Mulle C (2004) Subunit composition and alternative splicing regulate membrane delivery of kainate receptors. *J Neurosci* 24:2506-2515.
- Jennings CG, Dyer SM, Burden SJ (1993) Muscle-specific trk-related receptor with a kringle domain defines a distinct class of receptor tyrosine kinases. *Proc Natl Acad Sci U S A* 90:2895-2899.
- Jia XX, Gorczyca M, Budnik V (1993) Ultrastructure of neuromuscular junctions in *Drosophila*: comparison of wild type and mutants with increased excitability. *J Neurobiol* 24:1025-1044.
- Kennerdell JR, Carthew RW (2000) Heritable gene silencing in *Drosophila* using double-stranded RNA. *Nat Biotechnol* 18:896-898.
- Keshishian H, Broadie K, Chiba A, Bate M (1996) The *Drosophila* neuromuscular junction: a model system for studying synaptic development and function. *Annu Rev Neurosci* 19:545-575.
- Kiger AA, Baum B, Jones S, Jones MR, Coulson A, Echeverri C, Perrimon N (2003) A functional genomic analysis of cell morphology using RNA interference. *J Biol* 2:27.
- Kim YO, Park SJ, Balaban RS, Nirenberg M, Kim Y (2004) A functional genomic screen for cardiogenic genes using RNA interference in developing *Drosophila* embryos. *Proc Natl Acad Sci U S A* 101:159-164.
- Kirsch J, Betz H (1995) The postsynaptic localization of the glycine receptor-associated protein gephyrin is regulated by the cytoskeleton. *J Neurosci* 15:4148-4156.
- Kneussel M, Brandstatter JH, Laube B, Stahl S, Muller U, Betz H (1999) Loss of postsynaptic GABA(A) receptor clustering in gephyrin-deficient mice. *J Neurosci* 19:9289-9297.
- Koh YH, Gramates LS, Budnik V (2000) *Drosophila* larval neuromuscular junction: molecular components and mechanisms underlying synaptic plasticity. *Microsc Res Tech* 49:14-25.
- Kuusinen A, Abele R, Madden DR, Keinänen K (1999) Oligomerization and ligand-binding properties of the ectodomain of the alpha-amino-3-hydroxy-5-methyl-4-isoxazole propionic acid receptor subunit GluRD. *J Biol Chem* 274:28937-28943.
- LaRochelle WJ, Froehner SC (1986) Determination of the tissue distributions and relative concentrations of the postsynaptic 43-kDa protein and the acetylcholine receptor in Torpedo. *J Biol Chem* 261:5270-5274.
- Laube B, Kuhse J, Betz H (1998) Evidence for a tetrameric structure of recombinant NMDA receptors. *J Neurosci* 18:2954-2961.
- Li TR, White KP (2003) Tissue-specific gene expression and ecdysone-regulated genomic networks in *Drosophila*. *Dev Cell* 5:59-72.
- Li Z, Sheng M (2003) Some assembly required: the development of neuronal synapses. *Nat Rev Mol Cell Biol* 4:833-841.
- Liao D, Hessler NA, Malinow R (1995) Activation of postsynaptically silent synapses during pairing-induced LTP in CA1 region of hippocampal slice. *Nature* 375:400-404.
- Lin W, Burgess RW, Dominguez B, Pfaff SL, Sanes JR, Lee KF (2001) Distinct roles of nerve and muscle in postsynaptic differentiation of the neuromuscular synapse. *Nature* 410:1057-1064.
- Littleton JT (2000) A genomic analysis of membrane trafficking and neurotransmitter release in *Drosophila*. *J Cell Biol* 150:F77-82.
- Littleton JT, Ganetzky B (2000) Ion channels and synaptic organization: analysis of the *Drosophila* genome. *Neuron* 26:35-43.
- Luo ZG, Je HS, Wang Q, Yang F, Dobbins GC, Yang ZH, Xiong WC, Lu B, Mei L (2003) Implication of geranylgeranyltransferase I in synapse formation. *Neuron* 40:703-717.
- Luo ZG, Wang Q, Zhou JZ, Wang J, Luo Z, Liu M, He X, Wynshaw-Boris A, Xiong WC, Lu B, Mei L (2002) Regulation of AChR clustering by Dishevelled interacting with MuSK and PAK1. *Neuron* 35:489-505.
- Madden DR (2002) The structure and function of glutamate receptor ion channels. *Nat Rev Neurosci* 3:91-101.
- Mano I, Teichberg VI (1998) A tetrameric subunit stoichiometry for a glutamate receptor-channel complex. *Neuroreport* 9:327-331.

- Marangi PA, Forsayeth JR, Mittaud P, Erb-Vogtli S, Blake DJ, Moransard M, Sander A, Fuhrer C (2001) Acetylcholine receptors are required for agrin-induced clustering of postsynaptic proteins. *Embo J* 20:7060-7073.
- Marrs GS, Green SH, Dailey ME (2001) Rapid formation and remodeling of postsynaptic densities in developing dendrites. *Nat Neurosci* 4:1006-1013.
- Marrus SB, Portman SL, Allen MJ, Moffat KG, DiAntonio A (2004) Differential localization of glutamate receptor subunits at the *Drosophila* neuromuscular junction. *J Neurosci* 24:1406-1415.
- Matsuda K, Fletcher M, Kamiya Y, Yuzaki M (2003) Specific assembly with the NMDA receptor 3B subunit controls surface expression and calcium permeability of NMDA receptors. *J Neurosci* 23:10064-10073.
- McCabe BD, Marques G, Haghghi AP, Fetter RD, Crotty ML, Haerry TE, Goodman CS, O'Connor MB (2003) The BMP homolog Gbb provides a retrograde signal that regulates synaptic growth at the *Drosophila* neuromuscular junction. *Neuron* 39:241-254.
- McGee AW, Brecht DS (2003) Assembly and plasticity of the glutamatergic postsynaptic specialization. *Curr Opin Neurobiol* 13:111-118.
- McMahan UJ (1990) The agrin hypothesis. *Cold Spring Harb Symp Quant Biol* 55:407-418.
- Meguro H, Mori H, Araki K, Kushiya E, Kutsuwada T, Yamazaki M, Kumanishi T, Arakawa M, Sakimura K, Mishina M (1992) Functional characterization of a heteromeric NMDA receptor channel expressed from cloned cDNAs. *Nature* 357:70-74.
- Milner R, Campbell IL (2002) The integrin family of cell adhesion molecules has multiple functions within the CNS. *J Neurosci Res* 69:286-291.
- Missias AC, Mudd J, Cunningham JM, Steinbach JH, Merlie JP, Sanes JR (1997) Deficient development and maintenance of postsynaptic specializations in mutant mice lacking an 'adult' acetylcholine receptor subunit. *Development* 124:5075-5086.
- Missler M, Zhang W, Rohlmann A, Kattenstroth G, Hammer RE, Gottmann K, Sudhof TC (2003) Alpha-neurexins couple Ca²⁺ channels to synaptic vesicle exocytosis. *Nature* 423:939-948.
- Monyer H, Sprengel R, Schoepfer R, Herb A, Higuchi M, Lomeli H, Burnashev N, Sakmann B, Seeburg PH (1992) Heteromeric NMDA receptors: molecular and functional distinction of subtypes. *Science* 256:1217-1221.
- Mulle C, Sailer A, Swanson GT, Brana C, O'Gorman S, Bettler B, Heinemann SF (2000) Subunit composition of kainate receptors in hippocampal interneurons. *Neuron* 28:475-484.
- Nguyen T, Sudhof TC (1997) Binding properties of neuroligin 1 and neurexin 1beta reveal function as heterophilic cell adhesion molecules. *J Biol Chem* 272:26032-26039.
- Noakes PG, Phillips WD, Hanley TA, Sanes JR, Merlie JP (1993) 43K protein and acetylcholine receptors colocalize during the initial stages of neuromuscular synapse formation in vivo. *Dev Biol* 155:275-280.
- Noakes PG, Gautam M, Mudd J, Sanes JR, Merlie JP (1995) Aberrant differentiation of neuromuscular junctions in mice lacking s-laminin/laminin beta 2. *Nature* 374:258-262.
- O'Brien R, Xu D, Mi R, Tang X, Hopf C, Worley P (2002) Synaptically targeted narp plays an essential role in the aggregation of AMPA receptors at excitatory synapses in cultured spinal neurons. *J Neurosci* 22:4487-4498.
- O'Brien RJ, Xu D, Petralia RS, Steward O, Haganir RL, Worley P (1999) Synaptic clustering of AMPA receptors by the extracellular immediate-early gene product Narp. *Neuron* 23:309-323.
- Okabe S, Miwa A, Okado H (2001) Spine formation and correlated assembly of presynaptic and postsynaptic molecules. *J Neurosci* 21:6105-6114.
- Okabe S, Urushido T, Konno D, Okado H, Sobue K (2001) Rapid redistribution of the postsynaptic density protein PSD-Zip45 (Homer 1c) and its differential regulation by NMDA receptors and calcium channels. *J Neurosci* 21:9561-9571.
- Ono F, Higashijima S, Shcherbatko A, Fetcho JR, Brehm P (2001) Paralytic zebrafish lacking acetylcholine receptors fail to localize rapsyn clusters to the synapse. *J Neurosci* 21:5439-5448.
- Packard M, Koo ES, Gorczyca M, Sharpe J, Cumberledge S, Budnik V (2002) The *Drosophila* Wnt, wingless, provides an essential signal for pre- and postsynaptic differentiation. *Cell* 111:319-330.
- Parnas D, Haghghi AP, Fetter RD, Kim SW, Goodman CS (2001) Regulation of postsynaptic structure and protein localization by the Rho-type guanine nucleotide exchange factor dPix. *Neuron* 32:415-424.
- Pasterkamp RJ, Kolodkin AL (2003) Semaphorin junction: making tracks toward neural connectivity. *Curr Opin Neurobiol* 13:79-89.
- Perez-Otano I, Schulteis CT, Contractor A, Lipton SA, Trimmer JS, Sucher NJ, Heinemann SF (2001)

- Assembly with the NR1 subunit is required for surface expression of NR3A-containing NMDA receptors. *J Neurosci* 21:1228-1237.
- Petersen SA, Fetter RD, Noordermeer JN, Goodman CS, DiAntonio A (1997) Genetic analysis of glutamate receptors in *Drosophila* reveals a retrograde signal regulating presynaptic transmitter release. *Neuron* 19:1237-1248.
- Phillips GR, Huang JK, Wang Y, Tanaka H, Shapiro L, Zhang W, Shan WS, Arndt K, Frank M, Gordon RE, Gawinowicz MA, Zhao Y, Colman DR (2001) The presynaptic particle web: ultrastructure, composition, dissolution, and reconstitution. *Neuron* 32:63-77.
- Phillips WD, Maimone MM, Merlie JP (1991) Mutagenesis of the 43-kD postsynaptic protein defines domains involved in plasma membrane targeting and AChR clustering. *J Cell Biol* 115:1713-1723.
- Pinkstaff JK, Detterich J, Lynch G, Gall C (1999) Integrin subunit gene expression is regionally differentiated in adult brain. *J Neurosci* 19:1541-1556.
- Poodry CA, Edgar L (1979) Reversible alteration in the neuromuscular junctions of *Drosophila melanogaster* bearing a temperature-sensitive mutation, shibire. *J Cell Biol* 81:520-527.
- Prange O, Murphy TH (2001) Modular transport of postsynaptic density-95 clusters and association with stable spine precursors during early development of cortical neurons. *J Neurosci* 21:9325-9333.
- Prokop A (1999) Integrating bits and pieces: synapse structure and formation in *Drosophila* embryos. *Cell Tissue Res* 297:169-186.
- Prokop A, Landgraf M, Rushton E, Broadie K, Bate M (1996) Presynaptic development at the *Drosophila* neuromuscular junction: assembly and localization of presynaptic active zones. *Neuron* 17:617-626.
- Prokop A, Martin-Bermudo MD, Bate M, Brown N (1998) Absence of PS integrins or laminin A affects extracellular adhesion, but not intracellular assembly, of hemiadherens and neuromuscular junctions in *Drosophila* embryos. *Dev Biol* 196:58-76.
- Rao A, Cha EM, Craig AM (2000) Mismatched appositions of presynaptic and postsynaptic components in isolated hippocampal neurons. *J Neurosci* 20:8344-8353.
- Rao A, Kim E, Sheng M, Craig AM (1998) Heterogeneity in the molecular composition of excitatory postsynaptic sites during development of hippocampal neurons in culture. *J Neurosci* 18:1217-1229.
- Ren Z, Riley NJ, Needleman LA, Sanders JM, Swanson GT, Marshall J (2003) Cell surface expression of GluR5 kainate receptors is regulated by an endoplasmic reticulum retention signal. *J Biol Chem* 278:52700-52709.
- Rheuben MB, Yoshihara M, Kidokoro Y (1999) Ultrastructural correlates of neuromuscular junction development. *Int Rev Neurobiol* 43:69-92.
- Ritzenthaler S, Suzuki E, Chiba A (2000) Postsynaptic filopodia in muscle cells interact with innervating motoneuron axons. *Nat Neurosci* 3:1012-1017.
- Rosenberg M, Meier J, Triller A, Vannier C (2001) Dynamics of glycine receptor insertion in the neuronal plasma membrane. *J Neurosci* 21:5036-5044.
- Rosenmund C, Stern-Bach Y, Stevens CF (1998) The tetrameric structure of a glutamate receptor channel. *Science* 280:1596-1599.
- Roy PJ, Stuart JM, Lund J, Kim SK (2002) Chromosomal clustering of muscle-expressed genes in *Caenorhabditis elegans*. *Nature* 418:975-979.
- Ruegg MA, Bixby JL (1998) Agrin orchestrates synaptic differentiation at the vertebrate neuromuscular junction. *Trends Neurosci* 21:22-27.
- Safferling M, Tichelaar W, Kummerle G, Jouppila A, Kuusinen A, Keinänen K, Madden DR (2001) First images of a glutamate receptor ion channel: oligomeric state and molecular dimensions of GluRB homomers. *Biochemistry* 40:13948-13953.
- Saitoe M, Tanaka S, Takata K, Kidokoro Y (1997) Neural activity affects distribution of glutamate receptors during neuromuscular junction formation in *Drosophila* embryos. *Dev Biol* 184:48-60.
- Saitoe M, Schwarz TL, Umbach JA, Gundersen CB, Kidokoro Y (2001) Absence of junctional glutamate receptor clusters in *Drosophila* mutants lacking spontaneous transmitter release. *Science* 293:514-517.
- Sanes JR, Lichtman JW (1999) Development of the vertebrate neuromuscular junction. *Annu Rev Neurosci* 22:389-442.
- Sanes JR, Lichtman JW (2001) Induction, assembly, maturation and maintenance of a postsynaptic apparatus. *Nat Rev Neurosci* 2:791-805.
- Scannevin RH, Haganir RL (2000) Postsynaptic organization and regulation of excitatory synapses. *Nat*

- Rev Neurosci 1:133-141.
- Scheiffele P, Fan J, Choih J, Fetter R, Serafini T (2000) Neuroligin expressed in nonneuronal cells triggers presynaptic development in contacting axons. *Cell* 101:657-669.
- Schulze KL, Broadie K, Perin MS, Bellen HJ (1995) Genetic and electrophysiological studies of *Drosophila* syntaxin-1A demonstrate its role in nonneuronal secretion and neurotransmission. *Cell* 80:311-320.
- Schuster CM, Davis GW, Fetter RD, Goodman CS (1996) Genetic dissection of structural and functional components of synaptic plasticity. I. Fasciclin II controls synaptic stabilization and growth. *Neuron* 17:641-654.
- Schuster CM, Ultsch A, Schloss P, Cox JA, Schmitt B, Betz H (1991) Molecular cloning of an invertebrate glutamate receptor subunit expressed in *Drosophila* muscle. *Science* 254:112-114.
- Scott DB, Blanpied TA, Swanson GT, Zhang C, Ehlers MD (2001) An NMDA receptor ER retention signal regulated by phosphorylation and alternative splicing. *J Neurosci* 21:3063-3072.
- Shapira M, Zhai RG, Dresbach T, Bresler T, Torres VI, Gundelfinger ED, Ziv NE, Garner CC (2003) Unitary assembly of presynaptic active zones from Piccolo-Bassoon transport vesicles. *Neuron* 38:237-252.
- Shen K, Bargmann CI (2003) The immunoglobulin superfamily protein SYG-1 determines the location of specific synapses in *C. elegans*. *Cell* 112:619-630.
- Shen K, Fetter RD, Bargmann CI (2004) Synaptic specificity is generated by the synaptic guidepost protein SYG-2 and its receptor, SYG-1. *Cell* 116:869-881.
- Sheng M (2001) Molecular organization of the postsynaptic specialization. *Proc Natl Acad Sci U S A* 98:7058-7061.
- Sheng M, Lee SH (2001) AMPA receptor trafficking and the control of synaptic transmission. *Cell* 105:825-828.
- Sheridan DL, Berlot CH, Robert A, Inglis FM, Jakobsdottir KB, Howe JR, Hughes TE (2002) A new way to rapidly create functional, fluorescent fusion proteins: random insertion of GFP with an in vitro transposition reaction. *BMC Neurosci* 3:7.
- Sigrist SJ, Thiel PR, Reiff DF, Schuster CM (2002) The postsynaptic glutamate receptor subunit DGluR-IIA mediates long-term plasticity in *Drosophila*. *J Neurosci* 22:7362-7372.
- Sigrist SJ, Thiel PR, Reiff DF, Lachance PE, Lasko P, Schuster CM (2000) Postsynaptic translation affects the efficacy and morphology of neuromuscular junctions. *Nature* 405:1062-1065.
- Sone M, Suzuki E, Hoshino M, Hou D, Kuromi H, Fukata M, Kuroda S, Kaibuchi K, Nabeshima Y, Hama C (2000) Synaptic development is controlled in the periaxonal zones of *Drosophila* synapses. *Development* 127:4157-4168.
- Sprengel R, Aronoff R, Volkner M, Schmitt B, Mosbach R, Kuner T (2001) Glutamate receptor channel signatures. *Trends Pharmacol Sci* 22:7-10.
- Standley S, Baudry M (2000) The role of glycosylation in ionotropic glutamate receptor ligand binding, function, and trafficking. *Cell Mol Life Sci* 57:1508-1516.
- Stathopoulos A, Levine M (2002) Whole-genome expression profiles identify gene batteries in *Drosophila*. *Dev Cell* 3:464-465.
- Sudhof TC (2000) The synaptic vesicle cycle revisited. *Neuron* 28:317-320.
- Sweeney ST, Broadie K, Keane J, Niemann H, O'Kane CJ (1995) Targeted expression of tetanus toxin light chain in *Drosophila* specifically eliminates synaptic transmission and causes behavioral defects. *Neuron* 14:341-351.
- Tejedor FJ, Bokhari A, Rogero O, Gorczyca M, Zhang J, Kim E, Sheng M, Budnik V (1997) Essential role for dlg in synaptic clustering of Shaker K⁺ channels in vivo. *J Neurosci* 17:152-159.
- Thibault ST, Singer MA, Miyazaki WY, Milash B, Dompe NA, Singh CM, Buchholz R, Demsky M, Fawcett R, Francis-Lang HL, Ryner L, Cheung LM, Chong A, Erickson C, Fisher WW, Greer K, Hartouni SR, Howie E, Jakkula L, Joo D, Killpack K, Laufer A, Mazzotta J, Smith RD, Stevens LM, Stuber C, Tan LR, Ventura R, Woo A, Zakrajsek I, Zhao L, Chen F, Swimmer C, Kopczynski C, Duyk G, Winberg ML, Margolis J (2004) A complementary transposon tool kit for *Drosophila melanogaster* using P and piggyBac. *Nat Genet* 36:283-287.
- Thomas U, Kim E, Kuhlendahl S, Koh YH, Gundelfinger ED, Sheng M, Garner CC, Budnik V (1997) Synaptic clustering of the cell adhesion molecule fasciclin II by discs-large and its role in the regulation of presynaptic structure. *Neuron* 19:787-799.
- Togashi H, Abe K, Mizoguchi A, Takaoka K, Chisaka O, Takeichi M (2002) Cadherin regulates dendritic spine morphogenesis. *Neuron* 35:77-89.
- Valenzuela DM, Stitt TN, DiStefano PS, Rojas E, Mattsson K, Compton DL, Nunez L, Park JS, Stark JL, Gies DR, et al. (1995) Receptor tyrosine kinase specific for the skeletal muscle lineage: expression in embryonic muscle, at the neuromuscular junction, and after injury. *Neuron*

- 15:573-584.
- Vandenberghe W, Bredt DS (2004) Early events in glutamate receptor trafficking. *Curr Opin Cell Biol* 16:134-139.
- Varoqueaux F, Sigler A, Rhee JS, Brose N, Enk C, Reim K, Rosenmund C (2002) Total arrest of spontaneous and evoked synaptic transmission but normal synaptogenesis in the absence of Munc13-mediated vesicle priming. *Proc Natl Acad Sci U S A* 99:9037-9042.
- Verhage M, Maia AS, Plomp JJ, Brussaard AB, Heeroma JH, Vermeer H, Toonen RF, Hammer RE, van den Berg TK, Missler M, Geuze HJ, Südhof TC (2000) Synaptic assembly of the brain in the absence of neurotransmitter secretion. *Science* 287:864-869.
- Wallace BG (1989) Agrin-induced specializations contain cytoplasmic, membrane, and extracellular matrix-associated components of the postsynaptic apparatus. *J Neurosci* 9:1294-1302.
- Wan HJ, DiAntonio A, Fetter RD, Bergstrom K, Strauss R, Goodman CS (2000) Highwire regulates synaptic growth in *Drosophila*. *Neuron* 26:313-329.
- Washbourne P, Bennett JE, McAllister AK (2002) Rapid recruitment of NMDA receptor transport packets to nascent synapses. *Nat Neurosci* 5:751-759.
- Wenthold RJ, Petralia RS, Blahos J, II, Niedzielski AS (1996) Evidence for multiple AMPA receptor complexes in hippocampal CA1/CA2 neurons. *J Neurosci* 16:1982-1989.
- Weston C, Yee B, Hod E, Prives J (2000) Agrin-induced acetylcholine receptor clustering is mediated by the small guanosine triphosphatases Rac and Cdc42. *J Cell Biol* 150:205-212.
- Weston C, Gordon C, Teresa G, Hod E, Ren XD, Prives J (2003) Cooperative regulation by Rac and Rho of agrin-induced acetylcholine receptor clustering in muscle cells. *J Biol Chem* 278:6450-6455.
- White JG, Southgate E, Thomson JN, Brenner S (1976) The structure of the ventral nerve cord of *Caenorhabditis elegans*. *Philos Trans R Soc Lond B Biol Sci* 275:327-348.
- Wojtowicz JM, Marin L, Atwood HL (1994) Activity-induced changes in synaptic release sites at the crayfish neuromuscular junction. *J Neurosci* 14:3688-3703.
- Wucherpfennig T, Wilsch-Brauninger M, Gonzalez-Gaitan M (2003) Role of *Drosophila* Rab5 during endosomal trafficking at the synapse and evoked neurotransmitter release. *J Cell Biol* 161:609-624.
- Xia H, Hornby ZD, Malenka RC (2001) An ER retention signal explains differences in surface expression of NMDA and AMPA receptor subunits. *Neuropharmacology* 41:714-723.
- Xia H, von Zastrow M, Malenka RC (2002) A novel anterograde trafficking signal present in the N-terminal extracellular domain of ionotropic glutamate receptors. *J Biol Chem* 277:47765-47769.
- Yamagata M, Sanes JR, Weiner JA (2003) Synaptic adhesion molecules. *Curr Opin Cell Biol* 15:621-632.
- Yang X, Arber S, William C, Li L, Tanabe Y, Jessell TM, Birchmeier C, Burden SJ (2001) Patterning of muscle acetylcholine receptor gene expression in the absence of motor innervation. *Neuron* 30:399-410.
- Yoshihara CM, Hall ZW (1993) Increased expression of the 43-kD protein disrupts acetylcholine receptor clustering in myotubes. *J Cell Biol* 122:169-179.
- Yoshihara M, Rheuben MB, Kidokoro Y (1997) Transition from growth cone to functional motor nerve terminal in *Drosophila* embryos. *J Neurosci* 17:8408-8426.
- Zhai RG, Vardinon-Friedman H, Cases-Langhoff C, Becker B, Gundelfinger ED, Ziv NE, Garner CC (2001) Assembling the presynaptic active zone: a characterization of an active one precursor vesicle. *Neuron* 29:131-143.
- Zhang FL, Casey PJ (1996) Protein prenylation: molecular mechanisms and functional consequences. *Annu Rev Biochem* 65:241-269.
- Zhou H, Glass DJ, Yancopoulos GD, Sanes JR (1999) Distinct domains of MuSK mediate its abilities to induce and to associate with postsynaptic specializations. *J Cell Biol* 146:1133-1146.
- Zito K, Fetter RD, Goodman CS, Isacoff EY (1997) Synaptic clustering of Fascilin II and Shaker: essential targeting sequences and role of Dlg. *Neuron* 19:1007-1016.

Appendix

Genes enriched in larval body wall preparations

Abundance	Fold change	Gene description
23719.6	~26.8	FB:FBgn0031264 /sym=CG11835 /name= /prod= /func=DNA binding /map=21C6-21C6 /transc=CT33127 /len=2494 /GB:AE003589
102926.3	25.1	FB:FBgn0038943 /sym=CG5391 /name= /prod= /func= /map=94A12-94A13 /transc=CT17120 /len=755 /GB:AE003738
54625.7	20.3	FB:FBgn0038152 /sym=CG9792 /name= /prod= /func= /map=87E11-87E11 /transc=CT27648 /len=1695 /GB:AE003700
19700	20.2	FB:FBgn0025393 /sym=EG:196F3.3 /name= /prod= /func= /map=2B2-2B2 /transc=CT34605 /len=351 /GB:AE003421
95020.4	16.9	FB:FBgn0039299 /sym=CG11854 /name= /prod= /func= /map=96C4-96C4 /transc=CT33075 /len=1001 /GB:AE003751
11605.6	~15.3	FB:FBgn0037601 /sym=Cyp313b1 /name= /prod=cytochrome P450, CYP313B1 /func=cytochrome P45 /map=85A10-85A10 /transc=CT27472 /len=1494 /GB:AE003679
64568.5	15.1	FB:FBgn0003046 /sym=Pcp /name=Pupal cuticle protein /prod= /func=structural protein of pupal cuticle (<i>Drosophila</i>) /map=27D1-27D1 /transc=CT11573 /len=575 /GB:AE003615
15304.4	~14.7	FB:FBgn0039755 /sym=CG15531 /name= /prod= /func=enzyme /map=99E3-99E3 /transc=CT35646 /len=1005 /GB:AE003772
10859.7	~14.3	FB:FBgn0000422 /sym=Ddc /name=Dopa decarboxylase /prod=dopa decarboxylase /func=aromatic-L-amino-acid decarboxylase ; EC:4.1.1.28 /map=37C1-37C1 /transc=CT38799 /len=1889 /GB:AE003772
20881.3	13.6	FB:FBgn0016675 /sym=Lectin-galC1 /name=Galactose-specific C-type lectin /prod=galactose-specific C-type lectin /func=galactose binding lectin /map=37E1-37E1 /transc=CT28109 /len=746 /GB:AE003772
20429.4	13.5	FB:FBgn0038180 /sym=CG9307 /name= /prod= /func=enzyme /map=87F13-87F13 /transc=CT26495 /len=2109 /GB:AE003701 /note=3prime sequence from clone BDGP:LP08894.3prime-hit
25782.1	12.7	FB:FBgn0039030 /sym=CG6660 /name= /prod= /func= /map=94D4-94D4 /transc=CT20704 /len=819 /GB:AE003741
200301.9	11.9	FB:FBgn0037114 /sym=CG7160 /name= /prod=cuticle protein /func=structural protein /map=78F1-78F1 /transc=CT22123 /len=441 /GB:AE003595
15276.1	11.9	FB:FBgn0015565 /sym=yin /name=yin /prod=hydrogen/oligopeptide symporter /func=hydrogen/oligopeptide symporter /map=4A1-4A1 /transc=CT9924 /len=2544 /GB:AE003429 /note=3prime sequ
6628	~11.4	FB:FBgn0035711 /sym=CG8519 /name= /prod=RAS small GTPase-like /func=signal transduction /map=65C3-65C3 /transc=CT24887 /len=606 /GB:AE003561
6730.9	~11.3	FB:FBgn0036364 /sym=CG14109 /name= /prod= /func= /map=70A8-70A8 /transc=CT33704 /len=732 /GB:AE003538
8660.2	~10.9	FB:FBgn0033667 /sym=CG13183 /name= /prod= /func= /map=48D1-48D1 /transc=CT32424 /len=1356 /GB:AE003824
12992.1	10.8	FB:FBgn0029544 /sym=CG16994 /name= /prod= /func= /map=1D1-1D1 /transc=CT34390 /len=1155 /GB:AE003419
92230.8	10.5	FB:FBgn0037083 /sym=CG5656 /name= /prod=alkaline phosphatase-like /func=enzyme /map=78D5-78D5 /transc=CT17844 /len=1770 /GB:AE003594 /note=3prime sequence from clone BDGP:LP08894.3prime-hit
15667	10.4	FB:FBgn0030357 /sym=CG2471 /name= /prod= /func=actin binding /map=10F8-10F9 /transc=CT8171 /len=1103 /GB:AE003487 /note=3prime sequence from clone BDGP:LP11415.3prime-hit
10666	~10.3	FB:FBgn0023550 /sym=EG:103B4.2 /name= /prod= /func= /map=2E2-2E2 /transc=CT40356 /len=1517 /GB:AE003423
8699.1	~10.3	FB:FBgn0035813 /sym=CG8492 /name= /prod=lysozyme P /func=defense/immunity protein /map=66A10-66A10 /transc=CT14304 /len=2709 /GB:AE003558
8511.4	~10.0	FB:FBgn0033289 /sym=CG2121 /name= /prod= /func=transporter /map=44C1-44C1 /transc=CT6910 /len=1360 /GB:AE003837 /note=3prime sequence from clone BDGP:GH09628.3prime-hit
10694.8	9.9	FB:FBgn0033726 /sym=CG8836 /name= /prod=larval cuticle protein-like /func=structural protein /map=49A2-49A2 /transc=CT25408 /len=501 /GB:AE003822
11203.2	9.6	FB:FBgn0036264 /sym=CG11529 /name= /prod=trypsin-like /func=endopeptidase /map=68F8-68F8 /transc=CT21438 /len=864 /GB:AE003542
14520.8	9.6	FB:FBgn0038179 /sym=CG9312 /name= /prod= /func= /map=87F13-87F13 /transc=CT26517 /len=784 /GB:AE003701 /note=3prime sequence from clone BDGP:GH09754.3prime-hit
106759.7	9.5	FB:FBgn0034856 /sym=CG9891 /name= /prod= /func= /map=59D9-59D9 /transc=CT27880 /len=1266 /GB:AE003460

8081 ~9.1 FB:FBgn0032349 /sym=CG4779 /name= /prod= /func= /map=32D4-32D4 /transc=CT15337 /len=1272 /GB:AE003631
 7297.3 ~9.1 FB:FBgn0033858 /sym=CG13335 /name= /prod= /func= /map=50B7-50B7 /transc=CT32654 /len=408 /GB:AE003818
 6026.4 ~8.9 FB:FBgn0040868 /sym=CG15762 /name= /prod= /func= /map=12B10-12B10 /transc=CT36016 /len=240 /GB:AE003493
 10038.8 8.9 FB:FBgn0037319 /sym=CG2666 /name= /prod=chitin synthase-like /func=enzyme /map=83A5-83A5 /transc=CT9021 /len=3897 /GB:AE003603
 17201.8 8.6 FB:FBgn0034443 /sym=CG10460 /name= /prod= /func=endopeptidase /map=56D4-56D4 /transc=CT29364 /len=485 /GB:AE003796
 30755.5 8.5 FB:FBgn0035964 /sym=CG4665 /name=dihydropteridine reductase /prod=dihydropteridine reductase-like /func=dihydropteridine reductase /map=66F6-66F6 /transc=CT15055 /len=708 /GB:AE003500
 22531.1 8.3 FB:FBgn0035427 /sym=CG14959 /name= /prod= /func= /map=63C2-63C2 /transc=CT34804 /len=450 /GB:AE003477
 10634.5 8.2 FB:FBgn0029821 /sym=CG4020 /name= /prod= /func= /map=5C6-5C6 /transc=CT13322 /len=1485 /GB:AE003435
 11276.3 7.8 FB:FBgn0035300 /sym=CG1139 /name= /prod=amino-acid permease-like /func=transporter /map=62B11-62B11 /transc=CT1131 /len=1511 /GB:AE003473
 19312.7 7.7 FB:FBgn0038348 /sym=CG18519 /name= /prod= /func= /map=88F8-88F8 /transc=CT42266 /len=3671 /GB:AE003709
 7383.3 ~7.7 FB:FBgn0034253 /sym=CG10936 /name= /prod= /func=endopeptidase /map=54D3-54D4 /transc=CT30629 /len=4407 /GB:AE003802
 6329 ~7.4 FB:FBgn0038629 /sym=CG14304 /name= /prod= /func= /map=91B4-91B4 /transc=CT33934 /len=3585 /GB:AE003722
 19301.8 7.3 FB:FBgn0031791 /sym=CG9486 /name= /prod= /func=enzyme /map=26C1-26C1 /transc=CT26862 /len=651 /GB:AE003613
 7576.3 ~7.3 FB:FBgn0037503 /sym=CG14598 /name= /prod= /func= /map=84D3-84D3 /transc=CT34346 /len=690 /GB:AE003671
 22097.3 7.3 FB:FBgn0037761 /sym=CG8534 /name= /prod= /func= /map=85E10-85E10 /transc=CT24919 /len=818 /GB:AE003684
 63005.9 7.2 FB:FBgn0030326 /sym=CG2444 /name= /prod= /func= /map=10D4-10D4 /transc=CT8084 /len=635 /GB:AE003487
 5453.9 ~7.2 FB:FBgn0000594 /sym=Est-P /name=Esterase P /prod=carboxylesterase /func=carboxylesterase ; EC:3.1.1.1 /map=68F8-68F8 /transc=CT38084 /len=1635 /GB:AE003542
 101119.9 7.1 FB:FBgn0034162 /sym=CG6426 /name= /prod=calcium binding protein-like /func=ligand binding or carrier /map=53D15-53D15 /transc=CT19886 /len=426 /GB:AE003805
 6255.2 ~7.1 FB:FBgn0033136 /sym=CG12838 /name= /prod= /func= /map=42E2-42E2 /transc=CT31970 /len=633 /GB:AE003842
 5606.4 ~7.0 FB:FBgn0026190 /sym=prolyl-4-hydroxylase-alpha /name=prolyl 4-hydroxylase alpha /prod=procollagen-proline,2-oxoglutarate-4-dioxygenase, alpha subunit /func=procollagen-proline,2-oxoglutarate-4-dioxygenase, alpha subunit
 7498.3 7 FB:FBgn0037905 /sym=CG14703 /name= /prod= /func= /map=86E6-86E6 /transc=CT34493 /len=1397 /GB:AE003691
 5278.4 ~7.0 FB:FBgn0033099 /sym=CG9435 /name= /prod= /func= /map=42C3-42C3 /transc=CT26754 /len=594 /GB:AE003789
 5163.4 ~6.8 FB:FBgn0031564 /sym=CG2816 /name= /prod=chymotrypsin inhibitor-like /func=enzyme inhibitor /map=24A5-24A5 /transc=CT9603 /len=292 /GB:AE003579
 169802.4 6.7 FB:FBgn0033595 /sym=CG18337 /name= /prod= /func= /map=47E1-47E1 /transc=CT41641 /len=540 /GB:AE003826
 11072.1 6.7 FB:FBgn0022702 /sym=Cht2 /name=Chitinase 2 /prod=chitinase /func=chitinase ; EC:3.2.1.14 /map=62B1-62B1 /transc=CT6562 /len=1597 /GB:AE003472 /note=3prime sequence from clone BDGP:1
 19916.4 6.6 FB:FBgn0022770 /sym=Peritrophin-A /name=Peritrophin A /prod=peritrophin A /func=chitin binding /map=19C1-19C1 /transc=CT35567 /len=1232 /GB:AE003572 /note=3prime sequence from clone BDGP:1
 7115.8 6.6 FB:FBgn0010222 /sym=Nmdmc /name=NAD-dependent methylenetetrahydrofolate dehydrogenase /prod=NAD-dependent methylenetetrahydrofolate dehydrogenase /func=methylenetetrahydrofolate dehydrogenase
 2204.1 ~6.6 FB:FBgn0039098 /sym=CG13822 /name= /prod= /func= /map=95B1-95B1 /transc=CT33322 /len=651 /GB:AE003744
 4567.9 ~6.6 FB:FBgn0035553 /sym=CG13722 /name= /prod=prolin-rich protein-like /func=structural protein /map=64B12-64B12 /transc=CT33188 /len=2124 /GB:AE003481
 5343.8 ~6.6 FB:FBgn0027570 /sym=BcDNA:GH07643 /name= /prod=membrane-anchored zinc metalloendopeptidase-like (M13 peptidase) /func=endopeptidase /map=82D6-82D7 /transc=CT27583 /len=2739 /GB:AE003500
 78514.5 6.5 FB:FBgn0039482 /sym=CG14258 /name= /prod= /func= /map=97E6-97E6 /transc=CT33878 /len=777 /GB:AE003759
 80923 6.5 FB:FBgn0034517 /sym=CG18066 /name= /prod= /func= /map=57A8-57A8 /transc=CT40491 /len=625 /GB:AE003791 /note=3prime sequence from clone BDGP:GH09112.3prime-hit

18578.3	6.5	FB:FBgn0030976 /sym=CG7378 /name= /prod=protein phosphatase-like /func=protein phosphatase /map=17E8-17E8 /transc=CT22699 /len=738 /GB:AE003510
11156	6.5	FB:FBgn0033022 /sym=CG10398 /name= /prod= /func= /map=41C1-41C1 /transc=CT29180 /len=501 /GB:AE003786
14907.6	6.4	FB:FBgn0038053 /sym=CG18549 /name= /prod= /func= /map=87C1-87C1 /transc=CT17408 /len=1634 /GB:AE003696
10676.1	6.4	FB:FBgn0031542 /sym=CG15414 /name= /prod= /func= /map=23F3-23F3 /transc=CT35473 /len=963 /GB:AE003579
4298	~6.3	FB:FBgn0035755 /sym=CG14830 /name= /prod= /func= /map=65E10-65E10 /transc=CT34646 /len=972 /GB:AE003559
61989.6	6.3	FB:FBgn0035684 /sym=CG10461 /name= /prod=cuticle protein-like /func=structural protein /map=65A5-65A5 /transc=CT29366 /len=321 /GB:AE003563
36997.1	6.3	FB:FBgn0034860 /sym=CG9812 /name= /prod= /func= /map=59D10-59D11 /transc=CT42639 /len=611 /GB:AE003460
8959.2	6.3	FB:FBgn0030816 /sym=CG16700 /name= /prod=amino-acid permease-like /func=G protein linked receptor /map=15D2-15D3 /transc=CT37167 /len=1673 /GB:AE003504
5244.5	~6.3	FB:FBgn0038449 /sym=CG17562 /name= /prod= /func=enzyme /map=89D5-89D5 /transc=CT34716 /len=1416 /GB:AE003714
33816.6	6.2	FB:FBgn0030558 /sym=CG1461 /name= /prod=tyrosine aminotransferase /func=enzyme /map=12E1-12E1 /transc=CT3554 /len=1844 /GB:AE003495
5926.4	~6.1	FB:FBgn0039111 /sym=CG10371 /name= /prod= /func=protein phosphatase /map=95B7-95B7 /transc=CT29124 /len=585 /GB:AE003744
5751.7	6.1	FB:FBgn0039895 /sym=CG11288 /name= /prod=fibrillin-like /func=cell adhesion /map=102A3-102A3 /transc=CT31491 /len=914 /GB:AE003844
34282.6	6.1	FB:FBgn0031737 /sym=CG11142 /name= /prod=peritrophin-like /func=structural protein /map=26A1-26A1 /transc=CT31147 /len=1457 /GB:AE003611
36701.5	6	FB:FBgn0038366 /sym=CG4576 /name= /prod= /func= /map=89A8-89A8 /transc=CT14818 /len=2581 /GB:AE003710
4539.5	~6.0	FB:FBgn0023540 /sym=EG:152A3.3 /name= /prod= /func= /map=2E1-2E1 /transc=CT12189 /len=1918 /GB:AE003423 /note=3prime sequence from clone BDGP:HL01173.3prime-hit
9254.7	5.9	FB:FBgn0035936 /sym=CG4999 /name= /prod= /func= /map=66E3-66E3 /transc=CT16000 /len=1131 /GB:AE003553
68492.5	5.9	FB:FBgn0020439 /sym=fau /name= /prod=anoxia upregulated protein /func= /map=86C4-86C4 /transc=CT41978 /len=2121 /GB:AE003688
23518.7	5.8	FB:FBgn0027600 /sym=BcDNA:GH02976 /name= /prod=peritrophin-like /func=ligand binding or carrier /map=30F6-30F6 /transc=CT15349 /len=1095 /GB:AE003627 /note=3prime sequence from c
4834	~5.8	FB:FBgn0037186 /sym=CG11241 /name= /prod=pyridoxal-phosphate-dependent aminotransferase class-III /func=enzyme /map=79F2-79F2 /transc=CT31379 /len=1856 /GB:AE003598 /note=3prime
3240.1	~5.8	FB:FBgn0030595 /sym=CG14406 /name= /prod= /func= /map=13A1-13A1 /transc=CT34057 /len=312 /GB:AE003497
4244.5	~5.8	BDGP:GH188.3prime-hit /ESTpos=maps in FB:FBgn0036365 /sym=CG10732 /name= /prod= /func=signal transduction /map=7A8-7A8 /transc=CT369 /len=535
133216.6	5.8	FB:FBgn0010019 /sym=Cyp4g1 /name=Cytochrome P45-4g1 /prod=cytochrome P450, CYP4G1 /func=cytochrome P45 ; EC:1.14.14.1 /map=1B3-1B3 /transc=CT13187 /len=2267 /GB:AE003417 /no
223808.8	5.7	FB:FBgn0033725 /sym=CG8502 /name= /prod=cuticle protein /func=structural protein /map=49A2-49A2 /transc=CT24855 /len=1413 /GB:AE003822 /note=3prime sequence from clone BDGP:LP07
15326.8	5.7	FB:FBgn0029838 /sym=CG4666 /name= /prod= /func= /map=5D2-5D2 /transc=CT15013 /len=729 /GB:AE003436
6663.7	~5.6	FB:FBgn0035304 /sym=CG1282 /name= /prod=titin/twitchin-like /func=cell adhesion /map=62C3-62C3 /transc=CT2687 /len=2392 /GB:AE003473
4180.6	~5.6	FB:FBgn0028922 /sym=BG:DS00929.8 /name= /prod= /func= /map=35C1-35C1 /transc=CT12287 /len=1508 /GB:AE003646
30948	5.6	FB:FBgn0030394 /sym=CG2560 /name= /prod=cuticle protein-like /func=structural protein /map=11B7-11B7 /transc=CT8657 /len=893 /GB:AE003489
4313.6	~5.6	FB:FBgn0036185 /sym=CG7346 /name= /prod=ATP-binding cassette transporter /func=enzyme /map=68C10-68C11 /transc=CT22647 /len=1794 /GB:AE003544
2815.4	~5.6	FB:FBgn0033290 /sym=CG8698 /name= /prod= /func= /map=44C1-44C1 /transc=CT8775 /len=504 /GB:AE003837
4744	~5.5	FB:FBgn0035289 /sym=CG12026 /name= /prod= /func= /map=62B9-62B9 /transc=CT1797 /len=1455 /GB:AE003473 /note=3prime sequence from clone BDGP:LP10272.3prime-hit
4859.8	5.5	FB:FBgn0031872 /sym=CG9211 /name= /prod= /func=cell adhesion /map=27C5-27C6 /transc=CT26314 /len=3247 /GB:AE003615 /note=3prime sequence from clone BDGP:GH03927.3prime-hit
33949.7	5.5	FB:FBgn0032497 /sym=CG6043 /name= /prod= /func= /map=34A11-34B1 /transc=CT18935 /len=3263 /GB:AE003639

3265 ~5.5 FB:FBgn0035457 /sym=CG12604 /name= /prod= /func= /map=63E8-63E8 /transc=CT34822 /len=936 /GB:AE003479

10486.1 5.4 FB:FBgn0037534 /sym=CG2781 /name= /prod= /func=1,3-beta-glucan synthase /map=84E5-84E5 /transc=CT9465 /len=831 /GB:AE003677

46425 5.3 FB:FBgn0034920 /sym=CG5597 /name= /prod= /func= /map=60A8-60A8 /transc=CT17698 /len=897 /GB:AE003462 /note=3prime sequence from clone BDGP:GH04238.3prime-hit

109250.5 5.3 FB:FBgn0035985 /sym=CG3672 /name= /prod= /func=structural protein /map=67B2-67B2 /transc=CT12317 /len=997 /GB:AE003552 /note=3prime sequence from clone BDGP:GH12638.3prime-hit

5817 ~5.3 FB:FBgn0030065 /sym=CG12075 /name= /prod= /func=transcription factor /map=8B4-8B4 /transc=CT5152 /len=3406 /GB:AE003445 /note=3prime sequence from clone BDGP:LD23217.3prime-hit

5570.1 5.3 FB:FBgn0032230 /sym=CG13139 /name= /prod= /func= /map=31D10-31D10 /transc=CT32379 /len=807 /GB:AE003628

5566.8 ~5.3 FB:FBgn0037805 /sym=CG11871 /name= /prod= /func= /map=86A1-86A1 /transc=CT37022 /len=3575 /GB:AE003686

7060.1 5.3 FB:FBgn0035705 /sym=CG8352 /name= /prod= /func= /map=65B4-65B5 /transc=CT24625 /len=1728 /GB:AE003562 /note=3prime sequence from clone BDGP:LD26402.3prime-hit

54759.6 5.3 FB:FBgn0031971 /sym=CG7224 /name= /prod= /func= /map=28D11-28D11 /transc=CT22279 /len=755 /GB:AE003619 /note=3prime sequence from clone BDGP:GH18422.3prime-hit

16382.2 5.2 FB:FBgn0033509 /sym=CG12908 /name= /prod=nidogen-like /func=cell adhesion /map=47A1-47A1 /transc=CT32053 /len=4591 /GB:AE003830 /note=3prime sequence from clone BDGP:LD35637.3prime-hit

26464.9 5.2 FB:FBgn0036985 /sym=CG5847 /name= /prod= /func=structural protein /map=77B9-77B9 /transc=CT18331 /len=6855 /GB:AE003591

7616.8 5.2 FB:FBgn0022701 /sym=Cht3 /name=Chitinase 3 /prod=chitinase /func=chitinase ; EC:3.2.1.14 /map=40D5-40D5 /transc=CT40797 /len=3899 /GB:AE002743

5485.4 5.2 FB:FBgn0039690 /sym=CG1969 /name= /prod= /func=glucosamine-phosphate N-acetyltransferase ; EC:2.3.1.4 /map=99C1-99C1 /transc=CT4002 /len=1206 /GB:AE003771 /note=3prime sequence from clone BDGP:LD35637.3prime-hit

17808.5 5.2 FB:FBgn0029898 /sym=CG14439 /name= /prod=permease-like /func=transporter /map=6C11-6C11 /transc=CT34101 /len=1608 /GB:AE003438

9052.4 5.2 FB:FBgn0032993 /sym=CG18117 /name= /prod=chitinase-like /func=enzyme /map=40E1-40E1 /transc=CT40795 /len=1393 /GB:AE002743 /note=3prime sequence from clone BDGP:LP05745.3prime-hit

13143.1 5.2 FB:FBgn0032601 /sym=yellow-b /name=yellow-b /prod= /func= /map=36A8-36A8 /transc=CT39906 /len=1625 /GB:AE003652 /note=3prime sequence from clone BDGP:LD43175.3prime-hit

12986.1 5.1 FB:FBgn0035398 /sym=CG1869 /name= /prod=chitinase /func=enzyme /map=63B8-63B8 /transc=CT5720 /len=2346 /GB:AE003477

4051.1 ~5.1 FB:FBgn0039658 /sym=CG11956 /name= /prod= /func= /map=99A5-99A5 /transc=CT39158 /len=2937 /GB:AE003768 /note=3prime sequence from clone BDGP:LD35296.3prime-hit

5334.1 5.1 FB:FBgn0010388 /sym=Dro /name=Drosocin /prod=drosocin /func=antibacterial response protein /map=51C2-51C2 /transc=CT30318 /len=195 /GB:AE003813

197731.7 5 FB:FBgn0031908 /sym=CG5177 /name= /prod= /func=enzyme /map=27F6-27F6 /transc=CT16575 /len=980 /GB:AE003617 /note=3prime sequence from clone BDGP:LD18740.3prime-hit

2785.1 ~5.0 FB:FBgn0000152 /sym=Axs /name=Abnormal X segregation /prod= /func= /map=15A1-15A1 /transc=CT27428 /len=2396 /GB:AE003503

197877.5 5 FB:FBgn0032281 /sym=CG17107 /name= /prod= /func= /map=32A1-32A1 /transc=CT33651 /len=291 /GB:AE003629

53720.9 5 FB:FBgn0002440 /sym=l(3)mbn /name=lethal (3) malignant blood neoplasm /prod= /func= /map=65A4-65A4 /transc=CT29378 /len=1957 /GB:AE003563

12614.8 5 FB:FBgn0035103 /sym=CG7047 /name= /prod=arrestin-like /func= /map=61A5-61A5 /transc=CT42521 /len=1187 /GB:AE003467

13720.8 5 FB:FBgn0039894 /sym=CG10323 /name= /prod=fibulin/fibrillin-like /func=cell adhesion /map=102A1-102A3 /transc=CT7856 /len=1684 /GB:AE003844

8379.4 5 FB:FBgn0036271 /sym=CG10335 /name= /prod=porphobilinogen synthase-like /func=enzyme /map=69A3-69A3 /transc=CT29022 /len=984 /GB:AE003542

67255.1 5 FB:FBgn0034420 /sym=CG10737 /name= /prod=protein kinase-like /func=protein kinase /map=56B6-56C1 /transc=CT21097 /len=3105 /GB:AE003797 /note=3prime sequence from clone BDGP:GM003535

3691.1 ~4.9 FB:FBgn0013718 /sym=nuf /name=nuclear fallout /prod= /func=cytoskeletal structural protein /map=70D2-70D2 /transc=CT23449 /len=2261 /GB:AE003535

12605.8 4.9 FB:FBgn0033130 /sym=CG12843 /name=Tetraspanin 42Ei /prod=tetraspanin /func= /map=42E1-42E1 /transc=CT31975 /len=967 /GB:AE003842

17969.2 4.9 FB:FBgn0040631 /sym=CG13249 /name= /prod= /func= /map=77C2-77C2 /transc=CT32502 /len=432 /GB:AE003591 /note=3prime sequence from clone BDGP:LD43096.3prime-hit

3852.4 ~4.9 FB:FBgn0032382 /sym=CG14935 /name= /prod=maltase 2-like /func=enzyme /map=33B2-33B2 /transc=CT34763 /len=1790 /GB:AE003634

105433 4.9 FB:FBgn0038774 /sym=CG5023 /name= /prod=calponin-like /func=ligand binding or carrier /map=92D2-92D2 /transc=CT16114 /len=697 /GB:AE003729 /note=3prime sequence from clone BDGP:GM003535

84895.4 4.9 FB:FBgn0032774 /sym=CG17549 /name= /prod= /func= /map=37E1-37E1 /transc=CT38763 /len=1051 /GB:AE003662 /note=3prime sequence from clone BDGP:GH19142.3prime-hit

1602.3 ~4.9 FB:FBgn0035155 /sym=CG12015 /name= /prod= /func=transporter /map=61C9-61C9 /transc=CT1655 /len=728 /GB:AE003469

3659 ~4.8 FB:FBgn0036561 /sym=CG5891 /name= /prod=ankyrin-like /func=cytoskeletal structural protein /map=72D1-72D3 /transc=CT18415 /len=3517 /GB:AE003528

13249.8 4.8 FB:FBgn0038250 /sym=CG3505 /name= /prod= /func=endopeptidase /map=88C11-88C11 /transc=CT11805 /len=1161 /GB:AE003705 /note=3prime sequence from clone BDGP:LP10895.3prime-hit

11889.5 4.7 FB:FBgn0033724 /sym=CG8501 /name= /prod= /func= /map=49A2-49A2 /transc=CT24861 /len=902 /GB:AE003822 /note=3prime sequence from clone BDGP:HL07915.3prime-hit

9091.4 4.7 FB:FBgn0027617 /sym=Rbp9 /name= /prod= /func=RNA binding /map=23C1-23C2 /transc=CT38165 /len=3320 /GB:AE003581 /note=3prime sequence from clone BDGP:GH07919.3prime-hit

19529.2 4.7 FB:FBgn0036454 /sym=CG17839 /name= /prod= /func=cell adhesion /map=71A1-71A1 /transc=CT39634 /len=3570 /GB:AE003533

33251.3 4.7 FB:FBgn0034603 /sym=CG9480 /name= /prod=glycogenin glucosyltransferase-like /func=enzyme /map=57C7-57C7 /transc=CT26834 /len=950 /GB:AE003453

4041.9 ~4.7 FB:FBgn0003888 /sym=betaTub60D /name=betaTubulin6D /prod=beta-tubulin /func=cytoskeletal structural protein /map=60C5-60C5 /transc=CT11425 /len=1542 /GB:AE003463

12224.7 4.7 FB:FBgn0038151 /sym=CG17044 /name= /prod= /func= /map=87E11-87E11 /transc=CT37841 /len=1281 /GB:AE003700

9605 4.6 FB:FBgn0029662 /sym=CG12206 /name= /prod= /func= /map=3D6-3D6 /transc=CT10991 /len=1446 /GB:AE003427

2551.7 ~4.6 FB:FBgn0034112 /sym=CG3896 /name= /prod= /func=ligand binding or carrier /map=53A3-53A4 /transc=CT12657 /len=3264 /GB:AE003807

35881 4.6 FB:FBgn0037067 /sym=CG11310 /name= /prod= /func=structural protein /map=78C8-78C8 /transc=CT23453 /len=384 /GB:AE003594

66109.3 4.6 FB:FBgn0033679 /sym=CG8888 /name= /prod= /func=enzyme /map=48E4-48E6 /transc=CT25512 /len=1694 /GB:AE003823 /note=3prime sequence from clone BDGP:GH26015.3prime-hit

12875.6 4.6 FB:FBgn0033630 /sym=CG13200 /name= /prod= /func= /map=47F6-47F6 /transc=CT32444 /len=309 /GB:AE003826

6942.7 4.6 FB:FBgn0034522 /sym=CG13432 /name= /prod= /func= /map=57A9-57A10 /transc=CT32789 /len=1355 /GB:AE003791

80254.4 4.6 FB:FBgn0040992 /sym=CG10570 /name= /prod= /func= /map=37B1-37B1 /transc=CT29654 /len=802 /GB:AE003660 /note=3prime sequence from clone BDGP:GH23934.3prime-hit

4870.5 4.6 FB:FBgn0030798 /sym=CG13003 /name= /prod= /func= /map=15A10-15A10 /transc=CT32210 /len=3477 /GB:AE003503

5541.3 4.6 FB:FBgn0029843 /sym=CG5894 /name= /prod=endothelin-converting enzyme-like zinc metalloendopeptidase (M13 peptidase)-like /func=endopeptidase /map=5D2-5D2 /transc=CT18487 /len=2314

2715.6 ~4.5 FB:FBgn0038896 /sym=CG6328 /name= /prod= /func= /map=93F4-93F4 /transc=CT19790 /len=1317 /GB:AE003736

2903.8 ~4.5 FB:FBgn0038977 /sym=CG5376 /name= /prod= /func=motor /map=94B4-94B4 /transc=CT17018 /len=763 /GB:AE003739

4714.4 ~4.5 FB:FBgn0039433 /sym=CG5467 /name= /prod= /func= /map=97B9-97B9 /transc=CT17334 /len=2934 /GB:AE003757 /note=3prime sequence from clone BDGP:GH07007.3prime-hit

22217.6 4.5 FB:FBgn0037697 /sym=CG9363 /name= /prod= /func=enzyme /map=85D18-85D18 /transc=CT26609 /len=1037 /GB:AE003682 /note=3prime sequence from clone BDGP:GH17960.3prime-hit

12420.4 4.5 FB:FBgn0037721 /sym=CG9427 /name= /prod= /func= /map=85E1-85E2 /transc=CT26734 /len=836 /GB:AE003683 /note=3prime sequence from clone BDGP:GH19763.3prime-hit

6522.7 4.5 FB:FBgn0033917 /sym=CG8503 /name= /prod= /func= /map=50E8-50E8 /transc=CT24853 /len=1865 /GB:AE003815 /note=3prime sequence from clone BDGP:GH11294.3prime-hit

3016.2 ~4.5 FB:FBgn0031193 /sym=CG17602 /name= /prod= /func= /map=20A1-20A1 /transc=CT34368 /len=1152 /GB:AE003574

10559.3 4.4 FB:FBgn0038088 /sym=CG10126 /name= /prod=calcium binding protein-like /func=ligand binding or carrier /map=87D3-87D3 /transc=CT28495 /len=879 /GB:AE003697 /note=3prime sequence from clone BDGP:GH19182.3prime-hit

16478 4.4 FB:FBgn0015801 /sym=Reg-5 /name=Rhythmically expressed gene 5 /prod= /func= /map=60D15-60D16 /transc=CT9939 /len=1650 /GB:AE003465 /note=3prime sequence from clone BDGP:HL047

47971 4.4 FB:FBgn0036547 /sym=CG17032 /name= /prod= /func= /map=72C1-72C1 /transc=CT32296 /len=1007 /GB:AE003529

17963.1 4.4 FB:FBgn0033109 /sym=CG9446 /name= /prod= /func=chaperone /map=42C8-42C8 /transc=CT11617 /len=1880 /GB:AE003790

7878.7 4.4 FB:FBgn0035740 /sym=CG18138 /name= /prod= /func= /map=65E5-65E5 /transc=CT40868 /len=2170 /GB:AE003560 /note=3prime sequence from clone BDGP:GH12052.3prime-hit

219587.4 4.4 FB:FBgn0035917 /sym=CG6416 /name= /prod= /func=enzyme /map=66D9-66D10 /transc=CT20013 /len=1175 /GB:AE003554 /note=3prime sequence from clone BDGP:GH19182.3prime-hit

3588.9 ~4.4 FB:FBgn0036101 /sym=CG6449 /name= /prod=ninjurin /func=cell adhesion /map=67E5-67E5 /transc=CT20102 /len=591 /GB:AE003547
 2988.3 ~4.4 BDGP:SD1276.3prime-hit /ESTpos=maps 3prime of FB:FBgn0003638 /sym=su(w[a]) /name=suppressor of white-apricot /prod= /func=RNA binding /map=1E1-1E1 /transc=CT1162 /len=584
 110661.9 4.3 FB:FBgn0034044 /sym=CG12969 /name= /prod= /func=enzyme /map=52C7-52C8 /transc=CT32161 /len=1203 /GB:AE003809
 34249.9 4.3 FB:FBgn0032685 /sym=CG10211 /name= /prod=peroxidase-like /func=enzyme /map=37A1-37A1 /transc=CT28633 /len=3691 /GB:AE003659 /note=3prime sequence from clone BDGP:LD42267.3p
 25547.3 4.3 FB:FBgn0033033 /sym=CG11066 /name= /prod= /func=endopeptidase /map=41E3-41E4 /transc=CT30959 /len=1377 /GB:AE003785
 11289.1 4.3 FB:FBgn0030355 /sym=CG2467 /name= /prod= /func= /map=10F7-10F8 /transc=CT8145 /len=3418 /GB:AE003487 /note=3prime sequence from clone BDGP:GH09980.3prime-hit
 82296.8 4.3 FB:FBgn0031037 /sym=CG14207 /name= /prod=heat shock protein HSP20-like /func=chaperone /map=18D8-18D8 /transc=CT33820 /len=1175 /GB:AE003512 /note=3prime sequence from clone BL
 37898.4 4.3 FB:FBgn0000275 /sym=Pka-R1 /name=cAMP-dependent protein kinase R1 /prod=cAMP-dependent protein kinase, regulatory subunit /func=cAMP-dependent protein kinase regulator /map=77F1-77F1 /transc=CT33820 /len=1175 /GB:AE003512 /note=3prime sequence from clone BL
 11320.1 4.3 BDGP:GH4896.3prime-hit /ESTpos=maps in FB:FBgn0033462 /sym=CG12138 /name= /prod= /func=DNA binding /map=46C4-46C4 /transc=CT7814 /len=700
 3702.5 ~4.3 FB:FBgn0011656 /sym=Mef2 /name=Myocyte enhancing factor 2 /prod= /func=RNA polymerase II transcription factor /map=46C6-46C7 /transc=CT3413 /len=3211 /GB:AE003831 /note=3prime sequence from clone BDGP:GH17145.3p
 4432.4 4.3 FB:FBgn0031938 /sym=CG18590 /name= /prod= /func= /map=28C2-28C2 /transc=CT42499 /len=176 /GB:AE003618
 6566.3 4.3 FB:FBgn0036673 /sym=CG11915 /name= /prod= /func=ligand binding or carrier /map=73D3-73D3 /transc=CT37088 /len=2999 /GB:AE003525 /note=3prime sequence from clone BDGP:GH17145.3p
 1895.4 ~4.3 FB:FBgn0033936 /sym=CG17386 /name= /prod= /func=RNA binding /map=51A1-51A1 /transc=CT33484 /len=2609 /GB:AE003814
 16413.7 4.3 FB:FBgn0032456 /sym=CG6214 /name= /prod=ATP-binding cassette transporter; multidrug resistance protein-like /func=ion channel /map=33F2-33F3 /transc=CT19412 /len=6461 /GB:AE003637 /note=3prime sequence from clone BDGP:GH17145.3p
 26327.7 4.2 FB:FBgn0033133 /sym=CG12841 /name= /prod= /func= /map=42E1-42E1 /transc=CT31973 /len=648 /GB:AE003842
 3681.9 ~4.2 FB:FBgn0004620 /sym=Glu-RIIA /name=Glutamate receptor IIA /prod=glutamate receptor /func=glutamate receptor /map=25F1-25F1 /transc=CT21587 /len=3022 /GB:AE003610
 20932.2 4.2 FB:FBgn0029517 /sym=CG13377 /name= /prod= /func= /map=1A5-1A5 /transc=CT32709 /len=993 /GB:AE003417
 2247.7 ~4.2 FB:FBgn0038987 /sym=CG6926 /name= /prod= /func= /map=94B8-94B8 /transc=CT21454 /len=789 /GB:AE003739
 3098.4 ~4.2 FB:FBgn0032616 /sym=CG15131 /name= /prod= /func= /map=36A10-36A10 /transc=CT35026 /len=862 /GB:AE003652
 3047.3 ~4.2 FB:FBgn0022703 /sym=Cht1 /name=Chitinase 1 /prod=chitinase /func=chitinase ; EC:3.2.1.14 /map=40D5-40E1 /transc=CT39094 /len=1527 /GB:AE002743
 11736.9 4.2 FB:FBgn0038720 /sym=CG6231 /name= /prod=organic cation transporter /func=transporter /map=92A13-92A13 /transc=CT19536 /len=1743 /GB:AE003727
 23343.7 4.2 FB:FBgn0030876 /sym=CG6762 /name= /prod= /func= /map=16D7-16D7 /transc=CT20293 /len=580 /GB:AE003507
 175868.2 4.2 FB:FBgn0033729 /sym=CG8510 /name= /prod=cuticle protein-like /func=structural protein /map=49A3-49A3 /transc=CT24877 /len=381 /GB:AE003822
 99849.6 4.2 FB:FBgn0001258 /sym=ImpL3 /name=Ecdysone-inducible gene L3 /prod=L-lactate dehydrogenase /func=L-lactate dehydrogenase ; EC:1.1.1.27 /map=65A8-65A8 /transc=CT28577 /len=999 /GB:AE003662
 180907.8 4.1 FB:FBgn0032777 /sym=CG18576 /name= /prod= /func= /map=37E1-37E1 /transc=CT42454 /len=1593 /GB:AE003662
 58068.8 4.1 FB:FBgn0037069 /sym=CG7658 /name= /prod=cuticle protein-like /func=structural protein /map=78C8-78C8 /transc=CT23381 /len=511 /GB:AE003594
 10733.4 4.1 FB:FBgn0017397 /sym=how /name=held out wings /prod= /func=RNA binding /map=94A1-94A2 /transc=CT28865 /len=1922 /GB:AE003737
 3085.2 ~4.1 FB:FBgn0032851 /sym=CG13970 /name= /prod= /func= /map=38C1-38C1 /transc=CT33523 /len=618 /GB:AE003665
 3880.9 ~4.1 FB:FBgn0004852 /sym=Ac76E /name=Adenylyl cyclase 76E /prod=adenylate cyclase /func=adenylate cyclase ; EC:4.6.1.1 /map=76D8-76E1 /transc=CT23940 /len=5189 /GB:AE003515 /note=3prime sequence from clone BDGP:GH17145.3p
 6721 4.1 FB:FBgn0030759 /sym=CG13014 /name= /prod= /func= /map=14F2-14F2 /transc=CT32227 /len=699 /GB:AE003502
 23837.1 4.1 FB:FBgn0032025 /sym=CG7778 /name= /prod= /func= /map=29B1-29B2 /transc=CT23662 /len=1222 /GB:AE003620 /note=3prime sequence from clone BDGP:GH17475.3prime-hit
 201594.6 4.1 FB:FBgn0014863 /sym=Mlp84B /name=Muscle LIM protein at 84B /prod=muscle LIM protein at 84B /func=transcription factor /map=84C3-84C3 /transc=CT1058 /len=1863 /GB:AE003672

17444.3	4.1	FB:FBgn0038842 /sym=CG5630 /name= /prod= /func= /map=93A4-93A4 /transc=CT17794 /len=1360 /GB:AE003732
4902	4.1	FB:FBgn0037213 /sym=CG12581 /name= /prod= /func= /map=82A1-82A1 /transc=CT34405 /len=2382 /GB:AE003607 /note=3prime sequence from clone BDGP:GM02933.3prime-hit
3392.7	~4.1	FB:FBgn0031700 /sym=CG14022 /name= /prod= /func=enzyme /map=25D5-25D5 /transc=CT33581 /len=334 /GB:AE003609
20768.8	4.1	FB:FBgn0034067 /sym=CG8399 /name= /prod= /func= /map=52E1-52E3 /transc=CT18617 /len=2268 /GB:AE003808 /note=3prime sequence from clone BDGP:LD47639.3prime-hit
2482.5	~4.0	FB:FBgn0037275 /sym=CG14655 /name= /prod= /func=nucleic acid binding /map=82E1-82E1 /transc=CT34432 /len=2167 /GB:AE003605 /note=3prime sequence from clone BDGP:GH23506.3prime-hit
8908.3	4	FB:FBgn0034575 /sym=CG15652 /name= /prod= /func= /map=57B16-57B16 /transc=CT35836 /len=1311 /GB:AE003452 /note=3prime sequence from clone BDGP:GH14953.3prime-hit
4181.8	4	FB:FBgn0033532 /sym=CG18380 /name= /prod= /func= /map=47A11-47A11 /transc=CT41783 /len=657 /GB:AE003829
3507.7	~4.0	FB:FBgn0008649 /sym=dei /name=delilah /prod= /func=specific RNA polymerase II transcription factor /map=97B2-97B2 /transc=CT17256 /len=1862 /GB:AE003756 /note=3prime sequence from clone BDGP:GM02933.3prime-hit
5096.9	4	FB:FBgn0022800 /sym=HD-14 /name= /prod=fibroblast growth factor receptor-like /func=protein tyrosine kinase ; EC:2.7.1.11 inferred from sequence similarity /map=96C2-96C2 /transc=CT28777 /len=1000
8693.5	4	FB:FBgn0039667 /sym=CG2010 /name= /prod= /func= /map=99B3-99B3 /transc=CT6431 /len=1752 /GB:AE003769 /note=3prime sequence from clone BDGP:GH26184.3prime-hit
117753.4	4	FB:FBgn0004028 /sym=wupA /name=wings up A /prod=troponin I /func=cytoskeletal structural protein /map=16F7-17A1 /transc=CT40012 /len=389 /GB:AE003507
1575.9	~4.0	FB:FBgn0033345 /sym=CG13750 /name= /prod= /func= /map=44F9-44F9 /transc=CT33227 /len=228 /GB:AE003835
3776.4	~4.0	FB:FBgn0030758 /sym=CG9819 /name= /prod= /func=protein phosphatase /map=14F1-14F1 /transc=CT27722 /len=1724 /GB:AE003502
95430.6	4	FB:FBgn0032284 /sym=CG7294 /name= /prod= /func= /map=32A1-32A1 /transc=CT22525 /len=527 /GB:AE003629
43777.9	4	FB:FBgn0031097 /sym=CG17052 /name= /prod=peritrophin-like /func=structural protein /map=19C1-19C1 /transc=CT37860 /len=1383 /GB:AE003572
4267.8	4	FB:FBgn0032279 /sym=CG17104 /name= /prod= /func= /map=32A1-32A1 /transc=CT38006 /len=1746 /GB:AE003629 /note=3prime sequence from clone BDGP:LD16579.3prime-hit
11681.3	4	FB:FBgn0039742 /sym=CG15528 /name= /prod=protein phosphatase-like /func=protein phosphatase /map=99D5-99D5 /transc=CT35642 /len=639 /GB:AE003772
8955.5	4	FB:FBgn0036674 /sym=CG11916 /name= /prod= /func=transcription factor /map=73D4-73D4 /transc=CT37092 /len=707 /GB:AE003525
5826.7	4	FB:FBgn0022341 /sym=CG17467 /name= /prod= /func= /map=102E3-102E3 /transc=CT38621 /len=1002 /GB:AE003846
4154	4	FB:FBgn0034701 /sym=CG13505 /name= /prod= /func= /map=58C5-58C5 /transc=CT32873 /len=1011 /GB:AE003456
15797.8	3.9	FB:FBgn0036675 /sym=CG9959 /name= /prod= /func=transcription factor /map=73D4-73D5 /transc=CT28055 /len=883 /GB:AE003525
3352.7	~3.9	FB:FBgn0032178 /sym=CG4804 /name= /prod=serpin /func=serpin /map=31A1-31A1 /transc=CT15443 /len=1259 /GB:AE003627
32617.1	3.9	FB:FBgn0028855 /sym=BG:DS07721.3 /name= /prod= /func= /map=35B4-35B4 /transc=CT35230 /len=465 /GB:AE003644
6591.7	3.9	FB:FBgn0038674 /sym=CG14285 /name= /prod= /func=transcription factor binding /map=91E4-91E4 /transc=CT33914 /len=894 /GB:AE003724
77573.9	3.9	FB:FBgn0036572 /sym=CG5165 /name= /prod=phosphoglucosyltransferase-like /func=enzyme /map=72D7-72D7 /transc=CT16539 /len=1766 /GB:AE003528 /note=3prime sequence from clone BDGP:LD16579.3prime-hit
18985.9	3.9	FB:FBgn0035710 /sym=SP1173 /name= /prod= /func= /map=65C1-65C1 /transc=CT28481 /len=2494 /GB:AE003561 /note=3prime sequence from clone BDGP:GH14073.3prime-hit
182724	3.9	FB:FBgn0004507 /sym=GlyP /name=Glycogen phosphorylase /prod=glycogen phosphorylase /func=phosphorylase ; EC:2.4.1.1 inferred from direct assay /map=22C3-22C3 /transc=CT22383 /len=287
7012.9	3.9	FB:FBgn0032474 /sym=CG9828 /name= /prod= /func=chaperone /map=34A8-34A8 /transc=CT27734 /len=1253 /GB:AE003639
3224.5	~3.9	FB:FBgn0037972 /sym=CG10005 /name= /prod= /func= /map=87A8-87A8 /transc=CT28191 /len=684 /GB:AE003693
16608.7	3.9	FB:FBgn0004577 /sym=Pxd /name=Peroxidase /prod=peroxidase /func=peroxidase ; EC:1.11.1.7 /map=89E11-89E11 /transc=CT11695 /len=2071 /GB:AE003716
6882.7	3.8	FB:FBgn0035494 /sym=CG14993 /name= /prod=fumarylacetoacetase-like /func=enzyme /map=64A5-64A5 /transc=CT34846 /len=1050 /GB:AE003480
2827.4	~3.8	FB:FBgn0040587 /sym=CG17618 /name= /prod= /func= /map=94C4-94C4 /transc=CT38876 /len=576 /GB:AE003740

3936.3 3.8 FB:FBgn0032332 /sym=CG14917 /name= /prod= /func= /map=32D1-32D1 /transc=CT34744 /len=1863 /GB:AE003630

1295.5 ~3.8 FB:FBgn0035385 /sym=CG2114 /name= /prod=G-protein coupled receptor-like /func=G protein linked receptor /map=63B2-63B2 /transc=CT2366 /len=1650 /GB:AE003476

12277.7 3.8 BDGP:GH1742.3prime-hit /ESTpos=maps in FB:FBgn0033441 /sym=CG1776 /name= /prod=myosin light chain kinase /func=protein kinase /map=46A3-46A4 /transc=CT5322 /len=488

6657 3.8 FB:FBgn0037167 /sym=CG11425 /name= /prod=phosphatidate phosphohydrolase type 2-like /func=enzyme /map=79E4-79E4 /transc=CT21215 /len=956 /GB:AE003597

9002.7 3.8 FB:FBgn0032785 /sym=CG10026 /name= /prod=alpha-tocopherol transfer relative protein /func=transcription factor /map=37E3-37E3 /transc=CT28189 /len=1143 /GB:AE003663 /note=3prime sequ

100295 3.8 FB:FBgn0014141 /sym=cher /name=cheerio /prod=filamin /func=actin binding /map=89F1-89F1 /transc=CT12961 /len=7617 /GB:AE003716 /note=3prime sequence from clone BDGP:SD05640.3pri

3312.8 ~3.8 FB:FBgn0010015 /sym=CanA1 /name=Calcineurin A1 /prod=protein serine/threonine phosphatase /func=protein serine/threonine phosphatase ; EC:3.1.3.16 | inferred from sequence similarity /map=100

372610.8 3.8 FB:FBgn0032280 /sym=CG17105 /name= /prod= /func= /map=32A1-32A1 /transc=CT33652 /len=312 /GB:AE003629

2216.2 ~3.8 FB:FBgn0030586 /sym=CG12539 /name= /prod=glucose dehydrogenase (acceptor) /func=enzyme /map=13A1-13A1 /transc=CT34058 /len=1503 /GB:AE003497

241944.8 3.8 FB:FBgn0032283 /sym=CG7296 /name= /prod= /func= /map=32A1-32A1 /transc=CT22519 /len=575 /GB:AE003629

6626.8 3.8 FB:FBgn0036550 /sym=CG17026 /name= /prod= /func= /map=72C1-72C1 /transc=CT37805 /len=855 /GB:AE003529

3162.7 ~3.8 FB:FBgn0033092 /sym=CG9422 /name= /prod= /func= /map=42C1-42C1 /transc=CT26724 /len=621 /GB:AE003789

928.4 ~3.8 FB:FBgn0038451 /sym=CG14893 /name= /prod= /func=enzyme /map=89D6-89D6 /transc=CT34717 /len=1491 /GB:AE003714

70266.1 3.8 FB:FBgn0031198 /sym=CG13238 /name= /prod= /func= /map=20A1-20A1 /transc=CT32487 /len=405 /GB:AE003574

266780.6 3.8 FB:FBgn0011296 /sym=l(2)efl /name=lethal (2) essential for life /prod= /func=chaperone /map=59F4-59F4 /transc=CT14702 /len=717 /GB:AE003461 /note=3prime sequence from clone BDGP:GH0

8973.7 3.8 FB:FBgn0035303 /sym=CG5699 /name= /prod= /func=cell adhesion /map=62C3-62C3 /transc=CT2689 /len=1990 /GB:AE003473 /note=3prime sequence from clone BDGP:GH09541.3prime-hit

3651.8 3.8 FB:FBgn0031534 /sym=CG2774 /name= /prod=sorting nexin 1-like /func=transporter /map=23F2-23F2 /transc=CT9125 /len=1450 /GB:AE003579

6549.3 3.8 FB:FBgn0031421 /sym=CG9867 /name= /prod= /func= /map=22E1-22E2 /transc=CT27848 /len=1826 /GB:AE003583 /note=3prime sequence from clone BDGP:GH05422.3prime-hit

2570.4 ~3.8 FB:FBgn0039927 /sym=CG11155 /name= /prod=glutamate receptor-like /func=ion channel /map=102E7-102F1 /transc=CT30863 /len=2062 /GB:AE003846

2175 ~3.7 FB:FBgn0031080 /sym=CG12655 /name= /prod= /func= /map=19A3-19A3 /transc=CT35310 /len=496 /GB:AE002611

27906.3 3.7 FB:FBgn0033034 /sym=CG15900 /name= /prod= /func= /map=41E4-41E4 /transc=CT34160 /len=519 /GB:AE003785

38758.8 3.7 FB:FBgn0032422 /sym=CG6579 /name= /prod= /func= /map=33C3-33C4 /transc=CT20347 /len=834 /GB:AE003635

5936.9 3.7 FB:FBgn0023023 /sym=CRMP /name=Collapsin Response Mediator Protein /prod= /func=enzyme /map=83B3-83B4 /transc=CT3290 /len=2554 /GB:AE003602 /note=3prime sequence from clone BL

32297.6 3.7 FB:FBgn0038096 /sym=CG7340 /name= /prod= /func= /map=87D7-87D7 /transc=CT22347 /len=1953 /GB:AE003698 /note=3prime sequence from clone BDGP:LD13869.3prime-hit

189512.7 3.7 FB:FBgn0038009 /sym=CG17738 /name= /prod= /func= /map=87B8-87B8 /transc=CT34537 /len=333 /GB:AE003695

1592.8 ~3.7 FB:FBgn0037813 /sym=CG17100 /name= /prod= /func= /map=86A5-86A5 /transc=CT34464 /len=2030 /GB:AE003687

7700.4 3.7 FB:FBgn0034797 /sym=CG12781 /name= /prod= /func=protein kinase /map=59B4-59B4 /transc=CT36793 /len=4470 /GB:AE003459 /note=3prime sequence from clone BDGP:GH04942.3prime-hit

110642.8 3.7 BDGP:LD43683.3prime-hit /ESTpos=maps in FB:FBgn0031097 /sym=CG17052 /name= /prod=peritrophin-like /func=structural protein /map=19C1-19C1 /transc=CT3786 /len=595

19441.5 3.7 FB:FBgn0035550 /sym=CG11349 /name= /prod= /func=structural protein /map=64B12-64B12 /transc=CT31656 /len=1880 /GB:AE003481

15639.1 3.7 FB:FBgn0015276 /sym=Pcmt /name=Protein-L-isoaspartate (D-aspartate) O-methyltransferase /prod=protein-L-isoaspartate (D-aspartate) O-methyltransferase /func=protein-L-isoaspartate (D-aspartate)

5993.8 3.7 FB:FBgn0033309 /sym=CG8735 /name= /prod= /func=electron transfer /map=44D1-44D2 /transc=CT8725 /len=1421 /GB:AE003836 /note=3prime sequence from clone BDGP:GH24644.3prime-hit

1907.1 ~3.7 FB:FBgn0040874 /sym=CG15600 /name= /prod= /func= /map=13E12-13E12 /transc=CT35723 /len=153 /GB:AE003499

114720.4 3.7 FB:FBgn0036902 /sym=CG8748 /name= /prod= /func= /map=76C4-76C4 /transc=CT25246 /len=1263 /GB:AE003516

152922.3 3.7 FB:FBgn0036901 /sym=CG8756 /name= /prod=low-density lipoprotein-receptor-like /func=receptor /map=76C3-76C3 /transc=CT25252 /len=2157 /GB:AE003516 /note=3prime sequence from clone

1914 ~3.7 FB:FBgn0032469 /sym=CG9932 /name= /prod= /func=nucleic acid binding /map=34A5-34A5 /transc=CT27960 /len=6516 /GB:AE003638

2709.8 ~3.7 FB:FBgn0040981 /sym=CG15268 /name= /prod= /func= /map=35B9-35B9 /transc=CT35215 /len=195 /GB:AE003645

44801.9 3.7 FB:FBgn0034042 /sym=CG8242 /name= /prod= /func=transcription factor /map=52C7-52C7 /transc=CT24455 /len=4875 /GB:AE003809

5279 3.6 FB:FBgn0033502 /sym=CG12910 /name= /prod= /func= /map=46F7-46F7 /transc=CT32055 /len=1690 /GB:AE003830 /note=3prime sequence from clone BDGP:GH17442.3prime-hit

4003.4 3.6 FB:FBgn0031064 /sym=CG12531 /name= /prod=amino-acid permease /func=transporter /map=18E3-18E5 /transc=CT33850 /len=2415 /GB:AE003513

67759 3.6 FB:FBgn0035612 /sym=CG10625 /name= /prod= /func= /map=64E2-64E2 /transc=CT29764 /len=3883 /GB:AE003565 /note=3prime sequence from clone BDGP:LD39545.3prime-hit

4178.9 ~3.6 FB:FBgn0034194 /sym=CG15611 /name= /prod=guanyl-nucleotide exchange factor /func=signal transduction /map=53F12-53F13 /transc=CT35747 /len=1742 /GB:AE003804 /note=3prime sequence

12376.6 3.6 FB:FBgn0000565 /sym=Eip71CD /name=Ecdysone-induced protein 28/29kD /prod=protein-methionine-S-oxide reductase-like /func=protein-methionine-S-oxide reductase ; EC:1.8.4.6 | inferred from s

3134.6 ~3.6 FB:FBgn0004879 /sym=plx /name=pollux /prod= /func= /map=83B8-83B9 /transc=CT1567 /len=5472 /GB:AE003602

17922 3.6 FB:FBgn0034075 /sym=CG18658 /name= /prod=peptide-aspartate beta-dioxygenase-like /func=enzyme /map=52F1-52F1 /transc=CT18815 /len=1662 /GB:AE003808

3078.3 ~3.6 FB:FBgn0033942 /sym=CG10112 /name= /prod= /func=structural protein /map=51A6-51A6 /transc=CT28465 /len=435 /GB:AE003814

3734 3.6 FB:FBgn0037911 /sym=CG10898 /name= /prod=7,8-dihydro-8-oxoguanine-triphosphatase /func=DNA repair protein /map=86E13-86E13 /transc=CT30521 /len=1936 /GB:AE003692 /note=3prime

325929 3.6 FB:FBgn0040993 /sym=CG17325 /name= /prod= /func= /map=37B1-37B2 /transc=CT35069 /len=765 /GB:AE003660

60953.3 3.6 FB:FBgn0028915 /sym=BG:DS01068.5 /name= /prod=serine endopeptidase /func=endopeptidase /map=35A1-35A1 /transc=CT23067 /len=530 /GB:AE003643

24963.9 3.6 FB:FBgn0036659 /sym=CG9701 /name= /prod=beta-glucosidase-like /func=ion channel /map=73B5-73B5 /transc=CT27420 /len=1936 /GB:AE003526 /note=3prime sequence from clone BDGP:LP0

210172.5 3.6 FB:FBgn0004117 /sym=Tm2 /name=Tropomyosin 2 /prod=tropomyosin /func=motor /map=88E11-88E12 /transc=CT15467 /len=914 /GB:AE003708

36382.6 3.6 FB:FBgn0036875 /sym=CG9449 /name= /prod=acid phosphatase-like /func=enzyme /map=76B6-76B6 /transc=CT26772 /len=1179 /GB:AE003516

103801.4 3.6 FB:FBgn0033968 /sym=CG10200 /name= /prod= /func= /map=51C5-51C5 /transc=CT28697 /len=659 /GB:AE003813 /note=3prime sequence from clone BDGP:LP02570.3prime-hit

28797.2 3.5 FB:FBgn0033919 /sym=CG8547 /name= /prod= /func=DNA binding /map=50F1-50F1 /transc=CT24943 /len=1313 /GB:AE003815

2544.5 ~3.5 FB:FBgn0035590 /sym=CG10673 /name= /prod= /func=protein kinase /map=64C12-64C12 /transc=CT29894 /len=675 /GB:AE003567

34614.2 3.5 FB:FBgn0030745 /sym=CG4239 /name= /prod= /func= /map=14C3-14C4 /transc=CT13936 /len=1639 /GB:AE003502 /note=3prime sequence from clone BDGP:GH25683.3prime-hit

3598.4 ~3.5 FB:FBgn0000719 /sym=fog /name=fog /prod=fog /func= /map=20A4-20A5 /transc=CT16970 /len=3059 /GB:AE003573 /note=3prime sequence from clone BDGP:SD02223.3prime-hit

8478.4 3.5 FB:FBgn0031293 /sym=CG4226 /name= /prod=AMPA/kainate-selective ionotropic glutamate receptor-like /func=ion channel /map=21D4-21D4 /transc=CT13021 /len=2979 /GB:AE003588 /note=3

50264.3 3.5 FB:FBgn0026077 /sym=Gasp /name= /prod=peritrophin-like /func=chitin binding /map=83D4-83D4 /transc=CT28895 /len=1460 /GB:AE003600 /note=3prime sequence from clone BDGP:LD05259.3

93934.7 3.5 FB:FBgn0036051 /sym=CG8154 /name= /prod= /func= /map=67C2-67C2 /transc=CT24352 /len=1726 /GB:AE003550

16140.3 3.5 BDGP:LD31422.3prime-hit /ESTpos=maps in FB:FBgn0004624 /sym=CaMKII /name=Calcium/calmodulin-dependent protein kinase II /prod=calcium/calmodulin-dependent protein kinase II /func=cal

119048.6 3.5 FB:FBgn0038181 /sym=CG9297 /name= /prod= /func=enzyme /map=87F13-87F13 /transc=CT26475 /len=2985 /GB:AE003701

28001.9 3.5 FB:FBgn0031199 /sym=CG9557 /name= /prod= /func= /map=20A1-20A1 /transc=CT17180 /len=420 /GB:AE003574

252647.4 3.5 FB:FBgn0038294 /sym=CG6803 /name= /prod= /func= /map=88E6-88E6 /transc=CT21060 /len=1488 /GB:AE003707 /note=3prime sequence from clone BDGP:GH14252.3prime-hit

2958.1 ~3.5 FB:FBgn0033996 /sym=CG11807 /name= /prod= /func=receptor /map=51E7-51E7 /transc=CT14564 /len=1924 /GB:AE003811 /note=3prime sequence from clone BDGP:SD03973.3prime-hit

49425.3 3.4 FB:FBgn0032897 /sym=CG9336 /name= /prod= /func= /map=38F1-38F1 /transc=CT5238 /len=660 /GB:AE003668

4378.2 3.4 FB:FBgn0034632 /sym=CG15668 /name= /prod= /func= /map=57E8-57E9 /transc=CT35852 /len=1976 /GB:AE003454 /note=3prime sequence from clone BDGP:GH02495.3prime-hit

3609.3 3.4 FB:FBgn0035844 /sym=CG13676 /name= /prod= /func= /map=66B10-66B10 /transc=CT33112 /len=2625 /GB:AE003556

60507.2 3.4 FB:FBgn0036903 /sym=CG8747 /name= /prod=low-density lipoprotein-like /func=receptor /map=76C4-76C4 /transc=CT25242 /len=651 /GB:AE003516

324724.1 3.4 FB:FBgn0034819 /sym=CG9877 /name= /prod= /func= /map=59C4-59C4 /transc=CT27864 /len=267 /GB:AE003459

2420.7 ~3.4 FB:FBgn0003995 /sym=vvl /name=ventral veins lacking /prod= /func=RNA polymerase II transcription factor /map=65C5-65D1 /transc=CT28091 /len=2556 /GB:AE003561

5423.7 3.4 FB:FBgn0001123 /sym=G-salpa60A /name=G protein alpha 6A /prod=G protein alphas-subunit /func=heterotrimeric G protein /map=60A12-60A12 /transc=CT40310 /len=1626 /GB:AE003462 /no

4149.2 3.4 FB:FBgn0033872 /sym=CG6329 /name= /prod= /func= /map=50C12-50C12 /transc=CT19784 /len=1312 /GB:AE003817 /note=3prime sequence from clone BDGP:HL02087.3prime-hit

3506.4 3.4 FB:FBgn0003162 /sym=Pu /name=Punch /prod=GTP cyclohydrolase I /func=GTP cyclohydrolase I ; EC:3.5.4.16 /map=57C5-57C6 /transc=CT26766 /len=1623 /GB:AE003453 /note=3prime sequence

20389 3.4 FB:FBgn0038610 /sym=CG7675 /name= /prod= /func=enzyme /map=91A2-91A2 /transc=CT30419 /len=1100 /GB:AE003721 /note=3prime sequence from clone BDGP:GH26851.3prime-hit

21255.5 3.4 FB:FBgn0028694 /sym=Rpn11 /name= /prod=19S proteasome regulatory particle, non-ATPase protein, subunit S13 /func= /map=25C3-25C3 /transc=CT41032 /len=1165 /GB:AE003608

2246.4 ~3.4 FB:FBgn0036028 /sym=CG16717 /name= /prod= /func= /map=67B11-67B11 /transc=CT37199 /len=903 /GB:AE003551

18200.4 3.4 FB:FBgn0031200 /sym=CG9558 /name= /prod= /func= /map=20A1-20A1 /transc=CT17174 /len=261 /GB:AE003574

75341.7 3.4 FB:FBgn0039897 /sym=CG1674 /name= /prod= /func=motor /map=102A3-102A4 /transc=CT4686 /len=2388 /GB:AE003844

2626.5 ~3.3 FB:FBgn0011327 /sym=Uch-L3 /name=Ubiquitin C-terminal hydrolase /prod=ubiquitinyl hydrolase L3 /func=ubiquitinyl hydrolase 1 /map=67B5-67B5 /transc=CT11565 /len=1137 /GB:AE003552 /n

46788.1 3.3 FB:FBgn0030309 /sym=CG1572 /name= /prod= /func= /map=10C4-10C4 /transc=CT4080 /len=955 /GB:AE003486 /note=3prime sequence from clone BDGP:LD04844.3prime-hit

21879.9 3.3 FB:FBgn0016756 /sym=Ubp64E /name=Ubiquitin-specific protease 64E /prod=ubiquitin-specific protease /func=ubiquitin-specific protease /map=64E13-64F1 /transc=CT17382 /len=4202 /GB:AE00

34071.5 3.3 FB:FBgn0033446 /sym=CG1648 /name= /prod= /func= /map=46B10-46B10 /transc=CT4516 /len=960 /GB:AE003832 /note=3prime sequence from clone BDGP:GH20817.3prime-hit

3179.6 ~3.3 FB:FBgn0039335 /sym=CG5127 /name= /prod=vacuolar protein sorting-like /func=transporter /map=96E1-96E1 /transc=CT16445 /len=2021 /GB:AE003752 /note=3prime sequence from clone BDGP

438729.7 3.3 FB:FBgn0033596 /sym=CG7738 /name= /prod= /func= /map=47E1-47E1 /transc=CT23557 /len=405 /GB:AE003826

11510.6 3.3 FB:FBgn0032002 /sym=CG8353 /name= /prod=cytidine deaminase-like /func=enzyme /map=28F4-28F4 /transc=CT24599 /len=513 /GB:AE003620

1319.3 ~3.3 FB:FBgn0037542 /sym=CG2723 /name= /prod= /func= /map=84E6-84E6 /transc=CT9257 /len=1314 /GB:AE003677 /note=3prime sequence from clone BDGP:LD11958.3prime-hit

16648.6 3.3 FB:FBgn0019972 /sym=Ice /name=Ice /prod=caspase /func=caspase ; EC:3.4.22.- /map=99C4-99C4 /transc=CT4706 /len=1932 /GB:AE003771 /note=3prime sequence from clone BDGP:GH24292.3pr

3327.3 3.3 FB:FBgn0023517 /sym=EG:63B12.4 /name= /prod= /func= /map=2B13-2B13 /transc=CT34629 /len=1066 /GB:AE003422 /note=3prime sequence from clone BDGP:GH02880.3prime-hit

2842 ~3.3 FB:FBgn0036843 /sym=CG6812 /name= /prod= /func= /map=75F4-75F5 /transc=CT21117 /len=1585 /GB:AE003518

87949.8 3.3 FB:FBgn0039719 /sym=CG15515 /name= /prod=cuticle protein-like /func=structural protein /map=99D1-99D1 /transc=CT35628 /len=327 /GB:AE003771

8183.4 3.3 FB:FBgn0031821 /sym=CG9542 /name= /prod= /func= /map=26D7-26D7 /transc=CT26992 /len=903 /GB:AE003613

30450.3 3.3 FB:FBgn0039208 /sym=CG6643 /name= /prod= /func=enzyme /map=96A7-96A7 /transc=CT20638 /len=2769 /GB:AE003748 /note=3prime sequence from clone BDGP:GH21511.3prime-hit

2308.2 ~3.3 FB:FBgn0031502 /sym=CG3524 /name= /prod= /func=enzyme /map=23C5-23D1 /transc=CT11835 /len=7590 /GB:AE003581 /note=3prime sequence from clone BDGP:GH02912.3prime-hit

1664 ~3.3 FB:FBgn0035054 /sym=CG9189 /name= /prod= /func= /map=60D14-60D14 /transc=CT26264 /len=1121 /GB:AE003465

3378.5 3.3 FB:FBgn0039529 /sym=CG5612 /name= /prod= /func= /map=98A4-98A4 /transc=CT17752 /len=1352 /GB:AE003761

629.4 ~3.3 FB:FBgn0029542 /sym=CG3708 /name= /prod= /func= /map=1C5-1C5 /transc=CT12445 /len=1188 /GB:AE003419 /note=3prime sequence from clone BDGP:GH17085.3prime-hit

1703.3 ~3.3 FB:FBgn0040542 /sym=CG12815 /name= /prod= /func= /map=85F15-85F15 /transc=CT31943 /len=213 /GB:AE003686

6343.4 3.3 FB:FBgn0031695 /sym=Cyp4ac3 /name= /prod=cytochrome P450, CYP4AC3 /func=cytochrome P450 /map=25D2-25D2 /transc=CT33590 /len=939 /GB:AE003609 /note=3prime sequence from clone

2727 ~3.2 FB:FBgn0031153 /sym=CG15448 /name= /prod= /func=transmembrane receptor /map=19E7-19E7 /transc=CT35512 /len=669 /GB:AE003569

1114.8 ~3.2 FB:FBgn0031211 /sym=CG2776 /name= /prod= /func=ligand binding or carrier /map=21A4-21A4 /transc=CT9453 /len=615 /GB:AE003590

45992.9 3.2 FB:FBgn0027540 /sym=BcDNA:GH12504 /name= /prod= /func=transmembrane receptor /map=85B3-85B4 /transc=CT27712 /len=3771 /GB:AE003680 /note=3prime sequence from clone BDGP:GH

95943.1 3.2 BDGP:GH1453.3prime-hit /ESTpos=maps in FB:FBgn0031737 /sym=CG11142 /name= /prod=peritrophin-like /func=structural protein /map=26A1-26A1 /transc=CT31147 /len=899

2321.5 ~3.2 FB:FBgn0031251 /sym=CG4213 /name= /prod= /func=motor /map=21C2-21C2 /transc=CT13886 /len=3696 /GB:AE003589

10103 3.2 FB:FBgn0038407 /sym=CG6126 /name= /prod=sugar transporter /func=transporter /map=89B13-89B13 /transc=CT19169 /len=2108 /GB:AE003712 /note=3prime sequence from clone BDGP:GH092

4787 3.2 FB:FBgn0034525 /sym=CG13435 /name= /prod= /func=ligand binding or carrier /map=57B1-57B1 /transc=CT32792 /len=1983 /GB:AE003791

3986.5 3.2 FB:FBgn0003499 /sym=sr /name=stripe /prod= /func=RNA polymerase II transcription factor /map=90E1-90E2 /transc=CT23724 /len=4829 /GB:AE003720

1926.4 ~3.2 FB:FBgn0035772 /sym=CG8582 /name= /prod= /func= /map=65F4-65F4 /transc=CT14420 /len=1739 /GB:AE003559

2596.2 ~3.2 FB:FBgn0036562 /sym=CG5600 /name= /prod= /func= /map=72D3-72D4 /transc=CT17536 /len=1858 /GB:AE003528 /note=3prime sequence from clone BDGP:GH16214.3prime-hit

14451.8 3.2 FB:FBgn0039606 /sym=CG1448 /name= /prod= /func= /map=98E6-98E6 /transc=CT3509 /len=1544 /GB:AE003767 /note=3prime sequence from clone BDGP:LD34202.3prime-hit

13226.4 3.2 FB:FBgn0028690 /sym=Rpn5 /name= /prod=19S proteasome regulatory particle, non-ATPase protein, subunit p55 /func=endopeptidase /map=83C1-83C1 /transc=CT1623 /len=1874 /GB:AE003601

2769.3 ~3.2 FB:FBgn0028468 /sym=BcDNA:LD28419 /name= /prod=tetracycline transporter-like /func=transporter /map=93B12-93B12 /transc=CT18069 /len=1718 /GB:AE003733 /note=3prime sequence from

1479.1 ~3.2 FB:FBgn0039870 /sym=CG1896 /name= /prod= /func= /map=100E2-100E2 /transc=CT5870 /len=806 /GB:AE003779 /note=3prime sequence from clone BDGP:LD39576.3prime-hit

116129.1 3.2 FB:FBgn0010424 /sym=TpnC73F /name=Troponin C at 73F /prod=troponin C /func=calcium binding /map=73E4-73E5 /transc=CT23822 /len=935 /GB:AE003525

2807.4 ~3.2 FB:FBgn0034029 /sym=CG8190 /name= /prod=translation initiation factor 2B-gamma-like /func=translation factor /map=52A10-52A10 /transc=CT20341 /len=1503 /GB:AE003810 /note=3prime seq

2943.7 3.2 FB:FBgn0030028 /sym=CG10965 /name= /prod= /func= /map=7D21-7D21 /transc=CT7616 /len=1052 /GB:AE003443 /note=3prime sequence from clone BDGP:GH26991.3prime-hit

48151.9 3.2 FB:FBgn0038149 /sym=CG9796 /name= /prod= /func= /map=87E10-87E10 /transc=CT27692 /len=1109 /GB:AE003700 /note=3prime sequence from clone BDGP:LD47508.3prime-hit

2891.3 ~3.2 FB:FBgn0034045 /sym=CG8249 /name= /prod=glucose transporter-like /func=transporter /map=52D2-52D2 /transc=CT21797 /len=1807 /GB:AE003809

2661.8 ~3.2 FB:FBgn0034579 /sym=CG9353 /name= /prod= /func= /map=57B20-57B20 /transc=CT26571 /len=647 /GB:AE003452 /note=3prime sequence from clone BDGP:SD09147.3prime-hit

27155.9 3.2 FB:FBgn0011716 /sym=spdo /name=sanpodo /prod=tropomodulin /func=tropomyosin binding /map=100A1-100A1 /transc=CT3919 /len=5374 /GB:AE003774 /note=3prime sequence from clone BDGP

49739 3.2 FB:FBgn0032899 /sym=CG9338 /name= /prod= /func= /map=38F1-38F1 /transc=CT5240 /len=660 /GB:AE003668 /note=3prime sequence from clone BDGP:GH07967.3prime-hit

8500.4 3.2 FB:FBgn0029958 /sym=CG12151 /name= /prod=pyruvate dehydrogenase phosphatase /func=protein phosphatase /map=7B8-7B8 /transc=CT8439 /len=1910 /GB:AE003441 /note=3prime sequence fr

57308.7 3.2 FB:FBgn0032596 /sym=CG17331 /name= /prod=20S proteasome, beta2 subunit /func=endopeptidase /map=36A7-36A7 /transc=CT32562 /len=760 /GB:AE003652

5424 3.2 FB:FBgn0038817 /sym=CG18039 /name= /prod= /func= /map=92F1-92F1 /transc=CT13538 /len=961 /GB:AE003731

51231.5 3.2 FB:FBgn0027501 /sym=BcDNA:LD24639 /name= /prod=UDP-N-acetylglucosamine pyrophosphorylase-like /func=enzyme /map=26D5-26D5 /transc=CT26974 /len=2033 /GB:AE003613 /note=3prim

2850.4 3.2 FB:FBgn0039898 /sym=CG1748 /name= /prod=RHO GTPase activator-like /func=signal transduction /map=102A4-102A4 /transc=CT4742 /len=717 /GB:AE003844

159590.5 3.2 FB:FBgn0000667 /sym=Actn /name=alpha actinin /prod=actinin-alpha /func=actin bundling /map=2C2-2C3 /transc=CT14163 /len=3432 /GB:AE003422 /note=3prime sequence from clone BDGP:LD

1758.7 ~3.1 FB:FBgn0028428 /sym=lh /name= /prod=voltage-gated ion channel protein /func=voltage-gated ion channel /map=50F1-50F1 /transc=CT24973 /len=3924 /GB:AE003815

2533.3 ~3.1 FB:FBgn0038866 /sym=CG5810 /name= /prod= /func=cell adhesion /map=93C3-93C3 /transc=CT18214 /len=1287 /GB:AE003733

3027.6 ~3.1 FB:FBgn0037762 /sym=CG16905 /name= /prod= /func= /map=85E10-85E10 /transc=CT37510 /len=781 /GB:AE003684

6961.5 3.1 FB:FBgn0004586 /sym=grh /name=grainy head /prod= /func=specific RNA polymerase II transcription factor /map=54F1-54F4 /transc=CT42182 /len=4748 /GB:AE003801 /note=3prime sequence from

2132.7 ~3.1 FB:FBgn0034366 /sym=CG5489 /name= /prod= /func=enzyme /map=55E4-55E4 /transc=CT42577 /len=1577 /GB:AE003799

1882.1 ~3.1 FB:FBgn0028895 /sym=BG:DS02740.8 /name= /prod= /func=nucleic acid binding /map=35F8-35F8 /transc=CT32539 /len=1158 /GB:AE003650

1783.7 ~3.1 FB:FBgn0039807 /sym=CG15546 /name= /prod= /func= /map=100B1-100B1 /transc=CT35662 /len=1233 /GB:AE003775

2643.4 ~3.1 FB:FBgn0037817 /sym=Cyp12e1 /name= /prod=cytochrome P450, CYP12E1 /func=cytochrome P450 /map=86A7-86A7 /transc=CT34465 /len=1518 /GB:AE003687

10842.5 3.1 FB:FBgn0023548 /sym=msta /name= /prod= /func= /map=2E2-2E2 /transc=CT40358 /len=3150 /GB:AE003423

2581.7 ~3.1 FB:FBgn0032490 /sym=CG16813 /name= /prod= /func= /map=34A10-34A10 /transc=CT35578 /len=555 /GB:AE003639

872 ~3.1 FB:FBgn0031457 /sym=CG3077 /name= /prod= /func=ligand binding or carrier /map=23B1-23B1 /transc=CT10334 /len=1317 /GB:AE003582 /note=3prime sequence from clone BDGP:LD12265.3p

18259.7 3.1 FB:FBgn0024989 /sym=EG:125H10.1 /name= /prod= /func=motor /map=1A8-1A8 /transc=CT12604 /len=2479 /GB:AE003417

2355.4 ~3.1 FB:FBgn0031933 /sym=CG7068 /name= /prod= /func= /map=28C1-28C1 /transc=CT21827 /len=4745 /GB:AE003618 /note=3prime sequence from clone BDGP:GH05679.3prime-hit

3907.1 3.1 FB:FBgn0033807 /sym=CG12251 /name=aquaporin /prod=aquaporin /func=water transporter /map=49F11-49F11 /transc=CT14932 /len=1180 /GB:AE003819

28159.7 3.1 FB:FBgn0023175 /sym=Prosalph7 /name=Proteasome alpha7 subunit /prod=20S proteasome, alpha7 subunit /func=multicatalytic endopeptidase ; EC:3.4.99.46 /map=46B13-46B13 /transc=CT3927 /l

7392.9 3.1 FB:FBgn0030917 /sym=CG6267 /name= /prod= /func= /map=17A11-17A11 /transc=CT19600 /len=678 /GB:AE003508

1763.6 ~3.1 FB:FBgn0031027 /sym=CG14201 /name= /prod= /func=transcription factor /map=18D3-18D3 /transc=CT33814 /len=702 /GB:AE003512

2247.5 ~3.1 FB:FBgn0032330 /sym=CG12291 /name= /prod= /func= /map=32D1-32D1 /transc=CT19324 /len=382 /GB:AE003630

20001.2 3.1 FB:FBgn0034142 /sym=CG8306 /name= /prod= /func=enzyme /map=53C7-53C8 /transc=CT24503 /len=1937 /GB:AE003806

5308.7 3.1 FB:FBgn0001250 /sym=if /name=inflated /prod=integrin, alpha-subunit /func=cell adhesion receptor /map=15A3-15A5 /transc=CT27194 /len=5726 /GB:AE003503

8376.5 3.1 FB:FBgn0036370 /sym=CG14108 /name= /prod= /func= /map=70B1-70B1 /transc=CT33703 /len=435 /GB:AE003537

242886.2 3.1 FB:FBgn0003060 /sym=CG9757 /name= /prod= /func= /map=87F5-87F5 /transc=CT27573 /len=566 /GB:AE003701

2320.9 ~3.1 FB:FBgn0000014 /sym=abd-A /name=abdominal A /prod= /func=specific RNA polymerase II transcription factor /map=89E4-89E4 /transc=CT29034 /len=1931 /GB:AE003715

4535 3.1 FB:FBgn0026749 /sym=Yippee /name= /prod=zinc binding protein /func=zinc binding /map=11E11-11E11 /transc=CT6354 /len=1152 /GB:AE003492 /note=3prime sequence from clone BDGP:LD40

26315.9 3.1 FB:FBgn0038293 /sym=CG6904 /name= /prod= /func=enzyme /map=88E5-88E5 /transc=CT21366 /len=2705 /GB:AE003707 /note=3prime sequence from clone BDGP:LD46952.3prime-hit

4934.2 3.1 FB:FBgn0001112 /sym=Gld /name=Glucose dehydrogenase /prod=glucose dehydrogenase (acceptor) == EC 1.1.99.10 /func=glucose dehydrogenase (acceptor) ; EC:1.1.99.10 /map=84C7-84C8 /transc=

27221.3 3 FB:FBgn0003206 /sym=Ras64B /name=Ras oncogene at 64B /prod= /func=RAS small GTPase /map=64A10-64A10 /transc=CT1405 /len=588 /GB:AE003480

106718.4 3 FB:FBgn0033600 /sym=CG9077 /name= /prod=cuticle protein /func=structural protein /map=47E1-47E1 /transc=CT26058 /len=396 /GB:AE003826

2196.8 ~3.0 FB:FBgn0029585 /sym=CG11511 /name= /prod= /func=transcription factor /map=2B6-2B6 /transc=CT34608 /len=1000 /GB:AE003421

1073.6 ~3.0 FB:FBgn0003511 /sym=Sry-beta /name=Serendipity beta /prod= /func=RNA polymerase II transcription factor /map=99D5-99D5 /transc=CT5812 /len=1247 /GB:AE003772 /note=3prime sequence fr

79152.2 3 FB:FBgn0003071 /sym=Pfk /name=Phosphofructokinase /prod=6-phosphofructokinase /func=6-phosphofructokinase ; EC:2.7.1.11 /map=46E4-46E4 /transc=CT13302 /len=3176 /GB:AE003830 /note=

8211.2 3 FB:FBgn0040559 /sym=CG14359 /name= /prod= /func= /map=88B1-88B1 /transc=CT33994 /len=237 /GB:AE003703

19686.7 3 FB:FBgn0028693 /sym=Rpn12 /name= /prod=19S proteasome regulatory particle, non-ATPase protein, subunit S14 /func=endopeptidase /map=73A8-73A8 /transc=CT13736 /len=989 /GB:AE00352

2397.7 ~3.0 FB:FBgn0038536 /sym=CG7655 /name= /prod=multipass nuclear envelope protein-like /func=transmembrane receptor /map=90C1-90C1 /transc=CT23407 /len=965 /GB:AE003718 /note=3prime seq

44484.6 3 FB:FBgn0029533 /sym=CG5254 /name= /prod= /func= /map=1C1-1C1 /transc=CT16777 /len=993 /GB:AE003418

3552.4 3 FB:FBgn0032128 /sym=CG13115 /name= /prod= /func= /map=30B11-30B11 /transc=CT32352 /len=956 /GB:AE003625 /note=3prime sequence from clone BDGP:GH05993.3prime-hit

38368.3 3 FB:FBgn0035030 /sym=CG3541 /name= /prod= /func= /map=60D7-60D8 /transc=CT11882 /len=2417 /GB:AE003464 /note=3prime sequence from clone BDGP:GH12163.3prime-hit

41645.2 3 FB:FBgn0022359 /sym=Sodh-2 /name=Sorbitol dehydrogenase-2 /prod=L-itol 2-dehydrogenase /func=L-itol 2-dehydrogenase ; EC:1.1.1.14 /map=86C7-86C7 /transc=CT14906 /len=1345 /GB:AE003418

14310.2 3 FB:FBgn0028685 /sym=Rpt4 /name= /prod=19S proteasome regulatory particle, triple-A protein, subunit S10b /func=proteasome ATPase ; EC:3.6.4.8 /map=5E1-5E1 /transc=CT11623 /len=1453 /GB:AE003418

104072.4 3 BDGP:HL664.3prime-hit /ESTpos=maps 3prime of FB:FBgn0038181 /sym=CG9297 /name= /prod= /func=enzyme /map=87F13-87F13 /transc=CT26475 /len=608

30341.6 3 FB:FBgn0028691 /sym=Rpn4 /name= /prod=19S proteasome regulatory particle, non-ATPase protein, subunit S13 /func=endopeptidase /map=95B5-95B5 /transc=CT28751 /len=1330 /GB:AE00374

4080.2 3 FB:FBgn0005771 /sym=noc /name=no ocelli /prod= /func=RNA polymerase II transcription factor /map=35A4-35A4 /transc=CT14619 /len=2668 /GB:AE003644 /note=3prime sequence from clone BDGP:GH06479.3prime-hit

4064.4 3 FB:FBgn0031637 /sym=CG2950 /name= /prod= /func=RNA binding /map=25B3-25B3 /transc=CT40278 /len=2649 /GB:AE003575 /note=3prime sequence from clone BDGP:GH06479.3prime-hit

16524 3 FB:FBgn0040520 /sym=CG12447 /name= /prod= /func= /map=20A1-20A1 /transc=CT32486 /len=132 /GB:AE003574

3987 ~3.0 FB:FBgn0003944 /sym=Ubx /name=Ultrathorax /prod= /func=specific RNA polymerase II transcription factor /map=89D8-89E2 /transc=CT29154 /len=2204 /GB:AE003714

86366.2 3 FB:FBgn0034497 /sym=CG9090 /name= /prod=phosphate transporter /func=carrier type transporter /map=56F16-56F16 /transc=CT25968 /len=1371 /GB:AE003792

32359.3 2.9 FB:FBgn0029876 /sym=CG3960 /name= /prod= /func=actin binding /map=6B3-6C1 /transc=CT13158 /len=2129 /GB:AE003438 /note=3prime sequence from clone BDGP:GH02414.3prime-hit

2061.3 ~2.9 FB:FBgn0027550 /sym=BcDNA:GH10711 /name= /prod= /func=receptor /map=32A4-32A5 /transc=CT20185 /len=2550 /GB:AE003629 /note=3prime sequence from clone BDGP:GH10711.3prime-hit

29445.5 2.9 FB:FBgn0034399 /sym=CG15083 /name= /prod= /func= /map=55F3-55F3 /transc=CT34958 /len=453 /GB:AE003798

38242.4 2.9 FB:FBgn0033553 /sym=CG12323 /name= /prod= /func= /map=47C1-47C1 /transc=CT22275 /len=1114 /GB:AE003828 /note=3prime sequence from clone BDGP:LD08717.3prime-hit

29174.8 2.9 FB:FBgn0031307 /sym=CG4726 /name= /prod=sodium/phosphate cotransporter /func=transporter /map=21E4-21E4 /transc=CT15243 /len=2003 /GB:AE003587

6818 2.9 FB:FBgn0032129 /sym=CG4405 /name= /prod= /func=RNA binding /map=30B11-30B12 /transc=CT14344 /len=3801 /GB:AE003625

10857 2.9 FB:FBgn0035927 /sym=CG5775 /name= /prod= /func= /map=66E1-66E1 /transc=CT18132 /len=837 /GB:AE003554 /note=3prime sequence from clone BDGP:SD08909.3prime-hit

67758.7 2.9 FB:FBgn0034470 /sym=CG11218 /name= /prod=antennal binding protein X-like /func=ligand binding or carrier /map=56E4-56E4 /transc=CT31326 /len=574 /GB:AE003795

13006.7 2.9 FB:FBgn0036891 /sym=CG9372 /name= /prod=serine protease-like /func=endopeptidase /map=76B11-76B11 /transc=CT26619 /len=1569 /GB:AE003516

1649.5 ~2.9 FB:FBgn0039706 /sym=CG18040 /name= /prod= /func= /map=99C5-99C6 /transc=CT40392 /len=786 /GB:AE003771

34712.3 2.9 FB:FBgn0032427 /sym=CG5453 /name= /prod= /func= /map=33D4-33D4 /transc=CT17294 /len=819 /GB:AE003636 /note=3prime sequence from clone BDGP:GH02216.3prime-hit

25527.5 2.9 FB:FBgn0010397 /sym=LamC /name=Lamin C /prod=lamin C /func=cytoskeletal structural protein /map=51B1-51B1 /transc=CT28479 /len=2334 /GB:AE003814 /note=3prime sequence from clone BDGP:GH02216.3prime-hit

1435.5 ~2.9 FB:FBgn0001624 /sym=dlg1 /name=discs large 1 /prod=guanylate kinase /func=guanylate kinase ; EC:2.7.4.8 /map=10B11-10B12 /transc=CT41310 /len=631 /GB:AE003486 /note=3prime sequence from clone BDGP:GH02216.3prime-hit

32146.3 2.9 FB:FBgn0035517 /sym=CG1265 /name= /prod= /func= /map=64B4-64B4 /transc=CT2591 /len=549 /GB:AE003480

2417.1 ~2.9 FB:FBgn0032013 /sym=CG7851 /name= /prod= /func= /map=29A4-29A4 /transc=CT23800 /len=1391 /GB:AE003620

6095.4 2.9 FB:FBgn0030494 /sym=CG15757 /name= /prod=cuticle protein-like /func=structural protein /map=12A1-12A1 /transc=CT36009 /len=522 /GB:AE003492

22931.3 2.9 FB:FBgn0040575 /sym=CG15922 /name= /prod= /func= /map=92E10-92E10 /transc=CT35885 /len=159 /GB:AE003731

1923 ~2.9 FB:FBgn0035199 /sym=CG9134 /name= /prod=C-type lectin-like /func=ligand binding or carrier /map=61F4-61F4 /transc=CT10115 /len=1161 /GB:AE003471 /note=3prime sequence from clone BDGP:GH02216.3prime-hit

2417.5 ~2.9 FB:FBgn0004957 /sym=por /name=porcupine /prod= /func= /map=17A10-17A10 /transc=CT19254 /len=2331 /GB:AE003508

143693.8 2.9 FB:FBgn0003075 /sym=Pgk /name=Phosphoglycerate kinase /prod=phosphoglycerate kinase /func=phosphoglycerate kinase ; EC:2.7.2.3 /map=23A7-23A7 /transc=CT10484 /len=1361 /GB:AE003582

18527.2 2.9 FB:FBgn0035542 /sym=CG11347 /name= /prod= /func= /map=64B11-64B11 /transc=CT31652 /len=2045 /GB:AE003481 /note=3prime sequence from clone BDGP:GH28550.3prime-hit

6337.5 2.8 FB:FBgn0031914 /sym=CG5973 /name= /prod= /func=ligand binding or carrier /map=27F7-28A1 /transc=CT18751 /len=1519 /GB:AE003617 /note=3prime sequence from clone BDGP:HL01515.3prime-hit

26453.9 2.8 FB:FBgn0028688 /sym=Rpn7 /name= /prod=19S proteasome regulatory particle, non-ATPase protein, subunit S10a /func=endopeptidase /map=94B3-94B3 /transc=CT17076 /len=1374 /GB:AE003700

293564.7 2.8 FB:FBgn0035062 /sym=CG16914 /name= /prod=larval cuticle protein-like /func=structural protein /map=60D15-60D15 /transc=CT37520 /len=279 /GB:AE003465

35174.6 2.8 FB:FBgn0034064 /sym=CG8392 /name= /prod=20S proteasome, beta1 subunit /func=endopeptidase /map=52E1-52E1 /transc=CT18263 /len=829 /GB:AE003808 /note=3prime sequence from clone BDGP:HL01515.3prime-hit

319262 2.8 FB:FBgn0040941 /sym=CG15308 /name= /prod= /func= /map=9B6-9B6 /transc=CT35285 /len=249 /GB:AE003449

109269.9 2.8 FB:FBgn0031629 /sym=CG3244 /name= /prod=selectin-like /func=ligand binding or carrier /map=25B1-25B1 /transc=CT10874 /len=1267 /GB:AE003575

14307.5 2.8 FB:FBgn0032727 /sym=CG10623 /name= /prod= /func= /map=37B8-37B8 /transc=CT29758 /len=1114 /GB:AE003661

20257.5 2.8 FB:FBgn0020369 /sym=Pros45 /name=Saccharomyces cerevisiae UAS construct a of Cheng /prod=19S proteasome regulatory particle, triple-A protein, subunit S8 /func=proteasome ATPase ; EC:3.6.1.13

5637 2.8 FB:FBgn0034975 /sym=CG11290 /name= /prod=histone acetyltransferase-like /func=enzyme /map=60B5-60B5 /transc=CT31509 /len=6956 /GB:AE003463 /note=3prime sequence from clone BDGP:HL01515.3prime-hit

1625.5 ~2.8 FB:FBgn0024887 /sym=kin17 /name= /prod= /func=DNA binding /map=77B4-77B4 /transc=CT17834 /len=1241 /GB:AE003591

38932.5 2.8 BDGP:GH13437.3prime-hit /ESTpos=maps 3prime of FB:FBgn0039493 /sym=CG5889 /name= /prod= /func= /map=97E11-97F1 /transc=CT18483 /len=374

126510.4 2.8 FB:FBgn0028544 /sym=BG:DS00180.3 /name= /prod= /func= /map=34E1-34E1 /transc=CT25718 /len=1397 /GB:AE003641 /note=3prime sequence from clone BDGP:HL02234.3prime-hit

6355.6 2.8 FB:FBgn0031067 /sym=CG12533 /name= /prod= /func=actin binding /map=18F1-18F1 /transc=CT33853 /len=2079 /GB:AE003513

61064.6 2.8 FB:FBgn0034140 /sym=CG8317 /name= /prod= /func= /map=53C7-53C7 /transc=CT24573 /len=693 /GB:AE003806

276870 2.8 FB:FBgn0014869 /sym=Pglym78 /name=Phosphoglyceromutase /prod=phosphoglycerate mutase /func=phosphoglycerate mutase ; EC:5.4.2.1 /map=99A1-99A1 /transc=CT4904 /len=1125 /GB:AE003806

16360.6 2.8 FB:FBgn0004066 /sym=Pros28.1 /name=Proteasome 28kD subunit 1 /prod=20S proteasome, alpha4 subunit /func=multicatalytic endopeptidase ; EC:3.4.99.46 /map=14B11-14B11 /transc=CT11501 /len=11501

9989.2 2.8 FB:FBgn0000084 /sym=AnnX /name=Annexin X /prod=annexin X /func=calcium-dependent phospholipid binding /map=19C1-19C1 /transc=CT17636 /len=1216 /GB:AE002611 /note=3prime sequence from clone BDGP:HL01515.3prime-hit

18942.3 2.8 FB:FBgn0035334 /sym=CG8993 /name= /prod=mitochondrial thioredoxin-like /func=chaperone /map=62E1-62E1 /transc=CT25846 /len=484 /GB:AE003474

298292.1 2.8 FB:FBgn0032538 /sym=CG16885 /name= /prod= /func= /map=34E1-34E1 /transc=CT35249 /len=780 /GB:AE003641

15314.8 2.8 FB:FBgn0033959 /sym=CG18372 /name= /prod= /func= /map=51C2-51C2 /transc=CT41763 /len=674 /GB:AE003813

21340.1 2.8 FB:FBgn0031322 /sym=CG5001 /name= /prod= /func=chaperone /map=21F1-21F1 /transc=CT15884 /len=1356 /GB:AE003587

34689.7 2.8 FB:FBgn0026380 /sym=Prosbeta3 /name= /prod=20S proteasome, beta3 subunit /func=multicatalytic endopeptidase ; EC:3.4.99.46 /map=85C3-85C3 /transc=CT32122 /len=915 /GB:AE003681 /note=3prime sequence from clone BDGP:HL01515.3prime-hit

10981.8 2.8 BDGP:LD8622.3prime-hit /ESTpos=maps 3prime of FB:FBgn0013718 /sym=nuf /name=nuclear fallout /prod= /func=cytoskeletal structural protein /map=7D2-7D2 /transc=CT23449 /len=291

24154.1 2.8 FB:FBgn0035788 /sym=CG8541 /name= /prod=cuticle protein /func=ligand binding or carrier /map=66A1-66A1 /transc=CT15726 /len=828 /GB:AE003559

1572.4 ~2.8 FB:FBgn0038063 /sym=CG6989 /name= /prod=beta adrenergic receptor-like /func=G protein linked receptor /map=87C2-87C2 /transc=CT21650 /len=1224 /GB:AE003696

5162.2 ~2.8 FB:FBgn0000462 /sym=dl /name=dorsal /prod= /func=specific RNA polymerase II transcription factor /map=36C2-36C2 /transc=CT42418 /len=4565 /GB:AE003655

26681.8 2.8 FB:FBgn0036357 /sym=CG10724 /name= /prod= /func=enzyme /map=70A7-70A7 /transc=CT30041 /len=2260 /GB:AE003538 /note=3prime sequence from clone BDGP:LD27045.3prime-hit

2345.7 ~2.8 FB:FBgn0039484 /sym=CG6124 /name= /prod= /func=cell adhesion /map=97E6-97E6 /transc=CT19227 /len=2673 /GB:AE003759

14723 2.8 FB:FBgn0037744 /sym=CG8417 /name= /prod=mannose-6-phosphate isomerase /func=enzyme /map=85E8-85E8 /transc=CT24707 /len=1398 /GB:AE003684 /note=3prime sequence from clone BDGP:HL01515.3prime-hit

19142.5 2.8 FB:FBgn0020304 /sym=drongo /name=drongo /prod= /func=defense/immunity protein /map=21D2-21D2 /transc=CT42210 /len=2383 /GB:AE003588 /note=3prime sequence from clone BDGP:GH1000000000

11359.3 2.8 FB:FBgn0035390 /sym=CG1893 /name= /prod= /func= /map=63B5-63B5 /transc=CT5862 /len=834 /GB:AE003476

23109.6 2.8 FB:FBgn0005666 /sym=bt /name=bent /prod=projectin /func=cell adhesion /map=102D6-102E1 /transc=CT3598 /len=23764 /GB:AE003843 /note=3prime sequence from clone BDGP:GH07636.3prime

1097.1 ~2.8 FB:FBgn0037651 /sym=CG11978 /name= /prod= /func= /map=85C3-85C3 /transc=CT32124 /len=456 /GB:AE003681

2869 ~2.8 FB:FBgn0033526 /sym=CG12892 /name= /prod= /func=enzyme /map=47A9-47A9 /transc=CT32037 /len=2244 /GB:AE003829

5181.6 2.8 FB:FBgn0016762 /sym=angel /name=angel /prod= /func=enzyme /map=59F4-59F4 /transc=CT17360 /len=1184 /GB:AE003461 /note=3prime sequence from clone BDGP:GH06351.3prime-hit

3664 2.8 FB:FBgn0030526 /sym=CG11102 /name= /prod= /func= /map=12B9-12B9 /transc=CT31063 /len=1671 /GB:AE003493

187409.7 2.8 FB:FBgn0003738 /sym=Tpi /name=Triose phosphate isomerase /prod=triosephosphate isomerase /func=triosephosphate isomerase ; EC:5.3.1.1 /map=99E1-99E1 /transc=CT6334 /len=1186 /GB:AE003493

5399.5 2.8 BDGP:LD1876.3prime-hit /ESTpos=maps 3prime of FB:FBgn0038501 /sym=CG5319 /name= /prod= /func= /map=9A6-9A6 /transc=CT1693 /len=567

361575.5 2.8 FB:FBgn0002789 /sym=Mp20 /name=Muscle protein 2 /prod=calcium-binding protein /func=calcium binding /map=49F15-49F15 /transc=CT15161 /len=852 /GB:AE003819

24381.1 2.7 FB:FBgn0030753 /sym=CG4420 /name= /prod= /func=DNA binding /map=14D1-14D1 /transc=CT14402 /len=1880 /GB:AE003502 /note=3prime sequence from clone BDGP:GM04721.3prime-hit

6802.3 2.7 FB:FBgn0039914 /sym=CG1901 /name= /prod=transforming growth factor beta-like /func=signal transduction /map=102D1-102D1 /transc=CT5854 /len=2528 /GB:AE003843

107633.5 2.7 FB:FBgn0032282 /sym=CG7299 /name= /prod= /func= /map=32A1-32A1 /transc=CT22515 /len=534 /GB:AE003629

11917.3 2.7 FB:FBgn0037138 /sym=CG7145 /name= /prod=1-pyrroline-5-carboxylate dehydrogenase-like /func=enzyme /map=79A5-79A5 /transc=CT22083 /len=1890 /GB:AE003595

3937.3 ~2.7 FB:FBgn0036656 /sym=CG13026 /name= /prod= /func= /map=73B5-73B5 /transc=CT32244 /len=405 /GB:AE003526

27579.5 2.7 FB:FBgn0033593 /sym=CG9080 /name= /prod= /func= /map=47E1-47E1 /transc=CT26066 /len=435 /GB:AE003826

39799.4 2.7 FB:FBgn0000486 /sym=Dox-A2 /name=Diphenol oxidase A2 /prod=proteasome, regulatory subunit S3 /func=multicatalytic endopeptidase ; EC:3.4.99.46 | inferred from sequence similarity /map=37B

3954.7 2.7 FB:FBgn0035232 /sym=CG12099 /name= /prod= /func= /map=62A7-62A7 /transc=CT6023 /len=2445 /GB:AE003472

282709.9 2.7 FB:FBgn0010423 /sym=TpnC47D /name=Troponin C at 47D /prod=troponin C /func=calcium binding /map=47E1-47E1 /transc=CT26048 /len=586 /GB:AE003826

261112.7 2.7 FB:FBgn0004169 /sym=up /name=upheld /prod=troponin T /func=tropomyosin binding /map=12A2-12A4 /transc=CT41714 /len=1424 /GB:AE003493

2179.9 ~2.7 BDGP:GH27479.3prime-hit /ESTpos=maps in FB:FBgn0031850 /sym=CG11326 /name= /prod=thrombospondin-3 like /func=cell adhesion /map=26F6-27A1 /transc=CT31613 /len=523

9124.9 2.7 FB:FBgn0000568 /sym=Eip75B /name=Ecdysone-induced protein 75B /prod=nuclear receptor NR1D3 /func=ligand-dependent nuclear receptor /map=75A10-75B6 /transc=CT24290 /len=4527 /GB:A

1646.1 ~2.7 FB:FBgn0035345 /sym=CG16764 /name= /prod= /func= /map=62E5-62E6 /transc=CT37287 /len=577 /GB:AE003475

16248.5 2.7 FB:FBgn0037821 /sym=CG14682 /name= /prod= /func=nucleic acid binding /map=86C2-86C2 /transc=CT34468 /len=3926 /GB:AE003688 /note=3prime sequence from clone BDGP:GH12580.3prime

6856.8 2.7 FB:FBgn0039136 /sym=CG5902 /name= /prod= /func= /map=95D1-95D1 /transc=CT18529 /len=1603 /GB:AE003745 /note=3prime sequence from clone BDGP:SD10002.3prime-hit

6014.3 2.7 FB:FBgn0037747 /sym=CG8481 /name= /prod=N-acetyltransferase /func=enzyme /map=85E8-85E8 /transc=CT24815 /len=1390 /GB:AE003684 /note=3prime sequence from clone BDGP:GH04732.

23332.5 2.7 FB:FBgn0034412 /sym=CG15105 /name= /prod= /func=transcription factor /map=56A1-56A2 /transc=CT34980 /len=3668 /GB:AE003797 /note=3prime sequence from clone BDGP:GH06739.3prime

28735.4 2.7 FB:FBgn0038130 /sym=CG8630 /name= /prod= /func=enzyme /map=87E5-87E5 /transc=CT25031 /len=1227 /GB:AE003699

406983.7 2.7 FB:FBgn0002772 /sym=Mlc1 /name=Myosin alkali light chain 1 /prod=myosin muscle class II essential light chain /func=muscle motor protein /map=98A6-98A6 /transc=CT17694 /len=722 /GB:AE0

4438.3 2.7 FB:FBgn0039268 /sym=CG11819 /name= /prod= /func=protein kinase /map=96B15-96B16 /transc=CT36931 /len=2933 /GB:AE003750

1636.4 ~2.7 FB:FBgn0023180 /sym=Orc6 /name=Origin recognition complex subunit 6 /prod=origin recognition complex, subunit 6 /func=DNA replication factor /map=46B13-46B13 /transc=CT4175 /len=774

3209.9 2.7 FB:FBgn0032218 /sym=CG5381 /name= /prod= /func=transcription factor /map=31D8-31D8 /transc=CT17078 /len=1884 /GB:AE003628

29892.5 2.7 FB:FBgn0033631 /sym=CG9027 /name= /prod=superoxide dismutase-like /func=enzyme /map=47F6-47F7 /transc=CT25938 /len=477 /GB:AE003826

15442.6 2.7 FB:FBgn0004646 /sym=ogre /name=optic ganglion reduced /prod=innexin /func=ion channel /map=6E4-6E4 /transc=CT9674 /len=2219 /GB:AE003439 /note=3prime sequence from clone BDGP:HL

3280.1 ~2.7 FB:FBgn0038572 /sym=CG7901 /name= /prod= /func= /map=90E4-90E4 /transc=CT42545 /len=937 /GB:AE003721

17540.7 2.7 FB:FBgn0028695 /sym=Rpn1 /name= /prod=19S proteasome regulatory particle, non-ATPase protein, subunit S2 /func=endopeptidase /map=76D7-76D7 /transc=CT23606 /len=2967 /GB:AE003515

1747.9 ~2.7 FB:FBgn0037806 /sym=CG11872 /name= /prod= /func= /map=86A1-86A2 /transc=CT37024 /len=4311 /GB:AE003686

3248.6 2.7 FB:FBgn0034969 /sym=CG10485 /name= /prod=ribosomal protein L12-like /func=structural protein of ribosome /map=60B2-60B2 /transc=CT29426 /len=675 /GB:AE003462

19865.8 2.7 FB:FBgn0039909 /sym=CG1970 /name= /prod=NADH-ubiquinone oxidoreductase /func=enzyme /map=102C5-102C5 /transc=CT6146 /len=1482 /GB:AE003843

295117.9 2.7 FB:FBgn0003149 /sym=Prm /name=Paramyosin /prod=paramyosin /func=structural protein of muscle /map=66D14-66D14 /transc=CT18619 /len=2721 /GB:AE003554 /note=3prime sequence from c

226879.3 2.6 FB:FBgn0003178 /sym=PyK /name=Pyruvate kinase /prod=pyruvate kinase /func=pyruvate kinase ; EC:2.7.1.40 /map=94A15-94A15 /transc=CT21861 /len=2091 /GB:AE003738 /note=3prime sequenc
 FB:FBgn0016697 /sym=ProsMA5 /name=Proteasome alpha subunit /prod=20S proteasome, alpha5 subunit /func=multicatalytic endopeptidase ; EC:3.4.99.46 /map=54C1-54C1 /transc=CT30641 /len=

26236 2.6 BDGP:LD33318.3prime-hi

1734.5 ~2.6 FB:FBgn0038591 /sym=CG7150 /name= /prod=transcriptional adaptor-like /func=transcription factor binding /map=90F4-90F4 /transc=CT22097 /len=1876 /GB:AE003721

31369.2 2.6 FB:FBgn0032148 /sym=CG13122 /name= /prod= /func= /map=30D1-30D1 /transc=CT32359 /len=1567 /GB:AE003626 /note=3prime sequence from clone BDGP:HL02309.3prime-hit

94556.2 2.6 FB:FBgn0003074 /sym=Pgi /name=Phosphoglucose isomerase /prod=phosphogluconate dehydrogenase (decarboxylating) /func=phosphogluconate dehydrogenase (decarboxylating) ; EC:1.1.1.44 /map=

17250.2 2.6 FB:FBgn0031187 /sym=CG14619 /name= /prod=ubiquitin-specific protease /func=ubiquitin-specific protease /map=19F5-19F6 /transc=CT34376 /len=2865 /GB:AE003574 /note=3prime sequence fro

65019.7 2.6 FB:FBgn0033126 /sym=CG10106 /name= /prod= /func= /map=42E1-42E1 /transc=CT7946 /len=1113 /GB:AE003842

1930.1 ~2.6 FB:FBgn0037543 /sym=CG10903 /name= /prod= /func= /map=84E7-84E7 /transc=CT10979 /len=831 /GB:AE003677

1510.5 ~2.6 FB:FBgn0040733 /sym=CG15068 /name= /prod= /func= /map=55C9-55C9 /transc=CT34939 /len=189 /GB:AE003799

32265.4 2.6 FB:FBgn0034952 /sym=CG18021 /name= /prod= /func= /map=60A15-60A15 /transc=CT40326 /len=2017 /GB:AE003462 /note=3prime sequence from clone BDGP:GH20492.3prime-hit

226436.5 2.6 FB:FBgn0036108 /sym=CG7941 /name= /prod=cuticle protein-like /func=structural protein /map=67F4-67F4 /transc=CT23954 /len=405 /GB:AE003546

6757.5 2.6 FB:FBgn0035464 /sym=CG12006 /name= /prod= /func= /map=63F1-63F1 /transc=CT1387 /len=1873 /GB:AE003479 /note=3prime sequence from clone BDGP:LD47795.3prime-hit

3265.6 2.6 BDGP:LD23884.3prime-hit /ESTpos=maps in FB:FBgn0030430 /sym=CG4410 /name= /prod=chaperone-like protein /func=chaperone /map=11C4-11C4 /transc=CT4259 /len=500

3303 2.6 FB:FBgn0023215 /sym=EG:114E2.2 /name= /prod= /func=transcription factor binding /map=3F2-3F2 /transc=CT9776 /len=1830 /GB:AE003428 /note=3prime sequence from clone BDGP:GH28809.

3036.8 2.6 FB:FBgn0037252 /sym=CG14650 /name= /prod= /func=chaperone /map=82C1-82C1 /transc=CT34422 /len=3606 /GB:AE003606 /note=3prime sequence from clone BDGP:GH27269.3prime-hit

8684.4 2.6 FB:FBgn0033179 /sym=CG11139 /name= /prod= /func= /map=43C4-43C5 /transc=CT31143 /len=1419 /GB:AE003841 /note=3prime sequence from clone BDGP:GH01724.3prime-hit

31577.4 2.6 FB:FBgn0037314 /sym=CG12000 /name= /prod=20S proteasome, beta4 subunit-like /func=endopeptidase /map=83A4-83A4 /transc=CT1070 /len=1216 /GB:AE003603 /note=3prime sequence from

15346.3 2.6 FB:FBgn0028689 /sym=Rpn6 /name=Proteasome p44.5 subunit /prod=19S proteasome regulatory particle, non-ATPase protein, subunit S9 /func=multicatalytic endopeptidase ; EC:3.4.99.46 | inferred

10636.7 2.6 FB:FBgn0012042 /sym=AttA /name=Attacin-A /prod=attacin /func=antibacterial response protein /map=51C2-51C2 /transc=CT28545 /len=895 /GB:AE003813 /note=3prime sequence from clone BD

4029.3 2.6 FB:FBgn0022986 /sym=qkr58E-1 /name=quaking related 58E-1 /prod= /func=RNA binding /map=58D8-58D8 /transc=CT12115 /len=1618 /GB:AE003457 /note=3prime sequence from clone BDGP:

346314.5 2.6 FB:FBgn0032538 /sym=CG16885 /name= /prod= /func= /map=34E1-34E1 /transc=CT35249 /len=780 /GB:AE003641

3832 2.6 FB:FBgn0039110 /sym=CG10225 /name= /prod= /func=structural protein /map=95B7-95B7 /transc=CT28739 /len=1726 /GB:AE003744 /note=3prime sequence from clone BDGP:LD02979.3prime-h

13072 2.6 FB:FBgn0002787 /sym=Mov34 /name=Mov34 /prod=19S proteasome regulatory particle, non-ATPase protein, subunit S12 /func=multicatalytic endopeptidase ; EC:3.4.99.46 /map=60D1-60D1 /transc=

14695.1 2.6 FB:FBgn0030479 /sym=CG1987 /name= /prod=RNA binding protein-like /func=RNA binding /map=11E11-11E11 /transc=CT6330 /len=393 /GB:AE003492

11266.1 2.6 FB:FBgn0000480 /sym=Doa /name=Darkener of apricot /prod=protein serine/threonine kinase /func=protein kinase /map=98F1-98F2 /transc=CT4592 /len=2232 /GB:AE003767 /note=3prime sequenc

2739.1 ~2.6 FB:FBgn0039688 /sym=CG1964 /name= /prod=ADAM10 family metalloendopeptidase/disintegrin-like /func=endopeptidase /map=99C1-99C1 /transc=CT3146 /len=4614 /GB:AE003770

3005.4 2.6 FB:FBgn0002641 /sym=mal /name=maroon-like /prod=molybdopterin cofactor sulfurase-like /func=molybdopterin cofactor sulfurase /map=19D2-19D3 /transc=CT4746 /len=2717 /GB:AE003571 /nc

2590.6 2.6 FB:FBgn0039423 /sym=CG6166 /name= /prod= /func= /map=97A9-97A9 /transc=CT19364 /len=2031 /GB:AE003756 /note=3prime sequence from clone BDGP:GH14066.3prime-hit

1561.7 ~2.5 FB:FBgn0038041 /sym=CG6525 /name= /prod= /func=ligand binding or carrier /map=87B15-87B15 /transc=CT20279 /len=6051 /GB:AE003695

4086.6 2.5 FB:FBgn0034688 /sym=CG11474 /name= /prod= /func= /map=58C1-58C1 /transc=CT36283 /len=1521 /GB:AE003456 /note=3prime sequence from clone BDGP:LD03212.3prime-hit

8386.7 2.5 FB:FBgn0029851 /sym=CG14445 /name= /prod= /func= /map=5D6-5D6 /transc=CT34116 /len=1143 /GB:AE003437

2153.4 ~2.5 FB:FBgn0034242 /sym=CG14480 /name= /prod= /func= /map=54D1-54D1 /transc=CT34191 /len=750 /GB:AE003802

22995.3 2.5 FB:FBgn0028687 /sym=Rpt1 /name= /prod=19S proteasome regulatory particle, triple-A protein, subunit S7 /func=proteasome ATPase ; EC:3.6.4.8 /map=43E6-43E6 /transc=CT3016 /len=1397 /GB:A

1340.1 ~2.5 FB:FBgn0035081 /sym=CG2858 /name= /prod= /func=enzyme /map=60E5-60E5 /transc=CT9732 /len=1449 /GB:AE003465

1871.2 ~2.5 FB:FBgn0038688 /sym=CG3768 /name= /prod=calcium binding protein-like /func=ligand binding or carrier /map=91F8-91F8 /transc=CT12576 /len=1030 /GB:AE003725 /note=3prime sequence from

5012.1 2.5 FB:FBgn0029715 /sym=CG11444 /name= /prod= /func= /map=4C4-4C4 /transc=CT9463 /len=1230 /GB:AE003431 /note=3prime sequence from clone BDGP:GM14292.3prime-hit

3675.4 2.5 FB:FBgn0024988 /sym=EG:131F2.2 /name= /prod= /func=enzyme /map=2B12-2B12 /transc=CT34614 /len=2176 /GB:AE003422 /note=3prime sequence from clone BDGP:SD04906.3prime-hit

58654.6 2.5 FB:FBgn0037346 /sym=CG2922 /name= /prod= /func= /map=83B4-83B4 /transc=CT7240 /len=2082 /GB:AE003602 /note=3prime sequence from clone BDGP:LD21309.3prime-hit

47824.9 2.5 FB:FBgn0036109 /sym=CG18349 /name= /prod= /func= /map=67F4-67F4 /transc=CT41690 /len=536 /GB:AE003546

150789.1 2.5 *Drosophila* gene for Gapdh2 (_5, _M, _3 represent transcript regions 5 prime, Middle, and 3 prime respectively)

237211 2.5 FB:FBgn0001092 /sym=Gapdh2 /name=Glyceraldehyde 3 phosphate dehydrogenase 2 /prod=glyceraldehyde 3-phosphate dehydrogenase (phosphorylating) 2 /func=glyceraldehyde 3-phosphate dehydro

15429.8 2.5 FB:FBgn0038420 /sym=CG10311 /name= /prod= /func= /map=89B22-89B22 /transc=CT28967 /len=719 /GB:AE003713

1337.5 ~2.5 FB:FBgn0033745 /sym=CG8824 /name= /prod=beta-N-acetylhexosaminidase-like /func=enzyme /map=49A9-49A9 /transc=CT25388 /len=2555 /GB:AE003822 /note=3prime sequence from clone BL

6100.3 2.5 FB:FBgn0038878 /sym=CG3301 /name= /prod= /func=enzyme /map=93D4-93D4 /transc=CT11093 /len=913 /GB:AE003734 /note=3prime sequence from clone BDGP:GH01837.3prime-hit

1526.3 ~2.5 FB:FBgn0031206 /sym=CG12466 /name= /prod= /func=enzyme /map=20B1-20B1 /transc=CT32678 /len=1204 /GB:AE003573 /note=3prime sequence from clone BDGP:GH12380.3prime-hit

21705.6 2.5 FB:FBgn0030672 /sym=CG9281 /name= /prod=ATP-binding cassette transporter /func=enzyme /map=13E14-13E14 /transc=CT26402 /len=2568 /GB:AE003500 /note=3prime sequence from clone B

35348.3 2.5 FB:FBgn0026781 /sym=Prosalph1 /name=Proteasome alpha1 subunit /prod=20S proteasome alpha1 subunit /func=multicatalytic endopeptidase ; EC:3.4.99.46 /map=43F1-43F1 /transc=CT42048 /len=

2834.7 2.5 FB:FBgn0036811 /sym=CG6884 /name= /prod= /func= /map=75D4-75D4 /transc=CT21320 /len=610 /GB:AE003519

515.3 ~2.5 FB:FBgn0032574 /sym=CG18629 /name= /prod= /func= /map=35E1-35E1 /transc=CT41822 /len=588 /GB:AE003649

2330 2.5 FB:FBgn0034094 /sym=CG3666 /name= /prod=transferrin-like /func=ligand binding or carrier /map=52F10-52F10 /transc=CT12185 /len=2352 /GB:AE003807 /note=3prime sequence from clone BD

463382.8 2.5 FB:FBgn0038154 /sym=CG18290 /name= /prod= /func= /map=87E11-87E11 /transc=CT41497 /len=1195 /GB:AE003700

9847.6 2.5 FB:FBgn0000250 /sym=cact /name=cactus /prod= /func=transcription factor, cytoplasmic sequestering /map=35F8-35F9 /transc=CT18347 /len=1918 /GB:AE003650 /note=3prime sequence from clo

15853.4 2.5 FB:FBgn0040754 /sym=CG17059 /name= /prod= /func= /map=49F13-49F13 /transc=CT37898 /len=358 /GB:AE003819

119631.9 2.5 FB:FBgn0000045 /sym=Act79B /name=Actin 79B /prod=actin /func=muscle motor protein /map=79B3-79B3 /transc=CT22987 /len=1172 /GB:AE003596

42016.5 2.5 FB:FBgn0023174 /sym=Probeta2 /name=Proteasome beta2 subunit /prod=20S proteasome, beta2 subunit /func=multicatalytic endopeptidase ; EC:3.4.99.46 /map=71A3-71A3 /transc=CT10524 /len=1

7369.5 2.5 FB:FBgn0001301 /sym=kel /name=kelch /prod= /func=transcription factor /map=36E3-36E5 /transc=CT22235 /len=5604 /GB:AE003657 /note=3prime sequence from clone BDGP:LD29455.3prime-

2044.3 ~2.5 FB:FBgn0029872 /sym=CG12543 /name= /prod= /func= /map=6A2-6A2 /transc=CT34107 /len=684 /GB:AE003437

6487.2 2.4 FB:FBgn0032202 /sym=CG18619 /name= /prod= /func= /map=31C6-31C6 /transc=CT40890 /len=486 /GB:AE003628

396588.5 2.4 FB:FBgn0002531 /sym=Lcp1 /name=Larval cuticle protein 1 /prod=larval cuticle protein 1 /func=structural protein of larval cuticle (*Drosophila*) /map=44C1-44C1 /transc=CT36649 /len=543 /GB:AE003842

7853 2.4 FB:FBgn0033129 /sym=CG12844 /name= /prod= /func= /map=42E1-42E1 /transc=CT31976 /len=673 /GB:AE003842

1333.8 ~2.4 FB:FBgn0035649 /sym=CG10483 /name= /prod= /func= /map=64F5-64F5 /transc=CT29432 /len=2221 /GB:AE003564 /note=3prime sequence from clone BDGP:GH26628.3prime-hit

1728.4 ~2.4 BDGP:LD4689.3prime-hit /ESTpos=maps in FB:FBgn0037937 /sym=CG6913 /name= /prod= /func=DNA binding /map=86F1-86F1 /transc=CT21412 /len=536

8012.7 2.4 BDGP:LD1981.3prime-hit /ESTpos=maps 3prime of FB:FBgn0027356 /sym=amphiphysin /name=amphiphysin /prod=amphiphysin /func=protein kinase /map=49B3-49B3 /transc=CT259 /len=527

20242.2 2.4 FB:FBgn0015282 /sym=Pros26.4 /name=Proteasome 26S subunit subunit 4 ATPase /prod=19S proteasome regulatory particle, triple-A protein, subunit S4 /func=proteasome ATPase ; EC:3.6.4.8 /map=7A9-7A9

1105.9 ~2.4 FB:FBgn0030941 /sym=CG6531 /name= /prod= /func= /map=17C3-17C3 /transc=CT20295 /len=1260 /GB:AE003509

11202 2.4 FB:FBgn0029534 /sym=CG5273 /name= /prod= /func= /map=1C1-1C1 /transc=CT16821 /len=2072 /GB:AE003418

30822.1 2.4 FB:FBgn0015283 /sym=Pros54 /name=Proteasome 54kD subunit /prod=19S proteasome regulatory particle, non-ATPase protein, subunit S5a /func=multicatalytic endopeptidase ; EC:3.4.99.46 /map=7A9-7A9

1588.1 ~2.4 FB:FBgn0033026 /sym=CG12183 /name= /prod= /func=actin binding /map=41C4-41C4 /transc=CT9399 /len=1982 /GB:AE003786

2849.2 2.4 FB:FBgn0039238 /sym=CG7016 /name= /prod= /func= /map=96B4-96B4 /transc=CT21718 /len=1089 /GB:AE003749

2368.7 ~2.4 FB:FBgn0036359 /sym=CG14105 /name= /prod= /func= /map=70A8-70A8 /transc=CT33698 /len=558 /GB:AE003538

32750.7 2.4 FB:FBgn0035089 /sym=CG9358 /name= /prod= /func=ligand binding or carrier /map=60E7-60E7 /transc=CT26583 /len=366 /GB:AE003465

2937.6 2.4 FB:FBgn0038260 /sym=CG14855 /name= /prod=organic cation transporter-like /func=transporter /map=88D5-88D5 /transc=CT34672 /len=1671 /GB:AE003706

61689.5 2.4 FB:FBgn0029639 /sym=CG14419 /name= /prod= /func= /map=3C3-3C3 /transc=CT34076 /len=588 /GB:AE003425

359826.3 2.4 FB:FBgn0001091 /sym=Gapdh1 /name=Glyceraldehyde 3 phosphate dehydrogenase 1 /prod=glyceraldehyde 3-phosphate dehydrogenase (phosphorylating) 1 /func=glyceraldehyde 3-phosphate dehydrogenase (phosphorylating) 1

1642.5 ~2.4 FB:FBgn0030991 /sym=CG7453 /name= /prod= /func= /map=18B4-18B4 /transc=CT22925 /len=1285 /GB:AE003511

27834.9 2.4 FB:FBgn0035978 /sym=CG4347 /name= /prod= /func=UTP--glucose-1-phosphate uridylyltransferase /map=67A9-67B1 /transc=CT14147 /len=2009 /GB:AE003552 /note=3prime sequence from clone BDGP:LD16758.3prime-hit

996.5 ~2.4 FB:FBgn0024993 /sym=EG:100G10.6 /name= /prod= /func=transcription factor /map=3B4-3B5 /transc=CT9011 /len=1402 /GB:AE003425

11747.2 2.4 FB:FBgn0036111 /sym=CG6391 /name= /prod=diphosphoinositol polyphosphate phosphohydrolase /func=enzyme /map=67F4-67F4 /transc=CT19950 /len=1704 /GB:AE003546

2303.3 2.4 FB:FBgn0032392 /sym=CG17749 /name= /prod= /func= /map=33B9-33B9 /transc=CT39339 /len=476 /GB:AE003634

18248.8 2.4 FB:FBgn0036580 /sym=CG13072 /name= /prod= /func= /map=72D12-72D12 /transc=CT32291 /len=402 /GB:AE003528

13431.5 2.4 FB:FBgn0033683 /sym=CG18343 /name= /prod= /func= /map=48E10-48E10 /transc=CT41671 /len=463 /GB:AE003823

73558.1 2.4 FB:FBgn0039358 /sym=CG5028 /name= /prod= /func=enzyme /map=96E10-96E10 /transc=CT16155 /len=1312 /GB:AE003753

1327 ~2.4 FB:FBgn0015569 /sym=alpha-Est10 /name=alpha-Esterase-1 /prod=esterase, unknown substrate /func=esterase, unknown substrate ; EC:3.1.1.- /map=84D5-84D5 /transc=CT1811 /len=1650 /GB:AE003842

9558.3 2.4 FB:FBgn0024754 /sym=Flo /name=flotillin /prod=flotillin /func=ligand binding or carrier /map=52A13-52A13 /transc=CT37018 /len=1779 /GB:AE003810 /note=3prime sequence from clone BDGP:LD16758.3prime-hit

37048.3 2.4 FB:FBgn0030151 /sym=CG1354 /name= /prod=GTP-binding protein /func=ligand binding or carrier /map=8F10-8F10 /transc=CT3048 /len=1200 /GB:AE003448

14186.8 2.4 FB:FBgn0028686 /sym=Rpt3 /name= /prod=19S proteasome regulatory particle, triple-A protein, subunit S6b /func=proteasome ATPase ; EC:3.6.4.8 /map=10A6-10A6 /transc=CT35131 /len=1242 /GB:AE003564

357251.3 2.4 FB:FBgn0000064 /sym=Ald /name=Aldolase /prod=fructose-bisphosphate aldolase /func=fructose-bisphosphate aldolase ; EC:4.1.2.13 | inferred from direct assay /map=97A6-97A6 /transc=CT41919 /len=1000

26041.1 2.4 FB:FBgn0037007 /sym=CG5059 /name= /prod= /func= /map=77C4-77C4 /transc=CT16233 /len=939 /GB:AE003591

146254 2.4 FB:FBgn0004551 /sym=Ca-P60A /name=Calcium ATPase at 6A /prod=calcium-transporting ATPase, sarco/endoplasmic reticulum type /func=calcium-transporting ATPase ; EC:3.6.1.38 /map=60A11-60A11

8895.8 2.4 FB:FBgn0027591 /sym=BcDNA:GH04245 /name= /prod= /func= /map=41A1-41A2 /transc=CT9123 /len=3519 /GB:AE003787 /note=3prime sequence from clone BDGP:LD16758.3prime-hit

968.3 ~2.4 FB:FBgn0030563 /sym=CG18157 /name= /prod= /func= /map=12E2-12E2 /transc=CT40954 /len=594 /GB:AE003495

20212.5 2.4 FB:FBgn0040954 /sym=CG13779 /name= /prod= /func= /map=27D5-27D5 /transc=CT33267 /len=240 /GB:AE003616

5163.6 2.4 FB:FBgn0035981 /sym=CG4452 /name= /prod= /func=endopeptidase /map=67B1-67B1 /transc=CT14468 /len=1633 /GB:AE003552 /note=3prime sequence from clone BDGP:LD21662.3prime-hit

133490.6 2.4 FB:FBgn0040764 /sym=CG13230 /name= /prod= /func= /map=47D4-47D4 /transc=CT32474 /len=219 /GB:AE003827

253266.6 2.4 *Drosophila* gene for Gapdh2 (_5, _M, _3 represent transcript regions 5 prime, Middle, and 3 prime respectively)

10105.4 2.4 FB:FBgn0026777 /sym=Rad23 /name= /prod= /func=DNA repair protein /map=102A8-102A8 /transc=CT5572 /len=1477 /GB:AE003844 /note=3prime sequence from clone BDGP:LD10153.complet

556.8 ~2.4 FB:FBgn0036074 /sym=CG11965 /name= /prod= /func= /map=67D2-67D2 /transc=CT37129 /len=1464 /GB:AE003549

6578.4 2.4 FB:FBgn0015614 /sym=CanB2 /name=Calcineurin B2 /prod=calcineurin, calcium-binding, regulatory (B)-subunit 2 /func=calcium binding /map=43E16-43E16 /transc=CT31322 /len=718 /GB:AE003549

5794.3 2.3 FB:FBgn0024753 /sym=Flo-2 /name=flotillin 2 /prod=flotillin 2 /func= /map=13A3-13A4 /transc=CT34056 /len=1791 /GB:AE003497 /note=3prime sequence from clone BDGP:LP11503.3prime-hit

22177.6 2.3 FB:FBgn0027493 /sym=BcDNA:LD32788 /name= /prod=adenylosuccinate synthase /func=adenylosuccinate synthase ; EC:6.3.4.4 /map=92F13-92F13 /transc=CT35906 /len=1986 /GB:AE003732 /note=3prime sequence from clone BDGP:LD21662.3prime-hit

13759.5 2.3 FB:FBgn0039213 /sym=CG6668 /name= /prod= /func= /map=96A14-96A15 /transc=CT20689 /len=2852 /GB:AE003748 /note=3prime sequence from clone BDGP:GH09383.3prime-hit

1521 ~2.3 FB:FBgn0034946 /sym=CG3065 /name= /prod= /func=nucleic acid binding /map=60A14-60A14 /transc=CT10306 /len=1916 /GB:AE003462 /note=3prime sequence from clone BDGP:GM01315.3prime-hit

21415.1 2.3 FB:FBgn0033886 /sym=CG13349 /name= /prod= /func= /map=50C20-50C20 /transc=CT32670 /len=1170 /GB:AE003816

53208.4 2.3 FB:FBgn0002284 /sym=Pros26 /name=Proteasome 26kD subunit /prod=20S proteasome, beta6 subunit /func=multicatalytic endopeptidase ; EC:3.4.99.46 /map=73A10-73A10 /transc=CT13566 /len=944

109219.9 2.3 FB:FBgn0017565 /sym=Nacalpa /name=Nascent polypeptide associated complex protein alpha subunit /prod=nascent polypeptide associated complex protein alpha subunit /func= /map=49C2-49C2 /transc=CT35112 /len=612 /GB:AE003486

11393.2 2.3 FB:FBgn0030310 /sym=CG11709 /name= /prod=peptidoglycan recognition protein-like /func=defense/immunity protein /map=10C4-10C4 /transc=CT35112 /len=612 /GB:AE003486

29773.9 2.3 FB:FBgn0030724 /sym=CG9212 /name= /prod= /func=4-nitrophenylphosphatase /map=14A6-14A6 /transc=CT26318 /len=1359 /GB:AE003501 /note=3prime sequence from clone BDGP:LD01807.3prime-hit

1175.3 ~2.3 FB:FBgn0029970 /sym=CG17256 /name= /prod=protein serine/threonine kinase-like /func=protein kinase /map=7C6-7C6 /transc=CT38234 /len=2435 /GB:AE003442 /note=3prime sequence from clone BDGP:LD01807.3prime-hit

22793.7 2.3 FB:FBgn0036630 /sym=CG4561 /name= /prod= /func=tyrosine-tRNA ligase /map=73A1-73A1 /transc=CT14730 /len=1717 /GB:AE003527

1093 ~2.3 BDGP:GH06247.3prime-hit /maps to FB:FBgn0036239 (/sym=CG5684 /name= /prod= /func=transcription factor) and FB:FBgn0036238 (/sym=CG5688 /name= /prod= /func=motor)

21198.4 2.3 FB:FBgn0003151 /sym=Pros35 /name=Proteasome 35kD subunit /prod=20S proteasome, alpha6 subunit /func=multicatalytic endopeptidase ; EC:3.4.99.46 /map=31B3-31B4 /transc=CT15762 /len=944

24276.6 2.3 FB:FBgn0035206 /sym=CG9186 /name= /prod= /func= /map=61F6-61F6 /transc=CT8283 /len=1400 /GB:AE003471 /note=3prime sequence from clone BDGP:LP01162.3prime-hit

2027.2 2.3 FB:FBgn0010406 /sym=RNaseX25 /name=Ribonuclease X25 /prod=ribonuclease-like /func=ribonuclease /map=66A22-66A22 /transc=CT24383 /len=1658 /GB:AE003557 /note=3prime sequence from clone BDGP:LD01807.3prime-hit

1848.8 ~2.3 FB:FBgn0029798 /sym=CG4078 /name= /prod= /func=DNA repair protein /map=5B3-5B3 /transc=CT13546 /len=3246 /GB:AE003435

2933.2 2.3 FB:FBgn0005649 /sym=Rox8 /name=Rox8 /prod=nucleolysin-like /func=poly(A) binding /map=95D5-95D5 /transc=CT17178 /len=3165 /GB:AE003746

1385.8 ~2.3 FB:FBgn0039901 /sym=CG10322 /name= /prod= /func= /map=102A7-102A8 /transc=CT7685 /len=630 /GB:AE003844

2931.2 2.3 FB:FBgn0033352 /sym=CG8232 /name= /prod=PAB-dependent poly(A)-specific ribonuclease subunit /func=enzyme /map=44F9-44F11 /transc=CT8229 /len=3925 /GB:AE003835 /note=3prime sequence from clone BDGP:LD01807.3prime-hit

12984.9 2.3 FB:FBgn0039265 /sym=CG11790 /name= /prod= /func=chaperone /map=96B15-96B15 /transc=CT33049 /len=794 /GB:AE003750

10889.7 2.3 FB:FBgn0034618 /sym=CG9485 /name= /prod=glycogen debranching enzyme /func=enzyme /map=57D4-57D5 /transc=CT26790 /len=4780 /GB:AE003453 /note=3prime sequence from clone BDGP:LD01807.3prime-hit

33371.1 2.3 FB:FBgn0038922 /sym=CG6439 /name= /prod=isocitrate dehydrogenase [NAD] subunit /func=enzyme /map=93F14-93F14 /transc=CT20062 /len=1598 /GB:AE003737 /note=3prime sequence from clone BDGP:LD01807.3prime-hit

13683.2 2.2 FB:FBgn0016122 /sym=Acer /name=Angiotensin-converting enzyme-related /prod=angiotensin I-converting enzyme /func=peptidyl-dipeptidase A ; EC:3.4.15.1 /map=29D1-29D2 /transc=CT29700 /len=1000

254389.5 2.2 *Drosophila* gene for Gapdh2 (_5, _M, _3 represent transcript regions 5 prime, Middle, and 3 prime respectively)

1518.4 ~2.2 FB:FBgn0025186 /sym=ari2 /name=ariadne 2 /prod= /func= /map=58C7-58D1 /transc=CT17832 /len=3002 /GB:AE003456
FB:FBgn0004237 /sym=Hrb87F /name=Heterogeneous nuclear ribonucleoprotein at 87F /prod=heterogeneous nuclear ribonucleoprotein A1 /func=ribonucleoprotein /map=87F7-87F7 /transc=CT2725
9346.5 2.2 BDGP:GH05625.3
25443.2 2.2 FB:FBgn0003150 /sym=Pros29 /name=Proteasome 29kD subunit /prod=20S proteasome, alpha3 subunit /func=multicatalytic endopeptidase ; EC:3.4.99.46 /map=57B15-57B15 /transc=CT26525 /len=
367002.4 2.2 FB:FBgn0032537 /sym=CG18634 /name= /prod= /func= /map=34E1-34E1 /transc=CT42158 /len=552 /GB:AE003641
25780.9 2.2 FB:FBgn0035631 /sym=CG5495 /name=Thioredoxin-like /prod=thioredoxin-like /func=thioredoxin /map=64F1-64F1 /transc=CT17420 /len=957 /GB:AE003565 /note=3prime sequence from clone B
62260.5 2.2 FB:FBgn0027910 /sym=BcDNA:GM14618 /name= /prod= /func= /map=25C2-25C3 /transc=CT26154 /len=1161 /GB:AE003608
13850 2.2 FB:FBgn0033356 /sym=CG8229 /name= /prod= /func= /map=44F12-45A1 /transc=CT8591 /len=1918 /GB:AE003835 /note=3prime sequence from clone BDGP:LD27667.3prime-hit
252125.8 2.2 FB:FBgn0000579 /sym=Eno /name=Enolase /prod=phosphopyruvate hydratase /func=phosphopyruvate hydratase ; EC:4.2.1.11 /map=22B1-22B1 /transc=CT32526 /len=1931 /GB:AE003585
38831.3 2.2 FB:FBgn0040985 /sym=CG6115 /name= /prod= /func= /map=36A11-36A11 /transc=CT19203 /len=566 /GB:AE003653
22161.4 2.2 FB:FBgn0022959 /sym=yps /name=ypsilon schachtel /prod= /func= /map=68F4-68F4 /transc=CT17850 /len=2254 /GB:AE003542 /note=3prime sequence from clone BDGP:LD37574.3prime-hit
18395.1 2.2 FB:FBgn0032776 /sym=CG18061 /name= /prod= /func= /map=37E1-37E1 /transc=CT40481 /len=2027 /GB:AE003662 /note=3prime sequence from clone BDGP:SD04793.3prime-hit
FB:FBgn0011754 /sym=PhKgamma /name=Phosphorylase kinase gamma /prod=phosphorylase kinase, catalytic gamma subunit /func=phosphorylase kinase catalyst /map=10D2-10D4 /transc=CT55
6974.5 2.2 BDGP:GH28523.3pri
2303.3 2.2 FB:FBgn0032203 /sym=CG4946 /name= /prod= /func= /map=31C6-31C6 /transc=CT15842 /len=834 /GB:AE003628
116191.6 2.2 FB:FBgn0032941 /sym=CG8669 /name= /prod= /func= /map=39D2-39D2 /transc=CT5302 /len=1793 /GB:AE003670 /note=3prime sequence from clone BDGP:GH11210.3prime-hit
962.2 ~2.2 FB:FBgn0029913 /sym=CG3044 /name= /prod=chitinase /func=enzyme /map=6D3-6D3 /transc=CT10053 /len=1299 /GB:AE003439
900.8 ~2.2 FB:FBgn0004170 /sym=sc /name=scute /prod= /func=specific RNA polymerase II transcription factor /map=1B2-1B2 /transc=CT12777 /len=1038 /GB:AE003417
2967.8 2.2 FB:FBgn0037377 /sym=CG1218 /name= /prod= /func= /map=83C1-83C1 /transc=CT2292 /len=1479 /GB:AE003601 /note=3prime sequence from clone BDGP:LD28626.3prime-hit
1095.1 ~2.2 FB:FBgn0040737 /sym=CG14503 /name= /prod= /func= /map=55C5-55C5 /transc=CT34218 /len=177 /GB:AE003800
37391.6 2.2 FB:FBgn0028490 /sym=BcDNA:GH07269 /name= /prod= /func=DNA binding /map=33A2-33A2 /transc=CT20317 /len=3403 /GB:AE003632 /note=3prime sequence from clone BDGP:GH07269.3p
1499.3 ~2.2 FB:FBgn0028854 /sym=BG:DS07721.6 /name= /prod= /func= /map=35B5-35B5 /transc=CT35229 /len=3129 /GB:AE003644
106563 2.2 FB:FBgn0031024 /sym=CG12233 /name= /prod= /func=enzyme /map=18D3-18D3 /transc=CT13154 /len=1375 /GB:AE003512
20052.9 2.2 FB:FBgn0034110 /sym=CG3615 /name= /prod= /func= /map=53A2-53A2 /transc=CT12045 /len=2831 /GB:AE003807 /note=3prime sequence from clone BDGP:SD01812.3prime-hit
20912.8 2.2 FB:FBgn0037537 /sym=CG2767 /name= /prod=alcohol dehydrogenase /func=enzyme /map=84E5-84E6 /transc=CT9417 /len=1293 /GB:AE003677 /note=3prime sequence from clone BDGP:LD2467
7230.8 2.2 FB:FBgn0015239 /sym=Hr78 /name=Hormone-receptor-like in 78 /prod=nuclear receptor NR2D1 /func=ligand-dependent nuclear receptor /map=78D7-78D7 /transc=CT22217 /len=2246 /GB:AE003
8132.5 2.2 FB:FBgn0033128 /sym=CG12142 /name=Tetraspanin 42Eg /prod=tetraspanin /func= /map=42E1-42E1 /transc=CT7934 /len=1170 /GB:AE003842 /note=3prime sequence from clone BDGP:GM0696
10851 2.2 FB:FBgn0036661 /sym=CG9705 /name= /prod=calcium-regulated heat stable protein-like /func= /map=73C1-73C1 /transc=CT27440 /len=1386 /GB:AE003526 /note=3prime sequence from clone BD
5745.6 2.2 FB:FBgn0027108 /sym=inx2 /name= /prod=innexin 2 /func=neurotransmitter transporter /map=6E4-6E5 /transc=CT14874 /len=1819 /GB:AE003439
47271.9 2.2 FB:FBgn0035904 /sym=CG6776 /name= /prod=glutathione transferase /func=glutathione transferase /map=66D4-66D4 /transc=CT21027 /len=776 /GB:AE003555
171608.5 2.2 FB:FBgn0004432 /sym=Cyp1 /name=Cyclophilin 1 /prod=cyclophilin /func=cyclophilin /map=14B15-14B15 /transc=CT27926 /len=910 /GB:AE003501 /note=3prime sequence from clone BDGP:SD
2011.6 ~2.2 FB:FBgn0037190 /sym=CG7651 /name= /prod=P-type ATPase /func=transporter /map=79F3-79F3 /transc=CT22775 /len=3566 /GB:AE003598
12077.1 2.2 FB:FBgn0036299 /sym=CG10620 /name= /prod=transferrin-like /func=transporter /map=69C4-69C4 /transc=CT29752 /len=2860 /GB:AE003541 /note=3prime sequence from clone BDGP:LD22449.
42356.9 2.2 FB:FBgn0037245 /sym=CG14648 /name= /prod= /func=enzyme /map=82B3-82B3 /transc=CT34420 /len=1773 /GB:AE003606

22512 2.2 FB:FBgn0033385 /sym=CG8055 /name= /prod= /func= /map=45B1-45B1 /transc=CT8052 /len=1251 /GB:AE003834 /note=3prime sequence from clone BDGP:GH13992.3prime-hit

574.3 ~2.2 FB:FBgn0034578 /sym=CG15653 /name= /prod= /func= /map=57B20-57B20 /transc=CT35837 /len=513 /GB:AE003452

1624.6 ~2.2 FB:FBgn0025802 /sym=Sbf /name=SET domain binding factor /prod= /func=ligand binding or carrier /map=86F9-86F9 /transc=CT21495 /len=6619 /GB:AE003693 /note=3prime sequence from clone

1672.7 2.2 FB:FBgn0031454 /sym=CG9960 /name= /prod= /func= /map=23B1-23B1 /transc=CT28077 /len=799 /GB:AE003582 /note=3prime sequence from clone BDGP:GH13185.3prime-hit

798.8 ~2.2 FB:FBgn0039443 /sym=CG14242 /name= /prod= /func= /map=97C1-97C1 /transc=CT33862 /len=687 /GB:AE003757

13583.6 2.1 FB:FBgn0037465 /sym=CG1105 /name= /prod= /func= /map=84C1-84C1 /transc=CT1653 /len=1336 /GB:AE003673

1734.8 ~2.1 FB:FBgn0034494 /sym=CG10444 /name= /prod=sodium-dependent multivitamin transporter-like /func=transporter /map=56F15-56F16 /transc=CT29322 /len=2772 /GB:AE003792 /note=3prime sequ

38948.5 2.1 FB:FBgn0028684 /sym=Rpt5 /name=Tat-binding protein-1 /prod=19S proteasome regulatory particle, triple-A protein, subunit S6a /func=proteasome ATPase ; EC:3.6.4.8 /map=95B7-95B7 /transc=CT

73992.4 2.1 FB:FBgn0034583 /sym=CG10527 /name= /prod= /func= /map=57B20-57B20 /transc=CT29543 /len=1133 /GB:AE003452 /note=3prime sequence from clone BDGP:LD46156.3prime-hit

8442.3 2.1 FB:FBgn0016700 /sym=Rab1 /name=Rab-protein 1 /prod= /func=RHO small GTPase /map=93D4-93D4 /transc=CT11153 /len=1791 /GB:AE003734

4736.2 2.1 FB:FBgn0038298 /sym=CG18525 /name= /prod= /func= /map=88E7-88E7 /transc=CT42292 /len=1494 /GB:AE003708 /note=3prime sequence from clone BDGP:GH14439.3prime-hit

160299.1 2.1 FB:FBgn0037686 /sym=CG9354 /name= /prod=ribosomal protein L34-like /func=structural protein of ribosome /map=85D15-85D15 /transc=CT25494 /len=771 /GB:AE003682

836.4 ~2.1 FB:FBgn0036722 /sym=CG13729 /name= /prod= /func= /map=74C1-74C1 /transc=CT33196 /len=360 /GB:AE003524

296466.6 2.1 FB:FBgn0002626 /sym=Rpl32 /name=Ribosomal protein L32 /prod=ribosomal protein L32 /func=large-subunit cytosol ribosomal protein /map=99D5-99D5 /transc=CT6405 /len=505 /GB:AE003772

12782.7 2.1 FB:FBgn0030087 /sym=CG7766 /name= /prod= /func=protein kinase /map=8C13-8C14 /transc=CT23171 /len=3994 /GB:AE003446

15250.7 2.1 FB:FBgn0023211 /sym=Elongin-C /name=Elongin C /prod=elongin C /func=transcription factor /map=56D7-56D7 /transc=CT26431 /len=557 /GB:AE003796

1257.5 ~2.1 FB:FBgn0040974 /sym=CG9260 /name= /prod= /func= /map=34C1-34C1 /transc=CT26204 /len=460 /GB:AE003640

389648.8 2.1 FB:FBgn0002533 /sym=Lcp2 /name=Larval cuticle protein 2 /prod=larval cuticle protein 2 /func=structural protein of larval cuticle (*Drosophila*) /map=44C1-44C1 /transc=CT3631 /len=526 /GB:AE0

27381 2.1 FB:FBgn0026088 /sym=EG:63B12.12 /name= /prod= /func= /map=2B14-2B14 /transc=CT34631 /len=460 /GB:AE003422

1849.4 ~2.1 FB:FBgn0039353 /sym=CG5046 /name= /prod= /func=cell adhesion /map=96E10-96E10 /transc=CT16193 /len=840 /GB:AE003753

15969.5 2.1 FB:FBgn0011768 /sym=Fdh /name=Formaldehyde dehydrogenase /prod=formaldehyde dehydrogenase (glutathione) /func=formaldehyde dehydrogenase (glutathione) ; EC:1.2.1.1 | inferred from direct

16747.9 2.1 FB:FBgn0032725 /sym=CG10679 /name= /prod= /func=structural protein of ribosome /map=37B8-37B8 /transc=CT29904 /len=255 /GB:AE003661

40713.9 2.1 FB:FBgn0032134 /sym=CG3864 /name= /prod= /func= /map=30C1-30C2 /transc=CT12877 /len=966 /GB:AE003625 /note=3prime sequence from clone BDGP:SD03042.3prime-hit

5591.9 2.1 FB:FBgn0033635 /sym=CG7777 /name= /prod=water transporter /func=transporter /map=47F13-47F13 /transc=CT23658 /len=1371 /GB:AE003826 /note=3prime sequence from clone BDGP:LD273

400824.5 2.1 FB:FBgn0002535 /sym=Lcp4 /name=Larval cuticle protein 4 /prod=larval cuticle protein 4 /func=structural protein of larval cuticle (*Drosophila*) /map=44C1-44C1 /transc=CT6607 /len=682 /GB:AE0

288362.1 2.1 FB:FBgn0002741 /sym=Mhc /name=Myosin heavy chain /prod=myosin II heavy chain /func=muscle motor protein /map=36A8-36A9 /transc=CT39920 /len=5794 /GB:AE003652

48332.5 2.1 FB:FBgn0013770 /sym=Cp1 /name=Cysteine proteinase-1 /prod=cathepsin L /func=cathepsin L ; EC:3.4.22.15 /map=50C20-50C20 /transc=CT20780 /len=1502 /GB:AE003816 /note=3prime sequence

889.6 ~2.1 FB:FBgn0033024 /sym=CG10416 /name= /prod= /func=RNA-directed DNA polymerase, group II intron encoded /map=41C2-41C2 /transc=CT29248 /len=1195 /GB:AE003786

4395.3 2.1 FB:FBgn0030847 /sym=CG12991 /name= /prod= /func= /map=16B8-16B8 /transc=CT32195 /len=1380 /GB:AE003506

1345.9 ~2.1 FB:FBgn0035026 /sym=CG12252 /name= /prod=RNA polymerase CTD phosphatase /func=protein phosphatase /map=60D5-60D5 /transc=CT15027 /len=3150 /GB:AE003464 /note=3prime sequence

16739.2 2.1 FB:FBgn0037752 /sym=CG8495 /name= /prod=ribosomal protein S29-like /func=structural protein of ribosome /map=85E9-85E9 /transc=CT24837 /len=979 /GB:AE003684

20291.9 2.1 FB:FBgn0030350 /sym=CG1844 /name= /prod= /func= /map=10F4-10F4 /transc=CT5645 /len=828 /GB:AE003487 /note=3prime sequence from clone BDGP:GH03581.3prime-hit

18640.2 2.1 FB:FBgn0035549 /sym=CG11346 /name= /prod= /func=structural protein /map=64B12-64B12 /transc=CT31648 /len=564 /GB:AE003481

1344.2 ~2.1 BDGP:LD32469.3prime-hit /maps to FB:FBgn0032432 (/sym=CG5442 /name= /prod=/func=) and FB:FBgn0032431 (/sym=CG5435 /name= /prod=/func=)

67263 2.1 FB:FBgn0038570 /sym=CG7217 /name= /prod= /func= /map=90E4-90E4 /transc=CT22257 /len=728 /GB:AE003721 /note=3prime sequence from clone BDGP:LD45324.3prime-hit

2990.8 2.1 FB:FBgn0023081 /sym=gek /name=genghis khan /prod=protein serine/threonine kinase /func=protein serine/threonine kinase ; EC:2.7.1.37 /map=60B5-60B5 /transc=CT13314 /len=5090 /GB:AE00346

136706.6 2.1 FB:FBgn0037874 /sym=CG4800 /name= /prod= /func= /map=86D7-86D7 /transc=CT15437 /len=782 /GB:AE003690

21274.7 2.1 FB:FBgn0020249 /sym=stck /name=steamer duck /prod= /func=transcription factor /map=84F15-84F16 /transc=CT23960 /len=1335 /GB:AE003678 /note=3prime sequence from clone BDGP:LD393

1644.3 ~2.1 FB:FBgn0039333 /sym=CG11917 /name= /prod= /func= /map=96D2-96D2 /transc=CT37090 /len=718 /GB:AE003751

58741.5 2.1 FB:FBgn0024923 /sym=TER94 /name=Saccharomyces cerevisiae UAS construct a of McKearin /prod=transitional endoplasmic reticulum adenosinetriphosphatase /func=adenosinetriphosphatase ; EC:3

111848.8 2.1 FB:FBgn0027844 /sym=CAH1 /name=Carbonic anhydrase 1 /prod=carbonate dehydratase /func=carbonate dehydratase ; EC:4.2.1.1 /map=34D1-34D1 /transc=CT23642 /len=1439 /GB:AE003641 /note

737.1 ~2.1 FB:FBgn0033900 /sym=CG8257 /name= /prod=cysteine--tRNA ligase-like /func=enzyme /map=50E2-50E2 /transc=CT24479 /len=1770 /GB:AE003815 /note=3prime sequence from clone BDGP:GH

392081.5 2.1 FB:FBgn0000116 /sym=Argk /name=Arginine kinase /prod=arginine kinase /func=arginine kinase ; EC:2.7.3.3 /map=66F2-66F2 /transc=CT13858 /len=2106 /GB:AE003553 /note=3prime sequence from

8765.4 2 FB:FBgn0037253 /sym=CG9798 /name= /prod= /func= /map=82C1-82C2 /transc=CT27682 /len=1914 /GB:AE003606

13142.2 2 FB:FBgn0027066 /sym=BcDNA:LD08743 /name= /prod= /func=cytoskeletal structural protein /map=42C3-42C4 /transc=CT10989 /len=1860 /GB:AE003789

495060.3 2 FB:FBgn0030541 /sym=CG11584 /name= /prod= /func=ligand binding or carrier /map=12D3-12D3 /transc=CT36540 /len=3048 /GB:AE003495

27166.8 2 BDGP:GH18222.3prime-hit /ESTpos=maps in FB:FBgn0033295 /sym=CG8689 /name= /prod=maltase L-like /func=enzyme /map=44C3-44C3 /transc=CT6492 /len=521

102551.1 2 FB:FBgn0011726 /sym=tsr /name=twinstar /prod=cofilin /func=actin binding /map=60B2-60B2 /transc=CT13858 /len=733 /GB:AE003462

10619.8 2 FB:FBgn0033134 /sym=CG12840 /name=Tetraspanin 42E1 /prod=tetraspanin /func= /map=42E2-42E2 /transc=CT31972 /len=1034 /GB:AE003842 /note=3prime sequence from clone BDGP:GH1495

3500.4 2 FB:FBgn0026630 /sym=nes /name=nessy /prod= /func= /map=76A3-76A3 /transc=CT27290 /len=2247 /GB:AE003517

7369.6 2 FB:FBgn0039595 /sym=CG10001 /name= /prod=allatostatin receptor-like /func=allatostatin receptor /map=98E2-98E2 /transc=CT28187 /len=990 /GB:AE003766

114502.3 2 FB:FBgn0032518 /sym=CG9282 /name= /prod=ribosomal protein L24 /func=structural protein of ribosome /map=34B6-34B6 /transc=CT26439 /len=774 /GB:AE003640

13035.4 2 J04423 E coli bioD gene dethiobiotin synthetase (-5 and -3 represent transcript regions 5 prime and 3 prime respectively)

21381.4 2 FB:FBgn0010808 /sym=l(3)03670 /name= /prod= /func= /map=100B4-100B4 /transc=CT4906 /len=906 /GB:AE003776

3752.8 2 FB:FBgn0035272 /sym=CG13922 /name= /prod= /func=structural protein of ribosome /map=62B4-62B4 /transc=CT33461 /len=830 /GB:AE003472

5878.8 2 FB:FBgn0035201 /sym=CG9146 /name= /prod= /func= /map=61F5-61F5 /transc=CT26188 /len=4092 /GB:AE003471

16376.3 2 FB:FBgn0027525 /sym=BcDNA:LD21529 /name= /prod= /func= /map=47C3-47C3 /transc=CT23459 /len=1643 /GB:AE003828 /note=3prime sequence from clone BDGP:LD21529.3prime-hit

51256.2 2 FB:FBgn0025366 /sym=Ip259 /name=Intronic Protein 259 /prod= /func= /map=31E1-31E1 /transc=CT16819 /len=838 /GB:AE003628 /note=3prime sequence from clone BDGP:GM13959.3prime-hit

48807.2 2 FB:FBgn0033188 /sym=CG1600 /name= /prod= /func=enzyme /map=43D3-43D3 /transc=CT37723 /len=1747 /GB:AE003840 /note=3prime sequence from clone BDGP:GH18014.3prime-hit

37785.4 2 BDGP:LP11629.3prime-hit /ESTpos=maps 3prime of FB:FBgn0033505 /sym=CG3451 /name= /prod= /func=cell cycle regulator /map=46F9-46F9 /transc=CT7898 /len=250

61261.7 2 FB:FBgn0000261 /sym=Cat /name=Catalase /prod=catalase /func=catalase ; EC:1.11.1.6 | inferred from direct assay /map=75D7-75D8 /transc=CT21282 /len=1977 /GB:AE003519

11587.6 2 FB:FBgn0031213 /sym=CG11372 /name= /prod= /func=ligand binding or carrier /map=21A5-21A5 /transc=CT31742 /len=1517 /GB:AE003590

224678.7 2 FB:FBgn0025828 /sym=EG:EG0003.7 /name= /prod=cytosolic translation release factor-like /func=cytosolic translation release factor /map=53D14-53D15 /transc=CT19804 /len=790 /GB:AE003805

33829.9 2 FB:FBgn0025582 /sym=Int6 /name=Int6 homologue /prod=translation initiation factor 3, subunit 6 /func=cytosolic translation initiation factor /map=73C1-73C1 /transc=CT27364 /len=1560 /GB:AE003590

26729	2	FB:FBgn0030531 /sym=CG11058 /name= /prod= /func=enzyme /map=12B9-12B10 /transc=CT30929 /len=2254 /GB:AE003493 /note=3prime sequence from clone BDGP:GH10492.3prime-hit
22852.6	2	FB:FBgn0015268 /sym=Nap1 /name=Nucleosome assembly protein 1 /prod=nucleosome assembly protein 1 /func=nucleosome assembly chaperone /map=60A9-60A9 /transc=CT16956 /len=1381 /GB:AE003493
34734.6	2	FB:FBgn0025637 /sym=skpA /name= /prod= /func=cell cycle regulator /map=1B10-1B11 /transc=CT32694 /len=1059 /GB:AE003418 /note=3prime sequence from clone BDGP:HL01263.3prime-hit
21750	2	FB:FBgn0020236 /sym=ATPCL /name=ATP citrate lyase /prod=ATP-citrate (pro-S)-lyase /func=ATP-citrate (pro-S)-lyase ; EC:4.1.3.8 /map=52E1-52E1 /transc=CT18257 /len=3745 /GB:AE003808
10182.9	2	FB:FBgn0038446 /sym=CG14903 /name= /prod= /func= /map=89D3-89D3 /transc=CT34727 /len=360 /GB:AE003714
13919.3	2	FB:FBgn0035471 /sym=CG10849 /name= /prod= /func= /map=63F6-63F6 /transc=CT30379 /len=1056 /GB:AE003479 /note=3prime sequence from clone BDGP:SD09294.3prime-hit
39019.7	2	FB:FBgn0038826 /sym=CG17838 /name= /prod=RNA binding protein /func=RNA binding /map=92F10-92F10 /transc=CT39628 /len=1802 /GB:AE003732 /note=3prime sequence from clone BDGP:SD04477.3prime-hit
15475.2	2	FB:FBgn0003498 /sym=sqd /name=squid /prod= /func=ribonucleoprotein /map=87F7-87F7 /transc=CT39414 /len=1137 /GB:AE003701
2246.4	2	FB:FBgn0001297 /sym=kay /name=kayak /prod= /func=DNA binding /map=99C2-99C4 /transc=CT35622 /len=2642 /GB:AE003771 /note=3prime sequence from clone BDGP:SD04477.3prime-hit

Lebenslauf

Ich bin am 13.12.1975 in Tianjin, Volkrepublik China, geboren und habe die chinesische Staatsangehörigkeit. 1994 schloss ich die No.1 High School in Tianjin ab und begann im selben Jahr mein Studium an der Nankai Universität in Tianjin. 1998 erhielt ich den Bachelor of Science im Hauptfach Molekularbiologie. 2001 erhielt ich den Master of Science (First class honours degree) der Nankai Universität in Tianjin.

Am 15. August 2001 begann ich in der Abteilung von Dr. Stephan J. Sigrist am European Neuroscience Institute des Bereichs Humanmedizin der Georg-August-Universität Göttingen unter der Anleitung von Prof. Dr. Friedrich-Wilhelm Schürmann die Arbeit an der Dissertation mit dem Thema „Identification and functional characterization of novel ionotropic glutamate receptor subunits at *Drosophila* neuromuscular synapse“.

Table content	1
Summary	4
List of Figures	5
List of Tables	6
Acknowledgements	7
1 Introduction	8
1.1 Molecular basics of Synaptogenesis	8
1.1.1 The making of a synapse	8
1.1.2 Development of vertebrate NMJ	11
1.1.2.1 Initial AchR clustering	11
1.1.2.2 Agrin-MuSK signalling pathway	13
1.1.2.3 Developmental role of AchR per se	16
1.1.3 Development of mammalian CNS excitatory synapse	16
1.1.3.1 Cell adhesion molecules in the axon-dendrite contact	18
1.1.3.2 Assembly of synapse	21
1.1.3.2.1 Presynaptic assembly	21
1.1.3.2.2 Postsynaptic assembly	23
1.1.3.3 Time sequence of pre- and postsynaptic assembly	25
1.1.4 <i>Drosophila</i> NMJ as one model for synaptogenesis	25
1.1.4.1 Structural properties of <i>Drosophila</i> NMJ	25
1.1.4.2 Initiation and maintenance of neuromuscular connection	28
1.1.4.2.1 Initiation of neuromuscular contact---target recognition (pathfinding)	28
1.1.4.2.2 Stabilization and maintenance of neuromuscular connection by cell adhesion molecules	29
1.1.4.3 Synapse formation	31
1.2 Structure and functional relevance of ionotropic glutamate receptors	33
1.2.1 Modular design of ionotropic glutamate receptors during evolution	33
1.2.2 Molecular mechanisms underlying selective assembly and transport of ionotropic glutamate receptors	34
1.2.3 Properties of ionotropic glutamate receptors expressed at <i>Drosophila</i> neuromuscular synapses	36
1.3 The aim and strategy of this work	37

2	Materials and methods	39
2.1	Materials (Chemicals, enzymes and molecular kits)	39
2.2	Methods	39
2.2.1	Genechip analysis and quantitative real-time RT-PCR	39
2.2.1.1	Genechip analysis	39
2.2.1.2	Real-time RT-PCR	45
2.2.2	Fly stocks and genetics	46
2.2.2.1	Fly stocks, crosses and rearing conditions	46
2.2.2.2	Mutagenesis screening	47
2.2.3	Molecular constructs and transgenes	48
2.2.4	In situ hybridization	50
2.2.5	Biochemistry (collaborated with Tobias Schwarz)	53
2.2.6	Immunohistochemistry	54
2.2.6.1	Embryonic and Larval filet preparation	54
2.2.6.2	Confocal epifluorescent microscopy	56
2.2.7	Ultrastructural analysis (collaborated with Carolin Wichmann)	56
2.2.8	Electrophysiology (collaborated with Robert Kittle)	57
3	Results	58
3.1	Establishing the tissue specific transcriptome of <i>Drosophila</i> larval body wall muscle	58
3.2	Identification of novel ionotropic glutamate receptor subunits expressed at the <i>Drosophila</i> neuromuscular synapse	59
3.2.1	Enrichment of various transcripts encoding novel ionotropic glutamate receptor subunits in larval body wall muscles	60
3.2.2	Expression pattern of new ionotropic glutamate receptor genes	61
3.2.3	The GluR-IIID and GluR-IIIE represent a new type of muscle expressed glutamate receptor subunits	63
3.2.4	GluR-IIC, GluR-IIID and GluR-IIIE are specifically localized at postsynaptic densities of neuromuscular synapses	65
3.3	GluR-IIID and GluR-IIIE are essential for viability	67
3.4	Reciprocal dependence of all essential glutamate receptor subunits for glutamate receptor expression and function at synapse	70
3.4.1	Complete absence of all the other glutamate receptor subunits at synapse in knockout of any essential subunit genes	70
3.4.2	Genetically depriving the expression level of any single essential glutamate receptor subunits results into tight reduction of all of the other subunits at synapse	72
3.4.3	Depriving synaptic glutamate receptor subunits results into dramatic weakness of postsynaptic activity	77

3.5 Structural role of ionotropic glutamate receptor during pre- and postsynaptic differentiation of neuromuscular synapse	77
3.5.1 Normal differentiation of presynaptic transmitter release machinery at glutamate receptor deprived synapse	77
3.5.2 Defective assembly of PSD specialization at glutamate receptor deprived but not presynaptic neurotransmission deprived synapse	79
3.5.3 Ultrastructural evidence of abnormal synaptic differentiation at glutamate receptor deprived synapse	84
3.5.4 Defective compartmentation of the synaptic and perisynaptic area at glutamate receptor deprived but not neurotransmission deprived synapse	87
3.5.5 Similar defects in synaptic differentiation in the complete absence of glutamate receptors	89
4 Discussion	90
4.1 Genomic tools could speed up identifying essential genes involved in synapse formation and modulation	90
4.2 GluR-IID and GluR-IIIE are novel glutamate receptor subunits crucial for glutamate receptor assembly and thus neurotransmission at neuromuscular synapse	91
4.3 Implications in the in vivo stoichiometry of <i>Drosophila</i> glutamate receptor based on genetic analysis	93
4.4 Structural role of ionotropic glutamate receptor per se in organizing synaptic assembly and time sequence of pre- and postsynaptic assembly	95
References	99
Appendix: Genes enriched in larval body wall preparations	107
<i>Lebenslauf</i>	127

Summary

The molecular mechanisms triggering the formation of synapses *in vivo* are crucial for understanding the development as well as the activity dependent remodelling of synaptic circuits. The *Drosophila* neuromuscular junction (NMJ) provides an excellent platform for investigating fundamental aspects of how glutamatergic synapse form *in vivo*. The molecular mechanisms relevant to synaptogenesis and growth control of the *Drosophila* NMJ were addressed by combining genome-wide transcript analysis with functional genetics. This allowed the identification of two novel postsynaptic muscle expressed ionotropic glutamate receptor subunits, GluR-IIID and GluR-IIIE. Genetic elimination of either of the two novel subunits resulted in paralyzed lethal embryos, indicating that both new subunits are essential for forming the postsynaptic glutamate receptor complex. Further genetic, cell biological and electrophysiological studies then uncovered a tight interdependence of all NMJ glutamate receptor subunits for synaptic localization and function. These results imply that the NMJ glutamate receptor complex has strictly hetero-tetrameric stoichiometry. This so far was not described for mammalian ionotropic glutamate receptors which are usually considered to be dimers of dimers. In the second part of the thesis, glutamate receptor deprived synapses were closer inspected. Surprisingly, depleting glutamate receptors (but not depleting synaptic neurotransmission activity) provoked severe ultrastructural and molecular defects of postsynaptic membrane organization and compartment formation. Thus, the glutamate receptor complex *per se* but not its ligand-gated ion channel activity seemingly plays an instructive role for assembling mature postsynaptic specializations. Such a ‘structural’ role of glutamate receptor complexes in synaptic differentiation is novel. It might be relevant for the role

ionotropic glutamate receptors play during synaptic plasticity of the mammalian brain, which is considered to be a cellular correlate of learning and memory processes.

List of Figures

Fig.1-1 Basic structure of chemical synapse	9
Fig. 1-2 Representative molecular composition of CNS glutamatergic Synapse	10
Fig.1-3 Vertebrate neuromuscular junction	12
Fig. 1-4 Spiny dendrites from hippocampal pyramidal neuron	18
Fig. 1-5 Structure of <i>Drosophila</i> NMJ	27
Fig.1-6 Structure of iGluR subunit and model of iGluR assembly	34
Figure 3-1. <i>GluR-IID</i> and <i>GluR-IIE</i>: novel glutamate receptor subunits with muscle specific expression	62
Figure 3-2 Sequence analysis of <i>GluR-IID</i> and <i>GluR-IIE</i>	64
Fig.3-3 <i>GluR-IID</i> and <i>GluR-IIE</i> are expressed within postsynaptic Densities	66
Figure 3-4 Genetic analysis of <i>GluR-IID</i> and <i>GluR-IIE</i>	68
Figure 3-5 Interdependence between glutamate receptor subunits for NMJ expression	71
Figure 3-6 A partial reduction of either <i>GluR-IIE</i> or <i>GluR-IID</i> provokes a significant reduction of all glutamate receptor subunits at the NMJ	73
Fig.3-7 Minimal mounts of <i>GluR-IIA</i> and no- <i>IIB</i>: expression of all glutamate receptor subunits and postsynaptic sensitivity are strongly reduced	76
Fig. 3-8 Normal organization of presynaptic neurotransmitter release machinery components at glutamate receptor deprived synapses	79
Fig.3-9 Defective PSD assembly at glutamate receptor deprived but not transmission deprived synapses	81
Fig. 3-10 Glutamate receptor <i>per se</i> but not presynaptic vesicle release are important for proper synapse formation at embryo NMJ	84
Fig.3-11 Electron microscopy: defective postsynaptic assembly at glutamate receptor deprived synapses	85
Fig.3-12 Defective synaptic compartments at glutamate receptor deprived but not neurotransmission deprived synapses	88

List of Tables

Table 3-1 Described muscle / cuticle-specific transcripts displaying enrichment in gene chip analysis of body-wall-preparations	59
Table 3-2 GluR-IID and GluR-IIIE are enriched in larval body wall mRNA	61

Acknowledgements

First of all, I would like to express my gratitude to my advisors, Dr. Stephan Sigrist, Prof. Dr. F. W. Schürmann and Prof. Dr. H. Jäckle for their consistent support, helpful tips, kind advices and comments.

My very special thanks are to Dr. Stephan Sigrist, who provides me the opportunity to join his group and do exciting cutting-edge science. As one talented and serious scientist, Stephan taught me not only how to perform successful experiments but also how to ask the right question and address it in a logic way. During my whole thesis period, I was encouraged by our extensive and enthusiastic discussion, from which I really have learned a lot. Also, for me it is really nice to witness the rapid growth of our young group.

I would like to thank several collaborators, Robert Kittel for electrophysiology, Dr. Carolin Wichmann for Electron Microscopy and Tobias Schwarz for biochemistry. Without their excellent contributions, I could hardly reach current stage. The Gene Chip experiments were performed in Max-Planck Institute for Biophysical Chemistry, I am really indebted to Dr. Ronald Kühnlein and Dr. Sebastian Grönke for their warm and patient help.

I am also grateful to my colleagues Carlos Melino, Tobias Rasse, Andreas Schmid, Sara Mertel, Wernher, Laura Swan and Manuela Schmidt, with whom I can freely exchange ideas and reagents, which greatly facilitate my work. I want to express my kindest gratefulness to Christine Quentin, Miriam Richter and Jasmin for their highly professional technical assistance.

Finally, my very special thanks are addressed to my family and my friends.

1 Introduction

1.1 Molecular basics of Synaptogenesis

1.1.1 The making of a synapse

The human brain comprises a huge network of neurons (about 10^{11}) which link with each other structurally and functionally through the special type of cell-cell junctions called synapses. Synapses transmit electrical signals between neurons, mediating neuronal signaling and computation, also they are able to undergo long-term changes (synaptic plasticity) that underlie aspects of learning and memory (Li and Sheng, 2003). Although many of these synaptic contacts are highly specialized, all neurons make use of one of the two basic forms of synaptic transmission: electrical or chemical. Synaptic communication in the brain is mainly dependent on chemical mechanisms, that is, synaptic transmission is mediated via a chemical substance that is released by presynaptic terminal and diffuses through the synaptic cleft to activate relevant receptors on the postsynaptic membrane. Like other cell-cell junctions, synapses contain a wide variety of transmembrane proteins, cytoskeletal units and signaling components. However, they differ from most other junctions in being structurally asymmetric (Fig. 1-1): the presynaptic specialization, usually on the axon, contains a complex apparatus called active zone, which controls the transmitter-filled vesicles docking, fusing and the release of transmitter into the synaptic cleft. In contrast, the postsynaptic reception specialization, just juxtaposed to the active zone and recognized ultrastructurally by the presence of an electron-dense thickening called the postsynaptic density (PSD), is made of receptors, ion channels, signaling components and scaffold proteins clustered all together (Garner et al., 2002; Yamagata et al., 2003).

On average, each neuron forms about 1000 synaptic connections and receives even more, perhaps as many as 10,000 connections (Kandel ER et al. 2001). These synapses include excitatory, inhibitory and modulatory type. Most

of them are excitatory and utilize glutamate as neurotransmitter. The inhibitory neurotransmission is mediated by glycine or GABA, whereas modulatory neurotransmission is mediated by 5-HT, dopamine, acetylcholine (Ach) and neuropeptides etc. Notably, although presynaptic terminals from any given neuron generally release one type of transmitter, neurons usually receive multiple forms of synaptic input, which can be excitatory, inhibitory or modulatory. Moreover, anatomical evidence has shown that the number of cellular contacts often exceeds the number of synaptic connections formed onto a single cell, suggesting that neurons are able to distinguish synaptic contact site and nonsynaptic site (White et al., 1976; Benson et al., 2001). Thus, for efficient and accurate neurotransmission, the site where synaptic contact forms is carefully selected, and, within an individual synapse, appropriate pre- and postsynaptic apparatus is assembled highly coordinately and precisely.

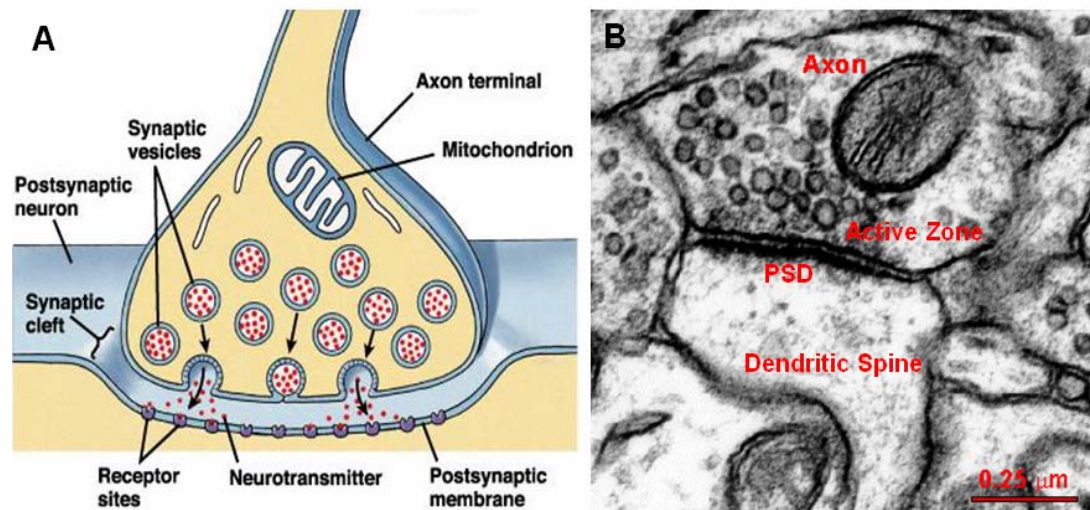


Fig.1-1 Basic structure of chemical synapse. A, diagram of a central nervous system chemical synapse. B, ultrastructure of a central chemical synapse (Adapted from www.synapses.mcg.edu/)

What is the molecular mechanisms controlling the site and type specific assembly of chemical synapses? To answer this fundamental question in neurobiology, extensive efforts have been invested to identify the molecular

constituents of synapses and define their functional significance via the combination of molecular, biochemical and genetic approaches (Fernandez-Chacon and Sudhof, 1999; Scannevin and Huganir, 2000; Phillips et al., 2001; Sheng, 2001; Garner et al., 2002) (Fig. 1-2). Furthermore, recently the adoption of newly developed optical imaging technique has provided a way to track the dynamics of individual synaptic protein trafficking and targeting during synapse formation even in real-time resolution (Ahmari et al., 2000; Okabe et al., 2001; Prange and Murphy, 2001; Rosenberg et al., 2001; Zhai et al., 2001).

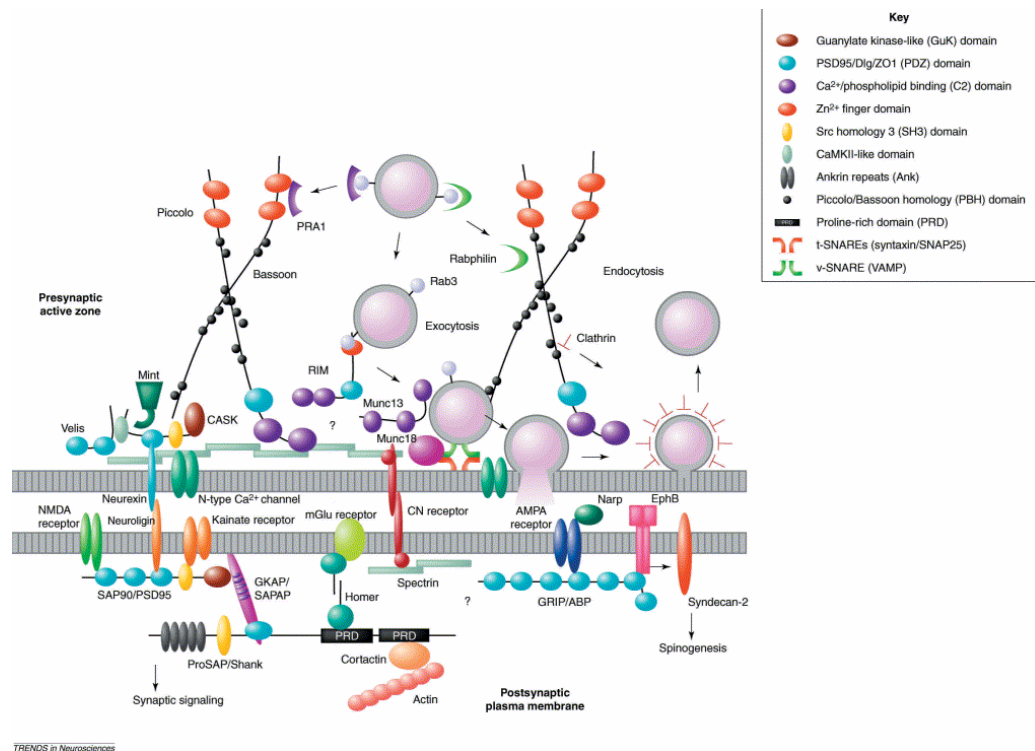


Fig. 1-2 Representative molecular composition of CNS glutamatergic synapse (Adapted from Garner et al., 2002).

Historically, much of what we know about the development of chemical synapses is based on studies of the vertebrate neuromuscular junction (NMJ)—a large peripheral synapse formed between a motor neuron and a skeletal muscle fibre. However, in recent years, with the incremental technical

advances a picture of the synaptogenesis in the mammalian central nervous system has also begun to emerge.

1.1.2 Vertebrate NMJ

The vertebrate NMJ (Fig. 1-3) is ideal for studying chemical synaptogenesis because it is large, relatively simple and unparalleled accessible to experimentation. During development (starting at about E11 in mice) multinucleated skeletal muscle fibres form by fusion of precursor myoblasts, shortly after myotubes begin to form (at E12-13 in mice), motor neurons innervate the muscle at a specialized region of the muscle membrane called the end-plate. At the region where the motor axon approaches the muscle fibre, the axon loses its myelin sheath and splits into several fine branches. The ends of the fine branches form multiple expansions or varicosities, called synaptic boutons, from which the neurotransmitter (here is Ach) is released from the motor neuron. Each bouton is positioned over a postjunctional fold, a deep and narrow depression of muscle cell membrane that contains high densities of transmitter receptors (here is acetylcholine receptors, AchRs), and this precise apposition of postsynaptic specializations to the motor nerve terminal insures that transmitter comes into contact with its receptor within microseconds after release, thereby facilitating efficient synaptic transmission.

1.1.2.1 Initial AchR clustering

Once the myotube forms, the AchR is starting to be expressed and inserted into the muscle surface, but with low density (usually about 1000 per μm^2); after synaptic maturation, by contrast, the AchRs are highly concentrated at the synaptic sites (to a density up to 10,000 per μm^2) and depleted at the extrasynaptic membrane (10 per μm^2 or less). One of the central questions is the contribution of muscle versus motor nerve in initiating

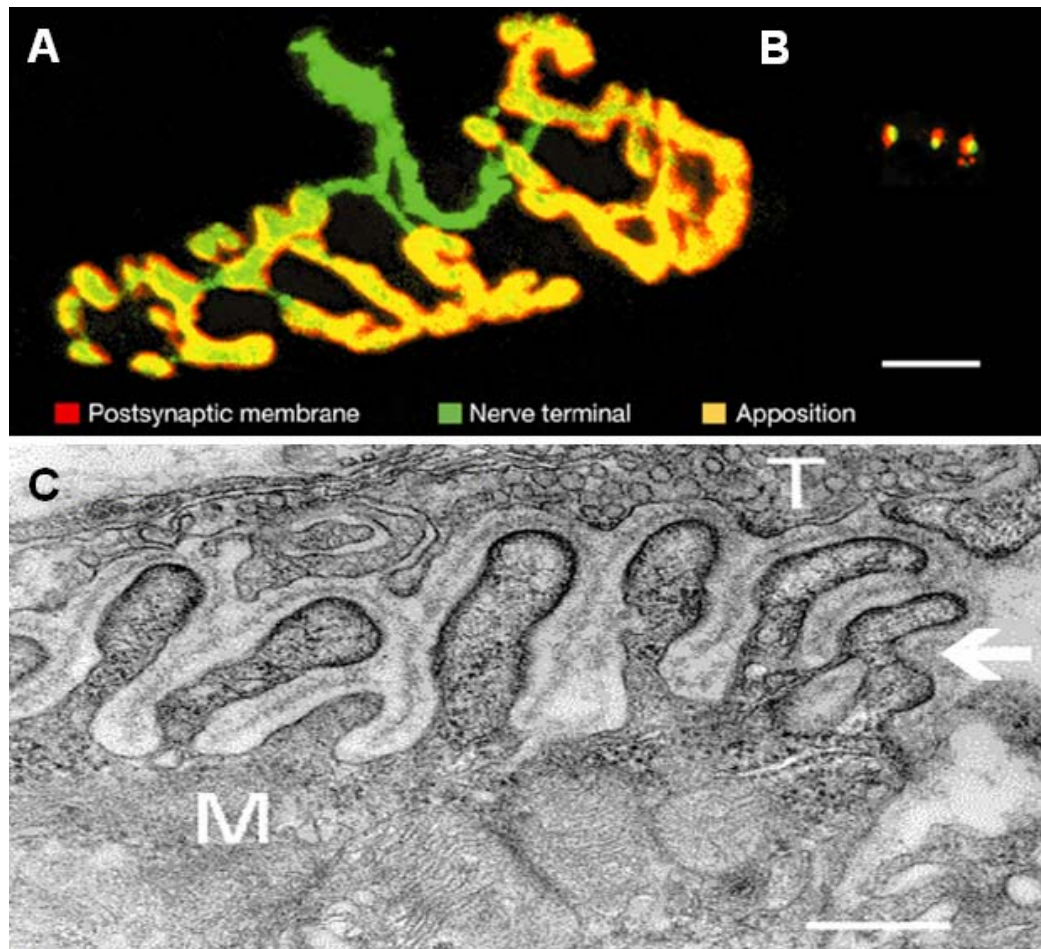


Fig.1-3 Vertebrate neuromuscular junction. A, The neuromuscular junction of an adult mouse. Scale = 5 μm . B, Three synapses on cultured mouse hippocampal neurons shown at the same scale (Adapted from Sanes J et al. 2001). C, Electron micrograph of motor end plate of abdominal muscle of frog. T - axon terminal, M - muscle fiber, arrow - foldings covered with basal lamina. Scale = 0.3 μm (Adapted from www.synapses.mcg.edu/)

and maintaining postsynaptic differentiation. Recently, more and more evidences suggest that the muscle itself has the capacity to be prepatterned. Particularly pertinent observations are, during the brief period when synaptogenesis begins in mouse muscle, some AchR clusters are not apposed by nerves and some nerve endings are not opposed to AchR clusters; moreover, the AchR clusters are present in muscles even without innervation, most of these

small clusters aggregate in the central end-plate band of the muscle, although this central band appears to be wider and more poorly defined than the one in innervated muscle (Lin et al., 2001; Yang et al., 2001).

1.1.2.2 Arin-MuSK Signaling Pathway

Upon innervation, AchR clusters are restricted to the central band of muscle. In the past three decades, numerous studies have established that motor nerve plays a major role in organizing this type of postsynaptic differentiation via two intramuscular mechanisms: clustering of AchRs at the synaptic contact sites; and selective transcription of AchR genes by myonuclei associated with synaptic sites (Burden, 1998; Sanes and Lichtman, 1999; Lin et al., 2001). Several nerve derived molecules have been identified and agrin is proved to be crucial *in vivo*. Agrin, isolated by McMahan and colleagues, is a large heparan sulphate proteoglycan that is synthesized by motor neurons, transported down motor axons, and released from nerve terminals, where it stably associates with the basal lamina of the synaptic cleft (Wallace, 1989; McMahan, 1990; Bowe and Fallon, 1995; Sanes and Lichtman, 2001). Agrin was identified from its ability to induce the aggregation AchRs on cultured myotubes, and was soon found to also aggregate many other components of the postsynaptic apparatus (Wallace, 1989). In Agrin-deficient mice, the number and density of AchR clusters, as well as synapse-specific transcription, are reduced markedly, which convincingly demonstrates that Agrin is crucial for AchR clustering in the muscle membrane opposite the presynaptic terminals (Gautam et al., 1996; Ruegg and Bixby, 1998).

MuSK, a transmembrane receptor tyrosine kinase, was discovered due to its selective abundance in synapse-rich Torpedo electric organ, whose principal cells are modified muscle cells that are innervated by cholinergic synapses (Jennings et al., 1993). Studies in mice reveal that MuSK is specifically expressed in skeletal muscles and is colocalized with AchRs in the postsynaptic membrane at the NMJ (Valenzuela et al., 1995).

Unexpectedly, muscles in MuSK-null mutant mice show totally no detectable signs of postsynaptic differentiation, although the AchR genes are expressed at normal level (DeChiara et al., 1996; Lin et al., 2001; Yang et al., 2001). Several studies have established the linkage between Agrin and Musk signaling: application of Agrin to myotubes leads to rapid activation of MuSK; expression of a dominant negative form of MuSK inhibits Agrin-induced cluster formation in cultured myotubes (Glass et al., 1996); MuSK^{-/-} myotubes are completely unresponsive to agrin, but agrin sensitivity is restored by introducing wild-type MuSK (Zhou et al., 1999). Taken together, these results demonstrate that MuSK is essential for agrin-induced postsynaptic differentiation.

A crucial component downstream of MuSK that affects the postsynaptic differentiation is rapsyn, a 43-kDa membrane associated cytoplasmic protein. Rapsyn is identified from its tight connection with AchR. It appears as soon as AchR starts clustering, perfectly colocalizes with AchR clusters, and in the electric organ it follows 1:1 stoichiometry (LaRochelle and Froehner, 1986; Noakes et al., 1993). Co-expression of AchR and rapsyn in all of the heterologous cells tested so far results into the formation of AchR- Rapsyn co-clusters, whereas AchRs are diffusely distributed when expressed alone (Froehner et al., 1990; Phillips et al., 1991). Consistently, in rapsyn mutant mice, no AchR clusters form on the muscle surface (Gautam et al., 1995). Thus, rapsyn is necessary for all forms of AchR clustering. Intriguingly, rapsyn can cluster AchRs when they are co-expressed in heterologous non-muscle cells that lack agrin and MuSK (Apel et al., 1997). By contrast, not even spontaneous (agrin-independent) AchR clusters form in MuSK deficient myotubes (Zhou et al., 1999), and overexpression of rapsyn in wild-type myotubes induces virtually no further cluster formation (Yoshihara and Hall, 1993; Han et al., 1999). This raises the possibility that muscles contain intrinsic activity to prevent the MuSK signaling independent clustering of rapsyn, which might be an efficient way to avoid the AchR clustering at the

wrong sites.

How does activation of Agrin-MuSK signaling lead to the clustering of AchRs? Previously it has been shown that cytoskeletal components are closely associated with AchR clusters, and disruption of cytoskeleton prevents the AchR cluster formation (Bloch and Pumplin, 1988). Thus, it is plausible that the activation of MuSK signaling upon agrin binding provide intrinsic cytoskeletal regulatory capacity required for remodelling and postsynaptic assembly. Consistent with this view, it has been found that agrin induces the polymerization of actin at the AchR clustering sites (Dai et al., 2000), moreover, it has been demonstrated that agrin-mediated clustering of AchRs depends on activation of Rac/ Cdc42, leading to the formation of AchR microclusters, followed by Rho activation, resulting in the consolidation of these microclusters into larger AchR clusters (Weston et al., 2000; Weston et al., 2003).

Although there is little doubt that Agrin/ MuSK signaling is the major pathway that is crucial for NMJ synaptogenesis, the intracellular signaling mechanisms downstream of MuSK have only begun to be elucidated recently. In response to agrin binding, MuSK undergoes tyrosine phosphorylation, this might create docking sites for signaling molecules or promote proper folding of the kinase. As an example, the juxtamembrane tyrosine (Y553) is required for agrin-induced AchR clustering (Zhou et al., 1999; Herbst and Burden, 2000). Very recently, the Abl kinases were shown to be required for the agrin/ MuSK dependant synaptic assembly, Abl kinases and MuSK can effect reciprocal tyrosine phosphorylation and form a complex after agrin engagement (Finn et al., 2003). Dishevelled (Dvl), a signaling molecule important for planar cell polarity, has also been found to interact directly with MuSK and PAK, forming a signaling scaffold which is important for agrin/ MuSK mediated AchR clustering (Luo et al., 2002). Additionally, evidences have been provided that geranylgeranyltransferase I (GGT), a zinc

metalloenzyme that tethers proteins to plasma membrane by prenylation (Zhang and Casey, 1996), serves as one important component in the agrin/MuSK pathway, which reveals an important role of prenylation in regulating synapse formation and/ or maintenance (Luo et al., 2003).

1.1.2.3 Developmental role of AchR *per se*

During postsynaptic differentiation, do AchRs only occupy the slots within assembled scaffold and contribute nothing for the assembly? In tested non-muscle cells, this seems true, but in muscle cells it is obviously not the case: Rapsyn fails to cluster at synaptic sites in zebrafish mutants deficient in the AchRs, suggesting the requirement of AchRs for proper synaptic localization of postsynaptic components (Ono et al., 2001); consistently, in the variants of C2 myotubes virtually lacking AchRs, agrin also fails to aggregate rapsyn (Marangi et al., 2001); moreover, in mutant mice that lack an adult AchR subunit, the postsynaptic membrane undergoes a profound reorganization in which levels of several membrane and cytoskeletal components decline in parallel with AchR loss, and residual material forms abnormal small islands at the NMJ (Missias et al., 1997). Therefore, the AchR *per se* is not merely a passive ligand, but plays an active role in organizing synaptic assembly. Interestingly, this is reminiscent of the assembly of inhibitory CNS synapses, in which GABA_A receptor subtypes are localized at synapses through their interaction with gephyrin (Kneussel et al., 1999). Gephyrin is not clustered at postsynaptic sites of mice lacking GABA_A receptor γ subunits, suggesting that gephyrin requires the presence of GABA_A receptors to efficiently form synaptic aggregates (Essrich et al., 1998). Thus, neurotransmitter receptors of both vertebrate NMJ and inhibitory CNS synapses are actively involved in postsynaptic assembly during synaptogenesis.

1.1.3 Mammalian CNS excitatory synapses

In the central nervous system, most excitatory synapses utilize glutamate

as the neurotransmitter. Glutamatergic synapses contain excitatory, glutamate responsive ionotropic and metabotropic receptors (Hollmann and Heinemann, 1994; McGee and Brecht, 2003). Ionotropic glutamate receptors are supposed to be tetrameric complexes, and are categorized into three major classes, on the basis of pharmacology, electrophysiology and sequence homology: AMPA (α -amino-3-hydroxy-5-methyl-4-isoxazolepropionic acid) receptors, NMDA (N-methyl-D-aspartic acid) receptors and kainate receptors.

Morphologically, most mature excitatory synapses are constructed on the characteristic tiny actin-rich structures---dendritic spines---the small lateral dendritic protrusions. Spines have variable size (up to a few μm in length and $0.8 \mu\text{m}^3$ in volume) and shape (such as thin, stubby or mushroom-like) (Harris and Kater, 1994; Hering and Sheng, 2001; Li and Sheng, 2003) (Fig. 1-4). During brain development, there is morphological transition in spines. During the first two postnatal weeks, synapses are frequently observed on the dendritic shaft, on stubby spines and on filopodia (Fiala et al., 1998), with maturation of the brain, such synapses are gradually substituted by, or converted to, synapses on mushroom-like spines (Harris and Kater, 1994).

As described before, the pre- and postsynaptic membrane of vertebrate NMJ are separated by an extracellular basal membrane, the extracellular-matrix molecule agrin is secreted from the nerve terminal and induces the postsynaptic differentiation. However, in central synapses, the extracellular matrix is not well characterized and, so far, no secreted molecules has been convincingly shown to be crucial for the development of mammalian central synapses. Narp (neuronal activity-regulated pentraxin), a secreted molecule that accumulates at synaptic sites, can interact with and cluster AMPA receptors (O'Brien et al., 1999; O'Brien et al., 2002). However, just as its name implied, Narp is a neuronal activity-regulated molecule, it recruits AMPA receptors only when a synapse is undergoing activity-dependant changes. Narp is less likely to play a major role during synaptogenesis, since AMPA receptor clustering is not essential for initial

synapse formation (see below for details).

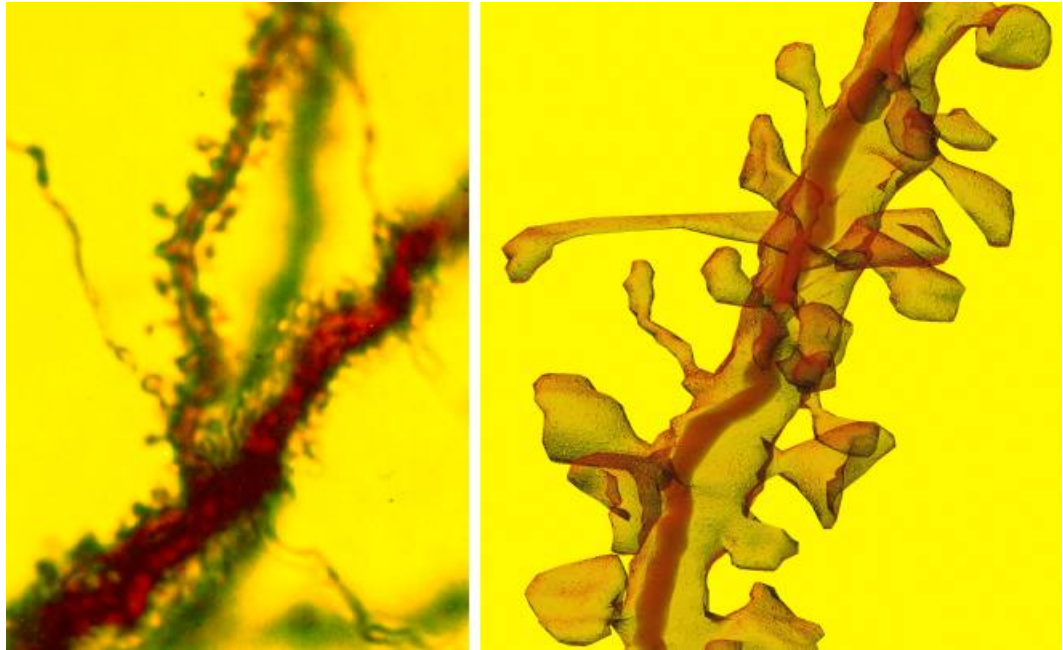


Fig. 1-4 Spiny dendrites from hippocampal pyramidal neuron.

Left: Light microscope image. *Right:* Reconstruction from serial electron microscopy (Adapted from www.synapses.mcg.edu/).

1.1.3.1 Cell adhesion molecules in the axon-dendrite contact

Synaptic assembly appears to be a multi-step process that is initiated from the axon-dendrite contact. Initial contact is followed by a stabilization step at the contact site and, subsequently, by further pre- and postsynaptic differentiation. Each process seems to require the interaction of various classes of cell adhesion molecules (CAMs). The Cadherin family of homophilic cell adhesion molecules is essential for the formation and stability of epithelial cell junctions. Cadherins are found to localize at both pre- and postsynaptic side, dominant-negative studies of the neuronal cadherins indicate that they are important for synapse integrity and morphological maturation of dendritic spines (Togashi et al., 2002). However, due to the large number of various Cadherin and Cadherin-related genes that are expressed in the central nervous system, it is still not possible to conclude

whether cadherin plays an initiating role in synapse formation or a promoting role in subsequent synaptic growth.

Various types of integrins are expressed in the brain with different distribution patterns (Pinkstaff et al., 1999). Integrins function as cell-matrix or cell-cell adhesion molecules by binding, respectively, to extracellular matrix proteins or to immunoglobulin superfamily proteins (Aplin et al., 1998). Based on our current understanding, integrins have diverse functions in early stage of CNS development, including neuronal migration (Milner and Campbell, 2002), axon pathfinding and outgrowth (Hoang and Chiba, 1998; Pasterkamp and Kolodkin, 2003), they also appear to have a role in synapse maturation (Chavis and Westbrook, 2001).

Immunoglobulin superfamily molecules contain certain numbers of extracellular cyctein-looped domains first found in immunoglobulins. Synaptic cell adhesion molecule (SynCAM) belongs to such a superfamily and is found to be localized on the synaptic membranes. Importantly, expression of SynCAM in nonneuronal cells both induces neighboring neurons to form functional presynaptic terminals and, if gluamate receptors are coexpressed, endows the postsynaptic membranes with the capacity of responding to glutamate (Biederer et al., 2002). Thus, SynCAM seems an ideal candidate initiating central synapse formation, although its *in vivo* role has yet to be examined. Very recently, another two immunoglobulin superfamily members, SYG-1 and SYG-2 were isolated in genetic screen for *C. elegans* mutants defective in targeting specificity during synaptogenesis (Shen and Bargmann, 2003; Shen et al., 2004). SYG-1 is present at the presynaptic neuron HSNL and localizes to synaptic sites at the early stages of synaptic formation, while SYG-2 is expressed transiently in the guidepost epithelial cells during synapse formation. SYG-2 can interact with SYG-1 and thus instruct the accumulation of synaptic vesicles and the subsequent synaptic assembly at proper site.

Presynaptic neurexins and postsynaptic neuroligins represent another group of synaptic CAMs proposed to function in synapse differentiation. The extracellular domain of presynaptic beta-neurexin interacts directly with the extracellular AchE-like domain of postsynaptic neuroligin (Nguyen and Sudhof, 1997). In a co-culture system, the overexpression of neuroligin in heterologous cells can induce the structural and functional presynaptic specialization in contacting axons (Scheiffele et al., 2000). More convincingly, in the context of intracellular interactions, the cytoplasmic tail of β -neurexin binds with PDZ protein CASK, a presynaptic scaffold protein; comparably, the intracellular part of neuroligin binds with PSD-95, which is an important PDZ domain scaffold protein of the postsynaptic density. Thus the direct ‘talk’ between β -neurexin and neuroligin across the synaptic cleft might bridge the adhesive and signaling components of both presynaptic transmitter release machinery and postsynaptic reception apparatus, allowing for a stepwise assembly of trans-synaptic complexes (Dean et al., 2003). Recent studies in knock-out mice have revealed that, in the absence of α -neurexins the central synapse morphology is largely normal, but the presynaptic calcium channel activity and neurotransmitter release are severely impaired (Missler et al., 2003). Therefore, α -neurexins probably have a role in organizing the molecular machinery at presynaptic side. Up to now, the in vivo role of β -neurexin in synaptic assembly remains to be answered.

Finally, Ephrin-Bs (EphB) are small transmembrane proteins identified as ligands for the EphB receptor tyrosine kinase. Through binding to EphB receptor, EphB can induce the clustering of NMDA receptors on the surface of fibroblasts and immature cultured hippocampal neurons (Dalva et al., 2000). The NMDA receptor clustering is mediated by a ligand-induced association of the extracellular domain of EphB receptor with the large extracellular domain of NR1 subunit, while the tyrosine kinase activity of EphB receptor are not necessary for this process. EphBs are unlikely to be the general inducers of postsynaptic differentiation, since in immature neurons it can only facilitate the

clustering of NMDA receptors and its partner Ca^{2+} -calmodulin-dependant protein kinase II (CaMKII) but not the other known PSD components (such as SAP90/ PSD95), moreover, although EpgB2 knock-out mice show deficits in activity-dependant synaptic plasticity, they have normal synapse density and structure, as well as largely intact synaptic function (Grunwald et al., 2001; Henderson et al., 2001). Syndecan2, a cell-surface heparan sulfate proteoglycan, is able to enhance the maturation of dendritic spines: when syndecan2 is overexpressed in cultured immature hippocampal neurons, dendritic spines display morphology typical of mature spines (Ethell and Yamaguchi, 1999). Interestingly, EphB receptor is shown to be the upstream activators of syndecan2 (Ethell et al., 2001), thus EphB receptor pathway might not only function during the initial formation of synapses but also participate in their maturation process.

1.1.3.2 Assembly of synapse

The development of the time-lapse imaging techniques has allowed one to obtain information on the dynamic behavior of essential biological processes in living cells. Synaptic transmission can be detected within an hour of initial axon-dendrite contact, so the accumulation of certain pre- and postsynaptic proteins must occur even earlier. The time-lapse studies have shown that many synaptic components are assembled within tens of minutes after the initial contact of axons and dendrites, much faster than previous estimation (Friedman et al., 2000; Okabe et al., 2001; Washbourne et al., 2002).

1.1.3.2.1 Presynaptic assembly

Recently, evidence is growing to support the opinion that the presynaptic specialization is constructed from essentially two types of preassembled ‘packets’ of vesicles and/ or proteins (Hannah et al., 1999; Jahn and Sudhof, 1999; Sudhof, 2000). The biogenesis of these two precursor complexes occurs in the soma, apparently through the Golgi body.

Using time-lapse imaging of green fluorescent protein (GFP) tagged VAMP (vesicle associated membrane protein, a synaptic vesicle protein), it has been found that even before the period of peak synaptogenesis in culture, VAMP-GFP is present in axons as mobile clusters (about 0.5-1.5 μm) larger than single synaptic vesicles. These VAMP labelled puncta have varied vesicular and tubular membrane structures, as shown by EM, and they colocalize with presynaptic membrane proteins (such as the voltage-gated calcium channels) and other synaptic vesicle associated proteins (such as synaptic vesicle protein 2 and synapsin I). It is estimated that the amount of VAMP required in a single presynaptic bouton corresponds to 1-4 such precursor packets (Ahmari et al., 2000).

A second type of precursor packet, which is associated with dense-core vesicles that have a diameter of about 80 nm, has been visualized and purified (Zhai et al., 2001). In contrast to synaptic vesicles, these dense-core vesicles contain many active zone components, including the presynaptic scaffold proteins Piccolo, Bassoon and RIM (Rab3-interacting molecule), the SNARE (soluble N-ethylmaleimide-sensitive-factor attachment protein receptor) proteins syntaxin and SNAP-25 (synaptosomal-associated protein 25), and the CAM N-Cadherin, suggesting that they constitute 'active zone precursor vesicles' that, upon fusing with the presynaptic plasma membrane, lead to rapid formation of active zones (Zhai et al., 2001). It was proposed that incorporation of only 2-3 of these transport vesicles supplies enough material for an active zone of average size (Shapira et al., 2003).

A common feature of these two types of precursor packets is that they are mobile along axons prior to synaptogenesis, but promptly immobilized at nascent synapses. During neuronal development, the Piccolo/ Bassoon dense-core vesicles are present earlier than the VAMP containing synaptic vesicle precursor packet, which might suggest that the formation of new neurotransmitter release sites is preceded by the recruitment and assembly of

active zone components. The molecular mechanisms that target these precursor complexes to the nascent synaptic site still remain elusive, however, studies from immunoglobulin superfamily proteins (SYG-1 and SYG-2, see above) have already provided possible clue.

1.1.3.2.2 Postsynaptic assembly

Compared to the assembly of presynaptic specialization, the process of postsynaptic assembly is not well characterized yet, which is at least partially due to the fact that postsynaptic specialization is more complex and heterogeneous than presynaptic active zone. One of the best-studied complexes is associated with NMDA receptors. This complex comprises molecules such as SAP90/ PSD95, alpha-actinin, and CaMKII, neuroligin, the microtubule-binding protein Cript, the guanylate kinase domain-binding proteins GKAP/ SAPAPs, and other proteins such as ProSAP/ Shank, Homer and cortactin (which provide additional links to the actin cytoskeleton and other glutamate receptor complexes (Garner et al., 2002). The rapid recruitment of PSD-95 and the presence of non-synaptic clusters of PSD-95 (Rao et al., 1998; Marrs et al., 2001) are consistent with the idea that ‘prefabricated’ complexes are used to assemble the PSD---which is analogous to presynaptic differentiation. However, it is not known whether the non-synaptic clusters of PSD-95 represent real packets of PSD proteins in delivery. In sharp contrast to this view, however, independent studies suggest that although some synaptic PSD-95 clusters might be derived from the transport of pre-existing non-synaptic precursor packets, the *de novo* accumulation of PSD-95 clusters at nascent synapses seems to usually occur from diffuse ‘cytoplasmic pools’ (Bresler et al., 2001; Marrs et al., 2001). Notably, this model is supported by an updated report in which more PSD components have been examined, all the tagged PSD components tested are recruited to new synaptic sites gradually, with no discernable discrete transport packets involved (Bresler et al., 2004). Interestingly, in this new study, the non-synaptic PSD clusters are also observed, but they appear no more mobile than synaptic clusters, hence unlikely representing the transport intermediates.

Ionotropic glutamate receptors are essential components of postsynaptic apparatus, in addition to converting the chemical signal released from presynaptic terminal to an electrical response in the postsynaptic neuron, they are critically involved in activity-dependant, long-term changes in synaptic strength, which may represent a central physiological correlate to learning and memory. Time-lapse imaging of GFP-tagged NR1 (one subunit of NMDA receptors) and GluR1 (one subunit of AMPA receptors) indicates that NMDA receptors and AMPA receptors are present in largely non-overlapping mobile clusters before synaptogenesis starts, NMDA receptors are recruited earlier than AMPA receptors to the axon-dendrite contact sites (Washbourne et al., 2002). It is still uncertain whether these glutamate receptor clusters represent prefabricated packets of synaptic components, or just reflect distinct classes of transport vesicles containing certain types of glutamate receptors. The fact that, the NMDA receptor scaffolding protein PSD-95 is transported to synaptic sites largely independently of NMDA receptors (Rao et al., 1998; Friedman et al., 2000; Rao et al., 2000; Washbourne et al., 2002), supports the latter interpretation. The non-overlapping of mobile AMPA and NMDA receptor clusters and the different dynamics of their recruitment to synaptic sites reflect the presence of distinct regulatory mechanisms controlling their synaptic traffic and localization. Consistently, the cytoplasmic parts of AMPA and NMDA receptor subunits bind to very different sets of structural and regulatory proteins (Scannevin and Huganir, 2000; Sheng, 2001; Sheng and Lee, 2001). The AMPA receptor binding protein, Stargazin, is crucial for the synaptic targeting of AMPA receptors, but not for the morphological development of synapses (Chen et al., 2000). Also combining with the discovery of 'silent synapses' present in rat hippocampus and somatosensory cortex, which only contain NMDA receptors but lack AMPA receptors (Liao et al., 1995; Isaac et al., 1997), it is clear that the AMPA receptor incorporation at the synaptic sites is not required for initial synaptic assembly.

1.1.3.3 Time sequence of pre- and postsynaptic assembly

Although more and more pre- and postsynaptic proteins have been tagged with fluorescent probes and recorded in living cells, there is incomplete agreement on the time course of pre- and postsynaptic assembly. For example, DsRed tagged NMDA receptors have been reported to cluster at nascent synapses within a few minutes of axon-dendrite contact in young cortical culture (3-4 days *in vitro*) (Washbourne et al., 2002). However, another study in more mature hippocampal neurons (about 14 days *in vitro*) showed that the accumulation of NMDA receptors at nascent synapses takes 1-2 hours, and therefore lags behind the accumulation of presynaptic markers (Okabe et al., 2001). Thus, it is still not absolutely sure whether one synaptic side differentiates before the other, or whether the synaptic assembly undergoes simultaneously on both sides. Because the discrepancy raised here is at least partially due to the difference of experimental materials, it is also possible that divergent mechanisms for synaptic assembly are used by different neuron types, or even different stages of the same type. Further studies are apparently required to determine this basic issue in synaptogenesis, and it will be much more beneficial to analyze, if possible, this process *in vivo*. Despite the uncertainty of the time course of pre- and postsynaptic assembly, as soon as a synapse is established, presynaptic active zone and PSD are exquisitely overlapped, indicating a close coordination of presynaptic and postsynaptic maintenance.

1.1.4 *Drosophila* NMJ as a model for studying synaptogenesis

1.1.4.1 Structural properties of *Drosophila* NMJ

The *Drosophila* neuromuscular junction (NMJ) is an excellent model system for addressing fundamental mechanisms governing synapse formation and growth. The advantageous features of *Drosophila* NMJ include its structural accessibility and amenability to powerful genetic, electrophysiological and microscopic techniques.

In *Drosophila* late stage embryo and larva, body wall musculature shows a segmentally repeated pattern of 30 muscle cells (in each symmetric hemisegment) innervated by about 45 motor axons. Each of these muscles is easily identified by its distinct position and size, and is innervated by specific motorneurons. The NMJ morphology is highly stereotyped, the axons of motorneurons spread onto the muscle surface, forming a synaptic arbor composed of series of varicosities connected by thin axonal processes (Fig. 1-5 A). These varicosities, or called synaptic boutons, are categorized by three classes (Gramates and Budnik, 1999; Rheuben et al., 1999). The major class of boutons (type I) contain clear vesicles and are glutamatergic, and at larval stage, they are surrounded by the characteristic subsynaptic reticulum (SSR), an elaborately layered structure formed from the muscle membrane at the junctional region (Atwood et al., 1993; Jia et al., 1993)(Fig. 1-5 B). All 30 body wall muscles are innervated by type I glutamatergic boutons, some muscles are also innervated by type II and type III boutons, which contain octopamine or peptide neurotransmitters (Koh et al., 2000). The neuromuscular contact differentiates into distinct boutons containing functional synapses in late stage embryo, and the boutons continuously grow and sprout throughout the whole larval life. Extensive studies have been made on the third instar larval type I glutamatergic synapses, detailed analysis revealed that type I boutons can be further divided into type I small (Is) and type I big (Ib) by size, the extent of the folding of SSR, and electrophysiological properties. Due to the tiny size of embryo, it is not used as frequently as larva, however, it has been proved to be invaluable in understanding molecular events relevant to initial synapse formation. Unlike the vertebrate NMJ, the NMJ of *Drosophila* is not covered by glial cells, leaving 10–20 μm of neuronal surface without insulation from the hemolymph. (Hall and Sanes, 1993; Auld et al., 1995).

Notably, *Drosophila* NMJ shares several important features with the excitatory central synapses in vertebrate brain: it is glutamatergic (unlike the cholinergic NMJ in vertebrate) and contains homologous ionotropic glutamate

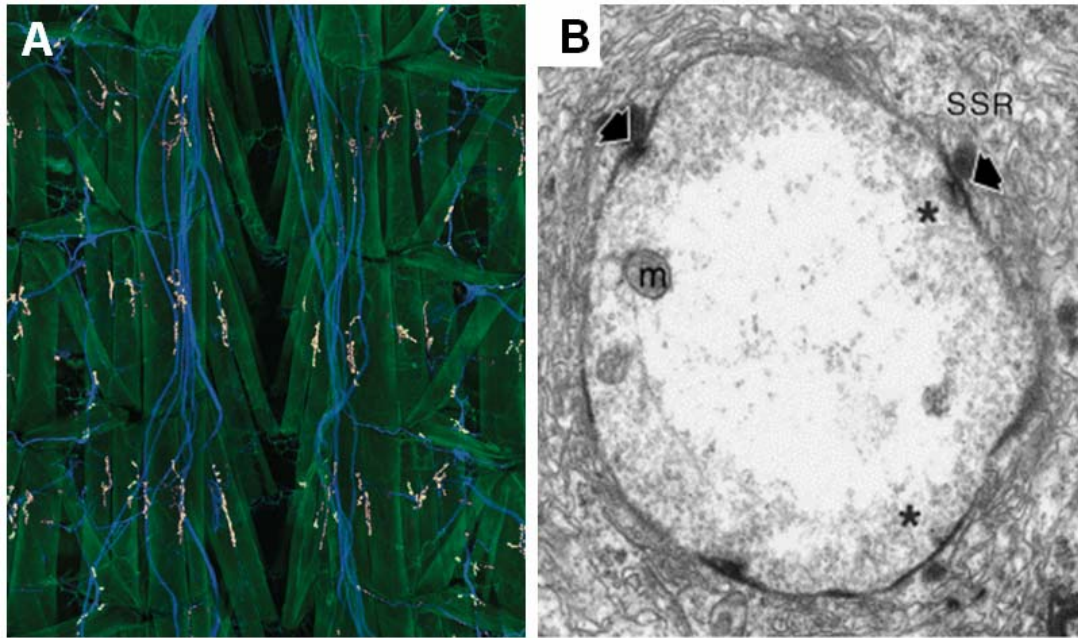


Fig.1-5 Structure of *Drosophila* NMJ.

A, Three segments of a dissected third instar *Drosophila* larva. Muscles are stained as green, neuromuscular junctions stained as red and nerves stained as blue (Adapted from (Daniels et al., 2004)). B, Electron micrographs depicting cross-sections through a type-I bouton on muscle 6 in wild-type larvae. The subsynaptic reticulum (SSR), active zones (asterisks), T-bars (thick arrows), and mitochondria (m) are marked (Adapted from (Aberle et al., 2002)).

receptors; there is no obvious basal lamina layer that separates pre- and postsynaptic membrane, so the synapse appears close membrane-membrane apposition ultrastructurally (Fig. 1-5 B); it is organized into a series of boutons that can be added or eliminated during development and plasticity (Petersen et al., 1997). During the period that larva grows from first instar to third instar, which normally takes several days, the muscles undergo a dramatic increase in size (more than 100 folds), therefore requiring a concomitant addition of more synaptic boutons and further elaboration of NMJ branches to efficiently depolarize the muscles.

Although the NMJ architecture changes dramatically during postembryonic

development, the characteristics of individual neuromuscular synapses are rather similar between embryo and larva at ultrastructural level (Prokop, 1999): the pre- and postsynaptic membranes appear smoother and more electron dense compared to the extrasynaptic areas, indicating that the molecular composition of synaptic fields differs from extrasynaptic membranes. The intracellular face of presynaptic membrane harbors active zones, which contain characteristic T-shaped electron-dense structures (T-bars) surrounded by clusters of synaptic vesicles (Fig. 1-5 B). T-bars can still be seen in neuronal terminals that are depleted of synaptic vesicles and therefore appear to be independent molecular structures (Poodry and Edgar, 1979). The exact molecular composition and function of T-bars still remain unclear.

1.1.4.2 Initiation and maintenance of neuromuscular connection

1.1.4.2.1 Initiation of neuromuscular contact---target recognition (pathfinding)

So far, most studies on NMJ formation have been carried out on the ventral longitudinal muscles 6 and 7, which are innervated exclusively by glutamatergic type I boutons. It is believed that most NMJs, if not all, develop in a similar way and share the common architecture. At embryonic stage 15/ 16, muscles start sending out myopodia preferentially from the future innervation site (Ritzenthaler et al., 2000), and they are contacted by filopodia sent out from the motoneuronal growth cones in a random fashion. Those motoneuronal processes which are in contact with inappropriate muscles are soon withdrawn (Broadie and Bate, 1993; Yoshihara et al., 1997). This specific targeting recognition process is suggested to be mediated by both repulsion from inappropriate target muscle and contact-mediated attraction to the right target muscle (Bate and Broadie, 1995; Keshishian et al., 1996). Example of repellent molecule is the Toll, which is present on the surfaces of certain muscles and can prevent innervating by irrelevant motoneurons, removal of Toll leads to the ectopic

innervation. Fasciclin III (FasIII), one homophilic cell adhesion molecule, appears to be mediate attractive cell-cell recognition, since misexpression of FasIII introduces innervation at the non-target cell. Up to now, many targeting cues have been identified, such as caspricious, semaphorins, connectin, neuromusculin and netrins (Bate and Broadie, 1995; Chiba and Rose, 1998), acting as either repellent or attractive molecules.

1.1.4.2.2 Stabilization and maintenance of neuromuscular connection by cell adhesion molecules

As soon as the initial neuromuscular contact is established, it has to be stabilized for further differentiation. This process, which should be also required for the new bouton growth during postembryonic period, is believed to be largely mediated by multiple cell adhesion molecules. Upon initial neuromuscular contact at embryonic stage 13, usually the junction consists of only short stretches of apposed membranes, often interrupted by stretches of non-connected cell surfaces (Schuster et al., 1996; Yoshihara et al., 1997; Prokop A et al., 1998). While at the mature NMJ of late stage 17 embryo such contact develops into an extended cell-cell junction, indicating that adhesive properties change during NMJ maturation. Consistent with this notion, FasIII, which contributes to target recognition and potentially also early phase of contact stabilization, disappears from NMJs of later stages (Broadie and Bate, 1993). In contrast, FasII, another homophilic CAM belonging to the immunoglobulin superfamily, is initially expressed strongly on the surfaces of all motor axons and at low levels in muscles during NMJ formation (Schuster et al., 1996). As synaptic connections are established, FasII is progressively clustered at pre- and postsynaptic membranes. The late junctional maintenance of FasII is largely, but not all, mediated by the scaffold protein Discs large (Dlg), the *Drosophila* Membrane-Associated Guanylate Kinase (MAGUK) homologous to mammalian PSD-95/ SAP90 family proteins (Budnik et al., 1996; Thomas et al., 1997; Zito et al., 1997), which itself is not detectable at the NMJ until late stage 17 (Guan et al., 1996). Deleting FasII does not interfere with

NMJ formation, but strongly affects postembryonic stabilization and maintenance of NMJs, suggesting its crucial role in controlling synaptic stability and growth (Schuster et al., 1996). Furthermore, it seems to be of developmental importance that FasII function is restricted to the late phase of NMJ differentiation: overexpression of FasII in muscles during initial NMJ formation seems to render muscle surfaces too 'sticky' and interferes with precise neuromuscular target recognition, as a result, ectopic motoneuronal branches (which normally occur only transiently) become trapped and form NMJs on inappropriate muscles (Davis et al., 1997). Apparently, there must exist other yet unidentified adhesion molecule(s) required for initial events of synapse formation.

Another example relevant to switch in adhesive properties at NMJ comes from analysis of *mef2* mutant embryos, where the initial neuromuscular contact can be genetically separated from the late phase of neuromuscular adhesion. In *mef2* mutant embryos, muscle founder cells form, and motoneurons establish initial contact with proper target cells (Prokop et al., 1996). However, the muscle founder cells remain immature and fail to acquire properties of general muscle differentiation. In late-stage 17 *mef2* mutant embryos, proper cell junctions between motoneurons and improperly differentiated muscle fibers are never observed, but instead the abnormal muscle surfaces are covered by basement membrane. This phenotype could be explained by lack of *mef2*-dependent late synaptic CAMs, which directly maintain the established neuromuscular connection. Alternatively, *mef2* might be required to exclude basement membrane receptors from the NMJ, thus preventing dissociation of the pre- and postsynaptic membranes from competitive invasion of basement membrane material. No matter which explanation is true, it is clear that appropriate adhesive strength is the prerequisite for proper NMJ maturation and further maintenance.

1.1.4.3 Synapse formation

Synapse formation involves the coordinated assembly of pre- and postsynaptic apparatus. Positioning cues are required to direct the juxtaposition of synaptic components at the pre- and postsynaptic membranes. In *Drosophila* NMJ, candidate that might serve as positioning cue is the special type of cleft-spanning adhesion molecules, as supposed by the function of Neuroligin/ Neuexin at vertebrate central synapses and immunoglobulin superfamily members SYG-1/ SYG-2 in *C. elegans* (see above), but this still remains to be proved.

In contrast to the essential role that nerve-secreted factor agrin plays in vertebrate NMJ differentiation, no agrin orthologue seems to be present in the *Drosophila* genome. However, recent evidence indicates that other sets of secreted molecules, Wnts and members of the TGF-beta family might take similar responsibility in the development of glutamatergic synapses at *Drosophila* NMJ. Wingless (Wg), a member of the Wnt family of ligands, is secreted from motorneuron, loss of Wg leads to dramatic impairment of synapse formation, with boutons lacking active zones and postsynaptic structures (Packard et al., 2002). In consistence with this, a mammalian Wg homologue Wnt7a has been implicated in presynaptic differentiation in the cerebellum (Hall et al., 2000). Wishful thinking (wit) encodes a BMP (bone-morphogenetic-protein) type II receptor, which is present in a subsets of neurons, including motorneurons; its ligand, the BMP ortholog Glass Bottom Boat (Gbb), mainly fuctions in muscles. Mutations in both wit and Gbb result in much smaller NMJs, defective synaptic transmission and presynaptic abnormalities (such as synaptic membrane detachment at active zone region, presence of floating T-bodies) (Aberle et al., 2002; McCabe et al., 2003). Taken together, these studies indicate that Wg and Gbb function in opposite directions at *Drosophila* NMJ to assure proper differentiation of pre- and postsynaptic structures.

Before motorneuron innervation, low amounts of glutamate receptors are already expressed in muscles and diffusely distributed over the muscle surfaces (Broadie and Bate, 1993; Currie et al., 1995; Saitoe et al., 1997). Upon the initial neuromuscular contact, glutamate receptors begin clustering rapidly at the innervation sites, and within a few hours, new glutamate receptors are synthesized and inserted into newly formed synapses. Compared to the innervation-independent spontaneous AchR clustering at vertebrate NMJ, the clustering of glutamate receptors is innervation-dependent, the aneural muscles neither cluster existing receptors nor synthesize additional receptors. Intriguingly, disruption or complete elimination of neurotransmission does not seem to inhibit glutamate receptor field formation (Broadie et al., 1995; Featherstone and Broadie, 2000), however, the glutamate receptors will not cluster if the action potential of the neuron is blocked genetically or with tetrodotoxin (Broadie and Bate, 1993). Thus, glutamate receptor clustering appears to require an electrical activity dependant signal derived from motorneuron, and this signal is not related to neurotransmission. The latter notion is completely consistent with findings in mammalian central synapses: in Munc-13 or Munc-18 null mutant mice, in which neurotransmitter release is completely absent, both brain anatomy and synapses appear normal (Verhage et al., 2000; Varoqueaux et al., 2002). Thus, evidences from both *Drosophila* and vertebrates highly suggest that, at least in glutamatergic synapses, synaptic activity is not necessary for initiating synaptogenesis.

Analysis on mutants deficient in muscle development indicates that the presynaptic apparatus can be assembled independently of the postsynaptic cell (Prokop et al., 1996), which again contrasts with vertebrate NMJ differentiation. In the latter case, muscular secretion of s-laminin into synaptic basement membrane is essential for the assembly of morphologically normal active zones (Noakes et al., 1995). Anyhow, although the assembly of active zones at *Drosophila* NMJ can be independent of muscle cells, the precise apposition of

pre- and postsynaptic apparatus must rely on the close communication between motorneuron and target muscle.

1.2 Structure and functional relevance of ionotropic glutamate receptors

The ionotropic glutamate receptors (iGluRs), including AMPA, NMDA and Kainate types, mediate excitatory synaptic transmission at most mammalian central synapses. In addition to converting transmitter released from presynaptic terminal to electrical response in the postsynaptic neuron, these receptors are thought to contribute to the activity-dependant, long-term changes in synaptic strength which is proposed to underlie learning and memory (Contractor and Heinemann, 2002). Besides the physiological importance of iGluRs, their dysfunction is implicated in various neuropathologies, including epilepsy, stroke damage and the perception of pain (Dingledine et al., 1999).

1.2.1 Modular design of ionotropic glutamate receptors during evolution

Ligand-gated ion channels are generally formed as homo- or hetero-oligomeric assemblies of integral membrane protein subunits. One important feature of iGluR structure is its modular construction. As illustrated in Fig.1-6 A, one typical iGluR subunit consists of an amino-terminal domain (NTD), a ligand-binding domain (S1S2), three transmembrane domains, a re-entrant pore loop, and a carboxy-terminal domain (Hollmann and Heinemann, 1994; Madden, 2002). The NTD shows homology to the leucine/ isoleucine/ valine-binding protein LIVBP, one of the bacterial periplasmic binding proteins (PBPs). In NR2 subunits, it forms or contributes to the binding site of many NMDA receptor modulators and affects receptor desensitization. For the non-NMDA receptors, it is supposed to be involved in receptor assembly. The S1S2 ligand-binding domain is formed by two sequences (the S1 region which is the N-terminal of transmembrane domain 1, and the S2 region which is C-terminal of transmembrane domain 2) sharing sequence and structural

homology with the glutamine-binding protein QBP. The re-entrant pore loop is homologous to the P-loop sequences of other channels, the P-loop sequence lines the channel and determines many of its electrophysiological properties. In addition, the cytoplasmic carboxy-terminal contains various interaction domains and phosphorylation sites, which likely controls the transport and localization of these receptors. The modular feature of iGluR indicates that it might have been assembled from discrete components during evolution, consistent with the ‘genes-in-pieces’ hypothesis (Gilbert, 1978). Supporting this notion, a prokaryotic glutamate receptor ion channel (GluR0) was found, which lacks NTD and has only two transmembrane domains but is indeed glutamate-gated and selective for potassium ions (Chen et al., 1999).

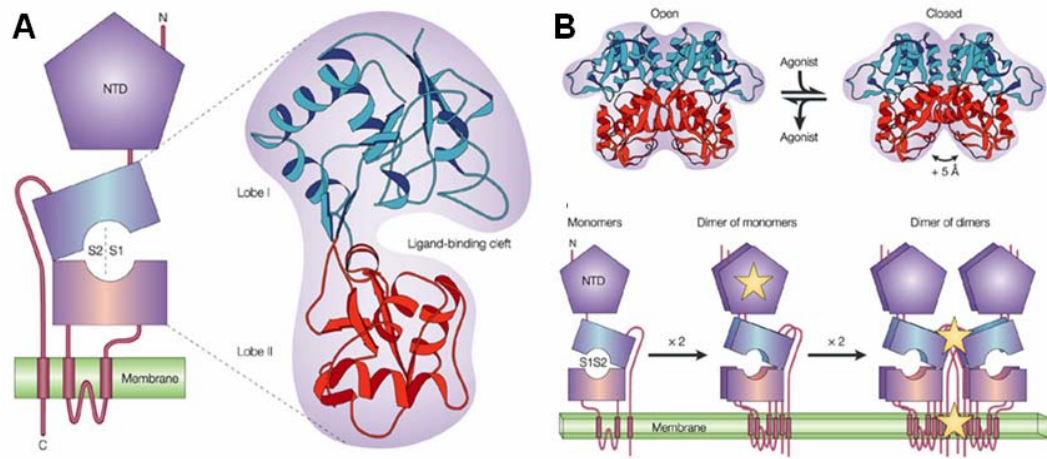


Fig.1-6 Structure of iGluR subunit and model of iGluR assembly. A, The modular structure of iGluR subunit. B, ‘Dimer of dimers’ model of iGluR assembly (Adapted from Madden, 2002).

1.2.2 Molecular mechanisms underlying selective assembly and transport of ionotropic glutamate receptors

Despite the schematic understanding of the sequence of building blocks that constitutes glutamate receptor subunits, still little is known about the spatial disposition of these domains within individual subunit and assembled functional

ion channel. Recently, dissecting the molecular details underlying the functional assembly and cell surface trafficking of various types of iGluRs has become one of the central focuses in molecular neuroscience.

On the basis of electrophysiological, biochemical and hydrodynamic analysis, iGluRs are proposed to be tetramers (Laube et al., 1998; Mano and Teichberg, 1998; Rosenmund et al., 1998; Kuusinen et al., 1999; Safferling et al., 2001). AMPA receptors are homo- or hetero-tetramers composed of GluR1-4 (Hollmann and Heinemann, 1994; Dingledine et al., 1999). Kainate receptors are homo- or hetero-tetramers of the subunits GluR5-7, KA1 and KA2. NMDA receptors require both NR1 and at least one type of the four NR2 subunits (A-D) to form functional channels, in some cases NR3 subunits are also included (Meguro et al., 1992; Monyer et al., 1992; Perez-Otano et al., 2001; Matsuda et al., 2003). Recently, using a series of epitope-tagged receptor chimeras (Ayalon and Stern-Bach, 2001), Ayalon and Stern-Bach provided evidence of sequential assembly of tetrameric iGluRs as dimmer of dimmers (Fig.1-7 B). In this model, initial subunit dimerization is mediated primarily by interactions between compatible NTDs. Then, assembly of functional receptors requires that these dimmers undergo a second dimerization, this time requiring compatibility between the S2 and transmembrane domains of the subunits. This secondary dimerization is not observed in the absence of NTD compatibility, indicating that it might be weaker than the primary dimerization. This dimmer-of-dimmers model of iGluR assembly is consistent with images of GluR2 homomers determined by electron microscopy (Safferling et al., 2001).

In non-neuronal cells, the step of exit from the endoplasmic reticulum (ER) is often under the most stringent control during transport of membrane proteins to the cell surface (Ellgaard and Helenius, 2003). Like other multimeric cell membrane proteins, glutamate receptors are synthesized, folded, assembled in the ER; similarly, traffic of glutamate receptors through ER is also tightly regulated, which decides the type and number of glutamate receptor at synapse

(Vandenberghe and Bredt, 2004). ER contains rigorous quality control system to ensure that only correctly folded and assembled proteins exit to the Golgi body, which in the case of glutamate receptors is evidenced by the presence of various ER retention and export signals in NMDA, AMPA and Kainate receptor subunits. For NMDA and Kainate receptors, both ER retention and export signals localize within the intracellular tails (Standley and Baudry, 2000; Scott et al., 2001; Xia et al., 2001; Ren et al., 2003; Hawkins et al., 2004; Jaskolski et al., 2004). Intriguingly, AMPA receptor subunit GluR2 contains a unique ER retention motif which just localizes in the re-entrant membrane loop (Greger et al., 2002), this single arginine (R607) is generated by mRNA editing and critically controls the ion permeability (Burnashev et al., 1992). Unlike other known ER export signal, the ER export signal of AMPA receptor subunit Glu1 appears within the extra-cellular NTD (Xia et al., 2002).

1.2.3 Properties of ionotropic glutamate receptors expressed at *Drosophila* neuromuscular synapses

In contrast to mammalian acetylcholinergic NMJ, the *Drosophila* type I junctional bouton is glutamatergic. So far, three ionotropic glutamate receptor subunits have been identified to be specifically expressed at the postsynaptic muscle cell (Schuster et al., 1991; Marrus et al., 2004). These glutamate receptor subunits are structurally and functionally similar to mammalian AMPA-/ Kainate-type receptors. *GluR-IIA* and *GluR-IIB* are genomic neighbors and their encoding proteins share 44% amino acid identity, animals with double knock-out of both genes die at late embryonic stage, while the lethality can be fully rescued by transgenic expression of either gene; moreover, modulation of subunit composition via genetically changing the copy number of *GluR-IIA* and *GluR-IIB* gene results into distinct single channel kinetic properties and is able to trigger long term changes of synaptic strength (Petersen et al., 1997; DiAntonio et al., 1999; Sigrist et al., 2002). GluRIII (also called GluR-IIC) is crucial for animal vitality and required for synaptic localization of GluR-IIA and GluR-IIB; while GluR-IIA and GluR-IIB do not precisely colocalize at

many synapses, they both perfectly colocalize with GluR-III, implicating that GluR-III acts as a obligate subunit for functional receptor assembly (Marrus et al., 2004).

1.3 The aim and strategy of this work

The purpose of this study is to improve our understanding of the molecular mechanisms relevant to the synaptogenesis and growth control/ regulation of *Drosophila* NMJ. To this end, newly developed DNA microarray technique was applied to sort potential genes relevant to the NMJ formation and functioning through the whole genome. Via RNA profiling of postsynaptic cell (here is the somatic body wall muscle), a pool of genes with specific or enriched expression pattern were obtained, which would greatly facilitate systematic characterization of certain interesting functional groups. Data mining from these obtained RNA profiles and online genomic resources resulted into the identification of several muscle expressed but uncharacterized ionotropic glutamate receptor subunit genes. The expression pattern of these subunits were further verified at both RNA and protein level, via quantitative RT-PCR, in situ hybridization and immunohistochemistry. Ionotropic glutamate receptors play the major roles in mediating the signal transmission at excitatory glutamatergic synapses in the central nervous system, moreover, these receptors are also thought to contribute to the activity-dependant, long-term plasticity of neuronal circuits which is proposed to underlie learning and memory (Contractor A et al., 2002). The *Drosophila* neuromuscular synapse provides an excellent platform for investigating the behavior of glutamate receptors, due to its structural and functional similarity to excitatory central synapse and its rather simple organization. Reasonably, characterizing the functional significance of these newly identified glutamate receptor subunits at *Drosophila* NMJ in principle would help better understand their orthologs in the central synapses and thus became the main body of this thesis work.

To study the *in vivo* roles of these novel glutamate receptor subunits, knock-out animals were generated via standard transposon-based mutagenesis screening. The null mutant animals of either subunit die at late embryonic stage, indicating that they are all essential genes. Further genetic, cell biological and electrophysiological studies were performed and uncovered a tight interdependence of all essential glutamate receptor subunits for synaptic localization and functioning, implying a novel “strictly hetero-tetrameric stoichiometry” model which is so far not reported in mammalian ionotropic glutamate receptors.

Closer inspection on glutamate receptor deprived synapses was also performed, with the combination of immunohistochemistry and electron microscopy based ultrastructural analysis. Surprisingly, it was found that with deprivation of glutamate receptors, the typical postsynaptic differentiation and synaptic compartmentation displayed severe defects, further analysis of a series of neurotransmission deficient mutant backgrounds excluded the involvement of neurotransmission activity in instructing differentiation of synaptic specializations. Thus, the glutamate receptor *per se*, but not its ligand-gated ion channel activity, is essential for normal synaptic construction. This important ‘structural’ role of glutamate receptor in organizing synaptic differentiation is firstly reported, raising highly interesting questions such as, which part of glutamate receptor is responsible for facilitating synaptic assembly? Do the ionotropic glutamate receptors in mammalian central synapses play similar roles during synaptogenesis?

1 Materials and methods

2.1 Materials (Chemicals, enzymes and molecular biology kits)

All of the chemicals were purchased from Roth and Sigma unless stated elsewhere. For molecular cloning, all of the enzymes, including various restriction endonuclease enzymes, T4 DNA ligases, Alkaline Phosphatase were purchased from Roche (Mannheim, Germany). The Vent polymerase used for PCR cloning was from NEB (USA). All of the oligonucleotides were synthesized from MWG (Germany). The E. Coli strains used for transformation were either self-made DH5 α chemical competent cell or SURE electroporation competent cell from Stratagene (USA). Unless described elsewhere all of the molecular biology kits were from Qiagen (Germany).

2.2 Methods

2.2.1 Genechip analysis and real-time RT-PCR

2.2.1.1 Genechip analysis

Part I Protocol for the Affymatrix GeneChip Target Preparation

Material and Reagents:

Qiagen RNeasy RNA purification kit

3M Sodium Acetate, pH 5.2 Sigma

80% ethanol kept cold

Absolute ethanol kept cold

Glycogen 5mg/ml, Roche

Ethidium bromide

7.5M Ammonium Acetate, Sigma

1). Synthesis of Double-Stranded cDNA from Total RNA

Materials and Reagents:

T7- (dT)₂₄ Primer, (MWG Corp) HPLC purified DNA

Phase lock Gel, Eppendorf

Phenol/ Chloroform/isoamyl alcohol, Roth
Superscript Choice System, Invitrogen
Ice bath
Heat/cool block for 70°C, 42°C, 16°C
PE 9700 PCR machine

1.1. First strand cDNA synthesis

Prepare an RNase- free 0.5 ml reaction tube containing the following reagents. They are to be added in the order listed. The total reaction volume is 20µl.

1. In a 0.5ml RNase-free tube add total volume of 10µl of total RNA sample (2.5µg).
2. Add 1µl of T7- (dT) 24 primer (100 pmol/µl).
3. Incubate at 70°C for 10 Min, quick spin and place on ice.
4. Add 4µl of 5X First strand cDNA buffer.
5. Add 2µl of 0.1 M DTT.
6. Then add 1µl of 10mM dNTP mix.
7. Add this mixture to the RNA sample then Incubate at 42°C for 2 min.
8. While in the bath Add 2µl SSII
9. Incubate for 1 hour at 42°C.
10. Place reaction on ice and proceed onto second strand synthesis.
11. Equilibrate a 16°C bath.

1.2. Second Strand Synthesis

12. Briefly centrifuge first strand reaction and return to ice.
13. Add the following reagents in the order listed to the first strand reaction.
14. Make sure to add the reagents while the reaction is on ice.

91µl of DEPC-treated dH₂O

30µl of 5X Second Strand Reaction Buffer

3µl of 10mM dATP, dCTP, dGTP, DTTP

1µl of DNA ligase (10U/µl)

4µl of DNA polymerase I (10U/µl)

1µl of Rnase H (2U/µl)

To yield a final reaction volume of 150µl.

15. Gently tap tube to mix. Briefly spin to remove condensation.
16. Incubate the reaction at 16°C for 2 hours in a cooling water bath
17. While in the bath add 2µl of T4 DNA Polymerase.
18. Incubate for an additional 5 minutes at 16°C.
19. Add 10µl of 0.5M Na₂EDTA

The reaction product can be stored at -20°C for later use.

1.3 Clean Up of Double-Stranded cDNA

STEP 1-Phase Lock Gels Phenol/Chloroform Extraction

1. Pellet the Phase lock gel in a micro-centrifuge tube by spinning it at full speed (1,3200rpm) for 20 to 30 seconds.
2. Add 162µl of Phenol: Chloroform: isoamyl alcohol (saturated with 10mM Tris-HCl pH 8.0/ 1mM EDTA) to the cDNA reaction sample, mix by vortexing for one minute.
3. Transfer the entire cDNA Phenol Chloroform mixture into the PLG tube. Spin the PLG tube at full speed for 2minutes
4. Avoiding contact with the gel transfer the aqueous upper phase to a fresh 1.5 ml tube (Tilt the tube for better recovery).

Proceed to step 2.

STEP 2 - Ethanol precipitation

1. Add 1µl of glycogen to the sample.
2. Add 0.5 volumes of 7.5M NH₄Ac plus 2.5 volumes of absolute ethanol (stored at -20°C) to the sample and vortex.
3. Immediately spin at full speed in a micro-centrifuge at room temp for 20 min, discard supernatant.
4. Wash pellet with 500µl of 80% ethanol (stored at -20°C)
5. Spin at full speed for 5minutes at room temp.
6. Remove the ethanol very carefully so as not to disturb the pellet and repeat the wash. (This is an optional stopping point. The pellet may be left in the wash

at -20°C overnight.)

7. Air dry the pellet at room temp completely (this may require over an hour).

8. Resuspend the pellet in 12µl of Rnase-free water.

9. Proceed onto Synthesis of biotin-labeled cRNA.

To reduce overdrying leave the pellet in a very small volume of the last wash.

2). Synthesis of biotin-labeled cRNA

Materials and Reagents:

Enzo RNA transcript labeling Kit 9 (BioArray High Yield RNA Transcript Labeling Kit)

Rneasy Mini Kit, Qiagen

DEPC-treated water

10X TBE, BioWhittaker

Reagent preparation

5X Fragmentation Buffer:

In an Rnase-free vessel combine

4.0 ml of 1M Tris-acetate pH 8.1 (adjusted with glacial acetic acid).

0.64 g MgOAc.

0.98 g KOAc.

DEPC-treated water to make a final volume of 20mL.

Mix thoroughly then filter through a 0.2µm vacuum filter unit. This reagent should be aliquoted and stored.

2.1 protocol for the IVT reaction

1. Equilibrate a 37°C bath / block

2. Thaw the Enzo reagents on ice.

3. When thawed check for precipitate, vortex if necessary.

4. The volume of cDNA to be used in the IVT reaction should correspond to the total RNA range of 8.0 and 16.0 µg.

5. From the Enzo BioArray RNA labeling kit add the following reagents in the

order listed.

Reagent Volume

Template DNA Variable to give 1 μg of cDNA (10 μl)

Deionized water To make final volume equal to 40 μl (~12 μl)

10X HY Buffer 4 μl

10X Biotin-labeled nucleotides 4 μl

10X DTT 4 μl

10X RNase inhibitor 4 μl

20X T7 RNA polymerase 2 μl

Total volume 40 μl

6. Carefully mix the reagents in the tube then spin the sample briefly
7. Immediately place the tube in a water bath at 37°C incubate for 5.5 hours gently mixing every 30 to 45 minutes
8. Remove 1 μl aliquot for gel analysis
9. At the end of the incubation the reaction may be stored at -20.0°C for later use.

2.2 Purification and Quantification of in vitro Transcription

STEP 1 - Column purification of RNA

1. Pre-heat a small working stock of RNase-free water at 60-65°C.
2. Pre-heat elution buffer at 60-65°C.
3. Aliquot one half (~20 μl) of the cRNA reaction into a 1.5 ml tube.
4. Adjust volume to 100 μl with RNase-free water.
5. Add 350 μl of buffer RLT (lysis buffer) to the sample. Mix thoroughly.
6. Add 250 μl of ethanol (96-100%) to the lysate and mix well by pipetting up and down.
7. Apply sample (700 μl) to RNeasy mini-spin column sitting in a 2ml-collection tube.
8. Centrifuge for 30 sec at 10,000 rpm.
9. Reapply the flow-through onto the column and spin again.
10. Transfer the column into a new 2ml-collection tube.
11. Add 500 μl of buffer RPE (ensure ethanol has been added to the buffer) and

let stand for 1 min.

12. Spin at max for 30s and discard flow-through.

13. Add another 500µl of buffer RPE onto the column and let it stand for 1 min.

14. Centrifuge and discard flow-through.

15. Spin at full speed for an additional 3min.

16. Transfer the column to a new 1.5 ml tube and pipet 33 µl of the pre-heated Rnase free water directly onto the membrane. Let stand for 1 min.

17. Spin at full speed for 1 min.

18. Repeat elution using the flow-through from the first elution.

STEP 2 - Ethanol precipitation: if the cRNA yield is poor

19. Add 0.5 volume of 7.5M Ammonium Acetate and 2.5 times volume of absolute ethanol

20. Incubate at -20°C for 60 min then spin at full speed for 30 minutes.

21. Decant the supernatant then wash the pellet by adding 500µl of 80% Ethanol and spin at full speed for 5 minutes.

22. Decant the supernatant and repeat the wash step

23. Decant the final wash and dry the pellet at room temperature.

STEP 3 – Electrophoresis

24. Prepare sample in a RNA gel-loading buffer.

25. Heat sample 65°C , 5 min.

26. Run one lane of unpurified labeled cRNA (0.5 µl) along side a lane of the purified labeled probe (1.5 µl) on standard 1% agarose gel.

Fragmentation of cRNA for target preparation

27. Add 2µl of 5X Fragmentation buffer to every 8µl of RNA plus water. The final RNA concentration in the reaction can range between 0.8 µg/µl and 2 µg/µl.

28. The following are guidelines that should be followed:

20µg cRNA 1 to 16µl

5X Fragmentation buffer 4µl

Rnase-free water to 20µL

Component Volume

15 µg cRNA (extreme case) 1 to 12 µl

5X Fragmentation buffer 3 µl

Rnase-free water 15 µl

29. Incubate the reaction at 94°C for 35min, quick spin and place on ice immediately following the incubation.

30. Run 1 µg of the fragmented RNA on a 1% agarose gel to check the completion of fragmentation.

31. The fragmented RNA is ready for hybridization.

Hybridization was performed in Affymetrix hybridization oven at 50°C for 16 hours. The hybridized Gene chips were then stained and washed in Affymetrix fluidics station following the standard program. Data analysis was performed via Microarray Suite 4.0 and exported via Excel.

2.2.1.2 Real-time RT-PCR

1. Extract total RNAs using QIAGEN's RNeasy kit (as described in 2.2.1.1), check the concentration of each sample.

2. Perform reverse transcription using QIAGEN's Omniscript Reverse Transcriptase:

Master mix:

10X Buffer RT	2.0µl
dNTP Mix (5mM each dNTP)	2.0µl
Random hexamer	2.0µl
Rnase inhibitor (40 units /µl)	0.25µl
Ominiscript Reverse Transcriptase	1.0µl
Rnase-free H ₂ O	Xµl

Template RNA 2 μ g

Incubate the mixture for 1 hour at 37°C, then inactivate the Reverse Transcriptase by heating the reaction mixture to 93°C for 5 min followed by rapid cooling on ice.

3. Perform the real-time PCR in 96 well plate :

Master mix (50 μ l):

2X PCR mixture 25 μ l

H₂O 22 μ l

Primer (forward) 1.0 μ l

Primer (reverse) 1.0 μ l

cDNA template 1.0 μ l

4. Quantitate the relative transcript level by analyzing Ct value of each sample.

5. Check the amplified products by agrose gel electrophoresis.

2.2.2 Fly stocks and genetics

2.2.2.1 Fly stocks, crosses and rearing conditions

Fly stocks used are: All of the wild type control strain used is w¹ (B) except stated elsewhere. w⁻;Df(2L)^{SP22} (*Gglur-IIA*^{-/-}, *Gglur-IIB*^{-/-})/ Cyo, Kr::GFP (Petersen et al., 1997). w⁻;Df(2L)c1^{h4}/ Cyo, Kr::GFP. w⁻;OK319-Gal4. w⁻;UAS-TNTE (Sweeney et al., 1995). *Syx*²²⁹ is a null mutation allele of *syx-IA* that completely eliminates mRNA and protein expression (Schulze et al., 1995). *Shi*^{ts1} mutants were shifted from a permissive (25°C) to a non-permissive temperature (32°C) after 13 h of embryogenesis (Featherstone D et al., 2002). III¹/ Gla Bc (Marrus et al., 2004).

Double mutants in *GluR-IIA* and *GluR-IIB* were described previously (Petersen et al., 1997; DiAntonio et al., 1999). In short, *GluR-IIA* and *GluR-IIB*

double mutant embryos were recovered by crossing *Df(2L)GluR-IIA&B^{SP22}* to *Df(2L)cl^{h4}*, mutant embryos were selected using GFP marked balancer chromosomes.

To generate *GluRIIA^{hypo}*, *GluR-IIB^{null}* condition having an extremely reduced amount of GluR-IIA and no GluR-IIB expression, genomic fragment of GluR-IIA encompassing promoter region and the whole open reading frame while missing most part of the 3'-UTR was used. This transgene still produces full length GluR-IIA while in dramatically reduced amount due a loss of message stability (see 3.4.2 for details). This construct was expressed from *pUAST* vector (using the *GluR-IIA* endogenous promoter). A single transgene copy rescues embryos null for both *GluR-IIA* and *GluR-IIB* (*Df(2L)GluRIIA&B^{SP22}/Df(2L)cl^{h4}*) giving *GluRIIA^{hypo}*, *GluR-IIB^{null}* larvae (see results).

Unless stated elsewhere, all of the crosses were established at 25 °C with 60% humidity.

2.2.2.2 Mutagenesis screening

The *GluR-IIID* and *GluR-IIIE* loci are situated at 92F4. In a recently released pBac transposon insertion collection (Thibault et al., 2004), a *piggyBac* transposon (pBac{RB}e01443, #17952,) was found to be inserted into intron 6 at amino acid position 427 of the *GluR-IIID* open reading frame. This allele *GluR-IIIDe⁰¹⁴⁴³* is embryonic lethal both homozygous or over *Df(3R)H-B79* (Bloomington *Drosophila* stock center) which deletes a large genomic region including the *GluR-IIID* and *GluR-IIIE* locus, and over deficiency *GluRIID&-IIIE^{E3}* (see below). For *GluR-IIIE*, imprecise excision screening was performed using the P element line GE28753 (commercially available with Genexcel), which is inserted ~150bp downstream of the end of the *GluR-IIIE* transcript. In brief, P-element GE28753 was remobilized by crossing to the Δ 2-3 transposase source, white eye progenies were selected and mated individually,

then single fly genomic PCR reactions were performed to map deletions flanking the P-element insertion site. Nearly 1,000 eye color revertants were checked, one line (*GluR-IIE^{E1}*) was found to delete 1.2 kb flanking region in direction of the *GluR-IIE* gene, removing the C-term and transmembrane domain 4 of GluR-IIE. *GluR-IIE^{E1}* is embryonic lethal homozygously, over *df(3R)H-B79* and over *GluR-IID&-IIE^{E3}*. *GluR-IID&-IIE^{E3}* is a larger deletion also recovered from excision mutagenesis of GE28753, which removes both *GluR-IIE* and *GluRIID* and thus was used in combination with either *GluR-IID^{e01443}* or *GluR-IIE^{E1}* as deficiency.

2.2.3 Molecular Constructs and Transgenes

A genomic fragment covering the DGluR-IIA gene (containing 1.3 kb sequence 5' of the ATG) was firstly subcloned into pSL1180 as EcoRI/ XhoI fragment (5.6 Kb) from a BAC clone RPCI-98-35L07. The wild type rescue construct was made by directly inserting the EcoRI/ XhoI fragment into pUAST (Brand and Perrimon, 1993). For the 3' UTR deleted version, the subclone was cut with NcoI and XhoI, end-blunted and religated, then the EcoRI/ Asp718 fragment (4.7 Kb) was inserted into pUAST. All constructs were confirmed by double-strand sequencing, transgenic flies were produced in w1 background via standard procedures and crossed into the Df(2L)c1^{h4}/ Gla, Bc background.

Genomic fragments covering the *GluR-IID* gene and *GluR-IIE* gene were generated by PCR using for IID

5'GGTCTAGAGCGGCCGCGGCCACGAAGTACCCACGGTTTC3' and

5'GCGGCCCTCGAGCGACGTCAAGGATGTGCCAC3'

and for IIE

5'GGTCTAGAGCGGCCGCACCTCCCCAAGCTGTCAACTTC3' and

5'GCGGCCCTCGAGACTGCTCAAAGCTGCTGCCCTG3'. The products

were double strand sequenced and cloned into *pUAST*. Several independent lines of transgenic animals were generated. For overexpression studies,

UAS-GluRIID and *UAS-GluRIIE* were generated by introducing the full length cDNA into the transformation vector *pUAST*. Full-length cDNAs of *GluR-IID* (RE24732) and *GluR-IIE* (RE07945) were obtained from Berkeley *Drosophila* Genome Project cDNA libraries.

The construct for inducible RNA interference (*RNAi-GluR-IIE*) was made based on the *pUASTi* plasmid (contains an intron between insertion sites for sense and antisense fragments; generous gift by Amin Ghabria, Krasnow lab). Selected cDNA fragments covering part of 5'-UTR and coding region were PCR-amplified by using the following primer pairs:

5'GCGCGCCTCGAGCTGTTCGGGAAACTCAAGAAT3' and
5'GGTCTAGAGCGGCCCGCCGTGGTTAGCTCGTTCAAATG3'
and

5'GCTGGTACCTGTTCGGGAAACTCAAGAAT3' and
5'GCGTCTAGATCGTGGTTAGCTCGTTCAAATG3'

The two fragments were inserted into *pUASTi* plasmid sequentially and verified by sequencing. Several independent lines of transgenic animals carrying *UAS-GluR-IIE* were generated.

To generate *GluR-IIE::EGFP* fusion. The EGFP ORF was inserted into the C-terminal of *GluR-IIE* coding sequence (the insertion site and the linker sequences are as described in (Sheridan et al., 2002) via 'blunt-end ligation' strategy. Briefly, a *HindIII* fragment covering the C-terminal region of *GluRIIE* was cut from full-length cDNA (RE07945) and subcloned into *pSL1180*; PCR reaction was performed to generate the whole length linear fragment using the following primers which are standing at the EGFP insertion site but opposite in direction:

GGCAGATGTGTATAAGAGACAGTCGCCAGTCCTCGATGTCAGTAGCTT
and

AGATGTGTATAAGAGACAGGACTGGCGACTGCGCGAGTAGATGG,

at the same time EGFP coding sequence was amplified from EGFP vector (Clontech) using the following primers with 5' phosphate modification:

pGGCGCGCCGAGCAAGGGCGAGGAGCTGTTACCCGG

and

pCGGGCGCGCCGCCCTTGTACAGCTCGTCCATGCCGAGA,

the two PCR products were put together for blunt-end ligation and the positive clones with right orientation of EGFP were verified by PCR and sequencing; then the HindIII fragment (now containing EGFP insert) was put back into the full-length cDNA backbone and the reading frame was verified by PCR and sequencing; finally the full-length DGluRIIE cDNA tagged with EGFP was PCR cloned into the NotI/ XbaI site of pUAST and pFasBac vector and verified by sequencing. Several independent lines of transgenic animals were generated from injecting the pUAST construct. The pFastBac construct was used for driving expression in Sf9 cells (for details see 2.2.5)

2.2.4 In Situ Hybridization

I. Preparation of embryos

1. Collect embryos every 3 hours for 24 hours and wash 3X with 0.02% Triton X (Tx)
(15ml for up to 2ml embryos in a 50ml falcon tube).
2. Dechorionate 3 min. in 50% bleach.
3. Wash 3X with 0.02% Tx.
4. Fill tube with equal parts heptane and 4% formaldehyde/PBS (filtered).
5. Incubate 25 min. with frequent shaking.
6. Remove LOWER aqueous phase and replace with equal volume methanol.
7. Shake for 1 min. allowing embryos to settle. Do not vortex.
8. Remove UPPER phase along with embryos and vitelline membranes and remaining at the interphase.
9. Rinse settled embryos 3X with methanol (Embryos can be stored at -20 degrees C at this point).
10. Rehydrate in 3:1 (MeOH: 4% formaldehyde/PBS) for 2 min., then 1:3 (MeOH: 4% formaldehyde/PBS) for 5 min.

11. Fix 10 min. in 4% formaldehyde/PBS.
12. Rinse 6X with PBS + 0.1% Tween 20 (PBT).

II. Preparation of Probe

1. Perform restriction digestion of the vectors containing the sequences of interest. For preparing antisense RNA probes of, GluR-IIID and GluR-IIIE, RE24732 (*GluR-IIID*) and RE07945 (*GluR-IIIE*) plasmids were cut with *NotI*, respectively.
2. Run the digest on agarose gel and extract the DNA (elute the DNA in 10 μ l of H₂O)
3. Run 1 μ l of DNA on a test gel.
4. In-vitro transcription:

Set the following reaction mixture:

DNA	9 μ l
RNase free water	3 μ l
10xTranscription Buffer	2 μ l
RNase inhibitor	2 μ l
DIG-labelling mix	2 μ l
T3 RNA polymerase	2 μ l

Incubate at 37°C for 2 hours.

5. Then add 2 μ l RNase free DNase and incubate at 37°C for 15 minutes.
6. Extract the RNAs by using RNAeasy Kit.
7. Fragmentation of RNA

RNA sample in Rnase free water	25 μ l
2xcarbonate buffer	25 μ l

8. Divide the above mixture into two parts. Incubate 25 μ l at 60°C for 5 min and incubate other 25 μ l at 60°C for 15 min.
9. Add Rnase free water to the fragmented RNA sample to get a final volume of 100 μ l, add 10 μ l of NaAc buffer (PH 5.2) and 1 μ l of LPA, and 250 μ l of

absolute ethanol. Mix and centrifuge for 5 min at full speed, remove supernatant and wash the pellet with 75% ethanol.

10. Dissolve the RNAs sample with 25µl of probe resuspension buffer.

III. Hybridisation of embryos (fillets)

1. Wash the prepared embryos (fillets) in 1ml Pre-hybridisation Buffer(-DS)

Formamide	25 ml
20x SSC	10ml
50x Denhardtts	1 ml
tRNA 10 mg/ml	1.25 ml
ssDNA 10 mg/ml	1.25 ml
(preheated for 10 min at 100°C, followed by chilling in icewater)	
Heparin 50 mg/ml	0.05 ml
20% Tween	0.25 ml
Water	6.20 ml

Combine 9 ml with 1 ml water to get the Pre-hybridisation Buffer (-DS)

2. Incubate the samples in 1 ml of Pre-hybridisation Buffer(-DS) for 1 hr at room temperature.

3. Add 1µl of probe to 0.5 ml hybridisation Buffer (+DS) (9:1). Incubate overnight at 55°C.

4. 2x wash with 0.5 ml Washbuffer prewarmed at 55°C.

Wash buffer:

Formamide	250 ml
20x SSC	50 ml
Water	200 ml
20% Tween 20	2.5 ml

5. 7x 0.5 ml warmed wash buffer 1hr at 55°C.

6. Incubate in 0.5 ml warmed wash buffer overnight at 55°C.

7. 2x wash with PBTw.

8. Incubate for 30 min in PBTw at RT.
9. Incubate in 0.5 ml PBTw + 5% NGS + Antikörper (1:2000) (anti-DIG-AP FAB-Frag.) for 2 hrs. at RT.
10. 2x wash with PBTw.
11. 9x 10 min. PBTw at RT.
12. 2x wash with Alkaline Phosphatase Buffer + 0.1% Tween-20
 - 100 mM NaCl (= 20 ml 5M NaCl)
 - 5 mM MgCl₂ (=5 ml MgCl₂)
 - 100 mM Tris/HCl pH 9.5 (= 100 ml 1M Tris + 875 ml water)
 - 1/100 V 10% Tween-20
13. 5 min of incubation in AP buffer at RT.
14. Transfer the samples into 24 well plates, wash one time with 0.2 ml of BM Purple AP substrate, then add 0.2 ml of BM Purple AP substrate.
15. At proper stages, stop staining by 3 times of wash with PBTw and add 80% Glycerin/ H₂O. Store the plate at 4 degrees.

III. Mounting and light microscopy

2.2.5 Biochemistry (collaborated with Tobias Schwarz)

GluR-IIID and GluR-IIIE-EGFP were inserted into pFastbac1 vector (Invitrogen) and transformed into DH10Bac cells. Then the recombinant bacmid DNA was used for transfecting Sf9 cells with the aid of the Bac-to-Bac Baculovirus expression system (Invitrogen). For immunoblot experiments Sf9 cells were infected with the recombinant GluR-IIID and GluR-IIIE-EGFP baculovirus at a MOI (multiplicity of infection) of 1. Sf9 cells were harvested 40 hours post-infection washed twice with PBS, denatured in Laemmli buffer and heated at 100°C for 10 minutes.

Drosophila wild-type embryos were collected and dechorionated 18h AEL, froze in liquid nitrogen and stored at -80°C. Embryo lysates were prepared as described (Gillespie and Wasserman, 1994). The embryonic debris was removed

by centrifugation at 13000rpm for 15minutes and the supernatant was transferred to a new tube and centrifuged again for further purification. A portion of both pellet and supernatant fraction were mixed with an equal volume of 2x Laemmli buffer and heated at 100°C for 10 minutes.

Standard western blot was performed as described before. Anti-IID (1:1000), anti-IIC (1:1000) and rabbit anti-GFP antibodies (1:2000, Abcam) were incubated for 2 hours with the blot membranes at 4°C. For the visualization of the bands horseradish peroxidase conjugated secondary antibodies were used with the ECL Western blot system (Amersham).

2.2.6 Immunohistochemistry

2.2.6.1 Embryonic and Larval preparation

Solutions used for dissection:

Haemolymph-like (HL-3) saline without Ca

14ml 5M NaCl

5ml 1M KCl

20ml 1M MgCl₂

5ml Trehalose

115ml 1M Sucrose

Add distilled and deionized water to 1000ml, adjust PH to 7.2

10X PBS (Phosphate-buffered saline)

80g NaCl

2g KCl

2g KH₂PO₄

11.5g Na₂HPO₄.2H₂O

Add distilled and deionized water to 1000ml, adjust PH to 7.4

PBT

1X PBS

0.05% Tween-20

4% PFA (Fixation solution)

4% paraformaldehyde

1X PBS

Bouwin Fixation solution

Antibodies

Rabbit anti-GluR-IIC/III antibodies were generated against a c-terminal peptide (PRRSLDKSLDRTPKS). Rabbit anti-GluR-IID antibodies were generated against a c-terminal peptide of GluR-IID (ESLKTDSEENMPVED). Both sera were affinity purified and used at 1:500 dilution. Other primary antibodies were used at the following concentrations: mouse monoclonal anti-GluR-IIA antibody (8B4D2, DSHB), 1:100; Goat anti-HRP-Cy5, 1:250; mouse anti-FasII (1D4, DSHB), 1:40; mouse anti-Dlg (DSHB), 1:500; Nc82 (generous gift of Erich Buchner, Würzburg), 1:100. Except for samples stained with 8B4D2, which were fixed for 5 min with cold methanol, all of the other stainings were fixed for 10 min with 4% paraformaldehyd.

Dissection and staining

Mid stage 3rd instar larvae were put on a dissection plate, both ends were fixed by fine pins and the specimen was covered by a drop of ice cold HL-3 solution (see below). Dissection scissors were used to make a small hole at the dorsal midline of the larva (near to the posterior end) which was then completely opened along the dorsal midline from the hole to the anterior end. The epidermis was stretched flat and pinned down, then the internal organs and central nervous system were removed carefully with forceps. Late stage embryos (20- 22hrs after egg laying) were dissected on sylgard plates, fixed

with fine clips and opened using a pair of sharp tungsten needles. The dissected samples were fixed and then incubated with primary antibodies overnight, followed by fluorescence-labelled secondary antibodies (Dianova) and mounted in VectaShield mounting media (Vector Laboratories).

2.2.6.2 Confocal and epifluorescent microscopy

Imaging of embryonic and larval body wall preparations was performed on a Leica DM IRE2 microscope equipped with a Leica TCS SP2 AOBS scan head, using a Leica HCX PL Apo CS 63x 1.32 NA OIL UV objective. Epifluorescence images were taken on a Zeiss Axioscope with Axiocam camera, using a 100x oil objective of NA 1.4. Image processing was performed using ImageJ and Photoshop software.

2.2.7 Ultrastructural analysis (collaborated with Carolin Wichmann)

Dissected preparations were primary fixed in a mixture of 4% paraformaldehyde and 0.5% glutaraldehyde in 0.1M PBS (pH7.2) for 10 min and fixed additionally 60 min with secondary fixative comprising of 2% glutaraldehyde in 0.1 M sodium cacodylate buffer (pH7.2), washed three times for 5min in sodium cacodylate buffer, and postfixed on ice for 1hr with 1% osmium tetroxide, followed by an 1hr washing step in sodium cacodylate buffer and three brief washing steps in distilled water. The samples were stained en bloc with 1% uranyl acetate in distilled water for 1hr on ice. After a brief wash with distilled water, the samples were dehydrated in increasing ethanol concentrations (30%, 50%, 70%, 95%, 100%), infiltrated in Epon resin (100% EtOH/Epon 1:1, 30 min and 90 min; 100% Epon, over night) and embedded for 24hr at 85°C.

The samples were trimmed, and series of 80nm ultrathin sections were cut from muscle 6/7, abdominal segment 2 and 3 with a diamond knife on a Reichert Ultracut Ultramicrotome and mounted on Formvar-coated grids.

The sections were stained in uranyl acetate (4%) and photographed with a Philips (EM 301) transmission electron microscope.

2.2.8 Electrophysiology (collaborated with Robert Kittel)

Intracellular recordings were made at 22°C from muscle fiber 6 of abdominal segments 2 and 3, of late third instar larvae. The larvae were dissected in ice-cold, calcium-free haemolymph-like saline (HL-3) according to Stewart et al. (1994). Larval filets were rinsed with 2ml of HL-3 saline containing 1 mM Ca^{2+} , before being transferred to the recording chamber where two-electrode voltage clamp (TEVC) recordings were performed in 1mM extra cellular Ca^{2+} . The larval NMJ was visualized with a fixed-stage upright microscope (Olympus, 40x water immersion lens). Whole muscle recordings of both miniature and evoked postsynaptic currents were recorded in TEVC mode (AxoClamp 2B, Axon Instruments) using sharp microelectrodes (borosilicate glass with filament, 1,5mm outer diameter) with resistances of 15-35 M Ω and filled with 3M KCL. All cells selected for analysis had resting potentials between -55 and -70 mV. For stimulation, the cut end of the segmental nerve was pulled into a fire-polished suction electrode and brief (300 μs) depolarizing pulses were passed at 0.2 Hz (npi stimulus generator and isolation unit). To ensure the stable recruitment of both innervating motoneurons, the amplitude of the pulse was determined by increasing the stimulation strength to 1.5 times the amplitude needed to reach the threshold of double motoneuron recruitment. The clamp was tuned such that it responded to a voltage step from -60 to -70 mV with settling times of 1ms for mEJCs and 500-750 μs for eEJCs, this gave voltage errors of maximally 4 mV for eEJCs of approx. 100nA. Both eEJCs (voltage clamp at -60mV) and mEJCs (voltage clamp at -80mV) were low-pass filtered at 1 kHz. For each cell, 20 eEJCs and 90s of mEJCs recordings were used for subsequent analysis (pClamp9, Axon Instruments). For the paired-pulse stimulation, responses to 20 consecutive paired stimuli (separated by 4s rest) with 20ms interpulse interval were averaged.

3 Results

3.1 Establishing the tissue specific transcriptome of *Drosophila* larval body wall muscles

The total number of genes in *Drosophila* genome is predicted to be approximately 14,000. The high-density DNA microarray technique provides a fast and high throughput way to identify genes expressed at specific tissues or involved in certain processes (Stathopoulos and Levine, 2002; Butler et al., 2003; Li and White, 2003). Here, initial goal was to obtain a whole genome scaled map of molecular components involved in the construction and regulation of the postsynaptic muscle cells. Thus, using a *Drosophila* wild type strain (CS10), the transcripts of 3rd instar larval epidermis preparations, mainly consisting of body wall somatic muscles (with cuticles) but not central nervous systems, were prepared, amplified, labeled and hybridized to the Affymetrix *Drosophila* Genome arrays, generating the RNA expression profiles. RNA expression profiles of total larvae of *Drosophila* CS10 strain were also produced and set as baseline to compare with those from epidermis samples. Since equal amount of RNAs were utilized for different samples, transcripts displaying higher expression level in epidermis samples might represent the muscle specific or enriched genes and were selected.

The transcripts were ranked by average fold increase. Transcripts showing 2 fold or greater enrichment in epidermis samples were collected and shown in the appendix. One direct way to check the specificity of the data obtained is to check those transcripts with known tissue distribution pattern. As expected, among the pool of nearly 700 transcripts showing increasing abundance in epidermis samples, about one tenth are already known to be specifically (or abundantly) present in muscles or cuticles, thus directly proving the reliability of the data. These genes are categorized into various groups, including RNA-binding proteins, transcription factors, cell adhesion molecules, enzymes,

motor proteins, receptors and ion channels, and structural proteins, etc.(representatively shown in Table 3-1).

Table 3-1 Described muscle / cuticle-specific transcripts displaying enrichment in gene chip analysis of body-wall-preparations

Gene	Fold change	Proposed Function
RNA binding proteins		
How (held out wings)	4.5	RNA binding
Transcription factors		
Mef2	4.4	RNA polymerase II transcription factor
Muscle LIM protein at 84B	4.4	transcription factor
Cell adhesion molecules		
neuromusculin	7.3	cell adhesion
Enzymes		
Mlc-k	12.2	myosin light chain kinse
myosin light chain Kinase	5	myosin light chain kinase
CamKII	3.8	Calcium/ Calmodulin-dependent protein kinase II
dlg1 (discs large 1)	2.9	Synaptic and muscular scaffolding
Motor proteins		
Tropomyosin 1	2.6	Molecular motor
Tropomyosin 2	3.6	Molecular motor
upheld (troponin T)	3.6	tropomyosin binding
sanpodo (tropomodulin)	5.8	tropomyosin binding
Mhc (myosin II heavy chain)	2.5	muscle motor protein
Mlc2 (myosin light chain 2)	2.1	muscle motor protein
Receptors and ion channels		
GluR-IIA	4.3	glutamate receptor
GluR-IIB	2.6	glutamate receptor
GluR-III/ IIC	3.5	glutamate receptor
Structural proteins		
Lcp65Ag1	3.3	structural constituent of larval cuticle
Lcp1	2.9	structural constituent of larval cuticle
Lcp2	2.8	structural constituent of larval cuticle
Lcp65Ag2	2.1	structural constituent of larval cuticle
Lcp4	2.1	structural constituent of larval cuticle
Lcp3	2	structural constituent of larval cuticle
Others		
Mp20 (muscle protein 20)	2.9	calcium-binding
TpnC73F (Troponin C)	4.3	calcium-binding
TpnC47D	2.7	calcium-binding

3.2 Identification of novel ionotropic glutamate receptor subunits expressed at the *Drosophila* neuromuscular synapse

3.2.1 Enrichment of various transcripts encoding novel ionotropic glutamate receptor subunits in larval body wall muscles

The *Drosophila* genome encodes about 30 potential ionotropic glutamate receptor subunits (Littleton, 2000; Littleton and Ganetzky, 2000; Sprengel et al., 2001). Using the Affymetrix *Drosophila* gene chip result, the expression level of each subunit gene was compared between larval body wall and whole larvae RNA pools. As expected, GluR-IIA and GluR-IIB mRNA (Schuster et al., 1991; Petersen et al., 1997) were found to be enriched in body wall preparations. Another subunit annotated as CG4226, first referred to as GluR-IIC (Saitoe et al., 2001) and later as GluR-III (Marrus et al., 2004) was found to be enriched in body walls as well. A recent publication has shown that GluR-III null mutants die at late embryonic stages most likely due to a defect of glutamatergic transmission. In addition to these already described subunits with muscle expression, another glutamate receptor (annotated as CG18039) was found to be also enriched in body wall preparations.

Since the probe design of the *Drosophila* gene chip used here is based on an earlier version of the *Drosophila* genome annotation database, some genes might be omitted. To check if there are any newly annotated glutamate receptor genes which were not represented by the chip used, each of these selected glutamate receptor genes was blasted against the updated *Drosophila* genome annotation database (www.Flybase.com). Indeed, when blasting CG18039 coding sequence one gene annotated as CG31201 was found, which is strikingly similar to CG18039 (see below, Fig3-2). Interestingly, these two genes are located as direct neighbors within the genome, which is reminiscent of the organization of *GluR-IIA* and *GluR-IIB* (Petersen et al., 1997). Recently, it has been found that genes with similar expression pattern often cluster at certain regions of genome (Boutanaev et al., 2002; Roy et al., 2002), likely facilitating

transcriptional control of to be co-expressed genes. Intuitively, CG31201 might thus be expressed in a similar pattern with its neighbor CG18039.

Next, real time quantitative RT-PCR was applied to independently quantify the expression level of these candidate glutamate receptor genes. As shown in table3-2, real time quantitative PCR data were consistent with the observation from gene chip analysis. Moreover, CG31201 was shown to be enriched within body wall mRNA pool as well. From now on we will refer to the locus encoding subunit CG18039 as GluR-IIID and the locus encoding CG31201 as GluR-IIIE. These names are meant to reflect their muscle expression (see below) along with GluR-IIA, -IIB and -IIC/III.

	C _t (body wall)	% control	C _t (total larva)	% control	Body wall /total larva
<i>GluR-IIA</i> (CG6992)	26,7	15,4	28,3	4,4	3,5
<i>GluR-IIB</i> (CG7234)	28,2	5,6	29,5	1,9	3,0
<i>GluR-IIC/III</i> (CG4226)	26,4	18,7	28,9	3,1	6,3
<i>GluR-IIID</i> (CG18039)	25,5	35,5	27,0	10,5	3,4
<i>GluR-IIIE</i> (CG31201)	24,5	73,7	26,3	17,5	4,2
<i>tbp-1</i> (internal control)	23,8	100,0	23,8	100,0	1,0

Table 3-2 GluR-IIID and GluR-IIIE are enriched in larval body wall mRNA.

Abundances of glutamate receptor subunit transcripts estimated using real time PCR. The control transcript (proteasome subunit *tbp-1*) had the same abundance in body wall preps and whole larvae. The glutamate receptor subunits shown were enriched in body wall RNA when compared to whole larva RNA. The abundances of mRNAs are expressed as C_t values indicating the cycle number with which amplification exceeds detection threshold (C_t difference of one indicates a two-fold difference in abundance). All data are averages of three independent experiments where each sample was run two times in parallel.

3.2.2 Expression pattern of new ionotropic glutamate receptor genes

To further confirm the muscle expression of these new subunit genes, *in situ* hybridization on *Drosophila* embryos and larvae was performed. In fact, the mRNAs of GluR-IIID (Fig.3-1A-D) and GluR-IIIE (Fig.3-1E, F) are specifically expressed in somatic muscles of both *Drosophila* embryo (Fig.3-1A-C, E, F) and larva (Fig.3-1D). Expression of GluR-IIID (Fig.3-1C-D) and GluR-IIIE (Fig.3-1E) starts in somatic muscles of late stage 12 embryos (Fig.3-1A, E) and extends throughout embryonic and larval development (Fig.3-1D, F), a pattern very similar to that of GluR-IIA, -IIB and -IIC/III (data not shown; Petersen et al., 1997; Marrus et al., 2004). Intriguingly, in addition to the somatic muscle expression GluR-IIID is also abundantly present in cardiac precursor cells (Fig.3-1A, C), which was not found for the other muscle subunit genes.

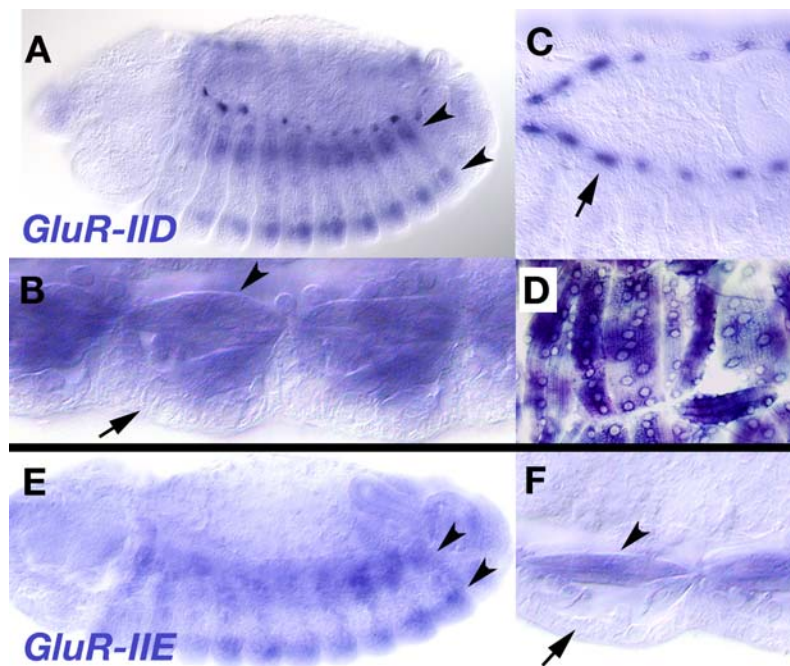


Figure 3-1. *GluR-IIID* and *GluR-IIIE*: novel glutamate receptor subunits with muscle specific expression

In situ hybridizations on *Drosophila* embryos (A-C, E,F) and larvae (D) for *GluRIID* (A-D) and *GluRIIE* mRNA (E,F). Both subunits are expressed specifically in presumptive somatic muscle cells (A, B, E, F, arrowheads) but are for example not found in the adjacent epidermis (A, B, F, arrows). Expression of *GluR-IIID* and *GluR-IIIE* transcript in the presumptive somatic muscles starts in late stage 12 and peaks at around stage 14 (A, E), to then persist during later embryogenesis (B: stage 16; E: stage 17) and larval development (D). *GluR-IIID* is also expressed within heart precursor cells (A and B, arrows).

3.2.3 GluR-IIID and GluR-IIIE represent a new type of muscle-expressed glutamate receptor subunit

In a 'simple' synaptic model system like the *Drosophila* NMJ the coexistence of so many distinct glutamate receptor subunits is somewhat unexpected. To get a closer view of the relationship among them, full-length cDNA clones of GluR-IIC, GluR-IIID and GluR-IIIE were obtained, the reading frames were verified by double strand sequencing and the deduced amino acid sequences compared. Clearly, these proteins encode all structural features typical in glutamate receptor subunits. Importantly, all putative transmembrane domains were found at similar positions (see Figure 3-2A). As previously noted (Marrus et al., 2004), the GluR-IIC/III sequence is closely related to GluR-IIA and IIB. GluR-IIID and GluR-IIIE are also highly related with each other (Fig. 3-2A, B). However, GluR-IIID and GluR-IIIE are distant from GluR-IIA, IIB and IIC/III group (Fig.3-2B). The fact is, GluR-IIID and GluR-IIIE are even slightly closer to human kainate receptor GluR6 than they are to the GluR-IIA, -IIB and -IIC/III group (see dendrogram in Fig.3-2B). Thus, in contrast to the GluR-IIA, -IIB, -IIC/III type, GluR-IIID and GluR-IIIE represent a new type of glutamate receptor subunits which is expressed in somatic *Drosophila* muscle. In a previous alignment entailing all identified ionotropic glutamate receptor subunits of the *Drosophila* genome, several other non-NMDA type subunits group in between GluR-IIID, -IIIE and GluR-IIA, -IIB, -IIC/III groups (Littleton and Ganetzky, 2000). Notably, all of the muscle glutamate receptor subunits (from GluR-IIA to -IIIE) have direct orthologs in *Drosophila Pseudoobscura* (data not shown), suggesting that the differentiation of the insect muscle-expressed glutamate receptor subunits into two structurally different groups might be conserved.

A

**GluR-IIC
GluR-IID
GluR-IIIE
GluR-6**



B

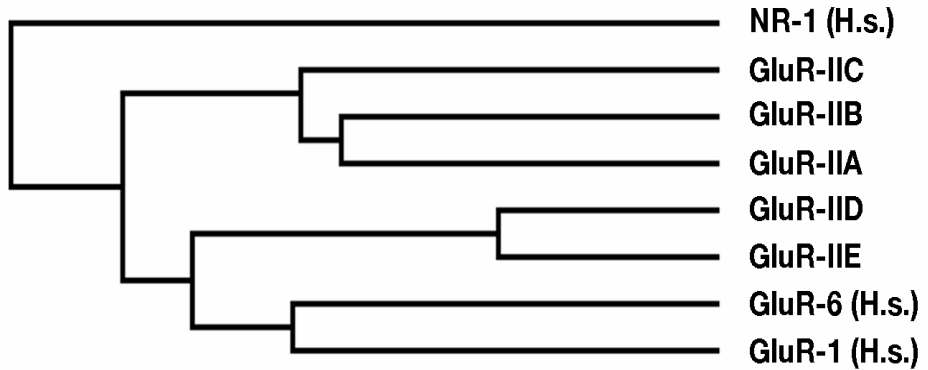


Figure 3-2 Sequence analysis of GluR-IID and GluR-IIIE

A, sequence alignment of predicted amino acid sequences of (from top to bottom) GluRIIC/III, GluR-IID, GluR-IIIE and human kainate receptor subunit GluR-6, similar amino acids are indicated by shaded boxes. Putative trans-membrane domains (TM1-4), the channel pore region and the c-terminal peptide of GluR-IID which was used for immunization are indicated as well.

B, dendrogram analysis comparing muscle expressed glutamate receptor subunits of *Drosophila*, together with AMPA receptor subunit GluR1, kainate receptor subunit GluR-6 and NMDA receptor subunit NR-1 (all Homo sapiens). Dendrogram was generated using MacVector software.

3.2.4 GluR-IIC, GluR-IID and GluR-IIIE are specifically localized at postsynaptic densities of neuromuscular synapses

To directly test the subcellular distribution of these novel glutamate receptor subunits, polyclonal antibodies were produced. In brief, rabbits were immunized with GluR-IIC/III C-terminus peptide (PRRSLDKSLDRTPKS) and GluR-IID C-terminus peptide (ESLKTDSEENMPVED) respectively. Collected sera were affinity-purified via their corresponding peptides. In western blotting assay, the antibodies against GluR-IIC/III and GluR-IID recognize a single band of about predicted 109 kD and 102 kD in wild type *Drosophila* embryo extracts respectively (Fig.3-3A, right lane). Cross reactivity of our sera between receptor subunits is not observed, since the antiserum against DGluR-IID can specifically recognize SF9-cells infected with recombinant virus containing GluR-IID cDNA but not the SF9-cells with expressing GluR-IIIE (Fig.3-3A, left lanes).

For immuno-fluorescence microscopy studies, previously a monoclonal antibody (8B4D2) against GluR-IIA has been characterized. In both late stage embryos and larvae 8B4D2 stains the postsynaptic membrane along the NMJ with a discrete dotted manner (Fethetherston et al., 2001; Packard et al., 2002). This antibody thus allows direct visualization of PSDs opposite the corresponding active zones. In the wild type larvae and embryos stained with our antibodies against GluR-IIC and GluR-IID, similar findings were obtained: localization of both GluR-IIC and GluR-IID is confined to typical punctae (Fig.3-3B, C, arrow heads) corresponding to individual postsynaptic densities (PSDs), which are surrounded by the HRP labels known to have perisynaptic expression (Sone et al., 2000). Moreover, these punctae are found directly opposite to the presynaptic Nc82 label. The Nc82 monoclonal antibody specifically recognizes the presynaptic active zone (Heimbeck et al., 1999; Wucherpfennig et al., 2003). Thus, it can be concluded that both GluR-IIC and GluR-IID are expressed within the PSD region of individual neuromuscular

synapses.

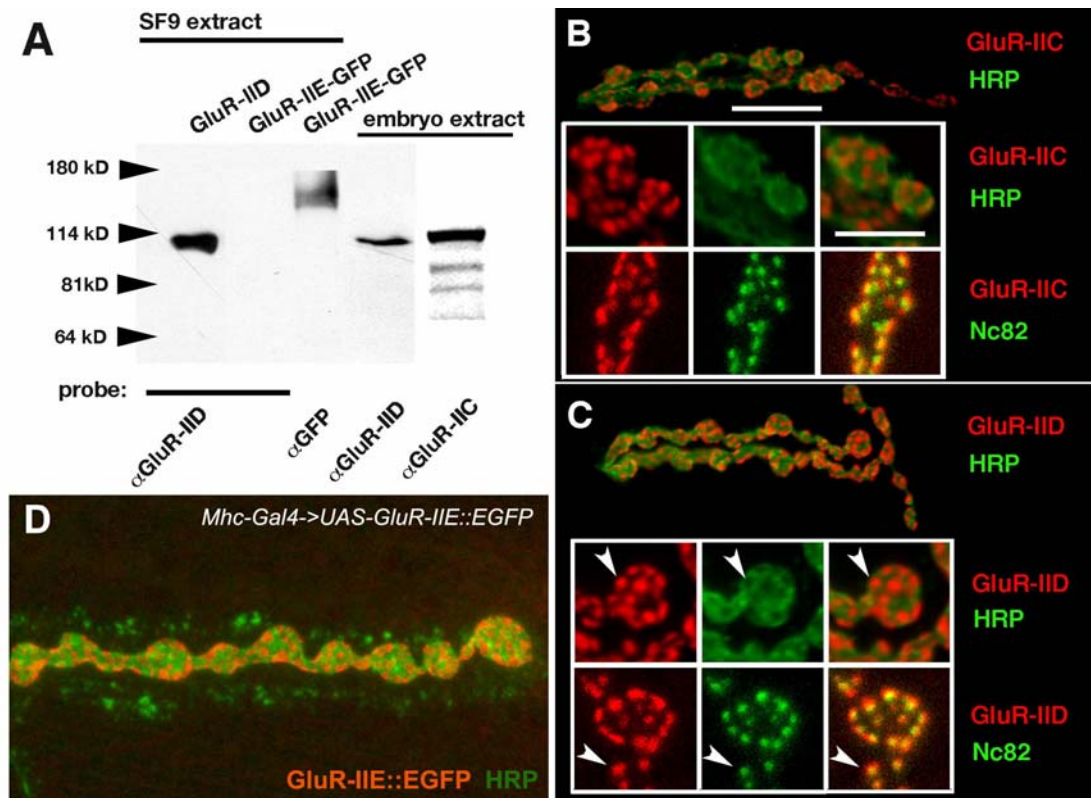


Fig.3-3 GluR-IIID and GluR-IIIE are expressed within postsynaptic densities

A: western blot analysis: the anti-IIID peptide antibody recognizes SF9-cell expressed GluR-IIID and endogenous GluR-IIID from *Drosophila* embryo extract. It does not cross react with the related GluR-IIIE protein, which is SF9-cell expressed as a GFP fusion and is recognized using anti-GFP antibody with the predicted size of about 145 kD. GluR-IIIC/III is recognized with our peptide antibody in *Drosophila* embryo extract with predicted size as well.

B-C, shown are epifluorescence pictures (upper two panels in B and C) and confocal pictures (lower panels in B and C) of receptor subunits GluR-IIIC/III (B, red) and GluR-IIID (C, red) together with the perisynaptic marker HRP (upper panels in B and C, green) or active zone marker Nc82 (lower panels in B and C, green), scale bars: 8 and 4 μ m.

D, confocal picture of GluR-IIIE::EGFP (red) together with perisynaptic marker HRP (green).

Several GluR-IIIE-specific peptides were used to immunize rabbits as well. Unfortunately, specific antibodies could not be obtained, mainly due to the fact that the GluR-IIIE amino acid sequence is closely related to GluR-IIID. In fact, it is hard to find a GluR-IIIE specific peptide sequence which would be proper for

immunization. To overcome this difficulty, the enhanced green fluorescent protein (EGFP) reading frame was inserted into the near C-terminus GluR-IIIE to generate an autofluorescent fusion protein. Fusion of EGFP into the same position of mammalian GluR2 has been previously shown not to interfere with glutamate receptor assembly and function (Sheridan et al., 2002). Indeed, upon overexpressing this GluR-IIIE::EGFP in larval muscle (driven by *MHC-Gal4*), an antibody directed against EGFP strongly labeled the postsynaptic density region (Fig3-3D). This result makes it very likely that the endogenous GluR-IIIE protein localizes to the PSD region as well.

3.3 GluR-IID and GluR-IIIE are essential for viability

To genetically investigate what roles GluR-IID and GluR-IIIE play in NMJ glutamatergic transmission, null mutants for each of the two genes were required. For *Drosophila* molecular genetics, transposon mediated mutagenesis often is an efficient way of knocking out a candidate gene function. In the presence of transposase activity, integrated transposons can be remobilized and randomly jump into other chromosomal locations. Upon remobilization, apart from the transposon sequence as well often genomic sequences flanking the insertion site of the mobilized transposon will be eliminated as well. Thus, transposon mapping in the near of candidate loci can be used to produce gene-specific deletions. Here, this strategy was used to obtain mutants of *GluR-IID* and *GluR-IIIE*.

From a collection of *piggyBac* transposon lines which covers 53% of all loci annotated for *Drosophila* (Thibault et al., 2004), one line (pBac{RB}e01443) was described to have an insertion in the *GluR-IID* locus. This line was obtained and genomic PCR was performed using one primer corresponding to the flanking region the proposed insertion site and another primer corresponding to the end of the *piggyBac* transposon. The resulting PCR

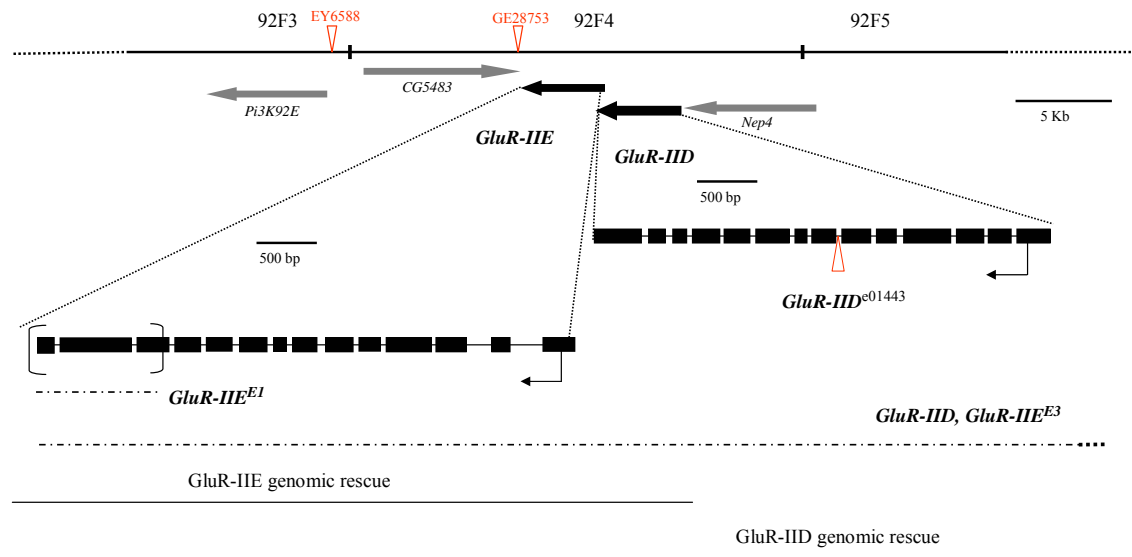


Figure 3-4 Genetic analysis of *GluR-IID* and *GluR-II*

GluR-IID and *GluR-II* map to position 92F on chromosome III. Exon-intron structure of both loci is shown, exons are boxed. The null allele *GluR-IID*^{e01443} is based on a piggyBac transposon insertion within the open reading frame of the *GluR-IID* locus. Null allele *GluR-II*^{E1} lacks c-terminal sequence of the protein including the last transmembrane domain of the receptor subunit. *GluR-II*^{E3} deletes at least *GluR-II* and *GluR-IID* alleles and thus is used as deficiency allele. The genomic stretches used for genomic rescue constructs are shown below.

product was purified and subjected to sequencing. It was found that in fact in this line the transposon has integrated directly into intron 6 of *DGluR-IID* (Fig.3-4). This could well interfere with normal transcript splicing and hence the generation of GluRIID protein. Interestingly, this line is embryonic lethal in homozygous condition. We from now on refer to this allele as *GluR-IID*^{e01443}.

For *GluR-IIE*, imprecise excision mutagenesis screening was performed using transposon line EY6588 (<http://flypush.imgen.bcm.tmc.edu/pscreen/>) and later GE28753 (<http://www.genexel.com>) whose insertion sites are located 14Kb and 150 bp downstream of the 3' end of *GluR-IIE* transcript, respectively (Fig.3-4). From the screening, about 30 imprecise excision events (Fig.3-4) were recovered, genomic PCR with a series of primer pairs corresponding to the flanking region of GE28753 insertion position were utilized to recover the deleted region in each line. Among them, a line called *GluR-IIE*^{E1} was found to have the genomic sequence encoding the C-terminal part of GluR-IIE including the last transmembrane domain deleted. Importantly however, the *GluR-IIE*^{E1} deletion does not extend into neighboring loci. Similar to *GluR-IID*^{e01443}, *GluR-IIE*^{E1} is also embryonic lethal in homozygous condition. In addition, no GluR-IID protein could be observed at the neuromuscular synapses of either *GluR-IID*^{e01443} or *GluR-IIE*^{E1} homozygous embryos (see 3.4.1 for details). *GluR-IID*^{e01443} and *GluR-IIE*^{E1} are also embryonic lethal over another independent excision allele *GluR-IID&IIE*^{E3} (Fig.3-4), a larger deficiency which deletes both *GluR-IID* and *GluR-IIE* genomic sequences. However, *GluR-IID*^{e01443} is fully viable when crossed over *GluR-IIE*^{E1}. Both *GluR-IID*^{e01443} and *GluR-IIE*^{E1} are fully rescued by transgenic addition of one copy of genomic *GluR-IID* or *GluR-IIE*, respectively; however, neither the *GluR-IID* mutant nor the *GluR-IIE* mutant can be rescued by the respective other transgene. Thus, several lines of evidence (here and 3.4.1) suggest that *GluR-IID*^{e01443} and *GluR-IIE*^{E1} represent specific null mutant alleles for *GluR-IID* and *GluR-IIE*, respectively. While the neighboring loci *GluR-IID* and *GluR-IIE* encode very similar proteins with largely overlapping expression pattern, both of them are essential for embryonic viability.

3.4 Reciprocal dependence of all essential glutamate receptor subunits for synaptic expression and function

3.4.1 Complete synaptic absence of all other glutamate receptor subunits after knockout of any essential subunit genes

Homozygous *GluR-IID*^{e01443} and *GluR-IIE*^{E1} embryos were subjected to further inspection. These embryos, while apparently developing normally, show no coordinated movements and do not hatch. The same phenotype is also observed previously within *GluR-IIC/III* single or *GluR-IIA&IIB* double null mutant embryos. This phenotype was interpreted as failure of neuromuscular neurotransmission due to the absence of functional postsynaptic glutamate receptors (Petersen et al., 1997; Marrus et al., 2004). Consistent with a role in synaptic transmission, *GluR-IID* and *GluR-IIE* mRNA expression starts within embryonic muscles well before the onset of neurotransmission (Fig.3-1), just like the cases of *GluR-IIA*, *-IIB* and *-IIC* (Petersen et al., 1997; Marrus et al., 2004).

In mammals, ionotropic glutamate receptors appear to be composed of rather closely related subunits (Wenthold et al., 1996; Mulle et al., 2000). Hence, whether the rather similar *GluR-IID* and *GluR-IIE* subunits directly form glutamate receptors was investigated via immuno-fluorescence microscopy. In principle, if the formation of a certain type of glutamate receptor fails, the synaptic localization of its constituent receptor subunits must be affected. In wild type late stage embryos, *GluR-IID* proteins stably localize at the PSD region of all NMJ synapses (Fig.3-5B, wild type). In *GluR-IIE*^{E1} embryos, neuromuscular contacts still form, as shown by staining against anti-HRP and Nc82 antibodies (Fig.3-5A, blue and green channel). However, *GluR-IID* is completely absent from *GluR-IIE*^{E1} embryonic NMJs (Fig.3-5B). This finding suggests that *GluR-IIE* and *GluR-IID* might join into a common glutamate receptor which in turn is essential for synaptic neurotransmission at the embryonic NMJ.

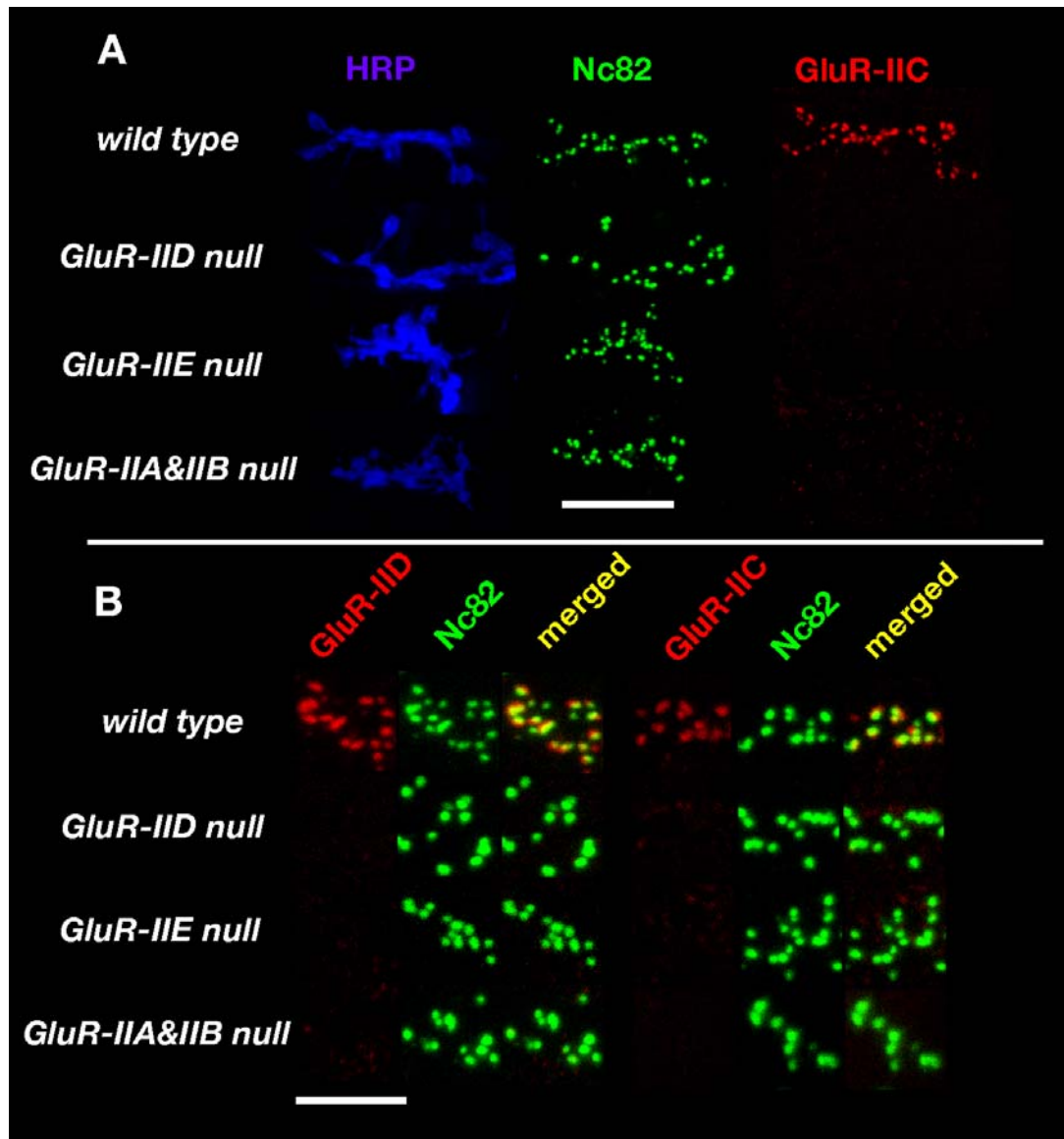


Figure 3-5 Interdependence between glutamate receptor subunits for NMJ expression

A, Confocal images of NMJs in wild-type, *GluR-IID* null, *GluR-IIE* null or *GluR-IIA&IIB* double null mutant embryos (20-22 hrs old) stained with antibodies against *GluR-IIC/III* (red), Nc82 (green) and HRP (blue). Nc82 staining indicates differentiation of presynaptic release sites at the mutant NMJs. Synaptic expression of all glutamate receptor subunits fails at the mutant NMJs. Scale bar: 10 μ m

B, Higher magnifications of confocal stainings similar as in A. Stainings of either *GluR-IID* (left panels) or *GluR-IIC/III* (right panels) are shown together with Nc82. Scale bar: 5 μ m.

Based on the analysis of *GluR-IIC/III* and *GluRII-A* hypomorphic larvae, it

has been suggested that GluR-IIC/III is an obligatory subunit, which associates with either GluR-IIA or GluR-IIB to form functionally distinct glutamate receptors (Marrus et al., 2004). This idea was tested again but **directly** by immunostaining *GluRII-A&IIB* double mutant embryos. Consistent with Marrus et al., GluR-IIC/III label is completely absent from NMJs of *GluR-IIA&IIB* null mutant embryos (Fig.3-5A and B). Thus GluR-IIA together with GluR-IIB can be considered a “synthetic essential subunit”. In principle, the two “groups” of subunits (GluR-IID, -IIE versus -IIA, -IIB, -IIC/III) could be independently essential for embryonic neurotransmission. Alternatively, synaptic localization and thus receptor function could be interdependent between both groups. To distinguish these two possibilities, it was first checked whether the synaptic localization of the GluRIIC/III glutamate receptor subunit is dependent on the presence of GluR-IID and GluR-IIE. Clearly, no synaptic localization of GluR-IIC/III can be found in either *GluR-IID* or *GluR-IIE* null mutant embryos (Fig.3-5A and B). *Vice versa*, the synaptic expression of GluR-IID was absent from *GluR-IIA&IIB* double null mutant embryos (Fig. 5B). Thus, at the embryonic NMJ, the synaptic expression of all essential glutamate receptor subunits is absolutely interdependent. The easiest explanation for these data is that at the *Drosophila* NMJ the glutamate receptor is formed by four different essential glutamate receptor subunits: GluR-IIC, GluR-IID, and GluR-IIE together with either GluR-IIA or GluR-IIB.

3.4.2 Genetically depriving the expression level of any single essential glutamate receptor subunit results into corresponding reduction of all other subunits

If the glutamate receptor is indeed assembled from four different subunits, partially suppressing the level of any single such subunit should interfere with the synaptic expression of the other essential subunits and the overall glutamate receptor formation. To test this, several independent experiments have been performed.

First, the expression of GluR-IIIE was knocked down in vivo via transgenic RNA interference technique (Kennerdell and Carthew, 2000). When RNA interference against *GluR-IIIE* was conducted in a muscle-specific manner, the *GluR-IIIE* transcript level was knocked down to about 20% of wild type level while the transcription level of all other muscle subunit genes remained unchanged (not shown), indicating the highly selective RNA degradation mediated by RNA interference. In contrast to the *GluR-IIIE* null mutants, these animals do not die at embryonic stage but instead develop into mature larvae and adult flies. So the effects on the distribution of other subunits in 3rd larvae were examined. Significantly, all of the other known subunits (GluR-IIA, GluR-IIB, GluR-IIC/III and GluR-IID) were greatly reduced at NMJ when the RNA interference was driven in muscles (using *G14-Gal4* or *MHC-Gal4*), while

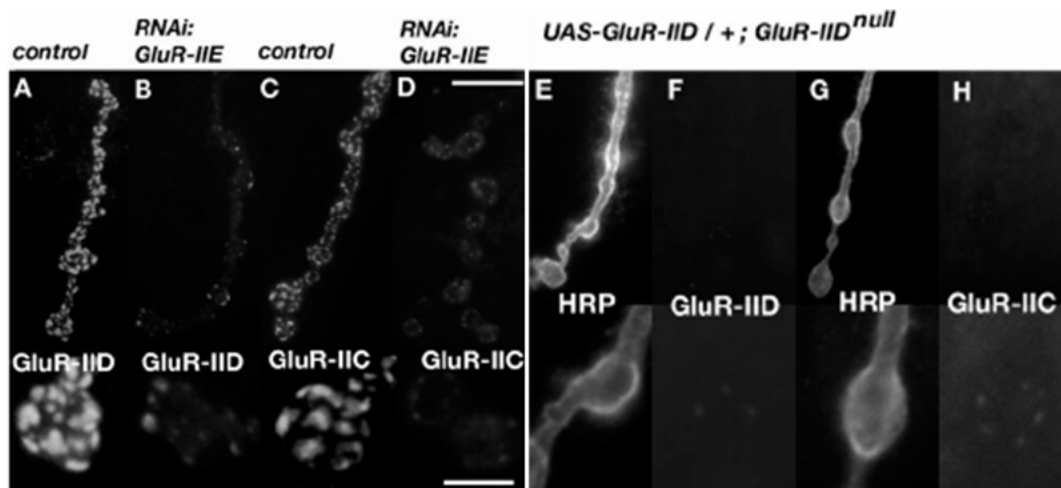


Figure 3-6 A partial reduction of either GluR-IIIE or GluR-IID provokes a significant reduction of all glutamate receptor subunits at the NMJ

(A-D) Larval NMJs (muscle 4, abdominal segment 2) stained for GluR-IID (A, B) or GluR-IIC/III (C, D) in control larvae (*G14-gal4/+*, A and C) or larvae experiencing muscle specific RNA interference against GluR-IIIE (*G14-gal4/+; UAS-GluR-IIIE-RNAi*, B and D). Suppression of *GluR-IIIE* leads also to a reduction in the NMJ expression of GluR-IIC/III and GluR-IID. Lower pictures represent higher magnifications.

(E-H) Shown are NMJs (muscle 4, abdominal segment 2) of *GluR-IID* null mutant larvae rescued with a single copy of *UAS-GluR-IID* (*UAS-GluR-IID/+; GluR-IID^{e01443}/GluR-IID&IIE^{E3}*). Only trace amounts of GluR-IID (F) and GluR-IIC (H) are expressed at the NMJ, HRP stainings (E, G) are added to visualize the NMJ. Non-linear contrasting had to be used to make the trace amounts of GluR-IID (F) and GluR-IIC (H) visible. Scale bar in upper panel 7,5 μm , in lower panel showing higher magnification 2,5 μm .

there is no obvious effects when driving the expression of RNA interference construct in the central nervous system (using *ELAV-Gal4*) (Fig.3-6B, D; data not shown)., which further verify that GluR-IIE functions specifically in somatic muscles and intrinsically associates with other subunits.

For a second experiment, it was found that minimal amounts of GluR-IID (produced by the “leaky” expression from pure *UAS-cDNA* transgenes) can already rescue *GluR-IID* null mutant embryos into mature larvae (Fig.3-6E-H). In these rescued larvae, both GluR-IID and all other glutamate receptor subunits were strongly reduced at the NMJs (Fig.3-6H). Re-expressing GluR-IID to **normal** level by using the muscle specific *Gal4*-driver line *Mhc-Gal4* at 18°C restored the synaptic localization of GluR-IID and all other glutamate receptor subunits (not shown; overexpression of GluR-IID cDNA in both wild type and *GluR-IID* null background at 25°C resulted into significant reduction of synaptic glutamate receptor level with abnormal accumulation of GluR-IID proteins within the ER). Thus, the levels of GluR-IID and GluR-IIE within the muscles directly control the overall amount of glutamate receptors that localize at the NMJ.

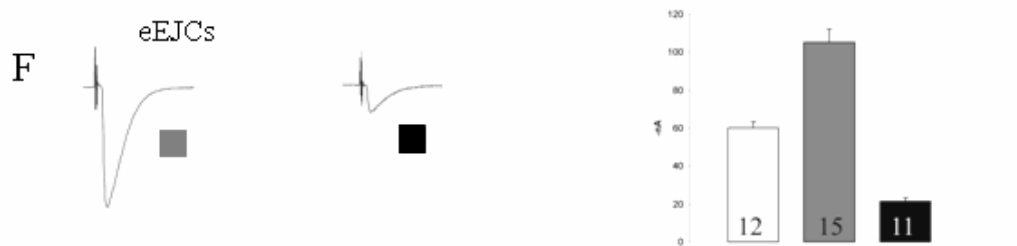
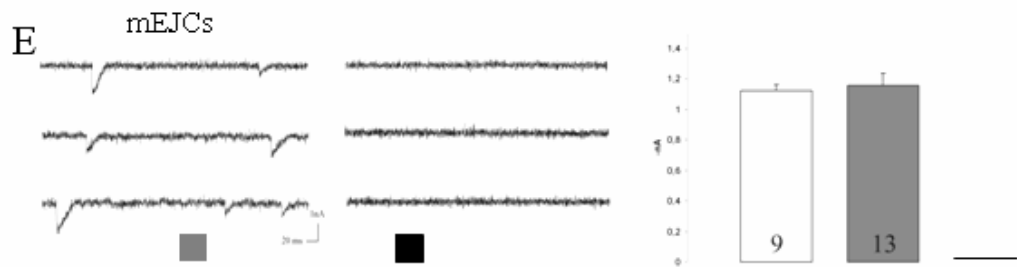
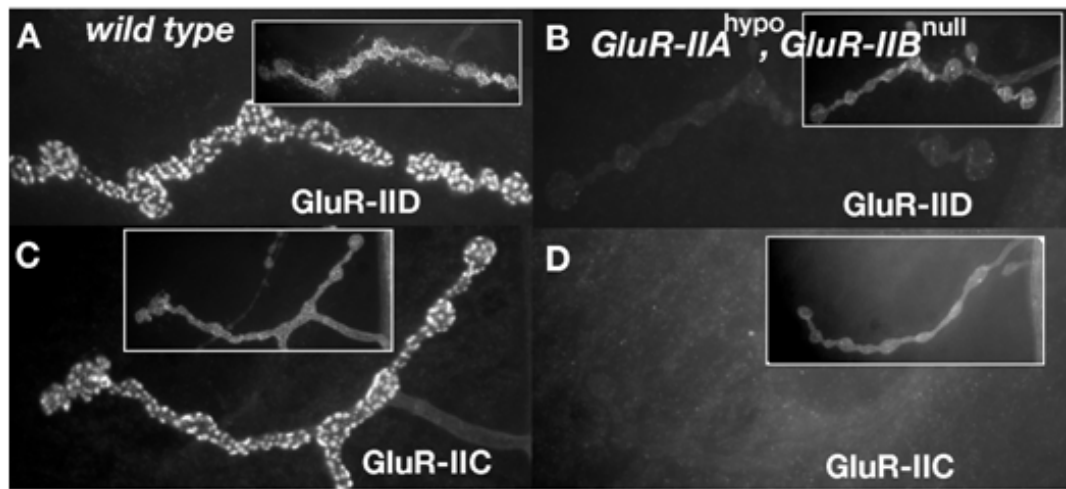
The next question addressed is, whether *vice versa* the amounts of muscle GluR-IIA, -IIB and -IIC/III can control synaptic level of GluR-IID and -IIE. To this end, a genetic situation in which *GluRIIB* was fully absent and simultaneously *GluR-IIA* was suppressed to dramatically low level (*GluRIIA^{hypo}*, *GluR-IIB^{null}*, see 2.2.2.1) was used. Previously it has been proposed that local postsynaptic translation plays important roles in controlling the growth and transmission efficacy of synapses at *Drosophila* NMJ. *GluR-IIA* appears might be a substrate under subsynaptic translational control (Sigrist et al., 2000). Since translational control elements often localize within the 3'UTR region of a gene, transgenic flies expressing *GluR-IIA* lacking most 3'UTR were produced and tested for their ability to rescue the *GluR-IIA&IIB* double null mutants, which is

embryonic lethal (Diantonio et al., 1999). Among several independent transgenic lines tested, only one of them could rescue the embryonic lethality with low rate and the rescued larvae were clearly paralyzed. Real-time quantitative PCR assay showed that the *GluR-IIA* message level was below 5% of endogenous level. In accordance with the low message level, the GluR-IIA protein was hardly detectable at the larval NMJ (not shown). Notably, the level of both GluR-IIC/III and GluR-IID were drastically low (Fig.3-7B, D). Collectively, all the above data suggest all essential glutamate receptor subunits together controls receptor formation and proper synaptic localization. Furthermore, this rule seems true for both initial formation and further development of NMJs, where many new synapses get added continuously (Schuster et al., 1996; Gramates and Budnik, 1999).

Fig.3-7 Minimal mounts of GluR-IIA and no- IIB: expression of all glutamate receptor subunits and postsynaptic sensitivity are strongly reduced

(A-D) Shown are 3rd instar larval NMJs (muscle 4, abdominal segment 2) stained for GluR-IID (A, B) or GluR-IIC/III (C, D) in wild type controls (A, C) or in animals having only about 5% GluR-IIA and no GluR-IIB (GluR-IIA^{hypo}, GluR-IIB^{null}, see Material and Methods). NMJ morphology in HRP labeling is shown in insets to allow NMJ visualization independent of receptor label. In GluR-IIA^{hypo}, GluR-IIB^{null} larvae, the synaptic localization of both GluR-IID and GluR-IIC/III is strongly reduced. Apparent differences in between residual GluR-IID and GluR-IIC/III are likely due to slightly different sensitivity of our antibodies.

E-G, Postsynaptic sensitivity is dramatically reduced at larval NMJs of GluR-IIA^{hypo},GluR-IIB^{null} larvae. E, F, Two-electrode voltage-clamp recordings of eEJCs and mEJCs from muscle 6 of abdominal segment A2 and A3. Representative traces of mEJC recordings (E) and average traces of 10 consecutively recorded eEJCs (F) of the indicated genotypes are shown. The mean amplitudes of mEJCs (white bars) are indistinguishable between wild type and GluR-IIA&IIB double mutant larvae rescued with a complete genomic GluR-IIA transgene (exact genotype: *df(2L)clh4, P[GluR-IIAΔ3'UTR] / GluR-IIA&BSP22*). In all muscle cells of GluR-IIA^{hypo},GluR-IIB^{null} larvae, no signs of mEJCs could be recorded despite extensive and sensitive recording. Evoked responses (F) are also dramatically reduced in GluR-IIA^{hypo},GluR-IIB^{null} larvae compared to both control groups. The increase in evoked response in animals rescued with wild type GluR-IIA (and thus without expressing of GluR-IIB) when compared to wild type has been described before (Petersen et al., 1997; DiAntonio et al., 1999). G, Paired pulses (stimulation interval ms) provoke slight facilitation in the controls but depression in GluR-IIA^{hypo},GluR-IIB^{-/-} larvae. Data are derived from the indicated number of cells (number in the column) and represent means ±SEM.



3.4.3 Depriving synaptic glutamate receptor subunits results into dramatic weakness of postsynaptic activity

To test whether the physiological function of glutamate receptor correlates well with its presence at synapse reflected from the above morphological data, electrophysiological analysis is highly necessary. Among the different genetic situations which partially deprive certain glutamate receptor subunits in embryos and larvae, the *GluRIIA^{hypo}*, *GluR-IIB^{null}* larvae maintain the lowest overall level of glutamate receptors (Fig.3-7 B, D) and display clear signs of paralysis. Thus *GluRIIA^{hypo}*, *GluR-IIB^{null}* larvae were subjected to two-electrode-voltage-clamp recordings in collaboration with Robert Kittle (Fig.3-7 E, F). As expected, compared to wild type conditions, spontaneous miniature junctional currents (mEJCs) in these animals were below the detection limit indicating an extreme drop of postsynaptic glutamate receptor function. Accordingly, evoked currents (eEJCs) were also significantly low (*wild type*: 61 nA, n=12, *GluRIIA^{hypo}*, *GluR-IIB^{null}*: 21 nA, n=11; $p < 0.00005$, Mann-Whitney, two-sided non-parametric test).

In conclusion, strongly reducing the expression of a single ‘essential’ glutamate receptor subunit is sufficient in severely downregulating the overall level of functional glutamate receptors at the NMJ, which in turn results into weakening of postsynaptic activity in response to neurotransmitter release.

3.5 Structural role of ionotropic glutamate receptor during pre- and postsynaptic differentiation of neuromuscular synapse

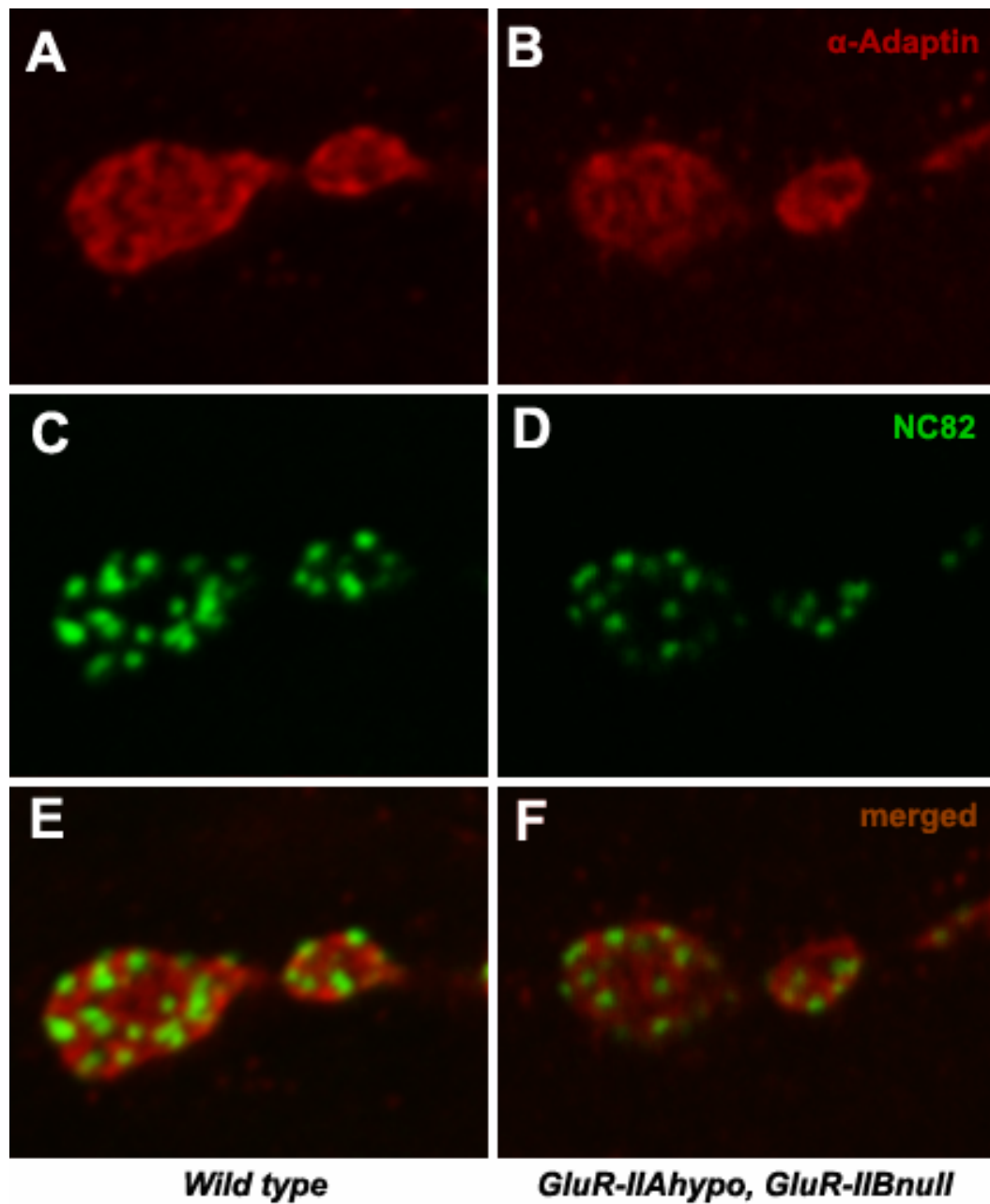
3.5.1 Normal differentiation of presynaptic transmitter release machinery at glutamate receptor deprived synapse

As shown in chapter 3.4, *GluRIIA^{hypo}*, *GluR-IIB^{null}* larval junctions produce evoked currents of about one third of that of wild type junctions. Even more drastically, the spontaneous currents are hardly detectable. We considered the fact that evoked responses appeared less affected than spontaneous responses in

GluRIIA^{hypo}, *GluR-IIB^{null}* larvae as indication of normal or even increased presynaptic transmitter vesicle release as compensation of severe postsynaptic defects. Consistent with the concomitant increase in presynaptic vesicle release, paired pulse stimulation of *GluRIIA^{hypo}*, *GluR-IIB^{null}* NMJ leads to depression of evoked currents while as for wild type controls the currents remain slightly increased in the same condition. The organization of presynaptic release machinery was further characterized morphologically. The active zone is the region of the presynaptic plasma membrane where synaptic vesicles dock, fuse, and release the neurotransmitters (Shapira et al., 2003). Monoclonal antibody NC82 was shown to specifically label the Active zones of synapses of *Drosophila* NMJ (Wucherpfennig et al., 2003) and central synapses (Heimbeck et al., 1999). In *GluRIIA^{hypo}*, *GluR-IIB^{null}* larvae, nc82 labels are clearly present at NMJ with both density and individual size comparable to wild type controls (Fig.3-8 C, D; Fig.3-9 D-E). α -Adaptin is essential for presynaptic endocytosis/vesicle retrieval (Gonzalez-Gaitan and Jackle, 1997) and is restricted to the presynaptic membrane, forming a network-like structure that surrounds the active zones (Gonzalez-Gaitan and Jackle, 1997) (Fig. 3-8 A-C). In *GluRIIA^{hypo}*, *GluR-IIB^{null}* larvae, subcellular distribution of α -Adaptin is not apparently distinct with that of wild type controls (Fig.3-8 A, B), suggesting that the differentiation of presynaptic release apparatus is not affected by depriving postsynaptic glutamate receptor.

Fig. 3-8 Normal organization of presynaptic neurotransmitter release machinery components at glutamate receptor deprived synapses

NMJs double-labeled with the antibodies against presynaptic component α -Adaptin (Gonzalez-Gaintan M et al., 1997; A-B) and Nc82 antibody recognizing an active zone epitope (Wucherpfennig et al., 2003, Heimbeck et al., 1999; C-D). In wild type animals, α -Adaptin is restricted to the presynaptic membrane, forming a network-like structure that surrounds the active zones represented by Nc82 spots (A, C, E). In *GluRIIA^{hypo}*, *GluRIIB^{-/-}* larvae, both Nc82 and α -Adaptin spots appear no different from wild type control (B, D, F).



3.5.2 Defective assembly of PSD specialization at glutamate receptor deprived but not presynaptic neurotransmission activity deprived synapse

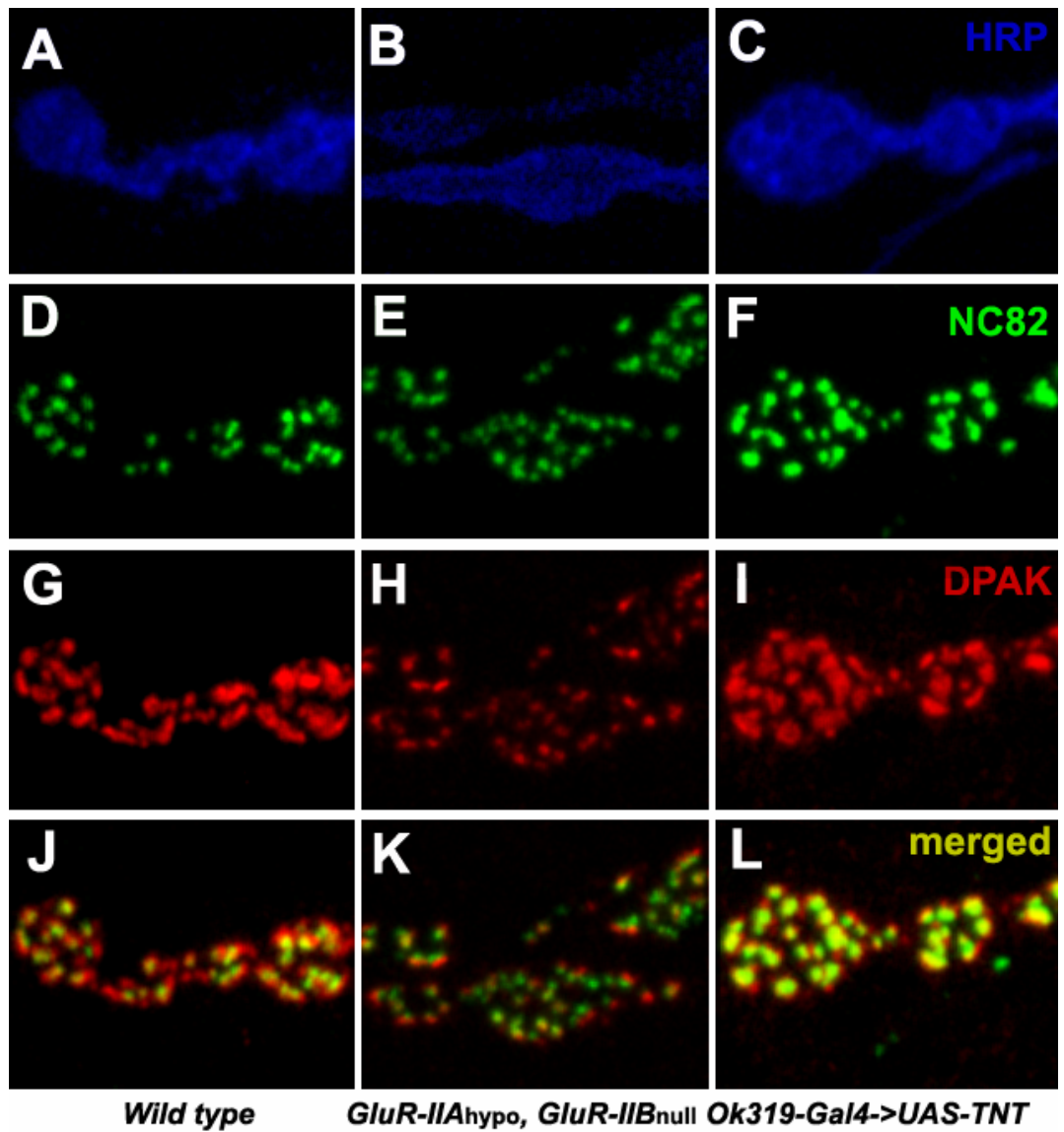
The differentiation of postsynaptic apparatus was also analyzed in *GluRIIA^{hypo}*, *GluR-IIB^{null}* larvae. So far, only a few PSD components have been identified and characterized at *Drosophila* NMJ (Sone et al., 2000; Wan et al.,

2000; Parnas et al., 2001). PAKs are a family of serine/threonine kinases that serve as targets for the small GTP-binding proteins Cdc42 and Rac, they are implicated in modulating the cytoskeleton organization (Bagrodia and Cerione, 1999). In *Drosophila*, dPak has been shown to specifically localize at the PSD of neuromuscular synapse at both immunofluorescence microscopic and immuno-EM level (Sone et al., 2000; Wan et al., 2000). In *dpak* mutants, the levels of DLG and GluRIIA at the synapse are reduced and the SSR folding is also disrupted (Parnas et al., 2001; Albin and Davis, 2004) In wild type larvae, dPAK antibodies labeled the well defined patches with approximately even distribution over the surface of bouton, (Fig. 3-9), and as expected NC82 perfectly colocalized with dPAK staining (Fig.3-9). In *GluRIIA^{hypo}*, *GluRIIB^{null}* bouton, however, the dPAK staining displayed apparently lower density, with the size of individual spots much more diverse---from huge irregular aggregates to tiny dots, and often, at some bouton areas the dPAK even did not aggregate at all but just ‘wrap’ the bouton like cloud, (Fig.3-9 , arrow).

The above data suggest that, when glutamate receptors are deprived from synapse other constitutive components of postsynaptic specialization can not be assembled efficiently. In principle, these defects could be either due to the absence of glutamate receptor *per se* or lack of glutamate mediated transmission activity. To distinguish these possibilities, several genetic situations in which the NMJ transmission was either strongly reduced (survival to larval stage) or

Fig.3-9 Defective PSD assembly at glutamate receptor deprived but not transmission deprived synapses

NMJs triple-labeled with the Nc82 antibody recognizing an active zone epitope (Wucherpfennig et al., 2003, Heimbeck et al., 1999; D-F), antibodies against PSD marker DPAK (Sone et al., 2000; G-I) and HRP (A-C). In wild type animals, Nc82 spots localize at presynaptically juxtaposed to postsynaptic DPAK spots (J). In *GluRIIA^{hypo}*, *GluRIIB^{-/-}* larvae, Nc82 spots localize normally (E), however, DPAK spots display significantly lower density and more variable individual size (H). In *OK319-Gal4->UAS-TNT* larvae, both Nc82 and DPAK spots appear no different from wild type control (F, I, L).



completely suppressed (lethal at late embryonic stage) were analyzed for postsynaptic assembly. Targeted expression of tetanus toxin light chain (TNT) in *Drosophila* neurons completely eliminates evoked, but not spontaneous synaptic vesicle release (Sweeney et al., 1995). When using the motor neuron driver *ok319-Gal4* to drive TNT expression, low number of animals can survive to 3rd instar larval stage (this survival is likely due to the mosaic property of the driver, Cahir O’Kane, personal communication). Surviving larvae were very strongly paralyzed, much stronger than *GluRIIA^{hypo}*, *GluR-IIB^{null}* larvae. However, the distribution of neither postsynaptic components dPAK nor glutamate receptor

show any discernible defects in all the NMJs checked, in contrast they both colocalize well with active zone shown by NC82 staining (Fig.3-9 F, I).

Since the expression of tetanus toxin does not fully eliminate spontaneous synaptic vesicle release (Sweeney et al., 1995), it might be argued that in the above *ok319-Gal4* driven situation remaining activity (especially spontaneous activity) could sufficiently induce the assembly of postsynaptic specializations at normal level. Indeed, recently a tight link between spontaneous vesicle exocytosis and glutamate receptor clustering during *Drosophila* embryonic development has been reported (Saitoe et al., 2001). It should be noted, however, that this report is clearly controversial to some other reports (Broadie et al., 1995; Featherstone et al., 2001). It has been proved previously that, in either null mutants of syntaxin or temperature sensitive allele of dynamin (*shi^{ts1}*) reared at nonpermissive temperature, both spontaneous and evoked vesicle exocytosis and hence synaptic transmission are completely eliminated (Broadie et al., 1995). Using these ‘cleaner’ conditions, the immuno-fluorescence microscopic analysis was performed with our antibodies against GluR-IIC and GluR-IID. In contrast to the findings of Saitoe M et al but consistent with those of Featherstone et al, the glutamate receptor localization within individual PSDs is essentially unaffected as seen in GluR-IIC and GluR-IID staining (Fig.3-10). Moreover, in these animals DPAK proteins also cluster at normal size at the PSD region as evidenced by colocalization with NC82 labels (Fig3-10). Therefore, it is the glutamate receptor per se but not synaptic transmission activity essential for the postsynaptic specialization (including glutamate receptor field) assembly.

Besides the main finding described above, another interesting phenomena found is found. At the NMJs of glutamate receptor deprived larvae (*GluRIIA^{hypo}*, *GluR-IIB^{null}*), often postsynaptic dPAK label was not opposed by presynaptic active zone marker (identified via NC82 staining) (Fig.3-9). One explanation is that these free NC82 labels might represent new synapse growth sites. However,

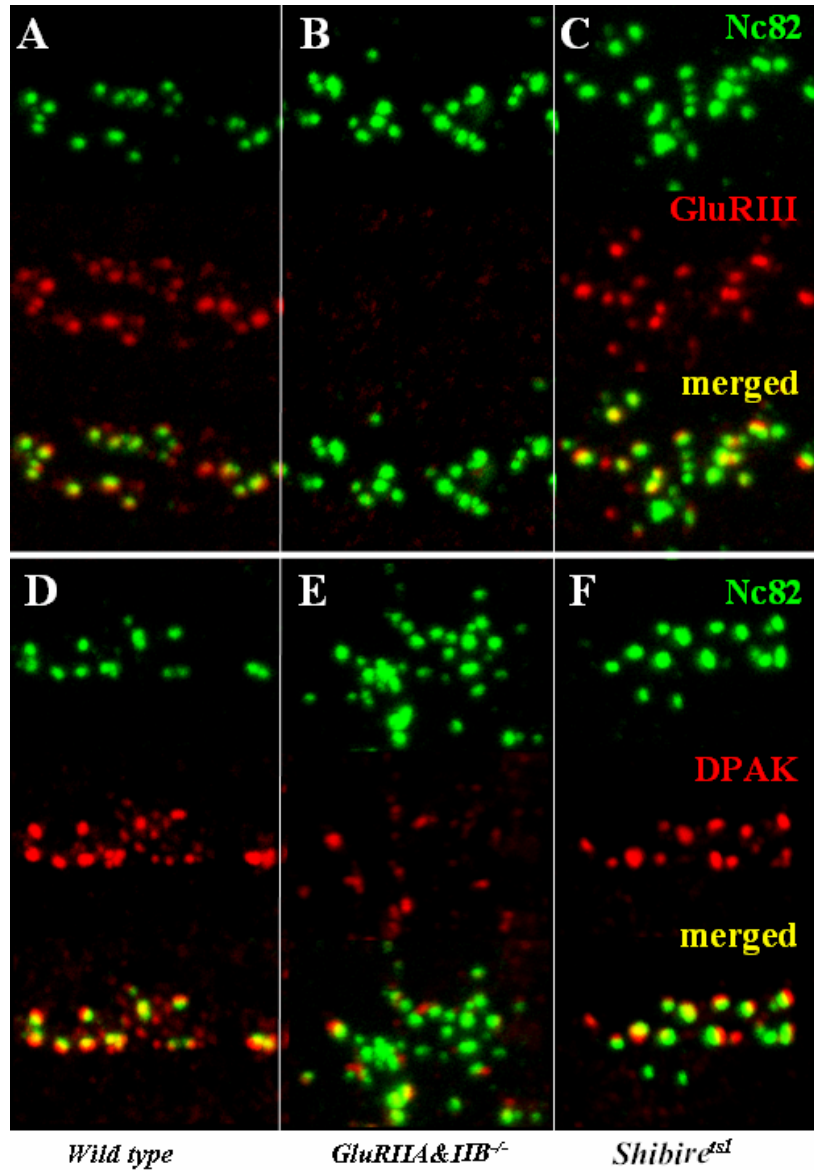
this is quite unlikely since in wild type NMJs stained with same antibodies, the free NC82 labels without aligned dPAK patches were very rarely found (Fig.3-9). Intriguingly, free dPAK labels could be stably detected in wide type NMJs, and in most cases such free dPAK patches are small and localize at the tips of junctions or the linkage regions between boutons, which likely represent the potential growth sites of new synapses. Thus, these free dPAK labels might reflect the precursors of new synapses, which implicates that, in contrast to the finding in synapses of cultured hippocampal neurons, at *Drosophila* NMJ the postsynaptic assembly might precede presynaptic assembly. In *GluRIIA^{hypo}*, *GluR-IIB^{null}* NMJs, the precise coordination of pre- and postsynaptic differentiation is strongly affected. However, it is unlikely that this coordination defect is merely due to absence of glutamate receptor per se, since in embryos with complete loss of presynaptic transmitter release, although individual PSDs are assembled rather normally, there also exist free active zones (Fig.3-10 F). Because the glutamate receptor null mutants lack both glutamate receptor and the concomitant transmission activity, it remains to be further addressed whether the precise coordination of pre- and postsynaptic differentiation is activity-dependant.

Fig. 3-10 Glutamate receptor *per se* but not presynaptic vesicle release are important for proper synapse formation at embryo NMJ

Confocal microscopy on embryonic NMJs (muscle 6 and 7), stained with the synaptic markers in wild type (A-D), in *GluR-IIA&IIB^{-/-}* double mutant embryos (B, E) and in *shibire* temperature sensitive mutant (*shi^{ts1}*) embryos reared at nonpermissive temperature (C, F).

A-C, Embryonic NMJs double labeled with active zone recognizing antibody Nc82, glutamate receptor subunits GluR-IIC/ III. In situation with defective presynaptic release (C), postsynaptic glutamate receptor fields appear identical as in wild type control. As expected, staining for GluR-IIC, which depends on the presence of either GluR-IIA or GluR-IIB expression, is absent from synapses of *dgluRIIA&IIB^{-/-}*(B).

D-F, Embryonic NMJs double labeled with the active zone recognizing antibody Nc82 and antibodies against PSD marker DPAK. Wild type embryos show typical DPAK patches juxtaposed to presynaptic Nc82 labels (D). In *GluR-IIA&IIB^{-/-}* and *shibire shi^{ts1}* embryos reared at nonpermissive temperature, Nc82 often is not associated with postsynaptic DPAK spots (E, F), DPAK spots are irregular in size and shape and show lower density in *GluR-IIA&IIB^{-/-}* embryos (E).



3.5.3 Ultrastructural evidence of abnormal synaptic differentiation at glutamate receptor deprived synapse

Next, to check whether such assembly defects of postsynaptic components at glutamate receptor deprived synapse could be directly visualized at the ultrastructural level, neuromuscular junctions 6 and 7 of 3rd instar *GluR-IIA^{hypo},GluR-IIB^{null}* larvae were subjected to transmission electron microscopy (collaborated with Carolin Wichman). At normal *Drosophila* neuromuscular synapses, active zones are characterized by the presence of

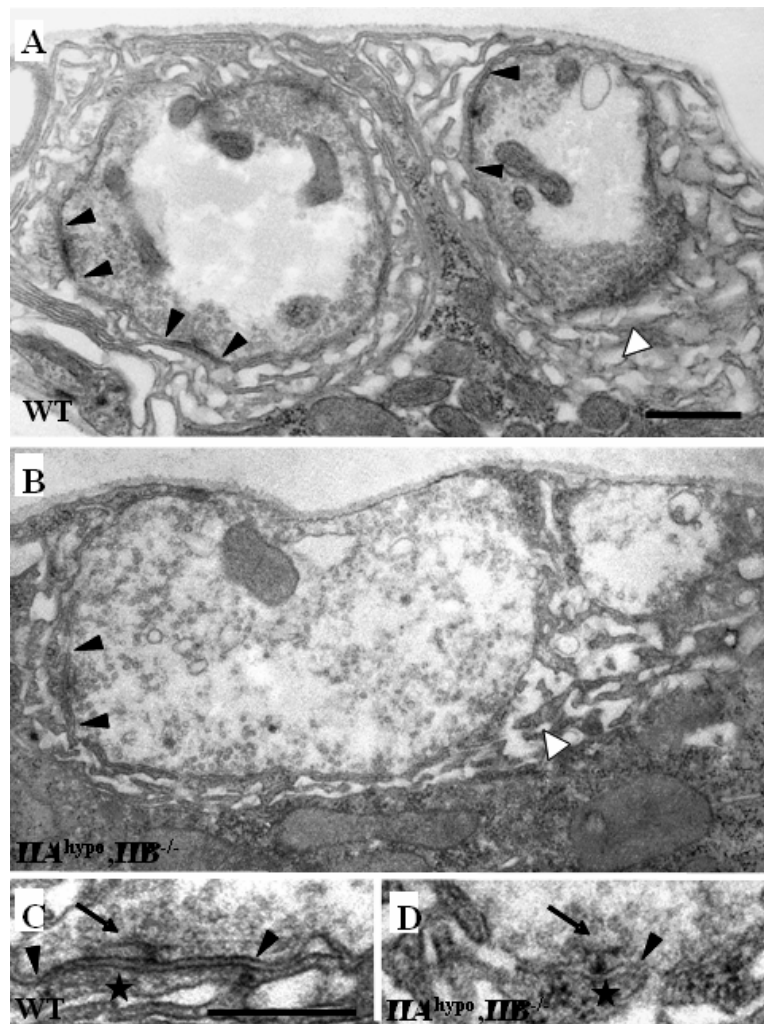


Fig.3-11 Electron microscopy: defective postsynaptic assembly at glutamate receptor deprived synapses

(A) Electron micrograph of type I nerve terminals of NMJ 6/7 in a wild type situation showing several clearly visible electron dense synapses (black arrowheads) and the SSR (white arrowhead). The synaptic vesicles are arranged along the presynaptic membrane. (B) *GluRIIA^{hypo},GluRIIB^{-/-}* type 1b bouton of NMJ 6/7, respectively. The black arrowheads indicate a mutant, clearly electron translucent synapses decorated with a T-bar. The SSR (white arrowhead) is significantly reduced. (C, D) Synaptic sites in wild type (C) and *GluRIIA^{hypo},GluRIIB^{-/-}* (D) larvae. The electron dense T-bars are indicated by arrows. The PSD, in wild type detectable as electron dense material (C, asterisk) is in *GluRIIA^{hypo},GluRIIB^{-/-}* synapses absent (D, asterisk) or in less frequent weaker cases dramatically reduced (not shown). In *GluRIIA^{hypo},GluRIIB^{-/-}* synapses the lack of PSD organization also affects the close alignment of the pre- and postsynaptic membranes, which usually extends over several 100 nm (C, arrowheads). In *GluRIIA^{hypo},GluRIIB^{-/-}* larvae this alignment is severely defective and the SSR formation already begins in direct vicinity to the T-bar (D, arrowhead) or extends asymmetrically.

electron-dense T-shaped structures called ‘T-bars’ at the presynaptic side (Wojtowicz et al., 1994; Cooper et al., 1995; Cooper et al., 1996). PSDs are opposite to the T-bars and easily recognized by electron dense linear membrane-membrane appositions (Fig.3-11), a characteristic structure also found in mammalian CNS glutamatergic synapses. Within the PSD region, pre- and postsynaptic membrane associate closely with each other and are visualized as linear apposition in cross section (Fig.3-11). At most synaptic sites, the PSD diameter clearly exceeds the diameter of the presynaptic T-bar. In region between individual PSDs (so called “perisynaptic region”), pre- and postsynaptic membrane (motorneuron and muscle membrane) are organized into various in-foldings and associate only at restricted contact points. This structure is continuous with the subsynaptic reticulum (SSR).

In *GluR-IIA^{hypo},GluR-IIB^{null}* larvae, apparently normal presynaptic T-bars were observed in boutons. However, PSD organization is severely defective (Fig.3-11) in these animals: the muscle membrane domains juxtaposed to the presynaptic T-bars, where typically PSDs should be formed, show very low amount or even complete absence of electron dense material (Fig. 3-11 D). Moreover, the typical extended and close alignment between pre- and postsynaptic membranes could not be found from *GluRIIA^{hypo},GluRIIB^{null}* larvae, in which with only significantly narrower and “wrinkled” apposition of membranes observed (Fig3-11 D). Thus, the ultrastructural analysis directly shows that in the absence of glutamate receptors, the PSD can not be efficiently assembled. In contrast, in the *dpak* mutants, despite the dramatic reduction of SSR foldings, the ultrastructure of individual synapse appeared rather normal, with smooth electron dense thickening at PSD region (Parnas et al., 2001). Rather normal ultrastructural active zone and PSD assembly was also found in embryos with neuronal TNT expression or lack of Syntaxin (Broadie et al., 1995). In combination of all these data, it is the glutamate receptor per se, obviously independent of transmission activity, controls the normal PSD assembly.

3.5.4 Defective compartmentation of the synaptic and perisynaptic zones at glutamate receptor deprived but not neurotransmission deprived synapse

The ultrastructural analysis showed that the close apposition in between pre- and postsynaptic membrane is largely abolished after reducing glutamate receptor level. It is thus interesting to know, whether the strong defects in ultrastructural PSD organization at glutamate receptor deprived synapses might also reflect defects in the molecular organization of synaptic compartments. Therefore, to address this issue, the *GluRIIA^{hypo},GluRIIB^{null}* larval NMJs were further investigated by antibody staining against compartment specific marker molecules. At normal *Drosophila* NMJ boutons, individual synapses are separated and surrounded by so called “perisynaptic” or “periaxial zone” compartment (Sone et al., 2000; Sigrist et al., 2002), characterized by the presence of various molecular markers such as Fasciclin II (FasII) and Disc Large (Dlg). FasII is one NCAM-related cell adhesion molecule involved in synaptic growth, stabilization and structural plasticity (Shuster et al., 1996). DLG is the *Drosophila* PSD95 homologue, it belongs to the membrane-associated guanylate kinase homologs (MAGUKs) family and is generally involved in synaptic clustering of various molecules such as potassium channel Shaker and FasII through the PDZ domains mediated interactions (Tejedor et al., 1997; Thomas et al., 1997; Zito et al., 1997). As reported previously, in wild type controls both FasII and DLG label the boutons in a characterized network pattern, which is clearly complementary with dPAK staining (Fig.3-12 A, D). Since normally presynaptic active zone is always precisely aligned with DPAK as evidenced by NC82 and DPAK double staining (see Fig.3-9), the perisynaptic components such as FasII and DLG clearly decorate the synaptic region.

At *GluRIIA^{hypo},GluRIIB^{null}* boutons, both FasII and DLG staining appear reduced and lose the typical network pattern, in contrast, they are distributed almost evenly throughout boutons (Fig.3-12 B, E). Notably, this homogeneous distribution pattern of Fas II and DLG indicates the intrusion of perisynaptic

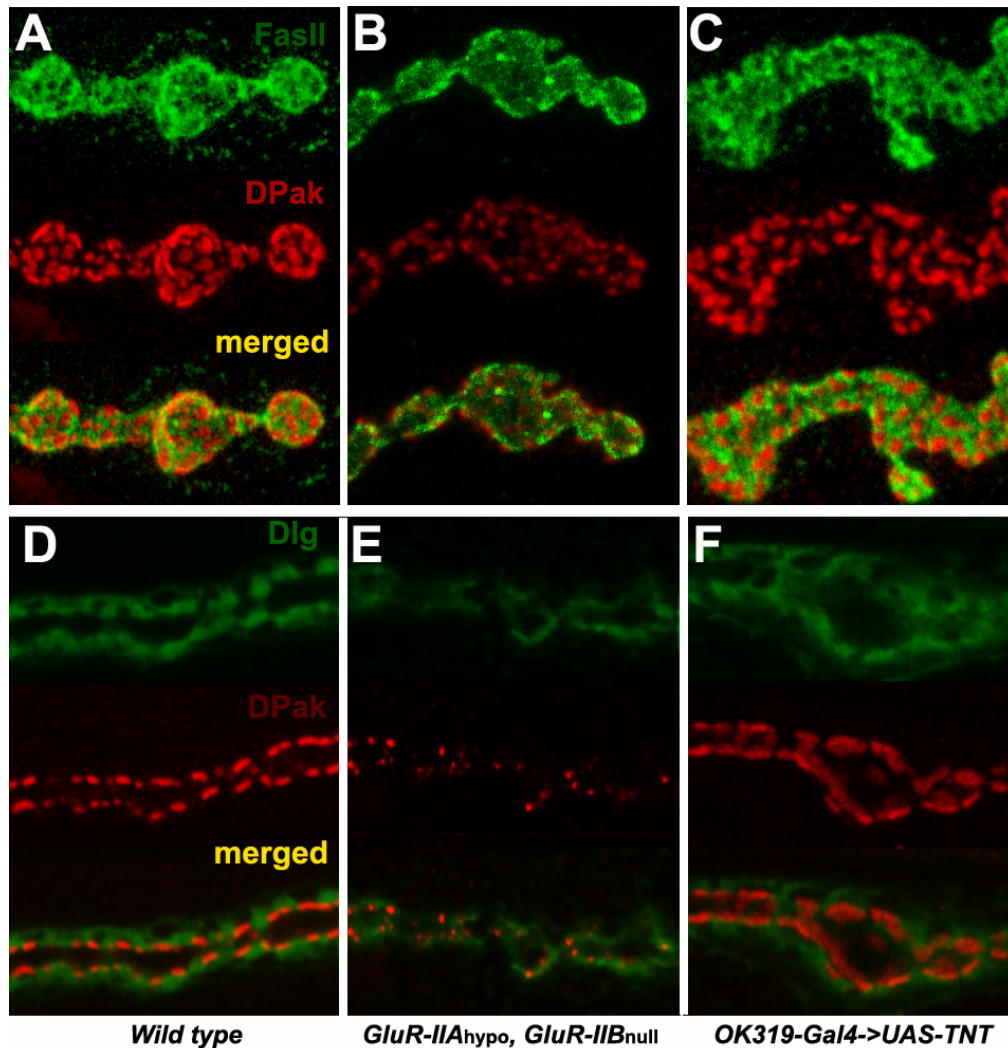


Fig.3-12 Defective synaptic compartments at glutamate receptor deprived but not neurotransmission deprived synapses

Confocal microscopy on NMJs of mid 3rd instar larvae at muscle 4, stained with compartment specific antibodies in wild type (A, D), *GluRIIA^{hypo}, GluRIIB^{-/-}* larvae (B, E) and animals with presynaptic expression of Tetanus-toxin light chain (*OK319-Gal4->UAS-TNT*, Sweeney, et al., 1995) (C, F).

A-C, NMJs double labeled with FASII together with DPAK. In wild type animals, FasII shows typical perisynaptic distribution surrounding individual PSDs which are marked by DPAK expression (A). In *GluRIIA^{hypo}, GluRIIB^{-/-}* larvae, FasII show rather even distribution over the whole bouton (B), DPAK spots display significantly lower density and more variable individual size (B). In *OK319-Gal4->UAS-TNT* larvae, both FasII and DPAK show normal distribution (C).

D-F, single cross section image of larval NMJs double labeled with DLG and DPAK. In wild type animals, DLG shows typical perisynaptic distribution surrounding individual PSDs which are marked by DPAK expression (D). In *GluRIIA^{hypo}, GluRIIB^{-/-}* larvae, DLG show rather even distribution over the whole bouton surface thus invade the synaptic area (E), DPAK spots display significantly lower density and more variable individual size and overlay with DLG labels (E). In *OK319-Gal4->UAS-TNT* larvae, both DLG and DPAK show normal distribution (F).

components into the synaptic/ active zone region, thus destroying the compartmentation of synaptic and perisynaptic area in boutons. Concerning the still rather normal localization of active zones within these boutons, clearly the major driving force to prevent perisynaptic components entering synaptic area comes from the efficiently assembled PSDs, glutamate receptors play either direct or indirect roles in this process.

3.5.5 Similar defects in synaptic differentiation in the complete absence of glutamate receptors

The above studies using glutamate receptor largely deprived larvae strongly support the structural role of glutamate receptor in organizing synaptic differentiation. To further confirm this finding, analysis on synapses with complete loss of all glutamate receptors is needed. To this end, the *GluR-IIA&IIB* double null mutant background was used. At late stage embryos of this mutant, none of any known muscle glutamate receptor subunits can be detected at NMJs (Fig.3-5 B; Fig.3-10). In consistent with the result obtained from *GluRIIA^{hypo},GluRIIB^{null}* larvae, although the active zone localize normally at the presynaptic terminal, much fewer amount of assemble dPAK aggregates are present at junctions compared to control conditions (Fig.3-10 E).

4 Discussion

4.1 Genomic tools could speed up identifying essential genes involved in synapse formation and modulation

Drosophila has long been an excellent model organism due to the availability of well established, classical genetic tools. With the recent release of the whole *Drosophila* genome sequence information and development of systematic functional genomic research tools, reverse genetics has further strengthened the power of this model organism. Recently genomic scale microarray screening has been stably applied to a wide range of studies to obtain molecular insights or identify novel relevant components of complicated regulatory processes (Furlong et al., 2001; Stathopoulos and Levine, 2002; Butler et al., 2003; Li and White, 2003).

Here, to screen genes relevant to synapse formation and growth control at whole genome scale, the microarray technique was applied to the *Drosophila* model synapse system, the NMJ. Thus, the *Drosophila* body wall filets which mainly consist of somatic muscles were sampled and the RNAs were extracted. Tissue specific RNA profiling was performed and pools of genes (about 700) with specific or enriched expression in postsynaptic muscles were obtained. These genes represent wide variety of functional groups, including enzymes, signal transduction components, receptors and ion channels, cell adhesion molecules, transcriptional factors, RNA-binding proteins, structural proteins and so on. Among them, some are previously already shown to be specifically or abundantly expressed within muscle cells, indicating that our strategy is absolutely feasible and the gene chip methodology is highly reliable. Notably, a large body of genes within the pools are not characterized yet, thus the challenge will be to study their functional significance in high-throughput way. To this end, the application of RNA interference (RNAi) will be the best choice since recently *Drosophila* whole genomic RNAi has been set up by various labs and proved to be very efficient assay (Kiger et al., 2003; Kim et al., 2004).

Undoubtedly, the microarray oriented reverse genetics platform can well complement the classical genetic screening based strategy and their application into neuronal system will greatly enhance our precise understanding of molecular details related to synapse construction and modulation. The main part of this thesis work is studying the molecular behaviors of glutamate receptor subunits, which is originated from the microarray screening and thus provide direct proof of its value.

4.2 GluR-IID and GluR-IIE are novel glutamate receptor subunits crucial for glutamate receptor assembly and thus neurotransmission at neuromuscular synapse

The glutamatergic neuromuscular synapses of *Drosophila*, rather similar to the excitatory CNS synapses of vertebrate brain in terms of ultrastructure and molecular composition, have been intensely utilized to investigate synaptic function *in vivo* capitalizing on the efficient genetics and superb experimental accessibility of this model system. At neuromuscular synapses three non-NMDA type glutamate receptor subunits (GluR-IIA, -IIB, -IIC/III) have been described previously. While only *GluR-IIA&IIB* double null mutants but not either single null mutants completely lack neurotransmission (Petersen et al., 1997; DiAntonio et al., 1999), lack of GluRIIC/ III alone is fatal with a phenotype consistent with the absence of neurotransmission at neuromuscular synapses (Marrus et al., 2004). The full picture of subunit composition of synaptic glutamate receptors at the NMJ still remains elusive.

Here via the genomic scale microarray screening, I report the identification of two additional non-NMDA glutamate receptor subunits, GluR-IID and GluR-IIE, which are proved to be specifically localized at the postsynaptic site of all neuromuscular synapses. Interestingly, while GluR-IID and GluR-IIE are genomic neighbors and very similar to each other, they are not particularly close to GluR-IIA, -IIB and -IIC/III. Specific null mutants for both *GluR-IID* and *GluR-IIE* have been obtained to further functional characterization. While both

GluR-IID and *GluR-IIE* null embryos still fully develop, they do not hatch and are incapable of performing any coordinated movement. Consistent with my finding, via embryonic electrophysiological recording, Featherstone et al. have recently demonstrated that no postsynaptic sensitivity to glutamate was detected at the embryonic muscles of one independent *GluR-IID* null mutant allele (personal communication). Thus, *GluR-IID* and *GluR-IIE* appear critically important for mediating glutamate-gated ionic currents at the postsynaptic site of neuromuscular synapses. Since in the case of *GluR-IIA&IIB* double as well as the *GluR-IIC/III* single mutant background the same paralysis phenotype was found, it is therefore most likely, that they also lack any glutamate gated ionic current.

Taken together, lack of either *GluR-IIC/III*, *-IID*, *-IIE* or both *-IIA* and *-IIB* leads to total loss of glutamate receptor function at the embryonic NMJ. The following evidences support that this is directly due to the loss of the respective glutamate receptor subunits hence all the functional glutamate receptors *within* the embryonic muscles. Firstly, despite the fact that *GluR-IID* is also present in cardio-precursor cells, the expression of *GluR-IIA*, *-IIB*, *-IIC/III* and *-IIE* is most likely restricted to the somatic muscles (Petersen et al., 1997; DiAntonio et al., 1999; Fig.3-1). Secondly, the paralysis phenotype of all these null mutants could always be fully rescued by a muscle-specific re-expression of the corresponding cDNAs (DiAntonio et al., 1999; Marrus et al., 2004; 3.4). Thirdly, muscle-specific down-regulation of *GluR-IIE* via RNA interference could effectively down-regulate synaptic expression of *GluR-IID*, *-IIA*, *-IIB* and *-IIC/III* as well. Last, in each of these null mutants, all of the other subunits are also completely absent at NMJ. Thus clearly, lack of any essential glutamate receptor subunits within the postsynaptic muscle cells will result into a complete loss of all glutamate receptors, which is the direct cause of embryonic paralysis.

4.3 Implications in the in vivo stoichiometry of *Drosophila* glutamate receptor based on genetic analysis

Several recent studies have suggested that the mammalian ionotropic glutamate receptors form as a tetramer of subunits (Kuusinen A et al., 1999; Rosenmund C et al., 1998; Laube B et al., 1998; Mano I et al., 1998; Safferling M et al., 2001). At the *Drosophila* Neuromuscular synapses, the synaptic expression of all glutamate receptor subunits is completely abolished after eliminating either *GluR-IID* or *IIE* alone or *GluR-IIA* and *IIB* together (Fig. 3-5), clearly indicating that essential glutamate receptor subunits (GluR-IIC/III, -IID and -IIE) are obligatory part of all postsynaptic glutamate receptors. In addition, the presence of either GluRIIA or GluR-IIB seems obligate for receptor formation as well. One likely scenario therefore is that the glutamate receptor population at the *Drosophila* NMJ is a mix of (IIA)(IIC/III)(IID)(IIE) receptors with (IIB)(IIC/III)(IID)(IIE) receptors. However, since the current tetrameric structure model of ionotropic glutamate receptors was suggested solely on the basis of either electrophysiological and biochemical studies in heterologous system or crystal structure analysis of ligand-binding domains, an unequivocal determination of the stoichiometry of functional glutamate receptor thus still awaits efficient method that reliably resolve the structure of the endogenous receptor itself. In theory, as was proposed in the past (Premkumar et al., 1997), pentameric (or higher) stoichiometry still cannot be totally excluded in the moment. Therefore, stoichiometry as (A)₂(C)(D)(E), (B)₂(C)(D)(E) or (A)(B)(C)(D)(E) still need to be considered.

Previous studies have established that GluR-IIA- and GluR-IIB-containing receptors differ strongly in their biophysical properties, with GluR-IIA-containing receptors showing slow desensitization kinetics and GluR-IIB-containing receptors showing fast desensitization kinetics (DiAntonio et al., 1999). Thus, GluR-IIA and GluR-IIB containing complexes are likely to play different roles in synaptic function and development. Accordingly, it has

been recently found that, increased postsynaptic GluR-IIA level or reduced GluR-IIB gene dosage results into an increased strength of NMJ transmission and an addition of boutons harboring increased numbers of synapses; this phenotypes were suppressed by overexpression of GluR-IIB (Sigrist et al., 2002). Thus, GluR-IIC/III, IID and IIE might establish a “receptor assembly platform” where the incorporation of either the GluR-IIA or the GluR-IIB subunit could determine the specific functions of the respective glutamate receptor.

As discussed above, the interdependency between all essential subunits observed for synaptic localization is easiest explained by assuming the existence of common glutamate receptor. Another possibility might be that eliminating a certain glutamate receptor subunit could provoke an early defect during the developmental set up of neuromuscular synapses, which in turn might interfere with the localization of other glutamate receptor complexes. This way, the genetic elimination of a certain subunit could also cause the loss of synaptic expression (and thus also synaptic function) of another subunit even if these two subunits would not be coassembled in the same glutamate receptor complex. At this juncture, such a scenario appears unlikely because of the following reasons. First, partial suppression of any essential glutamate receptor subunit always provokes a corresponding down-regulation of other essential glutamate receptor subunits at larval neuromuscular synapses (Fig.3-6 and 3-7; Marrus et al., 2004). This suggests that all essential subunits obey a tight stoichiometric relationship, where the availability of the least abundant subunit defines the overall amount of glutamate receptors, and that this relation exists throughout development. Secondly, Featherstone et al. have convincingly demonstrated a *complete* loss of glutamate mediated currents on embryonic muscle surfaces of one independent *GluR-IID* null mutant allele (Featherstone D et al., personal communication). In contrast, extrasynaptic glutamate receptor mediated currents have been stably detected on wild type embryonic muscle membranes using the same experimental settings (Broadie and Bate, 1993; Featherstone et al., personal

communication). Thus, elimination of GluR-IIID abolishes not only synaptic but also extrasynaptic populations of glutamate receptors on embryonic muscles. Therefore, if interaction between independently forming glutamate receptors is involved in their proper targeting, it would have to be absolutely essential already during the intracellular transport and insertion of glutamate receptors. Since all known muscle receptor subunits from GluR-IIA to GluR-IIID (GluR-IIIE also quite likely the case as evidenced by EGFP fusion protein distribution) are clearly expressed in substantial amounts within postsynaptic densities, the existence of subunits evolved only to mediate the intracellular transport or assembly of glutamate receptor complexes appears rather unlikely unless it was omitted from the Gene chip analysis.

Collectively, the *in vivo* data presented here clearly favor the notion that, at *Drosophila* neuromuscular synapses the functional glutamate receptors can be composed of four different subunits. To our knowledge, a “strictly hetero-tetrameric stoichiometry” has so far not been described for other types of ionotropic glutamate receptors in all model synapses. This finding thus potentially reveal that, apart from our current understanding on glutamate receptor behavior mainly based on heterologous studies, the *in vivo* glutamate receptors might have a rather fixed stoichiometry, which is reminiscent of that of other types of ligand-gated ion channels such as the nicotinic acetylcholine receptor (Colquhoun and Sivilotti, 2004).

4.4 Structural role of ionotropic glutamate receptor per se in organizing synaptic assembly

In the brain, huge amount of neurons are precisely connected via synapses, which display respectively characteristic structural properties at both pre and postsynaptic sides. Most excitatory synapses are glutamatergic, and their initial formation, stabilization, and elimination are under strict control all the time. Moreover, the local changes in synapse strength are proposed to be relevant to

the process of learning and memory. Apparently, it is of great importance to understand how the original synaptic contact is initiated at the proper site and how exquisite coordination of presynaptic and postsynaptic development is accomplished. Although up to now great efforts have been devoted in these directions with more and more synaptic components identified and characterized, still the molecular details driving synaptic assembly remain elusive.

At central excitatory synapses, synaptic transmission is mediated by various ionotropic glutamate receptors including AMPA, kainite and NMDA subfamilies. Recent work has revealed that certain classes of AMPA receptors recycle rapidly at the synaptic sites, suggesting that placeholders or 'slots' might be brought to, or assembled at the postsynaptic membrane with *de novo* insertion of AMPA receptors. The molecular identity of the slots is unknown, but is likely to involve one or more receptor-binding or scaffolding proteins (Barry and Ziff, 2002).

Taking the advantages of the powerful *Drosophila* genetic tools and the rather simpler architecture of NMJ, the consequences of losing synaptic glutamate receptor partially or completely *in vivo* were investigated. Despite the rather normal differentiation of transmitter release machinery at the presynaptic membrane, which is consistent with previous findings that the presynaptic differentiation can undergo at the nerve terminal even without contact with the postsynaptic cell (Prokop et al., 1996), the postsynaptic assembly is apparently deficient, as evidenced by not only inefficient clustering of other PSD component (dPAK) but also the intrusion of perisynaptic components (FASII and DLG) into synaptic (active zone) territory. PAK is known to regulate cytoskeleton dynamics, the cytoskeleton organization is crucial for the clustering of synaptic components and /or maintaining the synaptic structure at diverse types of synapses (Kirsch and Betz, 1995; Allison et al., 1998; Dai et al., 2000; Hirai, 2000). Recently it has been proposed that dPAK is important in

clustering glutamate receptors at *Drosophila* NMJ since in *dpak* hypomorphic mutant animals, glutamate receptor subunit GluR-IIA is significantly reduced but still localize normally at synapses (Parnas et al., 2001). Interestingly, the data presented here indicate that proper aggregation and synaptic distribution of dPAK is definitely dependant on the availability of glutamate receptors; with glutamate receptors depleted the dPAK is no longer able to cluster and localize properly. At mammalian neuromuscular synapse it has been shown that agrin-mediated clustering of AchR is mediated by the corporation of various signaling pathways: first the activation of Rac/ Cdc42, leading to formation of AchR microclusters, followed by Rho activation, resulting into combining these microclusters into larger clusters (Weston C et al., 2003). DPAK does not necessarily need to interact directly with glutamate receptors, but via various direct and indirect interactions glutamate receptors might be able to recruit various PSD components (including dPAK, other signaling molecules and scaffold proteins) during synaptogenesis, as soon as these components are recruited together, the relevant signaling cascades are efficiently activated and thus trigger the membrane and cytoskeleton remodeling which finally results into the stable development of mature synaptic structure; in depletion of glutamate receptors, either the dPAK signaling cascade is not efficiently activated to reorganize actin cytoskeleton essential for proper clustering, or activating dPAK cascade along is not sufficient for effective PSD components clustering and maintaining. Currently, it remains elusive whether other signaling pathways are involved in PSD formation, but based on the clear defects in synaptic compartmentation that perisynaptic components intrude into synaptic region, the cytoskeleton organization must have been improperly regulated. This notion is also supported from ultrastructural analysis, the electron dense material typical present at the PSD region is essentially absent from glutamate receptor deprived synapses, implicating that the components of postsynaptic scaffold are either not recruited together at all or no longer stable without the integration of glutamate receptors. Interestingly, at the neuromuscular synapses of *dpak* hypomorphic mutant, despite much fewer SSR, the ultrastructure of

both PSD and active zone appears quite normal, further supporting the relatively minor role of dPAK in postsynaptic differentiation. Notably, the role of glutamate receptor in synaptic development was shown not to be relevant to its ion channel activity, since in all the backgrounds tested which deprive presynaptic neurotransmitter release (partially or completely), the glutamate receptor can be clustered as effectively as wild type control. Correspondingly, the postsynaptic reception apparatus in these transmission depleted conditions appear functional since responses can be stably detected when applying glutamate at junctions (Broadie, 1996).

Another interesting phenomena at glutamate receptor deprived synapse is that the number of presynaptic specializations exceeds postsynaptic ones, thus resulting into free active zones without postsynaptic partners, which is hardly found in normal conditions. In principle, this can be due to either lack of glutamate receptor per se, or that of the transmission activity. The latter idea appears more likely since in complete transmitter release deficient situations, free active zones were also observed although certain levels of PSDs (glutamate receptor fields) were assembled normally.

In conclusion, apart from functioning as ligand-gated ion channel, the glutamate receptor at *Drosophila* NMJ also plays crucial role in organizing and /or maintaining the synaptic architecture, which is reminiscent of AchR at vertebrate NMJ (Ono F et al., 2001; Marangi PA et al., 2001; Missias AC et al., 1997) and glycin and GABA receptor at mammalian central synapses (Essrich et al., 1998). In mammalian CNS synapses similar roles of ionotropic glutamate receptors have not been reported, mainly due to the fact that there exist highly divergent classes of glutamate receptors at central synapses and each type of receptors play distinct roles, therefore it is not easy to obtain a condition with all types of glutamate receptors removed together.

Reference

- Aberle H, Haghighi AP, Fetter RD, McCabe BD, Magalhaes TR, Goodman CS (2002) wishful thinking encodes a BMP type II receptor that regulates synaptic growth in *Drosophila*. *Neuron* 33:545-558.
- Ahmari SE, Buchanan J, Smith SJ (2000) Assembly of presynaptic active zones from cytoplasmic transport packets. *Nat Neurosci* 3:445-451.
- Albin SD, Davis GW (2004) Coordinating structural and functional synapse development: postsynaptic p21-activated kinase independently specifies glutamate receptor abundance and postsynaptic morphology. *J Neurosci* 24:6871-6879.
- Allison DW, Gelfand VI, Spector I, Craig AM (1998) Role of actin in anchoring postsynaptic receptors in cultured hippocampal neurons: differential attachment of NMDA versus AMPA receptors. *J Neurosci* 18:2423-2436.
- Apel ED, Glass DJ, Moscoso LM, Yancopoulos GD, Sanes JR (1997) Rapsyn is required for MuSK signaling and recruits synaptic components to a MuSK-containing scaffold. *Neuron* 18:623-635.
- Aplin AE, Howe A, Alahari SK, Juliano RL (1998) Signal transduction and signal modulation by cell adhesion receptors: the role of integrins, cadherins, immunoglobulin-cell adhesion molecules, and selectins. *Pharmacol Rev* 50:197-263.
- Atwood HL, Govind CK, Wu CF (1993) Differential ultrastructure of synaptic terminals on ventral longitudinal abdominal muscles in *Drosophila* larvae. *J Neurobiol* 24:1008-1024.
- Auld VJ, Fetter RD, Broadie K, Goodman CS (1995) Gliotactin, a novel transmembrane protein on peripheral glia, is required to form the blood-nerve barrier in *Drosophila*. *Cell* 81:757-767.
- Ayalon G, Stern-Bach Y (2001) Functional assembly of AMPA and kainate receptors is mediated by several discrete protein-protein interactions. *Neuron* 31:103-113.
- Bagrodia S, Cerione RA (1999) Pak to the future. *Trends Cell Biol* 9:350-355.
- Barry MF, Ziff EB (2002) Receptor trafficking and the plasticity of excitatory synapses. *Curr Opin Neurobiol* 12:279-286.
- Bate M, Broadie K (1995) Wiring by fly: the neuromuscular system of the *Drosophila* embryo. *Neuron* 15:513-525.
- Benson DL, Colman DR, Huntley GW (2001) Molecules, maps and synapse specificity. *Nat Rev Neurosci* 2:899-909.
- Biederer T, Sara Y, Mozhayeva M, Atasoy D, Liu X, Kavalali ET, Sudhof TC (2002) SynCAM, a synaptic adhesion molecule that drives synapse assembly. *Science* 297:1525-1531.
- Bloch RJ, Pumplin DW (1988) Molecular events in synaptogenesis: nerve-muscle adhesion and postsynaptic differentiation. *Am J Physiol* 254:C345-364.
- Boutanaev AM, Kalmykova AI, Shevelyov YY, Nurminsky DI (2002) Large clusters of co-expressed genes in the *Drosophila* genome. *Nature* 420:666-669.
- Bowe MA, Fallon JR (1995) The role of agrin in synapse formation. *Annu Rev Neurosci* 18:443-462.
- Brand AH, Perrimon N (1993) Targeted gene expression as a means of altering cell fates and generating dominant phenotypes. *Development* 118:401-415.
- Bresler T, Ramati Y, Zamorano PL, Zhai R, Garner CC, Ziv NE (2001) The dynamics of SAP90/PSD-95 recruitment to new synaptic junctions. *Mol Cell Neurosci* 18:149-167.
- Bresler T, Shapira M, Boeckers T, Dresbach T, Futter M, Garner CC, Rosenblum K, Gundelfinger ED, Ziv NE (2004) Postsynaptic density assembly is fundamentally different from presynaptic active zone assembly. *J Neurosci* 24:1507-1520.
- Broadie K, Bate M (1993) Activity-dependent development of the neuromuscular synapse during *Drosophila* embryogenesis. *Neuron* 11:607-619.
- Broadie K, Bate M (1993) Innervation directs receptor synthesis and localization in *Drosophila* embryo synaptogenesis. *Nature* 361:350-353.
- Broadie K, Prokop A, Bellen HJ, O'Kane CJ, Schulze KL, Sweeney ST (1995) Syntaxin and synaptobrevin function downstream of vesicle docking in *Drosophila*. *Neuron* 15:663-673.
- Broadie KS (1996) Regulation of the synaptic vesicle cycle in *Drosophila*. *Biochem Soc Trans* 24:639-645.
- Budnik V, Koh YH, Guan B, Hartmann B, Hough C, Woods D, Gorczyca M (1996) Regulation of

- synapse structure and function by the *Drosophila* tumor suppressor gene dlg. *Neuron* 17:627-640.
- Burden SJ (1998) The formation of neuromuscular synapses. *Genes Dev* 12:133-148.
- Burnashev N, Khodorova A, Jonas P, Helm PJ, Wisden W, Monyer H, Seeburg PH, Sakmann B (1992) Calcium-permeable AMPA-kainate receptors in fusiform cerebellar glial cells. *Science* 256:1566-1570.
- Butler MJ, Jacobsen TL, Cain DM, Jarman MG, Hubank M, Whittle JR, Phillips R, Simcox A (2003) Discovery of genes with highly restricted expression patterns in the *Drosophila* wing disc using DNA oligonucleotide microarrays. *Development* 130:659-670.
- Chavis P, Westbrook G (2001) Integrins mediate functional pre- and postsynaptic maturation at a hippocampal synapse. *Nature* 411:317-321.
- Chen GQ, Cui C, Mayer ML, Gouaux E (1999) Functional characterization of a potassium-selective prokaryotic glutamate receptor. *Nature* 402:817-821.
- Chen L, Chetkovich DM, Petralia RS, Sweeney NT, Kawasaki Y, Wenthold RJ, Brecht DS, Nicoll RA (2000) Stargazin regulates synaptic targeting of AMPA receptors by two distinct mechanisms. *Nature* 408:936-943.
- Chiba A, Rose D (1998) "Painting" the target: how local molecular cues define synaptic relationships. *Bioessays* 20:941-948.
- Colquhoun D, Sivilotti LG (2004) Function and structure in glycine receptors and some of their relatives. *Trends Neurosci* 27:337-344.
- Contractor A, Heinemann SF (2002) Glutamate receptor trafficking in synaptic plasticity. *Sci STKE* 2002:RE14.
- Cooper RL, Marin L, Atwood HL (1995) Synaptic differentiation of a single motor neuron: conjoint definition of transmitter release, presynaptic calcium signals, and ultrastructure. *J Neurosci* 15:4209-4222.
- Cooper RL, Harrington CC, Marin L, Atwood HL (1996) Quantal release at visualized terminals of a crayfish motor axon: intraterminal and regional differences. *J Comp Neurol* 375:583-600.
- Currie DA, Truman JW, Burden SJ (1995) *Drosophila* glutamate receptor RNA expression in embryonic and larval muscle fibers. *Dev Dyn* 203:311-316.
- Dai Z, Luo X, Xie H, Peng HB (2000) The actin-driven movement and formation of acetylcholine receptor clusters. *J Cell Biol* 150:1321-1334.
- Dalva MB, Takasu MA, Lin MZ, Shamah SM, Hu L, Gale NW, Greenberg ME (2000) EphB receptors interact with NMDA receptors and regulate excitatory synapse formation. *Cell* 103:945-956.
- Daniels RW, Collins CA, Gelfand MV, Dant J, Brooks ES, Krantz DE, Diantonio A (2004) Increased Expression of the *Drosophila* Vesicular Glutamate Transporter Leads to Excess Glutamate Release and a Compensatory Decrease in Quantal Content. *J Neurosci* 24:10466-10474.
- Davis GW, Schuster CM, Goodman CS (1997) Genetic analysis of the mechanisms controlling target selection: target-derived Fasciclin II regulates the pattern of synapse formation. *Neuron* 19:561-573.
- Dean C, Scholl FG, Choih J, DeMaria S, Berger J, Isacoff E, Scheiffele P (2003) Neurexin mediates the assembly of presynaptic terminals. *Nat Neurosci* 6:708-716.
- DeChiara TM, Bowen DC, Valenzuela DM, Simmons MV, Poueymirou WT, Thomas S, Kinetz E, Compton DL, Rojas E, Park JS, Smith C, DiStefano PS, Glass DJ, Burden SJ, Yancopoulos GD (1996) The receptor tyrosine kinase MuSK is required for neuromuscular junction formation in vivo. *Cell* 85:501-512.
- DiAntonio A, Petersen SA, Heckmann M, Goodman CS (1999) Glutamate receptor expression regulates quantal size and quantal content at the *Drosophila* neuromuscular junction. *J Neurosci* 19:3023-3032.
- Dingledine R, Borges K, Bowie D, Traynelis SF (1999) The glutamate receptor ion channels. *Pharmacol Rev* 51:7-61.
- Dingledine R, Borges K, Bowie D, Traynelis SF (1999) The glutamate receptor ion channels. *Pharmacol Rev* 51:7-61.
- Ellgaard L, Helenius A (2003) Quality control in the endoplasmic reticulum. *Nat Rev Mol Cell Biol* 4:181-191.
- Essrich C, Lorez M, Benson JA, Fritschy JM, Luscher B (1998) Postsynaptic clustering of major GABAA receptor subtypes requires the gamma 2 subunit and gephyrin. *Nat Neurosci* 1:563-571.
- Ethell IM, Yamaguchi Y (1999) Cell surface heparan sulfate proteoglycan syndecan-2 induces the maturation of dendritic spines in rat hippocampal neurons. *J Cell Biol* 144:575-586.
- Ethell IM, Irie F, Kalo MS, Couchman JR, Pasquale EB, Yamaguchi Y (2001) EphB/syndecan-2

- signaling in dendritic spine morphogenesis. *Neuron* 31:1001-1013.
- Featherstone DE, Broadie K (2000) Surprises from *Drosophila*: genetic mechanisms of synaptic development and plasticity. *Brain Res Bull* 53:501-511.
- Fernandez-Chacon R, Sudhof TC (1999) Genetics of synaptic vesicle function: toward the complete functional anatomy of an organelle. *Annu Rev Physiol* 61:753-776.
- Fiala JC, Feinberg M, Popov V, Harris KM (1998) Synaptogenesis via dendritic filopodia in developing hippocampal area CA1. *J Neurosci* 18:8900-8911.
- Finn AJ, Feng G, Pendergast AM (2003) Postsynaptic requirement for Abl kinases in assembly of the neuromuscular junction. *Nat Neurosci* 6:717-723.
- Friedman HV, Bresler T, Garner CC, Ziv NE (2000) Assembly of new individual excitatory synapses: time course and temporal order of synaptic molecule recruitment. *Neuron* 27:57-69.
- Froehner SC, Luetje CW, Scotland PB, Patrick J (1990) The postsynaptic 43K protein clusters muscle nicotinic acetylcholine receptors in *Xenopus* oocytes. *Neuron* 5:403-410.
- Furlong EE, Andersen EC, Null B, White KP, Scott MP (2001) Patterns of gene expression during *Drosophila* mesoderm development. *Science* 293:1629-1633.
- Garner CC, Zhai RG, Gundelfinger ED, Ziv NE (2002) Molecular mechanisms of CNS synaptogenesis. *Trends Neurosci* 25:243-251.
- Gautam M, Noakes PG, Mudd J, Nichol M, Chu GC, Sanes JR, Merlie JP (1995) Failure of postsynaptic specialization to develop at neuromuscular junctions of rapsyn-deficient mice. *Nature* 377:232-236.
- Gautam M, Noakes PG, Moscoso L, Rupp F, Scheller RH, Merlie JP, Sanes JR (1996) Defective neuromuscular synaptogenesis in agrin-deficient mutant mice. *Cell* 85:525-535.
- Gilbert W (1978) Why genes in pieces? *Nature* 271:501.
- Gillespie SK, Wasserman SA (1994) Dorsal, a *Drosophila* Rel-like protein, is phosphorylated upon activation of the transmembrane protein Toll. *Mol Cell Biol* 14:3559-3568.
- Glass DJ, Bowen DC, Stitt TN, Radziejewski C, Bruno J, Ryan TE, Gies DR, Shah S, Mattsson K, Burden SJ, DiStefano PS, Valenzuela DM, DeChiara TM, Yancopoulos GD (1996) Agrin acts via a MuSK receptor complex. *Cell* 85:513-523.
- Gonzalez-Gaitan M, Jackle H (1997) Role of *Drosophila* alpha-adaptin in presynaptic vesicle recycling. *Cell* 88:767-776.
- Gramates LS, Budnik V (1999) Assembly and maturation of the *Drosophila* larval neuromuscular junction. *Int Rev Neurobiol* 43:93-117.
- Greger IH, Khatri L, Ziff EB (2002) RNA editing at arg607 controls AMPA receptor exit from the endoplasmic reticulum. *Neuron* 34:759-772.
- Grunwald IC, Korte M, Wolfer D, Wilkinson GA, Unsicker K, Lipp HP, Bonhoeffer T, Klein R (2001) Kinase-independent requirement of EphB2 receptors in hippocampal synaptic plasticity. *Neuron* 32:1027-1040.
- Guan B, Hartmann B, Kho YH, Gorczyca M, Budnik V (1996) The *Drosophila* tumor suppressor gene, *dlg*, is involved in structural plasticity at a glutamatergic synapse. *Curr Biol* 6:695-706.
- Hall AC, Lucas FR, Salinas PC (2000) Axonal remodeling and synaptic differentiation in the cerebellum is regulated by WNT-7a signaling. *Cell* 100:525-535.
- Hall ZW, Sanes JR (1993) Synaptic structure and development: the neuromuscular junction. *Cell* 72 Suppl:99-121.
- Han H, Noakes PG, Phillips WD (1999) Overexpression of rapsyn inhibits agrin-induced acetylcholine receptor clustering in muscle cells. *J Neurocytol* 28:763-775.
- Hannah MJ, Schmidt AA, Huttner WB (1999) Synaptic vesicle biogenesis. *Annu Rev Cell Dev Biol* 15:733-798.
- Harris KM, Kater SB (1994) Dendritic spines: cellular specializations imparting both stability and flexibility to synaptic function. *Annu Rev Neurosci* 17:341-371.
- Hawkins LM, Prybylowski K, Chang K, Moussan C, Stephenson FA, Wenthold RJ (2004) Export from the endoplasmic reticulum of assembled N-methyl-D-aspartic acid receptors is controlled by a motif in the c terminus of the NR2 subunit. *J Biol Chem* 279:28903-28910.
- Heimbeck G, Bugnon V, Gendre N, Haberlin C, Stocker RF (1999) Smell and taste perception in *Drosophila melanogaster* larva: toxin expression studies in chemosensory neurons. *J Neurosci* 19:6599-6609.
- Henderson JT, Georgiou J, Jia Z, Robertson J, Elowe S, Roder JC, Pawson T (2001) The receptor tyrosine kinase EphB2 regulates NMDA-dependent synaptic function. *Neuron* 32:1041-1056.
- Herbst R, Burden SJ (2000) The juxtamembrane region of MuSK has a critical role in agrin-mediated signaling. *Embo J* 19:67-77.
- Hering H, Sheng M (2001) Dendritic spines: structure, dynamics and regulation. *Nat Rev Neurosci*

- 2:880-888.
- Hirai H (2000) Clustering of delta glutamate receptors is regulated by the actin cytoskeleton in the dendritic spines of cultured rat Purkinje cells. *Eur J Neurosci* 12:563-570.
- Hoang B, Chiba A (1998) Genetic analysis on the role of integrin during axon guidance in *Drosophila*. *J Neurosci* 18:7847-7855.
- Hollmann M, Heinemann S (1994) Cloned glutamate receptors. *Annu Rev Neurosci* 17:31-108.
- Isaac JT, Crair MC, Nicoll RA, Malenka RC (1997) Silent synapses during development of thalamocortical inputs. *Neuron* 18:269-280.
- Jahn R, Sudhof TC (1999) Membrane fusion and exocytosis. *Annu Rev Biochem* 68:863-911.
- Jaskolski F, Coussen F, Nagarajan N, Normand E, Rosenmund C, Mulle C (2004) Subunit composition and alternative splicing regulate membrane delivery of kainate receptors. *J Neurosci* 24:2506-2515.
- Jennings CG, Dyer SM, Burden SJ (1993) Muscle-specific trk-related receptor with a kringle domain defines a distinct class of receptor tyrosine kinases. *Proc Natl Acad Sci U S A* 90:2895-2899.
- Jia XX, Gorczyca M, Budnik V (1993) Ultrastructure of neuromuscular junctions in *Drosophila*: comparison of wild type and mutants with increased excitability. *J Neurobiol* 24:1025-1044.
- Kennerdell JR, Carthew RW (2000) Heritable gene silencing in *Drosophila* using double-stranded RNA. *Nat Biotechnol* 18:896-898.
- Keshishian H, Broadie K, Chiba A, Bate M (1996) The *Drosophila* neuromuscular junction: a model system for studying synaptic development and function. *Annu Rev Neurosci* 19:545-575.
- Kiger AA, Baum B, Jones S, Jones MR, Coulson A, Echeverri C, Perrimon N (2003) A functional genomic analysis of cell morphology using RNA interference. *J Biol* 2:27.
- Kim YO, Park SJ, Balaban RS, Nirenberg M, Kim Y (2004) A functional genomic screen for cardiogenic genes using RNA interference in developing *Drosophila* embryos. *Proc Natl Acad Sci U S A* 101:159-164.
- Kirsch J, Betz H (1995) The postsynaptic localization of the glycine receptor-associated protein gephyrin is regulated by the cytoskeleton. *J Neurosci* 15:4148-4156.
- Kneussel M, Brandstatter JH, Laube B, Stahl S, Muller U, Betz H (1999) Loss of postsynaptic GABA(A) receptor clustering in gephyrin-deficient mice. *J Neurosci* 19:9289-9297.
- Koh YH, Gramates LS, Budnik V (2000) *Drosophila* larval neuromuscular junction: molecular components and mechanisms underlying synaptic plasticity. *Microsc Res Tech* 49:14-25.
- Kuusinen A, Abele R, Madden DR, Keinänen K (1999) Oligomerization and ligand-binding properties of the ectodomain of the alpha-amino-3-hydroxy-5-methyl-4-isoxazole propionic acid receptor subunit GluRD. *J Biol Chem* 274:28937-28943.
- LaRochelle WJ, Froehner SC (1986) Determination of the tissue distributions and relative concentrations of the postsynaptic 43-kDa protein and the acetylcholine receptor in Torpedo. *J Biol Chem* 261:5270-5274.
- Laube B, Kuhse J, Betz H (1998) Evidence for a tetrameric structure of recombinant NMDA receptors. *J Neurosci* 18:2954-2961.
- Li TR, White KP (2003) Tissue-specific gene expression and ecdysone-regulated genomic networks in *Drosophila*. *Dev Cell* 5:59-72.
- Li Z, Sheng M (2003) Some assembly required: the development of neuronal synapses. *Nat Rev Mol Cell Biol* 4:833-841.
- Liao D, Hessler NA, Malinow R (1995) Activation of postsynaptically silent synapses during pairing-induced LTP in CA1 region of hippocampal slice. *Nature* 375:400-404.
- Lin W, Burgess RW, Dominguez B, Pfaff SL, Sanes JR, Lee KF (2001) Distinct roles of nerve and muscle in postsynaptic differentiation of the neuromuscular synapse. *Nature* 410:1057-1064.
- Littleton JT (2000) A genomic analysis of membrane trafficking and neurotransmitter release in *Drosophila*. *J Cell Biol* 150:F77-82.
- Littleton JT, Ganetzky B (2000) Ion channels and synaptic organization: analysis of the *Drosophila* genome. *Neuron* 26:35-43.
- Luo ZG, Je HS, Wang Q, Yang F, Dobbins GC, Yang ZH, Xiong WC, Lu B, Mei L (2003) Implication of geranylgeranyltransferase I in synapse formation. *Neuron* 40:703-717.
- Luo ZG, Wang Q, Zhou JZ, Wang J, Luo Z, Liu M, He X, Wynshaw-Boris A, Xiong WC, Lu B, Mei L (2002) Regulation of AChR clustering by Dishevelled interacting with MuSK and PAK1. *Neuron* 35:489-505.
- Madden DR (2002) The structure and function of glutamate receptor ion channels. *Nat Rev Neurosci* 3:91-101.
- Mano I, Teichberg VI (1998) A tetrameric subunit stoichiometry for a glutamate receptor-channel complex. *Neuroreport* 9:327-331.

- Marangi PA, Forsayeth JR, Mittaud P, Erb-Vogtli S, Blake DJ, Moransard M, Sander A, Fuhrer C (2001) Acetylcholine receptors are required for agrin-induced clustering of postsynaptic proteins. *Embo J* 20:7060-7073.
- Marrs GS, Green SH, Dailey ME (2001) Rapid formation and remodeling of postsynaptic densities in developing dendrites. *Nat Neurosci* 4:1006-1013.
- Marrus SB, Portman SL, Allen MJ, Moffat KG, DiAntonio A (2004) Differential localization of glutamate receptor subunits at the *Drosophila* neuromuscular junction. *J Neurosci* 24:1406-1415.
- Matsuda K, Fletcher M, Kamiya Y, Yuzaki M (2003) Specific assembly with the NMDA receptor 3B subunit controls surface expression and calcium permeability of NMDA receptors. *J Neurosci* 23:10064-10073.
- McCabe BD, Marques G, Haghghi AP, Fetter RD, Crotty ML, Haerry TE, Goodman CS, O'Connor MB (2003) The BMP homolog Gbb provides a retrograde signal that regulates synaptic growth at the *Drosophila* neuromuscular junction. *Neuron* 39:241-254.
- McGee AW, Brecht DS (2003) Assembly and plasticity of the glutamatergic postsynaptic specialization. *Curr Opin Neurobiol* 13:111-118.
- McMahan UJ (1990) The agrin hypothesis. *Cold Spring Harb Symp Quant Biol* 55:407-418.
- Meguro H, Mori H, Araki K, Kushiya E, Kutsuwada T, Yamazaki M, Kumanishi T, Arakawa M, Sakimura K, Mishina M (1992) Functional characterization of a heteromeric NMDA receptor channel expressed from cloned cDNAs. *Nature* 357:70-74.
- Milner R, Campbell IL (2002) The integrin family of cell adhesion molecules has multiple functions within the CNS. *J Neurosci Res* 69:286-291.
- Missias AC, Mudd J, Cunningham JM, Steinbach JH, Merlie JP, Sanes JR (1997) Deficient development and maintenance of postsynaptic specializations in mutant mice lacking an 'adult' acetylcholine receptor subunit. *Development* 124:5075-5086.
- Missler M, Zhang W, Rohlmann A, Kattenstroth G, Hammer RE, Gottmann K, Sudhof TC (2003) Alpha-neurexins couple Ca²⁺ channels to synaptic vesicle exocytosis. *Nature* 423:939-948.
- Monyer H, Sprengel R, Schoepfer R, Herb A, Higuchi M, Lomeli H, Burnashev N, Sakmann B, Seeburg PH (1992) Heteromeric NMDA receptors: molecular and functional distinction of subtypes. *Science* 256:1217-1221.
- Mulle C, Sailer A, Swanson GT, Brana C, O'Gorman S, Bettler B, Heinemann SF (2000) Subunit composition of kainate receptors in hippocampal interneurons. *Neuron* 28:475-484.
- Nguyen T, Sudhof TC (1997) Binding properties of neuroligin 1 and neurexin 1beta reveal function as heterophilic cell adhesion molecules. *J Biol Chem* 272:26032-26039.
- Noakes PG, Phillips WD, Hanley TA, Sanes JR, Merlie JP (1993) 43K protein and acetylcholine receptors colocalize during the initial stages of neuromuscular synapse formation in vivo. *Dev Biol* 155:275-280.
- Noakes PG, Gautam M, Mudd J, Sanes JR, Merlie JP (1995) Aberrant differentiation of neuromuscular junctions in mice lacking s-laminin/laminin beta 2. *Nature* 374:258-262.
- O'Brien R, Xu D, Mi R, Tang X, Hopf C, Worley P (2002) Synaptically targeted narp plays an essential role in the aggregation of AMPA receptors at excitatory synapses in cultured spinal neurons. *J Neurosci* 22:4487-4498.
- O'Brien RJ, Xu D, Petralia RS, Steward O, Haganir RL, Worley P (1999) Synaptic clustering of AMPA receptors by the extracellular immediate-early gene product Narp. *Neuron* 23:309-323.
- Okabe S, Miwa A, Okado H (2001) Spine formation and correlated assembly of presynaptic and postsynaptic molecules. *J Neurosci* 21:6105-6114.
- Okabe S, Urushido T, Konno D, Okado H, Sobue K (2001) Rapid redistribution of the postsynaptic density protein PSD-Zip45 (Homer 1c) and its differential regulation by NMDA receptors and calcium channels. *J Neurosci* 21:9561-9571.
- Ono F, Higashijima S, Shcherbatko A, Fetcho JR, Brehm P (2001) Paralytic zebrafish lacking acetylcholine receptors fail to localize rapsyn clusters to the synapse. *J Neurosci* 21:5439-5448.
- Packard M, Koo ES, Gorczyca M, Sharpe J, Cumberledge S, Budnik V (2002) The *Drosophila* Wnt, wingless, provides an essential signal for pre- and postsynaptic differentiation. *Cell* 111:319-330.
- Parnas D, Haghghi AP, Fetter RD, Kim SW, Goodman CS (2001) Regulation of postsynaptic structure and protein localization by the Rho-type guanine nucleotide exchange factor dPix. *Neuron* 32:415-424.
- Pasterkamp RJ, Kolodkin AL (2003) Semaphorin junction: making tracks toward neural connectivity. *Curr Opin Neurobiol* 13:79-89.
- Perez-Otano I, Schulteis CT, Contractor A, Lipton SA, Trimmer JS, Sucher NJ, Heinemann SF (2001)

- Assembly with the NR1 subunit is required for surface expression of NR3A-containing NMDA receptors. *J Neurosci* 21:1228-1237.
- Petersen SA, Fetter RD, Noordermeer JN, Goodman CS, DiAntonio A (1997) Genetic analysis of glutamate receptors in *Drosophila* reveals a retrograde signal regulating presynaptic transmitter release. *Neuron* 19:1237-1248.
- Phillips GR, Huang JK, Wang Y, Tanaka H, Shapiro L, Zhang W, Shan WS, Arndt K, Frank M, Gordon RE, Gawinowicz MA, Zhao Y, Colman DR (2001) The presynaptic particle web: ultrastructure, composition, dissolution, and reconstitution. *Neuron* 32:63-77.
- Phillips WD, Maimone MM, Merlie JP (1991) Mutagenesis of the 43-kD postsynaptic protein defines domains involved in plasma membrane targeting and AChR clustering. *J Cell Biol* 115:1713-1723.
- Pinkstaff JK, Detterich J, Lynch G, Gall C (1999) Integrin subunit gene expression is regionally differentiated in adult brain. *J Neurosci* 19:1541-1556.
- Poodry CA, Edgar L (1979) Reversible alteration in the neuromuscular junctions of *Drosophila melanogaster* bearing a temperature-sensitive mutation, shibire. *J Cell Biol* 81:520-527.
- Prange O, Murphy TH (2001) Modular transport of postsynaptic density-95 clusters and association with stable spine precursors during early development of cortical neurons. *J Neurosci* 21:9325-9333.
- Prokop A (1999) Integrating bits and pieces: synapse structure and formation in *Drosophila* embryos. *Cell Tissue Res* 297:169-186.
- Prokop A, Landgraf M, Rushton E, Broadie K, Bate M (1996) Presynaptic development at the *Drosophila* neuromuscular junction: assembly and localization of presynaptic active zones. *Neuron* 17:617-626.
- Prokop A, Martin-Bermudo MD, Bate M, Brown N (1998) Absence of PS integrins or laminin A affects extracellular adhesion, but not intracellular assembly, of hemiadherens and neuromuscular junctions in *Drosophila* embryos. *Dev Biol* 196:58-76.
- Rao A, Cha EM, Craig AM (2000) Mismatched appositions of presynaptic and postsynaptic components in isolated hippocampal neurons. *J Neurosci* 20:8344-8353.
- Rao A, Kim E, Sheng M, Craig AM (1998) Heterogeneity in the molecular composition of excitatory postsynaptic sites during development of hippocampal neurons in culture. *J Neurosci* 18:1217-1229.
- Ren Z, Riley NJ, Needleman LA, Sanders JM, Swanson GT, Marshall J (2003) Cell surface expression of GluR5 kainate receptors is regulated by an endoplasmic reticulum retention signal. *J Biol Chem* 278:52700-52709.
- Rheuben MB, Yoshihara M, Kidokoro Y (1999) Ultrastructural correlates of neuromuscular junction development. *Int Rev Neurobiol* 43:69-92.
- Ritzenthaler S, Suzuki E, Chiba A (2000) Postsynaptic filopodia in muscle cells interact with innervating motoneuron axons. *Nat Neurosci* 3:1012-1017.
- Rosenberg M, Meier J, Triller A, Vannier C (2001) Dynamics of glycine receptor insertion in the neuronal plasma membrane. *J Neurosci* 21:5036-5044.
- Rosenmund C, Stern-Bach Y, Stevens CF (1998) The tetrameric structure of a glutamate receptor channel. *Science* 280:1596-1599.
- Roy PJ, Stuart JM, Lund J, Kim SK (2002) Chromosomal clustering of muscle-expressed genes in *Caenorhabditis elegans*. *Nature* 418:975-979.
- Ruegg MA, Bixby JL (1998) Agrin orchestrates synaptic differentiation at the vertebrate neuromuscular junction. *Trends Neurosci* 21:22-27.
- Safferling M, Tichelaar W, Kummerle G, Jouppila A, Kuusinen A, Keinänen K, Madden DR (2001) First images of a glutamate receptor ion channel: oligomeric state and molecular dimensions of GluRB homomers. *Biochemistry* 40:13948-13953.
- Saitoe M, Tanaka S, Takata K, Kidokoro Y (1997) Neural activity affects distribution of glutamate receptors during neuromuscular junction formation in *Drosophila* embryos. *Dev Biol* 184:48-60.
- Saitoe M, Schwarz TL, Umbach JA, Gundersen CB, Kidokoro Y (2001) Absence of junctional glutamate receptor clusters in *Drosophila* mutants lacking spontaneous transmitter release. *Science* 293:514-517.
- Sanes JR, Lichtman JW (1999) Development of the vertebrate neuromuscular junction. *Annu Rev Neurosci* 22:389-442.
- Sanes JR, Lichtman JW (2001) Induction, assembly, maturation and maintenance of a postsynaptic apparatus. *Nat Rev Neurosci* 2:791-805.
- Scannevin RH, Haganir RL (2000) Postsynaptic organization and regulation of excitatory synapses. *Nat*

- Rev Neurosci 1:133-141.
- Scheiffele P, Fan J, Choih J, Fetter R, Serafini T (2000) Neuroligin expressed in nonneuronal cells triggers presynaptic development in contacting axons. *Cell* 101:657-669.
- Schulze KL, Broadie K, Perin MS, Bellen HJ (1995) Genetic and electrophysiological studies of *Drosophila* syntaxin-1A demonstrate its role in nonneuronal secretion and neurotransmission. *Cell* 80:311-320.
- Schuster CM, Davis GW, Fetter RD, Goodman CS (1996) Genetic dissection of structural and functional components of synaptic plasticity. I. Fasciclin II controls synaptic stabilization and growth. *Neuron* 17:641-654.
- Schuster CM, Ultsch A, Schloss P, Cox JA, Schmitt B, Betz H (1991) Molecular cloning of an invertebrate glutamate receptor subunit expressed in *Drosophila* muscle. *Science* 254:112-114.
- Scott DB, Blanpied TA, Swanson GT, Zhang C, Ehlers MD (2001) An NMDA receptor ER retention signal regulated by phosphorylation and alternative splicing. *J Neurosci* 21:3063-3072.
- Shapira M, Zhai RG, Dresbach T, Bresler T, Torres VI, Gundelfinger ED, Ziv NE, Garner CC (2003) Unitary assembly of presynaptic active zones from Piccolo-Bassoon transport vesicles. *Neuron* 38:237-252.
- Shen K, Bargmann CI (2003) The immunoglobulin superfamily protein SYG-1 determines the location of specific synapses in *C. elegans*. *Cell* 112:619-630.
- Shen K, Fetter RD, Bargmann CI (2004) Synaptic specificity is generated by the synaptic guidepost protein SYG-2 and its receptor, SYG-1. *Cell* 116:869-881.
- Sheng M (2001) Molecular organization of the postsynaptic specialization. *Proc Natl Acad Sci U S A* 98:7058-7061.
- Sheng M, Lee SH (2001) AMPA receptor trafficking and the control of synaptic transmission. *Cell* 105:825-828.
- Sheridan DL, Berlot CH, Robert A, Inglis FM, Jakobsdottir KB, Howe JR, Hughes TE (2002) A new way to rapidly create functional, fluorescent fusion proteins: random insertion of GFP with an in vitro transposition reaction. *BMC Neurosci* 3:7.
- Sigrist SJ, Thiel PR, Reiff DF, Schuster CM (2002) The postsynaptic glutamate receptor subunit DGluR-IIA mediates long-term plasticity in *Drosophila*. *J Neurosci* 22:7362-7372.
- Sigrist SJ, Thiel PR, Reiff DF, Lachance PE, Lasko P, Schuster CM (2000) Postsynaptic translation affects the efficacy and morphology of neuromuscular junctions. *Nature* 405:1062-1065.
- Sone M, Suzuki E, Hoshino M, Hou D, Kuromi H, Fukata M, Kuroda S, Kaibuchi K, Nabeshima Y, Hama C (2000) Synaptic development is controlled in the periaxonal zones of *Drosophila* synapses. *Development* 127:4157-4168.
- Sprengel R, Aronoff R, Volkner M, Schmitt B, Mosbach R, Kuner T (2001) Glutamate receptor channel signatures. *Trends Pharmacol Sci* 22:7-10.
- Standley S, Baudry M (2000) The role of glycosylation in ionotropic glutamate receptor ligand binding, function, and trafficking. *Cell Mol Life Sci* 57:1508-1516.
- Stathopoulos A, Levine M (2002) Whole-genome expression profiles identify gene batteries in *Drosophila*. *Dev Cell* 3:464-465.
- Sudhof TC (2000) The synaptic vesicle cycle revisited. *Neuron* 28:317-320.
- Sweeney ST, Broadie K, Keane J, Niemann H, O'Kane CJ (1995) Targeted expression of tetanus toxin light chain in *Drosophila* specifically eliminates synaptic transmission and causes behavioral defects. *Neuron* 14:341-351.
- Tejedor FJ, Bokhari A, Rogero O, Gorczyca M, Zhang J, Kim E, Sheng M, Budnik V (1997) Essential role for dlg in synaptic clustering of Shaker K⁺ channels in vivo. *J Neurosci* 17:152-159.
- Thibault ST, Singer MA, Miyazaki WY, Milash B, Dompe NA, Singh CM, Buchholz R, Demsky M, Fawcett R, Francis-Lang HL, Ryner L, Cheung LM, Chong A, Erickson C, Fisher WW, Greer K, Hartouni SR, Howie E, Jakkula L, Joo D, Killpack K, Laufer A, Mazzotta J, Smith RD, Stevens LM, Stuber C, Tan LR, Ventura R, Woo A, Zakrajsek I, Zhao L, Chen F, Swimmer C, Kopczynski C, Duyk G, Winberg ML, Margolis J (2004) A complementary transposon tool kit for *Drosophila melanogaster* using P and piggyBac. *Nat Genet* 36:283-287.
- Thomas U, Kim E, Kuhlendahl S, Koh YH, Gundelfinger ED, Sheng M, Garner CC, Budnik V (1997) Synaptic clustering of the cell adhesion molecule fasciclin II by discs-large and its role in the regulation of presynaptic structure. *Neuron* 19:787-799.
- Togashi H, Abe K, Mizoguchi A, Takaoka K, Chisaka O, Takeichi M (2002) Cadherin regulates dendritic spine morphogenesis. *Neuron* 35:77-89.
- Valenzuela DM, Stitt TN, DiStefano PS, Rojas E, Mattsson K, Compton DL, Nunez L, Park JS, Stark JL, Gies DR, et al. (1995) Receptor tyrosine kinase specific for the skeletal muscle lineage: expression in embryonic muscle, at the neuromuscular junction, and after injury. *Neuron*

- 15:573-584.
- Vandenbergh W, Bredt DS (2004) Early events in glutamate receptor trafficking. *Curr Opin Cell Biol* 16:134-139.
- Varoqueaux F, Sigler A, Rhee JS, Brose N, Enk C, Reim K, Rosenmund C (2002) Total arrest of spontaneous and evoked synaptic transmission but normal synaptogenesis in the absence of Munc13-mediated vesicle priming. *Proc Natl Acad Sci U S A* 99:9037-9042.
- Verhage M, Maia AS, Plomp JJ, Brussaard AB, Heeroma JH, Vermeer H, Toonen RF, Hammer RE, van den Berg TK, Missler M, Geuze HJ, Südhof TC (2000) Synaptic assembly of the brain in the absence of neurotransmitter secretion. *Science* 287:864-869.
- Wallace BG (1989) Agrin-induced specializations contain cytoplasmic, membrane, and extracellular matrix-associated components of the postsynaptic apparatus. *J Neurosci* 9:1294-1302.
- Wan H, DiAntonio A, Fetter RD, Bergstrom K, Strauss R, Goodman CS (2000) Highwire regulates synaptic growth in *Drosophila*. *Neuron* 26:313-329.
- Washbourne P, Bennett JE, McAllister AK (2002) Rapid recruitment of NMDA receptor transport packets to nascent synapses. *Nat Neurosci* 5:751-759.
- Wenthold RJ, Petralia RS, Blahos J, II, Niedzielski AS (1996) Evidence for multiple AMPA receptor complexes in hippocampal CA1/CA2 neurons. *J Neurosci* 16:1982-1989.
- Weston C, Yee B, Hod E, Prives J (2000) Agrin-induced acetylcholine receptor clustering is mediated by the small guanosine triphosphatases Rac and Cdc42. *J Cell Biol* 150:205-212.
- Weston C, Gordon C, Teresa G, Hod E, Ren XD, Prives J (2003) Cooperative regulation by Rac and Rho of agrin-induced acetylcholine receptor clustering in muscle cells. *J Biol Chem* 278:6450-6455.
- White JG, Southgate E, Thomson JN, Brenner S (1976) The structure of the ventral nerve cord of *Caenorhabditis elegans*. *Philos Trans R Soc Lond B Biol Sci* 275:327-348.
- Wojtowicz JM, Marin L, Atwood HL (1994) Activity-induced changes in synaptic release sites at the crayfish neuromuscular junction. *J Neurosci* 14:3688-3703.
- Wucherpfennig T, Wilsch-Brauninger M, Gonzalez-Gaitan M (2003) Role of *Drosophila* Rab5 during endosomal trafficking at the synapse and evoked neurotransmitter release. *J Cell Biol* 161:609-624.
- Xia H, Hornby ZD, Malenka RC (2001) An ER retention signal explains differences in surface expression of NMDA and AMPA receptor subunits. *Neuropharmacology* 41:714-723.
- Xia H, von Zastrow M, Malenka RC (2002) A novel anterograde trafficking signal present in the N-terminal extracellular domain of ionotropic glutamate receptors. *J Biol Chem* 277:47765-47769.
- Yamagata M, Sanes JR, Weiner JA (2003) Synaptic adhesion molecules. *Curr Opin Cell Biol* 15:621-632.
- Yang X, Arber S, William C, Li L, Tanabe Y, Jessell TM, Birchmeier C, Burden SJ (2001) Patterning of muscle acetylcholine receptor gene expression in the absence of motor innervation. *Neuron* 30:399-410.
- Yoshihara CM, Hall ZW (1993) Increased expression of the 43-kD protein disrupts acetylcholine receptor clustering in myotubes. *J Cell Biol* 122:169-179.
- Yoshihara M, Rheuben MB, Kidokoro Y (1997) Transition from growth cone to functional motor nerve terminal in *Drosophila* embryos. *J Neurosci* 17:8408-8426.
- Zhai RG, Vardinon-Friedman H, Cases-Langhoff C, Becker B, Gundelfinger ED, Ziv NE, Garner CC (2001) Assembling the presynaptic active zone: a characterization of an active one precursor vesicle. *Neuron* 29:131-143.
- Zhang FL, Casey PJ (1996) Protein prenylation: molecular mechanisms and functional consequences. *Annu Rev Biochem* 65:241-269.
- Zhou H, Glass DJ, Yancopoulos GD, Sanes JR (1999) Distinct domains of MuSK mediate its abilities to induce and to associate with postsynaptic specializations. *J Cell Biol* 146:1133-1146.
- Zito K, Fetter RD, Goodman CS, Isacoff EY (1997) Synaptic clustering of Fascilin II and Shaker: essential targeting sequences and role of Dlg. *Neuron* 19:1007-1016.

Appendix

Genes enriched in larval body wall preparations

Abundance	Fold change	Gene description
23719.6	~26.8	FB:FBgn0031264 /sym=CG11835 /name= /prod= /func=DNA binding /map=21C6-21C6 /transc=CT33127 /len=2494 /GB:AE003589
102926.3	25.1	FB:FBgn0038943 /sym=CG5391 /name= /prod= /func= /map=94A12-94A13 /transc=CT17120 /len=755 /GB:AE003738
54625.7	20.3	FB:FBgn0038152 /sym=CG9792 /name= /prod= /func= /map=87E11-87E11 /transc=CT27648 /len=1695 /GB:AE003700
19700	20.2	FB:FBgn0025393 /sym=EG:196F3.3 /name= /prod= /func= /map=2B2-2B2 /transc=CT34605 /len=351 /GB:AE003421
95020.4	16.9	FB:FBgn0039299 /sym=CG11854 /name= /prod= /func= /map=96C4-96C4 /transc=CT33075 /len=1001 /GB:AE003751
11605.6	~15.3	FB:FBgn0037601 /sym=Cyp313b1 /name= /prod=cytochrome P450, CYP313B1 /func=cytochrome P45 /map=85A10-85A10 /transc=CT27472 /len=1494 /GB:AE003679
64568.5	15.1	FB:FBgn0003046 /sym=Pcp /name=Pupal cuticle protein /prod= /func=structural protein of pupal cuticle (<i>Drosophila</i>) /map=27D1-27D1 /transc=CT11573 /len=575 /GB:AE003615
15304.4	~14.7	FB:FBgn0039755 /sym=CG15531 /name= /prod= /func=enzyme /map=99E3-99E3 /transc=CT35646 /len=1005 /GB:AE003772
10859.7	~14.3	FB:FBgn0000422 /sym=Ddc /name=Dopa decarboxylase /prod=dopa decarboxylase /func=aromatic-L-amino-acid decarboxylase ; EC:4.1.1.28 /map=37C1-37C1 /transc=CT38799 /len=1889 /GB:AE003772
20881.3	13.6	FB:FBgn0016675 /sym=Lectin-galC1 /name=Galactose-specific C-type lectin /prod=galactose-specific C-type lectin /func=galactose binding lectin /map=37E1-37E1 /transc=CT28109 /len=746 /GB:AE003772
20429.4	13.5	FB:FBgn0038180 /sym=CG9307 /name= /prod= /func=enzyme /map=87F13-87F13 /transc=CT26495 /len=2109 /GB:AE003701 /note=3prime sequence from clone BDGP:LP08894.3prime-hit
25782.1	12.7	FB:FBgn0039030 /sym=CG6660 /name= /prod= /func= /map=94D4-94D4 /transc=CT20704 /len=819 /GB:AE003741
200301.9	11.9	FB:FBgn0037114 /sym=CG7160 /name= /prod=cuticle protein /func=structural protein /map=78F1-78F1 /transc=CT22123 /len=441 /GB:AE003595
15276.1	11.9	FB:FBgn0015565 /sym=yin /name=yin /prod=hydrogen/oligopeptide symporter /func=hydrogen/oligopeptide symporter /map=4A1-4A1 /transc=CT9924 /len=2544 /GB:AE003429 /note=3prime sequ
6628	~11.4	FB:FBgn0035711 /sym=CG8519 /name= /prod=RAS small GTPase-like /func=signal transduction /map=65C3-65C3 /transc=CT24887 /len=606 /GB:AE003561
6730.9	~11.3	FB:FBgn0036364 /sym=CG14109 /name= /prod= /func= /map=70A8-70A8 /transc=CT33704 /len=732 /GB:AE003538
8660.2	~10.9	FB:FBgn0033667 /sym=CG13183 /name= /prod= /func= /map=48D1-48D1 /transc=CT32424 /len=1356 /GB:AE003824
12992.1	10.8	FB:FBgn0029544 /sym=CG16994 /name= /prod= /func= /map=1D1-1D1 /transc=CT34390 /len=1155 /GB:AE003419
92230.8	10.5	FB:FBgn0037083 /sym=CG5656 /name= /prod=alkaline phosphatase-like /func=enzyme /map=78D5-78D5 /transc=CT17844 /len=1770 /GB:AE003594 /note=3prime sequence from clone BDGP:LP08894.3prime-hit
15667	10.4	FB:FBgn0030357 /sym=CG2471 /name= /prod= /func=actin binding /map=10F8-10F9 /transc=CT8171 /len=1103 /GB:AE003487 /note=3prime sequence from clone BDGP:LP11415.3prime-hit
10666	~10.3	FB:FBgn0023550 /sym=EG:103B4.2 /name= /prod= /func= /map=2E2-2E2 /transc=CT40356 /len=1517 /GB:AE003423
8699.1	~10.3	FB:FBgn0035813 /sym=CG8492 /name= /prod=lysozyme P /func=defense/immunity protein /map=66A10-66A10 /transc=CT14304 /len=2709 /GB:AE003558
8511.4	~10.0	FB:FBgn0033289 /sym=CG2121 /name= /prod= /func=transporter /map=44C1-44C1 /transc=CT6910 /len=1360 /GB:AE003837 /note=3prime sequence from clone BDGP:GH09628.3prime-hit
10694.8	9.9	FB:FBgn0033726 /sym=CG8836 /name= /prod=larval cuticle protein-like /func=structural protein /map=49A2-49A2 /transc=CT25408 /len=501 /GB:AE003822
11203.2	9.6	FB:FBgn0036264 /sym=CG11529 /name= /prod=trypsin-like /func=endopeptidase /map=68F8-68F8 /transc=CT21438 /len=864 /GB:AE003542
14520.8	9.6	FB:FBgn0038179 /sym=CG9312 /name= /prod= /func= /map=87F13-87F13 /transc=CT26517 /len=784 /GB:AE003701 /note=3prime sequence from clone BDGP:GH09754.3prime-hit
106759.7	9.5	FB:FBgn0034856 /sym=CG9891 /name= /prod= /func= /map=59D9-59D9 /transc=CT27880 /len=1266 /GB:AE003460

8081 ~9.1 FB:FBgn0032349 /sym=CG4779 /name= /prod= /func= /map=32D4-32D4 /transc=CT15337 /len=1272 /GB:AE003631
 7297.3 ~9.1 FB:FBgn0033858 /sym=CG13335 /name= /prod= /func= /map=50B7-50B7 /transc=CT32654 /len=408 /GB:AE003818
 6026.4 ~8.9 FB:FBgn0040868 /sym=CG15762 /name= /prod= /func= /map=12B10-12B10 /transc=CT36016 /len=240 /GB:AE003493
 10038.8 8.9 FB:FBgn0037319 /sym=CG2666 /name= /prod=chitin synthase-like /func=enzyme /map=83A5-83A5 /transc=CT9021 /len=3897 /GB:AE003603
 17201.8 8.6 FB:FBgn0034443 /sym=CG10460 /name= /prod= /func=endopeptidase /map=56D4-56D4 /transc=CT29364 /len=485 /GB:AE003796
 30755.5 8.5 FB:FBgn0035964 /sym=CG4665 /name=dihydropteridine reductase /prod=dihydropteridine reductase-like /func=dihydropteridine reductase /map=66F6-66F6 /transc=CT15055 /len=708 /GB:AE003500
 22531.1 8.3 FB:FBgn0035427 /sym=CG14959 /name= /prod= /func= /map=63C2-63C2 /transc=CT34804 /len=450 /GB:AE003477
 10634.5 8.2 FB:FBgn0029821 /sym=CG4020 /name= /prod= /func= /map=5C6-5C6 /transc=CT13322 /len=1485 /GB:AE003435
 11276.3 7.8 FB:FBgn0035300 /sym=CG1139 /name= /prod=amino-acid permease-like /func=transporter /map=62B11-62B11 /transc=CT1131 /len=1511 /GB:AE003473
 19312.7 7.7 FB:FBgn0038348 /sym=CG18519 /name= /prod= /func= /map=88F8-88F8 /transc=CT42266 /len=3671 /GB:AE003709
 7383.3 ~7.7 FB:FBgn0034253 /sym=CG10936 /name= /prod= /func=endopeptidase /map=54D3-54D4 /transc=CT30629 /len=4407 /GB:AE003802
 6329 ~7.4 FB:FBgn0038629 /sym=CG14304 /name= /prod= /func= /map=91B4-91B4 /transc=CT33934 /len=3585 /GB:AE003722
 19301.8 7.3 FB:FBgn0031791 /sym=CG9486 /name= /prod= /func=enzyme /map=26C1-26C1 /transc=CT26862 /len=651 /GB:AE003613
 7576.3 ~7.3 FB:FBgn0037503 /sym=CG14598 /name= /prod= /func= /map=84D3-84D3 /transc=CT34346 /len=690 /GB:AE003671
 22097.3 7.3 FB:FBgn0037761 /sym=CG8534 /name= /prod= /func= /map=85E10-85E10 /transc=CT24919 /len=818 /GB:AE003684
 63005.9 7.2 FB:FBgn0030326 /sym=CG2444 /name= /prod= /func= /map=10D4-10D4 /transc=CT8084 /len=635 /GB:AE003487
 5453.9 ~7.2 FB:FBgn0000594 /sym=Est-P /name=Esterase P /prod=carboxylesterase /func=carboxylesterase ; EC:3.1.1.1 /map=68F8-68F8 /transc=CT38084 /len=1635 /GB:AE003542
 101119.9 7.1 FB:FBgn0034162 /sym=CG6426 /name= /prod=calcium binding protein-like /func=ligand binding or carrier /map=53D15-53D15 /transc=CT19886 /len=426 /GB:AE003805
 6255.2 ~7.1 FB:FBgn0033136 /sym=CG12838 /name= /prod= /func= /map=42E2-42E2 /transc=CT31970 /len=633 /GB:AE003842
 5606.4 ~7.0 FB:FBgn0026190 /sym=prolyl-4-hydroxylase-alpha /name=prolyl 4-hydroxylase alpha /prod=procollagen-proline,2-oxoglutarate-4-dioxygenase, alpha subunit /func=procollagen-proline,2-oxoglutarate-4-dioxygenase, alpha subunit
 7498.3 7 FB:FBgn0037905 /sym=CG14703 /name= /prod= /func= /map=86E6-86E6 /transc=CT34493 /len=1397 /GB:AE003691
 5278.4 ~7.0 FB:FBgn0033099 /sym=CG9435 /name= /prod= /func= /map=42C3-42C3 /transc=CT26754 /len=594 /GB:AE003789
 5163.4 ~6.8 FB:FBgn0031564 /sym=CG2816 /name= /prod=chymotrypsin inhibitor-like /func=enzyme inhibitor /map=24A5-24A5 /transc=CT9603 /len=292 /GB:AE003579
 169802.4 6.7 FB:FBgn0033595 /sym=CG18337 /name= /prod= /func= /map=47E1-47E1 /transc=CT41641 /len=540 /GB:AE003826
 11072.1 6.7 FB:FBgn0022702 /sym=Cht2 /name=Chitinase 2 /prod=chitinase /func=chitinase ; EC:3.2.1.14 /map=62B1-62B1 /transc=CT6562 /len=1597 /GB:AE003472 /note=3prime sequence from clone BDGP:10038.8
 19916.4 6.6 FB:FBgn0022770 /sym=Peritrophin-A /name=Peritrophin A /prod=peritrophin A /func=chitin binding /map=19C1-19C1 /transc=CT35567 /len=1232 /GB:AE003572 /note=3prime sequence from clone BDGP:10038.8
 FB:FBgn0010222 /sym=Nmdmc /name=NAD-dependent methylenetetrahydrofolate dehydrogenase /prod=NAD-dependent methylenetetrahydrofolate dehydrogenase /func=methylenetetrahydrofolate dehydrogenase
 7115.8 6.6 /GB:AE003
 2204.1 ~6.6 FB:FBgn0039098 /sym=CG13822 /name= /prod= /func= /map=95B1-95B1 /transc=CT33322 /len=651 /GB:AE003744
 4567.9 ~6.6 FB:FBgn0035553 /sym=CG13722 /name= /prod=prolin-rich protein-like /func=structural protein /map=64B12-64B12 /transc=CT33188 /len=2124 /GB:AE003481
 5343.8 ~6.6 FB:FBgn0027570 /sym=BcDNA:GH07643 /name= /prod=membrane-anchored zinc metalloendopeptidase-like (M13 peptidase) /func=endopeptidase /map=82D6-82D7 /transc=CT27583 /len=2739 /GB:AE003579
 78514.5 6.5 FB:FBgn0039482 /sym=CG14258 /name= /prod= /func= /map=97E6-97E6 /transc=CT33878 /len=777 /GB:AE003759
 80923 6.5 FB:FBgn0034517 /sym=CG18066 /name= /prod= /func= /map=57A8-57A8 /transc=CT40491 /len=625 /GB:AE003791 /note=3prime sequence from clone BDGP:GH09112.3prime-hit

18578.3	6.5	FB:FBgn0030976 /sym=CG7378 /name= /prod=protein phosphatase-like /func=protein phosphatase /map=17E8-17E8 /transc=CT22699 /len=738 /GB:AE003510
11156	6.5	FB:FBgn0033022 /sym=CG10398 /name= /prod= /func= /map=41C1-41C1 /transc=CT29180 /len=501 /GB:AE003786
14907.6	6.4	FB:FBgn0038053 /sym=CG18549 /name= /prod= /func= /map=87C1-87C1 /transc=CT17408 /len=1634 /GB:AE003696
10676.1	6.4	FB:FBgn0031542 /sym=CG15414 /name= /prod= /func= /map=23F3-23F3 /transc=CT35473 /len=963 /GB:AE003579
4298	~6.3	FB:FBgn0035755 /sym=CG14830 /name= /prod= /func= /map=65E10-65E10 /transc=CT34646 /len=972 /GB:AE003559
61989.6	6.3	FB:FBgn0035684 /sym=CG10461 /name= /prod=cuticle protein-like /func=structural protein /map=65A5-65A5 /transc=CT29366 /len=321 /GB:AE003563
36997.1	6.3	FB:FBgn0034860 /sym=CG9812 /name= /prod= /func= /map=59D10-59D11 /transc=CT42639 /len=611 /GB:AE003460
8959.2	6.3	FB:FBgn0030816 /sym=CG16700 /name= /prod=amino-acid permease-like /func=G protein linked receptor /map=15D2-15D3 /transc=CT37167 /len=1673 /GB:AE003504
5244.5	~6.3	FB:FBgn0038449 /sym=CG17562 /name= /prod= /func=enzyme /map=89D5-89D5 /transc=CT34716 /len=1416 /GB:AE003714
33816.6	6.2	FB:FBgn0030558 /sym=CG1461 /name= /prod=tyrosine aminotransferase /func=enzyme /map=12E1-12E1 /transc=CT3554 /len=1844 /GB:AE003495
5926.4	~6.1	FB:FBgn0039111 /sym=CG10371 /name= /prod= /func=protein phosphatase /map=95B7-95B7 /transc=CT29124 /len=585 /GB:AE003744
5751.7	6.1	FB:FBgn0039895 /sym=CG11288 /name= /prod=fibrillin-like /func=cell adhesion /map=102A3-102A3 /transc=CT31491 /len=914 /GB:AE003844
34282.6	6.1	FB:FBgn0031737 /sym=CG11142 /name= /prod=peritrophin-like /func=structural protein /map=26A1-26A1 /transc=CT31147 /len=1457 /GB:AE003611
36701.5	6	FB:FBgn0038366 /sym=CG4576 /name= /prod= /func= /map=89A8-89A8 /transc=CT14818 /len=2581 /GB:AE003710
4539.5	~6.0	FB:FBgn0023540 /sym=EG:152A3.3 /name= /prod= /func= /map=2E1-2E1 /transc=CT12189 /len=1918 /GB:AE003423 /note=3prime sequence from clone BDGP:HL01173.3prime-hit
9254.7	5.9	FB:FBgn0035936 /sym=CG4999 /name= /prod= /func= /map=66E3-66E3 /transc=CT16000 /len=1131 /GB:AE003553
68492.5	5.9	FB:FBgn0020439 /sym=fau /name= /prod=anoxia upregulated protein /func= /map=86C4-86C4 /transc=CT41978 /len=2121 /GB:AE003688
23518.7	5.8	FB:FBgn0027600 /sym=BcDNA:GH02976 /name= /prod=peritrophin-like /func=ligand binding or carrier /map=30F6-30F6 /transc=CT15349 /len=1095 /GB:AE003627 /note=3prime sequence from c
4834	~5.8	FB:FBgn0037186 /sym=CG11241 /name= /prod=pyridoxal-phosphate-dependent aminotransferase class-III /func=enzyme /map=79F2-79F2 /transc=CT31379 /len=1856 /GB:AE003598 /note=3prime
3240.1	~5.8	FB:FBgn0030595 /sym=CG14406 /name= /prod= /func= /map=13A1-13A1 /transc=CT34057 /len=312 /GB:AE003497
4244.5	~5.8	BDGP:GH188.3prime-hit /ESTpos=maps in FB:FBgn0036365 /sym=CG10732 /name= /prod= /func=signal transduction /map=7A8-7A8 /transc=CT369 /len=535
133216.6	5.8	FB:FBgn0010019 /sym=Cyp4g1 /name=Cytochrome P45-4g1 /prod=cytochrome P450, CYP4G1 /func=cytochrome P45 ; EC:1.14.14.1 /map=1B3-1B3 /transc=CT13187 /len=2267 /GB:AE003417 /no
223808.8	5.7	FB:FBgn0033725 /sym=CG8502 /name= /prod=cuticle protein /func=structural protein /map=49A2-49A2 /transc=CT24855 /len=1413 /GB:AE003822 /note=3prime sequence from clone BDGP:LP07
15326.8	5.7	FB:FBgn0029838 /sym=CG4666 /name= /prod= /func= /map=5D2-5D2 /transc=CT15013 /len=729 /GB:AE003436
6663.7	~5.6	FB:FBgn0035304 /sym=CG1282 /name= /prod=titin/twitchin-like /func=cell adhesion /map=62C3-62C3 /transc=CT2687 /len=2392 /GB:AE003473
4180.6	~5.6	FB:FBgn0028922 /sym=BG:DS00929.8 /name= /prod= /func= /map=35C1-35C1 /transc=CT12287 /len=1508 /GB:AE003646
30948	5.6	FB:FBgn0030394 /sym=CG2560 /name= /prod=cuticle protein-like /func=structural protein /map=11B7-11B7 /transc=CT8657 /len=893 /GB:AE003489
4313.6	~5.6	FB:FBgn0036185 /sym=CG7346 /name= /prod=ATP-binding cassette transporter /func=enzyme /map=68C10-68C11 /transc=CT22647 /len=1794 /GB:AE003544
2815.4	~5.6	FB:FBgn0033290 /sym=CG8698 /name= /prod= /func= /map=44C1-44C1 /transc=CT8775 /len=504 /GB:AE003837
4744	~5.5	FB:FBgn0035289 /sym=CG12026 /name= /prod= /func= /map=62B9-62B9 /transc=CT1797 /len=1455 /GB:AE003473 /note=3prime sequence from clone BDGP:LP10272.3prime-hit
4859.8	5.5	FB:FBgn0031872 /sym=CG9211 /name= /prod= /func=cell adhesion /map=27C5-27C6 /transc=CT26314 /len=3247 /GB:AE003615 /note=3prime sequence from clone BDGP:GH03927.3prime-hit
33949.7	5.5	FB:FBgn0032497 /sym=CG6043 /name= /prod= /func= /map=34A11-34B1 /transc=CT18935 /len=3263 /GB:AE003639

3265 ~5.5 FB:FBgn0035457 /sym=CG12604 /name= /prod= /func= /map=63E8-63E8 /transc=CT34822 /len=936 /GB:AE003479

10486.1 5.4 FB:FBgn0037534 /sym=CG2781 /name= /prod= /func=1,3-beta-glucan synthase /map=84E5-84E5 /transc=CT9465 /len=831 /GB:AE003677

46425 5.3 FB:FBgn0034920 /sym=CG5597 /name= /prod= /func= /map=60A8-60A8 /transc=CT17698 /len=897 /GB:AE003462 /note=3prime sequence from clone BDGP:GH04238.3prime-hit

109250.5 5.3 FB:FBgn0035985 /sym=CG3672 /name= /prod= /func=structural protein /map=67B2-67B2 /transc=CT12317 /len=997 /GB:AE003552 /note=3prime sequence from clone BDGP:GH12638.3prime-hit

5817 ~5.3 FB:FBgn0030065 /sym=CG12075 /name= /prod= /func=transcription factor /map=8B4-8B4 /transc=CT5152 /len=3406 /GB:AE003445 /note=3prime sequence from clone BDGP:LD23217.3prime-hit

5570.1 5.3 FB:FBgn0032230 /sym=CG13139 /name= /prod= /func= /map=31D10-31D10 /transc=CT32379 /len=807 /GB:AE003628

5566.8 ~5.3 FB:FBgn0037805 /sym=CG11871 /name= /prod= /func= /map=86A1-86A1 /transc=CT37022 /len=3575 /GB:AE003686

7060.1 5.3 FB:FBgn0035705 /sym=CG8352 /name= /prod= /func= /map=65B4-65B5 /transc=CT24625 /len=1728 /GB:AE003562 /note=3prime sequence from clone BDGP:LD26402.3prime-hit

54759.6 5.3 FB:FBgn0031971 /sym=CG7224 /name= /prod= /func= /map=28D11-28D11 /transc=CT22279 /len=755 /GB:AE003619 /note=3prime sequence from clone BDGP:GH18422.3prime-hit

16382.2 5.2 FB:FBgn0033509 /sym=CG12908 /name= /prod=nidogen-like /func=cell adhesion /map=47A1-47A1 /transc=CT32053 /len=4591 /GB:AE003830 /note=3prime sequence from clone BDGP:LD35637.3prime-hit

26464.9 5.2 FB:FBgn0036985 /sym=CG5847 /name= /prod= /func=structural protein /map=77B9-77B9 /transc=CT18331 /len=6855 /GB:AE003591

7616.8 5.2 FB:FBgn0022701 /sym=Cht3 /name=Chitinase 3 /prod=chitinase /func=chitinase ; EC:3.2.1.14 /map=40D5-40D5 /transc=CT40797 /len=3899 /GB:AE002743

5485.4 5.2 FB:FBgn0039690 /sym=CG1969 /name= /prod= /func=glucosamine-phosphate N-acetyltransferase ; EC:2.3.1.4 /map=99C1-99C1 /transc=CT4002 /len=1206 /GB:AE003771 /note=3prime sequence from clone BDGP:LD35637.3prime-hit

17808.5 5.2 FB:FBgn0029898 /sym=CG14439 /name= /prod=permease-like /func=transporter /map=6C11-6C11 /transc=CT34101 /len=1608 /GB:AE003438

9052.4 5.2 FB:FBgn0032993 /sym=CG18117 /name= /prod=chitinase-like /func=enzyme /map=40E1-40E1 /transc=CT40795 /len=1393 /GB:AE002743 /note=3prime sequence from clone BDGP:LP05745.3prime-hit

13143.1 5.2 FB:FBgn0032601 /sym=yellow-b /name=yellow-b /prod= /func= /map=36A8-36A8 /transc=CT39906 /len=1625 /GB:AE003652 /note=3prime sequence from clone BDGP:LD43175.3prime-hit

12986.1 5.1 FB:FBgn0035398 /sym=CG1869 /name= /prod=chitinase /func=enzyme /map=63B8-63B8 /transc=CT5720 /len=2346 /GB:AE003477

4051.1 ~5.1 FB:FBgn0039658 /sym=CG11956 /name= /prod= /func= /map=99A5-99A5 /transc=CT39158 /len=2937 /GB:AE003768 /note=3prime sequence from clone BDGP:LD35296.3prime-hit

5334.1 5.1 FB:FBgn0010388 /sym=Dro /name=Drosocin /prod=drosocin /func=antibacterial response protein /map=51C2-51C2 /transc=CT30318 /len=195 /GB:AE003813

197731.7 5 FB:FBgn0031908 /sym=CG5177 /name= /prod= /func=enzyme /map=27F6-27F6 /transc=CT16575 /len=980 /GB:AE003617 /note=3prime sequence from clone BDGP:LD18740.3prime-hit

2785.1 ~5.0 FB:FBgn0000152 /sym=Axs /name=Abnormal X segregation /prod= /func= /map=15A1-15A1 /transc=CT27428 /len=2396 /GB:AE003503

197877.5 5 FB:FBgn0032281 /sym=CG17107 /name= /prod= /func= /map=32A1-32A1 /transc=CT33651 /len=291 /GB:AE003629

53720.9 5 FB:FBgn0002440 /sym=l(3)mbn /name=lethal (3) malignant blood neoplasm /prod= /func= /map=65A4-65A4 /transc=CT29378 /len=1957 /GB:AE003563

12614.8 5 FB:FBgn0035103 /sym=CG7047 /name= /prod=arrestin-like /func= /map=61A5-61A5 /transc=CT42521 /len=1187 /GB:AE003467

13720.8 5 FB:FBgn0039894 /sym=CG10323 /name= /prod=fibulin/fibrillin-like /func=cell adhesion /map=102A1-102A3 /transc=CT7856 /len=1684 /GB:AE003844

8379.4 5 FB:FBgn0036271 /sym=CG10335 /name= /prod=porphobilinogen synthase-like /func=enzyme /map=69A3-69A3 /transc=CT29022 /len=984 /GB:AE003542

67255.1 5 FB:FBgn0034420 /sym=CG10737 /name= /prod=protein kinase-like /func=protein kinase /map=56B6-56C1 /transc=CT21097 /len=3105 /GB:AE003797 /note=3prime sequence from clone BDGP:GM003535

3691.1 ~4.9 FB:FBgn0013718 /sym=nuf /name=nuclear fallout /prod= /func=cytoskeletal structural protein /map=70D2-70D2 /transc=CT23449 /len=2261 /GB:AE003535

12605.8 4.9 FB:FBgn0033130 /sym=CG12843 /name=Tetraspanin 42Ei /prod=tetraspanin /func= /map=42E1-42E1 /transc=CT31975 /len=967 /GB:AE003842

17969.2 4.9 FB:FBgn0040631 /sym=CG13249 /name= /prod= /func= /map=77C2-77C2 /transc=CT32502 /len=432 /GB:AE003591 /note=3prime sequence from clone BDGP:LD43096.3prime-hit

3852.4 ~4.9 FB:FBgn0032382 /sym=CG14935 /name= /prod=maltase 2-like /func=enzyme /map=33B2-33B2 /transc=CT34763 /len=1790 /GB:AE003634

105433 4.9 FB:FBgn0038774 /sym=CG5023 /name= /prod=calponin-like /func=ligand binding or carrier /map=92D2-92D2 /transc=CT16114 /len=697 /GB:AE003729 /note=3prime sequence from clone BDGP:GM003535

84895.4 4.9 FB:FBgn0032774 /sym=CG17549 /name= /prod= /func= /map=37E1-37E1 /transc=CT38763 /len=1051 /GB:AE003662 /note=3prime sequence from clone BDGP:GH19142.3prime-hit

1602.3 ~4.9 FB:FBgn0035155 /sym=CG12015 /name= /prod= /func=transporter /map=61C9-61C9 /transc=CT1655 /len=728 /GB:AE003469

3659 ~4.8 FB:FBgn0036561 /sym=CG5891 /name= /prod=ankyrin-like /func=cytoskeletal structural protein /map=72D1-72D3 /transc=CT18415 /len=3517 /GB:AE003528

13249.8 4.8 FB:FBgn0038250 /sym=CG3505 /name= /prod= /func=endopeptidase /map=88C11-88C11 /transc=CT11805 /len=1161 /GB:AE003705 /note=3prime sequence from clone BDGP:LP10895.3prime-hit

11889.5 4.7 FB:FBgn0033724 /sym=CG8501 /name= /prod= /func= /map=49A2-49A2 /transc=CT24861 /len=902 /GB:AE003822 /note=3prime sequence from clone BDGP:HL07915.3prime-hit

9091.4 4.7 FB:FBgn0027617 /sym=Rbp9 /name= /prod= /func=RNA binding /map=23C1-23C2 /transc=CT38165 /len=3320 /GB:AE003581 /note=3prime sequence from clone BDGP:GH07919.3prime-hit

19529.2 4.7 FB:FBgn0036454 /sym=CG17839 /name= /prod= /func=cell adhesion /map=71A1-71A1 /transc=CT39634 /len=3570 /GB:AE003533

33251.3 4.7 FB:FBgn0034603 /sym=CG9480 /name= /prod=glycogenin glucosyltransferase-like /func=enzyme /map=57C7-57C7 /transc=CT26834 /len=950 /GB:AE003453

4041.9 ~4.7 FB:FBgn0003888 /sym=betaTub60D /name=betaTubulin6D /prod=beta-tubulin /func=cytoskeletal structural protein /map=60C5-60C5 /transc=CT11425 /len=1542 /GB:AE003463

12224.7 4.7 FB:FBgn0038151 /sym=CG17044 /name= /prod= /func= /map=87E11-87E11 /transc=CT37841 /len=1281 /GB:AE003700

9605 4.6 FB:FBgn0029662 /sym=CG12206 /name= /prod= /func= /map=3D6-3D6 /transc=CT10991 /len=1446 /GB:AE003427

2551.7 ~4.6 FB:FBgn0034112 /sym=CG3896 /name= /prod= /func=ligand binding or carrier /map=53A3-53A4 /transc=CT12657 /len=3264 /GB:AE003807

35881 4.6 FB:FBgn0037067 /sym=CG11310 /name= /prod= /func=structural protein /map=78C8-78C8 /transc=CT23453 /len=384 /GB:AE003594

66109.3 4.6 FB:FBgn0033679 /sym=CG8888 /name= /prod= /func=enzyme /map=48E4-48E6 /transc=CT25512 /len=1694 /GB:AE003823 /note=3prime sequence from clone BDGP:GH26015.3prime-hit

12875.6 4.6 FB:FBgn0033630 /sym=CG13200 /name= /prod= /func= /map=47F6-47F6 /transc=CT32444 /len=309 /GB:AE003826

6942.7 4.6 FB:FBgn0034522 /sym=CG13432 /name= /prod= /func= /map=57A9-57A10 /transc=CT32789 /len=1355 /GB:AE003791

80254.4 4.6 FB:FBgn0040992 /sym=CG10570 /name= /prod= /func= /map=37B1-37B1 /transc=CT29654 /len=802 /GB:AE003660 /note=3prime sequence from clone BDGP:GH23934.3prime-hit

4870.5 4.6 FB:FBgn0030798 /sym=CG13003 /name= /prod= /func= /map=15A10-15A10 /transc=CT32210 /len=3477 /GB:AE003503

5541.3 4.6 FB:FBgn0029843 /sym=CG5894 /name= /prod=endothelin-converting enzyme-like zinc metalloendopeptidase (M13 peptidase)-like /func=endopeptidase /map=5D2-5D2 /transc=CT18487 /len=2314

2715.6 ~4.5 FB:FBgn0038896 /sym=CG6328 /name= /prod= /func= /map=93F4-93F4 /transc=CT19790 /len=1317 /GB:AE003736

2903.8 ~4.5 FB:FBgn0038977 /sym=CG5376 /name= /prod= /func=motor /map=94B4-94B4 /transc=CT17018 /len=763 /GB:AE003739

4714.4 ~4.5 FB:FBgn0039433 /sym=CG5467 /name= /prod= /func= /map=97B9-97B9 /transc=CT17334 /len=2934 /GB:AE003757 /note=3prime sequence from clone BDGP:GH07007.3prime-hit

22217.6 4.5 FB:FBgn0037697 /sym=CG9363 /name= /prod= /func=enzyme /map=85D18-85D18 /transc=CT26609 /len=1037 /GB:AE003682 /note=3prime sequence from clone BDGP:GH17960.3prime-hit

12420.4 4.5 FB:FBgn0037721 /sym=CG9427 /name= /prod= /func= /map=85E1-85E2 /transc=CT26734 /len=836 /GB:AE003683 /note=3prime sequence from clone BDGP:GH19763.3prime-hit

6522.7 4.5 FB:FBgn0033917 /sym=CG8503 /name= /prod= /func= /map=50E8-50E8 /transc=CT24853 /len=1865 /GB:AE003815 /note=3prime sequence from clone BDGP:GH11294.3prime-hit

3016.2 ~4.5 FB:FBgn0031193 /sym=CG17602 /name= /prod= /func= /map=20A1-20A1 /transc=CT34368 /len=1152 /GB:AE003574

10559.3 4.4 FB:FBgn0038088 /sym=CG10126 /name= /prod=calcium binding protein-like /func=ligand binding or carrier /map=87D3-87D3 /transc=CT28495 /len=879 /GB:AE003697 /note=3prime sequence from clone BDGP:GH19182.3prime-hit

16478 4.4 FB:FBgn0015801 /sym=Reg-5 /name=Rhythmically expressed gene 5 /prod= /func= /map=60D15-60D16 /transc=CT9939 /len=1650 /GB:AE003465 /note=3prime sequence from clone BDGP:HL047

47971 4.4 FB:FBgn0036547 /sym=CG17032 /name= /prod= /func= /map=72C1-72C1 /transc=CT32296 /len=1007 /GB:AE003529

17963.1 4.4 FB:FBgn0033109 /sym=CG9446 /name= /prod= /func=chaperone /map=42C8-42C8 /transc=CT11617 /len=1880 /GB:AE003790

7878.7 4.4 FB:FBgn0035740 /sym=CG18138 /name= /prod= /func= /map=65E5-65E5 /transc=CT40868 /len=2170 /GB:AE003560 /note=3prime sequence from clone BDGP:GH12052.3prime-hit

219587.4 4.4 FB:FBgn0035917 /sym=CG6416 /name= /prod= /func=enzyme /map=66D9-66D10 /transc=CT20013 /len=1175 /GB:AE003554 /note=3prime sequence from clone BDGP:GH19182.3prime-hit

3588.9 ~4.4 FB:FBgn0036101 /sym=CG6449 /name= /prod=ninjurin /func=cell adhesion /map=67E5-67E5 /transc=CT20102 /len=591 /GB:AE003547
 2988.3 ~4.4 BDGP:SD1276.3prime-hit /ESTpos=maps 3prime of FB:FBgn0003638 /sym=su(w[a]) /name=suppressor of white-apricot /prod= /func=RNA binding /map=1E1-1E1 /transc=CT1162 /len=584
 110661.9 4.3 FB:FBgn0034044 /sym=CG12969 /name= /prod= /func=enzyme /map=52C7-52C8 /transc=CT32161 /len=1203 /GB:AE003809
 34249.9 4.3 FB:FBgn0032685 /sym=CG10211 /name= /prod=peroxidase-like /func=enzyme /map=37A1-37A1 /transc=CT28633 /len=3691 /GB:AE003659 /note=3prime sequence from clone BDGP:LD42267.3p
 25547.3 4.3 FB:FBgn0033033 /sym=CG11066 /name= /prod= /func=endopeptidase /map=41E3-41E4 /transc=CT30959 /len=1377 /GB:AE003785
 11289.1 4.3 FB:FBgn0030355 /sym=CG2467 /name= /prod= /func= /map=10F7-10F8 /transc=CT8145 /len=3418 /GB:AE003487 /note=3prime sequence from clone BDGP:GH09980.3prime-hit
 82296.8 4.3 FB:FBgn0031037 /sym=CG14207 /name= /prod=heat shock protein HSP20-like /func=chaperone /map=18D8-18D8 /transc=CT33820 /len=1175 /GB:AE003512 /note=3prime sequence from clone BL
 37898.4 4.3 FB:FBgn0000275 /sym=Pka-R1 /name=cAMP-dependent protein kinase R1 /prod=cAMP-dependent protein kinase, regulatory subunit /func=cAMP-dependent protein kinase regulator /map=77F1-77F1 /transc=CT33820 /len=1175 /GB:AE003512 /note=3prime sequence from clone BL
 11320.1 4.3 BDGP:GH4896.3prime-hit /ESTpos=maps in FB:FBgn0033462 /sym=CG12138 /name= /prod= /func=DNA binding /map=46C4-46C4 /transc=CT7814 /len=700
 3702.5 ~4.3 FB:FBgn0011656 /sym=Mef2 /name=Myocyte enhancing factor 2 /prod= /func=RNA polymerase II transcription factor /map=46C6-46C7 /transc=CT3413 /len=3211 /GB:AE003831 /note=3prime sequence from clone BDGP:GH17145.3p
 4432.4 4.3 FB:FBgn0031938 /sym=CG18590 /name= /prod= /func= /map=28C2-28C2 /transc=CT42499 /len=176 /GB:AE003618
 6566.3 4.3 FB:FBgn0036673 /sym=CG11915 /name= /prod= /func=ligand binding or carrier /map=73D3-73D3 /transc=CT37088 /len=2999 /GB:AE003525 /note=3prime sequence from clone BDGP:GH17145.3p
 1895.4 ~4.3 FB:FBgn0033936 /sym=CG17386 /name= /prod= /func=RNA binding /map=51A1-51A1 /transc=CT33484 /len=2609 /GB:AE003814
 16413.7 4.3 FB:FBgn0032456 /sym=CG6214 /name= /prod=ATP-binding cassette transporter; multidrug resistance protein-like /func=ion channel /map=33F2-33F3 /transc=CT19412 /len=6461 /GB:AE003637 /note=3prime sequence from clone BDGP:GH17145.3p
 26327.7 4.2 FB:FBgn0033133 /sym=CG12841 /name= /prod= /func= /map=42E1-42E1 /transc=CT31973 /len=648 /GB:AE003842
 3681.9 ~4.2 FB:FBgn0004620 /sym=Glu-RIIA /name=Glutamate receptor IIA /prod=glutamate receptor /func=glutamate receptor /map=25F1-25F1 /transc=CT21587 /len=3022 /GB:AE003610
 20932.2 4.2 FB:FBgn0029517 /sym=CG13377 /name= /prod= /func= /map=1A5-1A5 /transc=CT32709 /len=993 /GB:AE003417
 2247.7 ~4.2 FB:FBgn0038987 /sym=CG6926 /name= /prod= /func= /map=94B8-94B8 /transc=CT21454 /len=789 /GB:AE003739
 3098.4 ~4.2 FB:FBgn0032616 /sym=CG15131 /name= /prod= /func= /map=36A10-36A10 /transc=CT35026 /len=862 /GB:AE003652
 3047.3 ~4.2 FB:FBgn0022703 /sym=Cht1 /name=Chitinase 1 /prod=chitinase /func=chitinase ; EC:3.2.1.14 /map=40D5-40E1 /transc=CT39094 /len=1527 /GB:AE002743
 11736.9 4.2 FB:FBgn0038720 /sym=CG6231 /name= /prod=organic cation transporter /func=transporter /map=92A13-92A13 /transc=CT19536 /len=1743 /GB:AE003727
 23343.7 4.2 FB:FBgn0030876 /sym=CG6762 /name= /prod= /func= /map=16D7-16D7 /transc=CT20293 /len=580 /GB:AE003507
 175868.2 4.2 FB:FBgn0033729 /sym=CG8510 /name= /prod=cuticle protein-like /func=structural protein /map=49A3-49A3 /transc=CT24877 /len=381 /GB:AE003822
 99849.6 4.2 FB:FBgn0001258 /sym=ImpL3 /name=Ecdysone-inducible gene L3 /prod=L-lactate dehydrogenase /func=L-lactate dehydrogenase ; EC:1.1.1.27 /map=65A8-65A8 /transc=CT28577 /len=999 /GB:AE003662
 180907.8 4.1 FB:FBgn0032777 /sym=CG18576 /name= /prod= /func= /map=37E1-37E1 /transc=CT42454 /len=1593 /GB:AE003662
 58068.8 4.1 FB:FBgn0037069 /sym=CG7658 /name= /prod=cuticle protein-like /func=structural protein /map=78C8-78C8 /transc=CT23381 /len=511 /GB:AE003594
 10733.4 4.1 FB:FBgn0017397 /sym=how /name=held out wings /prod= /func=RNA binding /map=94A1-94A2 /transc=CT28865 /len=1922 /GB:AE003737
 3085.2 ~4.1 FB:FBgn0032851 /sym=CG13970 /name= /prod= /func= /map=38C1-38C1 /transc=CT33523 /len=618 /GB:AE003665
 3880.9 ~4.1 FB:FBgn0004852 /sym=Ac76E /name=Adenylyl cyclase 76E /prod=adenylate cyclase /func=adenylate cyclase ; EC:4.6.1.1 /map=76D8-76E1 /transc=CT23940 /len=5189 /GB:AE003515 /note=3prime sequence from clone BDGP:GH17145.3p
 6721 4.1 FB:FBgn0030759 /sym=CG13014 /name= /prod= /func= /map=14F2-14F2 /transc=CT32227 /len=699 /GB:AE003502
 23837.1 4.1 FB:FBgn0032025 /sym=CG7778 /name= /prod= /func= /map=29B1-29B2 /transc=CT23662 /len=1222 /GB:AE003620 /note=3prime sequence from clone BDGP:GH17475.3prime-hit
 201594.6 4.1 FB:FBgn0014863 /sym=Mlp84B /name=Muscle LIM protein at 84B /prod=muscle LIM protein at 84B /func=transcription factor /map=84C3-84C3 /transc=CT1058 /len=1863 /GB:AE003672

17444.3		4.1	FB:FBgn0038842 /sym=CG5630 /name= /prod= /func= /map=93A4-93A4 /transc=CT17794 /len=1360 /GB:AE003732
4902		4.1	FB:FBgn0037213 /sym=CG12581 /name= /prod= /func= /map=82A1-82A1 /transc=CT34405 /len=2382 /GB:AE003607 /note=3prime sequence from clone BDGP:GM02933.3prime-hit
3392.7	~4.1		FB:FBgn0031700 /sym=CG14022 /name= /prod= /func=enzyme /map=25D5-25D5 /transc=CT33581 /len=334 /GB:AE003609
20768.8		4.1	FB:FBgn0034067 /sym=CG8399 /name= /prod= /func= /map=52E1-52E3 /transc=CT18617 /len=2268 /GB:AE003808 /note=3prime sequence from clone BDGP:LD47639.3prime-hit
2482.5	~4.0		FB:FBgn0037275 /sym=CG14655 /name= /prod= /func=nucleic acid binding /map=82E1-82E1 /transc=CT34432 /len=2167 /GB:AE003605 /note=3prime sequence from clone BDGP:GH23506.3prime-hit
8908.3		4	FB:FBgn0034575 /sym=CG15652 /name= /prod= /func= /map=57B16-57B16 /transc=CT35836 /len=1311 /GB:AE003452 /note=3prime sequence from clone BDGP:GH14953.3prime-hit
4181.8		4	FB:FBgn0033532 /sym=CG18380 /name= /prod= /func= /map=47A11-47A11 /transc=CT41783 /len=657 /GB:AE003829
3507.7	~4.0		FB:FBgn0008649 /sym=dei /name=delilah /prod= /func=specific RNA polymerase II transcription factor /map=97B2-97B2 /transc=CT17256 /len=1862 /GB:AE003756 /note=3prime sequence from clone BDGP:GM02933.3prime-hit
5096.9		4	FB:FBgn0022800 /sym=HD-14 /name= /prod=fibroblast growth factor receptor-like /func=protein tyrosine kinase ; EC:2.7.1.11 inferred from sequence similarity /map=96C2-96C2 /transc=CT28777 /len=1000
8693.5		4	FB:FBgn0039667 /sym=CG2010 /name= /prod= /func= /map=99B3-99B3 /transc=CT6431 /len=1752 /GB:AE003769 /note=3prime sequence from clone BDGP:GH26184.3prime-hit
117753.4		4	FB:FBgn0004028 /sym=wupA /name=wings up A /prod=troponin I /func=cytoskeletal structural protein /map=16F7-17A1 /transc=CT40012 /len=389 /GB:AE003507
1575.9	~4.0		FB:FBgn0033345 /sym=CG13750 /name= /prod= /func= /map=44F9-44F9 /transc=CT33227 /len=228 /GB:AE003835
3776.4	~4.0		FB:FBgn0030758 /sym=CG9819 /name= /prod= /func=protein phosphatase /map=14F1-14F1 /transc=CT27722 /len=1724 /GB:AE003502
95430.6		4	FB:FBgn0032284 /sym=CG7294 /name= /prod= /func= /map=32A1-32A1 /transc=CT22525 /len=527 /GB:AE003629
43777.9		4	FB:FBgn0031097 /sym=CG17052 /name= /prod=peritrophin-like /func=structural protein /map=19C1-19C1 /transc=CT37860 /len=1383 /GB:AE003572
4267.8		4	FB:FBgn0032279 /sym=CG17104 /name= /prod= /func= /map=32A1-32A1 /transc=CT38006 /len=1746 /GB:AE003629 /note=3prime sequence from clone BDGP:LD16579.3prime-hit
11681.3		4	FB:FBgn0039742 /sym=CG15528 /name= /prod=protein phosphatase-like /func=protein phosphatase /map=99D5-99D5 /transc=CT35642 /len=639 /GB:AE003772
8955.5		4	FB:FBgn0036674 /sym=CG11916 /name= /prod= /func=transcription factor /map=73D4-73D4 /transc=CT37092 /len=707 /GB:AE003525
5826.7		4	FB:FBgn0022341 /sym=CG17467 /name= /prod= /func= /map=102E3-102E3 /transc=CT38621 /len=1002 /GB:AE003846
4154		4	FB:FBgn0034701 /sym=CG13505 /name= /prod= /func= /map=58C5-58C5 /transc=CT32873 /len=1011 /GB:AE003456
15797.8		3.9	FB:FBgn0036675 /sym=CG9959 /name= /prod= /func=transcription factor /map=73D4-73D5 /transc=CT28055 /len=883 /GB:AE003525
3352.7	~3.9		FB:FBgn0032178 /sym=CG4804 /name= /prod=serpin /func=serpin /map=31A1-31A1 /transc=CT15443 /len=1259 /GB:AE003627
32617.1		3.9	FB:FBgn0028855 /sym=BG:DS07721.3 /name= /prod= /func= /map=35B4-35B4 /transc=CT35230 /len=465 /GB:AE003644
6591.7		3.9	FB:FBgn0038674 /sym=CG14285 /name= /prod= /func=transcription factor binding /map=91E4-91E4 /transc=CT33914 /len=894 /GB:AE003724
77573.9		3.9	FB:FBgn0036572 /sym=CG5165 /name= /prod=phosphoglucosyltransferase-like /func=enzyme /map=72D7-72D7 /transc=CT16539 /len=1766 /GB:AE003528 /note=3prime sequence from clone BDGP:LD16579.3prime-hit
18985.9		3.9	FB:FBgn0035710 /sym=SP1173 /name= /prod= /func= /map=65C1-65C1 /transc=CT28481 /len=2494 /GB:AE003561 /note=3prime sequence from clone BDGP:GH14073.3prime-hit
182724		3.9	FB:FBgn0004507 /sym=GlyP /name=Glycogen phosphorylase /prod=glycogen phosphorylase /func=phosphorylase ; EC:2.4.1.1 inferred from direct assay /map=22C3-22C3 /transc=CT22383 /len=287
7012.9		3.9	FB:FBgn0032474 /sym=CG9828 /name= /prod= /func=chaperone /map=34A8-34A8 /transc=CT27734 /len=1253 /GB:AE003639
3224.5	~3.9		FB:FBgn0037972 /sym=CG10005 /name= /prod= /func= /map=87A8-87A8 /transc=CT28191 /len=684 /GB:AE003693
16608.7		3.9	FB:FBgn0004577 /sym=Pxd /name=Peroxidase /prod=peroxidase /func=peroxidase ; EC:1.11.1.7 /map=89E11-89E11 /transc=CT11695 /len=2071 /GB:AE003716
6882.7		3.8	FB:FBgn0035494 /sym=CG14993 /name= /prod=fumarylacetoacetase-like /func=enzyme /map=64A5-64A5 /transc=CT34846 /len=1050 /GB:AE003480
2827.4	~3.8		FB:FBgn0040587 /sym=CG17618 /name= /prod= /func= /map=94C4-94C4 /transc=CT38876 /len=576 /GB:AE003740

3936.3 3.8 FB:FBgn0032332 /sym=CG14917 /name= /prod= /func= /map=32D1-32D1 /transc=CT34744 /len=1863 /GB:AE003630

1295.5 ~3.8 FB:FBgn0035385 /sym=CG2114 /name= /prod=G-protein coupled receptor-like /func=G protein linked receptor /map=63B2-63B2 /transc=CT2366 /len=1650 /GB:AE003476

12277.7 3.8 BDGP:GH1742.3prime-hit /ESTpos=maps in FB:FBgn0033441 /sym=CG1776 /name= /prod=myosin light chain kinase /func=protein kinase /map=46A3-46A4 /transc=CT5322 /len=488

6657 3.8 FB:FBgn0037167 /sym=CG11425 /name= /prod=phosphatidate phosphohydrolase type 2-like /func=enzyme /map=79E4-79E4 /transc=CT21215 /len=956 /GB:AE003597

9002.7 3.8 FB:FBgn0032785 /sym=CG10026 /name= /prod=alpha-tocopherol transfer relative protein /func=transcription factor /map=37E3-37E3 /transc=CT28189 /len=1143 /GB:AE003663 /note=3prime sequ

100295 3.8 FB:FBgn0014141 /sym=cher /name=cheerio /prod=filamin /func=actin binding /map=89F1-89F1 /transc=CT12961 /len=7617 /GB:AE003716 /note=3prime sequence from clone BDGP:SD05640.3pri

3312.8 ~3.8 FB:FBgn0010015 /sym=CanA1 /name=Calcineurin A1 /prod=protein serine/threonine phosphatase /func=protein serine/threonine phosphatase ; EC:3.1.3.16 | inferred from sequence similarity /map=100

372610.8 3.8 FB:FBgn0032280 /sym=CG17105 /name= /prod= /func= /map=32A1-32A1 /transc=CT33652 /len=312 /GB:AE003629

2216.2 ~3.8 FB:FBgn0030586 /sym=CG12539 /name= /prod=glucose dehydrogenase (acceptor) /func=enzyme /map=13A1-13A1 /transc=CT34058 /len=1503 /GB:AE003497

241944.8 3.8 FB:FBgn0032283 /sym=CG7296 /name= /prod= /func= /map=32A1-32A1 /transc=CT22519 /len=575 /GB:AE003629

6626.8 3.8 FB:FBgn0036550 /sym=CG17026 /name= /prod= /func= /map=72C1-72C1 /transc=CT37805 /len=855 /GB:AE003529

3162.7 ~3.8 FB:FBgn0033092 /sym=CG9422 /name= /prod= /func= /map=42C1-42C1 /transc=CT26724 /len=621 /GB:AE003789

928.4 ~3.8 FB:FBgn0038451 /sym=CG14893 /name= /prod= /func=enzyme /map=89D6-89D6 /transc=CT34717 /len=1491 /GB:AE003714

70266.1 3.8 FB:FBgn0031198 /sym=CG13238 /name= /prod= /func= /map=20A1-20A1 /transc=CT32487 /len=405 /GB:AE003574

266780.6 3.8 FB:FBgn0011296 /sym=l(2)efl /name=lethal (2) essential for life /prod= /func=chaperone /map=59F4-59F4 /transc=CT14702 /len=717 /GB:AE003461 /note=3prime sequence from clone BDGP:GH0

8973.7 3.8 FB:FBgn0035303 /sym=CG5699 /name= /prod= /func=cell adhesion /map=62C3-62C3 /transc=CT2689 /len=1990 /GB:AE003473 /note=3prime sequence from clone BDGP:GH09541.3prime-hit

3651.8 3.8 FB:FBgn0031534 /sym=CG2774 /name= /prod=sorting nexin 1-like /func=transporter /map=23F2-23F2 /transc=CT9125 /len=1450 /GB:AE003579

6549.3 3.8 FB:FBgn0031421 /sym=CG9867 /name= /prod= /func= /map=22E1-22E2 /transc=CT27848 /len=1826 /GB:AE003583 /note=3prime sequence from clone BDGP:GH05422.3prime-hit

2570.4 ~3.8 FB:FBgn0039927 /sym=CG11155 /name= /prod=glutamate receptor-like /func=ion channel /map=102E7-102F1 /transc=CT30863 /len=2062 /GB:AE003846

2175 ~3.7 FB:FBgn0031080 /sym=CG12655 /name= /prod= /func= /map=19A3-19A3 /transc=CT35310 /len=496 /GB:AE002611

27906.3 3.7 FB:FBgn0033034 /sym=CG15900 /name= /prod= /func= /map=41E4-41E4 /transc=CT34160 /len=519 /GB:AE003785

38758.8 3.7 FB:FBgn0032422 /sym=CG6579 /name= /prod= /func= /map=33C3-33C4 /transc=CT20347 /len=834 /GB:AE003635

5936.9 3.7 FB:FBgn0023023 /sym=CRMP /name=Collapsin Response Mediator Protein /prod= /func=enzyme /map=83B3-83B4 /transc=CT3290 /len=2554 /GB:AE003602 /note=3prime sequence from clone BL

32297.6 3.7 FB:FBgn0038096 /sym=CG7340 /name= /prod= /func= /map=87D7-87D7 /transc=CT22347 /len=1953 /GB:AE003698 /note=3prime sequence from clone BDGP:LD13869.3prime-hit

189512.7 3.7 FB:FBgn0038009 /sym=CG17738 /name= /prod= /func= /map=87B8-87B8 /transc=CT34537 /len=333 /GB:AE003695

1592.8 ~3.7 FB:FBgn0037813 /sym=CG17100 /name= /prod= /func= /map=86A5-86A5 /transc=CT34464 /len=2030 /GB:AE003687

7700.4 3.7 FB:FBgn0034797 /sym=CG12781 /name= /prod= /func=protein kinase /map=59B4-59B4 /transc=CT36793 /len=4470 /GB:AE003459 /note=3prime sequence from clone BDGP:GH04942.3prime-hit

110642.8 3.7 BDGP:LD43683.3prime-hit /ESTpos=maps in FB:FBgn0031097 /sym=CG17052 /name= /prod=peritrophin-like /func=structural protein /map=19C1-19C1 /transc=CT3786 /len=595

19441.5 3.7 FB:FBgn0035550 /sym=CG11349 /name= /prod= /func=structural protein /map=64B12-64B12 /transc=CT31656 /len=1880 /GB:AE003481

15639.1 3.7 FB:FBgn0015276 /sym=Pcmt /name=Protein-L-isoaspartate (D-aspartate) O-methyltransferase /prod=protein-L-isoaspartate (D-aspartate) O-methyltransferase /func=protein-L-isoaspartate (D-aspartate)

5993.8 3.7 FB:FBgn0033309 /sym=CG8735 /name= /prod= /func=electron transfer /map=44D1-44D2 /transc=CT8725 /len=1421 /GB:AE003836 /note=3prime sequence from clone BDGP:GH24644.3prime-hit

1907.1 ~3.7 FB:FBgn0040874 /sym=CG15600 /name= /prod= /func= /map=13E12-13E12 /transc=CT35723 /len=153 /GB:AE003499

114720.4 3.7 FB:FBgn0036902 /sym=CG8748 /name= /prod= /func= /map=76C4-76C4 /transc=CT25246 /len=1263 /GB:AE003516

152922.3 3.7 FB:FBgn0036901 /sym=CG8756 /name= /prod=low-density lipoprotein-receptor-like /func=receptor /map=76C3-76C3 /transc=CT25252 /len=2157 /GB:AE003516 /note=3prime sequence from clone

1914 ~3.7 FB:FBgn0032469 /sym=CG9932 /name= /prod= /func=nucleic acid binding /map=34A5-34A5 /transc=CT27960 /len=6516 /GB:AE003638

2709.8 ~3.7 FB:FBgn0040981 /sym=CG15268 /name= /prod= /func= /map=35B9-35B9 /transc=CT35215 /len=195 /GB:AE003645

44801.9 3.7 FB:FBgn0034042 /sym=CG8242 /name= /prod= /func=transcription factor /map=52C7-52C7 /transc=CT24455 /len=4875 /GB:AE003809

5279 3.6 FB:FBgn0033502 /sym=CG12910 /name= /prod= /func= /map=46F7-46F7 /transc=CT32055 /len=1690 /GB:AE003830 /note=3prime sequence from clone BDGP:GH17442.3prime-hit

4003.4 3.6 FB:FBgn0031064 /sym=CG12531 /name= /prod=amino-acid permease /func=transporter /map=18E3-18E5 /transc=CT33850 /len=2415 /GB:AE003513

67759 3.6 FB:FBgn0035612 /sym=CG10625 /name= /prod= /func= /map=64E2-64E2 /transc=CT29764 /len=3883 /GB:AE003565 /note=3prime sequence from clone BDGP:LD39545.3prime-hit

4178.9 ~3.6 FB:FBgn0034194 /sym=CG15611 /name= /prod=guanyl-nucleotide exchange factor /func=signal transduction /map=53F12-53F13 /transc=CT35747 /len=1742 /GB:AE003804 /note=3prime sequence

12376.6 3.6 FB:FBgn0000565 /sym=Eip71CD /name=Ecdysone-induced protein 28/29kD /prod=protein-methionine-S-oxide reductase-like /func=protein-methionine-S-oxide reductase ; EC:1.8.4.6 | inferred from s

3134.6 ~3.6 FB:FBgn0004879 /sym=plx /name=pollux /prod= /func= /map=83B8-83B9 /transc=CT1567 /len=5472 /GB:AE003602

17922 3.6 FB:FBgn0034075 /sym=CG18658 /name= /prod=peptide-aspartate beta-dioxygenase-like /func=enzyme /map=52F1-52F1 /transc=CT18815 /len=1662 /GB:AE003808

3078.3 ~3.6 FB:FBgn0033942 /sym=CG10112 /name= /prod= /func=structural protein /map=51A6-51A6 /transc=CT28465 /len=435 /GB:AE003814

3734 3.6 FB:FBgn0037911 /sym=CG10898 /name= /prod=7,8-dihydro-8-oxoguanine-triphosphatase /func=DNA repair protein /map=86E13-86E13 /transc=CT30521 /len=1936 /GB:AE003692 /note=3prime

325929 3.6 FB:FBgn0040993 /sym=CG17325 /name= /prod= /func= /map=37B1-37B2 /transc=CT35069 /len=765 /GB:AE003660

60953.3 3.6 FB:FBgn0028915 /sym=BG:DS01068.5 /name= /prod=serine endopeptidase /func=endopeptidase /map=35A1-35A1 /transc=CT23067 /len=530 /GB:AE003643

24963.9 3.6 FB:FBgn0036659 /sym=CG9701 /name= /prod=beta-glucosidase-like /func=ion channel /map=73B5-73B5 /transc=CT27420 /len=1936 /GB:AE003526 /note=3prime sequence from clone BDGP:LP0

210172.5 3.6 FB:FBgn0004117 /sym=Tm2 /name=Tropomyosin 2 /prod=tropomyosin /func=motor /map=88E11-88E12 /transc=CT15467 /len=914 /GB:AE003708

36382.6 3.6 FB:FBgn0036875 /sym=CG9449 /name= /prod=acid phosphatase-like /func=enzyme /map=76B6-76B6 /transc=CT26772 /len=1179 /GB:AE003516

103801.4 3.6 FB:FBgn0033968 /sym=CG10200 /name= /prod= /func= /map=51C5-51C5 /transc=CT28697 /len=659 /GB:AE003813 /note=3prime sequence from clone BDGP:LP02570.3prime-hit

28797.2 3.5 FB:FBgn0033919 /sym=CG8547 /name= /prod= /func=DNA binding /map=50F1-50F1 /transc=CT24943 /len=1313 /GB:AE003815

2544.5 ~3.5 FB:FBgn0035590 /sym=CG10673 /name= /prod= /func=protein kinase /map=64C12-64C12 /transc=CT29894 /len=675 /GB:AE003567

34614.2 3.5 FB:FBgn0030745 /sym=CG4239 /name= /prod= /func= /map=14C3-14C4 /transc=CT13936 /len=1639 /GB:AE003502 /note=3prime sequence from clone BDGP:GH25683.3prime-hit

3598.4 ~3.5 FB:FBgn0000719 /sym=fog /name=folded gastrulation /prod= /func= /map=20A4-20A5 /transc=CT16970 /len=3059 /GB:AE003573 /note=3prime sequence from clone BDGP:SD02223.3prime-hit

8478.4 3.5 FB:FBgn0031293 /sym=CG4226 /name= /prod=AMPA/kainate-selective ionotropic glutamate receptor-like /func=ion channel /map=21D4-21D4 /transc=CT13021 /len=2979 /GB:AE003588 /note=3

50264.3 3.5 FB:FBgn0026077 /sym=Gasp /name= /prod=peritrophin-like /func=chitin binding /map=83D4-83D4 /transc=CT28895 /len=1460 /GB:AE003600 /note=3prime sequence from clone BDGP:LD05259.3

93934.7 3.5 FB:FBgn0036051 /sym=CG8154 /name= /prod= /func= /map=67C2-67C2 /transc=CT24352 /len=1726 /GB:AE003550

16140.3 3.5 BDGP:LD31422.3prime-hit /ESTpos=maps in FB:FBgn0004624 /sym=CaMKII /name=Calcium/calmodulin-dependent protein kinase II /prod=calcium/calmodulin-dependent protein kinase II /func=cal

119048.6 3.5 FB:FBgn0038181 /sym=CG9297 /name= /prod= /func=enzyme /map=87F13-87F13 /transc=CT26475 /len=2985 /GB:AE003701

28001.9 3.5 FB:FBgn0031199 /sym=CG9557 /name= /prod= /func= /map=20A1-20A1 /transc=CT17180 /len=420 /GB:AE003574

252647.4 3.5 FB:FBgn0038294 /sym=CG6803 /name= /prod= /func= /map=88E6-88E6 /transc=CT21060 /len=1488 /GB:AE003707 /note=3prime sequence from clone BDGP:GH14252.3prime-hit

2958.1 ~3.5 FB:FBgn0033996 /sym=CG11807 /name= /prod= /func=receptor /map=51E7-51E7 /transc=CT14564 /len=1924 /GB:AE003811 /note=3prime sequence from clone BDGP:SD03973.3prime-hit

49425.3 3.4 FB:FBgn0032897 /sym=CG9336 /name= /prod= /func= /map=38F1-38F1 /transc=CT5238 /len=660 /GB:AE003668

4378.2 3.4 FB:FBgn0034632 /sym=CG15668 /name= /prod= /func= /map=57E8-57E9 /transc=CT35852 /len=1976 /GB:AE003454 /note=3prime sequence from clone BDGP:GH02495.3prime-hit

3609.3 3.4 FB:FBgn0035844 /sym=CG13676 /name= /prod= /func= /map=66B10-66B10 /transc=CT33112 /len=2625 /GB:AE003556

60507.2 3.4 FB:FBgn0036903 /sym=CG8747 /name= /prod=low-density lipoprotein-like /func=receptor /map=76C4-76C4 /transc=CT25242 /len=651 /GB:AE003516

324724.1 3.4 FB:FBgn0034819 /sym=CG9877 /name= /prod= /func= /map=59C4-59C4 /transc=CT27864 /len=267 /GB:AE003459

2420.7 ~3.4 FB:FBgn0003995 /sym=vvl /name=ventral veins lacking /prod= /func=RNA polymerase II transcription factor /map=65C5-65D1 /transc=CT28091 /len=2556 /GB:AE003561

5423.7 3.4 FB:FBgn0001123 /sym=G-salpa60A /name=G protein alpha 6A /prod=G protein alphas-subunit /func=heterotrimeric G protein /map=60A12-60A12 /transc=CT40310 /len=1626 /GB:AE003462 /no

4149.2 3.4 FB:FBgn0033872 /sym=CG6329 /name= /prod= /func= /map=50C12-50C12 /transc=CT19784 /len=1312 /GB:AE003817 /note=3prime sequence from clone BDGP:HL02087.3prime-hit

3506.4 3.4 FB:FBgn0003162 /sym=Pu /name=Punch /prod=GTP cyclohydrolase I /func=GTP cyclohydrolase I ; EC:3.5.4.16 /map=57C5-57C6 /transc=CT26766 /len=1623 /GB:AE003453 /note=3prime sequence

20389 3.4 FB:FBgn0038610 /sym=CG7675 /name= /prod= /func=enzyme /map=91A2-91A2 /transc=CT30419 /len=1100 /GB:AE003721 /note=3prime sequence from clone BDGP:GH26851.3prime-hit

21255.5 3.4 FB:FBgn0028694 /sym=Rpn11 /name= /prod=19S proteasome regulatory particle, non-ATPase protein, subunit S13 /func= /map=25C3-25C3 /transc=CT41032 /len=1165 /GB:AE003608

2246.4 ~3.4 FB:FBgn0036028 /sym=CG16717 /name= /prod= /func= /map=67B11-67B11 /transc=CT37199 /len=903 /GB:AE003551

18200.4 3.4 FB:FBgn0031200 /sym=CG9558 /name= /prod= /func= /map=20A1-20A1 /transc=CT17174 /len=261 /GB:AE003574

75341.7 3.4 FB:FBgn0039897 /sym=CG1674 /name= /prod= /func=motor /map=102A3-102A4 /transc=CT4686 /len=2388 /GB:AE003844

2626.5 ~3.3 FB:FBgn0011327 /sym=Uch-L3 /name=Ubiquitin C-terminal hydrolase /prod=ubiquitinyl hydrolase L3 /func=ubiquitinyl hydrolase 1 /map=67B5-67B5 /transc=CT11565 /len=1137 /GB:AE003552 /r

46788.1 3.3 FB:FBgn0030309 /sym=CG1572 /name= /prod= /func= /map=10C4-10C4 /transc=CT4080 /len=955 /GB:AE003486 /note=3prime sequence from clone BDGP:LD04844.3prime-hit

21879.9 3.3 FB:FBgn0016756 /sym=Ubp64E /name=Ubiquitin-specific protease 64E /prod=ubiquitin-specific protease /func=ubiquitin-specific protease /map=64E13-64F1 /transc=CT17382 /len=4202 /GB:AE00

34071.5 3.3 FB:FBgn0033446 /sym=CG1648 /name= /prod= /func= /map=46B10-46B10 /transc=CT4516 /len=960 /GB:AE003832 /note=3prime sequence from clone BDGP:GH20817.3prime-hit

3179.6 ~3.3 FB:FBgn0039335 /sym=CG5127 /name= /prod=vacuolar protein sorting-like /func=transporter /map=96E1-96E1 /transc=CT16445 /len=2021 /GB:AE003752 /note=3prime sequence from clone BDGP

438729.7 3.3 FB:FBgn0033596 /sym=CG7738 /name= /prod= /func= /map=47E1-47E1 /transc=CT23557 /len=405 /GB:AE003826

11510.6 3.3 FB:FBgn0032002 /sym=CG8353 /name= /prod=cytidine deaminase-like /func=enzyme /map=28F4-28F4 /transc=CT24599 /len=513 /GB:AE003620

1319.3 ~3.3 FB:FBgn0037542 /sym=CG2723 /name= /prod= /func= /map=84E6-84E6 /transc=CT9257 /len=1314 /GB:AE003677 /note=3prime sequence from clone BDGP:LD11958.3prime-hit

16648.6 3.3 FB:FBgn0019972 /sym=Ice /name=Ice /prod=caspase /func=caspase ; EC:3.4.22.- /map=99C4-99C4 /transc=CT4706 /len=1932 /GB:AE003771 /note=3prime sequence from clone BDGP:GH24292.3pr

3327.3 3.3 FB:FBgn0023517 /sym=EG:63B12.4 /name= /prod= /func= /map=2B13-2B13 /transc=CT34629 /len=1066 /GB:AE003422 /note=3prime sequence from clone BDGP:GH02880.3prime-hit

2842 ~3.3 FB:FBgn0036843 /sym=CG6812 /name= /prod= /func= /map=75F4-75F5 /transc=CT21117 /len=1585 /GB:AE003518

87949.8 3.3 FB:FBgn0039719 /sym=CG15515 /name= /prod=cuticle protein-like /func=structural protein /map=99D1-99D1 /transc=CT35628 /len=327 /GB:AE003771

8183.4 3.3 FB:FBgn0031821 /sym=CG9542 /name= /prod= /func= /map=26D7-26D7 /transc=CT26992 /len=903 /GB:AE003613

30450.3 3.3 FB:FBgn0039208 /sym=CG6643 /name= /prod= /func=enzyme /map=96A7-96A7 /transc=CT20638 /len=2769 /GB:AE003748 /note=3prime sequence from clone BDGP:GH21511.3prime-hit

2308.2 ~3.3 FB:FBgn0031502 /sym=CG3524 /name= /prod= /func=enzyme /map=23C5-23D1 /transc=CT11835 /len=7590 /GB:AE003581 /note=3prime sequence from clone BDGP:GH02912.3prime-hit

1664 ~3.3 FB:FBgn0035054 /sym=CG9189 /name= /prod= /func= /map=60D14-60D14 /transc=CT26264 /len=1121 /GB:AE003465

3378.5 3.3 FB:FBgn0039529 /sym=CG5612 /name= /prod= /func= /map=98A4-98A4 /transc=CT17752 /len=1352 /GB:AE003761

629.4 ~3.3 FB:FBgn0029542 /sym=CG3708 /name= /prod= /func= /map=1C5-1C5 /transc=CT12445 /len=1188 /GB:AE003419 /note=3prime sequence from clone BDGP:GH17085.3prime-hit

1703.3 ~3.3 FB:FBgn0040542 /sym=CG12815 /name= /prod= /func= /map=85F15-85F15 /transc=CT31943 /len=213 /GB:AE003686

6343.4 3.3 FB:FBgn0031695 /sym=Cyp4ac3 /name= /prod=cytochrome P450, CYP4AC3 /func=cytochrome P450 /map=25D2-25D2 /transc=CT33590 /len=939 /GB:AE003609 /note=3prime sequence from clone

2727 ~3.2 FB:FBgn0031153 /sym=CG15448 /name= /prod= /func=transmembrane receptor /map=19E7-19E7 /transc=CT35512 /len=669 /GB:AE003569

1114.8 ~3.2 FB:FBgn0031211 /sym=CG2776 /name= /prod= /func=ligand binding or carrier /map=21A4-21A4 /transc=CT9453 /len=615 /GB:AE003590

45992.9 3.2 FB:FBgn0027540 /sym=BcDNA:GH12504 /name= /prod= /func=transmembrane receptor /map=85B3-85B4 /transc=CT27712 /len=3771 /GB:AE003680 /note=3prime sequence from clone BDGP:GH

95943.1 3.2 BDGP:GH1453.3prime-hit /ESTpos=maps in FB:FBgn0031737 /sym=CG11142 /name= /prod=peritrophin-like /func=structural protein /map=26A1-26A1 /transc=CT31147 /len=899

2321.5 ~3.2 FB:FBgn0031251 /sym=CG4213 /name= /prod= /func=motor /map=21C2-21C2 /transc=CT13886 /len=3696 /GB:AE003589

10103 3.2 FB:FBgn0038407 /sym=CG6126 /name= /prod=sugar transporter /func=transporter /map=89B13-89B13 /transc=CT19169 /len=2108 /GB:AE003712 /note=3prime sequence from clone BDGP:GH092

4787 3.2 FB:FBgn0034525 /sym=CG13435 /name= /prod= /func=ligand binding or carrier /map=57B1-57B1 /transc=CT32792 /len=1983 /GB:AE003791

3986.5 3.2 FB:FBgn0003499 /sym=sr /name=stripe /prod= /func=RNA polymerase II transcription factor /map=90E1-90E2 /transc=CT23724 /len=4829 /GB:AE003720

1926.4 ~3.2 FB:FBgn0035772 /sym=CG8582 /name= /prod= /func= /map=65F4-65F4 /transc=CT14420 /len=1739 /GB:AE003559

2596.2 ~3.2 FB:FBgn0036562 /sym=CG5600 /name= /prod= /func= /map=72D3-72D4 /transc=CT17536 /len=1858 /GB:AE003528 /note=3prime sequence from clone BDGP:GH16214.3prime-hit

14451.8 3.2 FB:FBgn0039606 /sym=CG1448 /name= /prod= /func= /map=98E6-98E6 /transc=CT3509 /len=1544 /GB:AE003767 /note=3prime sequence from clone BDGP:LD34202.3prime-hit

13226.4 3.2 FB:FBgn0028690 /sym=Rpn5 /name= /prod=19S proteasome regulatory particle, non-ATPase protein, subunit p55 /func=endopeptidase /map=83C1-83C1 /transc=CT1623 /len=1874 /GB:AE003601

2769.3 ~3.2 FB:FBgn0028468 /sym=BcDNA:LD28419 /name= /prod=tetracycline transporter-like /func=transporter /map=93B12-93B12 /transc=CT18069 /len=1718 /GB:AE003733 /note=3prime sequence from

1479.1 ~3.2 FB:FBgn0039870 /sym=CG1896 /name= /prod= /func= /map=100E2-100E2 /transc=CT5870 /len=806 /GB:AE003779 /note=3prime sequence from clone BDGP:LD39576.3prime-hit

116129.1 3.2 FB:FBgn0010424 /sym=TpnC73F /name=Troponin C at 73F /prod=troponin C /func=calcium binding /map=73E4-73E5 /transc=CT23822 /len=935 /GB:AE003525

2807.4 ~3.2 FB:FBgn0034029 /sym=CG8190 /name= /prod=translation initiation factor 2B-gamma-like /func=translation factor /map=52A10-52A10 /transc=CT20341 /len=1503 /GB:AE003810 /note=3prime seq

2943.7 3.2 FB:FBgn0030028 /sym=CG10965 /name= /prod= /func= /map=7D21-7D21 /transc=CT7616 /len=1052 /GB:AE003443 /note=3prime sequence from clone BDGP:GH26991.3prime-hit

48151.9 3.2 FB:FBgn0038149 /sym=CG9796 /name= /prod= /func= /map=87E10-87E10 /transc=CT27692 /len=1109 /GB:AE003700 /note=3prime sequence from clone BDGP:LD47508.3prime-hit

2891.3 ~3.2 FB:FBgn0034045 /sym=CG8249 /name= /prod=glucose transporter-like /func=transporter /map=52D2-52D2 /transc=CT21797 /len=1807 /GB:AE003809

2661.8 ~3.2 FB:FBgn0034579 /sym=CG9353 /name= /prod= /func= /map=57B20-57B20 /transc=CT26571 /len=647 /GB:AE003452 /note=3prime sequence from clone BDGP:SD09147.3prime-hit

27155.9 3.2 FB:FBgn0011716 /sym=spdo /name=sanpodo /prod=tropomodulin /func=tropomyosin binding /map=100A1-100A1 /transc=CT3919 /len=5374 /GB:AE003774 /note=3prime sequence from clone BDGP:GH0967.3prime-hit

49739 3.2 FB:FBgn0032899 /sym=CG9338 /name= /prod= /func= /map=38F1-38F1 /transc=CT5240 /len=660 /GB:AE003668 /note=3prime sequence from clone BDGP:GH07967.3prime-hit

8500.4 3.2 FB:FBgn0029958 /sym=CG12151 /name= /prod=pyruvate dehydrogenase phosphatase /func=protein phosphatase /map=7B8-7B8 /transc=CT8439 /len=1910 /GB:AE003441 /note=3prime sequence fr

57308.7 3.2 FB:FBgn0032596 /sym=CG17331 /name= /prod=20S proteasome, beta2 subunit /func=endopeptidase /map=36A7-36A7 /transc=CT32562 /len=760 /GB:AE003652

5424 3.2 FB:FBgn0038817 /sym=CG18039 /name= /prod= /func= /map=92F1-92F1 /transc=CT13538 /len=961 /GB:AE003731

51231.5 3.2 FB:FBgn0027501 /sym=BcDNA:LD24639 /name= /prod=UDP-N-acetylglucosamine pyrophosphorylase-like /func=enzyme /map=26D5-26D5 /transc=CT26974 /len=2033 /GB:AE003613 /note=3prim

2850.4 3.2 FB:FBgn0039898 /sym=CG1748 /name= /prod=RHO GTPase activator-like /func=signal transduction /map=102A4-102A4 /transc=CT4742 /len=717 /GB:AE003844

159590.5 3.2 FB:FBgn0000667 /sym=Actn /name=alpha actinin /prod=actinin-alpha /func=actin bundling /map=2C2-2C3 /transc=CT14163 /len=3432 /GB:AE003422 /note=3prime sequence from clone BDGP:LD

1758.7 ~3.1 FB:FBgn0028428 /sym=lh /name= /prod=voltage-gated ion channel protein /func=voltage-gated ion channel /map=50F1-50F1 /transc=CT24973 /len=3924 /GB:AE003815

2533.3 ~3.1 FB:FBgn0038866 /sym=CG5810 /name= /prod= /func=cell adhesion /map=93C3-93C3 /transc=CT18214 /len=1287 /GB:AE003733

3027.6 ~3.1 FB:FBgn0037762 /sym=CG16905 /name= /prod= /func= /map=85E10-85E10 /transc=CT37510 /len=781 /GB:AE003684

6961.5 3.1 FB:FBgn0004586 /sym=grh /name=grainy head /prod= /func=specific RNA polymerase II transcription factor /map=54F1-54F4 /transc=CT42182 /len=4748 /GB:AE003801 /note=3prime sequence from

2132.7 ~3.1 FB:FBgn0034366 /sym=CG5489 /name= /prod= /func=enzyme /map=55E4-55E4 /transc=CT42577 /len=1577 /GB:AE003799

1882.1 ~3.1 FB:FBgn0028895 /sym=BG:DS02740.8 /name= /prod= /func=nucleic acid binding /map=35F8-35F8 /transc=CT32539 /len=1158 /GB:AE003650

1783.7 ~3.1 FB:FBgn0039807 /sym=CG15546 /name= /prod= /func= /map=100B1-100B1 /transc=CT35662 /len=1233 /GB:AE003775

2643.4 ~3.1 FB:FBgn0037817 /sym=Cyp12e1 /name= /prod=cytochrome P450, CYP12E1 /func=cytochrome P450 /map=86A7-86A7 /transc=CT34465 /len=1518 /GB:AE003687

10842.5 3.1 FB:FBgn0023548 /sym=msta /name= /prod= /func= /map=2E2-2E2 /transc=CT40358 /len=3150 /GB:AE003423

2581.7 ~3.1 FB:FBgn0032490 /sym=CG16813 /name= /prod= /func= /map=34A10-34A10 /transc=CT35578 /len=555 /GB:AE003639

872 ~3.1 FB:FBgn0031457 /sym=CG3077 /name= /prod= /func=ligand binding or carrier /map=23B1-23B1 /transc=CT10334 /len=1317 /GB:AE003582 /note=3prime sequence from clone BDGP:LD12265.3p

18259.7 3.1 FB:FBgn0024989 /sym=EG:125H10.1 /name= /prod= /func=motor /map=1A8-1A8 /transc=CT12604 /len=2479 /GB:AE003417

2355.4 ~3.1 FB:FBgn0031933 /sym=CG7068 /name= /prod= /func= /map=28C1-28C1 /transc=CT21827 /len=4745 /GB:AE003618 /note=3prime sequence from clone BDGP:GH05679.3prime-hit

3907.1 3.1 FB:FBgn0033807 /sym=CG12251 /name=aquaporin /prod=aquaporin /func=water transporter /map=49F11-49F11 /transc=CT14932 /len=1180 /GB:AE003819

28159.7 3.1 FB:FBgn0023175 /sym=Prosalph7 /name=Proteasome alpha7 subunit /prod=20S proteasome, alpha7 subunit /func=multicatalytic endopeptidase ; EC:3.4.99.46 /map=46B13-46B13 /transc=CT3927 /l

7392.9 3.1 FB:FBgn0030917 /sym=CG6267 /name= /prod= /func= /map=17A11-17A11 /transc=CT19600 /len=678 /GB:AE003508

1763.6 ~3.1 FB:FBgn0031027 /sym=CG14201 /name= /prod= /func=transcription factor /map=18D3-18D3 /transc=CT33814 /len=702 /GB:AE003512

2247.5 ~3.1 FB:FBgn0032330 /sym=CG12291 /name= /prod= /func= /map=32D1-32D1 /transc=CT19324 /len=382 /GB:AE003630

20001.2 3.1 FB:FBgn0034142 /sym=CG8306 /name= /prod= /func=enzyme /map=53C7-53C8 /transc=CT24503 /len=1937 /GB:AE003806

5308.7 3.1 FB:FBgn0001250 /sym=if /name=inflated /prod=integrin, alpha-subunit /func=cell adhesion receptor /map=15A3-15A5 /transc=CT27194 /len=5726 /GB:AE003503

8376.5 3.1 FB:FBgn0036370 /sym=CG14108 /name= /prod= /func= /map=70B1-70B1 /transc=CT33703 /len=435 /GB:AE003537

242886.2 3.1 FB:FBgn0003060 /sym=CG9757 /name= /prod= /func= /map=87F5-87F5 /transc=CT27573 /len=566 /GB:AE003701

2320.9 ~3.1 FB:FBgn0000014 /sym=abd-A /name=abdominal A /prod= /func=specific RNA polymerase II transcription factor /map=89E4-89E4 /transc=CT29034 /len=1931 /GB:AE003715

4535 3.1 FB:FBgn0026749 /sym=Yippee /name= /prod=zinc binding protein /func=zinc binding /map=11E11-11E11 /transc=CT6354 /len=1152 /GB:AE003492 /note=3prime sequence from clone BDGP:LD40

26315.9 3.1 FB:FBgn0038293 /sym=CG6904 /name= /prod= /func=enzyme /map=88E5-88E5 /transc=CT21366 /len=2705 /GB:AE003707 /note=3prime sequence from clone BDGP:LD46952.3prime-hit

4934.2 3.1 FB:FBgn0001112 /sym=Gld /name=Glucose dehydrogenase /prod=glucose dehydrogenase (acceptor) == EC 1.1.99.10 /func=glucose dehydrogenase (acceptor) ; EC:1.1.99.10 /map=84C7-84C8 /transc=

27221.3 3 FB:FBgn0003206 /sym=Ras64B /name=Ras oncogene at 64B /prod= /func=RAS small GTPase /map=64A10-64A10 /transc=CT1405 /len=588 /GB:AE003480

106718.4 3 FB:FBgn0033600 /sym=CG9077 /name= /prod=cuticle protein /func=structural protein /map=47E1-47E1 /transc=CT26058 /len=396 /GB:AE003826

2196.8 ~3.0 FB:FBgn0029585 /sym=CG11511 /name= /prod= /func=transcription factor /map=2B6-2B6 /transc=CT34608 /len=1000 /GB:AE003421

1073.6 ~3.0 FB:FBgn0003511 /sym=Sry-beta /name=Serendipity beta /prod= /func=RNA polymerase II transcription factor /map=99D5-99D5 /transc=CT5812 /len=1247 /GB:AE003772 /note=3prime sequence fr

79152.2 3 FB:FBgn0003071 /sym=Pfk /name=Phosphofructokinase /prod=6-phosphofructokinase /func=6-phosphofructokinase ; EC:2.7.1.11 /map=46E4-46E4 /transc=CT13302 /len=3176 /GB:AE003830 /note=

8211.2 3 FB:FBgn0040559 /sym=CG14359 /name= /prod= /func= /map=88B1-88B1 /transc=CT33994 /len=237 /GB:AE003703

19686.7 3 FB:FBgn0028693 /sym=Rpn12 /name= /prod=19S proteasome regulatory particle, non-ATPase protein, subunit S14 /func=endopeptidase /map=73A8-73A8 /transc=CT13736 /len=989 /GB:AE00352

2397.7 ~3.0 FB:FBgn0038536 /sym=CG7655 /name= /prod=multipass nuclear envelope protein-like /func=transmembrane receptor /map=90C1-90C1 /transc=CT23407 /len=965 /GB:AE003718 /note=3prime seq

44484.6 3 FB:FBgn0029533 /sym=CG5254 /name= /prod= /func= /map=1C1-1C1 /transc=CT16777 /len=993 /GB:AE003418

3552.4 3 FB:FBgn0032128 /sym=CG13115 /name= /prod= /func= /map=30B11-30B11 /transc=CT32352 /len=956 /GB:AE003625 /note=3prime sequence from clone BDGP:GH05993.3prime-hit

38368.3 3 FB:FBgn0035030 /sym=CG3541 /name= /prod= /func= /map=60D7-60D8 /transc=CT11882 /len=2417 /GB:AE003464 /note=3prime sequence from clone BDGP:GH12163.3prime-hit

41645.2 3 FB:FBgn0022359 /sym=Sodh-2 /name=Sorbitol dehydrogenase-2 /prod=L-itol 2-dehydrogenase /func=L-itol 2-dehydrogenase ; EC:1.1.1.14 /map=86C7-86C7 /transc=CT14906 /len=1345 /GB:AE003418

14310.2 3 FB:FBgn0028685 /sym=Rpt4 /name= /prod=19S proteasome regulatory particle, triple-A protein, subunit S10b /func=proteasome ATPase ; EC:3.6.4.8 /map=5E1-5E1 /transc=CT11623 /len=1453 /GB:AE003418

104072.4 3 BDGP:HL664.3prime-hit /ESTpos=maps 3prime of FB:FBgn0038181 /sym=CG9297 /name= /prod= /func=enzyme /map=87F13-87F13 /transc=CT26475 /len=608

30341.6 3 FB:FBgn0028691 /sym=Rpn4 /name= /prod=19S proteasome regulatory particle, non-ATPase protein, subunit S13 /func=endopeptidase /map=95B5-95B5 /transc=CT28751 /len=1330 /GB:AE00374

4080.2 3 FB:FBgn0005771 /sym=noc /name=no ocelli /prod= /func=RNA polymerase II transcription factor /map=35A4-35A4 /transc=CT14619 /len=2668 /GB:AE003644 /note=3prime sequence from clone BDGP:GH06479.3prime-hit

4064.4 3 FB:FBgn0031637 /sym=CG2950 /name= /prod= /func=RNA binding /map=25B3-25B3 /transc=CT40278 /len=2649 /GB:AE003575 /note=3prime sequence from clone BDGP:GH06479.3prime-hit

16524 3 FB:FBgn0040520 /sym=CG12447 /name= /prod= /func= /map=20A1-20A1 /transc=CT32486 /len=132 /GB:AE003574

3987 ~3.0 FB:FBgn0003944 /sym=Ubx /name=Ultrathorax /prod= /func=specific RNA polymerase II transcription factor /map=89D8-89E2 /transc=CT29154 /len=2204 /GB:AE003714

86366.2 3 FB:FBgn0034497 /sym=CG9090 /name= /prod=phosphate transporter /func=carrier type transporter /map=56F16-56F16 /transc=CT25968 /len=1371 /GB:AE003792

32359.3 2.9 FB:FBgn0029876 /sym=CG3960 /name= /prod= /func=actin binding /map=6B3-6C1 /transc=CT13158 /len=2129 /GB:AE003438 /note=3prime sequence from clone BDGP:GH02414.3prime-hit

2061.3 ~2.9 FB:FBgn0027550 /sym=BcDNA:GH10711 /name= /prod= /func=receptor /map=32A4-32A5 /transc=CT20185 /len=2550 /GB:AE003629 /note=3prime sequence from clone BDGP:GH10711.3prime-hit

29445.5 2.9 FB:FBgn0034399 /sym=CG15083 /name= /prod= /func= /map=55F3-55F3 /transc=CT34958 /len=453 /GB:AE003798

38242.4 2.9 FB:FBgn0033553 /sym=CG12323 /name= /prod= /func= /map=47C1-47C1 /transc=CT22275 /len=1114 /GB:AE003828 /note=3prime sequence from clone BDGP:LD08717.3prime-hit

29174.8 2.9 FB:FBgn0031307 /sym=CG4726 /name= /prod=sodium/phosphate cotransporter /func=transporter /map=21E4-21E4 /transc=CT15243 /len=2003 /GB:AE003587

6818 2.9 FB:FBgn0032129 /sym=CG4405 /name= /prod= /func=RNA binding /map=30B11-30B12 /transc=CT14344 /len=3801 /GB:AE003625

10857 2.9 FB:FBgn0035927 /sym=CG5775 /name= /prod= /func= /map=66E1-66E1 /transc=CT18132 /len=837 /GB:AE003554 /note=3prime sequence from clone BDGP:SD08909.3prime-hit

67758.7 2.9 FB:FBgn0034470 /sym=CG11218 /name= /prod=antennal binding protein X-like /func=ligand binding or carrier /map=56E4-56E4 /transc=CT31326 /len=574 /GB:AE003795

13006.7 2.9 FB:FBgn0036891 /sym=CG9372 /name= /prod=serine protease-like /func=endopeptidase /map=76B11-76B11 /transc=CT26619 /len=1569 /GB:AE003516

1649.5 ~2.9 FB:FBgn0039706 /sym=CG18040 /name= /prod= /func= /map=99C5-99C6 /transc=CT40392 /len=786 /GB:AE003771

34712.3 2.9 FB:FBgn0032427 /sym=CG5453 /name= /prod= /func= /map=33D4-33D4 /transc=CT17294 /len=819 /GB:AE003636 /note=3prime sequence from clone BDGP:GH02216.3prime-hit

25527.5 2.9 FB:FBgn0010397 /sym=LamC /name=Lamin C /prod=lamin C /func=cytoskeletal structural protein /map=51B1-51B1 /transc=CT28479 /len=2334 /GB:AE003814 /note=3prime sequence from clone BDGP:GH02216.3prime-hit

1435.5 ~2.9 FB:FBgn0001624 /sym=dlg1 /name=discs large 1 /prod=guanylate kinase /func=guanylate kinase ; EC:2.7.4.8 /map=10B11-10B12 /transc=CT41310 /len=631 /GB:AE003486 /note=3prime sequence from clone BDGP:GH02216.3prime-hit

32146.3 2.9 FB:FBgn0035517 /sym=CG1265 /name= /prod= /func= /map=64B4-64B4 /transc=CT2591 /len=549 /GB:AE003480

2417.1 ~2.9 FB:FBgn0032013 /sym=CG7851 /name= /prod= /func= /map=29A4-29A4 /transc=CT23800 /len=1391 /GB:AE003620

6095.4 2.9 FB:FBgn0030494 /sym=CG15757 /name= /prod=cuticle protein-like /func=structural protein /map=12A1-12A1 /transc=CT36009 /len=522 /GB:AE003492

22931.3 2.9 FB:FBgn0040575 /sym=CG15922 /name= /prod= /func= /map=92E10-92E10 /transc=CT35885 /len=159 /GB:AE003731

1923 ~2.9 FB:FBgn0035199 /sym=CG9134 /name= /prod=C-type lectin-like /func=ligand binding or carrier /map=61F4-61F4 /transc=CT10115 /len=1161 /GB:AE003471 /note=3prime sequence from clone BDGP:GH02216.3prime-hit

2417.5 ~2.9 FB:FBgn0004957 /sym=por /name=porcupine /prod= /func= /map=17A10-17A10 /transc=CT19254 /len=2331 /GB:AE003508

143693.8 2.9 FB:FBgn0003075 /sym=Pgk /name=Phosphoglycerate kinase /prod=phosphoglycerate kinase /func=phosphoglycerate kinase ; EC:2.7.2.3 /map=23A7-23A7 /transc=CT10484 /len=1361 /GB:AE003582

18527.2 2.9 FB:FBgn0035542 /sym=CG11347 /name= /prod= /func= /map=64B11-64B11 /transc=CT31652 /len=2045 /GB:AE003481 /note=3prime sequence from clone BDGP:GH28550.3prime-hit

6337.5 2.8 FB:FBgn0031914 /sym=CG5973 /name= /prod= /func=ligand binding or carrier /map=27F7-28A1 /transc=CT18751 /len=1519 /GB:AE003617 /note=3prime sequence from clone BDGP:HL01515.3prime-hit

26453.9 2.8 FB:FBgn0028688 /sym=Rpn7 /name= /prod=19S proteasome regulatory particle, non-ATPase protein, subunit S10a /func=endopeptidase /map=94B3-94B3 /transc=CT17076 /len=1374 /GB:AE003700

293564.7 2.8 FB:FBgn0035062 /sym=CG16914 /name= /prod=larval cuticle protein-like /func=structural protein /map=60D15-60D15 /transc=CT37520 /len=279 /GB:AE003465

35174.6 2.8 FB:FBgn0034064 /sym=CG8392 /name= /prod=20S proteasome, beta1 subunit /func=endopeptidase /map=52E1-52E1 /transc=CT18263 /len=829 /GB:AE003808 /note=3prime sequence from clone BDGP:HL01515.3prime-hit

319262 2.8 FB:FBgn0040941 /sym=CG15308 /name= /prod= /func= /map=9B6-9B6 /transc=CT35285 /len=249 /GB:AE003449

109269.9 2.8 FB:FBgn0031629 /sym=CG3244 /name= /prod=selectin-like /func=ligand binding or carrier /map=25B1-25B1 /transc=CT10874 /len=1267 /GB:AE003575

14307.5 2.8 FB:FBgn0032727 /sym=CG10623 /name= /prod= /func= /map=37B8-37B8 /transc=CT29758 /len=1114 /GB:AE003661

20257.5 2.8 FB:FBgn0020369 /sym=Pros45 /name=Saccharomyces cerevisiae UAS construct a of Cheng /prod=19S proteasome regulatory particle, triple-A protein, subunit S8 /func=proteasome ATPase ; EC:3.6.1.13

5637 2.8 FB:FBgn0034975 /sym=CG11290 /name= /prod=histone acetyltransferase-like /func=enzyme /map=60B5-60B5 /transc=CT31509 /len=6956 /GB:AE003463 /note=3prime sequence from clone BDGP:HL01515.3prime-hit

1625.5 ~2.8 FB:FBgn0024887 /sym=kin17 /name= /prod= /func=DNA binding /map=77B4-77B4 /transc=CT17834 /len=1241 /GB:AE003591

38932.5 2.8 BDGP:GH13437.3prime-hit /ESTpos=maps 3prime of FB:FBgn0039493 /sym=CG5889 /name= /prod= /func= /map=97E11-97F1 /transc=CT18483 /len=374

126510.4 2.8 FB:FBgn0028544 /sym=BG:DS00180.3 /name= /prod= /func= /map=34E1-34E1 /transc=CT25718 /len=1397 /GB:AE003641 /note=3prime sequence from clone BDGP:HL02234.3prime-hit

6355.6 2.8 FB:FBgn0031067 /sym=CG12533 /name= /prod= /func=actin binding /map=18F1-18F1 /transc=CT33853 /len=2079 /GB:AE003513

61064.6 2.8 FB:FBgn0034140 /sym=CG8317 /name= /prod= /func= /map=53C7-53C7 /transc=CT24573 /len=693 /GB:AE003806

276870 2.8 FB:FBgn0014869 /sym=Pglym78 /name=Phosphoglyceromutase /prod=phosphoglycerate mutase /func=phosphoglycerate mutase ; EC:5.4.2.1 /map=99A1-99A1 /transc=CT4904 /len=1125 /GB:AE003806

16360.6 2.8 FB:FBgn0004066 /sym=Pros28.1 /name=Proteasome 28kD subunit 1 /prod=20S proteasome, alpha4 subunit /func=multicatalytic endopeptidase ; EC:3.4.99.46 /map=14B11-14B11 /transc=CT11501 /len=11501

9989.2 2.8 FB:FBgn0000084 /sym=AnnX /name=Annexin X /prod=annexin X /func=calcium-dependent phospholipid binding /map=19C1-19C1 /transc=CT17636 /len=1216 /GB:AE002611 /note=3prime sequence from clone BDGP:HL01515.3prime-hit

18942.3 2.8 FB:FBgn0035334 /sym=CG8993 /name= /prod=mitochondrial thioredoxin-like /func=chaperone /map=62E1-62E1 /transc=CT25846 /len=484 /GB:AE003474

298292.1 2.8 FB:FBgn0032538 /sym=CG16885 /name= /prod= /func= /map=34E1-34E1 /transc=CT35249 /len=780 /GB:AE003641

15314.8 2.8 FB:FBgn0033959 /sym=CG18372 /name= /prod= /func= /map=51C2-51C2 /transc=CT41763 /len=674 /GB:AE003813

21340.1 2.8 FB:FBgn0031322 /sym=CG5001 /name= /prod= /func=chaperone /map=21F1-21F1 /transc=CT15884 /len=1356 /GB:AE003587

34689.7 2.8 FB:FBgn0026380 /sym=Prosbeta3 /name= /prod=20S proteasome, beta3 subunit /func=multicatalytic endopeptidase ; EC:3.4.99.46 /map=85C3-85C3 /transc=CT32122 /len=915 /GB:AE003681 /note=3prime sequence from clone BDGP:HL01515.3prime-hit

10981.8 2.8 BDGP:LD8622.3prime-hit /ESTpos=maps 3prime of FB:FBgn0013718 /sym=nuf /name=nuclear fallout /prod= /func=cytoskeletal structural protein /map=7D2-7D2 /transc=CT23449 /len=291

24154.1 2.8 FB:FBgn0035788 /sym=CG8541 /name= /prod=cuticle protein /func=ligand binding or carrier /map=66A1-66A1 /transc=CT15726 /len=828 /GB:AE003559

1572.4 ~2.8 FB:FBgn0038063 /sym=CG6989 /name= /prod=beta adrenergic receptor-like /func=G protein linked receptor /map=87C2-87C2 /transc=CT21650 /len=1224 /GB:AE003696

5162.2 ~2.8 FB:FBgn0000462 /sym=dl /name=dorsal /prod= /func=specific RNA polymerase II transcription factor /map=36C2-36C2 /transc=CT42418 /len=4565 /GB:AE003655

26681.8 2.8 FB:FBgn0036357 /sym=CG10724 /name= /prod= /func=enzyme /map=70A7-70A7 /transc=CT30041 /len=2260 /GB:AE003538 /note=3prime sequence from clone BDGP:LD27045.3prime-hit

2345.7 ~2.8 FB:FBgn0039484 /sym=CG6124 /name= /prod= /func=cell adhesion /map=97E6-97E6 /transc=CT19227 /len=2673 /GB:AE003759

14723 2.8 FB:FBgn0037744 /sym=CG8417 /name= /prod=mannose-6-phosphate isomerase /func=enzyme /map=85E8-85E8 /transc=CT24707 /len=1398 /GB:AE003684 /note=3prime sequence from clone BDGP:HL01515.3prime-hit

19142.5 2.8 FB:FBgn0020304 /sym=drongo /name=drongo /prod= /func=defense/immunity protein /map=21D2-21D2 /transc=CT42210 /len=2383 /GB:AE003588 /note=3prime sequence from clone BDGP:GH1000000000

11359.3 2.8 FB:FBgn0035390 /sym=CG1893 /name= /prod= /func= /map=63B5-63B5 /transc=CT5862 /len=834 /GB:AE003476

23109.6 2.8 FB:FBgn0005666 /sym=bt /name=bent /prod=projectin /func=cell adhesion /map=102D6-102E1 /transc=CT3598 /len=23764 /GB:AE003843 /note=3prime sequence from clone BDGP:GH07636.3prime

1097.1 ~2.8 FB:FBgn0037651 /sym=CG11978 /name= /prod= /func= /map=85C3-85C3 /transc=CT32124 /len=456 /GB:AE003681

2869 ~2.8 FB:FBgn0033526 /sym=CG12892 /name= /prod= /func=enzyme /map=47A9-47A9 /transc=CT32037 /len=2244 /GB:AE003829

5181.6 2.8 FB:FBgn0016762 /sym=angel /name=angel /prod= /func=enzyme /map=59F4-59F4 /transc=CT17360 /len=1184 /GB:AE003461 /note=3prime sequence from clone BDGP:GH06351.3prime-hit

3664 2.8 FB:FBgn0030526 /sym=CG11102 /name= /prod= /func= /map=12B9-12B9 /transc=CT31063 /len=1671 /GB:AE003493

187409.7 2.8 FB:FBgn0003738 /sym=Tpi /name=Triose phosphate isomerase /prod=triosephosphate isomerase /func=triosephosphate isomerase ; EC:5.3.1.1 /map=99E1-99E1 /transc=CT6334 /len=1186 /GB:AE003493

5399.5 2.8 BDGP:LD1876.3prime-hit /ESTpos=maps 3prime of FB:FBgn0038501 /sym=CG5319 /name= /prod= /func= /map=9A6-9A6 /transc=CT1693 /len=567

361575.5 2.8 FB:FBgn0002789 /sym=Mp20 /name=Muscle protein 2 /prod=calcium-binding protein /func=calcium binding /map=49F15-49F15 /transc=CT15161 /len=852 /GB:AE003819

24381.1 2.7 FB:FBgn0030753 /sym=CG4420 /name= /prod= /func=DNA binding /map=14D1-14D1 /transc=CT14402 /len=1880 /GB:AE003502 /note=3prime sequence from clone BDGP:GM04721.3prime-hit

6802.3 2.7 FB:FBgn0039914 /sym=CG1901 /name= /prod=transforming growth factor beta-like /func=signal transduction /map=102D1-102D1 /transc=CT5854 /len=2528 /GB:AE003843

107633.5 2.7 FB:FBgn0032282 /sym=CG7299 /name= /prod= /func= /map=32A1-32A1 /transc=CT22515 /len=534 /GB:AE003629

11917.3 2.7 FB:FBgn0037138 /sym=CG7145 /name= /prod=1-pyrroline-5-carboxylate dehydrogenase-like /func=enzyme /map=79A5-79A5 /transc=CT22083 /len=1890 /GB:AE003595

3937.3 ~2.7 FB:FBgn0036656 /sym=CG13026 /name= /prod= /func= /map=73B5-73B5 /transc=CT32244 /len=405 /GB:AE003526

27579.5 2.7 FB:FBgn0033593 /sym=CG9080 /name= /prod= /func= /map=47E1-47E1 /transc=CT26066 /len=435 /GB:AE003826

39799.4 2.7 FB:FBgn0000486 /sym=Dox-A2 /name=Diphenol oxidase A2 /prod=proteasome, regulatory subunit S3 /func=multicatalytic endopeptidase ; EC:3.4.99.46 | inferred from sequence similarity /map=37B

3954.7 2.7 FB:FBgn0035232 /sym=CG12099 /name= /prod= /func= /map=62A7-62A7 /transc=CT6023 /len=2445 /GB:AE003472

282709.9 2.7 FB:FBgn0010423 /sym=TpnC47D /name=Troponin C at 47D /prod=troponin C /func=calcium binding /map=47E1-47E1 /transc=CT26048 /len=586 /GB:AE003826

261112.7 2.7 FB:FBgn0004169 /sym=up /name=upheld /prod=troponin T /func=tropomyosin binding /map=12A2-12A4 /transc=CT41714 /len=1424 /GB:AE003493

2179.9 ~2.7 BDGP:GH27479.3prime-hit /ESTpos=maps in FB:FBgn0031850 /sym=CG11326 /name= /prod=thrombospondin-3 like /func=cell adhesion /map=26F6-27A1 /transc=CT31613 /len=523

9124.9 2.7 FB:FBgn0000568 /sym=Eip75B /name=Ecdysone-induced protein 75B /prod=nuclear receptor NR1D3 /func=ligand-dependent nuclear receptor /map=75A10-75B6 /transc=CT24290 /len=4527 /GB:A

1646.1 ~2.7 FB:FBgn0035345 /sym=CG16764 /name= /prod= /func= /map=62E5-62E6 /transc=CT37287 /len=577 /GB:AE003475

16248.5 2.7 FB:FBgn0037821 /sym=CG14682 /name= /prod= /func=nucleic acid binding /map=86C2-86C2 /transc=CT34468 /len=3926 /GB:AE003688 /note=3prime sequence from clone BDGP:GH12580.3prime

6856.8 2.7 FB:FBgn0039136 /sym=CG5902 /name= /prod= /func= /map=95D1-95D1 /transc=CT18529 /len=1603 /GB:AE003745 /note=3prime sequence from clone BDGP:SD10002.3prime-hit

6014.3 2.7 FB:FBgn0037747 /sym=CG8481 /name= /prod=N-acetyltransferase /func=enzyme /map=85E8-85E8 /transc=CT24815 /len=1390 /GB:AE003684 /note=3prime sequence from clone BDGP:GH04732.

23332.5 2.7 FB:FBgn0034412 /sym=CG15105 /name= /prod= /func=transcription factor /map=56A1-56A2 /transc=CT34980 /len=3668 /GB:AE003797 /note=3prime sequence from clone BDGP:GH06739.3prime

28735.4 2.7 FB:FBgn0038130 /sym=CG8630 /name= /prod= /func=enzyme /map=87E5-87E5 /transc=CT25031 /len=1227 /GB:AE003699

406983.7 2.7 FB:FBgn0002772 /sym=Mlc1 /name=Myosin alkali light chain 1 /prod=myosin muscle class II essential light chain /func=muscle motor protein /map=98A6-98A6 /transc=CT17694 /len=722 /GB:AE0

4438.3 2.7 FB:FBgn0039268 /sym=CG11819 /name= /prod= /func=protein kinase /map=96B15-96B16 /transc=CT36931 /len=2933 /GB:AE003750

1636.4 ~2.7 FB:FBgn0023180 /sym=Orc6 /name=Origin recognition complex subunit 6 /prod=origin recognition complex, subunit 6 /func=DNA replication factor /map=46B13-46B13 /transc=CT4175 /len=774

3209.9 2.7 FB:FBgn0032218 /sym=CG5381 /name= /prod= /func=transcription factor /map=31D8-31D8 /transc=CT17078 /len=1884 /GB:AE003628

29892.5 2.7 FB:FBgn0033631 /sym=CG9027 /name= /prod=superoxide dismutase-like /func=enzyme /map=47F6-47F7 /transc=CT25938 /len=477 /GB:AE003826

15442.6 2.7 FB:FBgn0004646 /sym=ogre /name=optic ganglion reduced /prod=innexin /func=ion channel /map=6E4-6E4 /transc=CT9674 /len=2219 /GB:AE003439 /note=3prime sequence from clone BDGP:HL

3280.1 ~2.7 FB:FBgn0038572 /sym=CG7901 /name= /prod= /func= /map=90E4-90E4 /transc=CT42545 /len=937 /GB:AE003721

17540.7 2.7 FB:FBgn0028695 /sym=Rpn1 /name= /prod=19S proteasome regulatory particle, non-ATPase protein, subunit S2 /func=endopeptidase /map=76D7-76D7 /transc=CT23606 /len=2967 /GB:AE003515

1747.9 ~2.7 FB:FBgn0037806 /sym=CG11872 /name= /prod= /func= /map=86A1-86A2 /transc=CT37024 /len=4311 /GB:AE003686

3248.6 2.7 FB:FBgn0034969 /sym=CG10485 /name= /prod=ribosomal protein L12-like /func=structural protein of ribosome /map=60B2-60B2 /transc=CT29426 /len=675 /GB:AE003462

19865.8 2.7 FB:FBgn0039909 /sym=CG1970 /name= /prod=NADH-ubiquinone oxidoreductase /func=enzyme /map=102C5-102C5 /transc=CT6146 /len=1482 /GB:AE003843

295117.9 2.7 FB:FBgn0003149 /sym=Prm /name=Paramyosin /prod=paramyosin /func=structural protein of muscle /map=66D14-66D14 /transc=CT18619 /len=2721 /GB:AE003554 /note=3prime sequence from c

226879.3 2.6 FB:FBgn0003178 /sym=PyK /name=Pyruvate kinase /prod=pyruvate kinase /func=pyruvate kinase ; EC:2.7.1.40 /map=94A15-94A15 /transc=CT21861 /len=2091 /GB:AE003738 /note=3prime sequenc
FB:FBgn0016697 /sym=ProsMA5 /name=Proteasome alpha subunit /prod=20S proteasome, alpha5 subunit /func=multicatalytic endopeptidase ; EC:3.4.99.46 /map=54C1-54C1 /transc=CT30641 /len=

26236 2.6 BDGP:LD33318.3prime-hi

1734.5 ~2.6 FB:FBgn0038591 /sym=CG7150 /name= /prod=transcriptional adaptor-like /func=transcription factor binding /map=90F4-90F4 /transc=CT22097 /len=1876 /GB:AE003721

31369.2 2.6 FB:FBgn0032148 /sym=CG13122 /name= /prod= /func= /map=30D1-30D1 /transc=CT32359 /len=1567 /GB:AE003626 /note=3prime sequence from clone BDGP:HL02309.3prime-hit

94556.2 2.6 FB:FBgn0003074 /sym=Pgi /name=Phosphoglucose isomerase /prod=phosphogluconate dehydrogenase (decarboxylating) /func=phosphogluconate dehydrogenase (decarboxylating) ; EC:1.1.1.44 /map=

17250.2 2.6 FB:FBgn0031187 /sym=CG14619 /name= /prod=ubiquitin-specific protease /func=ubiquitin-specific protease /map=19F5-19F6 /transc=CT34376 /len=2865 /GB:AE003574 /note=3prime sequence fro

65019.7 2.6 FB:FBgn0033126 /sym=CG10106 /name= /prod= /func= /map=42E1-42E1 /transc=CT7946 /len=1113 /GB:AE003842

1930.1 ~2.6 FB:FBgn0037543 /sym=CG10903 /name= /prod= /func= /map=84E7-84E7 /transc=CT10979 /len=831 /GB:AE003677

1510.5 ~2.6 FB:FBgn0040733 /sym=CG15068 /name= /prod= /func= /map=55C9-55C9 /transc=CT34939 /len=189 /GB:AE003799

32265.4 2.6 FB:FBgn0034952 /sym=CG18021 /name= /prod= /func= /map=60A15-60A15 /transc=CT40326 /len=2017 /GB:AE003462 /note=3prime sequence from clone BDGP:GH20492.3prime-hit

226436.5 2.6 FB:FBgn0036108 /sym=CG7941 /name= /prod=cuticle protein-like /func=structural protein /map=67F4-67F4 /transc=CT23954 /len=405 /GB:AE003546

6757.5 2.6 FB:FBgn0035464 /sym=CG12006 /name= /prod= /func= /map=63F1-63F1 /transc=CT1387 /len=1873 /GB:AE003479 /note=3prime sequence from clone BDGP:LD47795.3prime-hit

3265.6 2.6 BDGP:LD23884.3prime-hit /ESTpos=maps in FB:FBgn0030430 /sym=CG4410 /name= /prod=chaperone-like protein /func=chaperone /map=11C4-11C4 /transc=CT4259 /len=500

3303 2.6 FB:FBgn0023215 /sym=EG:114E2.2 /name= /prod= /func=transcription factor binding /map=3F2-3F2 /transc=CT9776 /len=1830 /GB:AE003428 /note=3prime sequence from clone BDGP:GH28809.

3036.8 2.6 FB:FBgn0037252 /sym=CG14650 /name= /prod= /func=chaperone /map=82C1-82C1 /transc=CT34422 /len=3606 /GB:AE003606 /note=3prime sequence from clone BDGP:GH27269.3prime-hit

8684.4 2.6 FB:FBgn0033179 /sym=CG11139 /name= /prod= /func= /map=43C4-43C5 /transc=CT31143 /len=1419 /GB:AE003841 /note=3prime sequence from clone BDGP:GH01724.3prime-hit

31577.4 2.6 FB:FBgn0037314 /sym=CG12000 /name= /prod=20S proteasome, beta4 subunit-like /func=endopeptidase /map=83A4-83A4 /transc=CT1070 /len=1216 /GB:AE003603 /note=3prime sequence from

15346.3 2.6 FB:FBgn0028689 /sym=Rpn6 /name=Proteasome p44.5 subunit /prod=19S proteasome regulatory particle, non-ATPase protein, subunit S9 /func=multicatalytic endopeptidase ; EC:3.4.99.46 | inferred

10636.7 2.6 FB:FBgn0012042 /sym=AttA /name=Attacin-A /prod=attacin /func=antibacterial response protein /map=51C2-51C2 /transc=CT28545 /len=895 /GB:AE003813 /note=3prime sequence from clone BD

4029.3 2.6 FB:FBgn0022986 /sym=qkr58E-1 /name=quaking related 58E-1 /prod= /func=RNA binding /map=58D8-58D8 /transc=CT12115 /len=1618 /GB:AE003457 /note=3prime sequence from clone BDGP:

346314.5 2.6 FB:FBgn0032538 /sym=CG16885 /name= /prod= /func= /map=34E1-34E1 /transc=CT35249 /len=780 /GB:AE003641

3832 2.6 FB:FBgn0039110 /sym=CG10225 /name= /prod= /func=structural protein /map=95B7-95B7 /transc=CT28739 /len=1726 /GB:AE003744 /note=3prime sequence from clone BDGP:LD02979.3prime-h

13072 2.6 FB:FBgn0002787 /sym=Mov34 /name=Mov34 /prod=19S proteasome regulatory particle, non-ATPase protein, subunit S12 /func=multicatalytic endopeptidase ; EC:3.4.99.46 /map=60D1-60D1 /transc=

14695.1 2.6 FB:FBgn0030479 /sym=CG1987 /name= /prod=RNA binding protein-like /func=RNA binding /map=11E11-11E11 /transc=CT6330 /len=393 /GB:AE003492

11266.1 2.6 FB:FBgn0000480 /sym=Doa /name=Darkener of apricot /prod=protein serine/threonine kinase /func=protein kinase /map=98F1-98F2 /transc=CT4592 /len=2232 /GB:AE003767 /note=3prime sequenc

2739.1 ~2.6 FB:FBgn0039688 /sym=CG1964 /name= /prod=ADAM10 family metalloendopeptidase/disintegrin-like /func=endopeptidase /map=99C1-99C1 /transc=CT3146 /len=4614 /GB:AE003770

3005.4 2.6 FB:FBgn0002641 /sym=mal /name=maroon-like /prod=molybdopterin cofactor sulfurase-like /func=molybdopterin cofactor sulfurase /map=19D2-19D3 /transc=CT4746 /len=2717 /GB:AE003571 /nc

2590.6 2.6 FB:FBgn0039423 /sym=CG6166 /name= /prod= /func= /map=97A9-97A9 /transc=CT19364 /len=2031 /GB:AE003756 /note=3prime sequence from clone BDGP:GH14066.3prime-hit

1561.7 ~2.5 FB:FBgn0038041 /sym=CG6525 /name= /prod= /func=ligand binding or carrier /map=87B15-87B15 /transc=CT20279 /len=6051 /GB:AE003695

4086.6 2.5 FB:FBgn0034688 /sym=CG11474 /name= /prod= /func= /map=58C1-58C1 /transc=CT36283 /len=1521 /GB:AE003456 /note=3prime sequence from clone BDGP:LD03212.3prime-hit

8386.7 2.5 FB:FBgn0029851 /sym=CG14445 /name= /prod= /func= /map=5D6-5D6 /transc=CT34116 /len=1143 /GB:AE003437

2153.4 ~2.5 FB:FBgn0034242 /sym=CG14480 /name= /prod= /func= /map=54D1-54D1 /transc=CT34191 /len=750 /GB:AE003802

22995.3 2.5 FB:FBgn0028687 /sym=Rpt1 /name= /prod=19S proteasome regulatory particle, triple-A protein, subunit S7 /func=proteasome ATPase ; EC:3.6.4.8 /map=43E6-43E6 /transc=CT3016 /len=1397 /GB:A

1340.1 ~2.5 FB:FBgn0035081 /sym=CG2858 /name= /prod= /func=enzyme /map=60E5-60E5 /transc=CT9732 /len=1449 /GB:AE003465

1871.2 ~2.5 FB:FBgn0038688 /sym=CG3768 /name= /prod=calcium binding protein-like /func=ligand binding or carrier /map=91F8-91F8 /transc=CT12576 /len=1030 /GB:AE003725 /note=3prime sequence from

5012.1 2.5 FB:FBgn0029715 /sym=CG11444 /name= /prod= /func= /map=4C4-4C4 /transc=CT9463 /len=1230 /GB:AE003431 /note=3prime sequence from clone BDGP:GM14292.3prime-hit

3675.4 2.5 FB:FBgn0024988 /sym=EG:131F2.2 /name= /prod= /func=enzyme /map=2B12-2B12 /transc=CT34614 /len=2176 /GB:AE003422 /note=3prime sequence from clone BDGP:SD04906.3prime-hit

58654.6 2.5 FB:FBgn0037346 /sym=CG2922 /name= /prod= /func= /map=83B4-83B4 /transc=CT7240 /len=2082 /GB:AE003602 /note=3prime sequence from clone BDGP:LD21309.3prime-hit

47824.9 2.5 FB:FBgn0036109 /sym=CG18349 /name= /prod= /func= /map=67F4-67F4 /transc=CT41690 /len=536 /GB:AE003546

150789.1 2.5 *Drosophila* gene for Gapdh2 (_5, _M, _3 represent transcript regions 5 prime, Middle, and 3 prime respectively)

237211 2.5 FB:FBgn0001092 /sym=Gapdh2 /name=Glyceraldehyde 3 phosphate dehydrogenase 2 /prod=glyceraldehyde 3-phosphate dehydrogenase (phosphorylating) 2 /func=glyceraldehyde 3-phosphate dehydro

15429.8 2.5 FB:FBgn0038420 /sym=CG10311 /name= /prod= /func= /map=89B22-89B22 /transc=CT28967 /len=719 /GB:AE003713

1337.5 ~2.5 FB:FBgn0033745 /sym=CG8824 /name= /prod=beta-N-acetylhexosaminidase-like /func=enzyme /map=49A9-49A9 /transc=CT25388 /len=2555 /GB:AE003822 /note=3prime sequence from clone BL

6100.3 2.5 FB:FBgn0038878 /sym=CG3301 /name= /prod= /func=enzyme /map=93D4-93D4 /transc=CT11093 /len=913 /GB:AE003734 /note=3prime sequence from clone BDGP:GH01837.3prime-hit

1526.3 ~2.5 FB:FBgn0031206 /sym=CG12466 /name= /prod= /func=enzyme /map=20B1-20B1 /transc=CT32678 /len=1204 /GB:AE003573 /note=3prime sequence from clone BDGP:GH12380.3prime-hit

21705.6 2.5 FB:FBgn0030672 /sym=CG9281 /name= /prod=ATP-binding cassette transporter /func=enzyme /map=13E14-13E14 /transc=CT26402 /len=2568 /GB:AE003500 /note=3prime sequence from clone B

35348.3 2.5 FB:FBgn0026781 /sym=Prosalph1 /name=Proteasome alpha1 subunit /prod=20S proteasome alpha1 subunit /func=multicatalytic endopeptidase ; EC:3.4.99.46 /map=43F1-43F1 /transc=CT42048 /len=

2834.7 2.5 FB:FBgn0036811 /sym=CG6884 /name= /prod= /func= /map=75D4-75D4 /transc=CT21320 /len=610 /GB:AE003519

515.3 ~2.5 FB:FBgn0032574 /sym=CG18629 /name= /prod= /func= /map=35E1-35E1 /transc=CT41822 /len=588 /GB:AE003649

2330 2.5 FB:FBgn0034094 /sym=CG3666 /name= /prod=transferrin-like /func=ligand binding or carrier /map=52F10-52F10 /transc=CT12185 /len=2352 /GB:AE003807 /note=3prime sequence from clone BD

463382.8 2.5 FB:FBgn0038154 /sym=CG18290 /name= /prod= /func= /map=87E11-87E11 /transc=CT41497 /len=1195 /GB:AE003700

9847.6 2.5 FB:FBgn0000250 /sym=cact /name=cactus /prod= /func=transcription factor, cytoplasmic sequestering /map=35F8-35F9 /transc=CT18347 /len=1918 /GB:AE003650 /note=3prime sequence from clo

15853.4 2.5 FB:FBgn0040754 /sym=CG17059 /name= /prod= /func= /map=49F13-49F13 /transc=CT37898 /len=358 /GB:AE003819

119631.9 2.5 FB:FBgn0000045 /sym=Act79B /name=Actin 79B /prod=actin /func=muscle motor protein /map=79B3-79B3 /transc=CT22987 /len=1172 /GB:AE003596

42016.5 2.5 FB:FBgn0023174 /sym=Probeta2 /name=Proteasome beta2 subunit /prod=20S proteasome, beta2 subunit /func=multicatalytic endopeptidase ; EC:3.4.99.46 /map=71A3-71A3 /transc=CT10524 /len=1

7369.5 2.5 FB:FBgn0001301 /sym=kel /name=kelch /prod= /func=transcription factor /map=36E3-36E5 /transc=CT22235 /len=5604 /GB:AE003657 /note=3prime sequence from clone BDGP:LD29455.3prime-

2044.3 ~2.5 FB:FBgn0029872 /sym=CG12543 /name= /prod= /func= /map=6A2-6A2 /transc=CT34107 /len=684 /GB:AE003437

6487.2 2.4 FB:FBgn0032202 /sym=CG18619 /name= /prod= /func= /map=31C6-31C6 /transc=CT40890 /len=486 /GB:AE003628

396588.5 2.4 FB:FBgn0002531 /sym=Lcp1 /name=Larval cuticle protein 1 /prod=larval cuticle protein 1 /func=structural protein of larval cuticle (*Drosophila*) /map=44C1-44C1 /transc=CT36649 /len=543 /GB:AE003842

7853 2.4 FB:FBgn0033129 /sym=CG12844 /name= /prod= /func= /map=42E1-42E1 /transc=CT31976 /len=673 /GB:AE003842

1333.8 ~2.4 FB:FBgn0035649 /sym=CG10483 /name= /prod= /func= /map=64F5-64F5 /transc=CT29432 /len=2221 /GB:AE003564 /note=3prime sequence from clone BDGP:GH26628.3prime-hit

1728.4 ~2.4 BDGP:LD4689.3prime-hit /ESTpos=maps in FB:FBgn0037937 /sym=CG6913 /name= /prod= /func=DNA binding /map=86F1-86F1 /transc=CT21412 /len=536

8012.7 2.4 BDGP:LD1981.3prime-hit /ESTpos=maps 3prime of FB:FBgn0027356 /sym=amphiphysin /name=amphiphysin /prod=amphiphysin /func=protein kinase /map=49B3-49B3 /transc=CT259 /len=527

20242.2 2.4 FB:FBgn0015282 /sym=Pros26.4 /name=Proteasome 26S subunit subunit 4 ATPase /prod=19S proteasome regulatory particle, triple-A protein, subunit S4 /func=proteasome ATPase ; EC:3.6.4.8 /map=7A9-7A9

1105.9 ~2.4 FB:FBgn0030941 /sym=CG6531 /name= /prod= /func= /map=17C3-17C3 /transc=CT20295 /len=1260 /GB:AE003509

11202 2.4 FB:FBgn0029534 /sym=CG5273 /name= /prod= /func= /map=1C1-1C1 /transc=CT16821 /len=2072 /GB:AE003418

30822.1 2.4 FB:FBgn0015283 /sym=Pros54 /name=Proteasome 54kD subunit /prod=19S proteasome regulatory particle, non-ATPase protein, subunit S5a /func=multicatalytic endopeptidase ; EC:3.4.99.46 /map=7A9-7A9

1588.1 ~2.4 FB:FBgn0033026 /sym=CG12183 /name= /prod= /func=actin binding /map=41C4-41C4 /transc=CT9399 /len=1982 /GB:AE003786

2849.2 2.4 FB:FBgn0039238 /sym=CG7016 /name= /prod= /func= /map=96B4-96B4 /transc=CT21718 /len=1089 /GB:AE003749

2368.7 ~2.4 FB:FBgn0036359 /sym=CG14105 /name= /prod= /func= /map=70A8-70A8 /transc=CT33698 /len=558 /GB:AE003538

32750.7 2.4 FB:FBgn0035089 /sym=CG9358 /name= /prod= /func=ligand binding or carrier /map=60E7-60E7 /transc=CT26583 /len=366 /GB:AE003465

2937.6 2.4 FB:FBgn0038260 /sym=CG14855 /name= /prod=organic cation transporter-like /func=transporter /map=88D5-88D5 /transc=CT34672 /len=1671 /GB:AE003706

61689.5 2.4 FB:FBgn0029639 /sym=CG14419 /name= /prod= /func= /map=3C3-3C3 /transc=CT34076 /len=588 /GB:AE003425

359826.3 2.4 FB:FBgn0001091 /sym=Gapdh1 /name=Glyceraldehyde 3 phosphate dehydrogenase 1 /prod=glyceraldehyde 3-phosphate dehydrogenase (phosphorylating) 1 /func=glyceraldehyde 3-phosphate dehydrogenase (phosphorylating) 1

1642.5 ~2.4 FB:FBgn0030991 /sym=CG7453 /name= /prod= /func= /map=18B4-18B4 /transc=CT22925 /len=1285 /GB:AE003511

27834.9 2.4 FB:FBgn0035978 /sym=CG4347 /name= /prod= /func=UTP--glucose-1-phosphate uridylyltransferase /map=67A9-67B1 /transc=CT14147 /len=2009 /GB:AE003552 /note=3prime sequence from clone BDGP:LD16758.3prime-hit

996.5 ~2.4 FB:FBgn0024993 /sym=EG:100G10.6 /name= /prod= /func=transcription factor /map=3B4-3B5 /transc=CT9011 /len=1402 /GB:AE003425

11747.2 2.4 FB:FBgn0036111 /sym=CG6391 /name= /prod=diphosphoinositol polyphosphate phosphohydrolase /func=enzyme /map=67F4-67F4 /transc=CT19950 /len=1704 /GB:AE003546

2303.3 2.4 FB:FBgn0032392 /sym=CG17749 /name= /prod= /func= /map=33B9-33B9 /transc=CT39339 /len=476 /GB:AE003634

18248.8 2.4 FB:FBgn0036580 /sym=CG13072 /name= /prod= /func= /map=72D12-72D12 /transc=CT32291 /len=402 /GB:AE003528

13431.5 2.4 FB:FBgn0033683 /sym=CG18343 /name= /prod= /func= /map=48E10-48E10 /transc=CT41671 /len=463 /GB:AE003823

73558.1 2.4 FB:FBgn0039358 /sym=CG5028 /name= /prod= /func=enzyme /map=96E10-96E10 /transc=CT16155 /len=1312 /GB:AE003753

1327 ~2.4 FB:FBgn0015569 /sym=alpha-Est10 /name=alpha-Esterase-1 /prod=esterase, unknown substrate /func=esterase, unknown substrate ; EC:3.1.1.- /map=84D5-84D5 /transc=CT1811 /len=1650 /GB:AE003842

9558.3 2.4 FB:FBgn0024754 /sym=Flo /name=flotillin /prod=flotillin /func=ligand binding or carrier /map=52A13-52A13 /transc=CT37018 /len=1779 /GB:AE003810 /note=3prime sequence from clone BDGP:LD16758.3prime-hit

37048.3 2.4 FB:FBgn0030151 /sym=CG1354 /name= /prod=GTP-binding protein /func=ligand binding or carrier /map=8F10-8F10 /transc=CT3048 /len=1200 /GB:AE003448

14186.8 2.4 FB:FBgn0028686 /sym=Rpt3 /name= /prod=19S proteasome regulatory particle, triple-A protein, subunit S6b /func=proteasome ATPase ; EC:3.6.4.8 /map=10A6-10A6 /transc=CT35131 /len=1242 /GB:AE003564

357251.3 2.4 FB:FBgn0000064 /sym=Ald /name=Aldolase /prod=fructose-bisphosphate aldolase /func=fructose-bisphosphate aldolase ; EC:4.1.2.13 | inferred from direct assay /map=97A6-97A6 /transc=CT41919 /len=1000

26041.1 2.4 FB:FBgn0037007 /sym=CG5059 /name= /prod= /func= /map=77C4-77C4 /transc=CT16233 /len=939 /GB:AE003591

146254 2.4 FB:FBgn0004551 /sym=Ca-P60A /name=Calcium ATPase at 6A /prod=calcium-transporting ATPase, sarco/endoplasmic reticulum type /func=calcium-transporting ATPase ; EC:3.6.1.38 /map=60A11-60A11

8895.8 2.4 FB:FBgn0027591 /sym=BcDNA:GH04245 /name= /prod= /func= /map=41A1-41A2 /transc=CT9123 /len=3519 /GB:AE003787 /note=3prime sequence from clone BDGP:LD16758.3prime-hit

968.3 ~2.4 FB:FBgn0030563 /sym=CG18157 /name= /prod= /func= /map=12E2-12E2 /transc=CT40954 /len=594 /GB:AE003495

20212.5 2.4 FB:FBgn0040954 /sym=CG13779 /name= /prod= /func= /map=27D5-27D5 /transc=CT33267 /len=240 /GB:AE003616

5163.6 2.4 FB:FBgn0035981 /sym=CG4452 /name= /prod= /func=endopeptidase /map=67B1-67B1 /transc=CT14468 /len=1633 /GB:AE003552 /note=3prime sequence from clone BDGP:LD21662.3prime-hit

133490.6 2.4 FB:FBgn0040764 /sym=CG13230 /name= /prod= /func= /map=47D4-47D4 /transc=CT32474 /len=219 /GB:AE003827

253266.6 2.4 *Drosophila* gene for Gapdh2 (_5, _M, _3 represent transcript regions 5 prime, Middle, and 3 prime respectively)

10105.4 2.4 FB:FBgn0026777 /sym=Rad23 /name= /prod= /func=DNA repair protein /map=102A8-102A8 /transc=CT5572 /len=1477 /GB:AE003844 /note=3prime sequence from clone BDGP:LD10153.complet

556.8 ~2.4 FB:FBgn0036074 /sym=CG11965 /name= /prod= /func= /map=67D2-67D2 /transc=CT37129 /len=1464 /GB:AE003549

6578.4 2.4 FB:FBgn0015614 /sym=CanB2 /name=Calcineurin B2 /prod=calcineurin, calcium-binding, regulatory (B)-subunit 2 /func=calcium binding /map=43E16-43E16 /transc=CT31322 /len=718 /GB:AE003549

5794.3 2.3 FB:FBgn0024753 /sym=Flo-2 /name=flotillin 2 /prod=flotillin 2 /func= /map=13A3-13A4 /transc=CT34056 /len=1791 /GB:AE003497 /note=3prime sequence from clone BDGP:LP11503.3prime-hit

22177.6 2.3 FB:FBgn0027493 /sym=BcDNA:LD32788 /name= /prod=adenylosuccinate synthase /func=adenylosuccinate synthase ; EC:6.3.4.4 /map=92F13-92F13 /transc=CT35906 /len=1986 /GB:AE003732 /note=3prime sequence from clone BDGP:LD32788.3prime-hit

13759.5 2.3 FB:FBgn0039213 /sym=CG6668 /name= /prod= /func= /map=96A14-96A15 /transc=CT20689 /len=2852 /GB:AE003748 /note=3prime sequence from clone BDGP:GH09383.3prime-hit

1521 ~2.3 FB:FBgn0034946 /sym=CG3065 /name= /prod= /func=nucleic acid binding /map=60A14-60A14 /transc=CT10306 /len=1916 /GB:AE003462 /note=3prime sequence from clone BDGP:GM01315.3prime-hit

21415.1 2.3 FB:FBgn0033886 /sym=CG13349 /name= /prod= /func= /map=50C20-50C20 /transc=CT32670 /len=1170 /GB:AE003816

53208.4 2.3 FB:FBgn0002284 /sym=Pros26 /name=Proteasome 26kD subunit /prod=20S proteasome, beta6 subunit /func=multicatalytic endopeptidase ; EC:3.4.99.46 /map=73A10-73A10 /transc=CT13566 /len=944

109219.9 2.3 FB:FBgn0017565 /sym=Nacalpha /name=Nascent polypeptide associated complex protein alpha subunit /prod=nascent polypeptide associated complex protein alpha subunit /func= /map=49C2-49C2 /transc=CT13566 /len=944

11393.2 2.3 FB:FBgn0030310 /sym=CG11709 /name= /prod=peptidoglycan recognition protein-like /func=defense/immunity protein /map=10C4-10C4 /transc=CT35112 /len=612 /GB:AE003486

29773.9 2.3 FB:FBgn0030724 /sym=CG9212 /name= /prod= /func=4-nitrophenylphosphatase /map=14A6-14A6 /transc=CT26318 /len=1359 /GB:AE003501 /note=3prime sequence from clone BDGP:LD01807.3prime-hit

1175.3 ~2.3 FB:FBgn0029970 /sym=CG17256 /name= /prod=protein serine/threonine kinase-like /func=protein kinase /map=7C6-7C6 /transc=CT38234 /len=2435 /GB:AE003442 /note=3prime sequence from clone BDGP:LD01807.3prime-hit

22793.7 2.3 FB:FBgn0036630 /sym=CG4561 /name= /prod= /func=tyrosine-tRNA ligase /map=73A1-73A1 /transc=CT14730 /len=1717 /GB:AE003527

1093 ~2.3 BDGP:GH06247.3prime-hit /maps to FB:FBgn0036239 (/sym=CG5684 /name= /prod= /func=transcription factor) and FB:FBgn0036238 (/sym=CG5688 /name= /prod= /func=motor)

21198.4 2.3 FB:FBgn0003151 /sym=Pros35 /name=Proteasome 35kD subunit /prod=20S proteasome, alpha6 subunit /func=multicatalytic endopeptidase ; EC:3.4.99.46 /map=31B3-31B4 /transc=CT15762 /len=944

24276.6 2.3 FB:FBgn0035206 /sym=CG9186 /name= /prod= /func= /map=61F6-61F6 /transc=CT8283 /len=1400 /GB:AE003471 /note=3prime sequence from clone BDGP:LP01162.3prime-hit

2027.2 2.3 FB:FBgn0010406 /sym=RNaseX25 /name=Ribonuclease X25 /prod=ribonuclease-like /func=ribonuclease /map=66A22-66A22 /transc=CT24383 /len=1658 /GB:AE003557 /note=3prime sequence from clone BDGP:LP01162.3prime-hit

1848.8 ~2.3 FB:FBgn0029798 /sym=CG4078 /name= /prod= /func=DNA repair protein /map=5B3-5B3 /transc=CT13546 /len=3246 /GB:AE003435

2933.2 2.3 FB:FBgn0005649 /sym=Rox8 /name=Rox8 /prod=nucleolysin-like /func=poly(A) binding /map=95D5-95D5 /transc=CT17178 /len=3165 /GB:AE003746

1385.8 ~2.3 FB:FBgn0039901 /sym=CG10322 /name= /prod= /func= /map=102A7-102A8 /transc=CT7685 /len=630 /GB:AE003844

2931.2 2.3 FB:FBgn0033352 /sym=CG8232 /name= /prod=PAB-dependent poly(A)-specific ribonuclease subunit /func=enzyme /map=44F9-44F11 /transc=CT8229 /len=3925 /GB:AE003835 /note=3prime sequence from clone BDGP:LD28328.3prim

12984.9 2.3 FB:FBgn0039265 /sym=CG11790 /name= /prod= /func=chaperone /map=96B15-96B15 /transc=CT33049 /len=794 /GB:AE003750

10889.7 2.3 FB:FBgn0034618 /sym=CG9485 /name= /prod=glycogen debranching enzyme /func=enzyme /map=57D4-57D5 /transc=CT26790 /len=4780 /GB:AE003453 /note=3prime sequence from clone BDGP:LD28328.3prim

33371.1 2.3 FB:FBgn0038922 /sym=CG6439 /name= /prod=isocitrate dehydrogenase [NAD] subunit /func=enzyme /map=93F14-93F14 /transc=CT20062 /len=1598 /GB:AE003737 /note=3prime sequence from clone BDGP:LD28328.3prim

13683.2 2.2 FB:FBgn0016122 /sym=Acer /name=Angiotensin-converting enzyme-related /prod=angiotensin I-converting enzyme /func=peptidyl-dipeptidase A ; EC:3.4.15.1 /map=29D1-29D2 /transc=CT29700 /len=1000

254389.5 2.2 *Drosophila* gene for Gapdh2 (_5, _M, _3 represent transcript regions 5 prime, Middle, and 3 prime respectively)

1518.4 ~2.2 FB:FBgn0025186 /sym=ari2 /name=ariadne 2 /prod=/func= /map=58C7-58D1 /transc=CT17832 /len=3002 /GB:AE003456
FB:FBgn0004237 /sym=Hrb87F /name=Heterogeneous nuclear ribonucleoprotein at 87F /prod=heterogeneous nuclear ribonucleoprotein A1 /func=ribonucleoprotein /map=87F7-87F7 /transc=CT2725
9346.5 2.2 BDGP:GH05625.3
25443.2 2.2 FB:FBgn0003150 /sym=Pros29 /name=Proteasome 29kD subunit /prod=20S proteasome, alpha3 subunit /func=multicatalytic endopeptidase ; EC:3.4.99.46 /map=57B15-57B15 /transc=CT26525 /len=
367002.4 2.2 FB:FBgn0032537 /sym=CG18634 /name=/prod=/func= /map=34E1-34E1 /transc=CT42158 /len=552 /GB:AE003641
25780.9 2.2 FB:FBgn0035631 /sym=CG5495 /name=Thioredoxin-like /prod=thioredoxin-like /func=thioredoxin /map=64F1-64F1 /transc=CT17420 /len=957 /GB:AE003565 /note=3prime sequence from clone B
62260.5 2.2 FB:FBgn0027910 /sym=BcDNA:GM14618 /name=/prod=/func= /map=25C2-25C3 /transc=CT26154 /len=1161 /GB:AE003608
13850 2.2 FB:FBgn0033356 /sym=CG8229 /name=/prod=/func= /map=44F12-45A1 /transc=CT8591 /len=1918 /GB:AE003835 /note=3prime sequence from clone BDGP:LD27667.3prime-hit
252125.8 2.2 FB:FBgn0000579 /sym=Eno /name=Enolase /prod=phosphopyruvate hydratase /func=phosphopyruvate hydratase ; EC:4.2.1.11 /map=22B1-22B1 /transc=CT32526 /len=1931 /GB:AE003585
38831.3 2.2 FB:FBgn0040985 /sym=CG6115 /name=/prod=/func= /map=36A11-36A11 /transc=CT19203 /len=566 /GB:AE003653
22161.4 2.2 FB:FBgn0022959 /sym=yps /name=ypsilon schachtel /prod=/func= /map=68F4-68F4 /transc=CT17850 /len=2254 /GB:AE003542 /note=3prime sequence from clone BDGP:LD37574.3prime-hit
18395.1 2.2 FB:FBgn0032776 /sym=CG18061 /name=/prod=/func= /map=37E1-37E1 /transc=CT40481 /len=2027 /GB:AE003662 /note=3prime sequence from clone BDGP:SD04793.3prime-hit
FB:FBgn0011754 /sym=PhKgamma /name=Phosphorylase kinase gamma /prod=phosphorylase kinase, catalytic gamma subunit /func=phosphorylase kinase catalyst /map=10D2-10D4 /transc=CT55
6974.5 2.2 BDGP:GH28523.3pri
2303.3 2.2 FB:FBgn0032203 /sym=CG4946 /name=/prod=/func= /map=31C6-31C6 /transc=CT15842 /len=834 /GB:AE003628
116191.6 2.2 FB:FBgn0032941 /sym=CG8669 /name=/prod=/func= /map=39D2-39D2 /transc=CT5302 /len=1793 /GB:AE003670 /note=3prime sequence from clone BDGP:GH11210.3prime-hit
962.2 ~2.2 FB:FBgn0029913 /sym=CG3044 /name=/prod=chitinase /func=enzyme /map=6D3-6D3 /transc=CT10053 /len=1299 /GB:AE003439
900.8 ~2.2 FB:FBgn0004170 /sym=sc /name=scute /prod=/func=specific RNA polymerase II transcription factor /map=1B2-1B2 /transc=CT12777 /len=1038 /GB:AE003417
2967.8 2.2 FB:FBgn0037377 /sym=CG1218 /name=/prod=/func= /map=83C1-83C1 /transc=CT2292 /len=1479 /GB:AE003601 /note=3prime sequence from clone BDGP:LD28626.3prime-hit
1095.1 ~2.2 FB:FBgn0040737 /sym=CG14503 /name=/prod=/func= /map=55C5-55C5 /transc=CT34218 /len=177 /GB:AE003800
37391.6 2.2 FB:FBgn0028490 /sym=BcDNA:GH07269 /name=/prod=/func=DNA binding /map=33A2-33A2 /transc=CT20317 /len=3403 /GB:AE003632 /note=3prime sequence from clone BDGP:GH07269.3p
1499.3 ~2.2 FB:FBgn0028854 /sym=BG:DS07721.6 /name=/prod=/func= /map=35B5-35B5 /transc=CT35229 /len=3129 /GB:AE003644
106563 2.2 FB:FBgn0031024 /sym=CG12233 /name=/prod=/func=enzyme /map=18D3-18D3 /transc=CT13154 /len=1375 /GB:AE003512
20052.9 2.2 FB:FBgn0034110 /sym=CG3615 /name=/prod=/func= /map=53A2-53A2 /transc=CT12045 /len=2831 /GB:AE003807 /note=3prime sequence from clone BDGP:SD01812.3prime-hit
20912.8 2.2 FB:FBgn0037537 /sym=CG2767 /name=/prod=alcohol dehydrogenase /func=enzyme /map=84E5-84E6 /transc=CT9417 /len=1293 /GB:AE003677 /note=3prime sequence from clone BDGP:LD2467
7230.8 2.2 FB:FBgn0015239 /sym=Hr78 /name=Hormone-receptor-like in 78 /prod=nuclear receptor NR2D1 /func=ligand-dependent nuclear receptor /map=78D7-78D7 /transc=CT22217 /len=2246 /GB:AE003
8132.5 2.2 FB:FBgn0033128 /sym=CG12142 /name=Tetraspanin 42Eg /prod=tetraspanin /func= /map=42E1-42E1 /transc=CT7934 /len=1170 /GB:AE003842 /note=3prime sequence from clone BDGP:GM0696
10851 2.2 FB:FBgn0036661 /sym=CG9705 /name=/prod=calcium-regulated heat stable protein-like /func= /map=73C1-73C1 /transc=CT27440 /len=1386 /GB:AE003526 /note=3prime sequence from clone BD
5745.6 2.2 FB:FBgn0027108 /sym=inx2 /name=/prod=innexin 2 /func=neurotransmitter transporter /map=6E4-6E5 /transc=CT14874 /len=1819 /GB:AE003439
47271.9 2.2 FB:FBgn0035904 /sym=CG6776 /name=/prod=glutathione transferase /func=glutathione transferase /map=66D4-66D4 /transc=CT21027 /len=776 /GB:AE003555
171608.5 2.2 FB:FBgn0004432 /sym=Cyp1 /name=Cyclophilin 1 /prod=cyclophilin /func=cyclophilin /map=14B15-14B15 /transc=CT27926 /len=910 /GB:AE003501 /note=3prime sequence from clone BDGP:SD
2011.6 ~2.2 FB:FBgn0037190 /sym=CG7651 /name=/prod=P-type ATPase /func=transporter /map=79F3-79F3 /transc=CT22775 /len=3566 /GB:AE003598
12077.1 2.2 FB:FBgn0036299 /sym=CG10620 /name=/prod=transferrin-like /func=transporter /map=69C4-69C4 /transc=CT29752 /len=2860 /GB:AE003541 /note=3prime sequence from clone BDGP:LD22449.
42356.9 2.2 FB:FBgn0037245 /sym=CG14648 /name=/prod=/func=enzyme /map=82B3-82B3 /transc=CT34420 /len=1773 /GB:AE003606

22512 2.2 FB:FBgn0033385 /sym=CG8055 /name= /prod= /func= /map=45B1-45B1 /transc=CT8052 /len=1251 /GB:AE003834 /note=3prime sequence from clone BDGP:GH13992.3prime-hit

574.3 ~2.2 FB:FBgn0034578 /sym=CG15653 /name= /prod= /func= /map=57B20-57B20 /transc=CT35837 /len=513 /GB:AE003452

1624.6 ~2.2 FB:FBgn0025802 /sym=Sbf /name=SET domain binding factor /prod= /func=ligand binding or carrier /map=86F9-86F9 /transc=CT21495 /len=6619 /GB:AE003693 /note=3prime sequence from clone

1672.7 2.2 FB:FBgn0031454 /sym=CG9960 /name= /prod= /func= /map=23B1-23B1 /transc=CT28077 /len=799 /GB:AE003582 /note=3prime sequence from clone BDGP:GH13185.3prime-hit

798.8 ~2.2 FB:FBgn0039443 /sym=CG14242 /name= /prod= /func= /map=97C1-97C1 /transc=CT33862 /len=687 /GB:AE003757

13583.6 2.1 FB:FBgn0037465 /sym=CG1105 /name= /prod= /func= /map=84C1-84C1 /transc=CT1653 /len=1336 /GB:AE003673

1734.8 ~2.1 FB:FBgn0034494 /sym=CG10444 /name= /prod=sodium-dependent multivitamin transporter-like /func=transporter /map=56F15-56F16 /transc=CT29322 /len=2772 /GB:AE003792 /note=3prime sequ

38948.5 2.1 FB:FBgn0028684 /sym=Rpt5 /name=Tat-binding protein-1 /prod=19S proteasome regulatory particle, triple-A protein, subunit S6a /func=proteasome ATPase ; EC:3.6.4.8 /map=95B7-95B7 /transc=CT

73992.4 2.1 FB:FBgn0034583 /sym=CG10527 /name= /prod= /func= /map=57B20-57B20 /transc=CT29543 /len=1133 /GB:AE003452 /note=3prime sequence from clone BDGP:LD46156.3prime-hit

8442.3 2.1 FB:FBgn0016700 /sym=Rab1 /name=Rab-protein 1 /prod= /func=RHO small GTPase /map=93D4-93D4 /transc=CT11153 /len=1791 /GB:AE003734

4736.2 2.1 FB:FBgn0038298 /sym=CG18525 /name= /prod= /func= /map=88E7-88E7 /transc=CT42292 /len=1494 /GB:AE003708 /note=3prime sequence from clone BDGP:GH14439.3prime-hit

160299.1 2.1 FB:FBgn0037686 /sym=CG9354 /name= /prod=ribosomal protein L34-like /func=structural protein of ribosome /map=85D15-85D15 /transc=CT25494 /len=771 /GB:AE003682

836.4 ~2.1 FB:FBgn0036722 /sym=CG13729 /name= /prod= /func= /map=74C1-74C1 /transc=CT33196 /len=360 /GB:AE003524

296466.6 2.1 FB:FBgn0002626 /sym=Rpl32 /name=Ribosomal protein L32 /prod=ribosomal protein L32 /func=large-subunit cytosol ribosomal protein /map=99D5-99D5 /transc=CT6405 /len=505 /GB:AE003772

12782.7 2.1 FB:FBgn0030087 /sym=CG7766 /name= /prod= /func=protein kinase /map=8C13-8C14 /transc=CT23171 /len=3994 /GB:AE003446

15250.7 2.1 FB:FBgn0023211 /sym=Elongin-C /name=Elongin C /prod=elongin C /func=transcription factor /map=56D7-56D7 /transc=CT26431 /len=557 /GB:AE003796

1257.5 ~2.1 FB:FBgn0040974 /sym=CG9260 /name= /prod= /func= /map=34C1-34C1 /transc=CT26204 /len=460 /GB:AE003640

389648.8 2.1 FB:FBgn0002533 /sym=Lcp2 /name=Larval cuticle protein 2 /prod=larval cuticle protein 2 /func=structural protein of larval cuticle (*Drosophila*) /map=44C1-44C1 /transc=CT3631 /len=526 /GB:AE0

27381 2.1 FB:FBgn0026088 /sym=EG:63B12.12 /name= /prod= /func= /map=2B14-2B14 /transc=CT34631 /len=460 /GB:AE003422

1849.4 ~2.1 FB:FBgn0039353 /sym=CG5046 /name= /prod= /func=cell adhesion /map=96E10-96E10 /transc=CT16193 /len=840 /GB:AE003753

15969.5 2.1 FB:FBgn0011768 /sym=Fdh /name=Formaldehyde dehydrogenase /prod=formaldehyde dehydrogenase (glutathione) /func=formaldehyde dehydrogenase (glutathione) ; EC:1.2.1.1 | inferred from direct

16747.9 2.1 FB:FBgn0032725 /sym=CG10679 /name= /prod= /func=structural protein of ribosome /map=37B8-37B8 /transc=CT29904 /len=255 /GB:AE003661

40713.9 2.1 FB:FBgn0032134 /sym=CG3864 /name= /prod= /func= /map=30C1-30C2 /transc=CT12877 /len=966 /GB:AE003625 /note=3prime sequence from clone BDGP:SD03042.3prime-hit

5591.9 2.1 FB:FBgn0033635 /sym=CG7777 /name= /prod=water transporter /func=transporter /map=47F13-47F13 /transc=CT23658 /len=1371 /GB:AE003826 /note=3prime sequence from clone BDGP:LD273

400824.5 2.1 FB:FBgn0002535 /sym=Lcp4 /name=Larval cuticle protein 4 /prod=larval cuticle protein 4 /func=structural protein of larval cuticle (*Drosophila*) /map=44C1-44C1 /transc=CT6607 /len=682 /GB:AE0

288362.1 2.1 FB:FBgn0002741 /sym=Mhc /name=Myosin heavy chain /prod=myosin II heavy chain /func=muscle motor protein /map=36A8-36A9 /transc=CT39920 /len=5794 /GB:AE003652

48332.5 2.1 FB:FBgn0013770 /sym=Cp1 /name=Cysteine proteinase-1 /prod=cathepsin L /func=cathepsin L ; EC:3.4.22.15 /map=50C20-50C20 /transc=CT20780 /len=1502 /GB:AE003816 /note=3prime sequence

889.6 ~2.1 FB:FBgn0033024 /sym=CG10416 /name= /prod= /func=RNA-directed DNA polymerase, group II intron encoded /map=41C2-41C2 /transc=CT29248 /len=1195 /GB:AE003786

4395.3 2.1 FB:FBgn0030847 /sym=CG12991 /name= /prod= /func= /map=16B8-16B8 /transc=CT32195 /len=1380 /GB:AE003506

1345.9 ~2.1 FB:FBgn0035026 /sym=CG12252 /name= /prod=RNA polymerase CTD phosphatase /func=protein phosphatase /map=60D5-60D5 /transc=CT15027 /len=3150 /GB:AE003464 /note=3prime sequence

16739.2 2.1 FB:FBgn0037752 /sym=CG8495 /name= /prod=ribosomal protein S29-like /func=structural protein of ribosome /map=85E9-85E9 /transc=CT24837 /len=979 /GB:AE003684

20291.9 2.1 FB:FBgn0030350 /sym=CG1844 /name= /prod= /func= /map=10F4-10F4 /transc=CT5645 /len=828 /GB:AE003487 /note=3prime sequence from clone BDGP:GH03581.3prime-hit

18640.2 2.1 FB:FBgn0035549 /sym=CG11346 /name= /prod= /func=structural protein /map=64B12-64B12 /transc=CT31648 /len=564 /GB:AE003481

1344.2 ~2.1 BDGP:LD32469.3prime-hit /maps to FB:FBgn0032432 (/sym=CG5442 /name= /prod=/func=) and FB:FBgn0032431 (/sym=CG5435 /name= /prod=/func=)

67263 2.1 FB:FBgn0038570 /sym=CG7217 /name= /prod= /func= /map=90E4-90E4 /transc=CT22257 /len=728 /GB:AE003721 /note=3prime sequence from clone BDGP:LD45324.3prime-hit

2990.8 2.1 FB:FBgn0023081 /sym=gek /name=genghis khan /prod=protein serine/threonine kinase /func=protein serine/threonine kinase ; EC:2.7.1.37 /map=60B5-60B5 /transc=CT13314 /len=5090 /GB:AE00346

136706.6 2.1 FB:FBgn0037874 /sym=CG4800 /name= /prod= /func= /map=86D7-86D7 /transc=CT15437 /len=782 /GB:AE003690

21274.7 2.1 FB:FBgn0020249 /sym=stck /name=steamer duck /prod= /func=transcription factor /map=84F15-84F16 /transc=CT23960 /len=1335 /GB:AE003678 /note=3prime sequence from clone BDGP:LD393

1644.3 ~2.1 FB:FBgn0039333 /sym=CG11917 /name= /prod= /func= /map=96D2-96D2 /transc=CT37090 /len=718 /GB:AE003751

58741.5 2.1 FB:FBgn0024923 /sym=TER94 /name=Saccharomyces cerevisiae UAS construct a of McKearin /prod=transitional endoplasmic reticulum adenosinetriphosphatase /func=adenosinetriphosphatase ; EC:3

111848.8 2.1 FB:FBgn0027844 /sym=CAH1 /name=Carbonic anhydrase 1 /prod=carbonate dehydratase /func=carbonate dehydratase ; EC:4.2.1.1 /map=34D1-34D1 /transc=CT23642 /len=1439 /GB:AE003641 /note

737.1 ~2.1 FB:FBgn0033900 /sym=CG8257 /name= /prod=cysteine--tRNA ligase-like /func=enzyme /map=50E2-50E2 /transc=CT24479 /len=1770 /GB:AE003815 /note=3prime sequence from clone BDGP:GH

392081.5 2.1 FB:FBgn0000116 /sym=Argk /name=Arginine kinase /prod=arginine kinase /func=arginine kinase ; EC:2.7.3.3 /map=66F2-66F2 /transc=CT13858 /len=2106 /GB:AE003553 /note=3prime sequence from

8765.4 2 FB:FBgn0037253 /sym=CG9798 /name= /prod= /func= /map=82C1-82C2 /transc=CT27682 /len=1914 /GB:AE003606

13142.2 2 FB:FBgn0027066 /sym=BcDNA:LD08743 /name= /prod= /func=cytoskeletal structural protein /map=42C3-42C4 /transc=CT10989 /len=1860 /GB:AE003789

495060.3 2 FB:FBgn0030541 /sym=CG11584 /name= /prod= /func=ligand binding or carrier /map=12D3-12D3 /transc=CT36540 /len=3048 /GB:AE003495

27166.8 2 BDGP:GH18222.3prime-hit /ESTpos=maps in FB:FBgn0033295 /sym=CG8689 /name= /prod=maltase L-like /func=enzyme /map=44C3-44C3 /transc=CT6492 /len=521

102551.1 2 FB:FBgn0011726 /sym=tsr /name=twinstar /prod=cofilin /func=actin binding /map=60B2-60B2 /transc=CT13858 /len=733 /GB:AE003462

10619.8 2 FB:FBgn0033134 /sym=CG12840 /name=Tetraspanin 42E1 /prod=tetraspanin /func= /map=42E2-42E2 /transc=CT31972 /len=1034 /GB:AE003842 /note=3prime sequence from clone BDGP:GH1495

3500.4 2 FB:FBgn0026630 /sym=nes /name=nessy /prod= /func= /map=76A3-76A3 /transc=CT27290 /len=2247 /GB:AE003517

7369.6 2 FB:FBgn0039595 /sym=CG10001 /name= /prod=allatostatin receptor-like /func=allatostatin receptor /map=98E2-98E2 /transc=CT28187 /len=990 /GB:AE003766

114502.3 2 FB:FBgn0032518 /sym=CG9282 /name= /prod=ribosomal protein L24 /func=structural protein of ribosome /map=34B6-34B6 /transc=CT26439 /len=774 /GB:AE003640

13035.4 2 J04423 E coli bioD gene dethiobiotin synthetase (-5 and -3 represent transcript regions 5 prime and 3 prime respectively)

21381.4 2 FB:FBgn0010808 /sym=l(3)03670 /name= /prod= /func= /map=100B4-100B4 /transc=CT4906 /len=906 /GB:AE003776

3752.8 2 FB:FBgn0035272 /sym=CG13922 /name= /prod= /func=structural protein of ribosome /map=62B4-62B4 /transc=CT33461 /len=830 /GB:AE003472

5878.8 2 FB:FBgn0035201 /sym=CG9146 /name= /prod= /func= /map=61F5-61F5 /transc=CT26188 /len=4092 /GB:AE003471

16376.3 2 FB:FBgn0027525 /sym=BcDNA:LD21529 /name= /prod= /func= /map=47C3-47C3 /transc=CT23459 /len=1643 /GB:AE003828 /note=3prime sequence from clone BDGP:LD21529.3prime-hit

51256.2 2 FB:FBgn0025366 /sym=Ip259 /name=Intronic Protein 259 /prod= /func= /map=31E1-31E1 /transc=CT16819 /len=838 /GB:AE003628 /note=3prime sequence from clone BDGP:GM13959.3prime-hit

48807.2 2 FB:FBgn0033188 /sym=CG1600 /name= /prod= /func=enzyme /map=43D3-43D3 /transc=CT37723 /len=1747 /GB:AE003840 /note=3prime sequence from clone BDGP:GH18014.3prime-hit

37785.4 2 BDGP:LP11629.3prime-hit /ESTpos=maps 3prime of FB:FBgn0033505 /sym=CG3451 /name= /prod= /func=cell cycle regulator /map=46F9-46F9 /transc=CT7898 /len=250

61261.7 2 FB:FBgn0000261 /sym=Cat /name=Catalase /prod=catalase /func=catalase ; EC:1.11.1.6 | inferred from direct assay /map=75D7-75D8 /transc=CT21282 /len=1977 /GB:AE003519

11587.6 2 FB:FBgn0031213 /sym=CG11372 /name= /prod= /func=ligand binding or carrier /map=21A5-21A5 /transc=CT31742 /len=1517 /GB:AE003590

224678.7 2 FB:FBgn0025828 /sym=EG:EG0003.7 /name= /prod=cytosolic translation release factor-like /func=cytosolic translation release factor /map=53D14-53D15 /transc=CT19804 /len=790 /GB:AE003805

33829.9 2 FB:FBgn0025582 /sym=Int6 /name=Int6 homologue /prod=translation initiation factor 3, subunit 6 /func=cytosolic translation initiation factor /map=73C1-73C1 /transc=CT27364 /len=1560 /GB:AE003590

26729	2	FB:FBgn0030531 /sym=CG11058 /name= /prod= /func=enzyme /map=12B9-12B10 /transc=CT30929 /len=2254 /GB:AE003493 /note=3prime sequence from clone BDGP:GH10492.3prime-hit
22852.6	2	FB:FBgn0015268 /sym=Nap1 /name=Nucleosome assembly protein 1 /prod=nucleosome assembly protein 1 /func=nucleosome assembly chaperone /map=60A9-60A9 /transc=CT16956 /len=1381 /GB:AE003493 /note=3prime sequence from clone BDGP:GH10492.3prime-hit
34734.6	2	FB:FBgn0025637 /sym=skpA /name= /prod= /func=cell cycle regulator /map=1B10-1B11 /transc=CT32694 /len=1059 /GB:AE003418 /note=3prime sequence from clone BDGP:HL01263.3prime-hit
21750	2	FB:FBgn0020236 /sym=ATPCL /name=ATP citrate lyase /prod=ATP-citrate (pro-S)-lyase /func=ATP-citrate (pro-S)-lyase ; EC:4.1.3.8 /map=52E1-52E1 /transc=CT18257 /len=3745 /GB:AE003808
10182.9	2	FB:FBgn0038446 /sym=CG14903 /name= /prod= /func= /map=89D3-89D3 /transc=CT34727 /len=360 /GB:AE003714
13919.3	2	FB:FBgn0035471 /sym=CG10849 /name= /prod= /func= /map=63F6-63F6 /transc=CT30379 /len=1056 /GB:AE003479 /note=3prime sequence from clone BDGP:SD09294.3prime-hit
39019.7	2	FB:FBgn0038826 /sym=CG17838 /name= /prod=RNA binding protein /func=RNA binding /map=92F10-92F10 /transc=CT39628 /len=1802 /GB:AE003732 /note=3prime sequence from clone BDGP:SD04477.3prime-hit
15475.2	2	FB:FBgn0003498 /sym=sqd /name=squid /prod= /func=ribonucleoprotein /map=87F7-87F7 /transc=CT39414 /len=1137 /GB:AE003701
2246.4	2	FB:FBgn0001297 /sym=kay /name=kayak /prod= /func=DNA binding /map=99C2-99C4 /transc=CT35622 /len=2642 /GB:AE003771 /note=3prime sequence from clone BDGP:SD04477.3prime-hit

Lebenslauf

Ich bin am 13.12.1975 in Tianjin, Volkrepublik China, geboren und habe die chinesische Staatsangehörigkeit. 1994 schloss ich die No.1 High School in Tianjin ab und begann im selben Jahr mein Studium an der Nankai Universität in Tianjin. 1998 erhielt ich den Bachelor of Science im Hauptfach Molekularbiologie. 2001 erhielt ich den Master of Science (First class honours degree) der Nankai Universität in Tianjin.

Am 15. August 2001 begann ich in der Abteilung von Dr. Stephan J. Sigrist am European Neuroscience Institute des Bereichs Humanmedizin der Georg-August-Universität Göttingen unter der Anleitung von Prof. Dr. Friedrich-Wilhelm Schürmann die Arbeit an der Dissertation mit dem Thema „Identification and functional characterization of novel ionotropic glutamate receptor subunits at *Drosophila* neuromuscular synapse“.